

Eugenio Fernández Cáceres

Assessment and measurement of
nox emissions in light diesel
vehicles during periodic technical
inspection

Director/es

Valero Delgado, Alicia
Ortego Bielsa, Abel

<http://zaguan.unizar.es/collection/Tesis>



Universidad de Zaragoza
Servicio de Publicaciones

ISSN 2254-7606

Tesis Doctoral

ASSESSMENT AND MEASUREMENT OF NOX
EMISSIONS IN LIGHT DIESEL VEHICLES DURING
PERIODIC TECHNICAL INSPECTION

Autor

Eugenio Fernández Cáceres

Director/es

Valero Delgado, Alicia
Ortego Bielsa, Abel

UNIVERSIDAD DE ZARAGOZA
Escuela de Doctorado

Programa de Doctorado en Energías Renovables y Eficiencia Energética

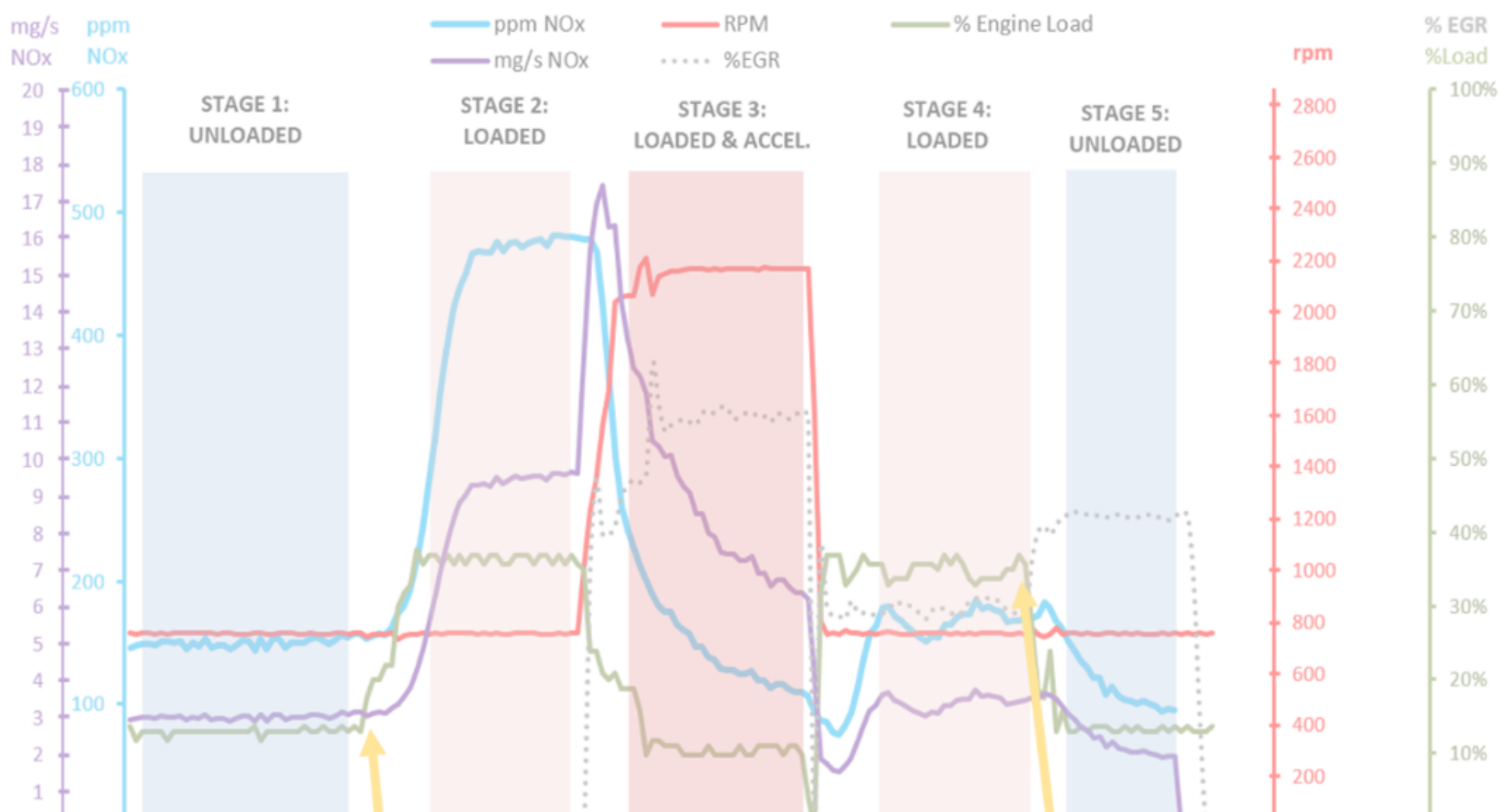
2024

Ph.D. DISSERTATION

ASSESSMENT AND MEASUREMENT OF NO_x EMISSIONS IN LIGHT DIESEL VEHICLES DURING PERIODIC TECHNICAL INSPECTION

Zaragoza, 2023

AUTHOR: Eugenio Fernández Cáceres



SUPERVISED BY:

Ph.D. Alicia Valero Delgado & Ph.D. Abel Ortego Bielsa



Universidad
Zaragoza



ASSESSMENT AND MEASUREMENT OF NO_x EMISSIONS IN LIGHT DIESEL VEHICLES DURING PERIODIC TECHNICAL INSPECTION

Zaragoza, 2023

Lord Kelvin:

"If you cannot measure it, you cannot improve it."

Enrico Fermi:

"There are two possible outcomes: if the result confirms the hypothesis, then you have made a measurement. If the result is contrary to the hypothesis, then you've made a discovery"

AGRADECIMIENTOS

Antes de comenzar una tarea de la envergadura de una Tesis Doctoral, no se es consciente (al menos yo no lo era) de cuánta gente te va a acompañar en el camino.

Al comienzo se asume como un reto personal, donde sólo tu esfuerzo y dedicación parecen necesarios para llevar a buen término el trabajo emprendido.

Sin embargo, al llegar al final del camino y echar la vista atrás, te das cuenta de toda la gente que ha estado involucrada, de una forma directa o indirecta, y sin cuya participación sencillamente habría sido imposible alcanzar el objetivo final.

Desde principios de 2017, hasta la finalización de la investigación en 2023, son muchas las personas a las que tengo que dar las gracias, y espero no olvidar a nadie. Si esto ocurriera ruego comprensión.

En primer lugar, sin duda, quiero dar las gracias a la persona que ha sufrido mis ausencias (no sólo las físicas, sino también las mentales) durante estos años. Laura, tú has hecho un doctorado en paciencia y comprensión, y la nota ha sido *Summa Cum Laude*. Ahora podrás tomarte unas merecidas vacaciones. Por supuesto, también Sofía y Alba tienen un trocito del diploma de su madre, dándole apoyo y compañía durante mis ausencias. Muchísimas gracias a las tres por vuestra comprensión.

Mi madre y mi hermana, que siempre están orgullosas de mí y sé que presumen de mis logros. Muchas gracias por vuestro apoyo y cariño. Se lo orgulloso que estaría mi padre viendo este momento. No hay día que no me acuerde de él, y me sirva de inspiración.

Una parte muy importante han sido mis compañeros y la empresa en la que trabajo. Muchas gracias a la dirección de GRUPO ITEVELESA por permitirme desarrollar la investigación en la estación de ITV donde trabajo, y poner a mi disposición todos los medios, tanto técnicos como humanos, que han sido necesarios para el desarrollo de la investigación. Nunca me ha faltado nada.

A Miguel Ángel Ubieto Pujalá, mi compañero, que se ha adaptado a mis continuos cambios de horarios, y que me ha puesto todas las facilidades del mundo para poder desarrollar la investigación. Muchas gracias, por esto y por muchas otras cosas.

A César de la Puente Gutiérrez, que me apoyó y animó con la investigación desde que solicité los primeros permisos, muchas gracias por orientar hacia CITA los trabajos que realizábamos. Fue un paso fundamental. Y a Juan Ramón González Rojo, que me acompañó y guio en las primeras reuniones en CITA, su apoyo fue de gran ayuda.

Y por supuesto, a todos mis compañeros de la estación de ITV 5001 de Malpica (y también de otras estaciones), que me han ayudado con los equipos, han cedido sus vehículos para hacer pruebas, han hecho mediciones a cientos de vehículos a pesar de la carga de trabajo, e incluso han acudido a Motorland para ayudarme a hacer mediciones en circulación, muchísimas gracias por vuestra ayuda.

Asimismo, agradecer también a Jorge Royo Mallén, Jefe de la Sección de Coordinación de Estaciones de ITV del Gobierno de Aragón, el interés y apoyo que me ha dado en todo este tiempo.

Una persona que ha sido fundamental para el desarrollo de la tesis es sin duda Rafael Baltasar Varela, de la empresa TEKBER (Centralauto). Su apoyo a nivel técnico ha sido impresionante, y aun así no es nada comparado con su apoyo a nivel humano. Sin el software desarrollado por él, hecho a medida para esta investigación, no habría sido posible alcanzar los resultados logrados.

En la Universidad de Zaragoza hay grandísimos profesionales, y además he tenido la suerte de conocer a algunos de los mejores. Alicia Valero Delgado y Abel Ortego Bielsa me han guiado, apoyado y ayudado desde el comienzo hasta el final, aportando su experiencia y saber hacer en el complejo trayecto que se debe recorrer para finalizar una investigación de este tipo. Me han facilitado ánimos, medios y recursos para poder llevar a cabo la investigación. Por ejemplo, las mediciones en Motorland Aragón y en CMT-Motores Térmicos de la Universitat Politècnica de Valencia no hubieran sido posibles sin ellos. Muchas gracias a los dos, este trabajo no hubiera sido posible sin vosotros.

Muchas gracias también a Juan José Alba López por su participación y sus ideas, ha sido un privilegio contar con su colaboración, y a Francisco Moreno Gómez por orientarnos en la mejor manera de acabar de validar el método y el equipo.

Además, agradecer a Antonio Valero Capilla su inspiración. El primer paso que me llevó a iniciar este viaje fueron sus clases en el Máster.

En el ámbito universitario, también tengo que dar las gracias al CMT-Motores Térmicos de la Universitat Politècnica de Valencia, y en especial a Vicente Bermúdez, por su colaboración y su gran generosidad, cediéndonos sus equipaciones, su ayuda y aún más importante, su tiempo, para realizar mediciones en sus instalaciones.

También quiero agradecer a Vicente Diaz López y a Susana Sanz Sánchez, de la Universidad Carlos III de Madrid, que me aportaron su valiosa experiencia y conocimiento. Su punto de vista me aportó nuevas perspectivas.

Para finalizar, me gustaría dar las gracias a todos los integrantes de CITA con los que he tenido el placer de colaborar. Poder presentar y defender los avances de la investigación en este foro, con un gran espíritu de crítica constructiva, me ha ayudado en gran medida a afianzar el método y hacerlo más robusto, además de darle visibilidad. En especial me gustaría agradecer a Eduard Fernández su excelente gestión y su amabilidad conmigo, a Thomas Ost por la gran labor realizada dirigiendo el grupo de trabajo de NO_x, a Pascal Buekenhoudt por su experiencia y excelente colaboración analizando métodos de medición de NO_x, y a Georges Petelet por su ayuda cediéndonos equipos para hacer pruebas. Ha sido un privilegio poder colaborar con todos ellos, y he aprendido mucho más de lo que yo haya podido aportar.

ACKNOWLEDGMENTS

Before embarking on a task of the magnitude of a Doctoral Thesis, one is not aware (at least I wasn't) of how many people will accompany you on the journey.

At the outset, it is assumed to be a personal challenge, where only your effort and dedication seem necessary to successfully complete the undertaken work.

However, upon reaching the end of the road and looking back, you realize all the people who have been involved, directly or indirectly, and without whose participation it would have simply been impossible to achieve the final goal.

From early 2017 to the completion of the research in 2023, there are many people I need to express my gratitude to, and I hope not to forget anyone. If this were to happen, I ask for your understanding.

First and foremost, undoubtedly, I want to thank the person who has endured my absences (not only physical but also mental) during these years. Laura, you have earned a doctorate in patience and understanding, and your grade is *Summa Cum Laude*. Now you can take a well-deserved vacation. Of course, Sofia and Alba also have a piece of their mother's diploma, providing support and companionship during my absences. Many thanks to all three of you for your understanding.

My mother and my sister, who are always proud of me and I know they boast about my achievements. Thank you very much for your support and affection. I know how proud my father would be witnessing this moment. Not a day goes by without me thinking of him and drawing inspiration from him.

A very important part has been played by my colleagues and the company I work for. Many thanks to the management of GRUPO ITEVELESA for allowing me to carry out the research at the ITV station where I work, and for providing me with all the necessary resources, both technical and human, for the research's development. I have never lacked anything.

To Miguel Ángel Ubieto Pujalá, my colleague, who has adapted to my constant changes in schedules and has made every effort to facilitate my research. Thank you very much for this and many other things.

To César de la Puente Gutiérrez, who supported and encouraged me in the research from the moment I requested the first permissions, thank you very much for guiding our work towards CITA. It was a pivotal step. And to Juan Ramón González Rojo, who accompanied and guided me in the initial meetings at CITA, his support was greatly beneficial.

And of course, to all my colleagues at the Malpica PTI Station No. 5001 (and at other stations), who have helped me with equipment, provided their vehicles for testing, conducted measurements on hundreds of vehicles despite their workload, and even went to Motorland to assist me with on-road measurements, thank you very much for your assistance.

Likewise, I'd like to thank Jorge Royo Mallén, Head of the Coordination Section of ITV Stations at the Government of Aragon, for the interest and support he has shown me throughout this time.

A person who has been fundamental to the development of this thesis is undoubtedly Rafael Baltasar Varela, from the company TEKBER (Centralauto). His technical support has been impressive, and yet it pales in comparison to his human support. Without the software he developed specifically for this research, achieving the results attained would not have been possible.

At the University of Zaragoza, there are outstanding professionals, and I've had the fortune of meeting some of the best. Alicia Valero Delgado and Abel Ortego Bielsa have guided, supported, and assisted me from beginning to end, contributing their experience and expertise to the complex journey required to finish research of this kind. They provided encouragement, resources, and means to carry out the research. For example, the measurements at Motorland Aragón and CMT-Motores Térmicos of the Universitat Politècnica de Valencia would not have been possible without them. Thank you both; this work wouldn't have been possible without you.

Many thanks also to Juan José Alba López for his participation and ideas. It has been a privilege to have his collaboration. Thanks to Francisco Moreno Gómez for guiding us in the best way to complete the method and equipment validation.

Additionally, I'd like to thank Antonio Valero Capilla for his inspiration. The first step that led me to embark on this journey was his classes in the Master's program.

In the academic sphere, I also need to express my gratitude to CMT-Motores Térmicos of the Universitat Politècnica de Valencia, and especially to Vicente Bermúdez, for their collaboration and great generosity in providing their facilities, assistance, and even more importantly, their time, for conducting measurements in their installations.

I would also like to thank Vicente Diaz López and Susana Sanz Sánchez from the Carlos III University of Madrid, who shared their valuable experience and knowledge. Their perspective brought new insights.

To conclude, I would like to express my gratitude to all members of CITA with whom I've had the pleasure of collaborating. Being able to present and defend research progress in this forum, with a spirit of constructive criticism, greatly aided in solidifying the method and making it more robust, while also giving it visibility. I would especially like to thank Eduard Fernández for his excellent management and kindness towards me, Thomas Ost for his outstanding work in leading the NO_x working group, Pascal Buekenhoudt for his experience and excellent collaboration in analyzing NO_x measurement methods, and Georges Petelet for his assistance. It has been a privilege to collaborate with all of them, and I have learned much more than I could have contributed myself.

RESUMEN

La contaminación atmosférica es, según la EEA (European Environment Agency), el mayor **riesgo medioambiental para la salud** en Europa, especialmente en las zonas urbanas donde el 72% de la población europea (el 40% en zonas densamente pobladas y el 32% en ciudades pequeñas y suburbios) está expuesta a altas concentraciones de contaminantes.

Uno de los principales contaminantes que se encuentran en esta contaminación atmosférica son los óxidos de nitrógeno, comúnmente conocidos como NO_x , los cuales se originan en procesos de combustión.

Entre los procesos de combustión donde se originan los NO_x , el principal por su contribución a la cantidad total de este contaminante son los motores de combustión de los vehículos de transporte por carretera. Estos son responsables del 40% de las emisiones totales, y de ellos los motores de compresión que utilizan combustible diesel generan el 85% del total de las emisiones debidas al transporte por carretera en Europa.

Para reducir los efectos de la exposición de la población a los NO_x , sería necesario reducir su presencia o concentración en la atmósfera, especialmente en los ambientes urbanos. Idealmente, se deberían eliminar totalmente las emisiones de NO_x , pero dado que esto a corto y medio plazo es inviable, se debe tratar al menos de minimizar dichas emisiones. Por tanto, es fundamental reducir las emisiones de NO_x de los vehículos diesel.

Conscientes de esta problemática las autoridades europeas han implementado, a lo largo de las últimas décadas, normativas cada vez más estrictas que teóricamente reducen las emisiones de NO_x de los vehículos. De esta forma, cada nueva generación de vehículos es menos contaminante que la anterior.

Sin embargo, en los últimos años se ha podido comprobar empíricamente que la reducción real en las emisiones de NO_x de los nuevos vehículos es mucho menor de la esperada con la implantación de estas normativas.

Además, la inexistencia de un mecanismo de control que permita monitorizar las emisiones de NO_x a lo largo de la vida útil de los vehículos, ha provocado que se haya tardado mucho tiempo en detectar esta situación.

En esta tesis se propone una herramienta que proporciona información fiable sobre las emisiones reales de NO_x de cada vehículo de la flota de vehículos, de forma periódica, y a lo largo de toda la vida útil de los vehículos. Para ello, se plantea la necesidad de realizar una **medición de NO_x** a los vehículos durante la **realización de la Inspección Técnica Periódica (ITV) obligatoria**.

La necesidad de esta prueba no es nueva, y a lo largo de los últimos años se han planteado varios posibles métodos de medición de NO_x en ITV. Sin embargo, hasta ahora no se ha implantado ninguno porque no ha habido propuestas que hayan demostrado cumplir con una serie de requisitos que son fundamentales:

- 1) El método debe cumplir los requisitos técnicos exigibles a las pruebas en ITV: la prueba debe ser rápida, sencilla y lo más económica posible en tiempo, recursos e intervención sobre el vehículo.

- 2) El resultado de la medición debe ser representativo de las emisiones reales del vehículo.
- 3) El método debe permitir establecer un valor límite que permita un nivel de rechazo adecuado de los vehículos en inspección, impidiendo la circulación de los vehículos con emisiones superiores al máximo nivel permitido.

El método propuesto de medición de NO_x se ha diseñado a partir del mecanismo de formación de NO_x, que es un proceso muy dependiente de la temperatura a la que se produce la combustión en el motor y por ello, de la demanda de par a que se somete a este.

Midiendo la demanda de par en el motor a través del OBD (mediante el valor "% engine load"), y midiendo las emisiones en la salida del escape a través de un equipo Analizador de Gases, se puede ejecutar el método de medición propuesto.

La medición de NO_x se ha planteado a régimen de ralentí, puesto que medir en esta situación aporta una serie de ventajas muy importantes para una medición en ITV:

- Simplicidad: hace el método de medición simple de aplicar, lo cual es un importante requisito para una prueba a realizar en ITV
- Reproducibilidad: se pueden reproducir las mediciones en las mismas condiciones de forma sencilla, obteniendo resultados similares
- Economía: permite realizar la prueba sin necesidad de complejos y costosos equipos, tanto en términos financieros como de tiempo, mantenimiento metrológico, requerimientos de personal,...
- Rapidez: permite realizar la prueba de forma rápida
- Representatividad: el resultado obtenido es representativo de una situación que se produce en condiciones de circulación urbana durante un tiempo significativo en cada trayecto, y según se comprueba a lo largo de la tesis, es representativo de las emisiones reales en circulación urbana
- Aplicabilidad: se puede aplicar del mismo modo a cualquier tipo de vehículo, independientemente de su configuración (manual o automático, 2x4 o 4x4, control de tracción no desconectable, ...)

En esta condición de ralentí, se generan dos estados distintos de demanda en el motor, mediante el uso de **los consumos generados por el equipamiento del propio vehículo**. De este modo, se genera un incremento en la demanda de par sobre el motor tal que permite observar una variación en la concentración de NO_x en la salida del tubo de escape.

Para validar el método, y justificar su aplicación, se han realizado diversas investigaciones que han arrojado importante información:

- Se ha aplicado el método a un grupo de 23 vehículos representativos de la flota de automóviles diesel.
- Se han realizado mediciones de las emisiones reales de los vehículos en circulación urbana, mediante simulaciones en un circuito de competición.
- Se ha realizado una amplia campaña de medición de vehículos en ITV, con más de 1880 vehículos analizados, la mayor de estas características desarrollada hasta la fecha.

- Se ha comparado el desempeño del equipo de medición empleado con un equipo de laboratorio, para valorar su idoneidad.

De la información obtenida de todas estas actividades, se desprende que el método propuesto se adapta perfectamente a los requisitos exigibles desde ITV para su implementación en el proceso de inspección, que los resultados obtenidos son representativos de las emisiones reales de NO_x en condiciones de circulación urbana, y que se puede definir un límite de rechazo que sería factible aplicar en el proceso de inspección.

Resumiendo, a lo largo de diversas investigaciones desarrolladas se ha planteado y validado un método para medir NO_x que es factible de implantar en ITV, que proporciona valores representativos de las emisiones reales en circulación urbana, que permite establecer un límite de rechazo en inspección, que puede ser aplicado con equipamiento sencillo y económico que dispone de suficiente precisión para realizar las medidas, y que podría implementarse en un corto espacio de tiempo.

Durante el transcurso de la investigación, se han generado diversos documentos relacionados con ella. Además de la presente tesis, los principales se pueden clasificar en dos categorías fundamentales:

- Artículos revisados por pares.
- Informes independientes.

Dentro de la primera categoría, se incluyen dos artículos publicados en revistas indexadas, *Sustainability* (IF: 3.889 [2021]) y *Vehicles* (IF: 2.2 [2022]), donde se expone el método y se analiza la idoneidad del equipo de medición utilizado.

En la segunda categoría, se encuentran tres informes independientes de esta investigación que han evaluado varias opciones para la medición de NO_x, incluyendo el método presentado en este estudio.

En uno de ellos, el Position Paper emitido por CITA (*International Motor Vehicle Inspection Committee*) sobre la monitorización de NO_x en ITV, se ha seleccionado el método presentado en esta tesis como el más apropiado entre los analizados para ser incorporado a la ITV en lo que respecta a la medición de NO_x en vehículos diésel actuales. En los otros dos informes, se ha comparado el método con otros existentes, y en ambos se han destacado las ventajas que su utilización presenta sobre otros métodos.

ABSTRACT

Air pollution is, according to the European Environment Agency (EEA), the primary environmental risk to health in Europe, particularly in urban areas where 72% of the European population (40% in densely populated areas and 32% in small cities and suburbs) is exposed to high concentrations of pollutants.

One of the key pollutants found in this air pollution is nitrogen oxides, commonly known as NO_x , which originate from combustion processes. Among the combustion processes giving rise to NO_x , the most significant contributor to the total amount of this pollutant is the combustion engines of road transport vehicles. They account for 40% of total emissions, with compression engines using diesel fuel responsible for 85% of the total road transport-related emissions in Europe.

To mitigate the effects of NO_x exposure on the population, it would be necessary to reduce its presence or concentration in the atmosphere, especially in urban environments. While the ideal would be complete elimination of NO_x emissions, this is not feasible in the short and medium term, making it essential to at least minimize such emissions. Therefore, it is crucial to decrease NO_x emissions from diesel vehicles.

Recognizing this issue, European authorities have implemented increasingly stringent regulations over the past decades to theoretically reduce vehicle NO_x emissions. As a result, each new generation of vehicles is less polluting than the previous one.

However, in recent years, it has been empirically demonstrated that the actual reduction in NO_x emissions from new vehicles is much less than expected with the implementation of these regulations.

Moreover, the absence of a monitoring mechanism for NO_x emissions throughout a vehicle's lifespan has led to a delay in detecting this situation.

This thesis proposes a tool that provides reliable information about the actual NO_x emissions of each vehicle in the vehicle fleet periodically throughout their entire lifespan. To achieve this, the need for **measuring NO_x emissions from vehicles during mandatory Periodic Technical Inspection (PTI)** is suggested.

The need for this test is not new, and over the past years, several possible methods for measuring NO_x in PTI have been considered. However, none have been implemented so far due to a lack of proposals that fulfill certain fundamental requirements:

- 1) The method must meet the technical requirements applicable to PTI tests: the test must be quick, simple, and as cost-effective as possible in terms of time, resources, and vehicle intervention.
- 2) The measurement result must be representative of the vehicle's actual emissions.
- 3) The method must allow the establishment of a limit value that enables an appropriate rejection level for vehicles in inspection, preventing vehicles with emissions exceeding the maximum permissible level from being on the road.

The proposed method for measuring NO_x has been designed based on the mechanism of NO_x formation, a process highly dependent on the combustion temperature in the engine and, consequently, the engine's torque demand.

By measuring the engine's torque demand through the On-Board Diagnostics (OBD) system (via the "% engine load" value) and measuring emissions at the exhaust outlet using a Gas Analyzer, the proposed measurement method can be executed.

The NO_x measurement is conducted at idle speed since measuring in this situation offers several significant advantages for an inspection measurement:

- Simplicity: This makes the measurement method straightforward to apply, which is a crucial requirement for a test conducted during PTI.
- Reproducibility: Measurements can be reproduced under the same conditions easily, yielding similar results.
- Cost-effectiveness: The test can be conducted without the need for complex and expensive equipment, both in financial terms and in time, metrological maintenance, personnel requirements, etc.
- Swiftness: The test can be performed quickly.
- Representativeness: The obtained result represents a situation that occurs in urban driving conditions over a significant time in each journey. As confirmed throughout the thesis, it is indicative of actual emissions in urban circulation.
- Applicability: It can be applied in the same manner to any type of vehicle, regardless of its configuration (manual or automatic, 2x4 or 4x4, non-disconnectable traction control, etc.).

In this idle condition, two distinct engine demand states are generated through the use of **consumption generated by the vehicle's own equipment**. This generates an increase in engine torque demand, allowing the observation of a variation in NO_x concentration at the exhaust pipe.

To validate the method and justify its application, various investigations have been carried out, providing important information:

- The method has been applied to a group of 23 vehicles representative of the diesel car fleet.
- Real vehicle emissions have been measured under urban circulation conditions through simulations on a race circuit.
- A comprehensive vehicle measurement campaign has been conducted during PTI, analyzing over 1880 vehicles, the largest of its kind developed to date.
- The performance of the measurement equipment used has been compared with laboratory equipment to assess its suitability.

From the information obtained from all these activities, it is evident that the proposed method aligns perfectly with the requirements demanded by PTI for its implementation in the inspection process. The results obtained are indicative of real NO_x emissions in urban circulation conditions, allowing the establishment of a rejection limit applicable in the inspection process. The method can be applied using

simple and economical equipment that offers sufficient accuracy for measurements and could be implemented in a short time frame.

In summary, throughout various conducted investigations, a method for measuring NO_x has been proposed and validated. This method is feasible for implementation in PTI, providing representative values of real emissions in urban circulation, allowing the establishment of a rejection limit in inspection, feasible with simple and economical equipment possessing sufficient accuracy for measurements, and could be implemented in a short time frame.

Throughout the course of the investigation, various documents related to it have been generated. In addition to the present thesis, the main ones can be categorized into two fundamental groups:

- Peer-reviewed papers.
- Independent reports.

Within the first category, there are two papers published in indexed journals, Sustainability (IF: 3.889 [2021]) and Vehicles (IF: 2.2 [2022]), where the method is presented and the suitability of the measurement equipment used is analyzed.

In the second category, there are three independent reports from this research that have assessed several options for NO_x measurement, including the method presented in this study.

In one of them, the Position Paper issued by CITA (International Motor Vehicle Inspection Committee) regarding NO_x monitoring in PTI, the method presented in this thesis has been selected as the most appropriate among those analyzed for incorporation into the PTI concerning the measurement of NO_x in current diesel vehicles. In the other two reports, the method has been compared with other existing ones, and in both cases, the advantages of its use over other methods have been highlighted.

CONTENT

AGRADECIMIENTOS.....	I
ACKNOWLEDGMENTS.....	III
RESUMEN	V
ABSTRACT.....	VIII
CONTENT.....	XI
LIST OF FIGURES.....	XVI
LIST OF TABLES.....	XXIII
LIST OF EQUATIONS.....	XXVI
ABBREVIATIONS.....	XXVIII
1. CONCEPTUAL FRAMEWORK, RESEARCH GOALS AND SCOPE OF THE THESIS.	2
1.1. INTRODUCTION.....	2
1.2. NO _x EMISSIONS: A HEALTH PROBLEM.....	2
1.3. WHY ARE DIESEL VEHICLES SO IMPORTANT TO CONTROL NO _x EMISSIONS?.....	10
1.4. NO _x EMISSIONS REGULATORY CONTROL, DISTRIBUTION, AND EVOLUTION.....	12
1.5. WHY IT IS IMPORTANT TO ASSESS AND MEASURE THE NO _x EMISSIONS AT PTI?.....	19
1.6. QUESTIONS ADDRESSED IN THE THESIS.....	20
1.6.1. IS NO _x MEASUREMENT IN PTI FEASIBLE?.....	20
1.6.2. IS NO _x MEASUREMENT IN PTI TECHNICALLY FEASIBLE? COMPLIANCE OF INSPECTION REQUIREMENTS AND AVAILABLE TECHNICAL RESOURCES.....	21
1.6.3. REPRESENTATIVENESS OF NO _x MEASUREMENT RESULTS: DOES THE MEASUREMENT REFLECT ACTUAL NO _x EMISSIONS?.....	22
1.6.4. ADVANTAGES OF NO _x MEASUREMENT IN PTI.....	23
1.7. OBJECTIVES OF THE THESIS.....	24
1.8. CONCLUSIONS.....	25
2. NO_x GENERATION, ANALYTICAL TECHNIQUES, MEASUREMENT METHODS, AND STUDIES FOR NO_x MEASUREMENT.....	27
2.1. INTRODUCTION.....	27
2.2. NO _x GENERATION PROCESS AND ITS DEPENDENCE ON ENGINE LOAD IN DIESEL VEHICLES.....	27
2.3. NO _x MEASUREMENT ANALYTICAL TECHNIQUES.....	33
2.3.1. CHEMILUMINESCENT ANALYZER (CLD).....	33
2.3.2. NON-DISPERSIVE ULTRAVIOLET ANALYZER (NDUV).....	35
2.3.3. NON-DISPERSIVE INFRA-RED ANALYZER (NDIR).....	36
2.3.4. INFRARED SUCH AS FOURIER-TRANSFORM INFRARED SPECTROSCOPY (FTIR).....	37
2.3.5. ELECTROCHEMICAL SENSORS.....	38
2.4. NO _x MEASUREMENT TESTS CURRENTLY IN USE.....	39

2.4.1.	UNLOADED TESTS	40
2.4.2.	TESTS WITH POWER DYNAMOMETER BENCH AT LOADED STEADY STATE.....	41
2.4.3.	TESTS WITH POWER DYNAMOMETER BENCH AT LOADED TRANSIENT	42
2.4.4.	ON-ROAD SIMULATION TESTS WITH POWER DYNAMOMETER BENCH AT LOADED TRANSIENT.....	43
2.4.5.	ON-ROAD TEST	47
2.4.6.	OTHER METHODS.....	47
2.5.	NO_x MEASUREMENT STUDIES.....	49
2.5.1.	REAL-WORLD NO _x MEASUREMENTS.....	49
2.5.1.1.	RSD MEASUREMENTS.....	49
2.5.1.2.	PEMS MEASUREMENTS.....	53
2.5.2.	NO _x MEASUREMENT AT PTI.....	59
2.6.	CONCLUSIONS.....	61
3.	TEST REQUIREMENTS FOR NO_x MEASUREMENT IN PTI.....	64
3.1.	INTRODUCTION	64
3.2.	PREMISES DESIGNING A NO _x EMISSIONS TEST FOR PTI.....	64
3.3.	PROPOSAL PRESENTATION	74
3.4.	TEST FEATURES OF IDLING MEASUREMENT.....	78
3.5.	CONCLUSIONS	80
4.	NO_x MEASUREMENT METHOD FOR PTI DESCRIPTION.....	83
4.1.	INTRODUCTION	83
4.2.	MEASUREMENT METHOD DESCRIPTION.....	83
4.2.1.	"% ENGINE LOAD" VALUE VARIATION ALONG WITH THE TEST	83
4.2.2.	STEP BY STEP OF THE TEST: MEASUREMENT PROTOCOL.....	87
4.2.3.	DATA AGGREGATION, UNLOADED, AND LOADED STATES.....	94
4.2.4.	CALCULATION OF THE MASS EMISSION OF NO _x	96
4.2.5.	TEST FINAL RESULT: 100% ENGINE LOAD NO _x EMISSIONS' EXTRAPOLATION.....	99
4.3.	SUMMARY OF THE MEASUREMENT PROTOCOL.....	106
4.4.	CONCLUSIONS	109
5.	PTI MEASUREMENT EQUIPMENT DESCRIPTION AND SUITABILITY	111
5.1.	INTRODUCTION	111
5.2.	GAS ANALYZER DESCRIPTION	111
5.3.	SUITABILITY OF NO _x MEASUREMENT WITH THE GAS ANALYZER.....	117
5.3.1.	MATERIALS AND METHODS.....	118
5.3.1.1.	DIESEL ENGINE AND ACCESSORIES.....	120
5.3.1.2.	PTI GAS ANALYZER.....	124
5.3.1.3.	LABORATORY GAS ANALYZER.....	124
5.3.1.4.	TESTS PERFORMED	126
5.3.1.5.	EQUIPMENT CALIBRATION	126
5.3.2.	RESULTS.....	127
5.3.2.1.	RESULTS OF STATIC IDLING INTERNAL LOAD TESTS.....	128
5.3.2.2.	RESULTS FOR FIXED ENGINE SPEED AND INCREASING LOAD TESTS.....	133
5.4.	CONCLUSIONS	143

6.	NO_x MEASUREMENT METHOD VALIDATION	146
6.1.	INTRODUCTION.....	146
6.2.	SET OF VEHICLES TESTED FOR METHOD VALIDATION.....	146
6.3.	QUALITY AND SIGNIFICANCE ANALYSIS	149
6.3.1.	R ² VALUE AND QUALITY.....	151
6.3.2.	P-VALUE AND SIGNIFICANCE.....	152
6.3.3.	QUALITY AND SIGNIFICANCE RESULTS.....	153
6.3.4.	SUMMARY OF QUALITY AND SIGNIFICANCE.....	157
6.4.	REPRODUCIBILITY ANALYSIS	159
6.4.1.	UNLOADED STATE REPRODUCIBILITY ANALYSIS.....	165
6.4.2.	LOADED STATE REPRODUCIBILITY ANALYSIS.....	173
6.4.3.	TMV REPRODUCIBILITY ANALYSIS.....	179
6.4.4.	TEMPERATURE REPRODUCIBILITY ANALYSIS.....	184
6.4.5.	SUMMARY OF THE REPRODUCIBILITY ANALYSIS.....	186
6.5.	VALIDATION OF THE MEASUREMENT PROCESS FROM THE RESULTS	188
6.5.1.	METHOD VALIDATION FROM LOAD STATE RESULTS.....	189
6.5.2.	METHOD VALIDATION BASED ON COMPARISON WITH EUROPEAN EMISSION STANDARDS.....	192
6.5.3.	SUMMARY OF VALIDATION OF THE MEASUREMENT PROCESS.....	201
6.6.	CONCLUSIONS	203
7.	URBAN ON-ROAD MEASUREMENTS	206
7.1.	INTRODUCTION.....	206
7.2.	DESIGNING VALIDATION OF IDLING NO _x MEASUREMENT TEST THROUGH URBAN ON-ROAD MEASUREMENTS.....	208
7.2.1.	DESCRIPTION OF VEHICLES.....	208
7.2.2.	DESCRIPTION OF CIRCUIT AND TEST CONDITIONS.....	210
7.2.3.	DESCRIPTION OF EQUIPMENT FOR THE ON-ROAD TEST.....	213
7.2.4.	DESCRIPTION OF THE TESTS.....	215
7.3.	ASSESSMENT OF RESULTS FROM ON-ROAD TESTS	218
7.3.1.	ASSESSMENT OF VEHICLE EMISSIONS IN THE SET OF TESTS.....	220
7.3.2.	ASSESSMENT OF VEHICLE EMISSIONS IN TEST #1.....	228
7.3.3.	DISCUSSION OF VEHICLE EMISSIONS ASSESSMENT IN ON-ROAD TESTS.....	233
7.4.	COMPARISON OF ON-ROAD EMISSIONS AND PTI NO_x MEASUREMENT	234
7.4.1.	COMPARISON OF RESULTS FROM VEHICLE No. 1.....	237
7.4.2.	DISCUSSION FROM THE COMPARISON OF RESULTS TO THE PTI PROPOSAL.....	242
7.5.	CONCLUSIONS	245
8.	NO_x MEASUREMENT CAMPAIGN IN PTI	248
8.1.	INTRODUCTION.....	248
8.2.	DEVELOPMENT OF THE NO_x MEASUREMENT CAMPAIGN	249
8.2.1.	LOCATIONS INVOLVED IN THE MEASUREMENT CAMPAIGN.....	249
8.2.2.	VEHICLES INVOLVED IN THE MEASUREMENT CAMPAIGN.....	251
8.2.3.	EQUIPMENT INVOLVED IN THE MEASUREMENT CAMPAIGN.....	257
8.3.	FEASIBILITY, QUALITY, SIGNIFICANCE, AND BEHAVIOR OF THE MEASUREMENT CAMPAIGN	260
8.3.1.	PERFORMANCE AND FEASIBILITY OF THE TEST FROM THE MEASUREMENT CAMPAIGN.....	260
8.3.2.	QUALITY AND SIGNIFICANCE OF THE MEASUREMENT CAMPAIGN.....	263
8.3.3.	ENGINE LOAD BEHAVIOR FROM THE MEASUREMENT CAMPAIGN.....	271
8.4.	RESULTS FROM THE MEASUREMENT CAMPAIGN	274

8.4.1.	NO _x EMISSION AVERAGE VALUES	275
8.4.2.	COMPARISON OF THE METHOD'S RESULTS TO ON-ROAD EMISSIONS.....	281
8.4.3.	COMPARISON OF THE METHOD'S RESULTS TO OTHER STUDIES.....	283
8.5.	NO _x THRESHOLDS DETERMINATION FOR PTI.....	289
8.6.	CONCLUSIONS.....	300
9.	ADDITIONAL VERIFICATION MEASURES OF THE PROPOSED PTI TEST	305
9.1.	INTRODUCTION.....	305
9.2.	CORRELATION ANALYSIS BETWEEN VARIABLES BASED ON THE MEASUREMENT CAMPAIGN.....	305
9.3.	COMPARATIVE ANALYSIS WITH MEASUREMENT AT POWER BENCH.....	319
9.3.1.	DESCRIPTION AND RESULTS OF THE TESTS.....	320
9.3.2.	DISCUSSION OF THE RESULTS.....	327
9.4.	MODELING AND ANALYSIS OF NO _x EMISSIONS IN URBAN CIRCULATION.....	330
9.5.	CONCLUSIONS.....	336
10.	CONCLUSIONS.....	339
10.1.	INTRODUCTION.....	339
10.2.	SUMMARY.....	339
10.3.	CONCLUSIONS.....	341
10.4.	PERSPECTIVES.....	346
10.5.	INFLUENCE AND VISIBILITY.....	348
11.	APPENDICES.....	355
11.1.	MEASUREMENT SOFTWARE DESCRIPTION	355
11.2.	MEASUREMENT WITH CAPELEC GAS ANALYZER.....	364
11.3.	MEASUREMENT ERROR ANALYSIS.....	368
11.3.1.	DEFINITIONS.....	369
11.3.2.	ERROR ANALYSIS FOR NO _x EMISSIONS MEASUREMENT.....	372
11.3.3.	ERROR ANALYSIS FOR MEASUREMENT RESULTS AVERAGING.....	373
11.3.4.	ERROR ANALYSIS FOR THE EXTRAPOLATION PROCESS	376
11.3.5.	ERROR ANALYSIS FOR THE NO _x MASS FLOW ESTIMATION	378
11.3.6.	SUMMARY OF ERROR ANALYSIS.....	382
11.4.	ASSESSMENT OF VEHICLE EMISSIONS FROM ON-ROAD TESTS.....	382
11.4.1.	ASSESSMENT OF VEHICLE EMISSIONS IN TEST #2	382
11.4.2.	ASSESSMENT OF VEHICLE EMISSIONS IN TEST #3.....	386
11.4.3.	ASSESSMENT OF VEHICLE EMISSIONS IN TEST #4.....	390
11.4.4.	ASSESSMENT OF VEHICLE EMISSIONS IN TEST #5 AND TEST #6.....	393
11.5.	COMPARISON OF ON-ROAD EMISSIONS AND PTI RESULTS.....	398
11.5.1.	COMPARISON OF RESULTS FROM VEHICLE No. 2.....	399
11.5.2.	COMPARISON OF RESULTS FROM VEHICLE No. 3.....	402
11.5.3.	COMPARISON OF RESULTS FROM VEHICLE No. 4.....	406
11.5.4.	COMPARISON OF RESULTS FROM VEHICLE No. 5.....	409
11.5.5.	COMPARISON OF RESULTS FROM VEHICLE No. 6.....	412
11.5.6.	COMPARISON OF RESULTS FROM VEHICLE No. 7.....	416
11.5.7.	COMPARISON OF RESULTS FROM VEHICLE No. 8.....	419

12. CONCLUSIONES.....	424
12.1. INTRODUCCIÓN.....	424
12.2. RESUMEN.....	424
12.3. CONCLUSIONES.....	426
12.4. PERSPECTIVAS.....	431
12.5. INFLUENCIA Y VISIBILIDAD.....	434
13. REFERENCES.....	439

LIST OF FIGURES

Chapter 1

Figure 1-1. Evolution of Premature Deaths and Years of Life Lost (YLL) by NO _x exposure in EU-28. Source: EEA Reports [19]–[22].	5
Figure 1-2. Evolution of Premature Deaths and Years of Life Lost (YLL) by O ₃ exposure in EU-28. Source: EEA Reports [19]–[22].	6
Figure 1-3. Evolution of Premature Deaths and Years of Life Lost (YLL) by PM _{2.5} exposure in EU-28. Source: EEA Reports [19]–[22].	7
Figure 1-4. Evolution of Premature Deaths and Years of Life Lost (YLL) related to air pollutants exposure in EU-28, compared to Road Traffic Deaths. Source: EEA Reports and Eurostat [19]–[22].	7
Figure 1-5. Evolution of Road Transport NO _x emissions in EU-27 compared to the evolution of diesel Approval Type NO _x emission limits. Data source: Eurostat.	10
Figure 1-6. Comparison of Euro emission limits and real-world NO _x emissions for petrol engines and diesel engines. Source: EEA(European Environment Agency) [5].	11
Figure 1-7. Diesel passenger cars fleet evolution in EU-28 from 2000 to 2019. Data source: Eurostat.	13
Figure 1-8. Comparison of fleet diesel passenger cars vs. population in EU-28 (2018) ordered by population. Data source: Eurostat.	14
Figure 1-9. Comparison of fleet diesel passenger cars vs. average NO _x concentration in every Capital City in EU-28 (2018) ordered by fleet diesel passenger cars. Data source: Eurostat.	15
Figure 1-10. Comparison between population, the fleet of diesel passenger cars, NO _x concentration in capital cities, and NO _x emissions in EU-28. Source: Eurostat.	16

Chapter 2

Figure 2-1. Relationship between NO _x formation process and combustion temperature (Source: Semakula et al., 2018) [70].	29
Figure 2-2. Variation of the cylinder head and exhaust manifold wall surface mean temperatures against engine load, for engine speeds of 1500, 2000, and 2500 rpm (Source: Rakopoulos et al., 2000) [74].	30
Figure 2-3. Flow Diagram for WCLD module measurement. Source: Emerson Process Management Rosemount Analytical Inc.[82].	34
Figure 2-4. Schematic of an NDUV gas analyzer. Source: Higashi et al., Proceedings of SPIE, 2014. [85].	35
Figure 2-5. Schematic of NDIR measurement equipment with filter for CO and CO ₂ detection. Source: www.cambustion.com.	36
Figure 2-6. FTIR spectrum. Source: Giechaskiel et al., 2021. [86].	38
Figure 2-7. Principle of operation of FTIR spectroscopy. Source: Giechaskiel et al., 2021. [86].	38
Figure 2-8. Scheme of Amperometric NO _x sensor operation. Source: Rheume, J., 2010. [87].	39
Figure 2-9. Free acceleration smoke (FAS) for opacity test. source: TNO.	40
Figure 2-10. Kick-down test with three accelerations. Source: KNESTEL.	40
Figure 2-11. ASM 2050 cycle.	41
Figure 2-12. Lug-down test. Source: Shenzhen Anche Technologies Co., Ltd.	42
Figure 2-13. NEDC cycle. Source: UN/ECE. [102].	43
Figure 2-14. WLTP cycle. Source: Delphi.	44
Figure 2-15. ERMES cycle. Source: Franco, V., 2014. [107].	44
Figure 2-16. ARTEMIS urban, rural-road, and motorway driving cycles and their structure in typical driving conditions. Source: André et al., 2004. [108].	45
Figure 2-17. Comparison of the speed pattern of NEDC and KDC. Source: Lee et al., 2013. [6].	45
Figure 2-18. Green NCAP Highway Cycle (BAB cycle). Source: Green NCAP 2019. [109].	46
Figure 2-19. US FTP-75 Urban Dynamometer Driving Schedule. Source: dieselnet.com.	46
Figure 2-20. Sample of RDE with PEMS test. Source: EMISIA S.A. [111].	47
Figure 2-21. Setup for RSD on-road measurements. Source: Pujadas et al., 2016. [31].	48

Figure 2-22. Plume chasing and NO _x emission calculation in the diluted plume. Source: AVL MTC Motortestcenter AB, 2020.[114].....	48
Figure 2-23. NO _x emission factors of gasoline (left) and diesel (right) passenger cars and light commercial vehicles (LCV). Source: Chen et al., 2014. [32].....	50
Figure 2-24. Average NO _x emissions from RSD CORETRA project. Source: Pujadas et al., 2017. [31].....	50
Figure 2-25. The number of RS records in the CONO _x database for petrol and diesel cars by Euro standard. Source: Borken-Kleefeld et al., 2018.[121].....	51
Figure 2-26. Results from RSD measurements in London. Source: TRUE, 2018. [124].....	52
Figure 2-27. Results from RSD measurements in Paris. Source: TRUE, 2019.[123].....	52
Figure 2-28. Results from RSD measurements in Krakow. Source: TRUE, 2020.[126].....	53
Figure 2-29. Results from RSD measurements in Brussels. Source: TRUE, 2021.[125].....	53
Figure 2-30. NO _x emissions [g] in the function of Vehicle Specific Power. Source: Varella et al., 2019. [140].....	57
Figure 2-31. Accumulated NO _x emissions from PEMS measurement with Urban, Rural, and Motorway emissions. Source: Luján et al. 2018. [141].....	58

Chapter 3

Figure 3-1. Some of the operating variables that affect vehicle NO _x emissions.....	67
Figure 3-2. Average NO _x emissions in summer and winter of four Euro 6 diesel vehicles. Source: Söderena et al., 2020. [51].....	68
Figure 3-3. Average NO _x emissions for each car on the five days with highest and lowest NO _x emissions, including trip distance and daily average temperature. Source: Söderena et al., 2020.[51].....	69
Figure 3-4. Operating variables that could affect vehicle NO _x emissions at the proposed static PTI test.....	71
Figure 3-5. Reduction of vehicle NO _x emissions from EGR and EATS (Source engine image: VAG).....	75

Chapter 4

Figure 4-1. Power and Torque plot from 1.9 liters 4-cylinder TDI Audi A3 engine (77 kW at 4000 min ⁻¹ , 250 N·m at 1900 min ⁻¹).....	86
Figure 4-2. Sample of fast increase and decrease of "% engine load" with free acceleration..	87
Figure 4-3. Gas analyzer probe into the exhaust pipe, and OBD reader connected.....	88
Figure 4-4. NO _x test for Euro 6 vehicle No. 20 and step-by-step test instructions.....	92
Figure 4-5. Data aggregation for Unloaded and Loaded states.....	95
Figure 4-6. "NO _x emission mass flow - % engine load" linear regression function.....	103
Figure 4-7. "NO _x concentration - % engine load" linear regression function.....	103
Figure 4-8. Graphical summary of the NO _x measurement protocol.....	107

Chapter 5

Figure 5-1. Centralauto Spektra 3011 Gas Analyzer.....	112
Figure 5-2. Test cell schema with Tekber and Horiba Gas Analyser installation.....	119
Figure 5-3. Test cell with the engine and the PTI Gas Analyzer.....	119
Figure 5-4. The performance curves of the PSA DW12 RU engines (Source: PSA).....	121
Figure 5-5. Sample of the test with EGR and low load conditions.....	129
Figure 5-6. Sample of the Test without EGR and low load conditions.....	131
Figure 5-7. Comparison of Tests with and without EGR and high load conditions.....	132
Figure 5-8. NO _x concentration with EGR activated: (a) @800 rpm, (b) @1000 rpm, (c) @1500 rpm, (d) @2000 rpm, (e) @2500 rpm, (f) @3000 rpm.....	134

Figure 5-9. Average differences in Absolute and Relative terms according to the load demand with the EGR activated: (a) @800 rpm, (b) @1000 rpm, (c) @1500 rpm, (d) @2000 rpm, (e) @2500 rpm, (f) @3000 rpm.	136
Figure 5-10. Correlation between concentration values from Tekber and Horiba equipment: (a) @800 rpm, (b) @1000 rpm, (c) @1500 rpm, (d) @2000 rpm, (e) @2500 rpm, (f) @3000 rpm.	137
Figure 5-11. Differences between Tekber and Horiba results according to the load demand with EGR.	141
Figure 5-12. Differences between Tekber and Horiba result according to the load demand without EGR.	143

Chapter 6

Figure 6-1. Best-Sellers Manufacturers in Spain (2019). Source of data: ANFAC [191].	148
Figure 6-2. Sections for analyzing R ² and p-value of the test.	150
Figure 6-3. Sample of NO _x test of vehicle No. 4.	155
Figure 6-4. Standard Deviation (SD) of NO _x concentration measurements in vehicle No. 20.	164
Figure 6-5. Standard Deviation for NO _x mass flow measurements in vehicle No. 20.	164
Figure 6-6. NO _x concentration and SD (red bar) for Unloaded State.	165
Figure 6-7. SD value for Unloaded State NO _x concentration.	166
Figure 6-8. NO _x mass flow emission and SD (red bar) for Unloaded State.	167
Figure 6-9. SD value for Unloaded State NO _x mass emission flow.	167
Figure 6-10. "% engine load" value and SD (red bar) for Unloaded State.	168
Figure 6-11. SD value for "% engine load" at Unloaded State.	169
Figure 6-12. CV at Unloaded State.	170
Figure 6-13. NO _x concentration and SD (red bar) for Loaded State.	173
Figure 6-14. SD value for Loaded State NO _x concentration.	174
Figure 6-15. NO _x mass flow emission and SD (red bar) for Loaded State.	174
Figure 6-16. SD value for Loaded State NO _x mass emission flow.	175
Figure 6-17. "% engine load" and SD (red bar) for Loaded State.	176
Figure 6-18. CV for variables at Loaded State.	177
Figure 6-19. NO _x concentration and SD (red bar) for TMV.	179
Figure 6-20. NO _x mass flow emission and SD (red bar) for TMV.	180
Figure 6-21. SD value for TMV NO _x concentration.	181
Figure 6-22. SD value for TMV NO _x mass emission flow.	181
Figure 6-23. CV for variables at TMV.	182
Figure 6-24. Average Temperature and SD (red bar) of Temperature along with the tests.	184
Figure 6-25. Coefficient of Variation (CV) for Temperature along with the test.	184
Figure 6-26. Percentage of increase of variables from unloaded to loaded state.	191
Figure 6-27. Sample of NO _x test of vehicle No. 12.	191
Figure 6-28. Vehicle's NO _x Emissions Factors according to Emission Level.	193
Figure 6-29. Vehicle's NO _x concentration from static measurement.	194
Figure 6-30. Vehicle's NO _x mass emission flow from static measurement.	194
Figure 6-31. Vehicles ordered according to NO _x concentration at Unloaded state.	195
Figure 6-32. Vehicles ordered according to NO _x mass emission flow at Unloaded state.	196
Figure 6-33. Vehicles ordered according to NO _x concentration at Loaded state.	197
Figure 6-34. Vehicles ordered according to NO _x mass emission flow at Loaded state.	198
Figure 6-35. Vehicles ordered according to NO _x concentration: TMV.	198
Figure 6-36. Vehicles ordered according to NO _x mass emission flow: TMV.	199
Figure 6-37. Vehicles are ordered according to the average "% engine load" values for the Unloaded state.	200
Figure 6-38. Vehicles are ordered according to the average "% engine load" values for the Loaded state.	200

Chapter 7

Figure 7-1. Vehicles No. 1-2 (right), No. 6 (middle), and No. 7 (left) the first test day.....	209
Figure 7-2. Vehicles No. 5 (right), No. 3 (middle right), No. 4 (middle left), and No.8 (left).....	209
Figure 7-3. Racetrack short variant (grey) design.....	211
Figure 7-4. Altitude and slope of the racetrack.....	211
Figure 7-5. Pressure first test day.....	212
Figure 7-6. Pressure second test day.....	212
Figure 7-7. Temperature first test day.....	212
Figure 7-8. Temperature second test day.....	213
Figure 7-9. Scheme of equipment connected to the vehicle for the on-road test.....	213
Figure 7-10. Measurement equipment installed into the trunk of vehicle No. 1.....	214
Figure 7-11. Gear shifting distribution in Test#1.....	216
Figure 7-12. Stops distribution in Test#2.....	217
Figure 7-13. Vehicle No. 1 on-road test results.....	221
Figure 7-14. Vehicle No. 2 on-road test results.....	222
Figure 7-15. Vehicle No. 3 on-road test results.....	223
Figure 7-16. Vehicle No. 4 on-road test results.....	224
Figure 7-17. Vehicle No. 5 on-road test results.....	225
Figure 7-18. Vehicle No. 6 on-road test results.....	226
Figure 7-19. Vehicle No. 7 on-road test results.....	227
Figure 7-20. Vehicle No. 8 on-road test results.....	228
Figure 7-21. NO _x emissions and "% engine load" from the set of vehicles in test #1.....	230
Figure 7-22. Vehicles ordered according to EF _{NO_x} for unloaded (up) and loaded (down) test #1.	232
Figure 7-23. Selection of Max. NO _x mass flow value from the test.....	237
Figure 7-24. Range of Avg. On-road emissions and Loaded PTI test result for Vehicle No. 1.	240
Figure 7-25. Range of Avg. On-road emissions and TMV PTI test results for Vehicle No. 1.....	241
Figure 7-26. Range of Max. On-road emissions and TMV PTI test results for Vehicle No. 1.....	241
Figure 7-27. The plot of the Range of average emissions from diesel vehicles.....	243
Figure 7-28. The plot of Range of Max. emissions from diesel vehicles.....	244

Chapter 8

Figure 8-1. Location of PTI stations from the measurement campaign.....	249
Figure 8-2. PTI stations involved in the measurement campaign: ITV 5001 (left upper), ITV 2831 (right upper), ITV 0825 (left down), ITV 3908 (middle down), ITV 3906 (right down).....	250
Figure 8-3. Statistical values of the sample size.....	251
Figure 8-4. Distribution of tested vehicles according to emissions Euro level.....	252
Figure 8-5. Distribution of tested vehicles according to manufacturers.....	252
Figure 8-6. Vehicles measured according to Engine Displacement (cm ³).....	253
Figure 8-7. Vehicles measured according to Engine Power (kW).....	254
Figure 8-8. Vehicles measured according to Mileage (km).....	255
Figure 8-9. Vehicles measured according to Age (years).....	255
Figure 8-10. Vehicles measured according to Approval Type.....	256
Figure 8-11. Gas Analyzer TEKBER CENTRALAUTO SPEKTRA 3011.....	257
Figure 8-12. TEKBER software for NO _x measurement for the proposed method.....	258
Figure 8-13. Example of files from NO _x measurement.....	261
Figure 8-14. Screenshots from Excel file used for NO _x data analysis.....	262
Figure 8-15. Distribution of Regression Factor values for the Initial Section.....	265
Figure 8-16. Distribution of Regression Factor values for the Final Section.....	267
Figure 8-17. Distribution of Regression Factor values for the Acceleration Section.....	267
Figure 8-18. Distribution of Regression Factor values for the Final Section.....	268
Figure 8-19. Distribution of p-value for the Initial Section.....	269
Figure 8-20. Distribution of p-value for the Final Section.....	269
Figure 8-21. Distribution of p-value for the Acceleration Section.....	270

Figure 8-22. Distribution of p-value for the Total Section.....	271
Figure 8-23. Avg. value of "% engine load" according to Displacement (cm ³).....	272
Figure 8-24. Avg. increase of "% engine load" from Unloaded to Loaded state.	274
Figure 8-25. Summary of avg. results: NO _x Mass Flow (left) and NO _x Concentration (right). ...	276
Figure 8-26. NO _x emissions from Euro level: Mass Flow (down) and Concentration (up).....	277
Figure 8-27. Euro 4 avg. results: NO _x Mass Flow (left) and NO _x Concentration (right).	278
Figure 8-28. Euro 5 avg. results: NO _x Mass Flow (left) and NO _x Concentration (right).....	278
Figure 8-29. Euro 5 avg. results: NO _x Mass Flow (left) and NO _x Concentration (right).....	279
Figure 8-30. Distribution of NO _x Loaded Emissions to On-Road Avg. Range.....	281
Figure 8-31. Distribution of NO _x TMV Emissions to On-Road Max. Range.....	282
Figure 8-32. Results from RSD measurements in London. Source: TRUE, 2018. [124].....	284
Figure 8-33. Results from RSD measurements in Paris. Source: TRUE, 2019. [123].....	285
Figure 8-34. 2019 Zurich Remote Sensing Campaign avg. results. Source: The ICCT [127].	286
Figure 8-35. 2020 Krakow Remote Sensing Campaign avg. results. Source: The ICCT [126]. ...	287
Figure 8-36. 2021 Brussels Remote Sensing Campaign avg. results. Source: The ICCT [125].....	287
Figure 8-37. Summary of NO _x emissions from PTI campaign, Concentration (up), and Mass Flow (down).....	288
Figure 8-38. The plot of Normal Distribution (a bell-shaped curve). Source: Wikipedia.	293
Figure 8-39. Definition of Thresholds from Normal Distribution. Source: sas.com, modified by the author.	294
Figure 8-40. Normal distribution and frequency distribution for Unloaded concentration results.	295
Figure 8-41. Normal distribution and frequency distribution for Loaded concentration results.	295
Figure 8-42. Normal distribution and frequency distribution for TMV concentration results.	296
Figure 8-43. Normal distribution and frequency distribution for Unloaded Mass Flow results.	296
Figure 8-44. Normal distribution and frequency distribution for Loaded Mass Flow results.	296
Figure 8-45. Normal distribution and frequency distribution for TMV Mass Flow results.	297
Figure 8-46. Thresholds for NO _x emissions in Concentration (up) and Mass Flow (down).	297
Figure 8-47. Threshold compared with the distribution of emissions in Concentration (up) and Mass Flow (down).....	299

Chapter 9

Figure 9-1. NO _x emissions to Displacement, in Concentration (up) and Mass Flow (down) ...	306
Figure 9-2. NO _x emissions to Weight, in Concentration (up) and Mass Flow (down).....	307
Figure 9-3. NO _x emissions to MMA, in Concentration (up) and Mass Flow (down).....	308
Figure 9-4. NO _x emissions to Power, in Concentration (up) and Mass Flow (down).....	309
Figure 9-5. NO _x emissions to Mileage, in Concentration (up) and Mass Flow (down).....	310
Figure 9-6. NO _x emissions to Age, in Concentration (up) and Mass Flow (down).....	311
Figure 9-7. NO _x emissions to CO ₂ emissions, in Concentration (up) and Mass Flow (down). ...	311
Figure 9-8. NO _x emissions to Approval type, in Concentration (up) and Mass Flow (down). ...	312
Figure 9-9. NO _x emissions to ratio Power/MOM (kW/kg), in Concentration (up) and Mass Flow (down).....	313
Figure 9-10. NO _x emissions to ratio Displacement/MOM (cm ³ /kg), in Concentration (up) and Mass Flow (down).....	314
Figure 9-11. NO _x emissions evolution along the year 2019-20, in Concentration (up) and Mass Flow (down).....	315
Figure 9-12. Manufacturers avg. NO _x emission.....	316
Figure 9-13. ASM2040 representation. Source: ACTIA.....	319
Figure 9-14. Data plots of NO _x measurements (ASM 2050) in Test Nr. 1.....	322
Figure 9-15. Test Nr. 2 (ASM 2050) complete test graphical representation.....	323
Figure 9-16. Static idling NO _x measurement test.....	326
Figure 9-17. Sample of a typical urban trip in Madrid center. Source: Google Maps.....	331
Figure 9-18. Plot results of sample trip.....	335

Chapter 10

Figure 10-1. Presentation of measurement proposal in the XXVII Jornadas Nacionales de ITV (Santander, 2018).....	348
Figure 10-2. Presentation of measurement proposal in the XXVIII Jornadas Nacionales de ITV (Zaragoza, 2019).....	349
Figure 10-3. Participation in Split Session during the 2023 CITA International Conference (Rotterdam, 2023).....	352
Figure 10-4. Participation in the conference "Vehicle Inspection and Society: Beyond Technology" (Brussels, 2023).....	353

Chapter 11

Figure 11-1. Generic acquisition software showing results from a measurement.	356
Figure 11-2. Vehicle data introduction screen previous to NO _x measurement.....	358
Figure 11-3. Measurement screen for Unloaded stage.....	360
Figure 11-4. Measurement screen for Loaded stage.	361
Figure 11-5. Measurement screen for Acceleration stage.....	362
Figure 11-6. Measurement finishing screen.....	363
Figure 11-7. Measurement results screen.....	364
Figure 11-8. CAPELEC Gas Analyzer model CAP3010+S.....	365
Figure 11-9. CAPELEC interface EOBD CAP 4250+S.....	366
Figure 11-10. The plot of results and Quality & Significance analysis for NO _x measurement with CAPELEC equipment.....	366
Figure 11-11. Final results and extrapolation of TMV for NO _x measurement with CAPELEC equipment.....	368
Figure 11-12. Distribution of measurement error.	369
Figure 11-13. Formal representation of accuracy and precision (Source: UN GTR 15) [105].....	371
Figure 11-14. Difference between accuracy and precision in the measurement process.	372
Figure 11-15. NO _x emissions and "% engine load" from the set of vehicles in test #2.....	383
Figure 11-16. Vehicles ordered according to EF _{NO_x} for unloaded (up) and loaded (down) test #2.....	385
Figure 11-17. NO _x emissions and "% engine load" from the set of vehicles in test #3.....	387
Figure 11-18. Vehicles ordered according to EF _{NO_x} for unloaded (up) and loaded (down) test #3.....	389
Figure 11-19. NO _x emissions and "% engine load" from the set of vehicles in test #4.....	392
Figure 11-20. Vehicles ordered according to EF _{NO_x} for unloaded (up) and loaded (down) test #4.....	393
Figure 11-21. NO _x emissions and "% engine load" from the set of vehicles in test #5.....	394
Figure 11-22. Vehicles ordered according to EF _{NO_x} for unloaded (up) and loaded (down) test #5.....	395
Figure 11-23. NO _x emissions and "% engine load" from the set of vehicles in test #6.....	397
Figure 11-24. Vehicles ordered according to EF _{NO_x} for unloaded (up) and loaded (down) test #6.....	398
Figure 11-25. Range of Avg. On-road emissions and Loaded PTI test result for Vehicle No. 2.	401
Figure 11-26. Range of Avg. On-road emissions and TMV PTI test results for Vehicle No. 2.	401
Figure 11-27. Range of Max. On-road emissions and TMV PTI test results for Vehicle No. 2.	402
Figure 11-28. Range of Avg. On-road emissions and Loaded PTI test result for Vehicle No. 3.	404
Figure 11-29. Range of Avg. On-road emissions and TMV PTI test results for Vehicle No. 3.	405
Figure 11-30. Range of Max. On-road emissions and TMV PTI test results for Vehicle No. 3.	405
Figure 11-31. Range of Avg. On-road emissions and Loaded PTI test result for Vehicle No. 4.	407
Figure 11-32. Range of Avg. On-road emissions and TMV PTI test results for Vehicle No. 4.	408

Figure 11-33. Range of Max. On-road emissions and TMV PTI test results for Vehicle No. 4.	409
Figure 11-34. Range of Avg. On-road emissions and Loaded PTI test result for Vehicle No. 5.	411
.....	411
Figure 11-35. Range of Avg. On-road emissions and TMV PTI test results for Vehicle No. 5.	411
Figure 11-36. Range of Max. On-road emissions and TMV PTI test results for Vehicle No. 5.	412
Figure 11-37. Range of Avg. On-road emissions and Loaded PTI test result for Vehicle No. 6.	414
.....	414
Figure 11-38. Range of Avg. On-road emissions and TMV PTI test results for Vehicle No. 6.	415
Figure 11-39. Range of Max. On-road emissions and TMV PTI test results for Vehicle No. 6.	415
Figure 11-40. Range of Avg. On-road emissions and Loaded PTI test result for Vehicle No. 7.	417
.....	417
Figure 11-41. Range of Avg. On-road emissions and TMV PTI test results for Vehicle No. 7.	418
Figure 11-42. Range of Max. On-road emissions and TMV PTI test results for Vehicle No. 7.	419
Figure 11-43. Range of Avg. On-road emissions and Loaded PTI test result for Vehicle No. 8.	421
.....	421
Figure 11-44. Range of Avg. On-road emissions and TMV PTI test results for Vehicle No. 8.	421
Figure 11-45. Range of Max. On-road emissions and TMV PTI test results for Vehicle No. 8.	422

LIST OF TABLES

Chapter 1

Table 1-1. OSHA exposure limits for NO ₂ . Source: www.osha.gov.....	3
Table 1-2. EEA standards exposition proposed for the protection of health. Source: EEA, 2020 [16]......	4
Table 1-3. WHO recommended AQG (Air Quality Guideline) levels. Source: WHO, 2021 Global AQG [17]......	4
Table 1-4. Emission thresholds for passenger cars (M1) in the EU.....	9

Chapter 2

Table 2-1. RDE boundary conditions from Regulation (EU) 2016/427/EC. Source: Hoofman et al., 2018. [128].....	54
Table 2-2. Specification of the RDE trip concerning speed and driving distance from Regulation (EU) 2016/427/EC. Source: Hoofman et al., 2018. [128].....	55

Chapter 3

Table 3-1. Vehicle operative variables that can affect NO _x emissions in a dynamic or static test.....	69
Table 3-2. Engine working ECU data registered from the vehicle through OBD.....	78

Chapter 4

Table 4-1. Load stages and engine working conditions for the test cycle.....	89
Table 4-2. Average measures in the static NO _x test.....	96
Table 4-3. Summary of final results in static NO _x test.....	100
Table 4-4. Stages and engine working conditions for the test cycle.....	108
Table 4-5. Sample of final results of the measurement procedure.....	109

Chapter 5

Table 5-1. NO _x sensor technical characteristics. Source: Tekber.....	114
Table 5-2. Gas Analyzer Environmental Requirements.....	115
Table 5-3. Gas Analyzer Error Parameters.....	116
Table 5-4. Maximum interference between gases.....	116
Table 5-5. General Technical Characteristics of the tested engine (Source: PSA).....	120
Table 5-6. Horiba Fuel Flow Measurement Specifications (Source: Horiba).....	122
Table 5-7. Horiba Dynamometer Specifications (Source: Horiba).....	123
Table 5-8. Horiba MEXA-ONE Analyzer Specifications (Source: Horiba).....	125
Table 5-9. Horiba MEXA-ONE System Specifications (Source: Horiba).....	126
Table 5-10. Summary of average concentrations and differences for the Static Idling Internal Load Test with EGR.....	130
Table 5-11. Summary of the average concentrations and differences for the Static Idling Internal Load Test without EGR.....	131
Table 5-12. Summary of Avg. concentration and differences between Horiba and Tekber equipment with EGR activated.....	135
Table 5-13. Summary of Avg. concentration and differences between Horiba and Tekber equipment with EGR deactivated.....	139
Table 5-14. Summary of Avg. absolute differences (ppm NO _x) between Tekber and Horiba equipment with EGR.....	140
Table 5-15. Summary of Avg. absolute differences (ppm NO _x) between Tekber and Horiba equipment without EGR.....	142

Chapter 6

Table 6-1. Set of vehicles and engines used for designing the method.....	147
Table 6-2. Statistical analysis of results from vehicles in static sections of NO _x test.....	156
Table 6-3. Statistical parameters calculated for the set of measurements for each vehicle.....	160
Table 6-4. Standard Deviation of the set of measurements from static NO _x test.....	161
Table 6-5. Coefficient of Variation of the set of measurements from static NO _x test.....	162
Table 6-6. Summary of results for the set of static NO _x tests for Vehicle No. 20.....	163
Table 6-7. Statistical parameters from the static NO _x tests for Vehicle No. 20.....	163
Table 6-8. Summary of dispersion values for Unloaded State.....	172
Table 6-9. Summary of dispersion values for Loaded State.....	178
Table 6-10. Summary of dispersion values for TMV State.....	183
Table 6-11. Summary of dispersion values for engine Temperature.....	185
Table 6-12. NO _x emissions average values for the unloaded idle state, loaded idle states, and TMV from static NO _x test.....	188
Table 6-13. Summary of avg. NO _x emissions from diesel vehicles.....	189
Table 6-14. Summary of avg. NO _x emissions from vehicles including the petrol one.....	189
Table 6-15. NO _x Emissions Factors according to Emissions level.....	193
Table 6-16. Standard uncertainty for measures and type of data.....	202

Chapter 7

Table 7-1. Vehicles selected for on-road urban circulation test.....	208
Table 7-2. Characteristics of the test racetrack.....	210
Table 7-3. Summary of On-Road tests characteristics.....	218
Table 7-4. NO _x emission Factor thresholds for M1 passenger cars.....	219
Table 7-5. Summary of avg. results from Test #1.....	231
Table 7-6. Set of vehicles and engines used for designing the method, Chapter 6.....	236
Table 7-7. NO _x emissions average values for the unloaded idle state, loaded idle states, and TMV from static NO _x test.....	236
Table 7-8. Summary of vehicle No. 1 results from on-road tests.....	238
Table 7-9. Summary of Static NO _x test on Vehicle No. 1.....	239
Table 7-10. Summary of Range values for Average emissions and Max. emissions.....	242

Chapter 8

Table 8-1. Date of entry into force Euro Emission Levels by vehicle category.....	256
Table 8-2. Comparison Avg. values of "% engine load" from sets of vehicles.....	273
Table 8-3. Example of results of a static NO _x measurement at PTI.....	275
Table 8-4. Summary of average results of the measurement campaign.....	275
Table 8-5. Summary of average results of measurement campaign for Euro 4 vehicles.....	277
Table 8-6. Summary of average results of measurement campaign for Euro 5 vehicles.....	278
Table 8-7. Summary of average results of measurement campaign for Euro 6 vehicles.....	279
Table 8-8. Summary NO _x emissions from the initial group of 22 diesel vehicles.....	280
Table 8-9. NO _x Concentration results campaign summary with statistical.....	292
Table 8-10. NO _x Mass Flow results campaign summary with statistical.....	293
Table 8-11. Results statistical and Threshold definition in concentration.....	296
Table 8-12. Results statistical and Threshold definition in mass flow.....	297
Table 8-13. Final Thresholds proposed for TMV value in the PTI test.....	298

Chapter 9

Table 9-1. Correlation between variables and NO _x emissions.....	318
Table 9-2. Average values from NO _x (ASM 2050) Test No 1.....	321
Table 9-3. Statistical values from NO _x (ASM 2050) Test No. 1.....	321
Table 9-4. Average values from NO _x (ASM 2050) Test No. 2.....	324

Table 9-5. Statistical values from NO _x (ASM 2050) Test No. 2	324
Table 9-6. R ² and p-value from NO _x (ASM 2050) Test Nr. 2	325
Table 9-7. Average values from NO _x static Test Nr. 3.....	326
Table 9-8. Statistical values from NO _x static Test Nr. 3.....	327
Table 9-9. R ² and p-value from NO _x static Test Nr. 3.....	327
Table 9-10. Main differences between dynamic and static tests.....	330
Table 9-11. European Driving Conditions. Source: André, 1997 [195].....	332
Table 9-12. Stop timing in sample trip.....	332
Table 9-13. Results of PTI test and estimation of sample trip emissions.....	334
Table 9-14. Emission thresholds for passenger cars (M1) in the EU.....	334

Chapter 11

Table 11-1. Data registered and associated error in instantaneous measurement.....	373
Table 11-2. Data registered and associated error in averaging measurement process.....	376
Table 11-3. Data registered and associated error in extrapolation measurement process.....	378
Table 11-4. Uncertainty for measures and type of data.....	379
Table 11-5. Summary of avg. results from Test #2.....	384
Table 11-6. Summary of avg. results from Test #3.....	388
Table 11-7. Summary of avg. results from Test #4.....	391
Table 11-8. Summary of avg. results from Test #5.....	396
Table 11-9. Summary of avg. results from Test #6.....	396
Table 11-10. Summary of vehicle No. 2 results from on-road tests.....	399
Table 11-11. Summary of Static NO _x test on Vehicle No. 2.....	400
Table 11-12. Summary of vehicle No. 3 results from on-road tests.....	403
Table 11-13. Summary of Static NO _x test on Vehicle No. 3.....	403
Table 11-14. Summary of vehicle No. 4 results from the on-road test.....	406
Table 11-15. Summary of Static NO _x test on Vehicle No. 4.....	407
Table 11-16. Summary of vehicle No. 5 results from the on-road test.....	410
Table 11-17. Summary of Static NO _x test on Vehicle No. 5.....	410
Table 11-18. Summary of vehicle No. 6 results from on-road test.....	413
Table 11-19. Summary of Static NO _x test on Vehicle No. 6.....	413
Table 11-20. Summary of vehicle No. 7 results from the on-road test.....	416
Table 11-21. Summary of Static NO _x test on Vehicle No. 7.....	417
Table 11-22. Summary of vehicle No. 8 results from the on-road test.....	420
Table 11-23. Summary of Static NO _x test on Vehicle No. 8.....	420

LIST OF EQUATIONS

Chapter 2	
Equation 2-1.....	28
Equation 2-2.....	28
Equation 2-3.....	28
Equation 2-4.....	28
Equation 2-5.....	28
Equation 2-6.....	28
Equation 2-7.....	28
Equation 2-8.....	28
Equation 2-9.....	31
Equation 2-10.....	31
Equation 2-11.....	31
Equation 2-12.....	31
Equation 2-13.....	31
Equation 2-14.....	31
Equation 2-15.....	32
Equation 2-16.....	32
Equation 2-17.....	32
Equation 2-18.....	33
Equation 2-19.....	34
Equation 2-20.....	34
Equation 2-21.....	34
Equation 2-22.....	35
Chapter 4	
Equation 4-1.....	97
Equation 4-2.....	97
Equation 4-3.....	98
Equation 4-4.....	98
Equation 4-5.....	99
Equation 4-6.....	101
Equation 4-7.....	101
Equation 4-8.....	101
Equation 4-9.....	101
Equation 4-10.....	101
Equation 4-11.....	102
Equation 4-12.....	102
Equation 4-13.....	102
Chapter 6	
Equation 6-1.....	151
Equation 6-2.....	159
Equation 6-3.....	160

Chapter 7

Equation 7-1..... 219
Equation 7-2..... 219

Chapter 11

Equation 11-1.....373
Equation 11-2.....374
Equation 11-3.....374
Equation 11-4.....374
Equation 11-5.....375
Equation 11-6.....375
Equation 11-7.....376
Equation 11-8.....376
Equation 11-9.....377
Equation 11-10.....377
Equation 11-11.....377
Equation 11-12.....378
Equation 11-13.....378
Equation 11-14.....378
Equation 11-15.....378

ABBREVIATIONS

AC	Air Conditioning
ADAC	Allgemeiner Deutscher Automobil-Club e.V.
AQG	Air Quality Guideline
ASL	Above Sea Level
BAB	Bundesautobahn
BEV	Battery Electric Vehicle
BMS	Battery Management System
CBA	Cost-Benefit Analysis
CF	Conformity Factor
CITA	International Motor Vehicle Inspection Committee
CV	Coefficient of Variation
EATS	Exhaust After-Treatment System
ECU	Engine Control Unit
EEA	European Environment Agency
EF	Emissions Factor
EGR	Exhaust Gas Recirculation
EU	European Union
FCEV	Fuel Cell Electric Vehicle
FTP	Federal Test Procedure (USA)
HDV	Heavy-Duty Vehicle
JRC	Joint Research Centre
LDV	Light-Duty Vehicle
LEZ	Low Emissions Zones
LNT	Lean NO _x Trap
MAF	Mass Air Flow
MIL	Malfunction Indicator Lamp
NEDC	New European Driving Cycle
NO	Nitrogen monoxide
NO ₂	Nitrogen dioxide
NO _x	Nitrogen oxides
OBD	On-Board Diagnosis

PC	Passenger Cars
PEMS	Portable Equipment Measurement System
PTI	Periodic Technical Inspection
RDE	Real Driving Emissions
RSD	Remote Sensing Device
<i>RSD</i>	<i>Relative Standard Deviation</i>
SCR	Selective Catalytic Reduction
SD	Standard Deviation
TMV	Theoretical Maximum Value
UDDS	Urban Dynamometer Driving Schedule
VERT	Verification of Emission Reduction Technologies
WHO	World Health Organization
WLTP	Worldwide Harmonized Light Vehicles Test Cycle
YLL	Years of Life Lost

CHAPTER 1

CONCEPTUAL FRAMEWORK, RESEARCH GOALS AND SCOPE OF THE THESIS

1. CONCEPTUAL FRAMEWORK, RESEARCH GOALS AND SCOPE OF THE THESIS

1.1. INTRODUCTION

The objective of this thesis is to present a valid proposal for a new NO_x measurement procedure for vehicles undergoing Periodic Technical Inspection (PTI).

Throughout this chapter, the existing problem with NO_x emissions from vehicles will be detailed, and the significance of NO_x measurement in PTI as a valid solution to this problem will be explained.

Lastly, the issues to be solved by the thesis will be listed and the research objectives that need to be accomplished to effectively address the raised issues will be enumerated.

1.2. NO_x EMISSIONS: A HEALTH PROBLEM

In recent years, frequent and striking episodes of pollutants' high concentrations in cities have increased public concern about urban pollution, some of which are recognized as being harmful to human health and the environment. In fact, air pollution is considered by the EEA (European Environment Agency) the single largest environmental health risk in Europe, particularly in urban areas [1].

NO_x is among the most dangerous pollutants, comprising both NO and NO₂. These compounds are primarily generated in the combustion process, accounting for road transport with a contribution of 40-70% of worldwide NO_x emissions [2], [3] and 39% within the EU-27 [4]. Diesel engines are responsible for about 85% of all NO_x emissions from road vehicles [5]–[7]. Despite the diesel vehicles fleet being significantly smaller than other fuels, like in the U.S.A. market, diesel vehicles are the dominant source of NO_x emissions [8].

NO_x emissions are dangerous because they have significant harmful effects on the health of people, both in short-term and long-term exposures as they are toxic gases, and they can damage the whole respiratory system.

NO_x low concentration exposure can irritate eyes, nose, throat, and lungs, causing cough, shortness of breath, tiredness, nausea, and can result in fluid build-up in the lungs one or two days after exposure.

Instead, exposure to high concentration levels can cause burning, spam, and swelling of tissues in the throat and upper respiratory tract, reduced oxygenation of body tissues, a build-up of fluid in the lungs (edema), and death. Skin or eye contact with liquid NO₂ can cause serious burns [9].

NO_x can react with vitamin B12, resulting in the inhibition of methionine synthase, and prolonged exposure could lead to megaloblastic bone marrow depression and other neurological diseases [10].

In general, we can say that NO_x exposure aggravates the consequences of pre-existing diseases and that it generates problems in the respiratory systems of healthy

people, organ disorders such as the liver or spleen, or systems such as the circulatory or immune systems, which in turn lead to lung infections and respiratory failures [11], [12]. Even diabetes and Alzheimer's disease have been related to NO_x exposure [13].

For this harmful influence on human health, several organisms, like OSHA (Occupational Safety and Health Administration, Table 1-1), EEA (European Environment Agency, Table 1-2), and WHO (World Health Organization, Table 1-3), have established restrictive exposure limits for NO_x. However, in 2019 most of the European urban population exceeded the WHO-recommended air pollution exposure [14].

Exposure Limits							
OSHA PEL 8-hour TWA (ST) STEL (C) Ceiling Peak		NIOSH REL Up to 10-hour TWA (ST) STEL (C) Ceiling		ACGIH TLV® 8-hour TWA (ST) STEL (C) Ceiling		CAL/OSHA PEL 8-hour TWA (ST) STEL (C) Ceiling Peak	
PEL-TWA		REL-TWA		TLV-TWA	0.2 ppm [2011]	PEL-TWA	
PEL-STEL		REL-STEL	1 ppm (1.8 mg/m ³)	TLV-STEL		PEL-STEL	1 ppm (1.8 mg/m ³)
PEL-C	5 ppm (9 mg/m ³)	REL-C		TLV-C		PEL-C	
Skin notation	N	Skin notation	N	Skin notation	N	Skin notation	N

Table 1-1. OSHA exposure limits for NO₂. Source: www.osha.gov

Pollutant	Averaging period	Legal nature and concentration	Comments
PM ₁₀	1 day	Limit value: 50 µg/m ³	Not to be exceeded on more than 35 days per year
	Calendar year	Limit value: 40 µg/m ³	
PM _{2.5}	Calendar year	Limit value: 25 µg/m ³	Average exposure indicator (AEI) (†) in 2015 (2013-2015 average) AEI (†) in 2020, the percentage reduction depends on the initial AEI
		Exposure concentration obligation: 20 µg/m ³ National exposure reduction target: 0-20 % reduction in exposure	
O ₃	Maximum daily 8-hour mean	Target value: 120 µg/m ³	Not to be exceeded on more than 25 days/year, averaged over 3 years (†)
		Long-term objective: 120 µg/m ³	
	1 hour	Information threshold: 180 µg/m ³ Alert threshold: 240 µg/m ³	
NO ₂	1 hour	Limit value: 200 µg/m ³ Alert threshold: 400 µg/m ³	Not to be exceeded on more than 18 hours per year To be measured over 3 consecutive hours over 100 km ² or an entire zone
	Calendar year	Limit value: 40 µg/m ³	

Table 1-2. EEA standards exposition proposed for the protection of health. Source: EEA, 2020 [15].

Pollutant	Averaging time	Interim target				AQG level
		1	2	3	4	
PM _{2.5} , µg/m ³	Annual	35	25	15	10	5
	24-hour ^a	75	50	37.5	25	15
PM ₁₀ , µg/m ³	Annual	70	50	30	20	15
	24-hour ^a	150	100	75	50	45
O ₃ , µg/m ³	Peak season ^b	100	70	–	–	60
	8-hour ^a	160	120	–	–	100
NO ₂ , µg/m ³	Annual	40	30	20	–	10
	24-hour ^a	120	50	–	–	25
SO ₂ , µg/m ³	24-hour ^a	125	50	–	–	40
CO, mg/m ³	24-hour ^a	7	–	–	–	4

^a 99th percentile (i.e. 3–4 exceedance days per year).

^b Average of daily maximum 8-hour mean O₃ concentration in the six consecutive months with the highest six-month running-average O₃ concentration.

Table 1-3. WHO recommended AQG (Air Quality Guideline) levels. Source: WHO, 2021 Global AQG [16].

As a consequence of this, according to the EEA Air Quality Report in 2017 [12], NO_x exposure was directly responsible for 75,000 premature deaths in EU-28 in the year 2014, which can be translated into 798,500 YLL (Years of Life Lost).

That year onwards, a decrease has been observed in the number of premature deaths and Years of Life Lost caused by NO_x exposure. According to the EEA Air Quality Reports, in 2021 46,150 premature deaths and 497,500 YLL [17] can be directly attributed to NO_x exposure in the EU-28 in 2019. The evolution in the last years of the number of premature deaths and YLL can be observed in Figure 1-1, where a decrease in mortality is observed, which could be influenced by the reduction in NO_x emissions.

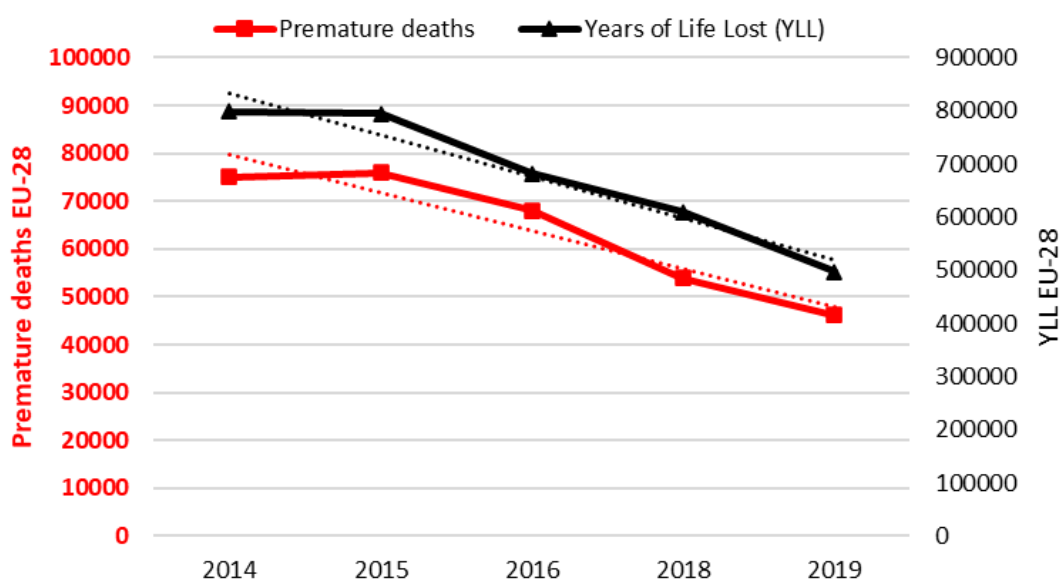


Figure 1-1. Evolution of Premature Deaths and Years of Life Lost (YLL) by NO_x exposure in EU-28. Source: EEA Reports [18]–[21].

In addition to this, NO_x emissions are responsible for the generation of Secondary Pollutants like tropospheric ozone (O₃) and Particulate Matter [22].

In the presence of hydrocarbons and ultraviolet light, NO_x is one of the main sources of tropospheric ozone [23], making this ground-level ozone highly harmful. According to the WHO in the Guide to Air Quality [11], several studies have shown there is a relationship between high levels of tropospheric ozone and daily mortality, regardless of the effects of other pollutants. Thus, it has been proven that mortality increases by 1-2% on days in which the average concentration of ozone over 8 hours reaches 100 µg/m³ concerning the mortality recorded when ozone levels remain at 70 µg/m³.

As a consequence of this, according to the EEA Air Quality Report in 2017, tropospheric ozone exposure was responsible for 13,600 premature deaths in EU-28 in 2014. Contrary to what has happened with deaths due to direct NO_x exposure, deaths due to exposure to tropospheric ozone have been maintained and even increased last

years, to a value of 17,680 deaths in 2019, with a total of 200,000 YLL in 2019 (see Figure 1-2).

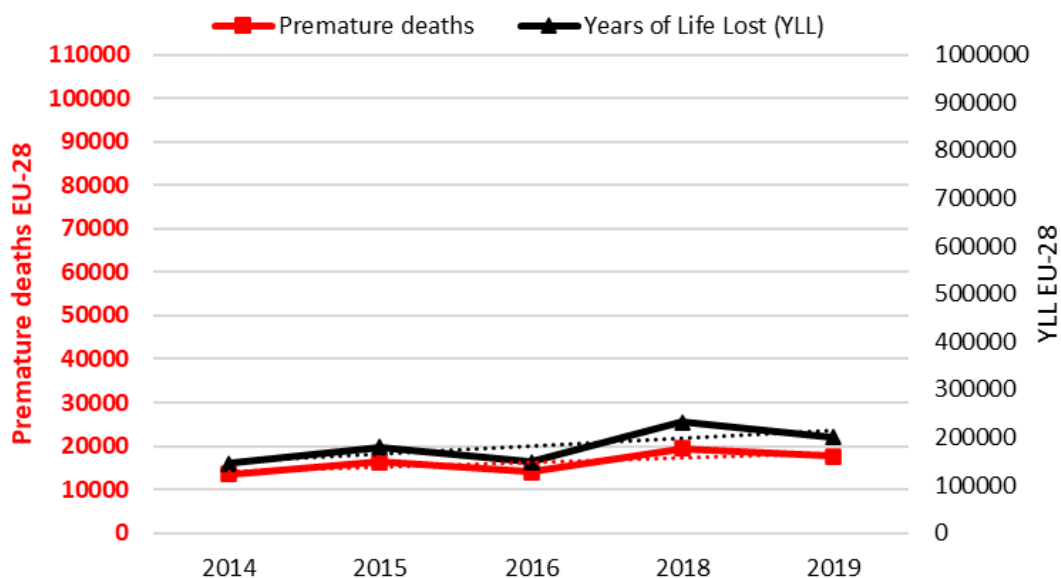


Figure 1-2. Evolution of Premature Deaths and Years of Life Lost (YLL) by O₃ exposure in EU-28. Source: EEA Reports [18]–[21].

As was previously said, NO_x is considered a Primary Pollutant because it generates other pollutants, e.g. the tropospheric ozone (O₃) or the HNO₃, which are then considered Secondary Pollutants.

These Secondary Pollutants generated from NO_x, working together with another secondary pollutant coming from diesel engine emissions (as the H₂SO₂, i.e.), are the cause of the effect of Acid Deposition. So, NO_x emissions are also responsible for Acid Deposition.

Acid Deposition is a recognized environmental problem that affects directly not only the forest ecosystems and cropland wealth through changes in the soil chemistry but also water reserves [24]. Besides the environment, it can also damage infrastructure, and affect human health [25].

Moreover, NO_x emissions contribute to the secondary formation of fine particles (less than 2.5 μm in size, PM_{2.5}) [22]. And according to the Air Quality Report in 2017 the EEA, exposure to PM_{2.5} caused 399,000 premature deaths in EU-28 in 2014.

As can be seen in Figure 1-3, premature deaths from exposure to PM_{2.5} show a moderate decreasing trend in the last years, although the number of demises is still high.

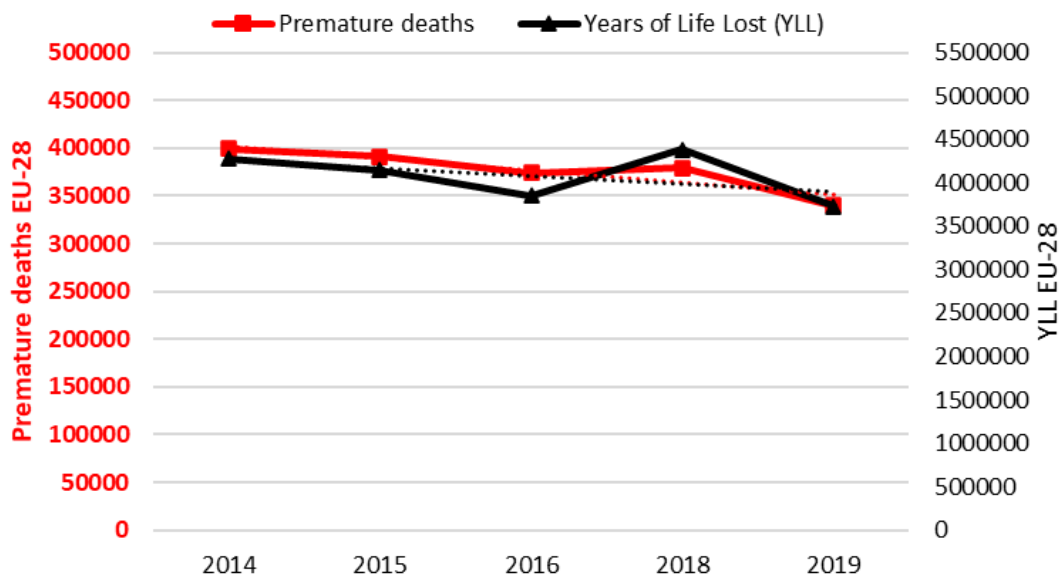


Figure 1-3. Evolution of Premature Deaths and Years of Life Lost (YLL) by $PM_{2.5}$ exposure in EU-28. Source: EEA Reports [18]–[21].

Combining all these data, NO_x emissions can be related, directly or indirectly, to 487,600 premature deaths and 5,222,500 YLL in EU-28 in 2014.

Combined premature deaths and YLL evolution show a decreasing trend, with 403,930 deaths and 4,423,400 YLL in 2019.

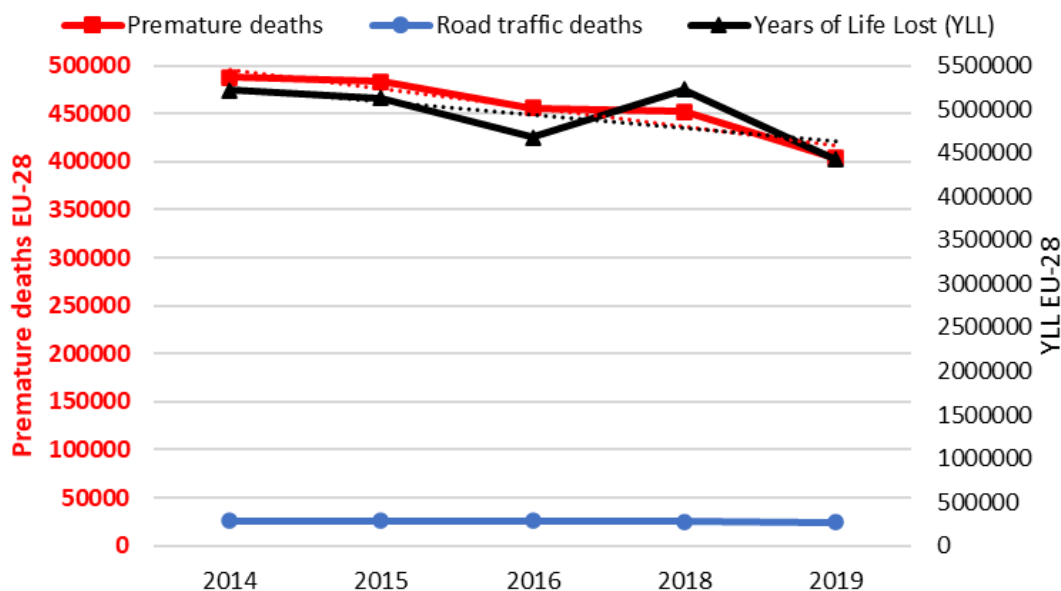


Figure 1-4. Evolution of Premature Deaths and Years of Life Lost (YLL) related to air pollutants exposure in EU-28, compared to Road Traffic Deaths. Source: EEA Reports and Eurostat [18]–[21].

However, the gravity of the mortality rate overshadows this positive decline. Each premature death signifies an average loss of approximately 11 years of life for individuals, which is deeply concerning.

To get an idea of what this amount means, the number of traffic accident casualties in the year 2014 in EU-28 was 25987 (Data from Eurostat <https://ec.europa.eu/eurostat/data/database>). That means, in the European Union NO_x emissions were related to 18.7 times higher mortality than traffic accidents in 2014. In 2019 the situation was slightly better but similar, with mortality related to NO_x 16.5 times higher than traffic accidents (Figure 1-4).

In addition to all these very serious consequences for human health, NO_x emissions and therefore the increase of NO₂ concentration in the atmosphere is of great importance. This is because NO₂ is an important trace gas since according to WHO [16], it:

- a. Contributes to impaired atmospheric visibility absorbing visible solar radiation
- b. Has a direct role in global climate change absorbing visible radiation
- c. Is a regulator of the oxidizing capacity of the troposphere
- d. Has a critical role in determining ozone concentration in the troposphere

In European cities, health impact assessments have suggested that reducing the concentration of pollutants could potentially prevent a significant number of premature deaths. These assessments indicate that there is no specific minimum threshold of pollutant concentration that can be considered completely safe. Therefore, any reduction in pollutant levels can contribute to a decrease in premature mortality. This highlights the importance of taking measures to minimize pollution and improve air quality to protect public health [26].

A modeling assessment has determined that the NO_x emission reductions expected with the implementation of the measures being proposed in the new Euro 7 emission standard in the period 2027-2050 would result in an annual reduction of even 98% from transport in 2050, with an estimated reduction of the number of premature deaths associated directly or indirectly with NO_x emissions between 34,000 and 41,000 [14].

Based on these findings, it becomes evident that controlling and decreasing NO_x emissions from the road transport sector is of utmost importance.

Recognizing this critical situation, the European Union has implemented a series of regulations over the past two decades intending to mitigate pollutant emissions from traffic, including a specific focus on reducing NO_x emissions.

Nevertheless, despite the implementation of stricter emissions regulations for vehicle approval [27], [28], it is important to note that the reduction in emission thresholds for NO_x has not been accompanied by an equivalent decrease in their concentration in the air. This suggests that while the regulations have targeted the control of theoretical emissions, there might be other factors contributing to the persistent levels of pollutants in the environment. Further efforts and measures may be necessary to effectively reduce the concentration of these pollutants and mitigate their potential impact on public health.

Emission Standard	Emission Thresholds (g/km)				
	CO	HC	HC+NO _x	NO _x	PM
Diesel (M1)					
Euro 1	2.72	--	0.97	--	0.14
Euro 2	1	--	0.7	--	0.08
Euro 3	0.64	--	0.56	0.5	0.05
Euro 4	0.5	--	0.3	0.25	0.025
Euro 5	0.5	--	0.23	0.18	0.005
Euro 6	0.5	--	0.17	0.08	0.005
Gasoline (M1)					
Euro 1	2.72	--	0.97	--	--
Euro 2	2.2	--	0.5	--	--
Euro 3	2.3	0.2	--	0.15	--
Euro 4	1	0.1	--	0.08	--
Euro 5	1	0.1	--	0.06	0.005
Euro 6	1	0.1	--	0.06	0.005

Table 1-4. Emission thresholds for passenger cars (M1) in the EU.

The emission limits in approval types for NO_x in diesel vehicles have been reduced from the 0.5 g/km allowed by the Euro 3 standard emission in 2000 to the 0.08 g/km established by the Euro 6 emission level in 2014 (see Table 1-4 and **Figure 1-5**). However, the emissions of NO_x have not only failed to decrease to the same extent, but in certain regions, the concentration levels have even remained stagnant [29].

From 2008 to 2019 the NO_x Approval Type emissions threshold became more than 3 times lower (a decrease of 68%). Instead, real Road Transport NO_x emissions in EU-27 have only decreased by 39% from the 2008 value, according to Eurostat data.

This means that the Approval Type emissions threshold reduction has not been translated into a real NO_x emission reduction with the same intensity, although road transport NO_x emissions showed a decreasing trend from 2008 onwards, as can be seen in Figure 1-5.

Comparing EU-27 data on road transport NO_x emissions with premature deaths previously attributed (directly and indirectly) to NO_x emissions, from 2014 to 2019 road transport NO_x emissions have decreased by 19%, while premature deaths have decreased by 17% at the same time. This could be an indicator of the importance of controlling and reducing road transport NO_x emissions to decrease the number of premature deaths caused by air pollution.

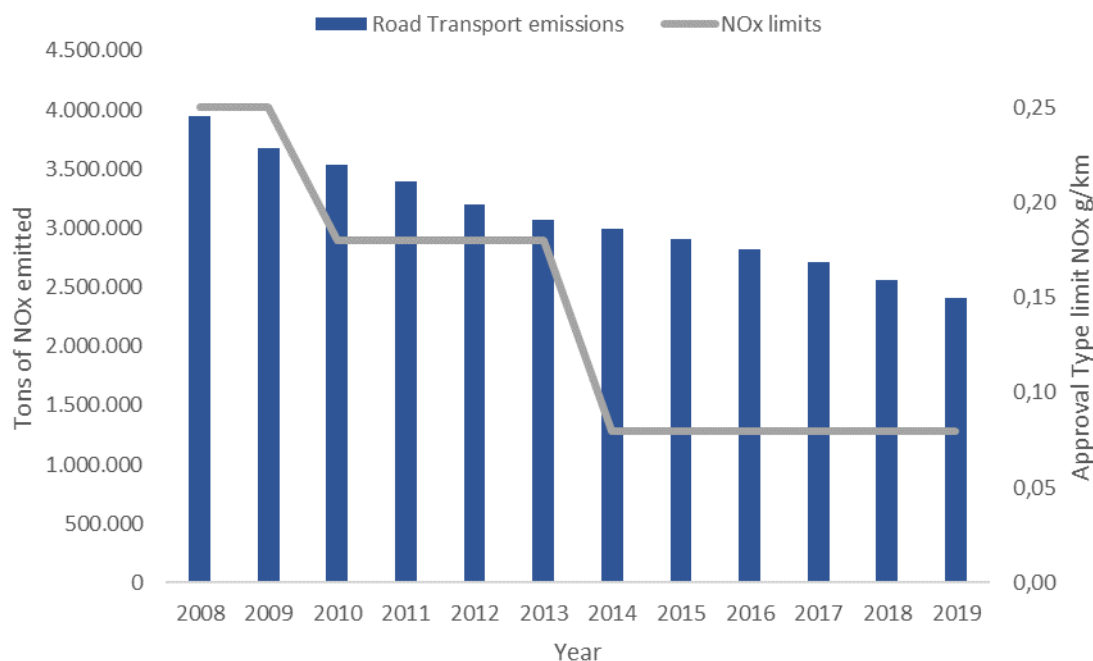


Figure 1-5. Evolution of Road Transport NO_x emissions in EU-27 compared to the evolution of diesel Approval Type NO_x emission limits. Data source: Eurostat.

It is estimated through modeling processes that reduction of NO_x emissions from vehicles (from the introduction of more severe normative as Euro 7/VII, or increasing the number of vehicles without emissions) will improve the air quality and reduce the premature deaths caused by air pollution [14].

To verify the accuracy of this claim, it is essential to monitor and regulate the actual emissions of nitrogen oxides (NO_x) from vehicles. Obtaining reliable information regarding which vehicles are contributing to NO_x emissions is the crucial first step towards controlling and reducing them. Therefore, a reliable tool is needed to measure NO_x emissions from vehicles, since Type Approval (the process through which a new vehicle is officially certified as meeting specific regulatory requirements and technical standards) has been demonstrated to be unreliable for this function (at least for NO_x).

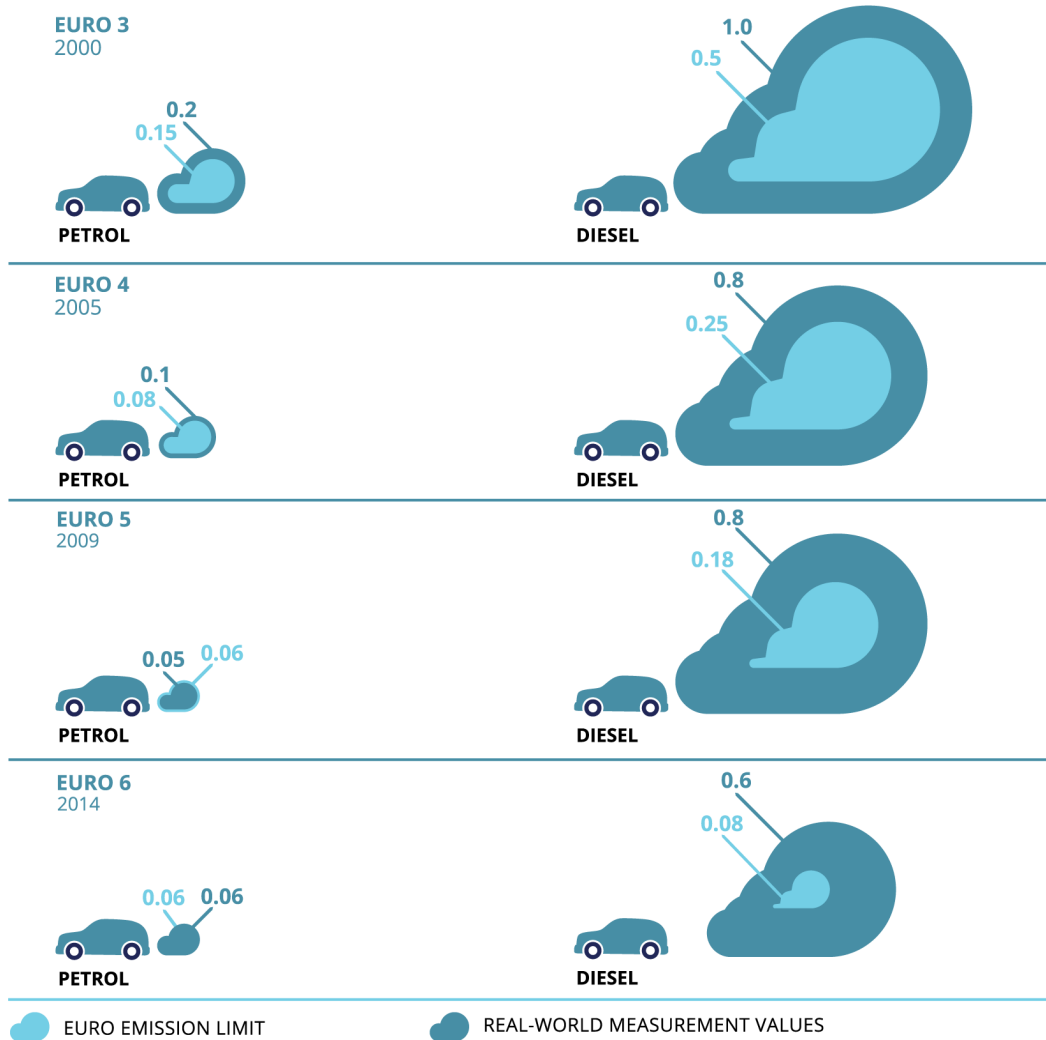
1.3. WHY ARE DIESEL VEHICLES SO IMPORTANT TO CONTROL NO_x EMISSIONS?

As noted above, about 85% of NO_x emissions from road transport come from diesel vehicles, so reducing them would have a strong impact on total NO_x emissions.

In contrast to the progress seen in reducing NO_x emissions from petrol engine vehicles, it has been substantiated that diesel engine vehicles have not achieved the expected reduction in NO_x emissions based on successive emissions control regulations [30], [31]. The introduction of Euro 3 emission standards and subsequent

regulations have not resulted in a significant decrease in NO_x emissions from certain newer diesel vehicles when evaluated under real-world driving conditions.

Comparison of NO_x emission standards for different Euro classes



Adapted from: ICCT, 2014a; Emisia, 2015

Nitrogen oxide (NO_x) emissions (in g/km)

Figure 1-6. Comparison of Euro emission limits and real-world NO_x emissions for petrol engines and diesel engines. Source: EEA(European Environment Agency) [4].

Figure 1-6 shows an estimation of average real emissions from petrol and diesel vehicles, compared with the emission standards thresholds. It graphically shows how emissions from diesel vehicles are higher than petrol ones, as well as the difference between real-world emissions and the limits of the various emission standards.

Surprisingly, it has been observed that some of these newer diesel vehicles exhibit NO_x emission levels comparable to older diesel vehicles [27]. Furthermore, certain

diesel vehicles subject to more stringent emissions control regulations may even exhibit similar or higher emissions compared to vehicles with fewer restrictions [30].

This fact has been confirmed through measurements of RDE (Real Driving Emissions) with PEMS (Portable Emissions Measurement Systems) [32]–[35], with RDS (Remote Sensing Detector) systems on a large number of vehicles [30], [31], [36], [37], as well as with theoretical models [35], [38], [39].

1.4. NO_x EMISSIONS REGULATORY CONTROL, DISTRIBUTION, AND EVOLUTION

At present, within the European Union, the regulation of NO_x emission levels in vehicles is limited to the homologation process.

To meet the EU regulations and receive the Type-Approval for a new vehicle, one of the procedures necessary for its commercialization involves conducting a specific test that measures the vehicle's emissions under predefined conditions. The purpose of this test is to ensure that the vehicle does not exceed a predetermined level of emissions for various pollutants, including NO_x. This process verifies compliance with the established emission standards before the vehicle can be sold in the market.

The aforementioned test is conducted on an individual vehicle, subject to specific and controlled conditions. However, setting aside cases like the Dieselgate scandal, where irregularities were found in vehicles to pass emissions tests [40], it has been proven that the maximum NO_x emission levels specified in the homologation test are significantly exceeded when vehicles are driven on public roads [27], [33], [41]. In other words, the test performed to assess vehicles' compliance with emission standards, particularly regarding NO_x emissions in diesel vehicles, does not accurately represent their real-world behavior [36], [39] (see Figure 1-6).

The significant issue in Europe lies in the fact that diesel-powered vehicles are the primary contributors to NO_x emissions, **surpassing the expected levels set by emission standards and approval types procedures**. This problem is aggravated by the higher prevalence of diesel vehicles in the EU compared to other regions worldwide. Approximately 70% of diesel passenger cars and vans sold globally are estimated to be within the EU [42].

This situation has been partly generated by **fuel taxation differences** between petrol and diesel fuels, which is a unique situation for Europe. This taxation became an indirect subsidy to diesel car owners, and together with the **higher fuel efficiency of diesel engines**, has promoted this situation of high penetration of diesel vehicles in European vehicles fleet [3].

Elsewhere the situation is different. For example, in the state of California, the main source of NO_x emissions from road transport is heavy-duty transport, consisting of gasoline and diesel vehicles, with 31% of total NO_x emissions, while road transport is responsible for 42% of the State's NO_x emissions. In other words, in California, 73% of NO_x emissions from road traffic are due to heavy-duty trucking [43].

Based on data from Eurostat, in 2015, the European Union registered a total of 6.6 million diesel vehicles, which represented 53% of all vehicle registrations. The dominance of diesel vehicles in the EU's automotive landscape experienced a slight decline from 55% in 2011 to 53% in both 2013 and 2014. Notably, certain European countries, including France, Spain, Belgium, and Ireland, had a significant portion of their passenger car fleets consisting of diesel vehicles, ranging from 65% to 72% [44].

In summary, an increasing trend can be observed from 2000 to the present day. The evolution from diesel passenger cars¹ in the EU28 fleet has increased from 17% of the passenger cars fleet in 2000 to 41% in 2018 (see Figure 1-7). Most of them are registered in the most populated countries of the EU (see Figure 1-8), where more than 70% of the population lives in an urban environment [45], exposed to a high concentration of NO_x and other air pollutants related to them (PM_{2.5} and O₃).

Fleet of diesel passenger cars registered in EU-28

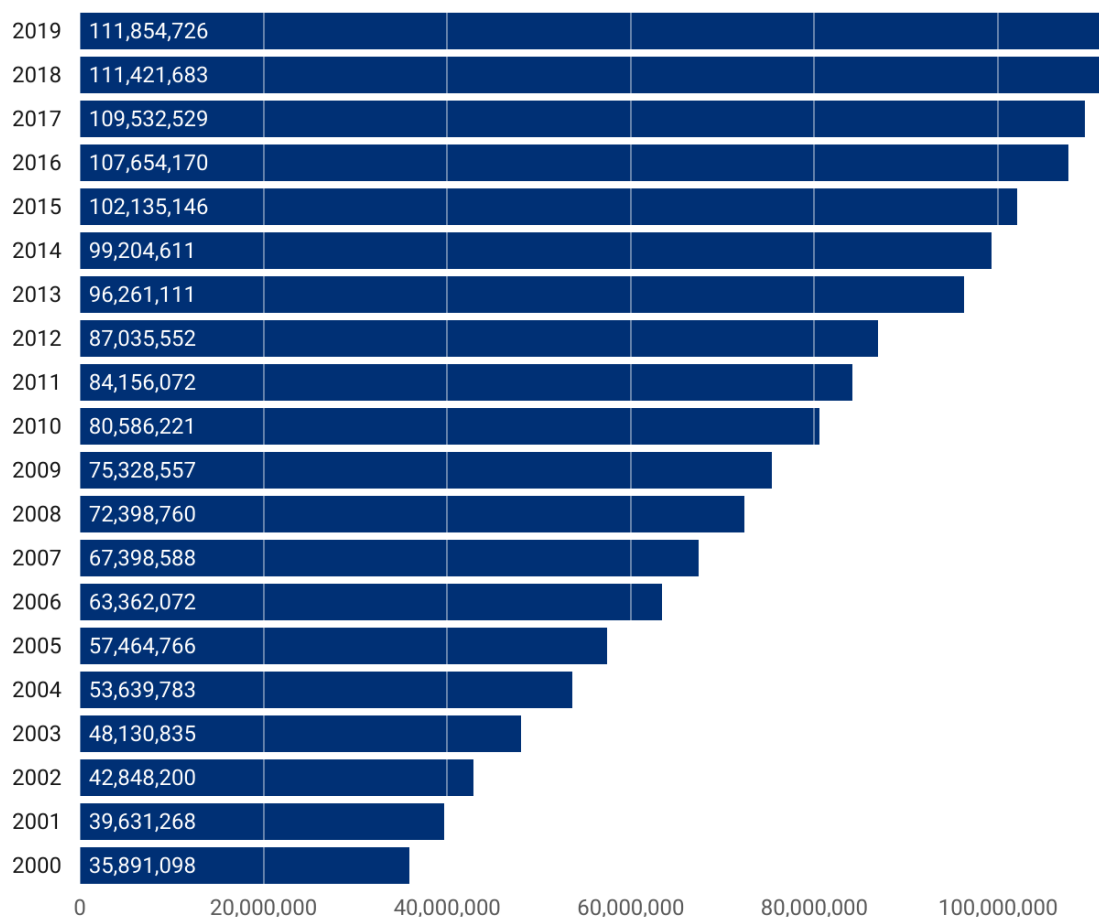


Figure 1-7. Diesel passenger cars fleet evolution in EU-28 from 2000 to 2019. Data source: Eurostat.

¹ Data from Eurostat <https://ec.europa.eu/eurostat/data/database>

The number of diesel vehicles is expected to remain stable, at least in the upcoming years. In 2019, the EU-28 had a fleet of over 111 million diesel passenger cars.

Checking the average NO_x concentration measured in European cities from Eurostat data, it can be seen how, except for Romania, the six countries more populated, and with more diesel passenger cars, have higher NO_x concentrations in cities (see Figure 1-9).



Figure 1-8. Comparison of fleet diesel passenger cars vs. population in EU-28 (2018) ordered by population. Data source: Eurostat.

In addition, nine of the 10 European cities with higher mortality burden related to NO_x belong to the 4 countries with higher diesel passenger car fleets [26]. Extending this assessment to the 50 European cities with a higher mortality burden, 38 of them

belong to the 4 countries with higher diesel passenger car fleets, the others from Belgium, Netherlands, and Poland.

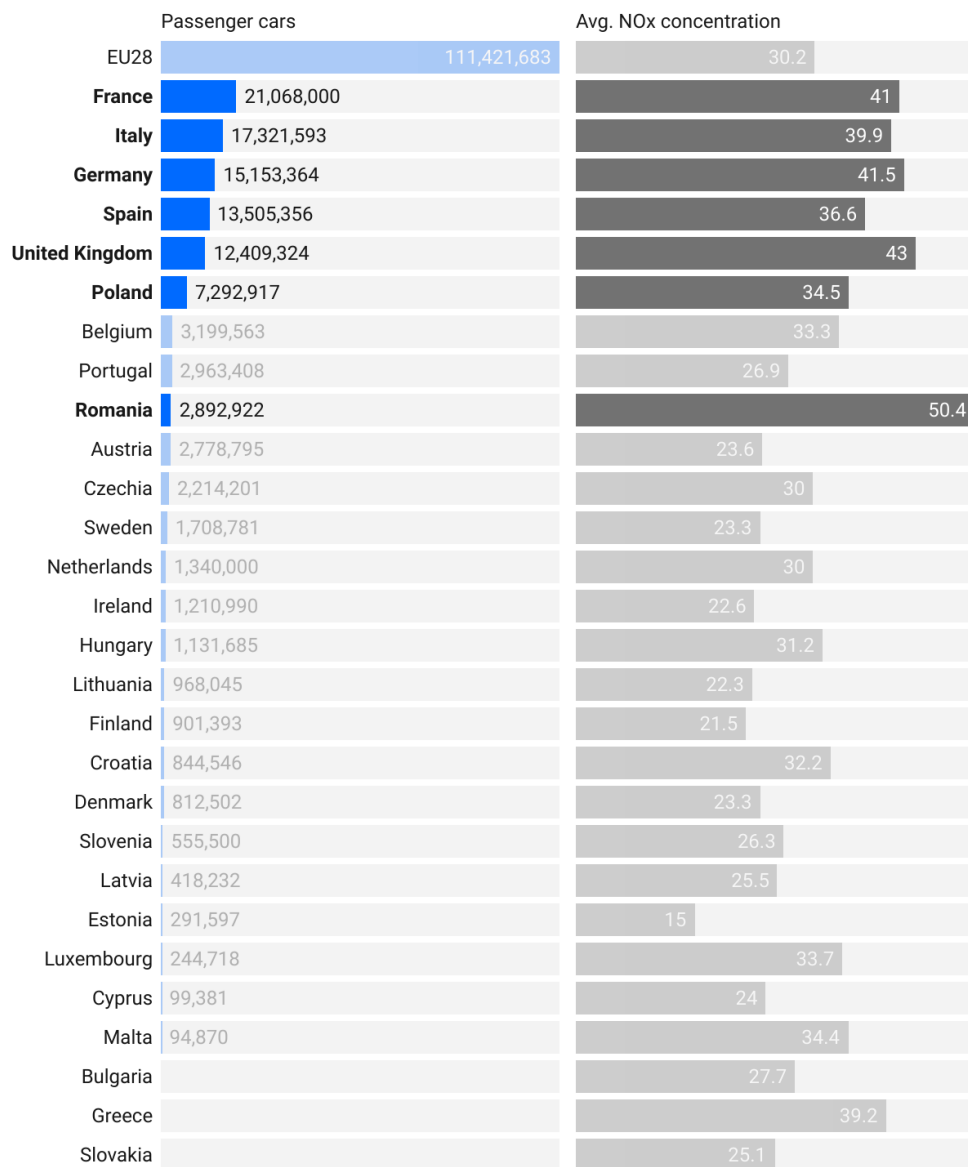


Figure 1-9. Comparison of fleet diesel passenger cars vs. average NO_x concentration in every Capital City in EU-28 (2018) ordered by fleet diesel passenger cars. Data source: Eurostat.

So, most diesel passenger cars (and light-duty vehicles) are registered in countries more populated and with a higher proportion of the population living in an urban environment, where more health problems can be generated, and where higher NO_x concentrations in big cities can be found (see Figure 1-10).

Not only is the number of vehicles growing, but the distance traveled is also increasing for both passenger and freight vehicles [3]. For the period 1995-2018, it has been settled an average annual increase rate of 1.2% for passenger kilometers traveled and

1.5% for freight tonne-kilometers traveled [46], [47]. More kilometers traveled means more NO_x emissions from road transport.

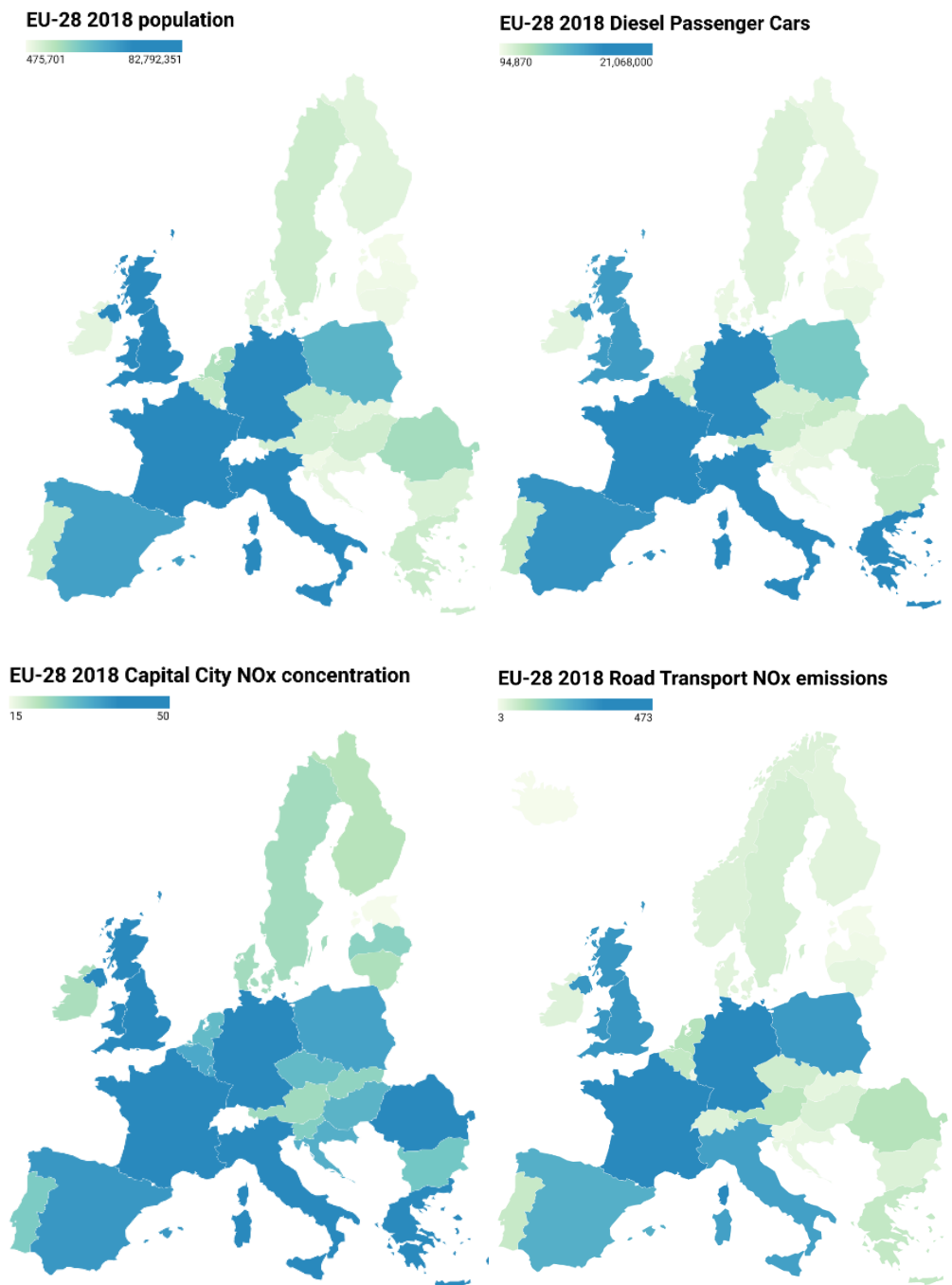


Figure 1-10. Comparison between population, the fleet of diesel passenger cars, NO_x concentration in capital cities, and NO_x emissions in EU-28. Source: Eurostat.

Light-duty vehicles showed a similar evolution, with an increase from 51% of the light-duty vehicles less than 1500 kg in 2003 to more than 85% in 2012, with more than 18 million light-duty vehicles fewer than 1500 kg. Most of these diesel light-duty vehicles

are used for the delivery of goods in the urban environment, where more harmful are the NO_x emissions, increasing NO_x concentration in the cities.

The NO_x emission limits for these vehicles are the same as passenger cars until a weigh-load of 1305 kg, and from 0.65 g/km to 0.105 g/km for light-duty vehicles between 1305 kg and 1760 kg, the same proportion of more than 6 times lower.

However, although NO_x emission limits have decreased over time, the real NO_x emissions reduction was lighter, compared with the reduction of the NO_x emissions thresholds.

As a result, the **concentration of NO_x in urban air has proven to be higher than anticipated**, leading to the previously mentioned adverse effects on human health.

By trying to improve efficiency and reduce vehicle emissions, EU regulations have been modified to make measurements during the type-approval process more representative of real vehicle emissions.

As a result, vehicles approved to Euro 6c Standard emissions level (from September 2018) and newer are subjected to the WLTP (Worldwide Harmonized Light Vehicles Test Procedure) cycle, during the type-approval process, instead of the NEDC (New European Driving Cycle) cycle previously used [48], [49].

Furthermore, Euro 6d-Temp standard vehicles are subjected to an RDE (Real Driving Emissions) measurement procedure with PEMS (Portable Emission Measurement System) to improve the representativeness of the homologation. Measurement results suggest that implementing this emission standard has improved the NO_x emission behavior of these vehicles concerning previous emission standards [50].

Even from September 2019, new Euro 6d-Temp vehicles may be subjected to ISC (In-Service Conformity) measurements to ensure that they continue to comply with the values measured in homologation once they are on the road [51].

Furthermore, since September 2020, the implementation of Regulation (EU) 2018/858 and (EU) 2020/683 has introduced the requirement for national authorities to carry out a Market Surveillance process that checks that vehicles and their components placed on the market comply with the requirements of the Union harmonization legislation.

The next Euro 7 emission standard is currently underway, which, among others, will likely reduce and equalize NO_x emission limits for diesel and gasoline vehicles and reduce the emission factor for the RDE test.

It is estimated that most pollutant emissions come from a proportionately small number of vehicles, which are known as "high emitters" [52]. Concerning NO_x emissions, according to the "Impact Assessment SWD (2012) 206 final" of the European Commission, if 5% of the most polluting vehicles were identified, it would reduce approximately 25% of the polluting emissions [53]. Therefore, it becomes key to develop a system that allows detecting this 5% of vehicles that account for 25% of total emissions.

In most countries in Europe (including all the European Union countries [54], [55], vehicles registered are subjected to Periodic Technical Inspection (PTI), the scope of

which varies according to the country of registration of the vehicle. That said, the minimum requirements for inspection (in European Union countries) are determined by European directives [56] and national regulations [57], [58].

The primary objective of vehicle technical inspections is twofold. Firstly, they aim to ensure the proper functioning of various vehicle systems, with a strong emphasis on ensuring road safety. Secondly, these inspections also focus on verifying that vehicles do not exceed the established limits for polluting emissions, thus contributing to environmental protection.

As is indicated in the European directive, testing should be relatively simple, quick, and inexpensive, while at the same time effective in achieving the objectives set by the established regulation [56].

In the case of petrol vehicles, PTI controls that the emissions of CO do not exceed the allowed percentages of % volume concentration in exhaust gases.

In the case of diesel vehicles, the opacity of the exhaust gases is measured, which theoretically allows checking the amount of soot generated in vehicles.

That means that currently the levels of NO_x emission in vehicles are not included in the scope of the diesel or petrol engine vehicles PTI. However, the last PTI European directive has contemplated the possibility of adding NO_x emissions on-road tests to the type-approval process (RDE test), and the establishment of NO_x levels measurements test methods at PTI [56].

Another modification incorporated in the application of the last European directive is the use of vehicle OBD systems as a support for the control and measurement of the vehicle's polluting emissions.

In this respect, several studies such as the one by CITA (International Motor Vehicle Inspection Committee), have tried to define and propose PTI inspection methods that allow controlling NO_x emissions and identifying EGR (Exhaust Gas Recirculation), LNT (Lean NO_x Trap), and SCR (Selective Catalytic Reduction) faults and tampering.

An example of such efforts was seen in 2011 with the TEDDIE Project [59], which concluded without establishing a specific procedure but emphasized the need for additional research. Similarly, in 2015, the SET Project [60], concluded with a recommendation to develop a cost-effective testing method for measuring NO_x, as well as determining applicable limit values for NO_x, although its primary focus was not solely on NO_x measurement.

In 2017, a new project was again carried out to try to determine a method for measuring NO_x emissions from vehicles with the SET II project [61], [62]. The results were presented in 2019, without a clear selection of a NO_x measurement method, although suggesting the use of a combination of the loaded ASM2050² method with an unloaded test method for EGR assessment.

Most of the procedures analyzed so far for measuring NO_x emissions in a vehicle have been based on protocols that pretend to simulate vehicle conditions in circulation. To

² ASM2050 method will be explained in Chapter 2

this end, a roller bench (usually reproducing a previously defined cycle) or free acceleration cycles in the static state have been used. Both kinds of procedures have presented similar reproducibility and representativity problems.

Furthermore, these approaches toward NO_x control primarily concentrate on identifying malfunctions or tampering with EGR and after-treatment systems. However, the underlying intention of the directive suggests that the primary emphasis should be on measuring (and understanding) the emissions level of vehicles. [56].

It has been found that EGR and EATS (Exhaust After-Treatment Systems) themselves are in many cases designed more to pass the type-approval test (especially in the case of NEDC) than to reduce emissions in real-life traffic conditions [33], [34], [39], [63]. Because of this, it seems more effective to focus efforts on knowing the actual level of emissions from vehicles, rather than on analyzing the proper functioning of these systems.

Focusing on the functioning of systems like the EGR can be counterproductive since these systems can operate correctly, and yet the vehicle may still have excessively high emissions. For example, it has been found that sometimes the SCR systems are ineffective in urban traffic [64], where NO_x emissions are more harmful to health. Therefore, verifying the proper functioning of a specific system (such as the SCR) may not be a good indicator of the level of NO_x emissions during urban vehicle operation.

Hence, after various experiments and tests over the last few years, a procedure that provides a feasible, reliable, reproducible, representative, simple, and fast NO_x measurement method to be performed in a PTI station has not yet been achieved.

15. WHY IT IS IMPORTANT TO ASSESS AND MEASURE THE NO_x EMISSIONS AT PTI?

The first step to setting up correct environmental and health policies is to obtain accurate information about real NO_x emissions. As the current theoretical information provided for the Type-approval process has been demonstrated as incorrect, it is necessary **to build a mechanism to measure and/or correctly estimate the real NO_x emissions from the whole fleet** of vehicles.

This mechanism could be a **PTI NO_x measurement**. The main reasons to use PTI to control NO_x emissions are the following:

- In the EU the whole fleet of vehicles must be periodically subjected to the procedure of inspection, so in a brief time it could be possible to measure and assess the NO_x emissions from all the vehicles considered, providing relevant information about NO_x emissions in a short period of time.
- As PTI is mandatory throughout the life of the vehicles, including NO_x emissions measurement at PTI will provide the historic register of the evolution of the whole fleet's NO_x emissions over the years. This is valuable feedback on the effectiveness of the environmental protection policies that could be implemented.

- PTI currently controls gaseous pollutant emissions from vehicles, so including NO_x emissions measurement is easier and less expensive in time and resources than creating a new system completely separated from PTI. By definition, PTI must be as quick and inexpensive as possible, so the cost-benefit ratio of implementation in PTI will be better than any other system.
- PTI is a system with high recognition and implementation in society. For example, currently, in Spain, the term PTI (ITV in Spanish) has been assumed as a synonym for technical revision, even though the said revision is not carried out on a vehicle. The system has proven its usefulness, as it has become a fundamental tool to guarantee minimum technical conditions for vehicles in circulation, with the consequent benefits that this entails in road safety [65] and protection of the environment. For this reason, the implementation of additional measurements in PTI will be more easily accepted by society than the creation of a new control process.

1.6. QUESTIONS ADDRESSED IN THE THESIS

Throughout the development of the thesis, a series of problems will have to be solved to demonstrate the feasibility of the proposed measurement method. These problems are intrinsic to the subject of the measurement, the NO_x, and to the site and time chosen for the measurement, the PTI.

Only through their resolution will it be possible to demonstrate that the proposed methodology is valid for the selected purpose: the NO_x measurement in PTI.

1.6.1. IS NO_x MEASUREMENT IN PTI FEASIBLE?

The PTI process is mandatory for registered vehicles in EU countries (and other countries worldwide).

The price of this process must be low enough not to be an excessive burden that causes absenteeism of the owners, and at the same time, it must be sufficient to allow the companies and organizations that perform it to afford the necessary personnel and equipment to carry out an adequate and quality inspection, which meets its fundamental objectives. This ensures that a thorough and high-quality inspection can be conducted, effectively fulfilling its core objectives.

In this way, the incorporation of NO_x measurement into the PTI process should not increase the cost of the inspection considerably.

It is important to incorporate the PTI process and equipment that provide a reliable NO_x measurement but fitting PTI requirements. The current equipment used for NO_x measurement has been designed more for Conformity Service or academic analysis, rather than for PTI use. Therefore, it must assess whether the existing NO_x measurement equipment is suitable for use in PTI (in terms of cost, maintenance, metrological control, facility of use, ...), or if it could be necessary to design a new type of equipment.

The same situation applies to the measurement process. It is necessary to keep in mind that a PTI NO_x test will be potentially performed millions of times each year so the time of preparation of equipment, execution of the test, and cost of performing the test have to be adequate. The suitability and longevity of equipment have to be also accounted for.

This thesis will address this question.

1.6.2. IS NO_x MEASUREMENT IN PTI TECHNICALLY FEASIBLE? COMPLIANCE OF INSPECTION REQUIREMENTS AND AVAILABLE TECHNICAL RESOURCES

The technical inspection has to be simple, inexpensive, and has to be done in a limited time. The PTI inspection process is very different from procedures of a Service Conformity: its objectives are different, and therefore the means used (both in equipment and personnel) are also different.

So, the accuracy and complexity of the equipment and measuring process of NO_x in PTI must be in accordance with the PTI's specific requirements. In this way, process and equipment have to be "PTI grade", meeting the standard expected in a PTI. The use of "laboratory grade" equipment will entail costs, staffing, and time requirements unassumable for PTI inspection, which could make the inspection meaningless and ineffective. The use of "mechanical workshop grade" equipment does not comply with PTI requirements.

Then, it is necessary to incorporate the PTI process and equipment that provide a reliable NO_x measurement but fitting PTI requirements. Until now, the equipment used for NO_x measurement has been designed more for Conformity Service or academic analysis than for PTI use. Therefore, it must be determined if the existing and available NO_x measurement equipment is suitable for use in PTI (in terms of cost, maintenance, metrological control, and facility of use...), or if it could be necessary to design a new type of equipment.

The suitability and longevity of equipment have to be also accounted for. The chosen equipment should be robust and durable enough to withstand the high volume of testing without frequent breakdowns or the need for extensive maintenance. This consideration is crucial to avoid disruptions in the testing process and to ensure reliable and consistent measurements over an extended period.

The same situation applies to the measurement process. It is necessary to keep in mind that a PTI NO_x test will be potentially performed more than a hundred million times each year. Therefore, it is crucial to ensure that the time of equipment preparation, test execution, and cost of performing the test is appropriate.

This thesis will address this question.

1.6.3. REPRESENTATIVENESS OF NO_x MEASUREMENT RESULTS: DOES THE MEASUREMENT REFLECT ACTUAL NO_x EMISSIONS?

A measurement method is useless if the result of the measurement cannot be translated into reality in any way.

PTI emissions tests specifically aim to identify vehicles that exceed a predetermined emission limit, which varies based on the type of engine. Consequently, a NO_x measurement test is designed to detect vehicles emitting NO_x above a specified threshold.

However, the current limits for NO_x emissions in type approvals have been found to be unrealistic. It has been demonstrated that vehicles that have successfully passed the type approval test, in real circulation exhibit significantly higher NO_x emissions than these limits. As a consequence, these limits can't be employed at PTI as a threshold for inspection.

Indeed, if a NO_x measurement test is to be included as part of PTI, it is necessary to establish specific rejection limits. These limits should be carefully defined to ensure that they can identify vehicles with excessive NO_x emissions, but only reject those vehicles that exhibit significantly higher emissions than they would under normal operating conditions. Striking the right balance is crucial to avoid false rejections while effectively identifying vehicles with substantial emission issues.

Therefore, a vehicle may be functioning correctly according to its design and performance standards, yet still have elevated NO_x emissions due to factors such as variations in real-world driving conditions or wear and tear over time. If the rejection threshold is set too low, there is a risk of rejecting vehicles that are operating properly but happen to exceed the limit due to these external factors.

To avoid this situation, it is crucial to establish rejection thresholds that strike a balance between detecting vehicles with significant emission issues and avoiding false rejections of vehicles that are functioning correctly under typical operating conditions.

Then, a general rejection threshold should be set high enough to avoid incorrectly rejecting vehicles that are operating within acceptable parameters under normal conditions. At the same time, it should be low enough to effectively identify and reject vehicles with excessive emissions, ensuring that high-emitter vehicles are appropriately flagged during PTI. Striking this balance ensures the reliability and effectiveness of the inspection process while minimizing the risk of false rejections.

Another possibility is the implementation of a specific rejection threshold for each vehicle. In this scenario, the collaboration of vehicle manufacturers with regulatory authorities is necessary, providing manufacturers with the appropriate limit of rejection for each vehicle model according to the test proposed.

By tailoring the rejection thresholds to individual vehicles, it becomes possible to more accurately identify excessive emissions on a case-by-case basis. This collaborative effort would ensure that vehicles with genuinely high emissions were detected and rejected while avoiding unnecessary rejections.

Finally, comparing vehicles with each other based on their emissions is a crucial aspect. By assessing the NO_x emissions of vehicles in urban traffic, where NO_x has the most significant impact on air quality and human health, the NO_x measurement test can serve as a tool for classifying vehicles according to their emission levels in urban environments. This information can be extremely valuable for policymakers in formulating effective policies to protect public health and the environment.

Additionally, such classification can aid in identifying high-emitting vehicles that should be prioritized for further inspections or targeted for emissions reduction initiatives. Overall, the NO_x measurement test can provide valuable insights into the emission performance of vehicles in real-world driving conditions and inform decision-making processes to mitigate the impact of vehicle emissions on urban air quality.

In this thesis, this question must be addressed.

1.6.4. ADVANTAGES OF NO_x MEASUREMENT IN PTI

Measuring NO_x emissions in PTI would provide significant advantages and benefits:

- **Emission Reduction:** By detecting and removing vehicles with excessive NO_x emissions from circulation, PTI can contribute to reducing overall air pollution and improving air quality in urban areas. This helps protect public health and the environment.
- **Targeted Inspection:** The NO_x measurement test enables the identification of high-emitting vehicles, allowing for targeted inspections and potential corrective actions. This approach efficiently allocates inspection resources and focuses on vehicles with the greatest impact on emissions.
- **Policy Informing Tool:** The data collected through PTI NO_x measurement can be valuable for policymakers, providing insights into the emission levels of vehicles in urban environments. This information can help shape policies and regulations aimed at reducing emissions, improving urban air quality, and safeguarding public health.

So, incorporating NO_x emissions measurement into PTI becomes a comprehensive tool for emission control, vehicle assessment, and policy formulation, ultimately leading to improved environmental outcomes. Since PTI is mandatory, the whole fleet of vehicles would be periodically subjected to NO_x measurement, providing comprehensive and timely information about NO_x emissions, including the time evolution of emissions, in a short period. It provides valuable insights into the overall emission levels and trends, enabling authorities to monitor the evolution of emissions over time.

This periodic control of emissions along the lifetime of the vehicle can hold significant importance (instead of a single value such as the data provided by the vehicle approval). Research indicates that NO_x emissions tend to increase with the age of vehicles, independent of factors such as maintenance and condition [66]. In addition, the monitoring over time of the whole fleet provides feedback on the effectiveness of environmental policies applied.

Moreover, the data collected from NO_x measurements during PTI can be utilized to detect potential manipulation or tampering on vehicles. Deviations from expected emission levels can indicate unauthorized modifications or attempts to deceive emission control systems. This can help identify non-compliant vehicles and discourage illegal activities related to emissions tampering.

Extending the existing controls within the PTI framework to incorporate the measurement of NO_x emissions is a more viable and cost-effective approach compared to creating a separate system solely dedicated to NO_x emissions measurement and control.

The PTI process is already established, widely implemented, and familiar to vehicle owners and regulatory authorities. It involves infrastructure, procedures, and personnel that can be leveraged to integrate NO_x measurement seamlessly, so the implementation of NO_x measurement through its incorporation in the PTI is easier to accept and assimilate than the creation of a new system that, also, has higher associated costs.

In summary, the implementation of NO_x measurement within the PTI process would indeed serve as a valuable tool to address the circulation of high-emission vehicles and provide comprehensive information on the NO_x emissions from the entire vehicle fleet. This contributes to improving air quality, protecting public health, and reducing the environmental impact of vehicle emissions.

In this thesis, this question must be addressed.

1.7. OBJECTIVES OF THE THESIS

This thesis will develop a new method different from the systems proposed until now for NO_x emissions test for PTI through a static, robust, and fast way.

The goals to be achieved in this thesis are the following:

- 1) Definition of a NO_x measurement procedure. This procedure has to accomplish PTI's technical and economic requirements. At the same time, it should ensure the quality, reproducibility, and accuracy of measurements. The measurement method should be applied, in the same way, and with the same equipment, as to any M1 (PC, Passenger Cars) and N1 (LDV, Light-Duty Vehicles) diesel engine vehicle (including 4x4 vehicles, automatic or manual gearbox vehicles, not disconnectable traction control vehicles,...) If possible, the measurement method (or similar) would be applied to M2, M3, N2, and N3³ vehicles (buses and trucks).
- 2) Results from the new measurement method have to be representative of the real NO_x emissions of vehicles. Accordingly, the method will be compared to real on-road NO_x emissions, to check how far or close the results of the PTI measurement are from reality. Results should be as close as possible to real NO_x emissions, or at least be representative of real emissions.

³ M2, M3: buses; N2, N3: trucks.

- 3) Equipment and staff requirements have to accomplish with PTI requirements, in technical and economical aspects.
- 4) The measurements of NO_x must demonstrate a level of representativeness and accuracy that is at least on par with other methods, while the requirements for the measurement process should be either equal to or less stringent.

These objectives must be reached to conclude that the proposal of measurement of NO_x emissions from diesel vehicles at PTI is feasible to be applied.

1.8. CONCLUSIONS

As a summary and main conclusions of this initial chapter, the following can be highlighted:

- For the proposed method in the thesis to be considered valid, it must demonstrate resolving a series of issues defined in the chapter.
- Vehicle emissions of NO_x, particularly from diesel vehicles, cause serious health effects on populations exposed to these emissions, especially in urban environments.
- In Europe, countries with larger populations, particularly in urban areas, have a higher number of diesel vehicles, exacerbating the aforementioned problem.
- Measuring NO_x emissions in Periodic Technical Inspections (PTI) would provide valuable information about the vehicle fleet's emissions, leading to improved environmental protection policies and reducing the consequences of NO_x exposure on the population.
- NO_x measurement in PTI would enable the identification of vehicles with higher emissions, facilitating their removal from circulation and promoting emission reduction.
- NO_x measurement in PTI must meet the technical and economic requirements of the inspection, while also being representative and accurate.

CHAPTER 2

NO_x GENERATION, ANALYTICAL TECHNIQUES, MEASUREMENT METHODS, AND STUDIES FOR NO_x MEASUREMENT

2. NO_x GENERATION, ANALYTICAL TECHNIQUES, MEASUREMENT METHODS, AND STUDIES FOR NO_x MEASUREMENT

2.1. INTRODUCTION

This chapter will provide the necessary background information required before initiating the design of the measurement method.

The initial part of this chapter will cover the fundamentals of NO_x formation in a compression engine, as well as how NO_x generation is influenced by different engine operating factors such as temperature and engine load. This understanding of the relationship between NO_x generation and these parameters will serve as the foundation for designing the measurement method being proposed.

Following, an overview will be provided regarding the different analytical techniques that can be utilized in NO_x measurement equipment.

A compilation of the frequently employed measurement methods for vehicle emissions, specifically focusing on NO_x (although they are not intended for use in PTI) will be detailed.

Upon understanding the process of NO_x generation in the engine and familiarizing it with the available measurement methods for vehicle emissions, the next step will involve examining the existing literature on NO_x emissions measurement from diesel vehicles. This review will encompass studies that specifically investigate NO_x measurement in PTI settings, as well as those that analyze emissions under real-world traffic conditions, with the most usual techniques: RSD and PEMS.

By presenting the scenario in which the new method for NO_x measurement in PTI will be introduced, it becomes possible to examine and understand the similarities and differences between the proposed method and the existing approaches.

2.2. NO_x GENERATION PROCESS AND ITS DEPENDENCE ON ENGINE LOAD IN DIESEL VEHICLES

The measurement and analysis of NO_x emissions from a diesel vehicle have to begin with knowledge about NO_x generation.

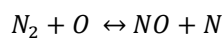
Nitrogen oxides, also known as NO_x, are a group of highly reactive gases composed of nitrogen and oxygen molecules. The two primary components of NO_x are nitric oxide (NO) and nitrogen dioxide (NO₂).

The primary source of NO_x is the Thermal NO, which is generated through the Zeldovich mechanism [67] (Equation 2-1, Equation 2-2, and Equation 2-3). Additionally, Prompt NO from the Extended Zeldovich Mechanism [68] serves as a secondary source. Usually, the other sources are of lesser importance compared with these NO_x sources.

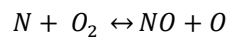
The most important source of NO_x generation from combustion in diesel engines as a whole is Thermal NO, but is not the only source. Part of the NO generated in combustion is subsequently combined with oxygen to get NO₂ (Equation 2-4) in the combustion chamber and along the exhaust line. The combination of the two compounds forms the NO_x pool (Equation 2-5) generated by the engine and emitted by the tailpipe.

While the majority of NO_x emissions produced by vehicles are in the form of NO, there has been an observed increase in the proportion of NO₂ in the exhaust gases of vehicles complying with the Euro 3 emission standard and newer models up to the present day [41].

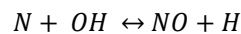
Equation 2-1



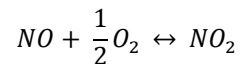
Equation 2-2



Equation 2-3



Equation 2-4

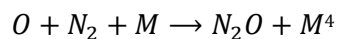


Equation 2-5

$$NO_x [ppm] = NO [ppm] + NO_2 [ppm]$$

The Zeldovich mechanism has also an intermediate N₂O route that generates NO in some lean fuel and low-temperature conditions, according to the following equations:

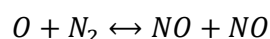
Equation 2-6



Equation 2-7



Equation 2-8



⁴ Organic residue.

The formation processes of Thermal NO are **strongly influenced by the temperature** within the combustion chamber [2], [67], [68], as well as the concentrations of oxygen and nitrogen and the duration of exposure.

Even in the case of gasoline vehicles (or other fuel types), higher temperatures directly contribute to increased NO_x generation and emissions [69].

As diesel engines work without throttle and usually with an excess of combustion air (lean combustion), the O₂ concentration is always ensured by combustion air, being modified the fuel-air ratio through the fuel injection. It has been also observed that NO_x emissions are related directly to the air-fuel ratio, decreasing the NO_x emission when decreasing this air-fuel ratio [70].

The nitrogen sources for the chemical reaction are both the nitrogen from the combustion of atmospheric air and the nitrogen bound in the fuel.

For lean combustion, almost 65% of fuel-bound nitrogen is converted to NO through the Thermal NO formation [70]. This is because nitrogen bonded in the fuel reacts with oxygen more readily than the molecular nitrogen supplied by the combustion air: the dissociation energy for the N₂ is 225,000 calories per gram-mole of nitrogen, whereas the dissociation energy for the carbon-nitrogen bonds in fuel molecules is between 60,000 to 150,000 calories per gram-mole of nitrogen [71].

The Thermal NO formation is temperature dependent because it is a highly endothermic process, in which higher equilibrium concentration occurs at higher temperatures near the stoichiometric combustion point.

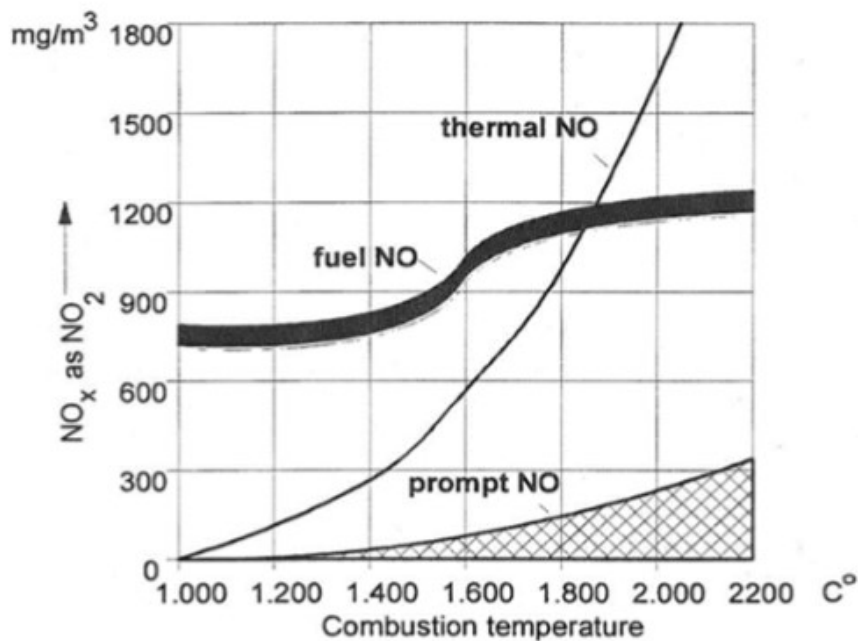


Figure 2-1. Relationship between NO_x formation process and combustion temperature (Source: Semakula et al., 2018) [70]

NO formation primarily takes place at temperatures exceeding 1,500°C within the flame front. When the temperature in the combustion chamber rises, such as when there is an increase in the vehicle's power demand, the concentration of generated NO also increases. Notably, raising the temperature in the combustion chamber beyond 1,600°C results in a substantial surge in NO generation [5], [70], [72], as illustrated in Figure 2-1.

The duration for which reacting gases are exposed to high temperatures also influences the generation of NO_x. The longer the gases remain in the conditions conducive to NO_x formation, the higher the amount of NO_x produced.

On the other hand, the engine load demand and the temperature in the combustion chamber are also related. The increase in load demand on the engine produces an increase in the fuel/air ratio (due to a higher proportion of fuel in-cylinder) and an increase in temperature, both in the combustion chamber and in the exhaust gases.

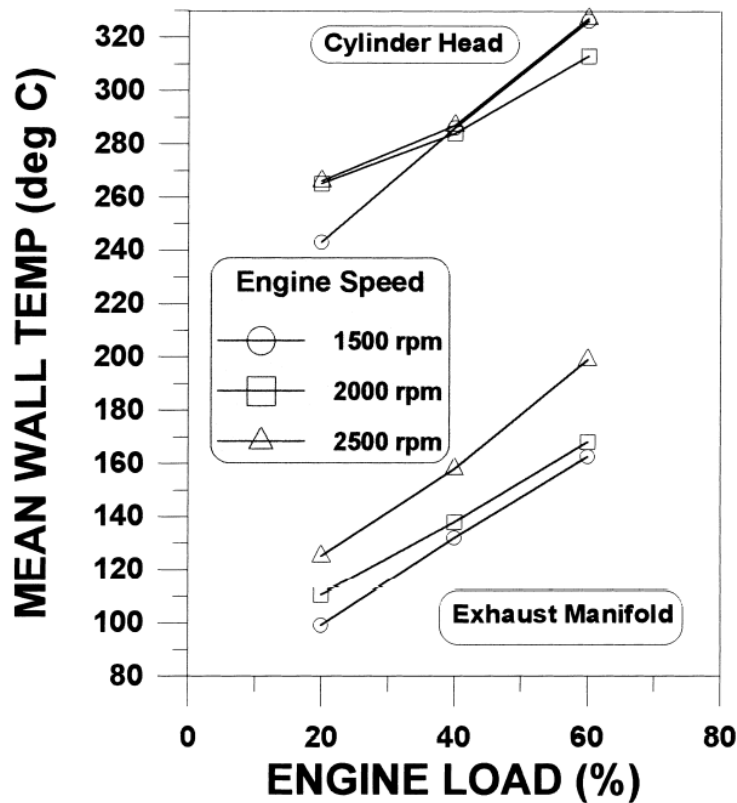


Figure 2-2. Variation of the cylinder head and exhaust manifold wall surface mean temperatures against engine load, for engine speeds of 1500, 2000, and 2500 rpm (Source: Rakopoulos et al., 2000) [73]

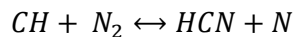
It can be checked experimentally that the increase of the load on the engine at a given engine speed produces an increase in the combustion chamber and exhaust gas temperature (see Figure 2-2). Instead, increasing the engine speed while maintaining a constant engine load has a marginal effect on the peak heat flow in the combustion chamber [73], [74].

Therefore, diesel vehicles' Thermal NO generation is strongly dependent on combustion chamber temperature, and this temperature is directly related to engine load demand, so **NO_x emissions are related to engine power demand through temperature in the combustion chamber, increasing NO_x emissions when load demand increases** [74], [75].

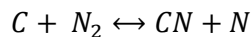
As was previously said, another important mechanism of NO_x generation is the Prompt NO, also known as Fenimore NO or Fenimore Mechanism, which is generated with the intervention of hydrocarbon fragments from fuel combustion. This source is more relevant in fuel-rich conditions when O₂ concentration is low and is more sensitive to fuel composition [29], and it is also formed at the flame front.

The hydrocarbon radicals react with molecular nitrogen, dissociating nitrogen molecules and creating cyano compounds as an intermediate step to NO formation, according to the following path [70]:

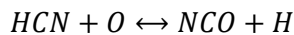
Equation 2-9



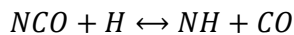
Equation 2-10



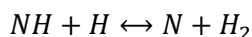
Equation 2-11



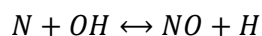
Equation 2-12



Equation 2-13



Equation 2-14



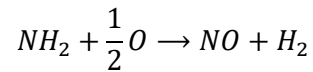
Another way of NO_x generation is the fuel NO_x formation, which is more dominant at low combustion temperatures, but when the temperature rises, it becomes negligible [71].

In the situation of a low fuel-air ratio, almost 60% of the nitrogen from the fuel is converted to NO, and the rest is converted into N₂ [76].

In high fuel-air ratios, fuel bounded nitrogen from N-H and N-C compounds is involved in the formation of ammonia and cyanohydrin acid (HCN). These compounds subsequently dissociate, forming NO when released into the atmosphere. This NO_x source cannot be controlled through combustion [70].

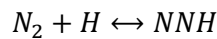
The amount of NO generated in this way depends on the percentage of nitrogen contained in the fuel because light distillate fuels contain approx. 0.06% volume of organic hydrogen and heavy distillate fuels can contain 1.5% volume or even higher. The path formation is with the following reactions:

Equation 2-15

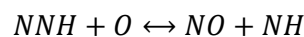


Finally, a new path to NO_x generation has been determined [77], the NNH mechanism, where two reactions of combustion of hydrogen and hydrocarbon fuels can generate NO by the following:

Equation 2-16



Equation 2-17



To summarize, although Prompt NO and Fuel NO can be, under certain circumstances, responsible for a significant amount of NO, usually **most of the NO generated in the combustion process comes from the Thermal NO, in a process highly dependent on temperature and load demand at the engine.** So, the use of low nitrogen fuel content does not guarantee low NO_x generation, because Thermal generation is the main mechanism of NO_x generation from diesel engines.

This **temperature dependence is the main way to control NO_x formation during the combustion process**, reducing peak temperatures in the flame. A usual way to reduce this temperature is retarding the fuel injection concerning the top dead center point [78]. Another way in lean combustions is to dilute the combustion gases with compounds that do not participate in the combustion reactions, such as exhaust gases. This reduces the adiabatic temperature of stoichiometric combustion [79]. This method is used in the control emissions method known as EGR (Exhaust Gas Recirculation).

Finally, due to this relationship between the NO generation, the temperature in the combustion chamber, and the load demand at the engine, it can be concluded that **it is important to know the behavior of the load demand to analyze NO_x emissions.** In this way, there is an important tool that provides information about the load demand in the engine and is easy to access and register in PTI: the "% engine load" value.

The "% engine load" is a parameter that relates the power demand to the fundamental operating parameters of the engine and can be easily read through the OBD (On-Board Diagnostic) port of the vehicle.

The "% engine load" is calculated (Equation 2-18) by the ECU of the vehicle according to SAE J1979/ ISO 15031-5 [80], through the relationship between the current airflow intake to the engine and the peak airflow intake at the given rpm for explosion engines. For the compression-ignition engines, the fuel flow is used in place of airflow for the calculations.

Equation 2-18

$$\% \text{ Engine Load} = \frac{\text{Current airflow}}{\text{Peak airflow}(rpm) \cdot \frac{\text{Baro}}{29.92} \cdot \sqrt{\frac{298}{T_{amb} + 273}}}$$

This value corresponds to the "Calculated load value" defined in European directives [81] and is a dimensionless number, which has the advantage that is not engine specific value, so can be used to compare engines with different characteristics.

The "% engine load" value indicates the percentage of peak available torque or, in other words, the percentage of the engine torque that is being used, as a function of rpm, by the power demand to which the engine is subjected.

It is a relative indicator that provides information on the use of the engine concerning its maximum capacity under given engine speed conditions, or as the directive explains is an indication of the proportion of engine capacity that is being used. This value is usually read at PID \$04 from the OBD communications system and is a generic output from ECU, both in diesel and petrol vehicles. Can be read without problems in all the Euro 6 vehicles, almost Euro 5 vehicles, and a high proportion of Euro 4 vehicles.

2.3. NO_x MEASUREMENT ANALYTICAL TECHNIQUES

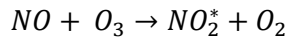
The main techniques used to measure nitrogen oxides are listed below. The various manufacturers of NO_x measurement equipment use these different techniques depending on their individual characteristics, and the main objectives to be met by the equipment.

- 1) Chemiluminescent Analyzer (CLD)
- 2) Non-Dispersive Ultraviolet Analyzer (NDUV)
- 3) Non-dispersive Infrared Analyzer (NDIR)
- 4) Infrared such as Fourier-Transform Infrared Spectroscopy (FTIR)
- 5) Electrochemical Sensors

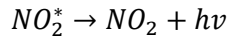
2.3.1. CHEMILUMINESCENT ANALYZER (CLD)

This technique can only be used to measure NO. It is based on the chemiluminescence reaction between ozone and nitric oxide to detect NO in a sample gas. It is based on the formation of NO₂ in an excited state from the reaction between the NO and the O₃ (see Equation 2-19).

Equation 2-19

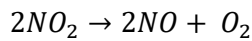


Equation 2-20



The intensity of the emitted light from the reaction in Equation 2-20 is proportional to the NO concentration in Equation 2-19.

Equation 2-21



If NO₂ exists in the sample gas, it must be converted to NO previously to the measurement process. In this case, a catalytic reduction is used to reduce the NO₂ to NO (see Equation 2-21).

Once NO₂ is converted to NO, it follows the measurement process from Equation 2-19 and Equation 2-20, being the emitted light intensity proportional to NO_x concentration.

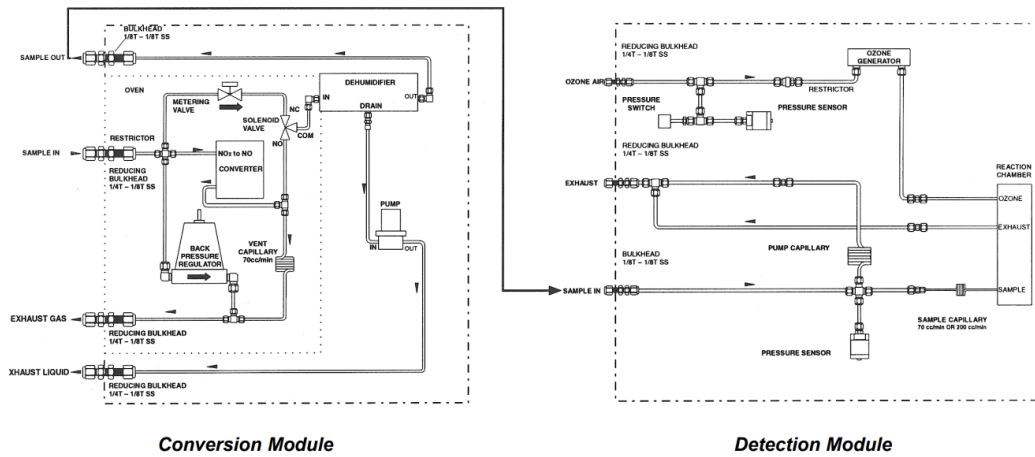


Figure 2-3. Flow Diagram for WCLD module measurement. Source: Emerson Process Management Rosemount Analytical Inc.[82]

This technique is commonly used in emission certifications and compliance testing. It is regulated by UN/ECE R83 (and EPA 1065).

It is characterized by a wide linear dynamic range, high accuracy, and fast response time. This technique can detect part per trillion concentrations of NO.

The main disadvantage is that this technique is usually used in complex and sensitive instruments, and it could be interfered with by other molecules based on nitrogen (NH₃, HNO₃, ...).

An important issue with this technique is the possible misreading caused by the vehicle's exhaust gases. In vehicles with SCR systems, NH₃ can be expected in the gas exhaust stream. In the catalytic converter of the CLD equipment, NH₃ will be converted to NO if the temperature is high enough, with subsequent positive bias in the measurement. However, if the temperature in the converter is not high enough, conversion efficiency decreases, and the NO_x measurement has a negative bias [83]. To avoid these problems, the conversion process needs to be periodically verified, the maintenance of equipment is complex, and the equipment is expensive.

To summarize, this measurement technique is more appropriate for laboratory testing [84] than for PTI requirements.

2.3.2. NON-DISPERSIVE ULTRAVIOLET ANALYZER (NDUV)

This technique consists of an ultraviolet source radiating the gas streams, while a detector is used to determine the amount of light energy absorbed. NO and NO₂ absorb UV light at different wavelengths, and this property can be used to measure the NO_x concentration in the sample gas stream.

Using the differential absorption technique, the radiant energy transmitted through the measuring cell is compared with the gas to be analyzed for two different UV bands. The absorption differential between the two wavelengths is measured and correlated with the concentration.

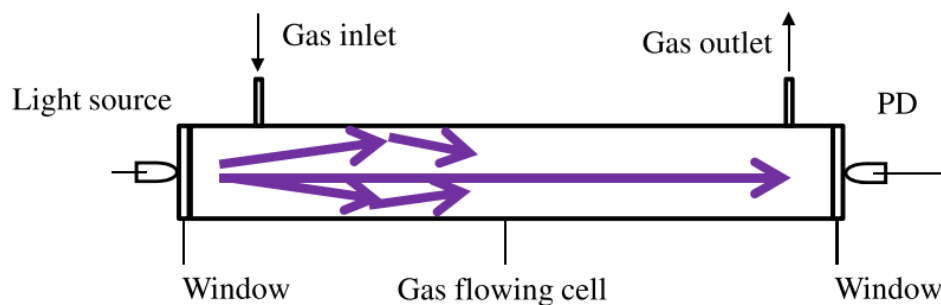


Figure 2-4. Schematic of an NDUV gas analyzer. Source: Higashi et al., Proceedings of SPIE, 2014. [85]

The absorption spectroscopy of a specific gas is realized through the Lambert-Beer law [85]:

Equation 2-22

$$I_1(\lambda) = I_0(\lambda)exp[-\sigma(\lambda)cL]$$

Being:

- λ the wavelength of light
- $I_o(\lambda)$ the initial light intensity
- $\sigma(\lambda)$ is the absorption cross-section of the gas
- c in the concentration of the gas
- L is the optical path length
- $I_t(\lambda)$ is the transmitted light intensity

The main advantage of the NDUV analyzers is that the equipment with this technology has a wide linear dynamic range and fast response time.

Compared to CLD, they present lower noise and CO₂ or H₂O interference, and are simpler and less expensive. However, they have been considered rather expensive for PTI [59]. Instead, this technique is used in PEMS [84].

The NDUV analyzers are regulated by UN/ECE R83 (and EPA 1065) for NO_x monitoring.

2.3.3. NON-DISPERSIVE INFRA-RED ANALYZER (NDIR)

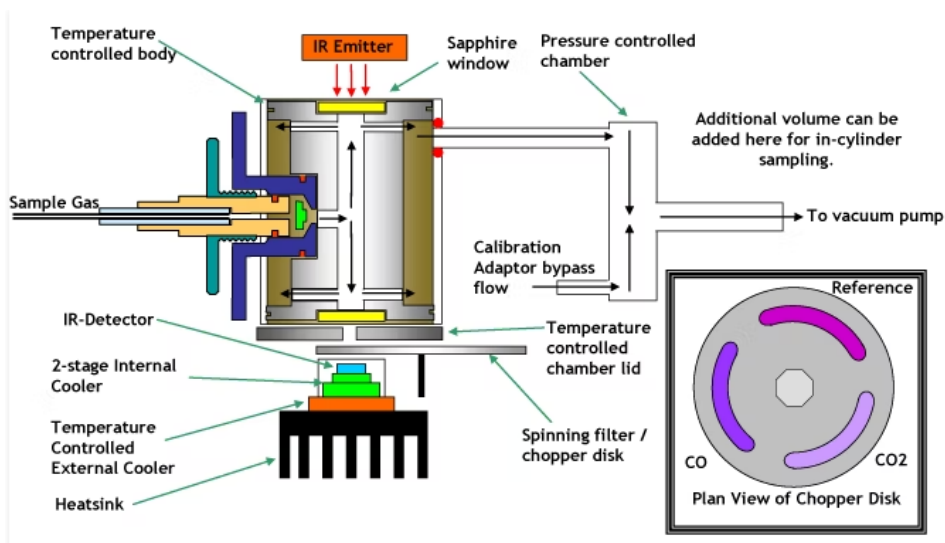


Figure 2-5. Schematic of NDIR measurement equipment with filter for CO and CO₂ detection.
 Source: www.cambustion.com

This technique is based on the measurement of the absorption of many molecules of infrared electromagnetic radiation. Each molecule absorbs this radiation in a discrete wavelength, which can be used to detect and measure the concentration of many gases in the gas stream.

However, this technique is not valid for the determination of NO_x in the exhaust gases of vehicles. A problem with this type of equipment is that NO₂ and H₂O absorb the IR radiation in a similar wavelength, which causes severe interference between NO₂ and water vapor.

In contrast, this technique is commonly used to measure CO, CO₂, and HC in gas analyzers for mechanical workshops. The equipment uses a monochromator to disperse the light into the different wavelengths and, in most equipment, a filter is used to transmit only the wavelengths of the target species to absorb (see Figure 2-5). Once the amount of IR absorbed by the sample gas is measured, the volumetric concentration of the species measured can be determined.

This technique is not used for transient engine testing because the dynamic response distorts the signal.

2.3.4. INFRARED SUCH AS FOURIER-TRANSFORM INFRARED SPECTROSCOPY (FTIR)

In this technique, infrared light is emitted through a gas sample, and the absorption of the infrared light is measured. The IR light is modulated in several wavelengths, allowing the measurement of different gases with the same instrument. The result of the measurement is a spectrum (see Figure 2-6) with the absorption of the different molecules in the sample gas, identifying the main compounds from the gas stream and their concentrations. The wavelengths absorbed correspond to the transition of vibrational levels of the molecule [86].

It can measure in real-time, which is an important advantage, in addition to the great advantage of simultaneously measuring separate compounds (e.g., NO and NO₂). This makes this technique a good option for real-time continuous monitoring.

However, the main disadvantages are the complexity of calibration and operation and the poor concentration accuracy compared with the other techniques. These types of equipment are relatively expensive. In general, this technique is considered less sensitive than CLD.

Anyway, this kind of NO_x measurement technique is used in static equipment for chassis dynamometer studies, and it is a good option for on-road applications.

An infrared light source (usually heated ceramic) emits IR light which is collected by a collimating mirror to make the rays parallel. Then, the light is divided and recombined in a single light beam with a beamsplitter and two mirrors (one fixed and another one moving mirror), interacting with the sample exhaust gas in a gas cell. The schematic of the operation is shown in Figure 2-7.

The signal from the interferometer is the result of the recombination of the divided original light, where both beams are interfering with each other. Finally, the signal from the interferometer is Fourier transformed to provide the spectrum of the analyzed gas (Figure 2-6).

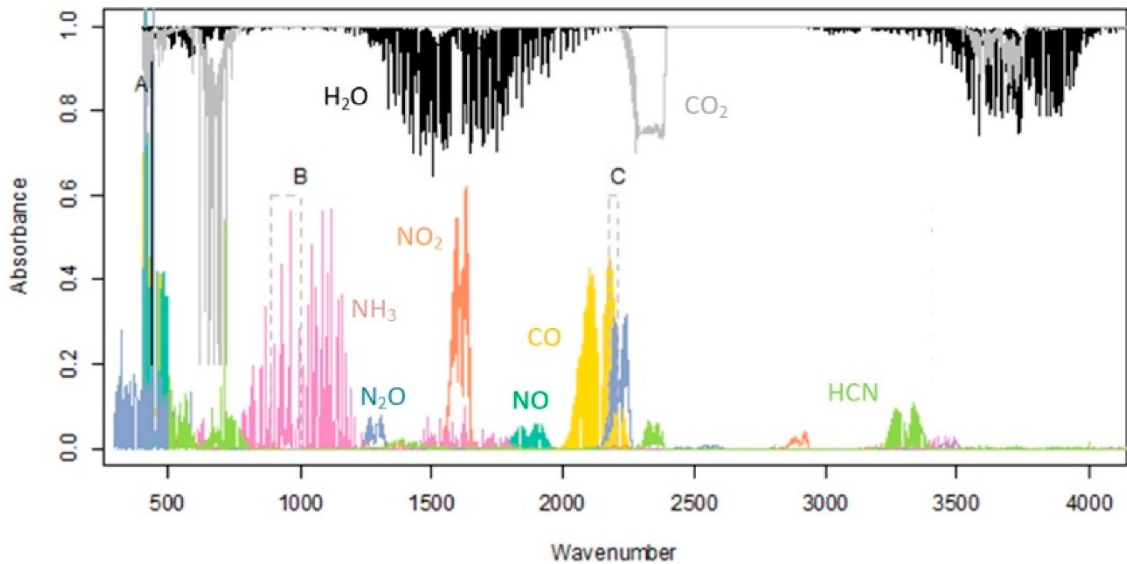


Figure 2-6. FTIR spectrum. Source: Giechaskiel et al.,2021. [86]

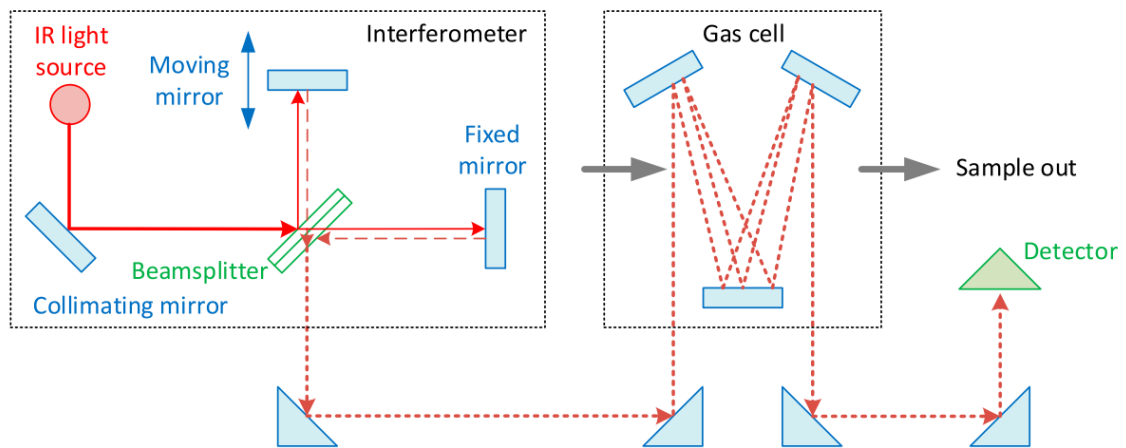


Figure 2-7. Principle of operation of FTIR spectroscopy. Source: Giechaskiel et al., 2021. [86]

2.3.5. ELECTROCHEMICAL SENSORS

This technology of NO_x sensors is commonly used as NO_x sensors onboard vehicles, to measure NO_x concentration in the exhaust stream and provide information to the ECU to manage the EATS.

Electrochemical sensors consist of a cell with electrodes and electrolytes. A chemical redox reaction with the exhaust stream gas involving electron transfer through ions transported by the electrolyte occurs into the cell, being the intensity of the current between electrodes proportional to the gas concentration.

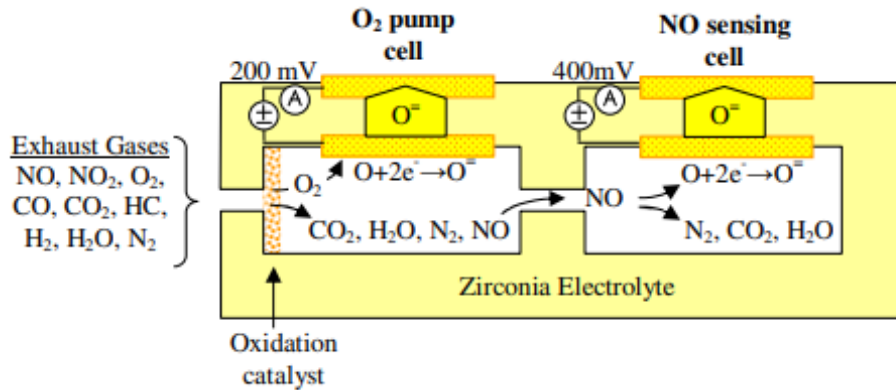


Figure 2-8. Scheme of Amperometric NO_x sensor operation. Source: Rheaume, J., 2010. [87]

In automotive applications, there are various types of sensors available, but the predominant type used for measuring NO_x emissions is the Amperometric sensor.

The main advantages of this technique are the fast response time and the low cost of the sensors. Also, they are available for different measurement ranges, even for low concentrations around 10 ppm [87].

As for disadvantages, they have relatively low accuracy, potential cross-sensitivity, and drift in sensitivity. Also, the lifetime of the sensor is reduced.

Accordingly, they are not used for compliance testing and certification processes. However, due to its characteristics, it may be the most suitable type of sensor for PTI use, because accuracy (± 10 ppm or better) and response time are correct for PTI purposes, and the cost of equipment is the lowest [59], [88]. The equipment used for the research was of this type.

2.4. NO_x MEASUREMENT TESTS CURRENTLY IN USE

There is a large variety of NO_x emissions tests, that focus on different aspects of NO_x emissions. Some of them are not suitable for PTI applications, but a sample of the most relevant used in various applications is listed below. According to the concepts or equipment used, they can be divided into the following groups [61], [62]:

- 1) Unloaded tests
- 2) Tests with Power Dynamometer Bench at loaded steady state
- 3) Tests with Power Dynamometer Bench at loaded transient
- 4) On-Road simulation tests with Power Dynamometer Bench at loaded transient
- 5) On-Road tests
- 6) Other methods

2.4.1. UNLOADED TESTS

In this set of tests, the vehicle remains free from any external load, and the analysis focuses on observing variations in engine speed.

- a) Idle tests. Usually, two engine speeds are measured [59].
- b) Free acceleration smoke (FAS) test. It is the test used in Europe to measure exhaust smoke opacity [59], [89]. Combinations of several free accelerations (Figure 2-9 and Figure 2-10) are suggested by equipment manufacturers to measure NO_x emissions [90].

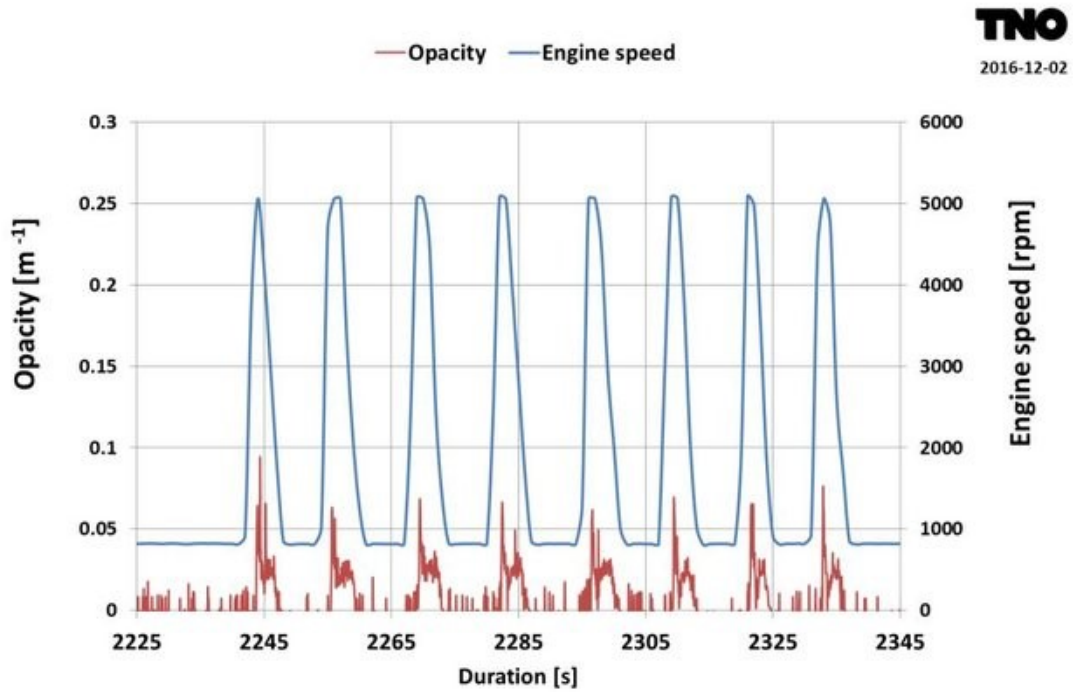


Figure 2-9. Free acceleration smoke (FAS) for opacity test. source: TNO.

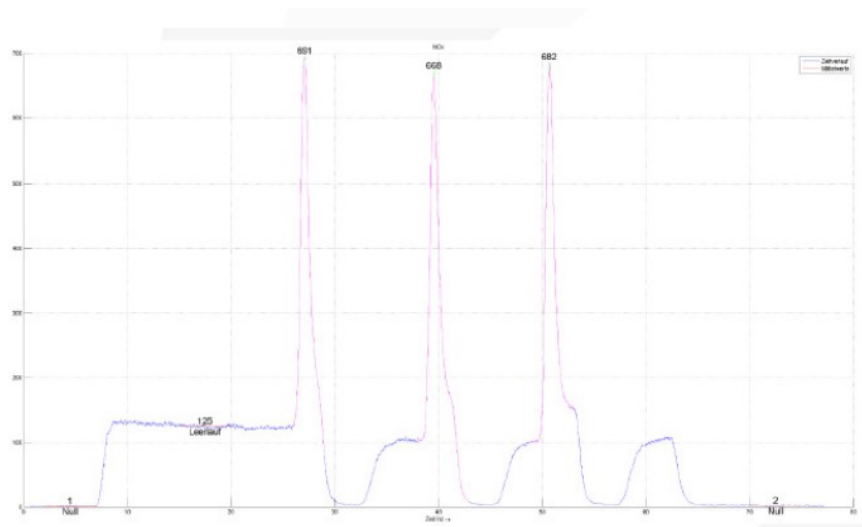


Figure 2-10. Kick-down test with three accelerations. Source: KNESTEL.

- c) INCOLL/AUTONAT. Both tests consist of rapid engine acceleration and deceleration [91].
- d) Norris. Based on gentle engine accelerations to operate the EGR system [92].
- e) CAPELEC and AVL. Combination of several free accelerations developed by these equipment manufacturers.

2.4.2. TESTS WITH POWER DYNAMOMETER BENCH AT LOADED STEADY STATE

In this group of tests, a power bench is used to place the vehicle. The vehicle can be operated at a specific speed while adjusting the brake load, establishing a consistent and loaded operating condition. Alternatively, the vehicle's speed can be altered while maintaining a constant brake load. These scenarios can be used individually or in combination to achieve different testing conditions.

- a) US Federal 3-Mode and CalVip, use a combination of vehicle speed and brake load, defined according to the characteristics of the vehicle [91].
- b) D550, uses a constant load (equivalent to a 5% road gradient) and 50 km/h of constant speed [93].
- c) ASM (Acceleration Simulation Mode), uses a constant load equivalent to the road load of the vehicle (except the rolling resistance) during acceleration [94]. It can be performed with various combinations of load and vehicle speed. The ASM2050 cycle analyses two speed points, 20 km/h and 50 km/h (see Figure 2-11). It is being used to study emissions in urban driving conditions.

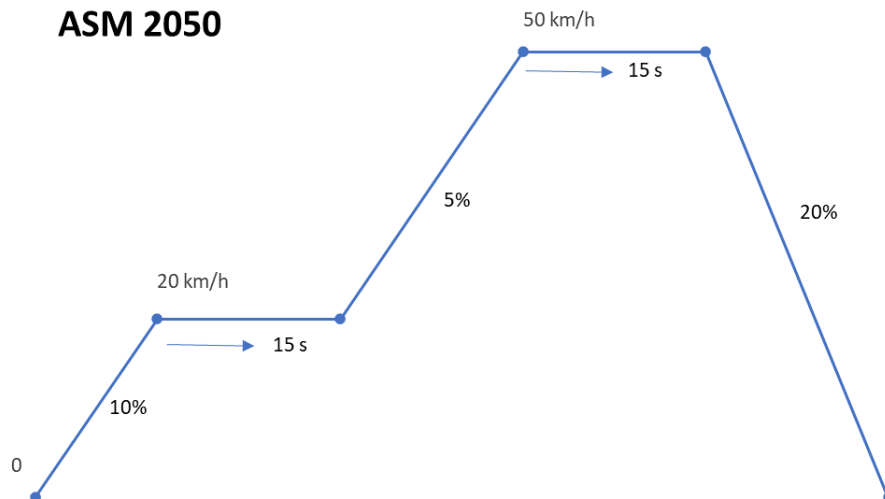


Figure 2-11. ASM 2050 cycle.

- d) The Lug-down test [95] uses a constant speed while the brake load increases to full-throttle vehicle condition. The brake load is gradually raised until the engine begins to struggle or stall. This is currently being used in China [96], according to GB 3847-2018 standard for diesel vehicles and GB18285-2018 for petrol vehicles. The threshold applied there for this measure is 1500 ppm of NO_x or 900 ppm of NO_x, depending on the location of the vehicle.

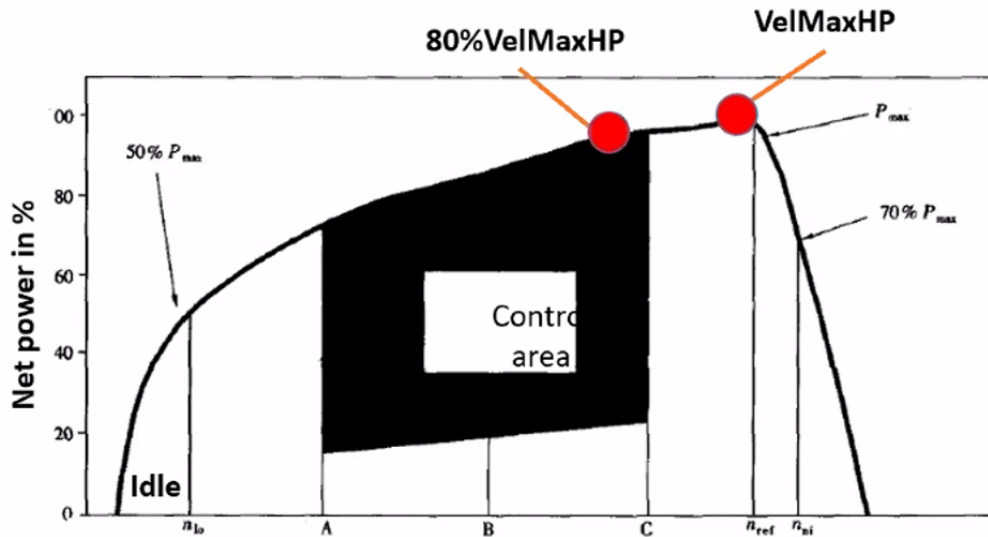


Figure 2-12. Lug-down test. Source: Shenzhen Anche Technologies Co., Ltd.

2.4.3. TESTS WITH POWER DYNAMOMETER BENCH AT LOADED TRANSIENT

In this group of tests, a power bench is used to place the vehicle [62]. The engine power and speed of vehicles vary throughout the cycle. The bench is used to reduce engine damage risk.

- Hot EUDC test, derived from the NEDC cycle (Extra-urban Driving Cycle part of the NEDC, see Figure 2-13) [97]. The manufacturer must provide the value to set the dynamometer inertia. During the driving cycle, one or more faults are introduced and should be detected by the EOBD system.
- DT80 test [93]. It is a mix-mode cycle, over a dynamometer bench with inertia simulation, that includes three full-load accelerations to 80 km/h, and a steady-state at 80 km/h.
- DT60 test [93]. It is similar to the DT80 test but with two full load accelerations at 60 km/h and a steady state at 60 km/h.
- AC5080 test [93]. It is similar to the DT80 test, with some important differences. A first full-load acceleration to 50 km/h is followed by a steady-state cruise at 50 km/h for 60 seconds, and then another full-load acceleration to 80 km/h with a final steady-state cruise at 80 km/h for 60 seconds.
- IM240 test [98]. A dynamometer bench with associated flywheels is needed. The cycle duration is 240 seconds and simulates a 3.1 km trip at an average speed of 47 km/h. It is a reduced version of the FTP-75 test.

2.4.4. ON-ROAD SIMULATION TESTS WITH POWER DYNAMOMETER BENCH AT LOADED TRANSIENT

In this group of tests, a power bench is used to place the vehicle. The vehicle reproduces defined speeds and acceleration patterns that simulate on-road circulation conditions.

- a) NEDC (New European Driving Cycle). It consists of two parts, an Urban Driving Cycle (UDC) and an Extra-Urban Driving Cycle (EUDC) (see Figure 2-13). Duration is 1180 seconds for Euro 3 and later vehicles (1220 seconds for previous), and the distance is 11 km. It consists of accelerations, steady speed, decelerations, and idling along with the two parts (in the EUDC there isn't idling) [97], [99]–[101].

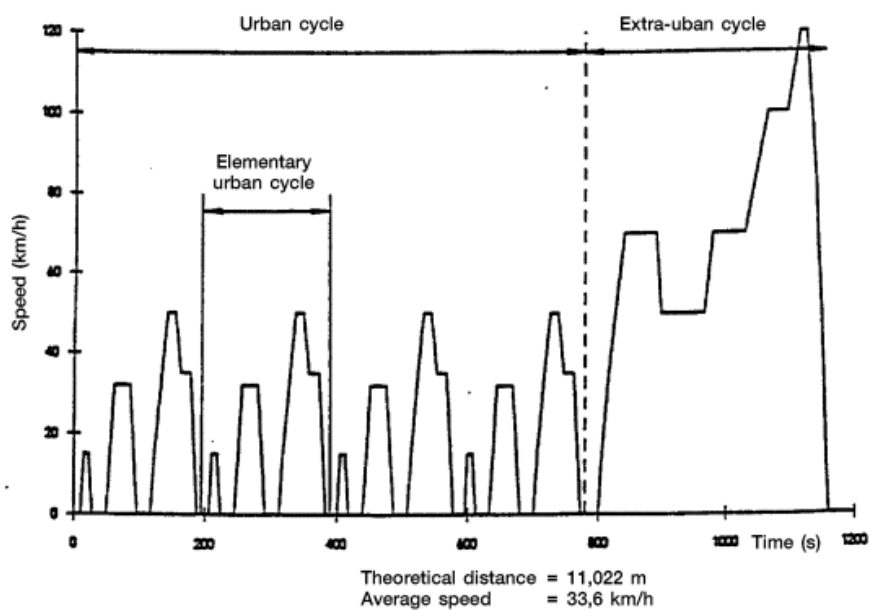


Figure 2-13. NEDC cycle. Source: UN/ECE. [102]

- b) WLTP (New Worldwide Harmonized Light Vehicles Test Procedure). It is based on UNECE GTR No. 15. It includes four parts (Low, Medium, High, and Extra High) (see Figure 2-14). The duration is 1,800 seconds, and the distance is 23.26 km. Like the NEDC, it consists of accelerations, steady speed, decelerations, and idling along with several parts. It was adopted in 2014 to replace the NEDC cycle [103]–[105].

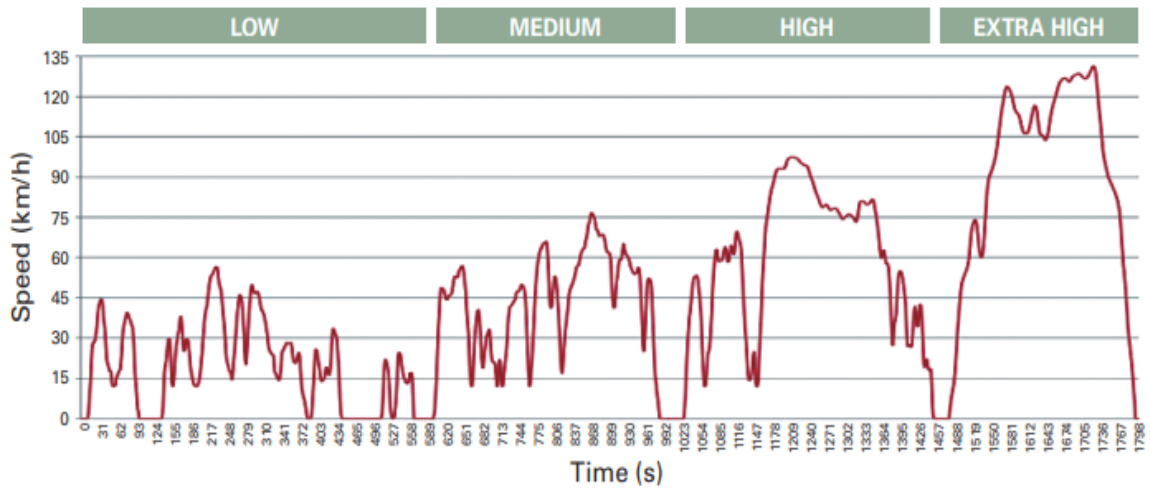


Figure 2-14. WLTP cycle. Source: Delphi.

- c) ERMES (European Research on Mobile Emission Sources) cycle is a real-world cycle that has been designed for emission modeling purposes, with a short duration (similar to NEDC) to increase schedule flexibility and reduce the cost of laboratory tests [106].

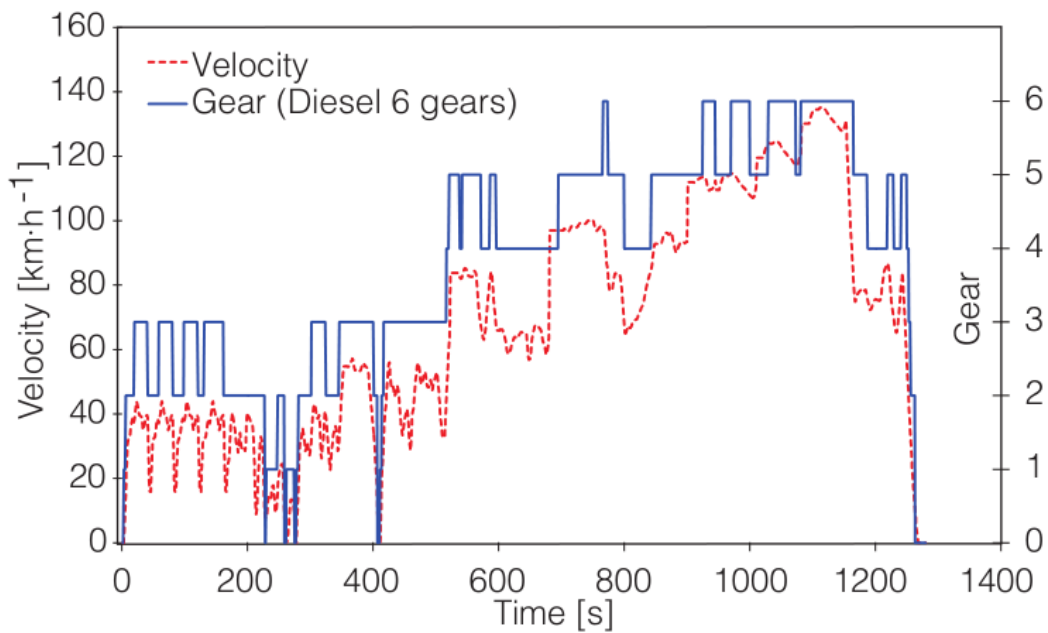


Figure 2-15. ERMES cycle. Source: Franco, V., 2014. [107]

- d) CADC (Common Artemis Driving Cycles) is a set of urban, rural, and motorway cycles (see Figure 2-16), with more dynamic characteristics than NEDC and WLTP cycles [108]. It is a result of the European ARTEMIS project.

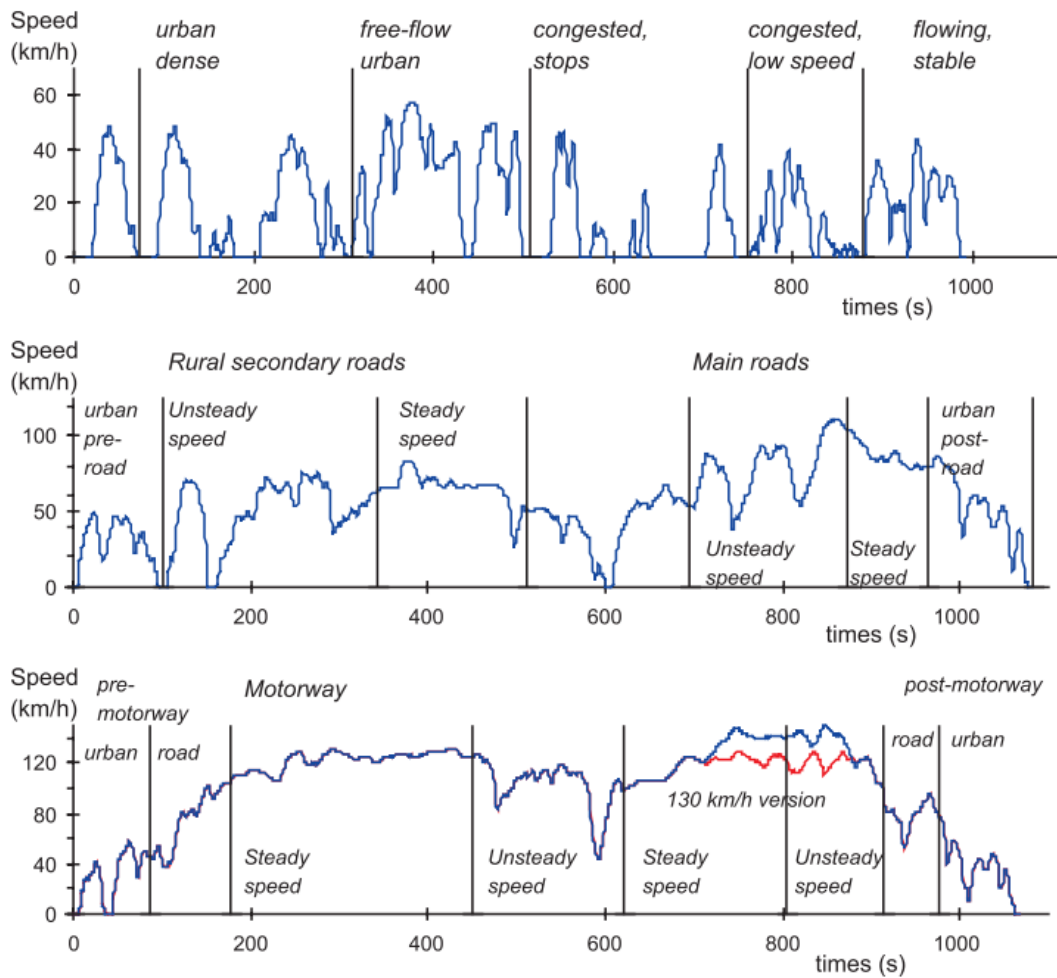


Figure 2-16. ARTEMIS urban, rural-road, and motorway driving cycles and their structure in typical driving conditions. Source: André et al., 2004. [108]

- e) KDC (Korean On-road Driving Cycle) is a combination of seven sub-cycles, considered similar to NEDC, but more representative and realistic as a driving pattern than NEDC [5].

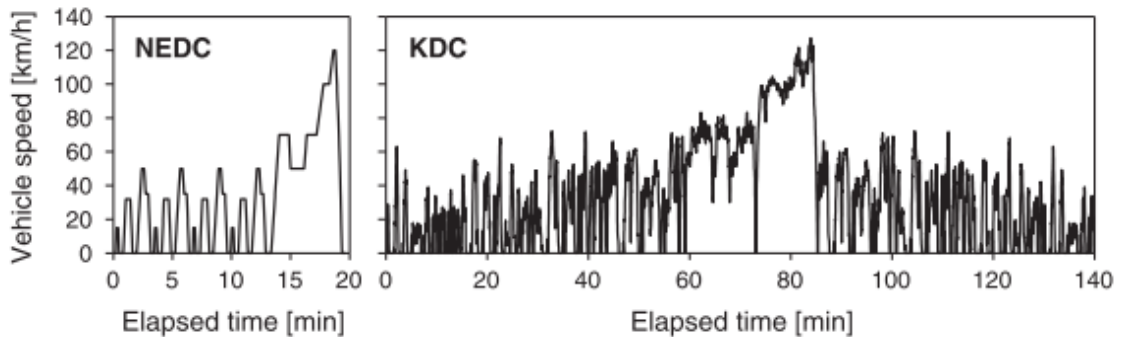


Figure 2-17. Comparison of the speed pattern of NEDC and KDC. Source: Lee et al., 2013. [5]

- f) BAB-cycle, or BAB-130 cycle, is a highway cycle for dynamometer tests developed by ADAC and part of the EcoTest car testing. It is performed with the A/C switch on, at highway speeds [109].

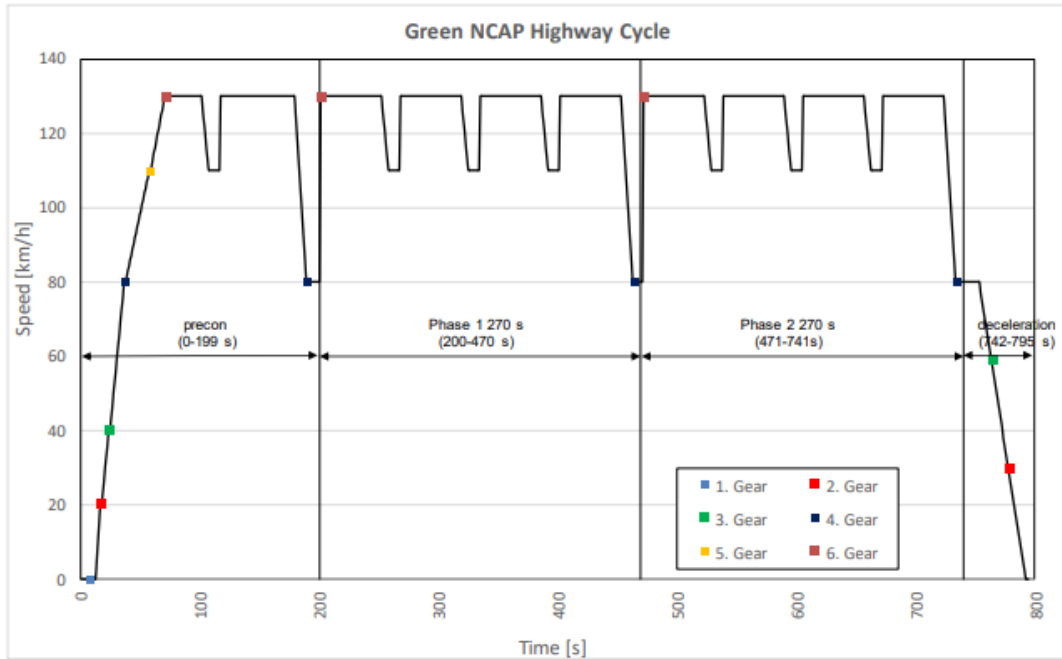


Figure 2-18. Green NCAP Highway Cycle (BAB cycle). Source: Green NCAP 2019. [109]

- g) The FTP-75 (or the variant FTP-72) is an urban circulation cycle used by the EPA in the USA as UDDS (Urban Dynamometer Driving Schedule).

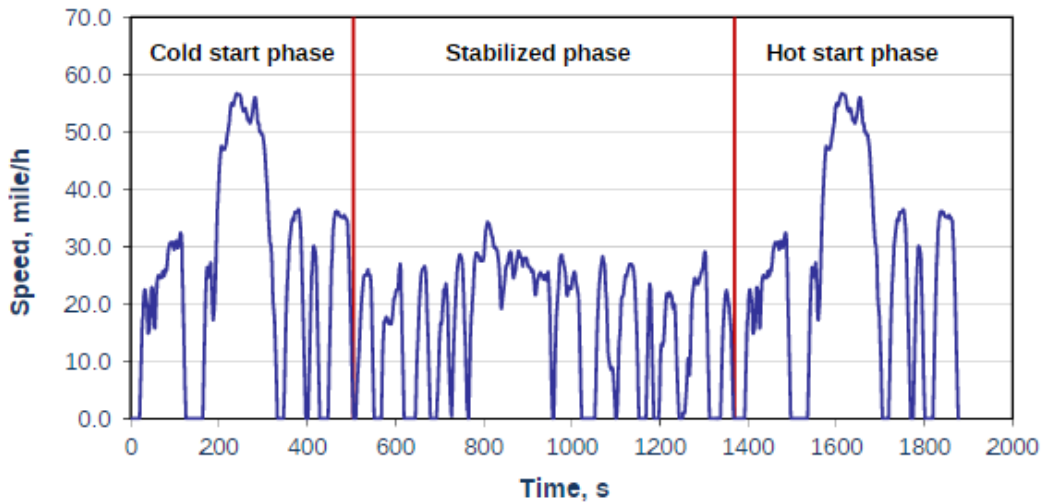


Figure 2-19. US FTP-75 Urban Dynamometer Driving Schedule. Source: dieselnet.com

Part of the EPA emission certification for vehicles, together with the HWFET cycle (Highway Fuel Economy Test), SFTP 06 (for aggressive and high-speed driving), and SFTP SC03 (use of air conditioning). The same cycle is used in

Australia with the name ADR 37 cycle (Australian Design Rules), and in Brazil is known as test standard NBR66015.

2.4.5. ON-ROAD TEST

- a) RDE (Real Driving Emissions) test with PEMS (Portable Emission Measurement System). Real emissions are measured from a vehicle with portable equipment while driving on a road with pre-defined characteristics [32]. The RDE is performed according to strict conditions. The PEMS is a complex system that reduces complete laboratory equipment to make it portable and to measure emissions while the vehicle is in real driving. So, the PEMS is capable of the acquisition of a great number of data when the vehicle is in circulation, both driving and emission data. Then, it could be a more precise system for determining the actual emissions of a specific vehicle during a specific trip, taking into account the particular environmental conditions and traffic situation at that time. However, this accuracy would only apply to that specific scenario and wouldn't necessarily reflect the vehicle's emissions in different circumstances. (see Figure 2-20). The equipment is expensive and time-consuming for preparation, maintenance, and performance. Because of that, the number of vehicles that can be tested is reduced [110].

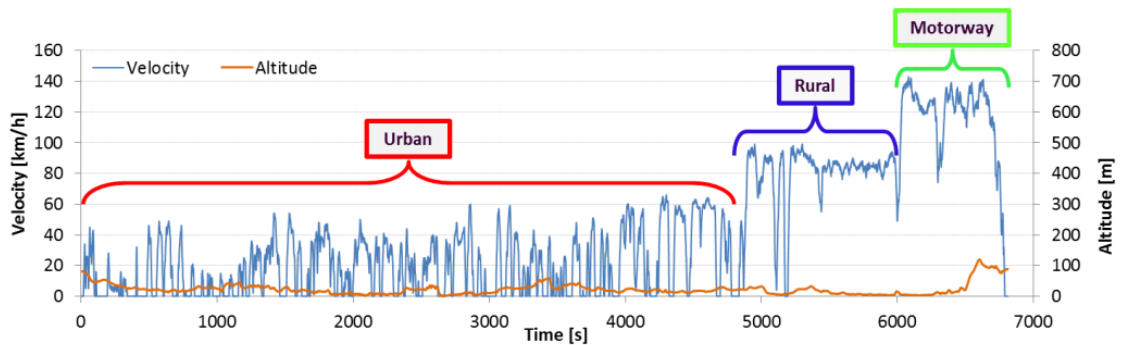


Figure 2-20. Sample of RDE with PEMS test. Source: EMISIA S.A. [111]

- b) A reduced version of the RDE test has been proposed for PTI with simpler components called miniPEMS. The test consists of measuring vehicle emissions driven over a short distance (inside the PTI station).

2.4.6. OTHER METHODS

- a) RSD (Remote Sensing Device). It is used to obtain a great number of measurements in a short time, in a fixed location in real driving conditions.

⁵ <https://www.transportpolicy.net/standard/us-light-duty-ftp-75/>

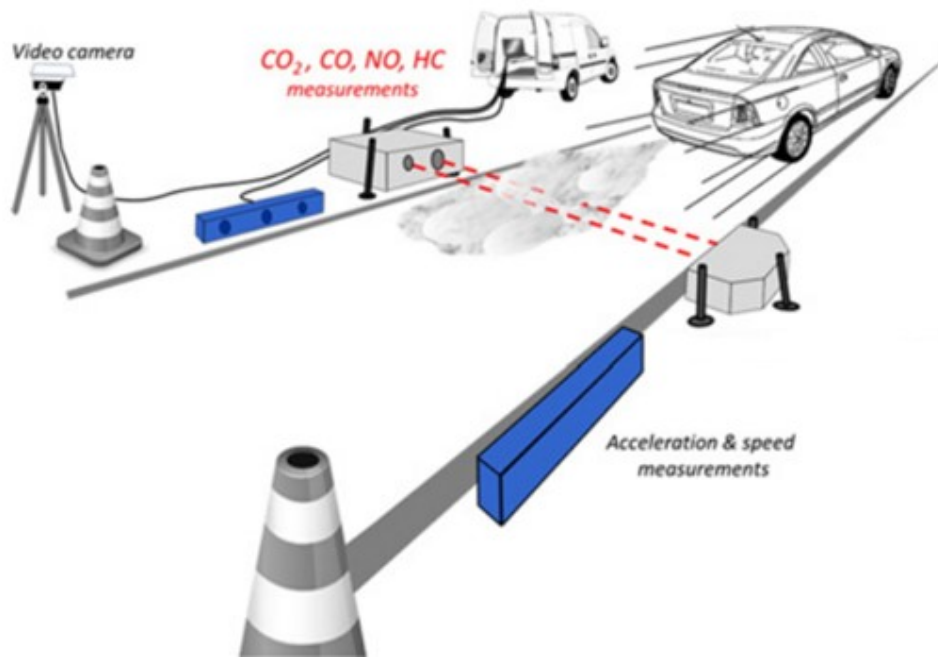


Figure 2-21. Setup for RSD on-road measurements. Source: Pujadas et al., 2016. [30]

It is a powerful tool to determine fleet emissions by location [30]. This concept has been proposed for PTI with an inspection called RSIS (Remote Sensing Inspection System).

- b) Plume Chasing is carried out from a vehicle driving behind the tested vehicle. This system is used for on-road monitoring of vehicle emissions (e.g., in several studies for the Færdselsstyrelsen in Denmark [112]–[114]).

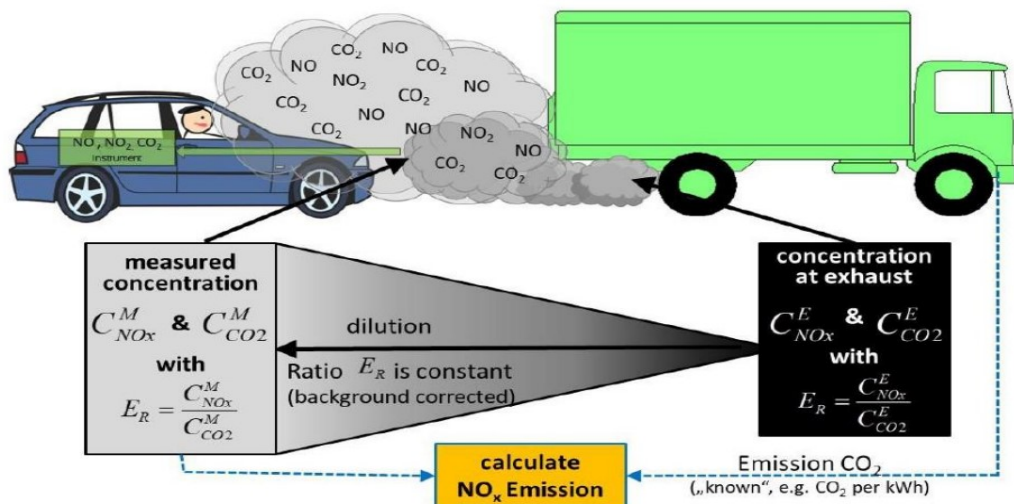


Figure 2-22. Plume chasing and NO_x emission calculation in the diluted plume. Source: AVL MTC Motortestcenter AB, 2020.[114]

2.5. NO_x MEASUREMENT STUDIES

The following are the main studies conducted on the measurement of NO_x, both focusing on NO_x measurement in PTI and those aimed at analyzing NO_x emissions in real-world vehicle circulation.

2.5.1. REAL-WORLD NO_x MEASUREMENTS

In addition to the previous studies that focused on NO_x measurement during PTI, numerous research projects and measurement campaigns have been conducted in recent years to evaluate current NO_x emissions from vehicles under real road conditions. A substantial amount of scientific publications on this topic exist, encompassing measurements carried out using various technologies and across different vehicle categories. While not an exhaustive list, here are some of the notable research studies categorized according to the technical solutions employed for NO_x measurement.

2.5.1.1. RSD MEASUREMENTS

RSD (Remote Sensing Device) measurement was first introduced in 1989 by studies conducted at the University of Denver [115], and it has played a significant role in identifying the NO_x problem in road transportation. This method involves placing measurement equipment at a fixed location (see Figure 2-21). The selection of the location is crucial and should align with the specific emission control objectives. Typically, areas, where vehicles operate under substantial loads, are chosen. This technique enables a large number of measurements to be collected, forming a comprehensive database for drawing conclusions. However, a key drawback is that the exact working conditions of the vehicles are unknown, with only speed and acceleration data available.

The equipment utilized for RSD measurements is founded on the principle of differential absorption spectroscopy. It is capable of detecting various pollutants such as CO, CO₂, NO_x, HC, and NH₃ in the exhaust plumes emitted by vehicles passing through the measurement point. The setup involves two light beams intersecting perpendicularly across the road, allowing for the measurement of exhaust plumes from vehicles as they pass through these beams of light. Complementary equipment measures the speed and acceleration of each vehicle, while a camera system captures the license plates for cross-referencing with the traffic database to retrieve technical information about each vehicle.

In this way, in 2004 an RSD measurement campaign was performed in Las Vegas (USA) as an approximation to NO_x control (and another pollutant) through RSD [116], [117].

The research conducted by Carlaw et al. using Remote Sensing Devices (RSD) revealed compelling evidence of diesel vehicles exceeding the approved limits for NO_x emissions [27], [118]–[120].

Also, the works of Chen et al. from 13 years of remote sensing data and later measurements pointed in the same direction [31], [66], [110].

Figure 2-23 shows one of the main conclusions from this research, diesel vehicles' NO_x emissions were higher than homologation thresholds, instead, gasoline vehicles show NO_x emissions reductions according to the threshold reduction.

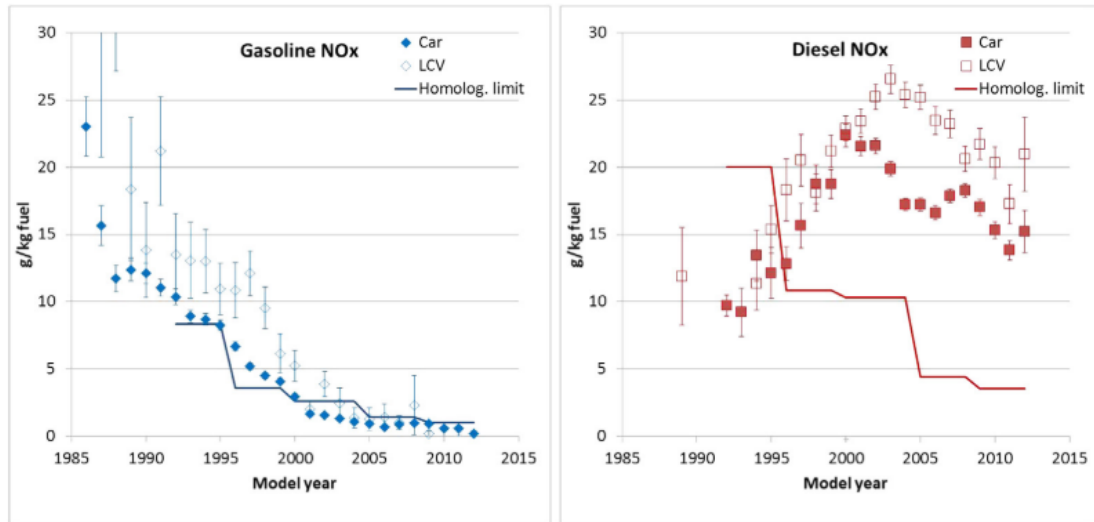


Figure 2-23. NO_x emission factors of gasoline (left) and diesel (right) passenger cars and light commercial vehicles (LCV). Source: Chen et al., 2014. [31]

In Spain, during 2014 and 2015 two field measurement campaigns were developed in Madrid, in the CORETRA project, with more than 190,000 vehicles tested. Pujadas et al. [30], came to similar conclusions about the evolution of NO_x emissions.

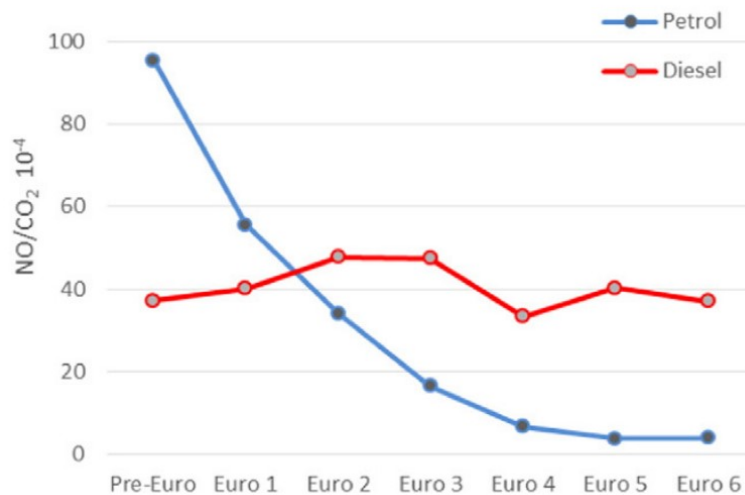


Figure 2-24. Average NO_x emissions from RSD CORETRA project. Source: Pujadas et al., 2017. [30]

RSD has been used in Europe since the 1990s, mainly in Sweden, Switzerland, and the UK, and lately also in Spain and France. Most of these measurements were performed for research purposes. Until 2017, about 750,000 records were obtained [121].

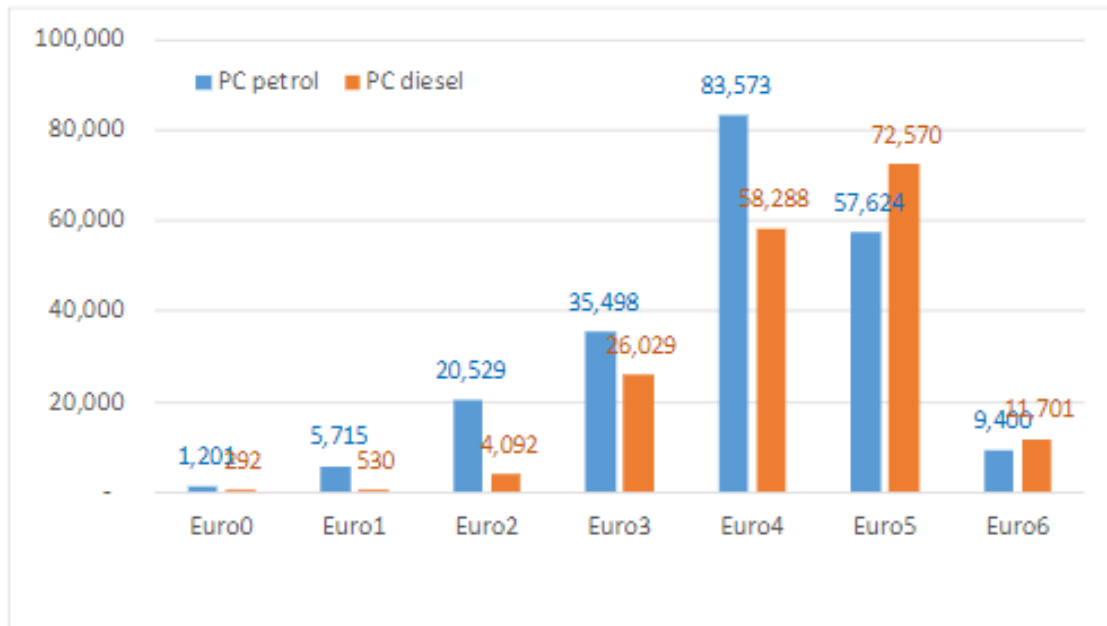


Figure 2-25. The number of RS records in the CONO_x database for petrol and diesel cars by Euro standard. Source: Borcken-Kleefeld et al., 2018.[121]

The CONO_x project serves as a coordinating body for remote sensing databases across Europe, enabling regular measurements to assess the long-term effectiveness of EATS (Emission Aftertreatment Systems) in diesel vehicles. It collects and analyzes data obtained from remote sensing campaigns conducted in Europe from 2011 to 2017 [121], [122]. This database encompasses a significant portion of the European vehicle fleet, including information on manufacturers, models, vehicle ages, Euro standards, and more. It provides comprehensive coverage of various driving and ambient conditions. At the inception of the database, it already contained the aforementioned 750,000 measurements, further enhancing its richness and representativeness.

In the last years, maybe the more relevant RSD campaigns were performed by the TRUE Initiative (The Real Urban Emissions), the FIA Foundations, and the ICCT (International Council on Clean Transportation). Important RSD measurement campaigns were developed in London, Paris, Brussels, and Krakow [123]–[127].

In these studies, the same behavior of fleet NO_x emissions can be observed:

- a) Lower emissions from petrol vehicles than from diesel vehicles.
- b) NO_x emissions from petrol vehicles are close to approval-type thresholds for Euro 6 vehicles.
- c) Decreasing NO_x emissions from Euro 2 to Euro 6 is related to the reduction of approval type thresholds for petrol vehicles (see Figure 2-23, Figure 2-26, Figure 2-27).

- d) NO_x emissions from diesel vehicles show much higher levels than homologation thresholds.
- e) NO_x reduction from diesel vehicles has been lower than the reduction from homologation thresholds (see Figure 2-23, Figure 2-26, Figure 2-27).
- f) In diesel vehicles, from Euro 4 to Euro 5 NO_x reduction is non-existent (see Figure 2-26) or, in some cases, even an increase can even be observed (see Figure 2-27, Figure 2-28, and Figure 2-29).
- g) Euro 6 shows a significant decrease in NO_x emissions for diesel vehicles. Reduction is even more remarkable for Euro 6 d-temp and newer (see Figure 2-28 and Figure 2-29).

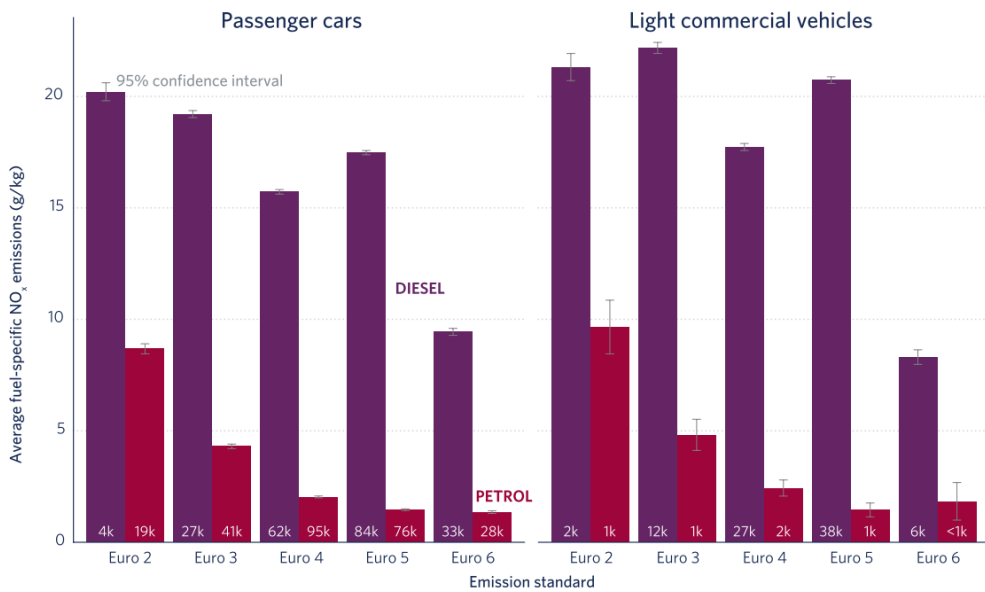


Figure 2-26. Results from RSD measurements in London. Source: TRUE, 2018. [124]

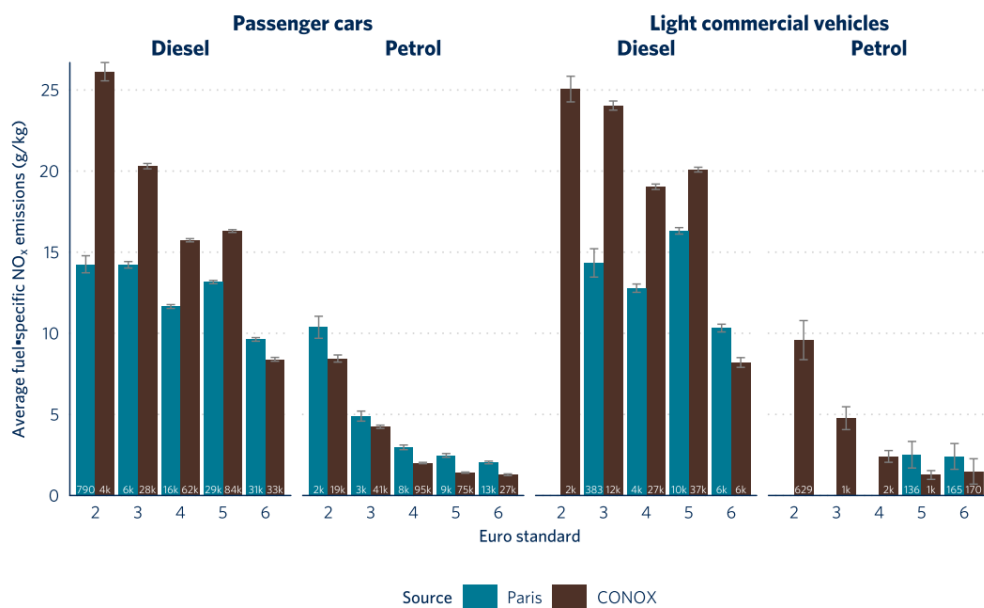


Figure 2-27. Results from RSD measurements in Paris. Source: TRUE, 2019.[123]

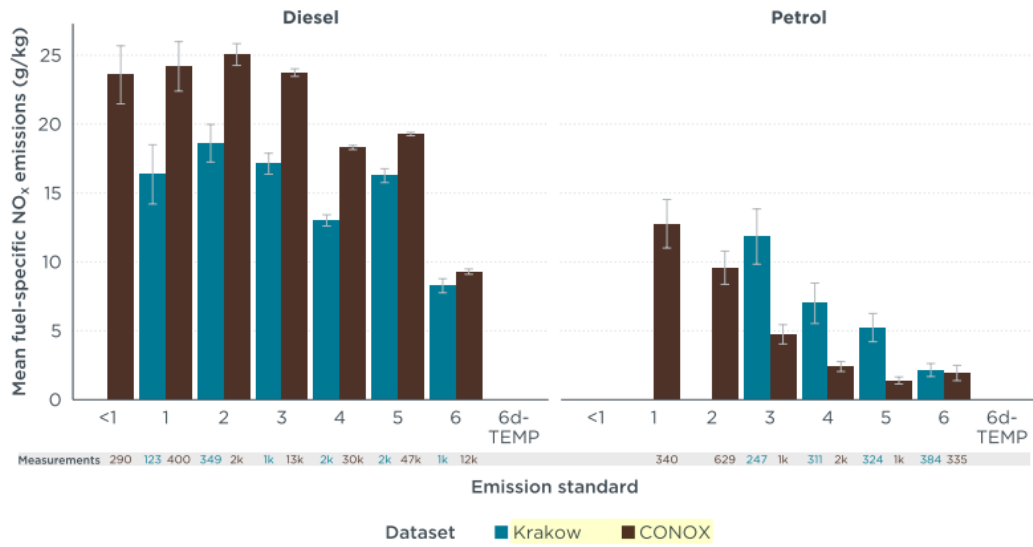


Figure 2-28. Results from RSD measurements in Krakow. Source: TRUE, 2020.[126]

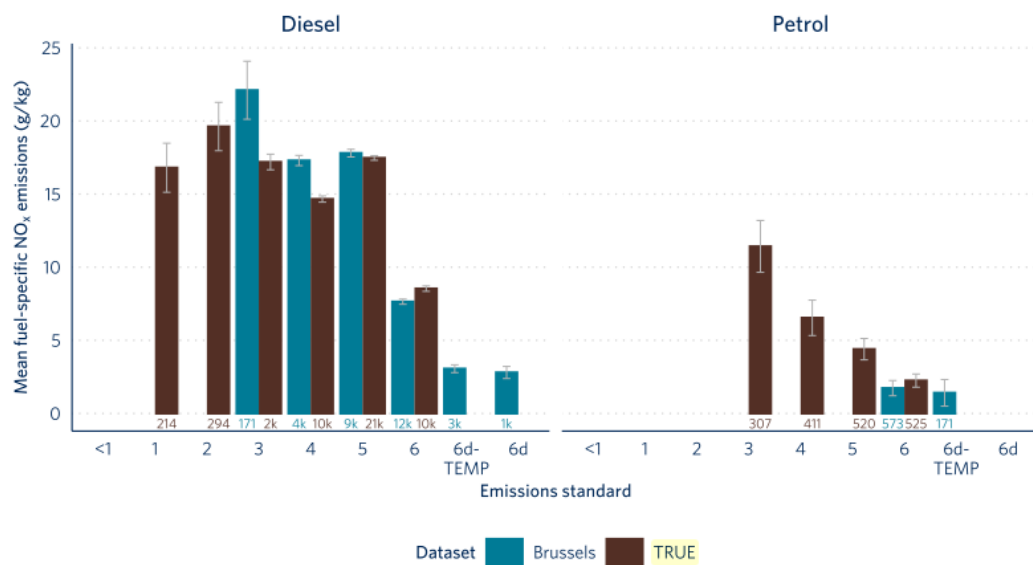


Figure 2-29. Results from RSD measurements in Brussels. Source: TRUE, 2021.[125]

2.5.1.2. PEMS MEASUREMENTS

PEMS (Portable Emissions Measurement Systems) measurements offer a significant advantage over other measurement techniques as they capture real-time emissions from vehicles while they are on the road, yielding detailed and valuable information.

However, conducting PEMS measurements is a resource-intensive process in terms of time, equipment, and personnel. Consequently, the number of vehicles that can be evaluated using this method is limited due to the demands associated with its implementation.

Moreover, PEMS measurements are highly sensitive to external factors such as driving style, environmental conditions, and trip design variables (including road type, traffic congestion, and road gradient). These factors, known as exogenous variables, can significantly impact the reproducibility of this measurement method. Thus, it becomes challenging to achieve consistent and comparable results across different testing scenarios due to the influence of these variables.

Despite the challenges mentioned, PEMS has been a widely employed technique in recent years to assess and evaluate the actual NO_x emissions of diverse vehicle types. It serves the purpose of examining whether the NO_x emission values obtained during the approval process are upheld in real-world usage. Additionally, PEMS enables the investigation of how variations in on-road conditions impact a vehicle's NO_x emissions, whether they increase or decrease. This technique provides valuable insights into the actual environmental performance of vehicles under real-world operating conditions.

Due to its ability to provide accurate information regarding real-world emissions, PEMS measurements have been integrated into the homologation process. This integration ensures that the emissions thresholds established during the approval phase are met in actual on-road conditions. For a comprehensive understanding of the implementation of PEMS in regulations, including a detailed chronology, reference can be made to the work of Hooftman et al., 2018 [128].

Parameter	Requirements Regulation (EU) 2016/427/EC	
Altitude	Moderate: 0 to 700 m < 100 m altitude difference between start and finish The cumulative elevation gain is limited to 1200 m/100 km ^a	(Extended: 700 to 1300 m)
Ambient temp.	Moderate: 0°C to 30°C	(Extended: -7°C-0°C and 30°C-35°C)
Dynamics^a	Max: 95th percentile of v*a (speed*positive acceleration)	Min: RPA (relative positive acceleration)
Maximum speed	145 km/h (160 km/h for 3% of the motorway driving time)	
Payload	Maximum 90% of the maximum vehicle weight (driver + equipment)	
Stop percentage	Between 6% and 30% of the urban driving time	
Use of auxiliary systems	Operated as in real life (air conditioning etc.), not to be recorded	

^aAdded through the 2nd RDE package.

Table 2-1. RDE boundary conditions from Regulation (EU) 2016/427/EC. Source: Hooftman et al., 2018. [128]

PEMS used for on-road testing have also been implemented for trucks since 2003 in the USA. One year later the use of PEMS for HDV (Heavy-Duty Vehicles) began in the EU through Regulation 595/2009.

The incorporation of PEMS technology in Light-Duty Vehicles (LDVs) took some time to be implemented, primarily due to technical and economic considerations. However, efforts to develop a PEMS measurement system had already started in 2004, as described in a project undertaken by the Joint Research Centre (JRC) [129]. This project outlined the existing technical landscape and identified the necessary areas of development for PEMS technology to be effectively utilized in LDV emissions measurement.

In a publication by the Joint Research Centre (JRC) in 2011, PEMS measurements revealed substantial disparities between Euro emission standards and real-world emissions [130]. This finding was subsequently supported by several studies conducted in both the European Union (EU) and the United States. Notably, one of these studies [40] provided the evidence that triggered the infamous "Dieselgate" scandal, exposing widespread discrepancies between laboratory emission tests and actual on-road emissions of diesel vehicles.

Trip Characteristics		Requirements Regulation (EU) 2016/427/EC
Average Speeds	Urban	15 km/h to 40 km/h
	Rural	60 km/h to 90 km/h
	Motorway	> 90 km/h
Distance	Urban	> 16 km
	Rural	> 16 km
	Motorway	> 16 km
Trip Composition	Urban	29% to 44% of the total distance
	Rural	23% to 43% of the total distance
	Motorway	23% to 43% of the total distance
Total Trip Duration		90 to 120 min

Table 2-2. Specification of the RDE trip concerning speed and driving distance from Regulation (EU) 2016/427/EC. Source: Hooftman et al., 2018. [128]

In China, the implementation of PEMS for controlling NO_x emissions from Heavy-Duty Vehicles (HDVs) dates back to 2009. Several test programs have been conducted to develop an inventory of emission sources, particularly in urban driving environments [131]. Starting from Euro II standards, diesel HDVs have been evaluated using PEMS due to their significant contribution to overall vehicle emissions [132]. PEMS measurements have not been limited to diesel vehicles alone but have also been employed to assess NO_x emissions from diesel hybrid, compressed natural gas (CNG),

and liquefied natural gas (LNG) vehicles [133]. These measurements have helped analyze the impact of various operating conditions, such as traffic congestion, speed, and air conditioning usage, on NO_x emissions.

Finally, in the EU, PEMS measurements have been included in the approval type process from September 2017 and Euro 6 vehicles as a complementary test to control NO_x and other pollutants emissions. The first regulation about RDE measurement with PEMS was established with Regulation (EU) 2016/427 [134]. From this European Regulation, the main conditions and boundaries of the RDE test were fixed, the most important indicated in Table 2-1 and Table 2-2.

Apart from the use of RDE in the homologation process, PEMS has been frequently used in scientific research, to analyze different aspects of pollutant emissions. One prominent application is the calculation of Emission Factors (EF) using PEMS data, which is crucial for emission modeling studies [135]. By analyzing the emissions captured by PEMS during real-world driving, researchers can derive EF values that contribute to a better understanding of pollutant emissions and facilitate more accurate emission modeling.

To assess the disparities between test results obtained during approval-type chassis dynamometer tests and real-world on-road emissions, numerous studies have compared measurements from the same vehicles using both chassis dynamometer tests and PEMS. One noteworthy example is the meta-analysis conducted by the International Council on Clean Transportation (ICCT) that examined European diesel vehicles (Euro 6) and US diesel vehicles (TIER 2 BIN 5/ULEV II) using PEMS measurements [38]. This study confirmed the NO_x discrepancy revealed by remote sensing device (RSD) measurements, indicating that average NO_x emissions under real-world conditions exceeded the homologation thresholds by a significant margin. These findings underscore the need to address the issue of higher-than-expected NO_x emissions in real-world driving situations.

As mentioned earlier, the primary advantage of PEMS measurements is their ability to directly measure and record real NO_x emissions from vehicles in actual on-road conditions. However, a drawback of this method is the substantial resources required in terms of equipment and time, which limits the number of vehicles that can be analyzed. For instance, in the current study, a total of 15 vehicles were analyzed. Similar conclusions were reached by TNO in the Netherlands, where they analyzed over 16 vehicles, highlighting the limited scope of analysis due to the resource-intensive nature of PEMS measurements [136].

In a comprehensive analysis conducted in 2017 involving a substantial sample size of over 149 vehicles, it was observed that there was a reduction in NO_x emissions from Euro 5 to Euro 6 vehicles. However, it was found that there was no uniform relationship between engine size and NO_x emissions [7]. The significant variation in real-world NO_x emissions among vehicles complying with the same Euro emission standard highlights the ineffectiveness of type approval in standardizing vehicle fleet emissions or reducing NO_x emissions in urban conditions. In fact, the study revealed that real-world urban NO_x emissions were as high as 450% above the Euro standard limits, indicating the urgent need for further measures to curb NO_x emissions. Authors indicate that the **Euro standards are not adequate to discriminate against vehicles because arbitrary, and a better option will be a real measure of emissions.**

Recent studies utilizing this methodology have been conducted on modern diesel vehicles, yielding consistent findings. While the WLTP cycle results are closer to real-world on-road emissions compared to the previous NEDC, it is the RDE test that serves as a significant improvement in bridging the gap between approval-type limits and actual emissions [33]. However, even with the CF (Conformity Factor)⁶ of 2.1, which allows for a certain margin of compliance, the **majority of vehicles surpassed this threshold on RDE-compliant routes**, emphasizing the influence of driving style on emissions outcomes [111]. In contrast, **gasoline vehicles tend to meet the approval-type thresholds within RDE-compliant routes**.

PEMS analysis also allows for the examination of various factors that influence NO_x emissions. One significant variable is driving style, which has a notable impact on NO_x emissions. For instance, a PEMS measurement conducted in 2010 investigated the influence of different driving styles on pollutant emissions and found that aggressive driving significantly increases NO_x emissions [137]. Another study conducted in 2012 examined the effect of vehicle speed on NO_x emissions [138]. More recent research using PEMS measurements has explored how driving style and road gradient can affect NO_x emissions [139]. These studies revealed that a severe driving style can lead to a staggering 255% increase in NO_x emissions, and an increase in road gradient from 0% to 5% can result in a 115% rise in NO_x emissions. These findings highlight the importance of considering driving behavior and road conditions when assessing and addressing NO_x emissions.

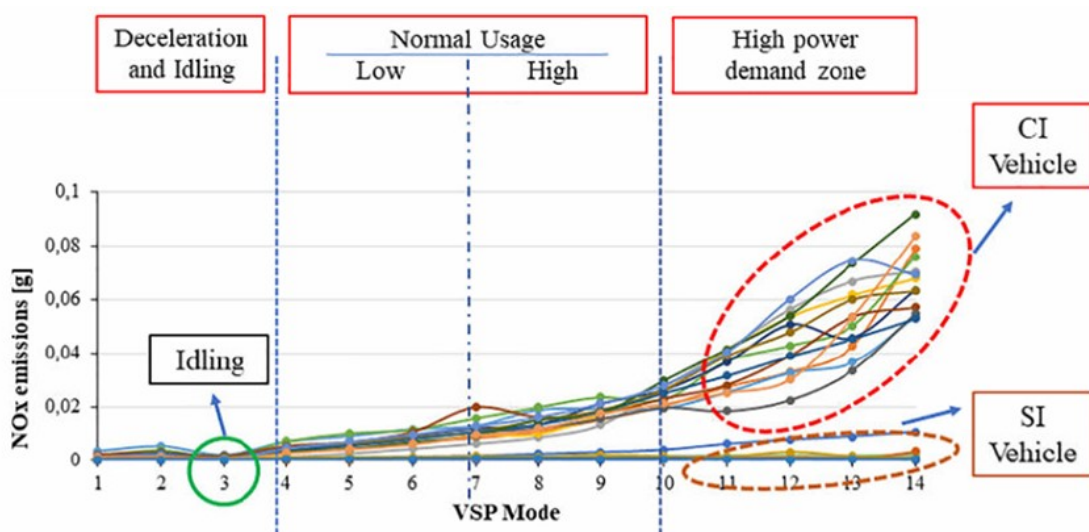


Figure 2-30. NO_x emissions [g] in the function of Vehicle Specific Power. Source: Varella et al., 2019. [140]

Ambient temperature, cold starts, and cold operation are additional factors that significantly impact NO_x emissions, resulting in an average increase of 55%. PEMS measurements have been instrumental in confirming this observation [140]. Moreover, it has been established that diesel vehicles emit significantly higher levels of NO_x

⁶ CF is a NTE (Not To Exceed) value proportional to increase the approval type threshold to be used for the RDE test. From January 2021 this value is reduced to 1.5.

compared to gasoline vehicles, and this difference becomes more pronounced as the engine's power demand increases.

In recent years, numerous studies employing PEMS measurements have examined the evolution of NO_x emissions from diesel vehicles in response to increasingly stringent emission regulations and the implementation of new emission after-treatment systems (EATS) in newly manufactured vehicles. These studies have provided valuable insights into the effectiveness of these technologies in reducing NO_x emissions.

Furthermore, studies have demonstrated that urban traffic conditions contribute significantly to the accumulation of NO_x emissions (see Figure 2-31), even for comparable distances traveled [141]. The combination of low speeds and frequent positive relative accelerations, which increase the power demand on the engine, has been identified as a key factor in elevating NO_x emissions levels.

PEMS-based NO_x measurements have also provided insights into the significance of Emission Aftertreatment Systems (EATS) behavior in reducing NO_x emissions, often surpassing the importance of the specific type of EATS employed. An example of this is seen in a software update to the Engine Control Unit (ECU) of a Euro 6b vehicle, which resulted in a threefold reduction in the average NO_x concentration emitted by the vehicle [142]. These emissions were even lower than those of a Euro 6 d-temp vehicle. This finding raises concerns since only manufacturers possess detailed knowledge of the EATS behavior through ECU programming.

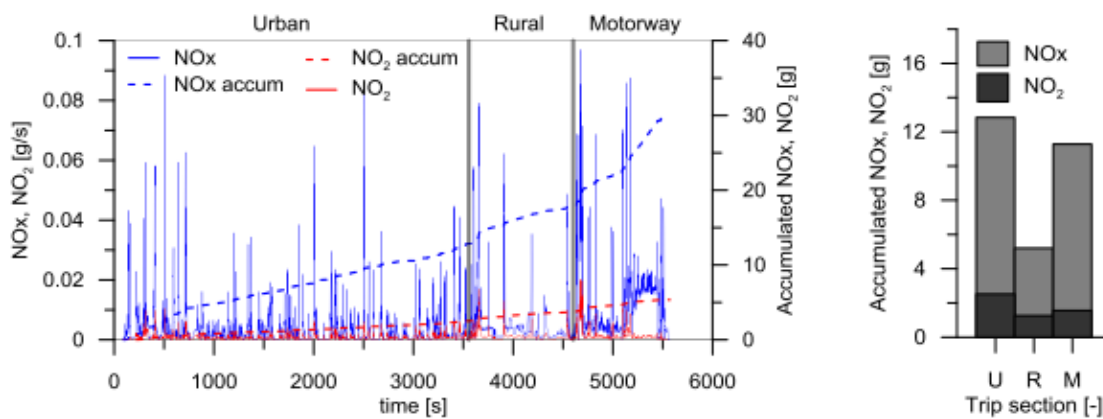


Figure 2-31. Accumulated NO_x emissions from PEMS measurement with Urban, Rural, and Motorway emissions. Source: Luján et al. 2018. [141]

To address this issue, one proposed measure for future regulations in the automotive sector is for manufacturers to share more technical data on vehicle operations with vehicle control systems. This would enable more effective control measures, such as those implemented during PTI, to detect malfunctions and tampering with anti-pollution systems.

PEMS measurements have revealed a significant finding regarding the accumulated instantaneous peaks of NO_x emissions. It has been observed that these peaks

contribute to approximately 80% of the total accumulated NO_x emissions, despite occurring within only 20% of the total travel time [143]. These instantaneous peaks are brief events characterized by high concentrations of NO_x emissions. This finding holds crucial implications for the forthcoming proposal, as it highlights the importance of addressing these short-duration, high-concentration emission events to effectively mitigate overall NO_x emissions.

The use of PEMS equipment allows for a detailed understanding of the actual emissions behavior under the exact driving conditions of the vehicle. Due to the high precision and accuracy of the results provided by these devices, and the representativeness of the measurements taken under real driving conditions, the findings obtained from these types of studies are highly reliable for the assessment of knowledge about vehicle emissions.

2.5.2. NO_x MEASUREMENT AT PTI

Over the last years, several studies have been conducted trying to define a NO_x measurement method applicable to PTI. Among these studies, the ones carried out by CITA (International Motor Vehicle Inspection Committee) are particularly significant. CITA has extensively examined and compared various emission control solutions, specifically focusing on NO_x emissions. Notably, the most relevant studies related to pollutant emissions conducted by CITA include TEDDIE, SET, and SET II.

In the TEDDIE (TEst(D)DIesel) project [88], performed in 2011, several types of equipment and procedures designed for NO_x and PM measurement were analyzed. The study's findings indicate that NDUV (Non-Dispersive Ultraviolet) equipment was technically viable for NO_x measurement during PTI. However, due to cost considerations, it was not selected as the preferred option. On the other hand, electrochemical cells showed potential to meet PTI requirements, but further refinement is necessary to enhance their capabilities. Regarding procedures, the study primarily focused on reviewing the existing tests used during the project, without proposing a specific method for implementation in PTI.

The SET (Sustainable Emission Test) study [60], performed in 2015, focused on exhaust emission measurement rather than specifically targeting NO_x control. However, the study recommended the incorporation of mandatory exhaust emission measurement, along with data retrieval through the vehicle's On-Board Diagnostics (OBD) system. It also emphasized the need for further research to determine cost-effective methods for NO_x measurement during PTI, as well as the establishment of NO_x emission limits for PTI control. Furthermore, the study highlighted the significant benefit-cost ratio associated with controlling pollutant emissions during PTI.

SET II study (Sustainable Emission Test) [61], [62], was performed in 2019. The study examined various NO_x measurement methods, both with and without load simulation. It was concluded that test methods incorporating load simulation have a higher potential for detecting vehicle failures and tampering compared to methods without load simulation. The study emphasized the importance of conditioning the vehicle to ensure optimal working temperatures for selective catalytic reduction (SCR) and lean

NO_x trap (LNT) systems. However, it was noted that the exact working conditions during the test, as well as before and after the test, are unknown.

In summary, the study emphasized the importance of obtaining specific technical information from the vehicle manufacturer to ensure accurate NO_x measurements. This information is crucial for properly preconditioning the vehicle before testing. Additionally, the study concluded that loaded tests, which simulate real-world driving conditions, provide more meaningful results compared to unloaded tests.

Despite extensive research, the study did not identify a specific method as the most suitable for NO_x measurement during PTI, highlighting the complexity of the task. Further testing is necessary to gain confidence in the study's results.

An important finding from the study was the Cost-Benefit Analysis (CBA), which demonstrated that regardless of the method employed for NO_x measurement, consistently favourable cost-benefit ratios were obtained. This underscores the justification for implementing effective NO_x measurement methods during PTI, as the benefits outweigh the associated costs.

Finally, the study concludes that *"it seems appropriate to combine the loaded ASM2050 method with the unloaded test method for EGR assessment and OBD readout for better evaluation"* [61].

So, after nine years and the completion of three important studies, the main conclusion was the pressing need to establish a method for measuring NO_x emissions at PTI. The Cost-Benefit Analysis consistently showed excellent ratios, reinforcing the importance of implementing such a method. However, **there is currently no clear candidate for the method to be used.**

In addition to these studies, other agencies and institutions have also developed studies and proposed solutions, trying to define methods for NO_x measurement in PTI.

In this way, from the Vienna University of Technology, there is a proposal for a short test for NO_x and PN to perform at PTI with load creation by constant idle speeds [144].

The VERT (Verification of Emission Reduction Technologies) Association has proposed a new PTI including NO_x and PN measurement [145]. For the NO_x measurement, the use of a power bench is proposed.

Applying a different approach, ÖAMTC has proposed the measurement of NO_x through the Q_{NO_x} ratio [146]. The Q_{NO_x} is the ratio between CO₂ and NO_x emissions, reading NO_x emissions through the OBD from the vehicle's onboard NO_x sensors, and calculating CO₂ emissions from the fuel consumption. This method can only be applied to new vehicles with NO_x sensors, and need access to this data from the vehicle, which is currently inaccessible.

In 2019, the VdTÜV performed a study commissioned by the Umweltbundesamt (German Environmental Agency), to analyze three procedures of NO_x measurement: ASM2050, On-Road test with mini-PEMS, and CAPELEC unloaded test. On one hand, the findings suggest that NO_x measurements should be carried out when the vehicle is under load, either through roller bench testing or on-road tests. However, it doesn't explicitly specify a specific method to be used, and it is noted that further studies are required to establish the procedure statistically [147]. On the other side, the most

relevant conclusion of the study was the CBA performed, which shows an excellent ratio (greater than 3 in the worst scenario), again justifying the need and usefulness of implementing NO_x measurement in the periodic inspection.

Also, in Germany, DEKRA has performed some research comparing several NO_x measurement methods and their ability to detect tampering in vehicles. Methods analyzed were a short on-road test called "2-stage driving ramp" (20 m trip from 0 km/h to 20 km/h), an unloaded test called "rotation speed-pump method" (5 accelerations at increasing engine speed), and a roller bench method ASM2050. From the comparison, the unloaded test gets better-pondered results.

The most recent studies, with a high interest in the topic, are being developed in France, Belgium, and Spain. The French study has not published any results yet, but Belgian and Spanish studies have been recently published.

In France, UTAC-CERAM is performing a study about NO_x measurements with a power bench [148].

In Belgium, GOCA Vlaanderen has performed a study comparing several methods of NO_x measurement for PTI (including this proposal) [149], proposing the measurement of the ratio between NO_x emissions and CO₂ emissions as the optimal option.

In Spain, Carlos III University has performed a study comparing several methods of NO_x and PN measurement for PTI (including this proposal) [150], also proposing a static method for measuring NO_x.

JRC is researching a measurement method for Euro 6 temp-d and newer diesel vehicles, consisting on measure NO_x emissions at idling after a period of driving the vehicle [151].

The most recent research conducted before the completion of this thesis has been carried out by the company 3DATX. Their study suggests the use of their PEMS equipment (3DATX parSYNC) to measure NO_x during PTI. The proposed method involves measuring various phases, including idling and accelerated speed, and even measuring emissions while the vehicle is in motion [152].

2.6. CONCLUSIONS

Throughout this chapter, it has been evident that there is abundant literature and experimentation focused on measuring NO_x emissions from diesel vehicles. Even the measurement of NO_x emissions in PTI (Portable Emissions Testing) has been analyzed in recent years.

Various measurement methods, some simple and quick, others more extensive and complex, are used to measure NO_x in various settings, ranging from measurements under real driving conditions to laboratory measurements.

However, to date, there is no widely adopted method for measuring NO_x in PTI.

As a summary and main conclusions of this chapter, the following can be highlighted:

- Engine NO_x generation is related to engine power demand through temperature in the combustion chamber, increasing NO_x emissions when engine load demand increases.
- The engine load demand can be easily determined through the "% engine load" parameter, which is measured through the vehicle's OBD system.
- There is a wide range of methods available to measure vehicle NO_x emissions, utilizing various procedures to generate engine load and focusing on measurement in different contexts (certification, research, etc.).
- Over the past years, several studies and analyses have been conducted on the existing methods and technologies to determine the most suitable way to measure NO_x in PTI
- There is currently no widespread and widely used method for measuring NO_x in PTI.
- Measurements and emission studies of NO_x from the vehicle fleet have been carried out using various methods and equipment, confirming the existing issue with NO_x emissions in diesel vehicles.
- The most suitable technology for measuring NO_x in PTI (Portable Emissions Testing) is electrochemical sensor-based technology.

CHAPTER 3

TEST REQUIREMENTS FOR NO_x MEASUREMENT IN PTI

3. TEST REQUIREMENTS FOR NO_x MEASUREMENT IN PTI

3.1. INTRODUCTION

The earlier sections have provided an explanation of the ongoing issue concerning NO_x emissions from diesel vehicles, along with the suggestion that implementing a measurement test during the PTI could serve as a valuable tool in mitigating the impact of these emissions.

This test would enable the detection of vehicles with higher emissions and offer insights into the emission patterns of the entire vehicle fleet.

The techniques and methods currently available for measuring NO_x in PTI have also been described. As explained, there is currently no widely selected method for conducting such measurements due to the complexities involved, and the existing methods have not been able to address these challenges.

In this chapter, the requirements and premises that a NO_x measurement method must meet to be effectively applied in PTI will be explained. PTI is a very specific activity, and both the equipment and inspection methods to be used must be perfectly adapted to their application in PTI.

Subsequently, a brief introduction to the proposed measurement method will be provided, outlining the technical foundations of the method without going into details, which will be explained and analyzed in later sections. Of course, the proposed method will meet the requirements set forth for its application in PTI.

Finally, the main features of the proposed method will be described, which make it suitable for the intended purpose and enable its practical application for controlling NO_x emissions from diesel vehicles in PTI.

3.2. PREMISES DESIGNING A NO_x EMISSIONS TEST FOR PTI

A test for PTI presents significant differences and particularities concerning emission tests oriented to other objectives (laboratory measurements, test for approval type homologation, control of pollution at a fixed location, ...).

In the first place, when developing a new test for PTI, it is essential to ensure compliance with inspection standards and requirements. According to the PTI directive [56], "*testing during the life cycle of a vehicle should be relatively simple, quick, and inexpensive, while at the same time effective in achieving the objectives of this Directive*". Likewise, the regulations of European countries (e.g., Spanish regulations [57], [58]) establish requirements in the same sense: "Testing should be as simple and direct as possible, and the inspection should be possible in a limited time".

Certainly, there are additional requirements that overlap with other types of tests, such as accuracy, sensitivity, precision, significance, and reproducibility, albeit to varying degrees. However, simplicity holds significant importance, as the PTI test primarily

aims to address a fundamental question effortlessly: "Is the vehicle in roadworthy condition or should it be rejected?"

The simplicity of the PTI test offers significant benefits. Firstly, it enables quick inspections, allowing a large number of vehicles to be assessed efficiently. Secondly, it minimizes the likelihood of errors during the execution of the test.

According to Eurostat data, in 2019 there were in EU-28 more than 111 million diesel passenger cars and more than 268 million passenger cars of any fuel type, with more than 15 million new registrations of passenger cars in 2018 according to ACEA (European Automobile Manufacturers Association) data. Based on this data, it can be inferred that the PTI test needs to be conducted over a hundred million times annually in the EU. This is in contrast to Approval Type homologation tests, which may be carried out only a few hundred times per year. Therefore, the attributes of simplicity and quickness are crucial for the PTI test.

Another advantage of simplicity is its impact on staff and equipment requirements. A simple test typically necessitates less complex and more affordable equipment compared to a more intricate test. Additionally, it does not demand highly qualified staff to conduct the tests.

This advantage of the simplicity of the test can be really important on some occasions. For example, in the situation of the COVID-19 pandemic, PTI procedures in Spain have been exceptionally modified [3] to allow vehicle inspection while the vehicle driver and PTI inspector are protected from infection. The PTI worker could not get access to the inner of the vehicle, and the driver had to personally carry out, under the supervision of the PTI worker some of the tests that are usually performed by PTI staff. In this way, the emission test and the brake efficiency test were performed by the vehicle driver. If these tests were complicated and hard to carry out, they couldn't be performed by the owner of the vehicle. Therefore, the simplicity of the test enables it to be implemented even in challenging circumstances, providing a viable solution for exceptional situations. Despite the difficult conditions, the PTI test can still be conducted effectively.

Another condition that must be ensured during the PTI test is safety: vehicle inspection can't be a risk for people or vehicle integrity.

By employing a simple test that involves minimal manipulations of the vehicle, the probability of errors during the test decreases significantly. Moreover, the likelihood of mechanical failures, safety incidents during the inspection, and the severity of consequences in the event of an accident are also reduced.

Instead, complex test procedures that involve a high number of manipulations over the vehicle or even manipulation of the vehicle under driving conditions (such as a power bench test at 20 km/h or even 50 km/h) have a higher probability of errors, mechanical failures and accidents compared to a static test. Furthermore, the severity of consequences in the event of such occurrences is significantly greater.

Despite the initial low probability of accidents, the sheer volume of tests that need to be conducted (over 275 million tests annually in the EU when including gasoline vehicles) means that even a slight increase in the risk of accidents during the testing process could eventually elevate the overall likelihood of occurrence. Moreover, the

severity of consequences in the event of an accident is notably higher when a significant number of vehicle manipulations are involved. For these reasons, simplicity is an important attribute to promoting safety in vehicle inspection.

Certainly, while ensuring simplicity, it is important to maintain a balance with the other defining characteristics of measurement. However, simplicity should be a key consideration when designing the PTI test.

It is more important to design a simple test than one that has greater accuracy or sensitivity. The cost in resources of complicating the procedure and/or using equipment that significantly increases the time, preparation, safety risks, and/or cost of the inspection would make the test meaningless.

Fitness for purpose implies that the quality of the measurement carried out is adequate so that, taking into account the needs of each sector, correct decisions can be made based on the test results. That means, fitness for purpose does not necessarily represent the best quality that test methods can give, since this approach could involve unnecessary expense or time for measuring (e.g., if the bias and precision are too small, the results may lack practical utility or significance) [153].

Maintaining a balance between these variables is indeed a complex task. However, it is crucial to remember that the purpose of the PTI test is not to replace Service Conformity testing. Rather, its objective is to monitor the operational and maintenance conditions of the entire vehicle fleet throughout its lifecycle.

If we had to define in a few sentences what PTI is and is not, they could be:

- PTI is not a Type-Approval procedure
- PTI is not a Conformity of Production assessment
- PTI is not a calibration
- PTI has to identify defective or worn-out parts
- PTI should be effective, relatively simple, quick, and inexpensive

To summarize, when designing a NO_x PTI test the main target must be to focus on guaranteeing simplicity and accomplishing regulation requirements.

Additionally, when designing a measurement procedure, it is important to know the process to be measured (in this case the NO_x emissions of the vehicle) and to analyze which variables or parameters can impact these emissions, thereby affecting the measurement results.

Existing methods for NO_x measurement, as described in section 2.4, tried to simulate in different ways the on-road conditions in vehicles to relate test results with real emissions. Yet these methods face a problem that is difficult to solve.

The engine NO_x generation mainly depends on O₂ concentration and temperature in the combustion chamber [2], [67], [68]. But a vehicle is a complex combination of interacting systems regulated by the ECU (Engine Control Unit), and the real on-road NO_x emission from the vehicle at the exhaust pipe depends on a large number of variables [154] (see Figure 3-1) which are continuously changing in real on-road circulation.

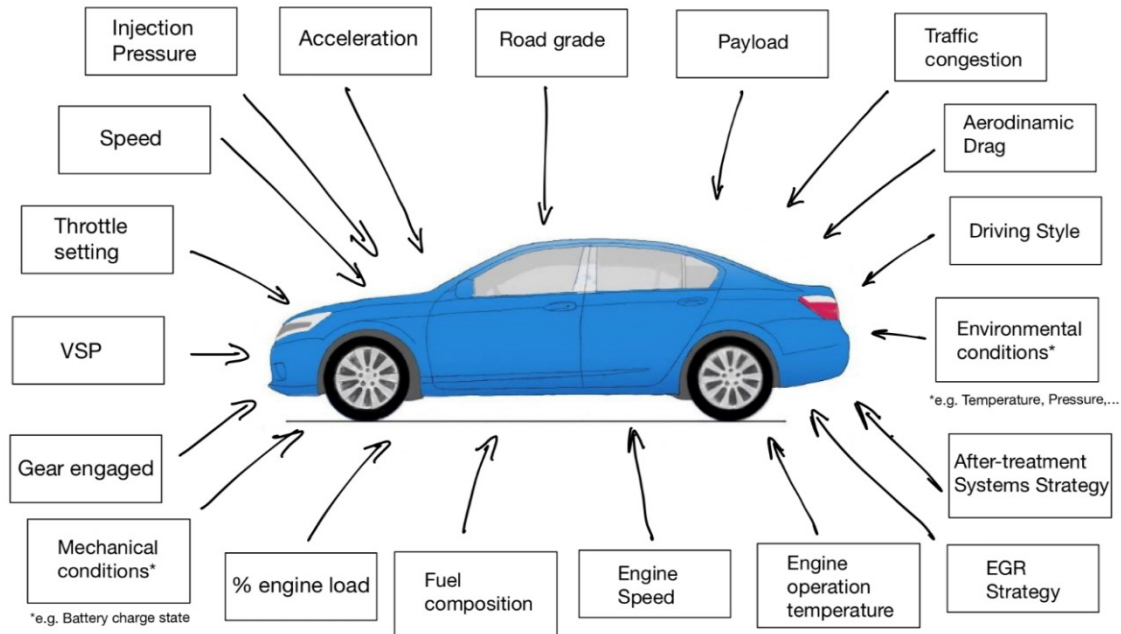


Figure 3-1. Some of the operating variables that affect vehicle NO_x emissions.

These variables can be divided into exogenous and endogenous [155]. The exogenous variables are those affected by the external engine working conditions, like traffic congestion, road condition, road grade, driving style, and fuel composition, among others. The endogenous variables are vehicle or engine inner working variables that affect emissions like engine speed, gear engaged, the power demanded, engine temperature, etc.

A change in any of these variables causes a significant variation in the vehicle's NO_x emissions [50]. For example, a severe driving style can increase NO_x emission from 40-50% to even more than 250%, and the increase of road grade from 0% to 5% could mean a NO_x emission increase of 115% [137], [139], cold operation of the vehicle could mean an increase of 55% of NO_x emissions [140], vehicle operation at low or very low temperatures also increases NO_x emissions [84], [156], and variations on traffic conditions, average speed or frequency of accelerations and decelerations can lead to increases of NO_x emissions [141], [157]. Even the aging of the vehicle influences the NO_x emissions, increasing when vehicles get older [66], [116], [158].

Also, altitude Above Sea Level (ASL) plays an important role in NO_x emissions, increasing the emission rate with altitude. This has been checked empirically in a pressure chamber [159], and more recently a study conducted in Switzerland with remote sensing emission measurement over passenger cars and LDVs, showed significant increases of 100% or higher in emissions at altitudes above 1,500 m ASL [160].

As a result of all of these influences, a vehicle that theoretically will emit a smaller amount of pollutants, depending on the influence of some variables can be converted into a high emitter.

A sample of these "inconsistencies" can be observed in the following research. Some Euro 6 vehicles (cars A, B, and C were Euro 6b, and car D was Euro 6 d-temp) were tested with PEMS. Results in Figure 3-2 show that car C and car D were the vehicles with lower average NO_x emissions from the set of vehicles [142].

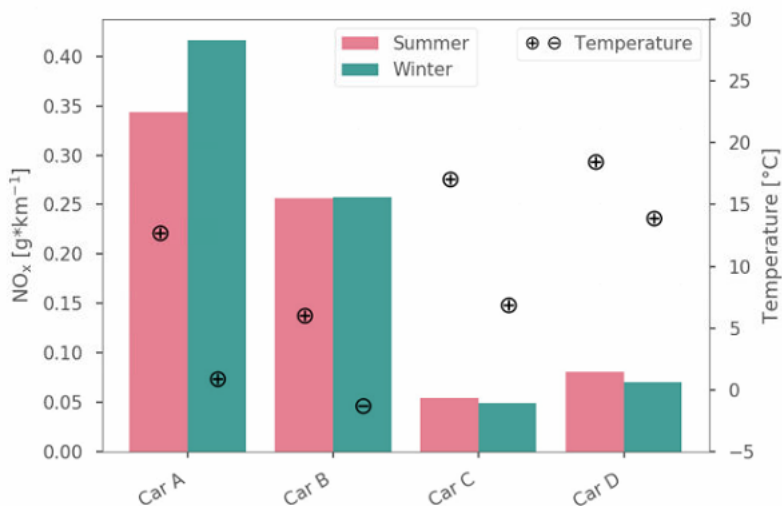


Figure 3-2. Average NO_x emissions in summer and winter of four Euro 6 diesel vehicles. Source: Söderena et al., 2020. [50]

These vehicles were subjected to a series of standardized routes (all vehicles were subjected to the same routes) and NO_x emissions were controlled in a continuous pattern. When comparing the 5 days of each vehicle with the lowest emissions and the 5 days of each vehicle with the highest emissions, it could be checked that the vehicles with the lower average values of NO_x emissions, vehicles C and D (Figure 3-2), were the vehicles with the highest NO_x emissions (Figure 3-3) in their worst days, in some trips and temperature conditions.

As a result, due to the variability of NO_x emissions from vehicles, it is complicated to design and carry out a NO_x test that takes into account all these variables (see Table 3-1) and also allows reproducing the test by keeping all these variables at values such that the results of two tests over the same vehicle are similar (for the same conditions) and comparable, that is, a test with consistency and good enough reproducibility.

When conducting NO_x emissions tests on power benches or RDE approach, which aims to simulate various on-road conditions, the main challenge arises from the multitude of variables that can affect the test results. As a result, the obtained values do not provide a straightforward basis for ranking vehicles due to the complexity of modifying factors. That means, the influence of differences from the great number of variables involved in the tests over two vehicles may be larger than the difference between the performance of the engine and/or EATS [161].

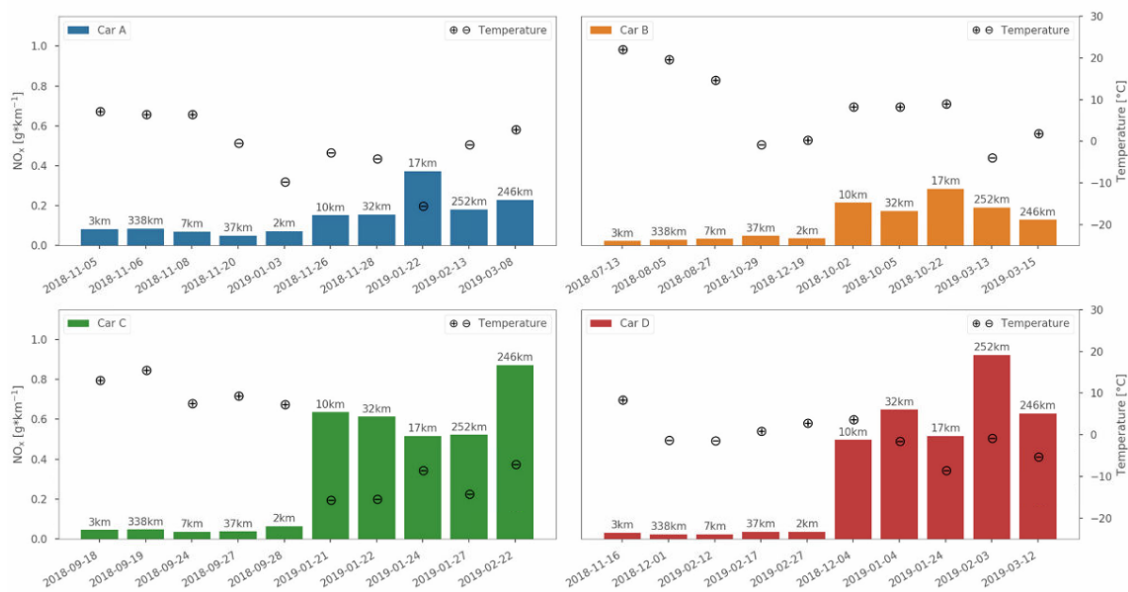


Figure 3-3. Average NO_x emissions for each car on the five days with highest and lowest NO_x emissions, including trip distance and daily average temperature. Source: Söderena et al., 2020.[50]

Type of variable	Variable	Origin of variable	Dynamic test	Static test
Endogenous	Engine speed	Operational	Yes	No
	Gear engaged	Operational	Yes	No
	Power demand	Operational	Yes	No
	Engine temperature	Operational	Yes	No
	EGR strategy	ECU	Yes	Yes
	EATS strategy	ECU	Yes	Yes
	% engine load	ECU	Yes	No
	Throttle setting	Operational	Yes	No
	Injection pressure	Operational	Yes	No
Exogenous	Traffic congestion	Road	Yes	No
	VSP	Vehicle	Yes	No
	Road condition	Road	Yes	No
	Road grade	Road	Yes	No
	Driving style	Driver	Yes	No
	Fuel composition	Vehicle	Yes	Yes
	Temperature	Environmental	Yes	Yes
	Atmospheric pressure	Environmental	Yes	Yes
	Humidity	Environmental	Yes	Yes
	Aerodynamic drag	Vehicle	Yes	No
	Payload	Vehicle	Yes	No
	Mechanical conditions	Vehicle	Yes	No
	Speed	Driver	Yes	No
Acceleration	Driver	Yes	No	

Table 3-1. Vehicle operative variables that can affect NO_x emissions in a dynamic or static test.

In response to this situation, a possible approach to simplify the test would be to predefine or limit the variables involved. By establishing these variables beforehand or reducing their number, the complexity of the test can be mitigated.

The first way introduces a high complexity to the test. For example, in a power bench test, most of the variables are predefined. While certain variables like aerodynamic drag or rolling resistance are technically determined by the equipment used in the test, other factors such as vehicle speed, acceleration, and "% engine load" are specified in the test protocol but rely on the driver's execution during the measurement. Small variations in throttle actuation from the driver cause significant differences in the behavior of these variables, which ultimately leads to different results when repeating the tests. To avoid these differences, either an expert driver or a technical solution is necessary to ensure the throttle actuation. Currently, even the Approval Type homologation process does not use this technical solution, but an expert driver to execute the test. This solution is not focused on simplicity and does not guarantee the reproducibility of the test for PTI.

On the other hand, the option to limit, omit, or ignore some variables can simplify the test, but the precision, accuracy, reproducibility, and representativity of the test are alarmingly reduced.

Moreover, as explained in Figure 3-3, even if these drawbacks can be overcome, there is no guarantee that even the result obtained in these tests is representative of the overall vehicle emissions.

To overcome the challenges posed by the previous options, an alternative is to conduct the test under conditions where several variables that typically affect NO_x emissions have minimal influence. This can be achieved by conducting the test while the engine is in an **idle state**.

When the vehicle is idling, the gear engaged, the speed, the acceleration, the VSP, the throttle position, the road grade, the payload, the weight, the aerodynamic drag, or the driving style, among others, do not influence NO_x emissions (see Figure 3-4 and Table 3-1).

As will be seen in the method description, the "% engine load" variation can be easily and accurately reproduced, making it a controlled variable during the test.

The engine speed remains the same and it is easy to reach (idling), and the engine operation temperature variation is small (or inexistent) because the preparation of the vehicle is the same.

The fuel composition is a variable that falls outside the control of the test (in PTI, the fuel composition is not analyzed for emission testing in gasoline or diesel engines). However, it is worth noting that the composition of commercial fuels is generally similar across suppliers, particularly when using "standard" diesel fuel. Therefore, significant differences arising from this variable are not anticipated. However, this is a variable that may be relevant in the event of a fuel change, since the use of biodiesel fuel instead of "standard" diesel fuel leads to increasing NO_x emissions by up to 68% with respect to diesel emissions [74], [162]–[164].

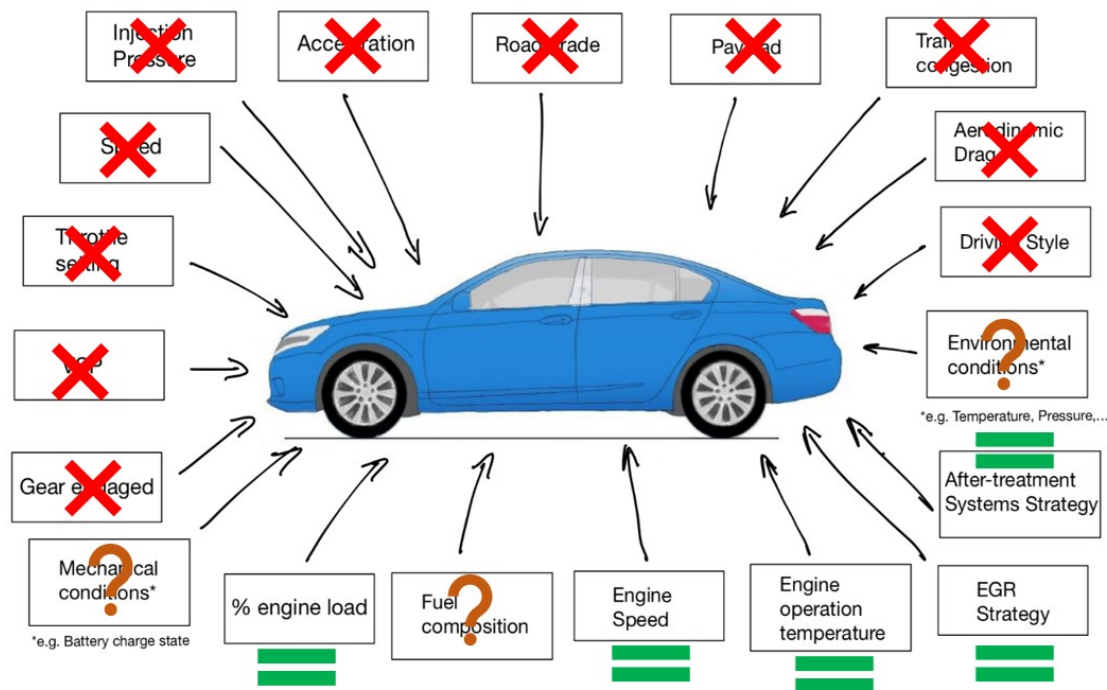


Figure 3-4. Operating variables that could affect vehicle NO_x emissions at the proposed static PTI test.

Other variables outside the test control, such as the EGR behavior and the EATS (Exhaust After-Treatment Systems) strategy, are controlled by the ECU's programming. But by reproducing the same engine behavior (at idle) and load demand (defined by the test), these strategies should work in the same way when the test is repeated. So, although it is not possible to control directly its behavior, it can be reproduced through the "% engine load" and engine speed behavior.

As such, only environmental and mechanical conditions could affect NO_x emissions without control during the idling test, although in a similar way to other PTI tests.

For example, low ambient temperatures are associated with higher NO_x emissions [84], [156]. On one hand, the use of EGR increases the water vapor concentration in the exhaust gas, and at lower ambient temperatures there are problems in the recirculating system when a high EGR rate is used because water vapor condensation can cause severe problems in the EGR line and/or the DPF system. For that reason, at low temperatures, EGR rates are reduced or even canceled to avoid the EGR component's failure. The result of the EGR rate decreasing is a higher NO_x emission at low ambient temperatures [41].

On the other hand, it has been observed a high dependence of NO_x emission at ambient temperatures below 25°C for diesel vehicles (that means below the temperature of the NEDC test) with higher emissions at lower temperatures, being more relevant in Pre-Euro 6 vehicles than for Euro 6 ones, and higher dependence for LNT Euro 6 vehicles than SCR Euro 6 vehicles [165], [166].

According to this, if the PTI test is performed with lower ambient temperatures, higher results from the NO_x emission test are expected. The interval between inspections typically ranges from 1 to 2 years, which means that the weather conditions during the PTI test may be similar when it is repeated throughout the vehicle's lifespan. As a result, the impact of this variation is minimized.

Consequently, the potential impact of such variations becomes significant only for vehicles that undergo inspections every 6 months. Nevertheless, additional research is needed to thoroughly examine the effects of fluctuations in ambient temperature, pressure, and relative humidity on the test results.

This variable is a condition that will affect any method used to measure NO_x emissions in PTI in the same way and only could be reduced if NO_x measurement will be carried out in an environmentally controlled space, which is far from the requirements indicated for a PTI test.

Mechanical conditions such as the battery's state of charge, which are not considered significant for other tests conducted during PTI inspections and are not assessed during the vehicle's preconditioning, could potentially impact both CO₂ and NO_x emissions in a similar manner [33]. It is important to investigate the extent to which these factors can contribute to variations in NO_x emissions, and further research is needed to determine their influence.

To develop a NO_x measurement method for PTI, the idle measurement approach offers a highly valuable attribute: simplicity. By minimizing the number of variables to be managed during the process, it allows for a streamlined measurement procedure. As mentioned earlier, this simplicity leads to a safer and quicker test with reduced potential for execution errors, ultimately ensuring enhanced test reproducibility.

The NO_x measurement at idling speed has another important advantage when it is compared with other methods: it represents a measurement of an actual driving condition. This helps to solve the problem of the representativeness of the measurement with respect to the overall emissions of the vehicle because the result is directly the actual emission value of the vehicle in a real driving situation, which is easily reproducible during PTI.

With this measurement, the result obtained corresponds to the actual emission value of the vehicle while it remains stopped along circulation in an urban area. That means, through this test, is possible to know the real NO_x emissions of a vehicle when it is stopped at a traffic red light. And even more, this particular situation is one of the most harmful to the health of people in the urban environment, because of the low dilution of the emissions of NO_x at low speeds and the high density of NO₂, increasing the NO_x concentration in the location where vehicles are stopped.

The average stop time of a vehicle in urban circulation can fluctuate between 6% of the trip time in very fluid traffic conditions, up to 60% of the time in case of congested traffic, being realistic values to assume a stopped time in urban traffic between 24% and 34% of the time, increasing to 40%-50% of the time when traffic density increase and traffic average speed decrease [50], [108], [166], [167].

Accordingly, with this measurement is possible to assess in a realistic way the current NO_x emissions value from a vehicle in approx. 30% or even more of the time on urban

circulation. **No other combination of "% engine load" and engine speed values that could be easily reproduced in a test occurs in real circulation as the conditions in the measurement at idling.**

It is complex to reproduce in a real way a situation of urban traffic (the kind of traffic circulation where NO_x emissions are most harmful to people's health), which occurs for such a long time throughout the vehicle's circulation.

Any other driving condition of the vehicle that can be reproduced will not last as long in time when driving as the situation of the vehicle stopped with the engine running or can't be reproduced as accurately.

For example, it has been shown that in very low-speed driving situations, there is a large difference between the values obtained through a simulation cycle on a roller bench and the real values obtained by measuring the emissions in circulation (the real emissions being much higher than those obtained on the roller bench) [167].

Additionally, the NO_x measurement at idling conditions provides another important advantage. It represents the same relative condition for all the vehicles independently of their mechanical configuration, and the lowest possible engine load demand so is a perfect point for the comparison between engines and vehicles with different technical and mechanical characteristics.

Measuring the NO_x emissions at idling would be the equivalent of measuring the heart rate at rest, i.e., to know the behavior in the condition of less effort, compared to a stress test. Both tests (engine idling test and heart rate rest test) have the advantage that they are very easy to perform and provide information that is simple, easy to understand, and allows for comparison with another vehicle although they are different because both remain in the same situation of lowest power demand.

The equivalent of the stress test would be to place the vehicle on the roller bench and subject the vehicle to a protocolized behavior, like gradually increasing the resistance of the rollers until the point of maximum engine power is reached (e.g., lug-down test), or performing a pattern of accelerations and speed over the vehicle (e.g., ASM test) to check the NO_x emissions.

Comparing the results of this type of test between two vehicles with distinct characteristics is similarly challenging as comparing the results of a stress test between two individuals with different body types and physical conditions.

It is not the same running 5 km for a 25 years old trained person as for a 40 years old non-trained person. The results of the test will be very different (O₂ consumption, maximum heart rate, the power developed...), although both persons were healthy.

In the same way, the pattern of NO_x emissions from a 1400 cm³ diesel engine in a familiar hatchback vehicle when accelerated from 20 km/h to 50 km/h will be very different from a 2500 cm³ diesel engine in a sport coupe vehicle in the same situation, although both vehicles were equally in good mechanical condition, being complicated to compare the values of emissions because there is a high number of variables involved in the NO_x emissions.

Indeed, obtaining simple and fundamental information about NO_x emissions through idle condition testing provides an uncomplicated and standardized approach to acquiring basic and comparable data.

While other types of tests may offer more specific information, they can pose challenges in terms of precise analysis and may not be suitable for straightforward comparisons of emissions between vehicles, which is a key requirement for PTI measurements. It is important to bear in mind that the primary objective is to establish a NO_x test method for PTI that enables easy and meaningful comparisons of emissions among vehicles.

Finally, an additional challenge in designing a NO_x measurement test for PTI is the limited availability of prior knowledge or information regarding the accurate measurement results and the anticipated behavior or patterns of NO_x emissions and corresponding actions. This lack of comprehensive understanding adds complexity to the development of an effective and reliable test method.

For example, when performing the gas analysis test for a gasoline vehicle, it is known in advance that, if the vehicle is in perfect condition, the CO value measured in % vol. will be close to 0, and the lambda value will be around 1 with defined tolerance.

This information is known before the test is performed and allows the test measurement to be designed in such a way that it is performed in the best way to check this behavior.

However, in a NO_x measurement on a vehicle, there is not enough information *a priori* to know the emission values that the vehicle will present during the test if its operating condition is correct.

The fact that each vehicle model (depending on the engine, onboard EATS systems, electronic management of these systems, etc.) may present a different emissions behavior greatly complicates the design of a test that can cover all the variety of emissions that may occur.

3.3. PROPOSAL PRESENTATION

As was previously explained in section 2.2, NO_x emissions have a strong relationship with engine power demand through the temperature of the combustion process, being the “% engine load” an ECU parameter that provides information from the vehicle about the engine power demand.

This proposal of NO_x measurement at PTI is based on the analysis of **the variation of the NO_x concentration at the vehicle exhaust pipe and its relationship with the variation of the “% engine load” demand at idling**. Due to the relationship between NO_x emissions and engine power demand, it is expected that if all the rest of the operating parameters of the engine remain at a constant value, the variation of load demand causes a variation in NO_x emissions of the engine. This variation in NO_x emissions of the engine directly translates into a variation of the NO_x concentration in the exhaust pipe, which can be measured with equipment available at PTI stations, and the analysis from this set of data allows us to perform a measurement process to estimate a full load state situation and compare in this way emissions between vehicles. **The**

engine idle state is chosen to simplify the test and to ensure reproducibility, for the reasons explained in section 3.2.

It should be noted that the test focuses on the NO_x concentration measurement at the vehicle's exhaust pipe, not on the NO_x generated by the engine. This is crucial because the aim of PTI is to evaluate the vehicle's emissions, not those of the engine.

NO_x emissions produced within the engine can undergo variations before being emitted through the vehicle's exhaust pipe. This is due to the influence of Exhaust Gas Recirculation (EGR) and other exhaust after-treatment systems (EATS), which are designed to lower the NO_x concentration from the engine exhaust to the vehicle's exhaust pipe. The extent of this reduction relies on the performance of EATS, which is controlled by the vehicle's Electronic Control Unit (ECU) based on input from various sensors measuring multiple parameters within the vehicle. The ECU's programming plays a crucial role in governing the behavior of the EATS.

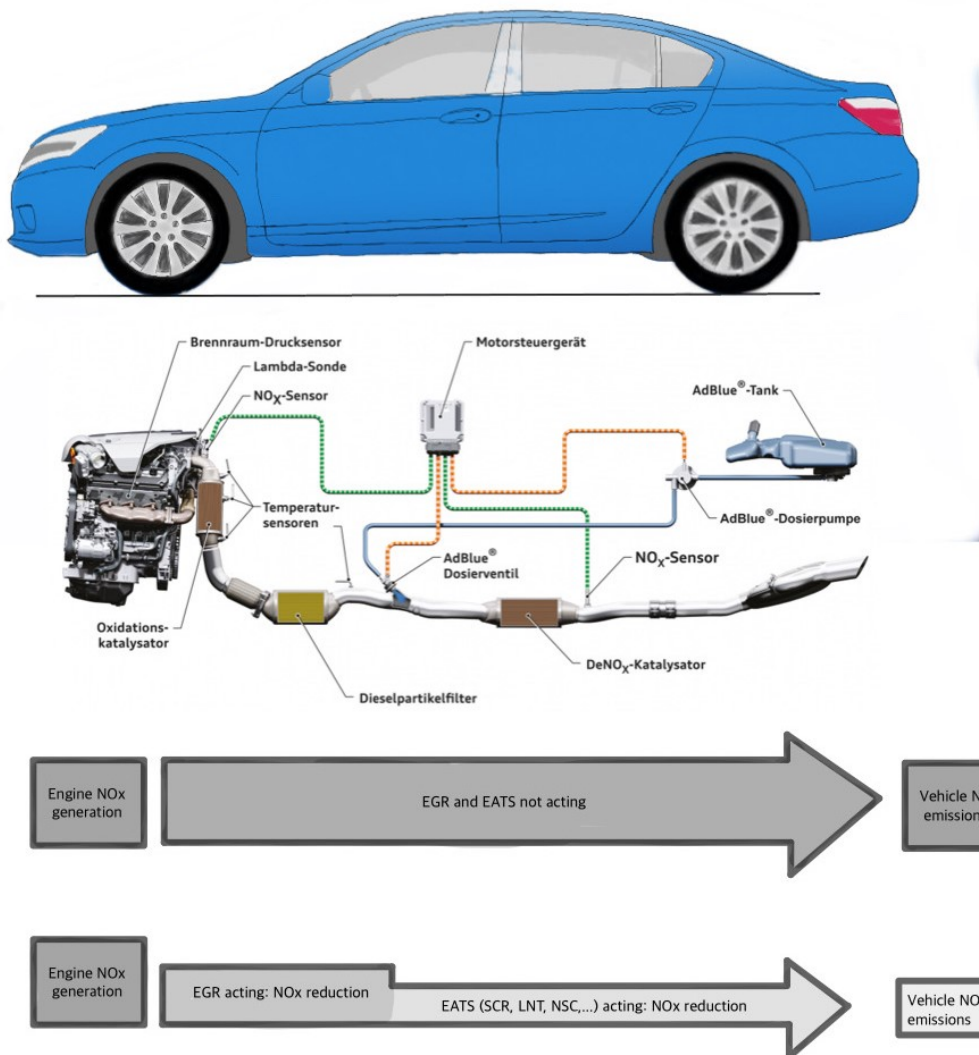


Figure 3-5. Reduction of vehicle NO_x emissions from EGR and EATS (Source engine image: VAG).

The PTI lacks the necessary tools to directly measure or assess⁷ the functioning of EATS, as they are exclusively controlled by the vehicle's ECU. However, by replicating the same engine speed (idling) and engine load conditions during the test, it is expected that the EATS will exhibit similar behavior. So, although from PTI there is no access to the vehicle's data to quantify the NO_x emission reduction from the EATS, if the vehicle's operating conditions are the same, the behavior of EATS will be the same, and the NO_x emission reduction will be the same. In this way, the reproducibility of the test is ensured.

Analyzing the NO_x emissions before and after engine acceleration (the Accelerated State that is included in the measurement proposal), it is possible to incorporate (and analyze) into the final result the reduction of emissions due to the action of EATS because it will reduce the emissions in the last part of the test, and the average value of emissions will be lower.

When the engine is in idling condition, it can be easily subjected to two significantly different engine states of load, which are defined and controlled through the measurement of the "% engine load" value through the OBD system.

As was said previously, this parameter is related to the engine load demand and provides information about the proportion of the capacity of the engine used. The variation of the engine load demand between both states causes a variation in the NO_x emissions between them, which can be analyzed in addition to the various engine working parameters that are read and registered through the OBD system.

Based on research findings, it has been observed that when a vehicle is in static conditions, the most effective way to increase the "% engine load" is not through free acceleration from idling. Such acceleration, which resembles an increase in engine speed without a corresponding increase in engine load, does not lead to a significant rise in combustion chamber temperature [73]). Instead, a more effective approach involves increasing the power demand from the equipment installed in the vehicle.

When the engine is started and operating at its natural idle speed, a portion of the available torque is utilized by essential engine accessories such as the water pump and generator. This consumption directly corresponds to a "% engine load" value, indicating the proportion of torque being utilized compared to the maximum available torque at the engine's natural idle speed. This value is different for each type of engine. Henceforth, we will refer to this state of the engine with minimal power demand as the "Unloaded state".

Increasing the power demand when the vehicle is idling will increase the "% engine load" value in a significant way. As the power available at idle is not very large, even an internal consumption could mean a power demand large enough to generate a significant increase in the "% engine load".

Activating different vehicle equipment like the Air Conditioning (A/C) system, lighting and signaling system, and rear window heater system is one of the easiest ways to

⁷ EGR operation can be known through the OBD system of vehicle on some occasions, but access to this value is not mandatory, so there are vehicles with EGR value not available.

increase load demand. These components draw additional power from the engine, effectively raising the load demand.

The power demand from the Air Conditioning system and the electric equipment of the vehicle are not considered in the type approval NEDC test, although it is estimated that it may vary the CO₂ emissions. Instead, an Air Conditioning test is used, for example, by the USA SC03 to control the pollutant emissions of vehicles.

Several previous measurements demonstrate that the A/C system use increases the engine load and the NO_x emissions [168], and the on-road NO_x emission with the A/C system connected can be from 68% to 85% higher than the situation with the A/C system disconnected [156], due to the increase in engine load demand. So, the use of the A/C system is an effective way to increase the engine load demand.

Furthermore, the battery's state of charge at the start of the NEDC test can vary by as much as 3% of the CO₂ emissions, so for the tests to be consistent between measurements, a full battery charge must be ensured before [33]. This observation highlights the impact that electrical consumption can have on pollutant emissions from a vehicle during idle conditions. Henceforth, we will refer to the state of the engine with the vehicle's equipment connected as the "Loaded state".

By following this procedure, it is feasible to increase the "% engine load" from the initial Unloaded state to the Loaded state, potentially even surpassing the values achieved during power bench simulation tests. Depending on the vehicle, it is possible to attain a "% engine load" exceeding 50% while the vehicle is at its natural idle speed. On average, the increase in "% engine load" from the Unloaded state to the Loaded state is approximately 100%.

Instead, free acceleration from natural engine idle speed without a gear engaged increases the "% engine load" for a short time, decreasing immediately to a lower natural engine idle speed level. When the engine speed is increased, the peak available torque and power also increase but the torque and power consumed by the engine remain constant if there are no new consumptions. As a consequence, the "% engine load" decreases. The initial increase of "% engine load" comes from the inertial forces of the engine that are necessary to overcome. But when the new engine speed is reached, the "% engine load" value decreases.

The OBD connector is used by the measurement equipment to gauge and record the "% engine load" of the vehicle. This connector is plugged into the OBD port of the vehicle and sends the necessary parameters to the measurement equipment [80], [89], [169], [170].

Not only the "% engine load" is registered from the ECU of the vehicle. Other relevant parameters could be registered through the vehicle's OBD port, being mandatory to register at least the engine speed and the engine oil temperature. If available, the % EGR opening and the MAF (Mass Air Flow intake) could be registered for better information from the test (see Table 3-2).

These data are standardized by the SAE J1979/ ISO 15031-5 [80], being the ECU PID the codes (Parameter ID) used to request information and get data access from the ECU in a standardized way.

Item	Units	ECU PID	Description
% Engine load	%	\$04	% of peak available torque
Engine speed	rpm	\$0C	Angular speed of the engine crankshaft
% EGR aperture	%	\$2C	% of commanded position of EGR valve
Air Flow Rate	g/s	\$10	Mass airflow intake of the engine
Engine Temperature	°C	\$05	Engine oil temperature

Table 3-2. Engine working ECU data registered from the vehicle through OBD.

To summarize, through the OBD port several working parameters are read from the vehicle's ECU, being the "% engine load" the most important. Simultaneously, a gas analyzer measures NO_x concentration from the vehicle's exhaust pipe synchronized with the OBD data.

Combining the OBD data and the NO_x concentration measures from the gas analyzer it is possible to analyze the relationship between the exhaust gas NO_x concentration from the vehicle and the functioning engine parameters, specifically the "% engine load".

3.4. TEST FEATURES OF IDLING MEASUREMENT

One of the main features of the idling test is allowing a comparison between different vehicles in a **similar relative condition** using the relationship between the NO_x emissions and the adimensional non-specific vehicle engine parameter "% engine load". This ensures that the measurements remain consistent and comparable across all vehicles, regardless of their specific characteristics.

Testing vehicles under idling conditions provides a standardized method to evaluate them regardless of their brand, engine size, engine type, or any other vehicle characteristic. While the specific value of "% engine load" may vary among different vehicles during idle, the initial condition of the test is consistent for all vehicles, the Unloaded State with no additional power demand. Achieving this starting point is straightforward for any vehicle, ensuring the easy reproducibility of this aspect of the test under identical conditions.

To get a significant increase in the engine load demand, and subsequently, the value from "% engine load", connecting some equipment of the vehicle is necessary: the Air Conditioning system and Lighting and Signaling system must be switched on. Since increasing the load through connecting this equipment is simple, the Loaded State of the test is easily achievable, and the reproducibility of this part of the test is also guaranteed.

As part of the test, it is necessary to accelerate and maintain the engine to a range of 2500 ± 500 rpm, which is relatively simple to accomplish. Therefore, achieving a high level of reproducibility in this particular phase of the test is readily attainable.

In conclusion, due to the ease with which the various components of the test can be conducted, it becomes feasible to ensure the reproducibility of the entire test. Therefore, simplicity and reproducibility are essential attributes of this test.

As reproducibility is a crucial aspect of a measurement method, the Standard Deviation and the Coefficient of Variation will be employed as statistical indicators to assess the method's reproducibility throughout the research.

The test is based on the relationship between the load demand through the "% engine load" value in the engine and the NO_x emissions from the vehicle in the exhaust pipe, so an important attribute of this method will be to demonstrate this relationship. To check the significance of this relationship the p-value between both variables will be studied with the test data, using a significance level of $p=0.01$ (a stringent value commonly used in medical research). This value can be checked for every test performed.

Another important feature of the test must be the link between the test and the emissions in the real world. In this regard, idling measurement is more representative of real emissions than it may initially appear.

A substantial portion of urban travel time (depending on traffic conditions) involves the vehicle being stationary with the engine idling. As mentioned in section 3.2, when it comes to urban traffic, the average duration of vehicle stops can reach as high as 60% of the total time, especially during congested conditions. A realistic average value to consider could be a range of stopped time between 24% and 34% of the total time. [50], [108], [166], [167].

This is very important because **most of the journeys made with a vehicle are urban, or at least can be estimated as such, based on the distance traveled**. Approximately **30% of car journeys in the EU were journeys of 3 km or less, and 50% of journeys were less than 5 km** [171]. Therefore, idling measurement is representative of a situation that occurs for a significant amount of time during a significant portion of the journeys undertaken by vehicles.

In addition, it must be taken into account that in this type of short urban trip, the temperatures of the EATS (as the SCR) do not usually reach the correct working temperatures, so they are in cold start emission conditions, which compromises the efficiency of these systems (both for NO_x and PN) [128]. This situation is characteristic of urban trips and contributes to increasing the NO_x emissions by diesel vehicles.

The proposed test, which measures NO_x emissions in an operating condition (before acceleration) in which in most cases the EATS systems are not working, provides valuable data on vehicle NO_x emissions in situations where the EATS are not operating as designed, which means the same situation in cold start condition.

For all these reasons, the proposed idling measurement is highly representative of actual vehicle emissions.

Moreover, the consequences on human health from NO_x emissions depend on the concentration in the environment, being more harmful when concentration increases. This concentration of NO_x can be affected by vehicle speed due to the lack of dilution of pollutants in the atmosphere [172], in similar behavior to forced ventilation in a

tunnel [173], [174]. In this way, NO_x concentration increases if vehicle speed decreases, and maximizes when the vehicle remains stopped.

The number of emitting vehicles also increases concentration. Because of that, vehicles stopped at idling (e.g. in a traffic jam) is a situation that increases the NO_x concentration at certain locations.

Additionally, the NO₂ relative density concerning air is 1.58⁸, which means that in an environment without dilution mechanisms (e.g. low speed of vehicles) and with high concentrations of pollutants (e.g. in a traffic jam), **the NO₂ will remain in the lowest layer of the environment**, where it is the most harmful to people's health. In fact, due to this particularity, one of the age groups most affected by this distribution of NO₂ in the lower layer is children.

As a result, assessing NO_x emissions during idling conditions of a vehicle allows us to determine the real NO_x emissions of that vehicle, in one of the worst scenarios for human health in an urban environment, characterized by congested traffic and high levels of pollutant emissions from vehicles. So, this is an important feature.

To summarize, some of the main features of this test are:

- Easy measurement method, and therefore suitable for fast implementation in the PTI process, allowing the measurement and control of NO_x emissions in a large number of vehicles in a short time.
- Equipment required for the measurement process that is simple to use, inexpensive to purchase and maintain, and similar to that currently used in the inspection process.
- Measurement of vehicle's NO_x emissions in the same operating condition, using an adimensional non-specific vehicle engine parameter: the "% engine load" value. This provides a suitable tool for the comparison of emissions from vehicles with different characteristics.
- The simplicity of the test likely provides great reproducibility.
- The test relies on the verifiable relationship between the "% engine load" value and the NO_x concentration in the exhaust pipe.
- The test provides representative information about the real NO_x emissions of vehicles in urban and congested circulation, which is one of the worst human health situations related to pollutant emissions.

3.5. CONCLUSIONS

This chapter concludes the first part of the thesis, in which the general framework on which the research will be developed has been presented.

In these chapters, we have provided a comprehensive overview of the present state concerning the issue of NO_x emissions from vehicles. We have covered a range of topics, including the current status of the problem, available options for controlling these emissions (including techniques, equipment, and measurement methods), and an extensive review of the existing literature on the subject.

⁸O'Neil, M.J. (ed.). *The Merck Index - An Encyclopedia of Chemicals, Drugs, and Biologicals*. Whitehouse Station, NJ: Merck and Co., Inc., 2006., p. 1142

It has been elucidated how the measurement of NO_x in Periodic Technical Inspections (PTIs) can serve as a valuable mechanism for managing emissions in vehicles. This approach enables the identification and elimination of highly polluting vehicles from circulation while providing up-to-date data on the overall emissions from the vehicle fleet. This information would contribute to the development of more impactful environmental control policies, thereby enhancing their effectiveness.

In this chapter, it has been outlined the challenges that must be addressed for a NO_x measurement method in PTI to be successful. The method proposed in this thesis has been described, emphasizing its key characteristics and distinctive features.

The main conclusions of this chapter are as follows:

- A measurement method in PTI must be simple and safe, as well as accurate and representative
- The proposed method is based on idle measurement, to meet the requirements of simplicity and safety, and incorporates the application of engine power demand to improve the accuracy and representativeness of the results
- The proposed method is technically based on the NO_x generation process in compression engines
- The measurement at idle speed and the use of the "% engine load" provide the method with important features

Subsequent chapters will delve into a comprehensive explanation of the proposed measurement method, meticulously assessing how the characteristics outlined in this chapter are upheld throughout the entire process. Additionally, the chapters will elucidate the tools employed to validate the method's feasibility and the obtained results. The objective is to ensure the reliability, utility, representativeness, and reproducibility of the proposed method, providing a solid foundation for its application.

CHAPTER 4

NO_x MEASUREMENT METHOD FOR PTI DESCRIPTION

4. NO_x MEASUREMENT METHOD FOR PTI DESCRIPTION

4.1. INTRODUCTION

In this chapter, the method for measuring NO_x in PTI will be described in detail, explaining all the steps required to complete the measurement on a vehicle.

Not only the measurement itself but also the complete process of data processing until obtaining the final result will be detailed.

With the information provided in this chapter, it is possible to replicate the measurement process, provided that the appropriate equipment is available for conducting the measurement, as well as the means for proper data handling.

The comprehensive version presented below provides a detailed description of the NO_x measurement method in PTI, encompassing all the elements considered in its design. While the information in this section was previously published in a condensed and summarized form in a peer-reviewed paper in the journal Sustainability [175], it is now expanded upon for a more thorough understanding.

4.2. MEASUREMENT METHOD DESCRIPTION

The measurement method proposed, which will be described in-depth below, is a process focused on its applicability in PTI, thus seeking simplicity in execution as a fundamental premise, along with test reproducibility and representativeness of the obtained result.

It is based on the relationship between the engine load demand and the concentration of NO_x in the vehicle's exhaust. Therefore, the first step involves a thorough analysis of the relationship between these variables and how this relationship is utilized in the design of the measurement method. Next, the step-by-step execution of the measurement method is detailed. Subsequently, the complete process of data processing obtained from the measurement is described, leading to the final result.

4.2.1. "% ENGINE LOAD" VALUE VARIATION ALONG WITH THE TEST

NO_x emissions from diesel engines have a strong relationship with engine power demand [41] through the temperature reached in the combustion process. Power demand can be controlled through the "% engine load" value. This value is an ECU parameter indicating relative engine power demand, accessible through OBD. It is pivotal for assessing torque demand in real-time.

The measurement method focuses on NO_x concentration changes during idle, generated by variations in "% engine load." This idle state guarantees reproducibility and test simplicity, as was explained in the previous chapter. Different load states are achieved by manipulating "% engine load," causing the NO_x concentration changes, while OBD reads engine parameters.

The working hypothesis is that once an engine working condition is settled (in this case the engine idle speed and other working parameters are fixed, as was explained in section 3.1), the variation in the power demand (that can be measured through the "% engine load" value) on the engine generates a variation in the engine NO_x emissions. Therefore, a variation in the NO_x concentration can be measured at the vehicle's exhaust pipe.

If there are no external factors (here external factors refer to influences external to the engine working condition), the **relationship between the values from these two parameters** (the "% engine load" value and the NO_x concentration in the exhaust pipe) seems to be a **linear function**, increasing the NO_x concentration as the "% engine load" (because of the increase of engine power demand) on the engine increases.

In the presence of external factors, the most usually:

- the variation of the engine speed,
- the EGR valve aperture,
- the Exhaust After-Treatment Systems (EATS) actuation,

The correlation between both variables can be altered, with a stronger alteration when the external factor is more prominent.

The variation of engine rotation speed affects directly the NO_x generation from the engine, by the variation of endogenous variables. This variation, depending on the working conditions of the engine and the entity of the variation can reduce or increase the engine NO_x generation, and therefore the vehicle NO_x emissions.

In contrast, the functioning of the EGR system consistently diminishes the production of NO_x from the engine when compared to its inactive state, thereby leading to a reduction in NO_x emissions from the vehicle.

Finally, the operation of the EATS system integrated into the vehicle reduces the quantity of NO_x emissions originating from the engine, resulting in a decrease in vehicle NO_x emissions through the exhaust pipe.

With the knowledge of the linear function governing the correlation between the measured NO_x concentration in the exhaust pipe and the "% engine load" value, it becomes feasible to **estimate** the NO_x concentration in the exhaust pipe for any given engine load percentage value during idling conditions. This approach enables the estimation of the highest possible NO_x emissions during idling conditions when the engine is operating at a 100% "% engine load".

This maximum value of NO_x emissions at idling can serve as a benchmark for comparing the emissions of different vehicles, as it allows for measurements to be taken under the same operating conditions (vehicle stopped and idling) and with an equivalent power demand applied to the engine (not the net value, but the relative demand of connected equipment).

In a static situation, the appropriate way to raise the "% engine load" value on the engine (i.e. the engine load demand) is not through free acceleration from idling but by increasing the power demand from the equipment of the vehicle, as was explained in the Proposal Presentation section (3.3).

As a result of the increase of power demand from equipment, the percentage of the torque consumed compared with the peak torque available at natural engine idle speed increases too (see Figure 4-1, loaded blue dotted line, 38% engine load in the sample). Henceforth, we will refer to this engine state, with the connected vehicle equipment, as the "Loaded state".

In this way, two power demand levels are defined, the "Unloaded State" (Figure 4-1, unloaded green dotted line), where the engine is working with the minimum possible power demand (it cannot be lower), and the "Loaded State" (Figure 4-1, loaded blue dotted line), where fixed power demand is applied to the engine. These two levels of power demand provide different "% engine load" values depending on the engine speed, but the net value of power demanded in each of both states remains fixed.

Through this straightforward approach, it is possible to increase the engine load demand, as indicated by the "% engine load" value, by twofold at idle from the initial unloaded state to the loaded state, and even surpass the "% engine load" value achieved in a simulated bench scenario. Depending on the vehicle, a "% engine load" value of more than 50% can be reached with the vehicle at the natural engine idle speed. The average increase of the "% engine load" value from the Unloaded state to the Loaded state is about 100% on average.

The "% engine load" value indicates the percentage of peak available torque during normal, fault-free conditions [80]. When the vehicle is at idling conditions, the peak available torque is lower than, for example, when the engine is at 2500 rpm, wherein the sample (see Figure 4-1) available torque is near its maximum value.

In this situation at 2500 rpm, the same power demand from the idling represents a lower percentage of the peak available (17% engine load in the sample). So, with the same power demand in the vehicle, accelerating the engine not only does not increase the "% engine load" value, but it decreases.

A free acceleration from natural engine idle speed without a gear engaged can increase the "% engine load" value for a short time, but it will decrease immediately to a lower natural engine idle speed level, as can be seen in Figure 4-2. The initial rise in the "% engine load" value can be attributed to the inertial forces that the engine must overcome. However, once the engine reaches the new speed, the "% engine load" value decreases.

If the engine speed is increased from idling, the peak available torque is increased too, but the torque consumed from the engine remains constant because there are no new consumptions, and as a consequence the "% engine load" value decreases.

Therefore, to increase the "% engine load" value during testing, the method employed is to connect equipment to the vehicle rather than relying on unrestricted acceleration from idle.

To measure and register the "% engine load" value of the vehicle, the gas analyzer uses an OBD connector. This connector plugs into the OBD port of the vehicle and transmits the required parameters to the measurement equipment [80], [8g], [16g], [170] through a Bluetooth connection.

Summarizing, through the OBD system, several working parameters are read and registered from the vehicle's ECU, being the "% engine load" value the most important. Simultaneously, a gas analyzer measures NO_x concentration from the vehicle's exhaust pipe. The details of the equipment used are shown in section Chapter 5.

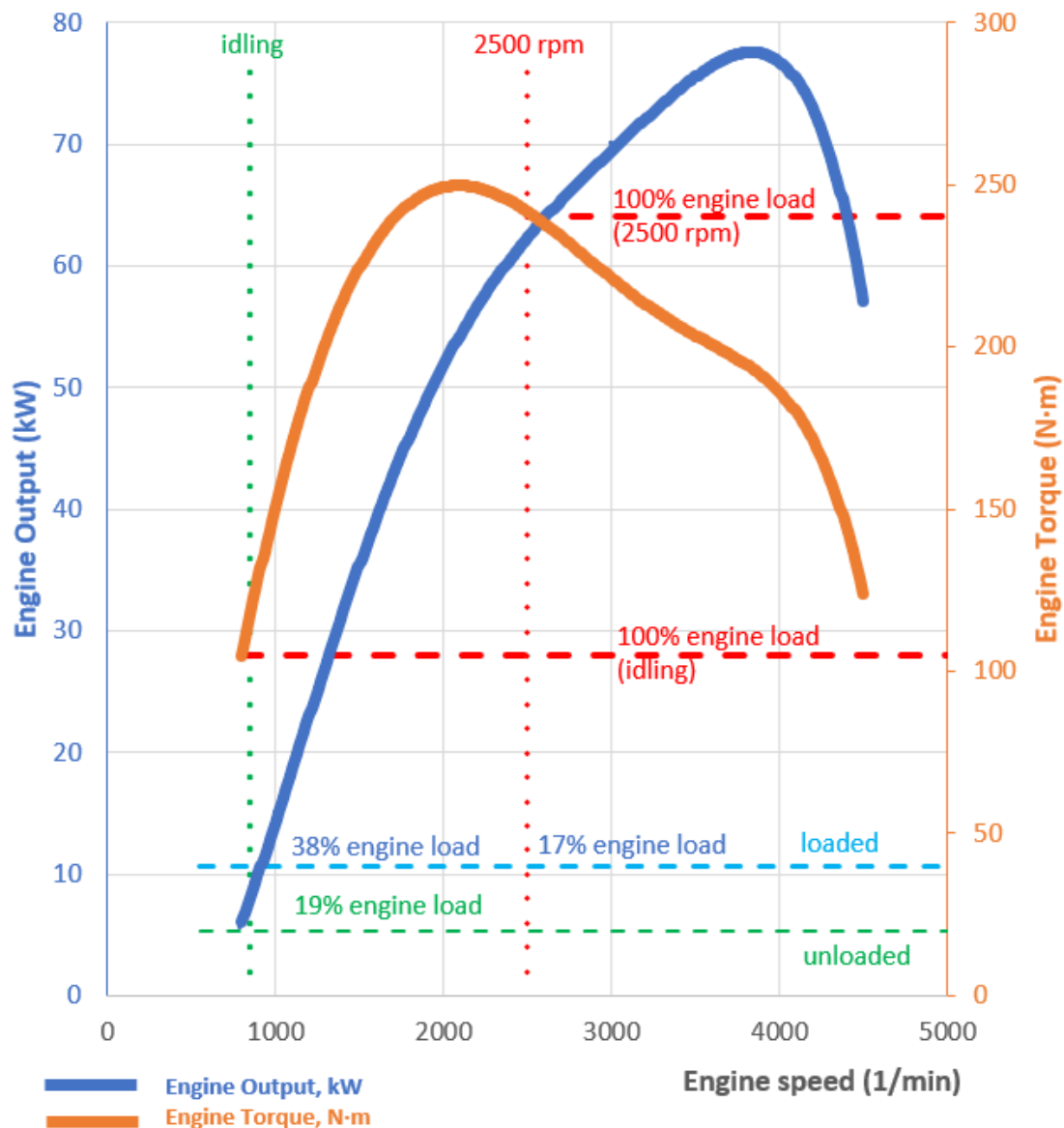


Figure 4-1. Power and Torque plot from 1.9 liters 4-cylinder TDI Audi A3 engine (77 kW at 4000 min⁻¹, 250 N·m at 1900 min⁻¹)

Combining the OBD data and the NO_x concentration measurement from the gas analyzer it is possible to analyze the behavior and relationship between the exhaust gas NO_x concentration from the vehicle and the operating engine parameters, specifically the "% engine load".

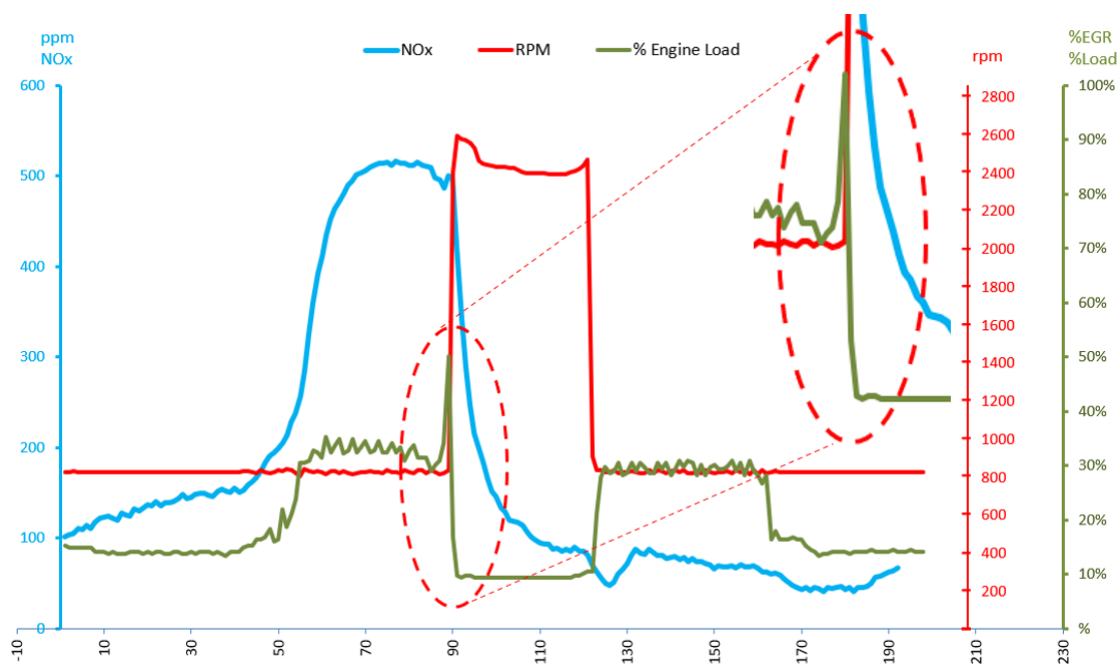


Figure 4-2. Sample of fast increase and decrease of "% engine load" with free acceleration.

4.2.2. STEP BY STEP OF THE TEST: MEASUREMENT PROTOCOL

In order to conduct research, design, and verify the measurement method, a group of diesel vehicles was utilized. Various tests have been conducted for each vehicle to compare the consistency of the results and ensure that the tests can be replicated.

To carry out the measurements, a protocol must be followed to ensure that every test is performed in the same way. This measurement protocol consists of the following steps:

- a) verification of vehicle conditions for the performance of the test.
- b) preconditioning of the vehicle.
- c) execution of the defined cycle for the test (Table 4-1).

The first and second steps, which can be defined as the **Preparation** of the vehicle for the test, are common with the current PTI opacity measurement procedure [89]. The only difference is the measurement equipment used: for the current measure of opacity in diesel vehicles an opacimeter is used, and for the NO_x measurement, equipment able to measure NO_x concentration will be used.

For the first step (verification), the conditions of the vehicle must be verified, to ensure that the vehicle is suitable and is prepared to be subjected to the test. The engine must be switched on and the following aspects must be checked:

- the state of the exhaust system is correct and does not show any apparent damage or modifications (check with a visual inspection),
- the absence of unusual noises,

- any extra loads and equipment of the vehicle are disconnected,
- the vehicle shows adequate mechanical and electrical condition,
- the vehicle does not indicate faults using the MIL (Malfunction Indicator Lamp)

In the second step (preconditioning), it must be checked that the engine is in normal working condition, using the engine oil temperature. At this point, vehicle manufacturer information must be used, but if it is not available, at least 80°C for the engine oil temperature will be necessary, or the engine crankcase temperature measured by the level of infrared radiation must be at least equal to it, to be considered as an appropriate value (in the same way that in the opacity test is required).

Usually, an infrared thermometer can be used, or a temperature sensor in the engine crankcase. Using the OBD system, it is possible to retrieve this information directly from the vehicle's ECU, making it the most reliable and efficient method for obtaining temperature readings. If the temperature falls below the required threshold, the engine should idle until the oil temperature rises to an appropriate level.

During the third step of the process, a specific cycle (defined in Table 4-1) is performed. To start, the measurement equipment's probe is inserted into the vehicle's exhaust pipe, and the OBD reader is connected to the vehicle's OBD port (as shown in Figure 4-3). Once the measurement equipment is set up to record the test data, the test follows five stages outlined in Table 4-1 while continuously measuring the NO_x concentration.



Figure 4-3. Gas analyzer probe into the exhaust pipe, and OBD reader connected.

To conduct the test, it is essential to read OBD data from the vehicles. Therefore, only vehicles equipped with an OBD port and supported communication protocol are eligible for the test. Most Euro 4 vehicles (but not all), as well as Euro 5 and Euro 6 vehicles, meet these criteria and can be tested. However, some Euro 3 vehicles can also be suitable for this type of measurement, though it is not guaranteed that OBD reading will be available in all of them.

During the test, for each stage defined in Table 4-1, at least the engine speed (rpm), the NO_x concentration (ppm NO_x), the engine load ("% engine load" value), the EGR valve aperture ("% EGR" value, if available) and the engine temperature (°C) have to be registered through the Gas Analyser and the OBD system. The test results are collected and organized according to the guidelines provided in Table 4-1.

The instructions in this table are followed to compile and present the data obtained from the various stages of the test, ensuring a structured and systematic approach to analyzing and reporting the results.

	Stage 1: Unloaded	Stage 2: Loaded	Stage 3: Loaded & Accelerated	Stage 4: Loaded	Stage 5: Unloaded
Engine speed	Idling	Idling	2500±500 rpm	Idling	Idling
Vehicle Equipment	Disconnected	Connected	Connected	Connected	Disconnected
Engine load value	<25%*	>25%*	Irrelevant	>25%*	<25%*

*Reference values, depending on the vehicle.

Table 4-1. Load stages and engine working conditions for the test cycle.

By utilizing all the data gathered from the test, it becomes possible to create the graph plotted in Figure 4-4. This graph is constructed using the compiled results, and it provides a visual representation of the data, allowing for a clearer understanding and analysis of the patterns and trends observed during the testing process.

To make the measurement process clearer, Figure 4-4 illustrates the various measurement phases graphically, accompanied by the corresponding actions listed in Table 4-1. This visual representation helps clarify the sequence of operations during the measurement.

The time of measurement is along the x-axis, NO_x concentration and NO_x mass flow are on the left y-axis, and engine speed, "% engine load", and % EGR aperture are on the right y-axis.

Once the probe is inserted into the exhaust pipe and the OBD reader is plugged into the OBD port, there is only one thing left to do. From the preparation of the vehicle, all the equipment has to be disconnected. Anyway, before starting, it is necessary to check this point again.

Once the engine is idling and all equipment is disconnected, **Stage 1** of the test can be started, with the equipment recording data.

The duration of the test reading time can be considered a matter of convenience, yet allocating 20 seconds for each stage is generally sufficient to accurately compute an average value for every stage. With the engine working at a steady state, it is not necessary to wait for a long time to get enough representative values. Yet if the engine working is irregular, a longer time might be required to get enough measurements to reach a representative average. The simplicity of the method allows for using as much time as necessary to get a correct measurement.

The employed software has been designed to ensure the ongoing recording of a 20-second test cycle, in accordance with the stipulated criteria for each Stage, as outlined in Table 4-1. If any alterations in the engine's operational circumstances transpire during the measurement process, causing any of the obligatory parameters to deviate from the prescribed conditions, the test procedure is temporarily suspended. Although data continues to be logged during this interval, it is not factored into the calculation of emission averages.

Once the engine conditions return to the required parameters, the measurement process automatically restarts. A new 20-second measurement is initiated to ensure a complete set of continuous 20-second measurements that adhere to the specified requirements. This approach guarantees the collection of accurate and consistent data by ensuring that measurements are taken under the appropriate conditions as outlined in the testing protocol.

When the reading time for this first stage is over, conditions for **Stage 2** must be reached. To achieve this, while keeping the engine at idle, the vehicle's equipment must be connected in the following sequence:

- 1) Air conditioning system, set to cold mode with the minimum temperature selected and the highest fan speed engaged.
- 2) The lighting and signaling system, including the Driving-beam headlamp, the Front and Rear position lamps, and the Front fog and Rear fog lamps.
- 3) Rear window heating system and Front windshield antifogging system.

When this equipment is switched on, it is noticed that the "% engine load" value starts to rise. This increase in engine load may take a few seconds before reaching its maximum value, as it depends on when the main power-consuming component, such as the air conditioning compressor, begins to demand maximum power.

The "% engine load" value may experience slight variations based on environmental conditions: higher temperatures and humidity levels can lead to increased power demand from the air conditioning compressor, impacting the engine load. However, the most significant differences in the "% engine load" value are primarily influenced by the connection-disconnection strategy of the air conditioning compressor during the journey [176].

Once all the described equipment has been connected, the "% engine load" value rises to approximately twice its initial value. Based on the complete set of tests conducted during the research, the average increase in "% engine load" from the unloaded stage to the loaded stage was 98%.

To provide some context, the average "% engine load" value at unloaded idle was measured at 20%, while the average "% engine load" value at loaded idle reached 38%.

This indicates that when the engine transitions from an unloaded state to a loaded state, it experiences a substantial increase in load, reaching approximately twice the initial value.

These findings demonstrate the significant impact that activating certain equipment, such as the air conditioning compressor, can have on the engine's load, and it highlights the importance of understanding these variations during testing and research.

Continuing with the test, once the allotted reading time for Stage 2 has elapsed, the conditions for **Stage 3** need to be established. To bring about this scenario, while keeping all the vehicle's equipment connected, the engine's rotational speed must be raised and sustained at 2500±500 rpm. The duration of this stage is identical to that of the preceding one.

Once the reading time for Stage 3 is completed, conditions for **Stage 4** must be met. To achieve this, all that is required is to stop accelerating the engine, allowing it to return to an idle state, while keeping the vehicle equipment connected.

Finally, once the reading time for Stage 4 concludes, in order to fulfill the conditions of **Stage 5**, all the equipment must be disconnected following the reverse order of the second stage. This process will revert the conditions back to those of Stage 1:

- 1) Rear window heating system and Front windshield antifogging system.
- 2) The lighting and signaling system, including the Driving-beam headlamp, the Front and Rear position lamps, and the Front fog and Rear fog lamps.
- 3) Air conditioning system, in cold mode at minimum temperature selection and with higher fan speed selected.

For each stage, the average values of the recorded parameters are computed. The key data for the measurement are derived from the combination of the average "% engine load" value and the average concentration of NO_x value. To calculate these averages, only the steady NO_x emissions and "% engine load" values are selected, specifically the data from the 20-second interval determined by the software during the test.

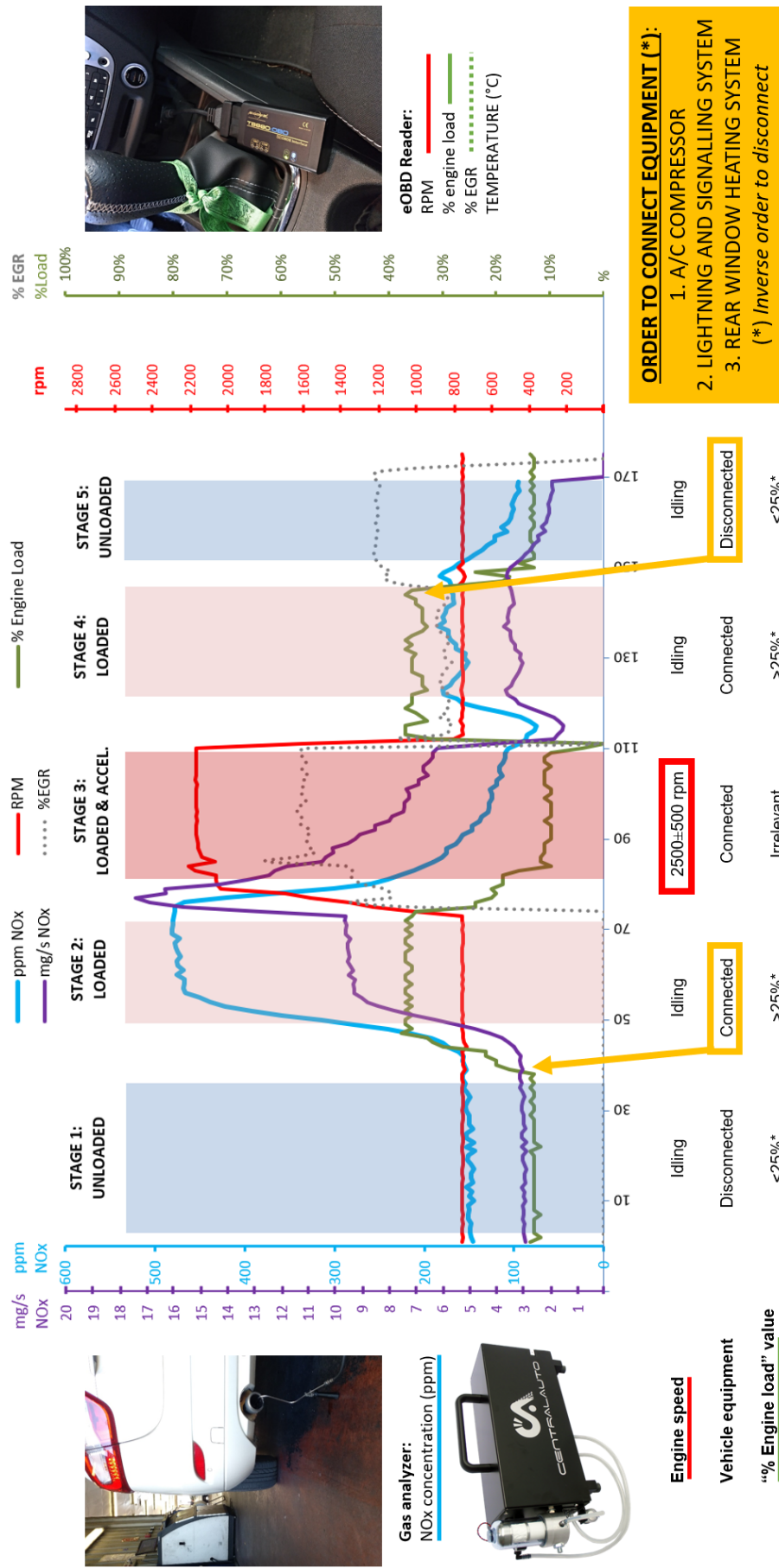


Figure 4-4. NO_x test for Euro 6 vehicle No. 20 and step-by-step test instructions.

Transient sections of data, where emissions are fluctuating due to changing engine load (between the stages), are avoided in this process. By focusing on the steady-state data points, the average values obtained more accurately represent the NO_x emissions corresponding to each engine load state. This approach ensures that the measurement results are reliable and reflect the true emission levels for each specific engine load condition.

To provide a clear illustration of the testing process, a specific vehicle is provided as an example (vehicle No. 20 from Table 6-1).

In Figure 4-6, the graphical representation illustrates the measurement results from the five previously described stages. To begin, we observe the initial Unloaded stage, where the average engine load stands at 13%, and the average NO_x concentration measures approximately 150 ppm. In the subsequent stage (Loaded state), the "% engine load" value rises to an average of 36%, accompanied by an increase in the average NO_x concentration to 465 ppm.

In these two stages, both the EGR and EATS systems were inactive, ensuring that the NO_x concentration reading remains unaffected by the emissions control system (refer to Figure 4-1). Notably, the % EGR aperture remains at zero until the commencement of stage 3.

Accordingly, the correlation between NO_x concentration and "% engine load", if exists, is not modified by the influence of other variables. The results of the tests carried out show that the indicators of the correlation (R^2 and p-value, see sections 6.3.1 and 6.3.2) between data of both variables are generally higher in these two stages than in other parts of the cycle, where other parameters may affect the concentration of NO_x.

The fact that the correlation between both variables is so significant in the absence of other influences at this stage seems to be evidence that there is a relationship between NO_x concentration and the "% engine load" value at idling.

During stage 3, the engine is accelerated to an average speed of 2163 rpm, and this modification in engine speed resulted in certain alterations in the engine's behavior.

Firstly, free acceleration leads to a decrease in the "% engine load" value. As mentioned earlier, when the engine speed rises, the available torque also increases (see Figure 4-1). However, in stage 3, despite the increase in engine speed, the power demand remains the same as in stage 2.

As a result, when both available torque and power increase, but the power demand remains constant, the "% engine load" value decreases. This pattern is evident in both Figure 4-2 and Figure 4-4, where an increase in engine speed leads to a decrease in the "% engine load" value. This observation was consistent in all the conducted tests.

Another notable change was observed: as the engine speed increases, the NO_x concentration decreases. This reduction is partly attributed to the decrease in the "% engine load" value.

This is another confirmation of the relationship between NO_x concentration and "% engine load". Although the absolute value of power demand is the same in stages 2 and 3, the NO_x concentration in stage 3 decreases. So, this reduction **is related to the**

"% engine load" value reduction, and **not to the absolute value of power demand**. The same behavior was observed in every test carried out.

Besides this, the engine acceleration may cause the opening of the EGR valve, which produces an additional reduction of NO_x concentration. In fact, this is the objective of the acceleration stage, trying to "wake up" the EGR valve and the other EATS of the vehicle.

This is a common operating pattern for vehicles. When a vehicle is in motion if it comes to a stop and idles the EGR and EATS also stop functioning while the vehicle remains stationary. However, when the vehicle starts moving again (upon shifting into gear and accelerating the engine), the anti-pollution systems recommence their action based on the parameters provided by the Engine Control Unit (ECU).

As can be seen in Figure 4-4, in the Loaded & Accelerated section the EGR valve is 56% opened on average. As a consequence, and in combination with the reduction from the engine acceleration, the average NO_x concentration in this 3rd stage is similar to the 1st stage, but with the following difference: in the 1st stage, the NO_x concentration is steady and continuous, while in the 3rd stage, the NO_x concentration is strongly decreasing from a maximum value of 478 ppm to a value near to 100 ppm. Meanwhile, the "% engine load" is reduced and maintained at 11% throughout this stage (slightly lower than at unloaded conditions, although the power demand is higher).

In the 4th stage, the engine speed returns to 750 rpm, the same speed as in the 1st and 2nd stages, and the engine load returns to 35% engine load, the same level as the 2nd loaded stage. However, the NO_x concentration in the 4th stage is lower than in the 2nd stage. This is because the EGR valve remains open at 30%, reducing the NO_x emissions of the engine, and by this, of the vehicle. As a result, the average NO_x concentration in the 4th stage is slightly higher than in the 1st stage and significantly lower than in the 2nd stage.

Finally, in the 5th stage, the EGR valve remains open (even more than in the 4th stage), while the "% engine load" value is reduced to the same level as in the 1st stage. As a consequence, NO_x concentration in the 5th stage is lower than in the 1st stage.

This behavior supports the hypothesis that NO_x concentration is related to the "% engine load" value at idling and checks that EGR action reduces the NO_x concentration in the vehicle exhaust gas.

4.2.3. DATA AGGREGATION, UNLOADED, AND LOADED STATES

As a result of the static measurement from the NO_x test, data to build Table 4-2 are obtained. To build this table, data from Stage 1 and Stage 5 are joined in the "Idle Unloaded" state, and data from Stage 2 and Stage 4 are joined in the "Idle Loaded" state, while data from Stage 3 are placed in the "Loaded & Accelerated" state (see Figure 4-5). The average values of NO_x concentration, "% engine load" and the other emissions and parameters are summarized and calculated for each one of the three states.

In order to ensure that the EGR system or other EATS are functioning during the measurement process (which is typically not the case initially), an accelerated section

is included. Although the NO_x values obtained during this section are not used to determine the NO_x emissions level, they serve the purpose of activating and assessing the operation of EGR and other EATS throughout Stages 4 and 5. This mimics their behavior in real driving conditions according to the ECU programming. By doing so, the influence of these systems on NO_x concentration is taken into account through the average values in the final result.

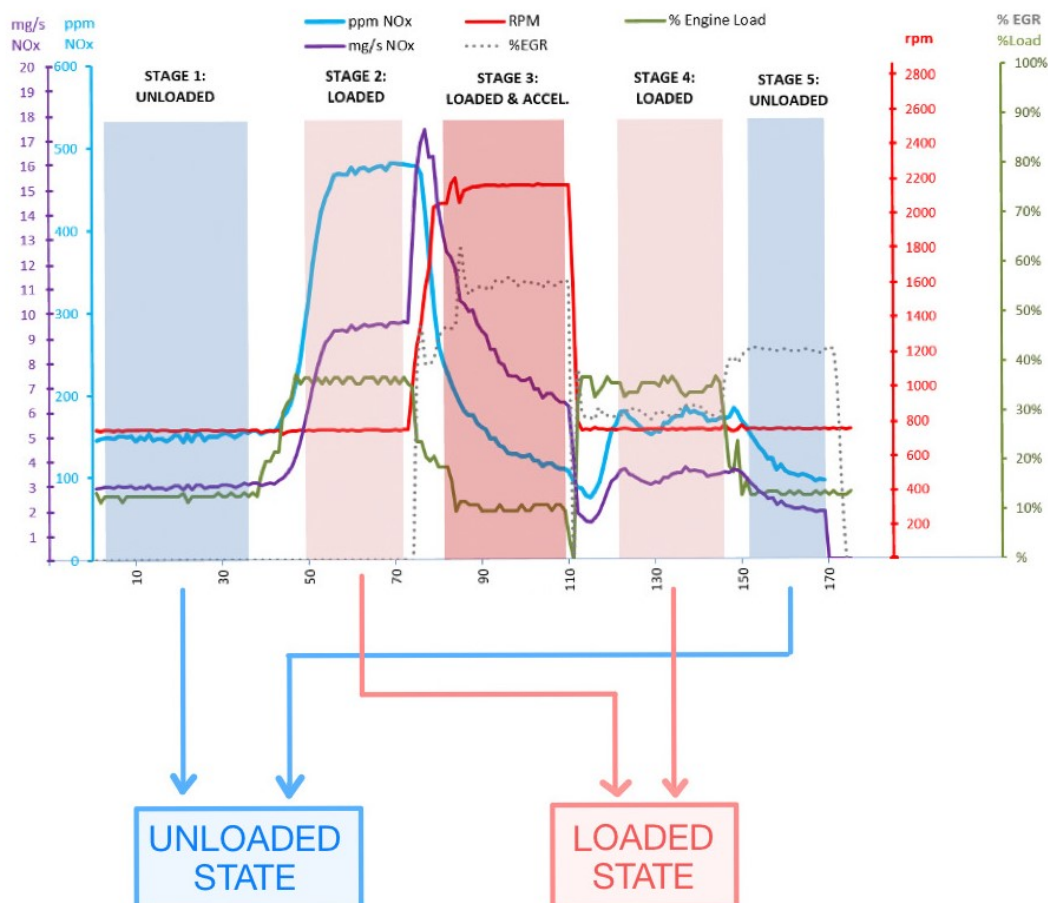


Figure 4-5. Data aggregation for Unloaded and Loaded states.

In essence, this simulation replicates the behavior observed in real urban driving. This setup ensures that the measurement process captures a more realistic representation of the vehicle's behavior and emission patterns during actual urban driving conditions.

As mentioned, in real urban circulation, the time that vehicles are stopped and idling can be even 60% of the time [108] at traffic jams, being a realistic approximation between 24% and 34% of the time [50], [166] in usual urban driving. Furthermore, for most of this idling time, the real conditions will be the same as stage 1 or stage 2, before acceleration.

On the other hand, calculating the average value using data before and after the acceleration provides a proper approximation to average the diverse scenarios encountered in real urban traffic. This approach considers both instances when the

vehicle is stationary, waiting to move, and when it starts to move with the EATS in action. By doing so, the influence of the EATS is appropriately accounted for in the final test result. Vehicles equipped with more efficient EATS can reflect their positive impact on the overall test outcome through this method.

State		Engine speed (rpm)	NO _x (ppm)	% Engine load	% EGR	Engine Temp. (°C)
Idle Unloaded	Av.	750	136	13	21	77
	Max.	774	178	24	43	79
Idle Loaded	Av.	750	306	36	30	77
	Max.	755	481	37	31	79
Loaded & Accelerated	Av.	2157	147	10	56	76
	Max.	2203	200	12	63	76

Table 4-2. Average measures in the static NO_x test.

From these results, it is possible to use the average NO_x concentration at both states as a simple indicator of NO_x concentration level, and Unloaded state concentration or Loaded state concentration could be used to make a comparison between vehicles (Bold data in Table 4-2).

Although these are the average values that are used to determine the NO_x emissions level, the results summary includes the maximum value of NO_x concentration read in the test because it will be used to estimate the maximum value of NO_x concentration (maximum value in the Unloaded and the Loaded state will be used, not in the accelerated state), by extrapolation with the unloaded and loaded values.

4.2.4. CALCULATION OF THE MASS EMISSION OF NO_x

Even though NO_x concentration can be used to compare the level of NO_x emissions between vehicles (most of the NO_x measurement test methods used until now provide NO_x concentration as a result), the most interesting data to do this comparison is not the concentration, but the mass emissions of the pollutants, in mg/s.

When comparing emissions between two vehicles with the same NO_x concentration at the exhaust pipe, it is important to consider that the vehicle with a larger engine size and/or higher engine idle speed will be actually emitting a greater quantity (mass) of NO_x. As a result, this vehicle has a more significant contribution to the overall pollutant concentration in the environment. If we solely rely on comparing the NO_x concentration, we might erroneously conclude that both vehicles emit the same amount, which is an incorrect assessment.

In approval-type procedures, the Emission Factor (g/km) value is used to compare pollutant emissions, yet from a static test, this value cannot be obtained. Instead, the

NO_x mass emissions flow can be used to compare emissions. This value is not directly obtained from the measurement equipment and should be calculated.

After understanding how to calculate the NO_x mass emission from the test data, it becomes possible to determine the instantaneous value of the NO_x emission mass flow in mg/s at each point of the test (refer to Figure 4-6). With these data, it is possible to calculate the average value for the "Unloaded Idle" state, for the "Loaded Idle" state, and the maximum value read in both states, in the same way, that the NO_x concentration average values were calculated.

Once these values are calculated and aggregated, there are two kinds of values to analyze the emissions of the vehicle: the value of concentration and the value of mass flow emission of NO_x.

As the measurement equipment does not provide the value of NO_x emission mass flow, but the NO_x concentration, it must be estimated from NO_x concentration and exhaust gas flow.

Since the test is developed for a quick measurement at PTI, not for a laboratory or homologation process, the accuracy from the following estimation method is considered enough for the test purpose.

In the first place, the Molar Volume of the exhaust gas is calculated with Equation 4-1.

Equation 4-1

$$V_m = \frac{n \cdot R \cdot T}{P}$$

V_m : Molar Volume of exhaust gas (l/mol)

n : the amount of substance (1 mol)

R : Ideal gas constant $\left(\frac{\text{mmHg}\cdot\text{l}}{\text{mol}\cdot^\circ\text{K}}\right)$

T : Gas temperature ($^\circ\text{K}$)

P : Gas pressure (mmHg)

With this value, NO_x concentration in mg/m³ in the exhaust gas flow is obtained from ppm concentration through Equation 4-2.

Equation 4-2

$$X_i = \frac{M_i}{V_m} \cdot x_i$$

X_i = NO_x concentration (mg/m³)

M_i = NO_x molecular weight (g/mol)

x_i = NO_x concentration (ppm)

At this point, as the measuring equipment employed utilizes solely a NO_x sensor, lacking differentiation between NO and NO₂ and offering a combined NO_x concentration value encompassing both compound concentrations (as per Equation 4-3), a determination must be made regarding the appropriate molecular weight value, M_i , for utilization in the calculation of Equation 4-2.

Equation 4-3

$$NO_x [ppm] = NO [ppm] + NO_2 [ppm]$$

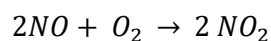
There were some possibilities:

- 1) Considering NO_x concentration as only NO
- 2) Considering NO_x concentration as only NO₂
- 3) Considering NO_x concentration as a proportion of NO and a proportion of NO₂

Option 3, which involved estimating the NO_x molecular weight as a proportion of both compounds (i.e., 50% NO and 50% NO₂) and subsequently calculating it using the molecular weights of both compounds (NO: 30 g/mol, NO₂: 46 g/mol), was thoroughly evaluated. However, there were three primary reasons for rejecting this option and ultimately selecting option 2:

- a) The proportion of both compounds is, in itself, an estimation, and this value varies for each vehicle.
- b) The measurement of NO_x concentration takes place in the exhaust pipe, where exhaust gases are released into the atmosphere. NO is a gas that readily oxidizes to NO₂ (as shown in Equation 4-4) at or above ambient temperatures. As a result, a significant portion of emitted NO is eventually converted to NO₂. Moreover, when expressing NO_x emissions in mass units, the same criterion is widely adopted in studies [50], [79], [83]
- c) NO₂ is more detrimental to human health compared to NO. Thus, for the sake of health protection, it is considered preferable to overestimate its value rather than underestimating it.

Equation 4-4



Summarizing, calculating the value of M_i based on the real proportion of NO and NO₂ present in the exhaust gases would be a more accurate option if the measurement equipment provided both values (being an easy improvement to implement), but since the equipment used for the development of the test only provides the aggregate NO_x data without disaggregating the measurement between the two components, using a theoretical proportion would be equally inaccurate but could lead to an underestimation of the emissions, so it has been considered a better option

to use the above criterion of considering all NO_x as NO₂, using the NO₂ molecular weight 46 g/mol to calculate the NO_x concentration in mass mode (mg/m^3).

Finally, the NO_x emission mass flow in mg/s is calculated with Equation 4-5 from the exhaust gas flow and the NO_x concentration.

Equation 4-5

$$\dot{m}_i = \dot{m}_e \cdot X_i$$

\dot{m}_i = NO_x emission mass flow (mg/s)

\dot{m}_e = Exhaust gas flow (m³/s)

X_i = NO_x concentration (mg/m³)

Although the exhaust gas flow (\dot{m}_e) is not measured in the test by the equipment, it can be estimated from the read test data with the OBD system. This approach is deemed sufficiently accurate for the measurement method's purpose, offering the added advantage of eliminating the need for an exhaust flowmeter. This reduction in equipment requirements not only lowers the overall cost but also simplifies the test execution process, making it a more favorable option.

Even for the PEMS equipment (used for the homologation process), there are accepted methods to estimate the exhaust gas flow without using a direct flowmeter read. These alternative estimation methods include using data from fuel consumption, intake airflow, vehicle speed, and O₂ concentration. The accuracy of the results obtained from these estimation methods is comparable to the values obtained using flowmeters or pitot tubes, making them reliable alternatives [50], [129], [155], [177].

The intake airflow could be measured through OBD, but sometimes these data are not available. Therefore, the method used is to **estimate** the intake airflow from the engine size and engine speed.

It can be assumed that, under a specific engine speed condition, a diesel engine's intake airflow is maximized, aiming to achieve the highest possible air intake. Furthermore, it is considered that the engine's **volume** of intake airflow is equal to the volume of exhaust gas exiting the engine [178]. Consequently, based on the engine size and speed, it becomes possible to estimate the volume of exhaust gas flow at the outlet.

4.2.5. TEST FINAL RESULT: 100% ENGINE LOAD NO_x EMISSIONS' EXTRAPOLATION

The average values for the "Unloaded Idle" and "Loaded Idle" states, including NO_x concentration and NO_x emission mass flow, are shown in Table 4-3 for a complete overview of NO_x emissions. The other values registered in Table 4-2 is not included because they are not relevant for the calculation of NO_x emissions, although they

provide relevant information that could be used for other purposes such as academic research.

Once the set of values for both states including the maximum instantaneous value read from both states (only from the Unloaded and Loaded states, not from the Accelerated state) is completed, it is possible to define a linear regression function to extrapolate values from NO_x concentration and NO_x mass emission related to the "% engine load" value.

	NO _x (mg/s)	NO _x (ppm)	% Engine load
Avg. Idle Unloaded	2.72	136	13
Avg. Idle Loaded	6.10	306	36
Maximum Read	9.59	481	37
Theoretical Maximum	21.84	1096	100

Table 4-3. Summary of final results in static NO_x test.

Finally, once both linear regression functions are available, Table 4-3 can be completed. The TMV (Theoretical Maximum Value) of NO_x emission mass flow (mg/s) is the estimation from the regression function of NO_x emissions mass flow if the vehicle was at 100% engine load at the idling state and is the estimated data that define the NO_x emissions level and can be used to compare NO_x emissions between vehicles. It is an indicator of NO_x emissions and it could be helpful to detect NO_x high emitters and to classify the fleet according to this NO_x emissions level. This calculation could be easily incorporated into measurement software as the final result of the test. The same value can be calculated for NO_x concentration, with the same interpretation and usefulness.

The mathematical process to calculate the regression function and estimate the TMV is outlined as follows.

From the measurement process, after the aggregation process of the measured values of NO_x emissions and "% engine load" in the Unloaded State and Loaded State (see Figure 4-5) as was explained in 4.2.3, a table like Table 4-3 is obtained. This table summarizes the average values of NO_x concentration in ppm and NO_x emission flow in mg/s for each of these states, related to the average value of the "% engine load" for these states.

In other words, after the measurement and aggregation process, the set of values measured throughout the test has been reduced to two values representing the average value of the emissions in two different states of power demand for a specific engine operating condition, i.e. idling.

In addition to these two values, the maximum emission value recorded from any of these two states (unloaded or loaded) is also available for the regression, with its correspondence value of "% engine load".

Finally, also point (0,0) is used to define the linear function, since according to the definition of "% engine load", its value is 0% at engine off and, at this point, the NO_x emissions are null.

From these 4 different values, a linear extrapolation can be performed to determine the estimated value of NO_x emissions (both in concentration and mass emission flow) when the "% engine load" reaches the maximum value of 100%.

To do this, a linear function must be defined from the previously selected data. This linear function will have the form of a straight line (Equation 4-6), which will be calculated as a regression of the dependent variable Y (NO_x emissions, either in the form of concentration or in the form of mass emission flow) on the independent variable X (the "% engine load" value).

Equation 4-6

$$Y = a + bX$$

For this purpose, the Least Squares method is used, which consists of minimizing the sum of the squares of the residuals (Equation 4-7), being residuals the difference between current values y_i and estimated values \hat{y}_i .

Equation 4-7

$$\sum_{i=1}^n e_i^2 = \sum_{i=1}^n (y_i - \hat{y}_i)^2$$

Through the application of this method, the following expressions are obtained, to build:

Equation 4-8

$$a = \bar{y} - b\bar{x}$$

Equation 4-9

$$b = \frac{S_{XY}}{S_X^2}$$

being \bar{x} and \bar{y} the average values from both variables,

Equation 4-10

$$\bar{x} = \frac{\sum_{i=1}^n x_i}{n} \quad x_i = \text{"\% engine load" value}$$

Equation 4-11

$$\bar{y} = \frac{\sum_{i=1}^n y_i}{n} \quad y_i = \text{NO}_x \text{ emissions value (ppm or } \frac{\text{mg}}{\text{s}})$$

and S_X^2 the variance of X and S_{XY} the covariance between X and Y.

Equation 4-12

$$S_X^2 = \frac{\sum_{i=1}^n (x_i - \bar{x})^2}{n}$$

Equation 4-13

$$S_{XY} = \frac{\sum_{i=1}^n (x_i - \bar{x})(y_i - \bar{y})}{n}$$

As a result, once the linear function is defined according to Equation 4-8, the value of NO_x emissions can be estimated for 100% value of "% engine load", and the linear function can be drawn for the graphical representation of the NO_x emissions at idling, both for mass flow (see Figure 4-6), and concentration (see Figure 4-7), and the R² value of relationship calculated to define the quality of the linear regression.

The high quality and significance of the relationship between "% engine load" and NO_x concentration make possible the extrapolation from these 4 pairs of values (x_i, y_i).

Furthermore, the recorded NO_x emissions and "% engine load" values for both Unloaded and Loaded states are averages derived from 20 seconds of measurements. These averages encapsulate a substantial volume of data, yet they are presented in a simplified manner that is easily comprehensible.

As mentioned earlier, the average NO_x emissions mass flow during Idle Unloaded and Idle Loaded conditions offers a highly accurate estimation of the actual NO_x emissions from the vehicle when it comes to a halt at a red light or gets stuck in a traffic jam during urban driving.

The insights gained from the entire vehicle fleet can be very valuable for quantifying anticipated NO_x emissions at specific locations. This data could prove essential when evaluating the installation of traffic lights or determining the optimal duration for a red light, preventing emissions from stationary vehicles from reaching hazardous levels. This information is particularly advantageous when assessing the viability of traffic lights in proximity to sensitive areas like hospitals or schools.

Furthermore, this knowledge finds utility in scrutinizing and confirming the outcomes of implementing Low Emissions Zones (LEZ) within urban areas. In essence, the data can contribute to informed decision-making for urban planning, emission control, and public health enhancement.

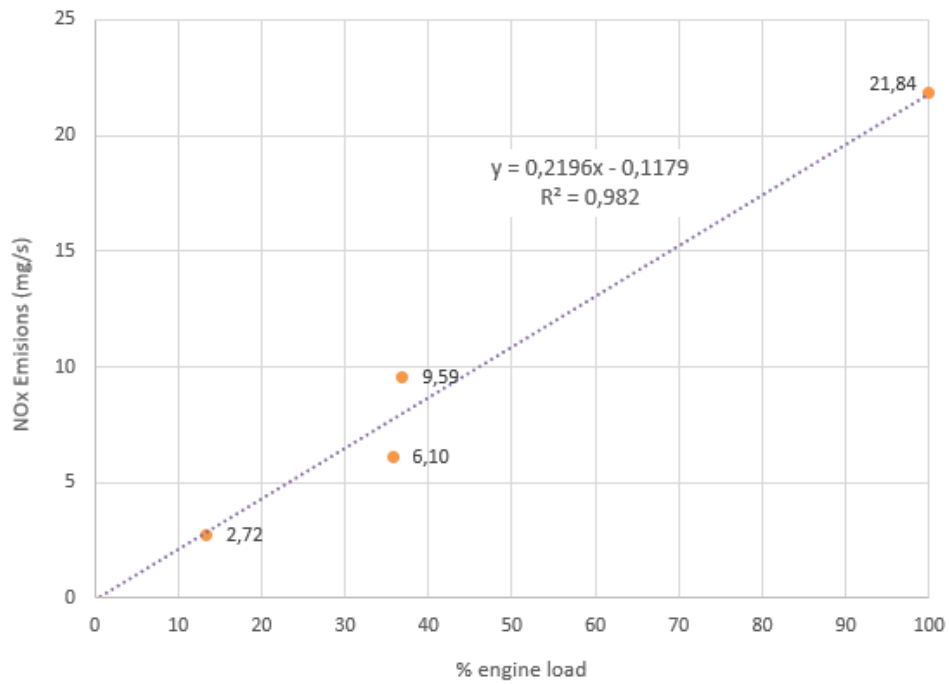


Figure 4-6. "NO_x emission mass flow - % engine load" linear regression function.

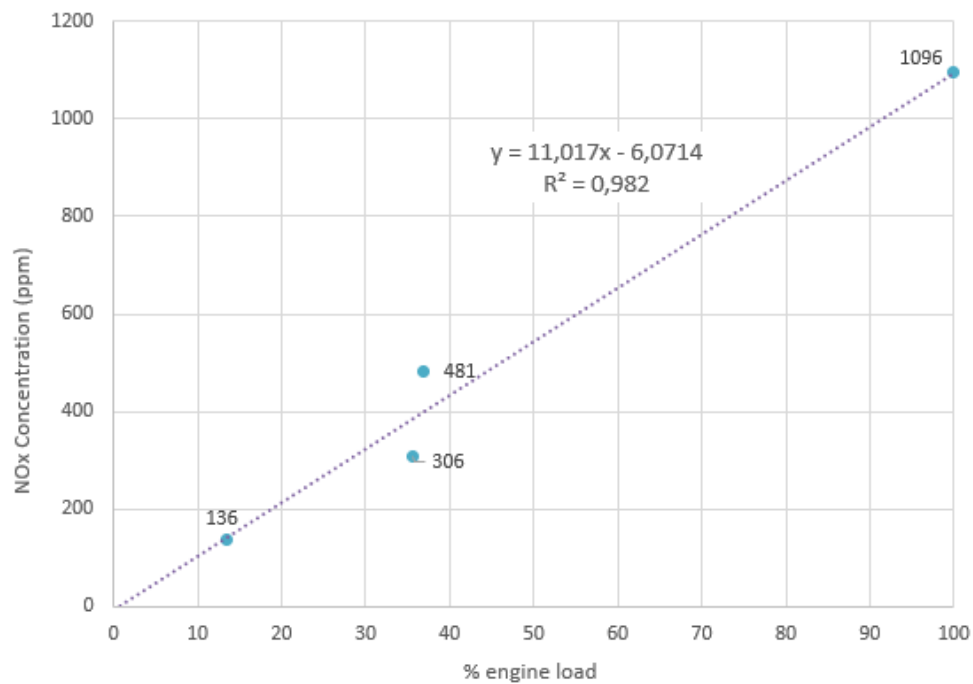


Figure 4-7. "NO_x concentration - % engine load" linear regression function.

In conclusion, the average values obtained from the test provide a reliable estimate of the actual NO_x emissions when the vehicle comes to a stop in real traffic conditions, but: *what is the meaning of the TMV (Theoretical Maximum Value) of NO_x emission?*

The difference in NO_x emissions between the "Unloaded Idle" and "Loaded Idle" states, along with the values collected during phases where the EGR and EATS are operational (as determined by the ECU programming) after acceleration, serves as an informative "footprint." This footprint offers valuable insights into how NO_x emissions could behave when the engine operates under a load.

The TMV of NO_x emission (both in concentration and mass flow) does not reflect a real value of emissions that the vehicle will present in circulation: the vehicle will never be, under normal driving conditions, at idle speed and subjected to "100% engine load".

Nonetheless, this theoretical value can be readily calculated based on the average data collected during the measurement for the "unloaded" and "loaded" states. These "unloaded" and "loaded" data correspond to real-life scenarios frequently encountered during vehicle operations in urban settings. This insight helps determine whether the vehicle's emissions will rise to a greater or lesser extent based on the variation between emissions in the "unloaded" and "loaded" states.

In other words, a vehicle that presents a small variation in emissions between both load states will have a regression line with a small slope (inclination of the regression line), and therefore, as the power demand from the engine increases, NO_x emissions will increase as indicated in that line.

Instead, a vehicle with a greater variation in emissions between both load states will have a steeper regression line and, therefore, the increases in NO_x emissions will be greater for similar increases in engine power demand than in the above case.

By using the average emissions values measured before and after the acceleration state, which triggers the activation of EATS in the latter part of the test, it becomes possible to assess whether vehicles equipped with improved EATS achieve a greater reduction in emissions. In essence, this test allows us to verify whether theoretically superior vehicles (Euro 6 standard or other advanced emission control systems) exhibit lower emissions compared to other vehicles.

The change in the slope of the regression line occurs as a result of the emission reduction observed in the second part of the test when the EATS are activated (if they are effective). This change is directly linked to the significant reduction in emissions achieved through the efficient operation of the EATS.

A vehicle equipped with highly effective emission control systems, which become active from the moment of engine acceleration, exhibits lower emission values in the second part of the test compared to the first part. This leads to a regression line that tends towards a horizontal orientation. In other words, the steeper emission reduction in the second part of the test contributes to a shallower slope in the regression line, indicating the superior performance of the vehicle's emission control systems.

When calculating the regression line, this implies that the slope of the function representing the maximum value has a shallower incline (and hence, the estimated

maximum value is lower) in comparison to a vehicle with less effective anti-pollution systems.

This characteristic of the regression line often has a more significant influence on the estimated maximum emissions value than the actual measured emissions value during the test. In simpler terms, a vehicle with higher concentrations of emissions in both the unloaded and loaded states might have a lower estimated value at 100% load compared to another vehicle with lower measured emissions values. However, the latter vehicle could show a steeper regression line due to a greater difference between loaded and unloaded emissions. Consequently, the estimated maximum value is more affected by the slope of the regression line rather than solely relying on the measured emissions value itself.

From the experience gained while presenting the proposed measurement method in various forums, it seems necessary to specifically justify the need to carry out an extrapolation from the emission values measured in the inspection, and the suitability and feasibility of this extrapolation to provide a value of NO_x emissions at 100% engine load.

The first part, the necessity of extrapolation, has already been extensively justified previously when considering and demonstrating that the value of emissions at 100% engine load is an adequate indicator to be used in the comparison of emissions between vehicles and that it is, therefore, necessary to estimate its value.

Regarding the second segment, the practice of extrapolating the emission value at 100% "% engine load" is deemed accurate. This judgment stems from the validation process of the method's development, along with subsequent measurements. These examinations have affirmed a robust correlation between the "percent engine load" metric and both the NO_x concentration in the exhaust pipe and the calculated mass flow of NO_x within the exhaust pipe. This correlation is established given that the mass flow is deduced from the NO_x concentration. This relationship shows high quality with high R² values and a high significance with a p-value below 0.01.

However, the question may arise as to whether the extrapolation of this value based only on 4 known values provides sufficient quality of estimation for the value to be valid.

At this point, it must be remembered that the test is designed and conceived for its application in PTI. This implies that, as indicated by the ISO 21069-1:2004 [179] standard, the adequacy for the intended purpose does not necessarily represent a search for the best quality that the test methods can give, since this approach could entail unnecessary expenditure on the performing measurements (for example, with too small a bias and precision, which might not be of practical use).

Applying this principle, the calculation in PTI of the braking efficiency of vehicles of categories M2, M3, N2, N3, O3, and O4 is carried out through a procedure similar to that proposed here to determine the maximum NO_x emissions value, which, based on empirical measurement, and knowing an initial data before the actuation of the brake system, an extrapolation is carried out to estimate the maximum braking force value that the vehicle will perform and, with this value, calculate the braking efficiency achieved for the maximum load assumption.

This extrapolation can be performed, according to ISO 21069-1:2004 standard, with only one braking force measurement point, as the starting point of the extrapolation is standardized and assumed to be a fixed value for all braking threshold pressures.

In case this starting point is not standardized, a low-pressure measurement of the actuator should be made and subsequently, a measurement using the maximum applicable braking force.

In either situation, the extrapolation is carried out from only two known values, this method is accepted and applied in the determination of the braking efforts and applied in the PTI because is considered accurate enough. This is possible because the standard applies the assumption that braking forces increase predictably with increasing pressure.

In the case of NO_x emissions, it is not necessary to apply the "assumption" that NO_x emissions increase predictably with increasing "% engine load", because the quality and representativeness of such a relationship can be checked at each measurement by using the p-value and calculating the R² of such a relationship.

Furthermore, the extrapolation process in the case of NO_x emissions is carried out based on 4 known values (instead of the two accepted values in the braking test):

- 0% of "% engine load", 0 ppm (0 mg/s) of NO_x emissions
- Average emissions at Unloaded Idle State
- Average emissions at Loaded Idle State
- The maximum value of emissions measured in either of the two states

It is important to remember that the averages of the emissions in the unloading and loading states represent 20 seconds of stable data in each of the two states. As a result, the regression function obtained from these four points has R² values of the order of 0.97 or higher, guaranteeing the quality of the extrapolation carried out from the average values.

In summary, the process of extrapolation from empirically obtained values to estimate a maximum value is standardized and is used in PTI because it is considered sufficient for the estimation of maximum braking values from only one measurement. Therefore, and given that the existence of a relationship between the value of "% engine load" and the concentration of NO_x measured in the exhaust of vehicles has been justified, it is considered that the process of extrapolation of NO_x emissions, based on 3 values obtained from measuring directly in the vehicle is adequate and accurately enough to estimate the NO_x emissions of vehicles in the case of reaching a value of 100% "engine load", and it is also considered appropriate to use this value as an indicator of the level of NO_x emissions of the vehicle and its use for the comparison of the level of emissions between different vehicles.

4.3. SUMMARY OF THE MEASUREMENT PROTOCOL

The essential tasks required to perform the measurement can be grouped into four main categories. To provide a simplified overview of the entire measurement procedure, the key steps for conducting an accurate measurement are presented as a concise summary of the measurement protocol.

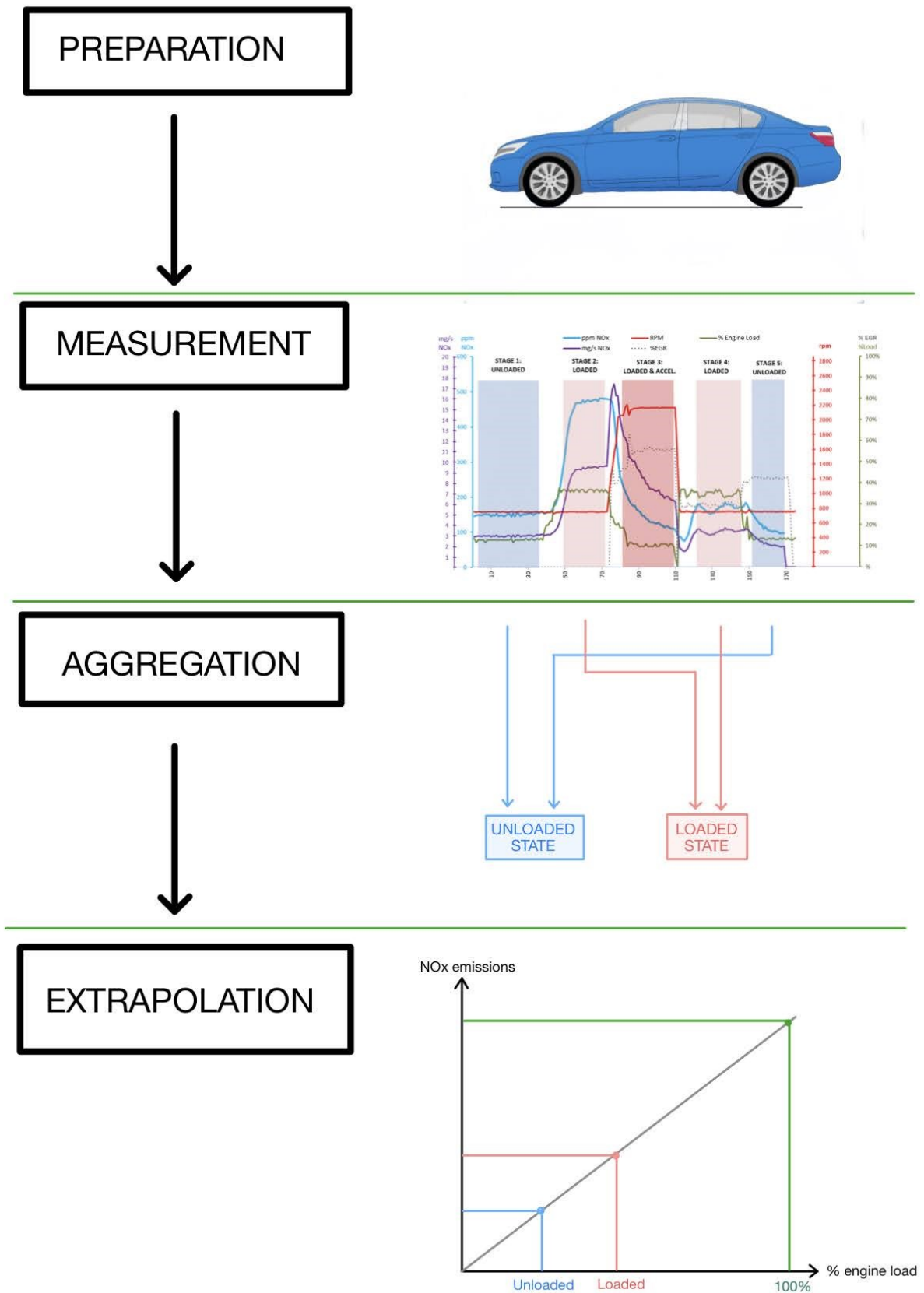


Figure 4-8. Graphical summary of the NO_x measurement protocol.

The four main categories (see Figure 4-8) are as follows:

- 1) **Vehicle Preparation**, as detailed in section 4.2.2 involves verifying the vehicle's conditions and preparing it accordingly.
- 2) **Exhaust NO_x Concentration Measurement** in five stages (see section 4.2.2.)
- 3) **Data Aggregation**, as outlined in section 4.2.3, both in the Unloaded and Loaded states
- 4) **Extrapolation to 100%** engine load as defined in 4.2.5

Figure 4-4 illustrates the measurement process in a graphical manner to simplify the execution of the procedure. It indicates the specific points at which adjustments to power demand and engine rotational speed should be made, as specified in Table 4-4.

Before performing the Aggregation and Extrapolation steps, it is necessary to estimate the mass flow emissions of NO_x based on the NO_x concentration, as specified in section 4.2.4.

Following the **Aggregation** process, the average NO_x emissions values are determined for both the Unloaded Idle State and Loaded Idle State. This provides valuable insights into the actual emissions of the vehicle during urban driving conditions. The calculation involves averaging the NO_x **concentration (ppm)** and the corresponding NO_x **mass flow (mg/s)**.

As a result of the **Extrapolation** step, the anticipated values for NO_x **concentration (ppm)** and **mass flow emissions (mg/s)** under 100% engine load at idling (referred to as TMV) are derived. These TMV values can be regarded as the ultimate outcomes of the test, serving the purpose of comparing NO_x emission levels among different vehicles and establishing a threshold for rejection.

Both sets of results, including the average values and TMV calculations, are compiled and summarized in the

Table 4-5 alongside the corresponding "% engine load" values. This comprehensive presentation aids in providing a clear overview of the emissions data obtained from the measurement procedure.

	Stage 1: Unloaded	Stage 2: Loaded	Stage 3: Loaded & Accelerated	Stage 4: Loaded	Stage 5: Unloaded
Engine speed	Idling	Idling	2500±500 rpm	Idling	Idling
Vehicle Equipment	Disconnected	Connected	Connected	Connected	Disconnected
Engine load value	<25%*	>25%*	Irrelevant	>25%*	<25%*

*Reference values, depending on the vehicle.

Table 4-4. Stages and engine working conditions for the test cycle.

	NO _x (mg/s)	NO _x (ppm)	% Engine load
Avg. Idle Unloaded	2.72	136	13
Avg. Idle Loaded	6.10	306	36
TMV (Theor. Max. Value)	21.84	1096	100

Table 4-5. Sample of final results of the measurement procedure.

4.4. CONCLUSIONS

In this chapter, the proposed NO_x measurement method has been described in detail. Starting with a step-by-step description of the method's execution for the measurement process, it elaborates on how to perform data aggregation and the procedure for estimating the TMV.

Throughout the chapter, all the necessary information has been provided to replicate the measurement method, including the mechanisms to verify the validity of the measurements.

The key highlights are as follows:

- The measurement process consists of four phases: preparation, measurement, data aggregation, and extrapolation of the maximum value.
- The measurement process provides two types of results: actual emission values when the vehicle is idling (unloaded and loaded), and the TMV when idling, which is used for comparing emissions levels among vehicles.
- The measurement method yields two types of values for each result: NO_x concentration values (ppm) and emitted NO_x mass flow values (mg/s).
- The method allows for assessing the quality of the relationship between the analyzed variables and their significance based on the data obtained during the measurement. This ensures that each measurement is conducted correctly, and the results are statistically significant.

The following chapter will analyze the measurement equipment, and ITS suitability to perform the NO_x measurement in PTI. This analysis will encompass its compliance with the usage requirements within the PTI context, as well as the validity of the yielded results.

CHAPTER 5

PTI MEASUREMENT EQUIPMENT DESCRIPTION AND SUITABILITY

5. PTI MEASUREMENT EQUIPMENT DESCRIPTION AND SUITABILITY

5.1. INTRODUCTION

After defining, describing, and validating the method in the previous two chapters, the current chapter will cover all aspects related to the measurement equipment.

The selection of measurement equipment holds paramount importance as it directly influences the suitability of the measurement for the PTI process.

Throughout the chapter, a detailed description of the utilized measurement equipment and its technical characteristics will be provided to ensure that it meets the necessary requirements for use in PTI.

Finally, the performance of the equipment will be compared with a reference gas analyzer used for measuring NO_x emissions in certification processes. This reference device is theoretically designed to meet the highest standards and possesses the highest precision in NO_x measurement.

Through this comparison, it will be determined whether the results obtained with the equipment used in PTI are suitable for the objective of measuring NO_x emissions in PTI.

5.2. GAS ANALYZER DESCRIPTION

The test, as defined in its simplest terms, can be performed using any gas analyzer capable of quantifying the concentration of NO_x (or separately, NO and NO₂) within the exhaust pipe. Moreover, the equipment should possess the capacity to capture these measured values at a minimum frequency of 1 Hz. Concurrently, it is essential to log engine operational parameters via the OBD system, and these logged data must be synchronized with the NO_x concentration readings.

Indeed, it's important to note that not every equipment that meets the specified criteria can be employed for NO_x measurement during the PTI. The main objective revolves around establishing a distinct measurement protocol tailored for PTI. Consequently, the emphasis is on leveraging equipment that is either currently present at PTI stations or shares similarities with the commonly used devices in those settings. This strategic approach serves to maintain uniformity and familiarity with the equipment among PTI staff, facilitating the seamless integration of the NO_x measurement procedure during inspection operations.

The PTI has strong requirements that must be complied with, about the time and cost of the process along with the inspection. Equipment used in PTI has to be according to these requirements, so most of the equipment is "PTI grade", which means, specifically designed to be used in PTI with **intensive use, minimum maintenance costs, ensured metrological control, and without intervention over the vehicle to perform the inspection.**

Although it could be simple, this means that most of this equipment has to be specifically designed for this function, not being on many occasions adequate because they do not meet all the requirements of the equipment used in mechanical workshops or homologation laboratories.

During the initial phases of test development, several types of NO_x measurement equipment were taken into account. Nevertheless, after a thorough evaluation, the conclusion was reached that the optimal choice would involve utilizing the pre-existing gas analyzers equipped with NO_x measurement functionalities, which are currently accessible at PTI stations. This decision was made to leverage the equipment that is already in place, ensuring efficiency and familiarity with the tools among PTI personnel, and thereby facilitating the implementation of the NO_x measurement process. This choice was also facilitated by the fact that most of the main manufacturers of PTI emissions equipment have some piece of equipment with the capacity to measure NO_x.

For the definition of the proposal, the choice was the gas analyzer TEKBER CENTRALAUTO model SPEKTRA 3011, equipment commonly used in PTI stations in Spain. It is used for the measurement of CO emissions and lambda values in the exhaust gases of petrol engine vehicles. The equipment used has Model Test (Class I) No. 370-B-57/12-M [40], is following the UNE 82501, and for the realization of the measurements has been equipped with an electrochemical NO_x sensor manufactured by IT (International Technologies Dr. Gambert GmbH), which is included in the Model Test approval.

The gas analyzer is based on the Andros 6900 subsystem, which exceeds worldwide gas-measurement performance specifications for automotive emissions, including EPA ASM, ASM/BAR-g7, OIML Class 0, and OIML Class 1. Additional technical characteristics of the Andros 6900 subsystem can be found in the appendix section.

The quality and accordance with international specifications of the equipment guarantee correct measurements from the equipment and validity of data registered.



Figure 5-1. Centralauto Spektra 3011 Gas Analyzer

The NO_x sensor works as a potentiostatic-driven cell backed up by an onboard battery and has a measurement range of 0 to 5000 ppm vol., an accuracy of ± 20 ppm abs. and ± 4% rel., and an annual deviation of less than 5% of the signal, according to the manufacturer's specifications. This sensor is included in the Model Examination of the gas analyzer. The operating range of the sensor is suitable for the measurements to be made, given that the usual values to measure move within the range of 0-2000 ppm. The most important characteristics of the NO_x sensor are related in Table 5-1.

As per the manufacturer's recommendations, calibrating the NO_x channel is advised after replacing the NO_x sensor and should be conducted monthly during regular operations. In scenarios involving intensive usage, more frequent calibrations might be necessary. Simultaneously, during the process of designing and validating the measurement method, the equipment has been subjected to **weekly calibration** using a certified standard gas cylinder. This practice aims to mitigate measurement errors stemming from sensor signal deterioration.

The Certificate of Calibration of the gas cylinder is included in the appendix section, being the concentration of NO_x used for the calibration process 2002,9 ppm NO_x. This value is included in the span calibration gas range declared by the equipment manufacturer.

The functioning of the NO_x measurement potentiostatic cell is as follows: The gas sample under analysis flows through the cell, initiating an electrochemical reaction. This reaction leads to the generation of an electrical signal at the sensor's output, which corresponds proportionally to the concentration of the target gas (NO_x) within the analyzed gas sample. The sensor produces a linear output ranging from 45 to 75 nA for each part per million (ppm) of NO_x concentration detected in the gas sample.

The NO_x sensor output is sent to the ADC converter, providing a digital value of the gas concentration (in ppm). This concentration is determined by a comparison between the sensor output at calibration (with the certified standard gas cylinder) and the output of the measurement performed.

Utilizing this equipment provides multiple benefits, mainly due to its status as the standard apparatus commonly used for emission assessments in PTI stations. Its routine implementation causes minimal disruption to the regular PTI station operations during such tests. This advantage was significant throughout the test for method definition and could be deemed a prerequisite for any future NO_x measurement equipment: **the equipment used for NO_x measurement must integrate into the PTI process easily.**

The complete measurement arrangement comprises the previously mentioned Gas Analyzer equipment and a computer running specialized software developed by the manufacturer of the analyzer. This software takes charge of reading and capturing the data, overseeing the test process, and producing a set of files containing the logged data for subsequent analysis.

The combination of the Gas Analyzer and the dedicated software ensures a comprehensive and efficient measurement process, allowing for accurate data collection and analysis during the test.

Characteristics	
Operating Principle:	Potentiostatic-driven cell backed up by an onboard battery
Electrical Connector:	4-pin Molex
Gas Connector:	M 16 × 1
Measurement Range:	0 to 5000 ppm
Output Signal:	45 to 75 nA/ppm
Response Time:	<5 s
Drift:	<5% of signal per annum
Operating Temperature:	0 to 50 °C
Pressure Range:	750 to 1750 hPa
Linearity Error:	±3% from 0 to 2000 ppm ±5% over 2000 ppm to full scale
Repeatability:	±2% of the signal, 20 ppm absolute
Recommended Load:	10 Ohm
Interferences:	±20 ppm NO response to: 16% CO ₂ balance N ₂ 10% CO balance N ₂ 100% rare gases 3000 ppm C ₃ H ₂ balance N ₂ 75 ppm H ₂ S balance N ₂ 75 ppm SO ₂ balance N ₂ 1000 ppm Benzene balance N ₂
All characteristics are based on conditions at 25 °C RH and 1013 hPa	

Table 5-1. NO_x sensor technical characteristics. Source: Tekber.

Furthermore, the equipment concurrently carries out the retrieval of a sequence of engine operational parameters via the OBD port of the vehicle. The utilization and attributes of the measurement software are detailed in section 11.1.

The essential operational details for the equipment are outlined below. The proper functioning and storage of the equipment require adherence to specific environmental conditions, which are specified in Table 5-2.

Environmental condition	Operating range	Storage range
Temperature	0°C to 50°C	-20°C to 70°C ⁽¹⁾
Humidity	5% to 95% (non-condensing) ⁽²⁾	
Atmospheric pressure	930 mbar ± 130 mbar	
Altitude	-300 m to 3000 m	
Vibration	1.0g senoidal, 5 to 1000 Hz	0.01g ² /Hz
Shock	1.22 m on a concrete floor	
EMI/EMC	CRF Title 47, Part 15, Subpart J, Class A y B. CFR Title 47, Part 68.	

⁽¹⁾ The storage temperature range for the NO_x sensor is from -20°C to 50°C. These sensors can be stored in this range for more than 10 days. The optimum temperature of storage of this type of sensor is between 5°C to 20°C.

⁽²⁾ For the NO_x sensor the specific humidity range is 15% to 90% RH.

Table 5-2. Gas Analyzer Environmental Requirements.

The gas analyzer provides measurement ranges and associated errors as outlined in Table 5-3 for various gases it is capable of measuring. The definitions employed are as follows:

Measurement range. The range is measured by the sensors. It applies to both measurement and noise.

Error. Difference between the measured value and the true value.

Repetition. Individual tolerance when repeating the same measurement.

Noise. Transients in the measurement produced by the analyzer.

Resolution. The smallest increment that is returned.

Gas	Measurement range	Error	Repetition	Noise	Resolution
HC n-Hexane	0 to 2000 ppm	±4 ppm abs. or ±3% rel.	±3 ppm abs. or ±2% rel.		
	2001 to 7000 ppm	±5% rel.	3% rel.		
	7001 to 15000 ppm	±15% rel.	5% rel.	2 ppm abs. or 0.8% rel.	1 ppm
	15001 to 30000 ppm	Not specified	Not specified		
HC Propane	0 to 4000 ppm	±8 ppm abs. or ±3% rel.	±6 ppm abs. or ±2% rel.		
	4001 to 30000 ppm	±15% rel.	±5% rel.	4 ppm abs. or 0.8% rel.	1 ppm
	30001 to 60000 ppm	Not specified	Not specified		
CO	0.00 to 10.00%	±0.02% abs. or ±3% rel.	±0.02 abs. or ±2% rel.	0.01% abs. or 0.8% rel.	0.001vol.%
	10.01 to 15.00%	±5% rel.	±3% rel.		
CO ₂	0.00 to 16.00%	±0.3% abs. or ±3% rel.	±0.1 abs. or ±2% rel.	0.1% abs. or 0.8% rel.	0.01vol.%
	16.01 to 20.00%	±5% rel.	±3% rel.		
NO _x	0 to 4000 ppm	±25 ppm abs. or ±4% rel.	±20 ppm abs. or ±3% rel.	10 ppm abs. or 1% rel.	1 ppm
	4001 to 5000 ppm	±5% rel.	±4% rel.		
O ₂	0.00 to 25.00%	±0.1% abs. or ±3% rel.	±0.1% abs. or ±3% rel.	0.1% abs. or 1.5% rel.	0.01vol.%

Table 5-3. Gas Analyzer Error Parameters.

In this equipment designed for measuring gases in a mixed stream, it is important to consider that the presence of one type of gas can potentially cause errors in the measurement of another gas.

Gas	Maximum interference
HC	±4 ppm
CO	±0.02%
CO ₂	±0.20%
NO _x	±20 ppm

Table 5-4. Maximum interference between gases.

In this equipment designed for measuring gases in a mixed stream, it is important to consider that the presence of one type of gas can potentially cause errors in the measurement of another gas.

The interactions between different gases in the mixed stream can influence the accuracy of the measurements. The Centralauto SPEKTRA 3011 has interference values between gases that follow OIML Class 0/1 and BAR-g7 specifications, which are shown in Table 5-4.

It can be observed that the error from the equipment for the NO_x measurement is similar ($\pm 4\%$ rel.) to the error from the equipment for the CO measurement ($\pm 3\%$ rel.)

The specific attributes of the equipment should not be regarded as mandatory criteria for the test, except for the measurement range, which must encompass a minimum range of 0-3000 ppm NO_x. It is advisable, however, that the Error and Resolution values align closely with those outlined in Table 5-3. Furthermore, it is essential to ensure that the reading frequency of the equipment is set at a minimum of 1 Hz.

To fulfill these requirements, any equipment with similar characteristics to those indicated should be suitable for performing the measurement method described.

5.3. SUITABILITY OF NO_x MEASUREMENT WITH THE GAS ANALYZER

The following section is basically the transcription of the paper published in Vehicles journal [180].

The measurement of NO_x emissions in vehicles has so far been exclusively carried out during the type-approval process. For this purpose, high-precision gas measurement laboratory equipment and Portable Emission Measurement Systems (PEMS) are used.

For the NO_x emissions measurement in PTI, the PEMS or laboratory equipment are unsuitable because both types of equipment are costly in terms of price, maintenance, complexity, and time of use (calibration and maintenance requirements). Instead, PTI-grade equipment has to be used.

Although CO and O₂ are currently being reliably measured with this PTI-grade equipment, there is not enough information about its accuracy for NO_x measurements.

In 2011, CITA published the TEDDIE study [59], [88], which analyzed the various technologies existing at that time for NO_x measurement, trying to determine which was most suitable for use in PTI. The recommendation was that the most appropriate technologies for PTI in terms of accuracy and stability were an electrochemical cell or Non-Dispersive Ultra Violet (NDUV) spectroscopy, the latter being more expensive. The NDUV analyzers highly correlated with Chemiluminescence Detectors (CLD), but no studies have yet compared electrochemical cell analyzers with other instruments. The study showed that electrochemical cells need to improve but it was expected that they would meet PTI requirements.

Currently, there are no defined requirements or specifications for NO_x measurement equipment in the inspection and/or maintenance of in-use vehicles, as observed in OIML publications [181].

To validate the appropriateness of the equipment currently in use at the PTI, an examination of the equipment's measurement capabilities is essential. This involves a comprehensive comparison with a benchmark value derived from the measurements conducted using laboratory equipment employed during the analysis and certification procedures of engines, vehicles, and components.

Using this laboratory equipment as a reference, it is possible to assess the accuracy and reliability of the measurements obtained with PTI-grade equipment. Reliability has to be understood as the ability of the equipment to be trustworthy or perform consistently well, taking into account that the main objective of the equipment is to measure in PTI. The accuracy level needs to be also consistent with PTI activities. Deviations of less than 10% rel. and/or 10 ppm in absolute terms are considered acceptable.

The objective of this research section has been to evaluate the appropriateness of the aforementioned equipment for the measurement of NO_x emissions. This assessment was carried out by comparing its performance against that of precise laboratory equipment.

5.3.1. MATERIALS AND METHODS

To compare the accuracy of a PTI-grade gas analyzer with a Laboratory-grade gas analyzer, facilities of the *CMT-Motores Térmicos* of *Universitat Politècnica de Valencia*, a prestigious research and postgraduate educational center involved in the R + D of Applied Thermo-Fluid Science, were used. These facilities are widely used for advanced research publications [182]–[184].

In this facility, a test cell with a diesel engine connected to an electric dynamometer allows for modifying the behavior of the load demand of the engine. A complex monitoring system provides detailed information about the working conditions of the engine and a laboratory gas analyzer measures the gaseous emissions from the exhaust. The test installation is shown in Figure 5-2 and Figure 5-3.

A PTI gas analyzer, when connected to the engine's exhaust pipe at the same location as the laboratory gas analyzer, facilitates concurrent measurement of gas emissions from the engine. This setup enables the simultaneous measurement of NO_x concentrations in the engine's exhaust gases using both equipment pieces, thereby allowing for result comparison.

Various engine scenarios were examined to conduct a comprehensive comparison of outcomes generated by both measurement devices across a diverse array of engine operational conditions. This comprehensive analysis served to verify the PTI gas analyzer's capability in accurately gauging NO_x emissions.

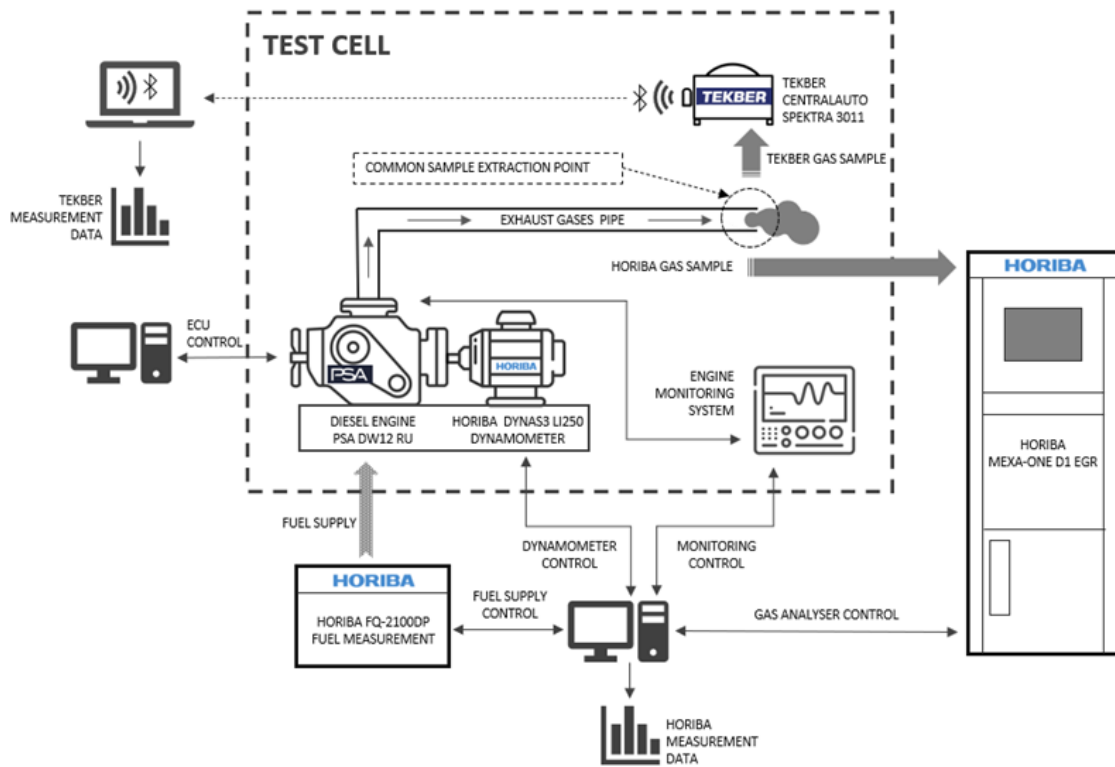


Figure 5-2. Test cell schema with Tekber and Horiba Gas Analyser installation.

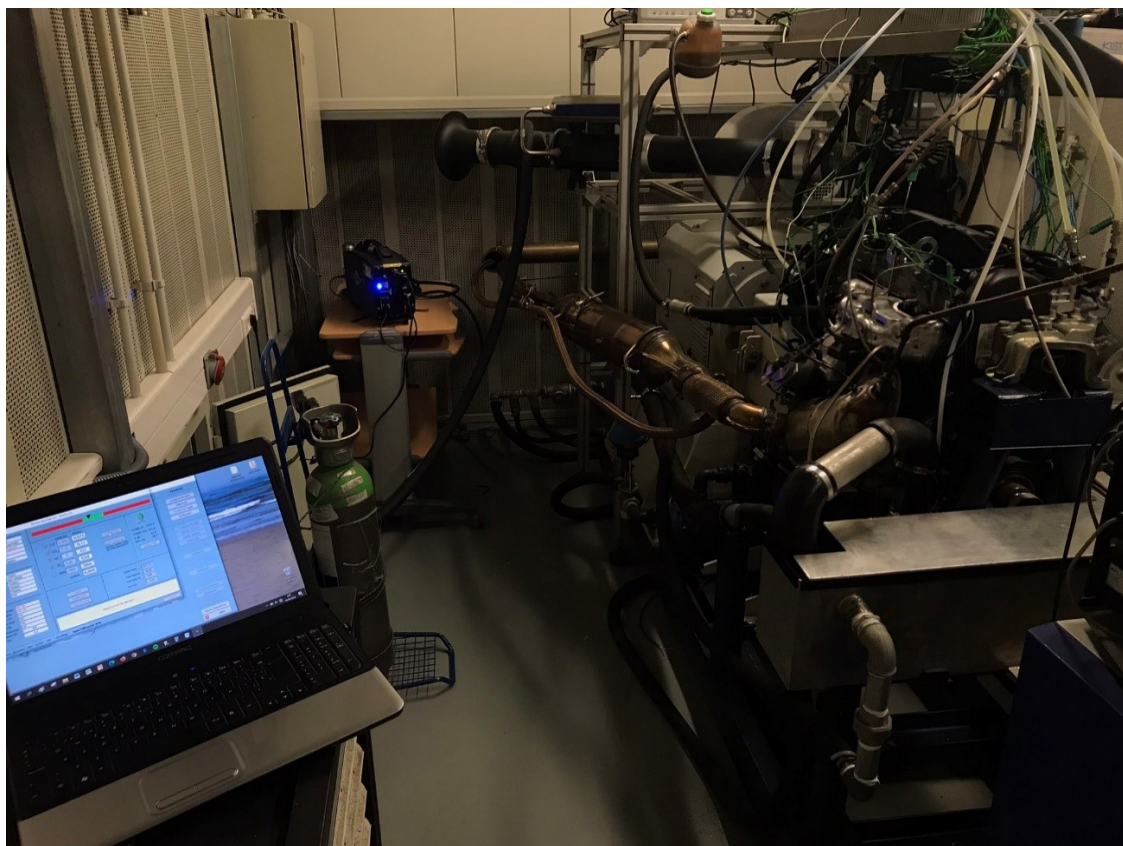


Figure 5-3. Test cell with the engine and the PTI Gas Analyzer

5.3.1.1. DIESEL ENGINE AND ACCESSORIES

A commercial diesel engine from the PSA group (PSA DW12 RU) was used, with the technical characteristics indicated in

Table 5-5. Specifically, it is a turbocharged 16-valve diesel engine from the DW12 family of PSAs, with 2179 cm³ of engine size, updated to meet the Euro 6d-TEMP emission standard. It has been commonly used in LDVs such as the Citroën Jumper and Peugeot Boxer since 2019 and later.

PSA DW12 RU General Technical Characteristics	
Fuel	Diesel
Bore	85mm
Stroke	96mm
Piston rod centreline distance	152mm
Displacement	2179cm ³
Engine architecture	4cylinders in-line
Number of camshafts	2
Number of valves	4valves per cylinder
Compression ratio	16:1
Base engine weight	183kg
Maximum Power	121kW @ 3775 rpm
Maximum Torque	370N·m @ 2000 rpm
Injection system	Delphi
High-pressure pump	Delphi DFP 6.1E
Turbocharger	BWTS
EGR valve	Yes
EGR cooler	Yes
Intercooler	Yes
Catalyst	Yes
DPF	Yes
SCR	Yes

Table 5-5. General Technical Characteristics of the tested engine (Source: PSA).

The version of the engine analyzed was the 370 N·m torque, with its performance curve shown in Figure 5-4.

The only difference between it and the standard engine is the necessary modifications to install it into the test cell, where a wide variety of variables and conditions can be measured and controlled.

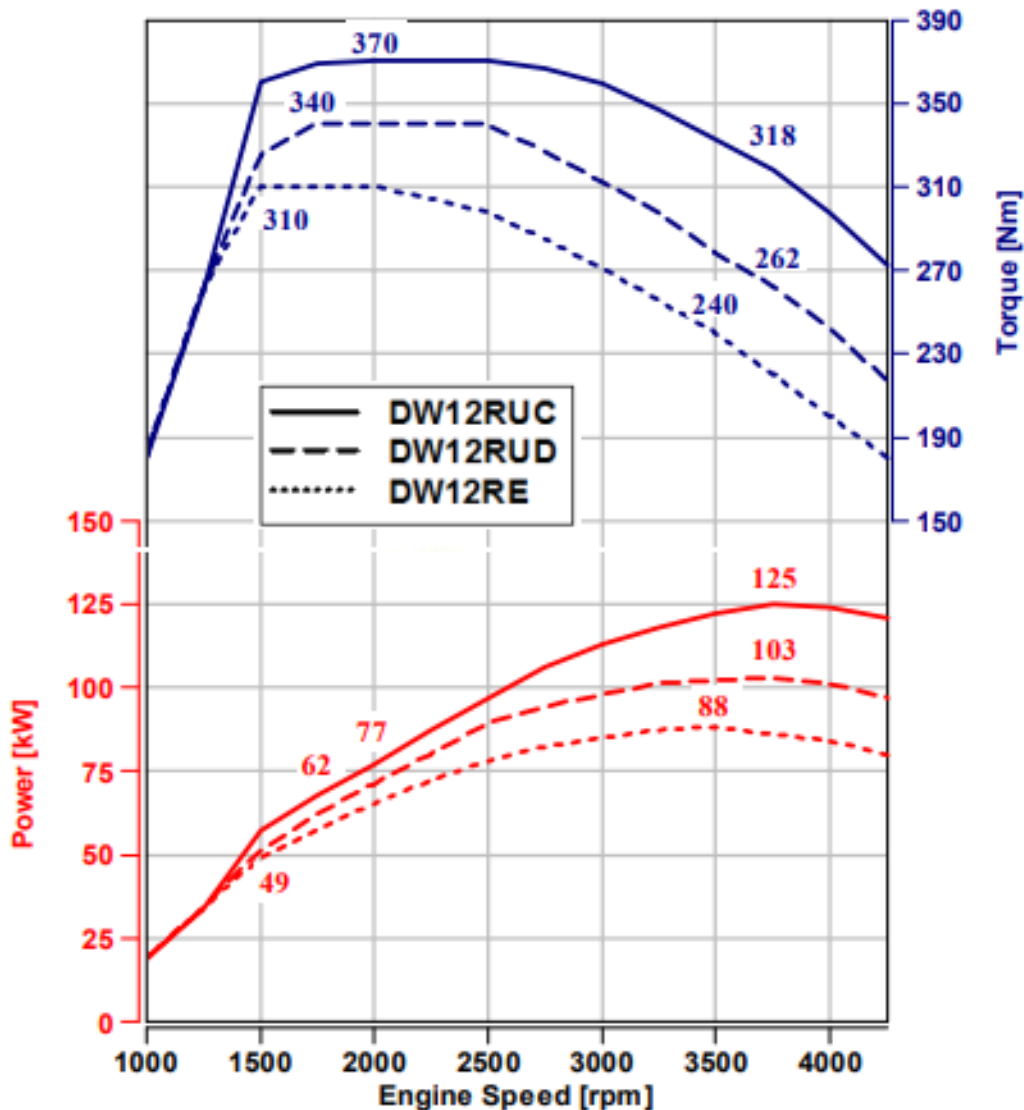


Figure 5-4. The performance curves of the PSA DW12 RU engines (Source: PSA).

Since the primary goal of the test was to compare NO_x measures from the two gas analyzers, the Selective Catalytic Reduction (SCR) system of the engine was disconnected, to avoid the NO_x reduction by this system and to ensure a minimum amount of NO_x emissions.

The Exhaust Gas Recirculation system (EGR) was connected and disconnected in different tests to provide a variety of NO_x emission behaviors. When connected, the

EGR was commanded by the Electronic Control Unit (ECU) of the engine, according to the engine manufacturer program.

Horiba FQ-2100DP Fuel Flow Measurement Specifications	
Measuring range	0.2...220 L/h (300 L/h)
	0.15...165 kg/h (225 kg/h)
Temperature control range ***	+15 °...+40 °C **
with optional heating module	max. 60 °C
Temperature Measurement uncertainty	0.5 °C
Temperature Control stability (steady-state conditions)	0.05 °C
Pressure control range fuel outlet	-0.3...9 bar -0.5...9 bar
with option vacuum controller	
Fuel return pressure	-0.5...2 bar relative ****
Fuel circulation rate adjustable	60 ... 360 L/h (optional up to 940 L/h)
Fuel Supply pressure	0.5... 1 bar
with option inlet Pressure Regulator	max. 5 bar
Fuel supply temperature	15...30 °C
Fuel supply feed	max. 350 L/h
Cooling water supply pressure	0.2...4 bar
Cooling water supply/return temperature	6...15 °C/12...21 °C
Cooling water supply feed	ca. 800 L/h
Electrical supply voltage	230 V
Electrical supply frequency	50/60 Hz
Electrical supply current (without heating)	4 A
Overall dimensions W × H × D	1150 × 1320 × 360 mm
Weight	ca. 200 kg
Ambient temperature	+5...+40 °C
Type of protection (electr. Part)	IP 44
Color	RAL 7035

* Depending on cooling water. ** Depending on heat returned by the engine. *** Max. heat transfer from engine: 2 kW.
**** Typical -0.1...1.5 bar; the return pressure is depending on the additional pressure loss in the return pipe caused by the circulation volume and the diameter of the pipe. There is the possibility of gas evolution in the fuel if the return pressure is too low adjusted.

Table 5-6. Horiba Fuel Flow Measurement Specifications (Source: Horiba).

The rest of the equipment of the engine (injection system, turbocharger...) was also controlled by the ECU. The engine fuel supply was provided through a Horiba FQ-2100DP Fuel Consumption Measurement System to control the mass and volumetric flow rate continuously. This equipment allows for accurately measuring the fuel consumption of combustion engines on chassis, engine, and powertrain test stands, or even altitude simulations on chassis dynamometers. Technical characteristics for the fuel consumption system can be found in Table 5-6.

Horiba DYNAS ₃ Dynamometer Specifications		
Rated power (absorbing)	[kW]	250
Rated speed (absorbing)	[rpm]	4980
Rated torque (absorbing)	[Nm]	480
Rated power (driving)	[kW]	225
Rated speed (driving)	[rpm]	4860
Rated torque (driving)	[Nm]	442
Overload factor, absorbing		1.2
Maximum speed n_{max}	[rpm]	10,000
Power at n_{max} (absorbing)	[kW]	200
Moment of inertia, machine without attachments	[kgm ²]	0.33
Max. Speed gradient up to rated speed incl. Overload	[rpm/s]	16,580

Table 5-7. Horiba Dynamometer Specifications (Source: Horiba).

The load demand on the engine was generated and regulated through a Horiba Dynas3-LI250 air-cooled dynamometer connected to the engine power output. In this way, the torque demanded by the engine could be controlled with high precision. Technical characteristics for the dynamometer can be found in Table 5-7.

With full control of the engine's ECU, multiple engine operating parameters can be known in real time. In addition, a complete engine monitoring system (such as intake air of the engine) allows for measuring temperatures and pressures in several components of the engine (such as turbocharging system, admission system, exhaust system, and EGR system...), providing a wide range of working data on the engine. Moreover, the test cell conditions were measured to control the air temperature and pressure in the test cell at any point.

5.3.1.2. PTI GAS ANALYZER

The equipment selected is the gas analyzer TEKBER CENTRALAUTO model SPEKTRA 3011, widely described in section 5.2, and commonly used in PTI stations in Spain. The equipment used has Model Test (Class I) No. 370-B-57/12-M and follows the UNE 82501 (equivalent to ISO 3930:2000 [185]). For the tests, it was equipped with an electrochemical NO_x sensor, which is included in the Model Test approval of the equipment. The cross-sensitivity of the NO_x sensor, as well as the rest of the technical characteristics, are detailed in Table 5-1). The gas analyzer is based on the Andros 6900 subsystem, which complies with worldwide gas-measurement performance specifications for automotive emissions, including EPA ASM, ASM/BAR-g7, OIML Class 0, and OIML Class 1.

5.3.1.3. LABORATORY GAS ANALYZER

The diesel engine's test cell is equipped with a motor exhaust gas analyzer Horiba MEXA-ONE D1 EGR vers. 1.12.5 HGS 4CW/5MTg, and NO_x analyzers, specifically model CLA-02OV-3-RBYNCY6M. This complex equipment allows for the simultaneous measurement of several pollutants in the exhaust gas stream, being a flexible measurement system for a wide range of applications.

Technical specifications of the pollutants measured by the equipment are listed in Table 5-8, and the system specifications are listed in Table 5-9.

The NO_x measurement technology in this equipment (CLD) is commonly used in emission certifications and compliance testing and is regulated by UN/ECE R83 [102] and EPA CFR Part 1065 [186] and Part 1066 [187]. CLD technique is characterized by a wide linear dynamic range, high accuracy (this technique can detect parts per trillion concentrations of NO), and fast response time. Specifically, optimal nitrogen compound measurements comprise one of the main capabilities of the equipment, even when performing multipoint sampling. The Dual-CLD method used by the equipment detects NO_x and NO simultaneously, calculating the NO₂ concentration by subtracting the NO from the NO_x concentration.

According to the manufacturer, this type of motor exhaust gas analyzer can be used for RDE tests on a chassis dynamometer, catalyst testing in automobiles and components, engine testing in automobiles and components, and measuring vehicle emissions on a chassis dynamometer.

For these applications of validation and verification of vehicles, components, and subsystems, equipment with high measurement accuracy and reliability is required. The equipment calibration is optimized with a Gas Divider Controller (GDC-one) to ensure the accuracy of measurements and a fixed installation to supply certified calibration gases to the equipment.

Component	Principle	Range
CO	NDIR	0-50 to 0-5,000 ppm
CO	NDIR	0-0.5 to 0-12 vol%
CO	NDIR	0-3 to 0-20 vol%
CO ₂	NDIR	0-0.1 to 0-6 vol%
CO ₂	NDIR	0-0.5 to 0-20 vol%
CO ₂	NDIR	0-3 to 0-20 vol%
HC	NDIR	0-100 to 0-5,000 ppm
HC	NDIR	0-5000 to 0-10,000 ppm
N ₂ O	NDIR	0-100 to 0-5,000 ppm
O ₂	MPD	0-1 to 0-25 vol%
THC	FID	0-10 to 0-30,000 ppmC
NO/NO _x	CLD	0-10 to 0-10,000 ppm
NO/NO _x	Heated-CLD	0-10 to 0-10,000 ppm
NO, NO _x , NO ₂	Dual heated-CLD	NO 0-10 to 0-10,000 ppm NO _x 0-10 to 0-10,000 ppm NO ₂ is measured by dual detector
CH ₄	GC-FID	0-10 to 0-3,000 ppm
THC	Heated-FID	0-10 to 0-60,000 ppmC
THC, CH ₄ , NMHC	Heated-FID NMC-FID	THC 0-50 to 0-60,000 ppmC CH ₄ 0-50 to 0-25,000 ppm NMHC is measured by dual detector

NDIR: Non-Dispersive Infrared Detector

FID: Flame Ionization Detector

GC-FID: Flame Ionization Detector with Gas Chromatography

NMC-FID: Flame Ionization Detector with Non-Methane Cutter

CLD: Chemiluminescence Detector (Type: Wet, Dry, Wet/Dry Switchable)

MPD : Magnetopneumatic Detector

Table 5-8. Horiba MEXA-ONE Analyzer Specifications (Source: Horiba)

System specifications	
Dimensions:	
Standard 19-inch Rack	655(W)x855(D)x1970(H) mm
Oven Type Heated Analyzer	430(W)x550(D)x1100(H) mm
Requirements:	
Ambient temperature	5°C to 40°C
Ambient humidity	80% or less as relative humidity
Ambient pressure	80 kPa to 102 kPa (abs)
Altitude	below 2,000m above sea level

Table 5-9. Horiba MEXA-ONE System Specifications (Source: Horiba)

5.3.1.4. TESTS PERFORMED

Diverse types of measurements were performed to assess the measurement capability of the PTI equipment under the broadest possible range of operating conditions:

- By modifying the load demand to which the engine is subjected, acting through the dynamometer over the engine.
- By modifying engine operating parameters such as engine speed and allowing or not allowing the EGR to be commanded by the ECU programming (by accessing directly through the ECU).

With the variation of these parameters, two different types of tests have been performed to compare the gas analyzers. Technical descriptions of the test are included in Sections 5.3.2.1 and 5.3.2.2.

The value of NO_x concentration was simultaneously measured with both gas analyzers to compare results, assuming the value measured from the Horiba gas analyzer as the reference value.

5.3.1.5. EQUIPMENT CALIBRATION

Both types of equipment were calibrated daily, according to the respective manufacturer's instructions, to ensure measurement accuracy during the tests.

The Tekber gas analyzer, which has a span calibration gas range from 100 to 5000 ppm NO_x was calibrated with a span calibration-Certified gas bottle with a concentration of 2002.9 ppm of NO_x (according to ISO/IEC 17025:2005 [188]). For the calibration process, the gas must be supplied with a flow rate of 1 liter/min, and

pressure must be regulated to 5 PSIG. Before the span calibration, a Zero calibration is required [189].

The Horiba gas analyzer was calibrated according to the manufacturer's protocol through a fixed installation connected to the certified calibration gas for the several calibration gases needed.

The first step for the NO_x calibration process is to use Zero gas calibration (nitrogen) in the minimal calibration range (10 ppm). The following step is to perform the span calibration in the certified gas bottle range. In this case, the span calibration-certified gas bottle concentration was 853 ppm, and the range for calibration was 1000 ppm. Finally, Zero gas is used again in the range of the span calibration-certified gas bottle (1000 ppm). This process can be performed manually or in an automated way.

5.3.2. RESULTS

This section shows the results from the set of tests performed. Although the Horiba equipment can provide NO, NO₂, and NO_x values, the Tekber equipment only provides NO_x concentration values, so the comparison was made exclusively with the NO_x concentration.

Another difference between the equipment is the data acquisition frequency. The Horiba gas analyzer can measure with a 10 Hz frequency, while the Tekber gas analyzer can only measure with a 1 Hz frequency. This difference can be significant when analyzing the behavior of both devices because the Tekber equipment could not detect some fast variations in NO_x concentration (e.g., instantaneous peak values).

The Horiba gas analyzer provides results of NO_x concentration on a dry basis, while the Tekber gas analyzer provides results on a wet basis. For the same sample, the dry basis concentration value is higher than the wet basis concentration value.

No correction has been made in the results of either equipment (dry basis to wet basis, or *vice versa*) because the objective of the analysis was to compare the direct result obtained by the PTI equipment (the value that was obtained when measuring during the vehicle inspection) with the real concentration value (the reference value, the most accurate possible measurement provided by laboratory equipment). Hence, the aim was not to validate or reproduce the homologation process of vehicles by applying corrections to the measurements from this process [102].

Currently, the gas emission measurements in PTI are always on a wet basis since the equipment must be as economical as possible. Consequently, the cost of installing (and maintaining) the necessary means for an accurate dry basis measurement is not justified by the advantage provided by the increase in accuracy. Converting the dry measurement obtained by the Horiba to a wet basis measurement would imply introducing uncertainty to the results obtained by the equipment. Moreover, it does not provide significant additional information to the objective of the analysis (which is to assess the suitability of the equipment for measuring NO_x in PTI) that would justify the increase of uncertainty.

5.3.2.1. RESULTS OF STATIC IDLING INTERNAL LOAD TESTS

The Static Idling Internal Load Test has been extensively expounded upon within Chapter 4, as well as in reference [175]. The concentration of nitrogen oxides in the pipe exhaust stream is quantified employing a gas analyzer, while manipulation of the engine's load requisites is controlled via the OBD system. The specific parameter of interest, the "% engine load," is furnished by the ECU of the engine, designated as PID \$04 according to the specifications delineated in SAE J1979/ISO 15031-5 [80].

The test is a five-stage measurement protocol, as outlined in the instructions presented in Figure 4-4. The temporal span allocated to each individual stage is purposefully chosen to amass a dataset of sufficient magnitude, thereby enabling the derivation of a statistically significant mean value. Typically, a duration of no less than 20 seconds during which the engine load remains consistently stable is documented and retained for analysis.

Tests were carried out in four different conditions for a wide range of results:

1. Static Idling Internal Load Test with EGR, low load condition;
2. Static Idling Internal Load Test with EGR, high load condition;
3. Static Idling Internal Load Test without EGR, low load condition;
4. Static Idling Internal Load Test without EGR, high load condition.

As explained, the method is designed to be performed on diesel vehicles in PTI. However, the test carried out in the test cell procedure cannot be exactly the same because there was no vehicle but only its engine. Therefore, it was necessary to simulate the variations of load demand generated over the engine by connecting and disconnecting the vehicle's auxiliary equipment. In this way, load demand over the vehicle has been modified through the dynamometer connected to the engine's power output.

If engine speed follows the instructions in Table 4-1, and load demand behavior is similar to the profile observed in Figure 4-4, the measurement test can be performed in the test cell.

Sequences of 20 consecutive cycles were programmed to optimize the timing of the tests. Since a computer program commands the implementation of the test, the duration of every stage is the same for every cycle.

At the same time, the NO_x concentration was measured simultaneously by the two gas analyzers. The blue-dotted square in Figure 5-5 shows the five stages described in Figure 4-4 that correspond to one single Static Idling Internal Load Test.

Figure 5-5 shows one of the tests performed with activated EGR. The purple line represents the load demand on the engine generated by the dynamometer, the red line is the engine speed, the green dotted line is the EGR aperture percentage, and the red and blue dotted lines are the exhaust gas temperature and engine oil temperature, respectively. Finally, the continuous orange line is the NO_x concentration (ppm) from the Horiba gas analyzer, and the continuous blue line is the NO_x concentration (ppm) from the Tekber gas analyzer.

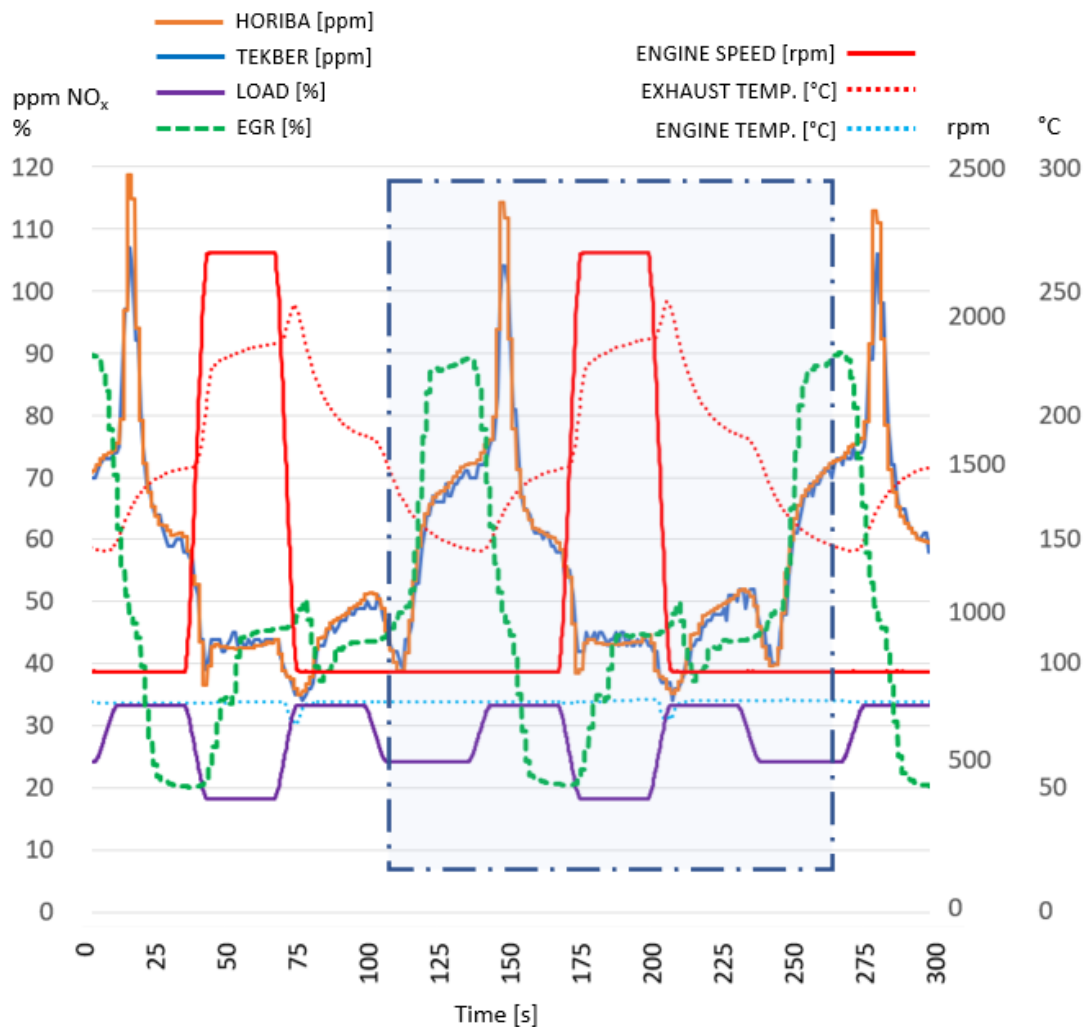


Figure 5-5. Sample of the test with EGR and low load conditions.

When the Static Idling Internal Load Test was performed at low load conditions for the unloaded stages, the dynamometer demand was set at a 24% level (torque demand in the range of 10–12 Nm), increasing to 33% in the loaded stages (torque demand in the range 37–40 Nm). When the Static Idling Internal Load Test was carried out at high load conditions, in the unloaded stages the engine brake demand was set at a 27% level (torque demand in the range of 19–22 Nm), increasing to 46% in the loaded stages (torque demand in the range 72–75 Nm).

Performing the test with and without EGR had two goals:

1. To check the Tekber gas analyzer behavior in two different situations
2. To check if the Tekber gas analyzer can detect that the EGR is not working through the NO_x concentration measurements.

Every test conducted shows that the results of both analyzers have the same trend and performance in each measurement section.

For the tests with the EGR activated and commanded by the engine's ECU, the NO_x concentration in the exhaust gas stream was reduced, usually in the interval of 30 to 70 ppm, although some peaks of higher concentration until 120 ppm could be detected. For this range of concentration, the behavior of the Tekber gas analyzer is similar to the Horiba gas analyzer.

Figure 5-5 shows a sample of the tests performed, where it can be observed that the measured concentrations from Tekber and Horiba gas analyzers are similar, without significant differences. Only for the peak values can differences of 10 ppm abs. and 11% rel. be found. The difference in the acquisition frequency (10 Hz for the Horiba vs. 1 Hz for the Tekber) can be responsible for the discrepancy between both measures. The average difference for this set of cycles between values of both devices was 1.7 ppm, which is an average of 3% rel. the difference, in the sample, shown. A similar behavior was observed when the test was repeated in the same conditions and when the engine load demand was increased.

A summary of results from the tests performed with the EGR activated is shown in Table 5-10.

The average absolute differences measured between the two devices with the activated EGR are 2.6 ppm for the low load tests and 8.6 ppm for the high load test, which, for the purpose of NO_x measurement in PTI, are not significant.

When the same tests were carried out with deactivated EGR, the NO_x concentration in the exhaust gas stream was up to seven times higher than in the first tests when the EGR was correctly working. In this situation, the NO_x concentration usually varied between 150 ppm at the minimum point and more than 500 ppm, with only a few peak emissions over 600 ppm.

	LOW LOAD	HIGH LOAD
HORIBA Average NO _x [ppm]	53.7	44.3
TEKBER Average NO _x [ppm]	53.6	36.2
Avg. Absolute Diff. [ppm]	2.6	8.6
Avg. Relative Diff. [%]	4.8%	20.6%

Table 5-10. Summary of average concentrations and differences for the Static Idling Internal Load Test with EGR.

As seen in the idling test without EGR and low load conditions in Figure 5-6, the NO_x concentrations from the Tekber gas analyzer and the Horiba gas analyzer were quite similar. The concentration values were 150 ppm in the lower zones and between 300 ppm and 350 ppm in the upper zones. When the test was repeated with high load demand, the average concentration measured and the concentration values for the lower and upper zones increased.

A summary of results from the tests performed with a deactivated EGR is shown in Table 5-11. The values of the absolute and relative differences between the results of both devices were low enough to evaluate the performance of the Tekber analyzer as adequate for measuring NO_x emissions in PTI.

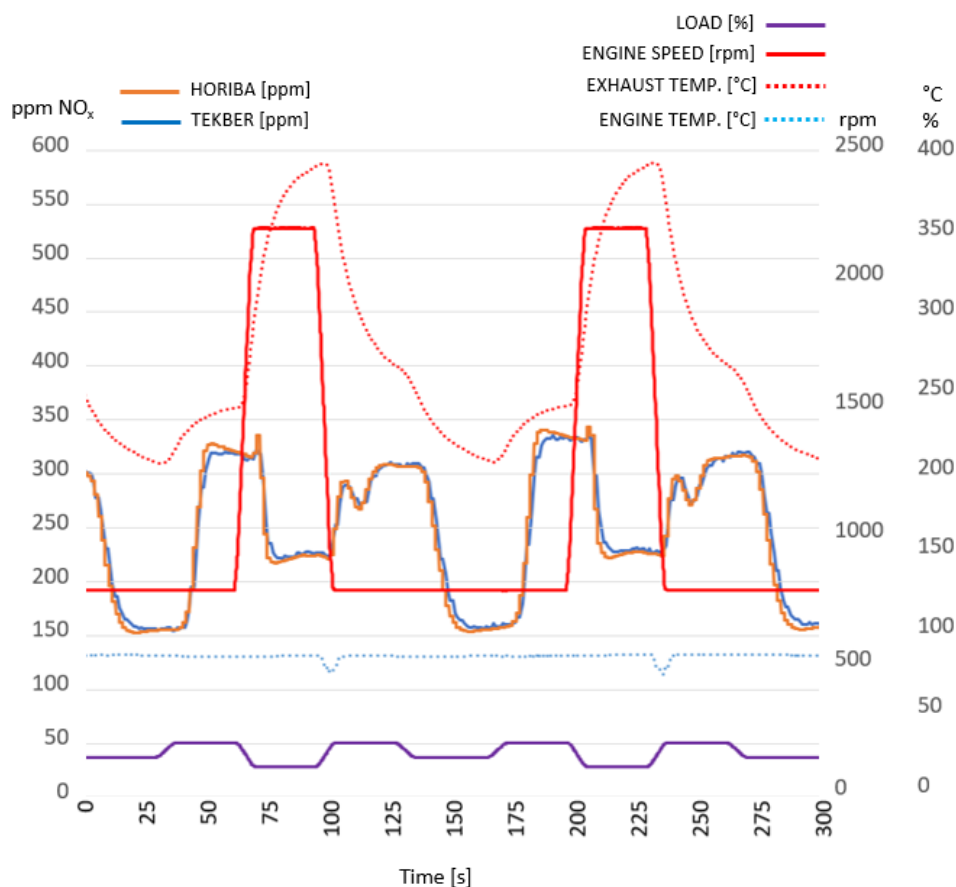


Figure 5-6. Sample of the Test without EGR and low load conditions.

From the point of view of PTI measurement, the behavior of both devices was similar for the EGR activated and deactivated, as can be observed in Figure 5-7.

	LOW LOAD	HIGH LOAD
HORIBA Average NO _x [ppm]	325.0	405.6
TEKBER Average NO _x [ppm]	339.8	430.2
Avg. Absolute Diff. [ppm]	20.8	29.1
Avg. Relative Diff. [%]	5.9%	7.1%

Table 5-11. Summary of the average concentrations and differences for the Static Idling Internal Load Test without EGR.

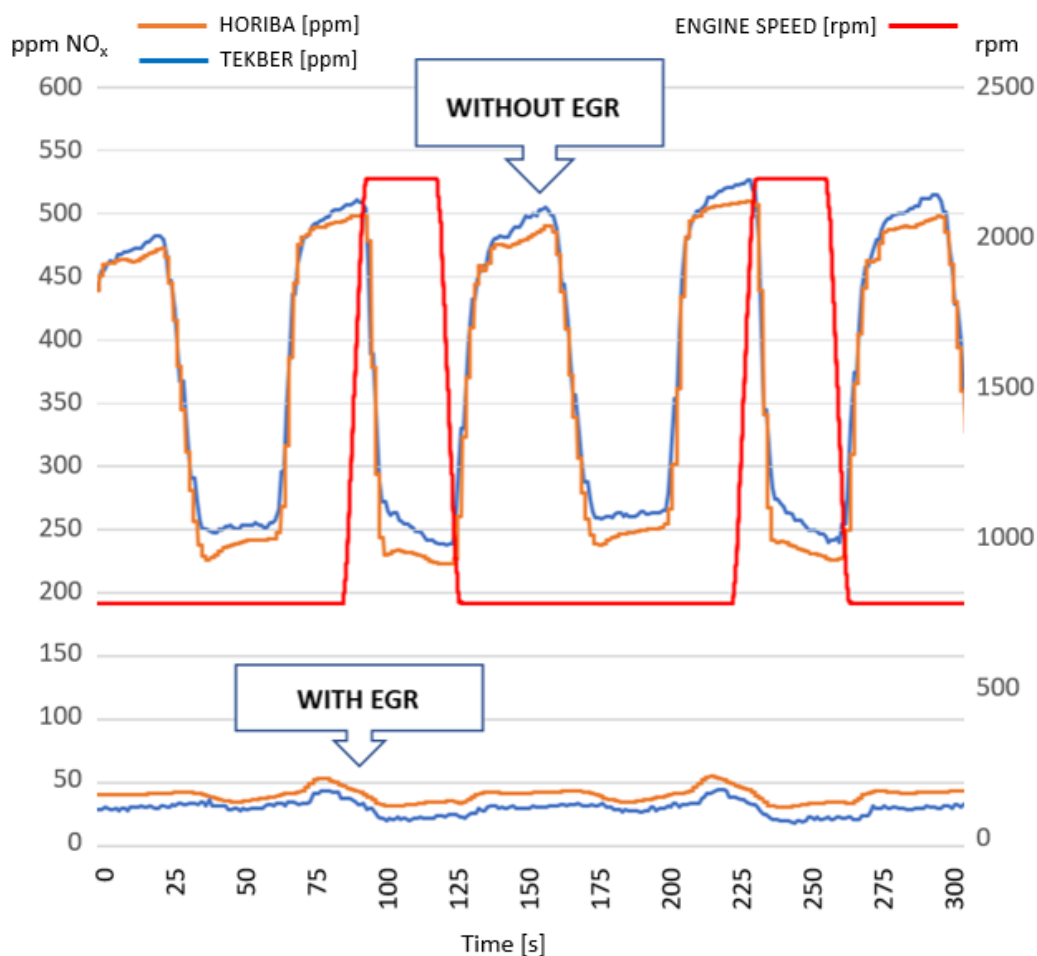


Figure 5-7. Comparison of Tests with and without EGR and high load conditions.

For the Static Idling Internal Load Test, the average relative differences that are lower than 8% in the tests with the EGR deactivated, when the NO_x concentration is higher, can be considered correct enough for PTI purposes. Absolute differences lower than 9 ppm for the EGR-activated tests when the NO_x concentration is lower are also correct enough to get the same test result in PTI: assuring the roadworthiness of the vehicle.

From this point of view, the performance of the Tekber device can be considered satisfactory, increasing or decreasing the value measured of NO_x concentration with a similar response to the Horiba device, even though the frequency is different: 1 Hz for the Tekber device and 10 Hz for the Horiba system. Although the PTI test is stationary, this is an important equipment feature.

The accuracy of the measurements may be the most important issue when analyzing the suitability of this type of equipment. From the results of the measurements reproducing the Static Idling Internal Load Tests, the performance of the Tekber equipment, in the measurement range covered by the Static Idling Internal Load Test, is satisfactory.

In the test with the EGR activated the average difference of the measurements was 8.6 ppm for the high-load tests and only 2.6 ppm for the low-load tests. These differences are not significant for determining the level of emissions of the vehicle.

When the engine was tested with the EGR deactivated, the average difference between measurements from both devices was 20.8 ppm for the low load test and 29.1 ppm for the high load test. The relative difference for the high load test was 7.1%, and even lower for the low load test, with a relative difference of 5.9%.

To summarise, the slight differences between both pieces of equipment, when the Static Idling Internal Load Test was performed, did not affect the test result because the concentration values obtained from both devices gave similar results.

5.3.2.2. RESULTS FOR FIXED ENGINE SPEED AND INCREASING LOAD TESTS

Another kind of test was performed to check the performance of the Tekber measurements compared to the Horiba equipment: the engine was subjected to gradual increases in power demand while maintaining a fixed engine speed in two different conditions:

1. Fixed engine speed, increasing the load demand, with EGR;
2. Fixed engine speed, increasing the load demand, without EGR.

In this way, the variation profile of the engine NO_x concentration could be analyzed with changing torque demand. The wide variety of conditions (engine speed, load demand, EGR aperture, the temperature of exhaust gases...) provides crucial information about the behavior of the Tekber gas analyzer.

These tests were conducted for 800 rpm, and from 1000 rpm to 3000 rpm with 500 rpm increments. The engine was subjected to an increase in torque demand for each of these speed conditions through the dynamometer coupled to the engine power output. The increase in torque demand was performed in 10% increments of the demand capacity of the dynamometer. Due to the system's technical requirements, measurements were started with a demand of 20%.

All the tests carried out with the EGR activated and commanded by the ECU show similar behavior. When load demand is low or medium, the %EGR opening is higher. It gradually closes as the power demand increases until it reaches the minimum value defined by the ECU at these conditions.

It can also be observed that the %EGR aperture is lower as engine speed increases. If at 1000 rpm and 20% of load demand the EGR value is 40%, with the same 20% of load demand at 3000 rpm the EGR value is 20%.

Figure 5-8 shows how the behavior of the Tekber results is similar to Horiba's measurements for every engine speed.

For the first test at 800 rpm with an activated EGR and at a dynamometer load demand of 80%, the difference in the NO_x concentration values from both types of equipment was lower than 10 ppm abs., until the concentration increased to 900 ppm (Figure 5-8 a). From this concentration, the discrepancies increased until a maximum

difference of 229 ppm abs. These average differences are represented in Figure 5-9 for every engine speed. Although the relative differences are over 20%, this value corresponds to a NO_x concentration of 9 ppm, which can be considered to be a low deviation.

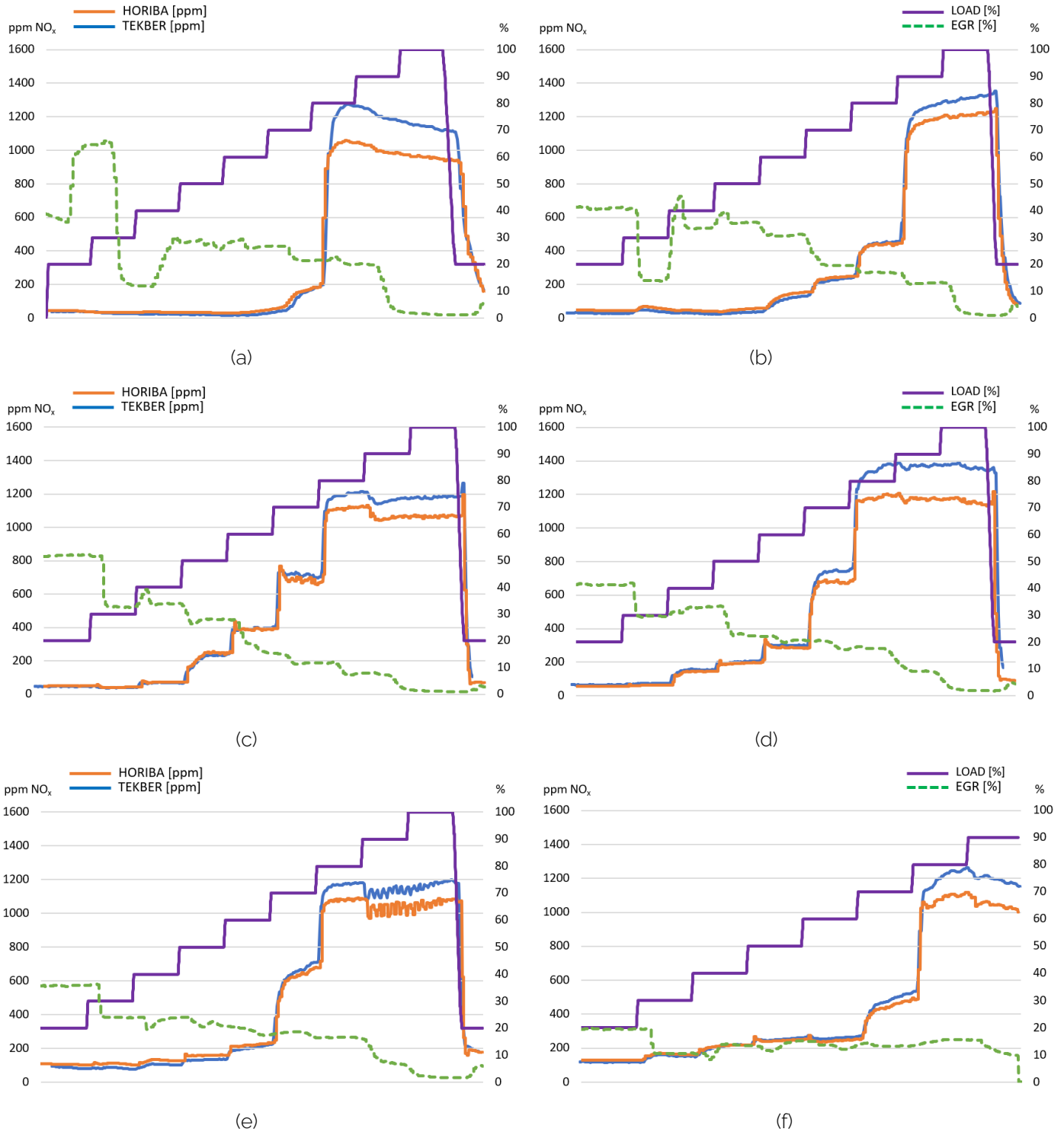


Figure 5-8. NO_x concentration with EGR activated: (a) @800 rpm, (b) @1000 rpm, (c) @1500 rpm, (d) @2000 rpm, (e) @2500 rpm, (f) @3000 rpm.

Engine speed	Load demand	20%	30%	40%	50%	60%	70%	80%	90%	100%
800 rpm	Avg. Horiba [ppm]	44.0	34.8	36.1	34.0	35.6	102.9	960.4	1008.5	966.4
	Avg. Tekber [ppm]	45.6	35.5	30.7	27.4	26.5	95.7	1189.6	1209.2	1150.1
	Avg. dif. Abs. [ppm]	1.6	0.7	-5.4	-6.6	-9.0	-7.2	229.2	200.8	183.7
	Avg. dif. Rel. [%]	3.6	1.9	-15.0	-19.4	-25.4	-7.0	23.9	19.9	19.0
1000 rpm	Avg. Horiba [ppm]	46.8	59.7	45.6	51.0	122.9	241.5	435.0	1135.9	1208.8
	Avg. Tekber [ppm]	29.2	42.1	28.6	35.3	111.2	230.5	444.9	1203.8	1303.6
	Avg. dif. Abs. [ppm]	-17.5	-17.6	-17.0	-15.7	-11.7	-11.0	10.0	67.8	94.8
	Avg. dif. Rel. [%]	-37.5	-29.5	-37.2	-30.8	-9.6	-4.5	2.3	6.0	7.8
1500 rpm	Avg. Horiba [ppm]	49.5	42.3	72.4	248.3	388.4	685.0	1110.8	1056.5	1064.6
	Avg. Tekber [ppm]	46.0	42.8	62.5	230.3	392.1	715.0	1196.6	1169.1	1182.8
	Avg. dif. Abs. [ppm]	-3.5	0.5	-9.9	-18.0	3.7	30.0	85.8	112.6	118.2
	Avg. dif. Rel. [%]	-7.1	1.2	-13.6	-7.2	1.0	4.4	7.7	10.7	11.1
2000 rpm	Avg. Horiba [ppm]	56.1	61.7	141.8	193.3	287.9	681.0	1179.9	1175.0	1162.6
	Avg. Tekber [ppm]	63.2	71.2	154.5	202.6	301.7	746.6	1349.8	1382.9	1384.2
	Avg. dif. Abs. [ppm]	7.1	9.5	12.7	9.3	13.8	65.6	170.0	207.9	221.6
	Avg. dif. Rel. [%]	12.6	15.4	9.0	4.8	4.8	9.6	14.4	17.7	19.1
2500 rpm	Avg. Horiba [ppm]	106.1	111.0	130.8	159.4	224.0	639.1	1080.7	1025.9	1057.1
	Avg. Tekber [ppm]	101.0	86.5	106.5	135.7	211.5	669.5	1174.4	1134.0	1180.8
	Avg. dif. Abs. [ppm]	-5.1	-24.5	-24.4	-23.7	-12.5	30.4	93.7	108.1	123.7
	Avg. dif. Rel. [%]	-4.8	-22.1	-18.6	-14.8	-5.6	4.8	8.7	10.5	11.7
3000 rpm	Avg. Horiba [ppm]	128.3	164.2	215.3	245.2	243.6	444.0	1080.2	1054.5	n.a.*
	Avg. Tekber [ppm]	120.8	158.3	213.1	255.3	262.6	498.7	1230.3	1183.1	n.a.*
	Avg. dif. Abs. [ppm]	-7.5	-5.9	-2.2	10.1	19.0	54.7	150.1	128.5	n.a.*
	Avg. dif. Rel. [%]	-5.9	-3.6	-1.0	4.1	7.8	12.3	13.9	12.2	n.a.*

*For technical reasons, the 100% load demand section couldn't be performed, so data are unavailable.

Table 5-12. Summary of Avg. concentration and differences between Horiba and Tekber equipment with EGR activated

Regarding the emissions behavior, it can be observed how the action of the EGR makes NO_x emissions decrease (to below 100 ppm) until demand rises to 70%. At this point, an increase in NO_x concentration to 200 ppm occurs. Above 90% load demand, the EGR closes, leading to the values included in Table 5-12, where average results

for the whole set of tests are summarised. Figure 5-10 shows the correlation between results from Tekber equipment and Horiba, with $R^2 > 0.98$ for every engine speed.

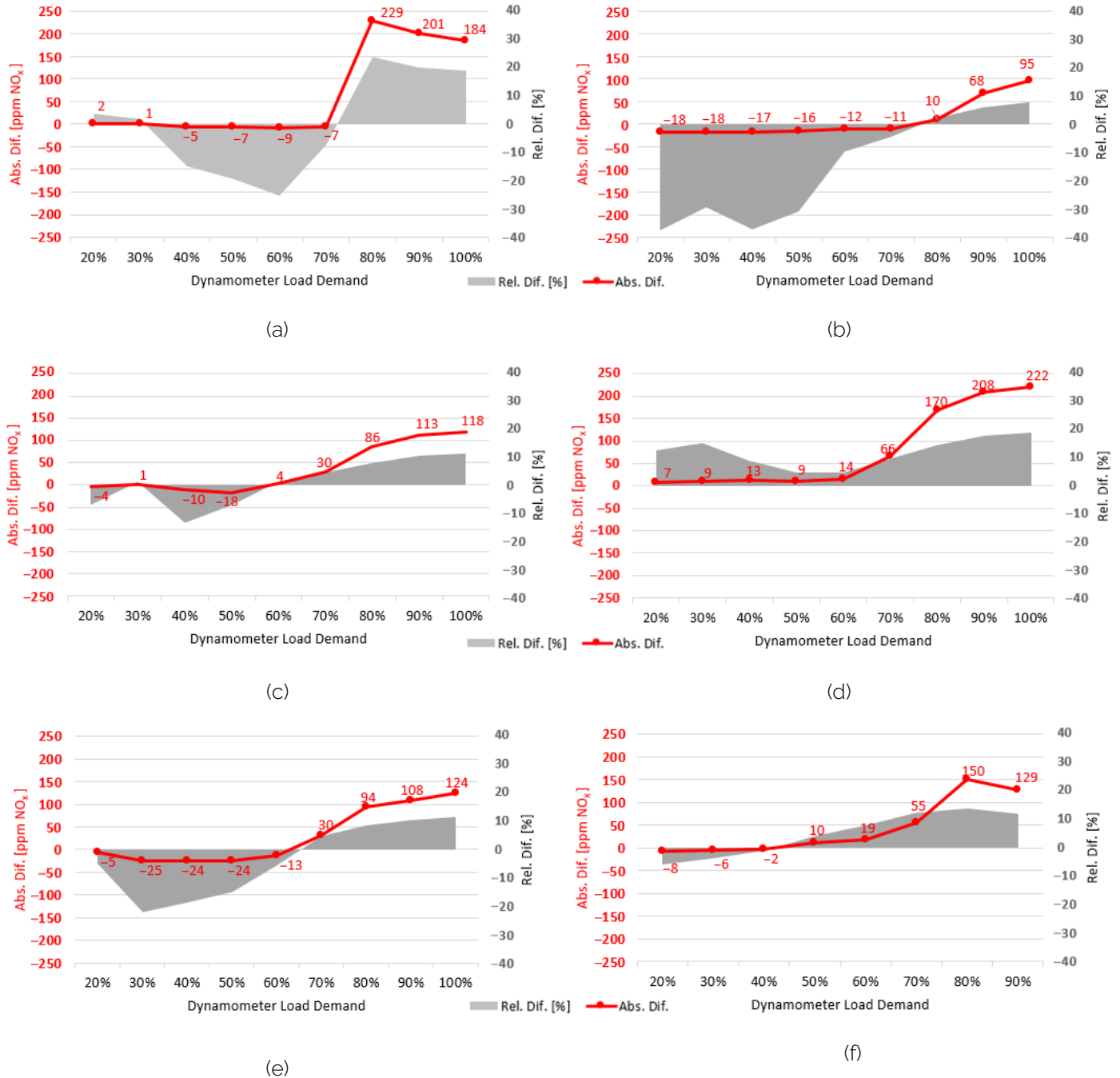


Figure 5-9. Average differences in Absolute and Relative terms according to the load demand with the EGR activated: (a) @800 rpm, (b) @1000 rpm, (c) @1500 rpm, (d) @2000 rpm, (e) @2500 rpm, (f) @3000 rpm.

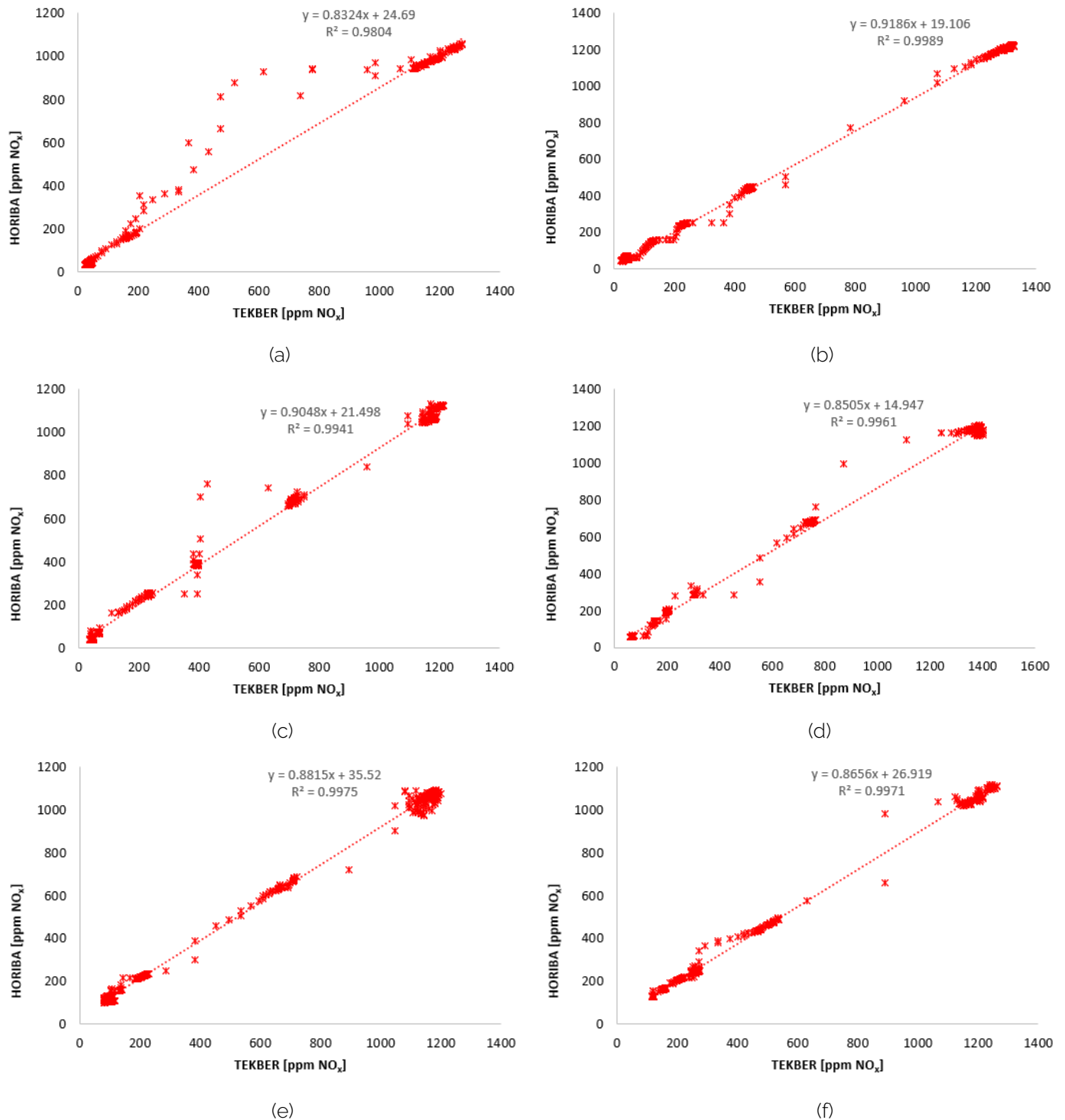


Figure 5-10. Correlation between concentration values from Tekber and Horiba equipment: (a) @800 rpm, (b) @1000 rpm, (c) @1500 rpm, (d) @2000 rpm, (e) @2500 rpm, (f) @3000 rpm.

The same situation could be observed for the test at 1000 rpm with EGR, Figure 5-8 b, where the difference between values from both types of equipment was close until reaching 1000 ppm (when load demand is at 90%). Until this point, the average difference between Horiba and Tekber devices was in the range of 10–18 ppm abs.

From this point upwards, the difference increased but was lower than 100 ppm abs, and less than 8% rel.

For the test carried out at @1500 rpm, as shown in Figure 5-8 c, it was again observed how the Tekber analyzer accurately reproduced the behavior of the Horiba analyzer. From 20% to 40% of load demand, the average difference was lower than 10 ppm. Once the concentration was stabilized, the section of 50% of load demand showed an average difference of 18 ppm, and for the 60% section, the average difference was lower than 4 ppm. When reaching 70% of the demanded load and NO_x concentrations reached 700 ppm level, the average difference increased to 30 ppm. From this power demand value onwards, the absolute value of the measurement difference increased up to 120 ppm, although the relative difference stabilized at values of 11% rel.

The test at 2000 rpm shows again how the Tekber results reproduce the behavior of the Horiba measures (as seen in Figure 5-8 d). Until reaching 70% load demand, the average absolute difference between them was lower than 15 ppm.

Table 5-10 d shows that the difference between both devices is small for NO_x concentrations under 600 ppm (that is until 60% load demand). With higher load demands and NO_x concentrations exceeding 600 ppm, the difference between the Tekber equipment and Horiba increases (in absolute and relative values). This behavior could be observed in this kind of test every time it was carried out.

In the test at 2500 rpm, as can be observed in Figure 5-8 e, not only was the same profile of concentration obtained, but the behavior of NO_x concentration in the sections of 90% and 100% was faithfully reproduced by both devices, with the only difference being the measured value. Again, the sections with concentrations below 600 ppm showed a reduced difference between both devices, with 25 ppm and 11% rel. being the highest average difference for these sections, as shown in Table 5-10 e.

Another issue to be mentioned is that the exhaust gas temperature for the sections with higher concentrations reached between 600 °C and 700 °C. The Horiba equipment is designed to work under such conditions. However, the Tekber equipment is focused on another kind of measurement, where the time duration of the measurement is shorter. Moreover, the gas temperature of the sample is usually much lower than 300 °C. In the Static Idling Internal Load Test, the engine at 2500 rpm is not subjected to any load, so the gas temperature is below 300 °C.

Finally, the last test was carried out at 3000 rpm with the behavior of NO_x concentration shown in Figure 5-8 f and the differences summarised in Figure 5-9 f. As can be seen, the last section of the 100% load demand could not be performed for technical reasons, so no data are available for this situation. The results of this last test were similar to the previous ones. The behavior of both types of equipment was similar, with an absolute difference between values being lower than 20 ppm (and a relative difference below 8%) until reaching 60% load demand. From 70% of load demand, the relative difference was, on average, around 13%, and the absolute difference was at a maximum of 150 ppm.

From this set of six tests, it can be concluded that the behavior of the Tekber gas analyzer faithfully reproduces the behavior of the Horiba gas analyzer.

The difference in measurement precision varies depending on the concentration values measured. Still, the variation is typically low when the concentration of NO_x in the gas stream is below 600 ppm, with an average value of 15 ppm for this condition.

Engine speed	Load demand	20%	30%	40%	50%	60%	70%	80%	90%	100%
800 rpm	Avg. Horiba [ppm]	93.8	207.3	391.0	639.7	796.4	873.0	917.7	904.1	888.5
	Avg. Tekber [ppm]	91.3	350.6	566.1	713.2	813.0	836.2	1042.5	1458.0	1464.1
	Avg. dif. Abs. [ppm]	-2.5	143.3	175.1	73.5	16.6	-36.8	124.8	553.9	575.6
	Avg. dif. Rel. [%]	-2.7	69.1	44.8	11.5	2.1	-4.2	13.6	61.3	64.8
1,000 rpm	Avg. Horiba [ppm]	194.1	488.3	584.4	748.7	1007.9	1011.5	1069.1	1180.0	1166.5
	Avg. Tekber [ppm]	188.2	498.8	603.9	813.0	1106.2	1110.4	1193.5	1311.5	1281.1
	Avg. dif. Abs. [ppm]	-5.8	10.5	19.6	64.3	98.3	98.9	124.4	131.5	114.5
	Avg. dif. Rel. [%]	-3.0	2.1	3.3	8.6	9.8	9.8	11.6	11.1	9.8
1,500 rpm	Avg. Horiba [ppm]	271.9	375.9	647.5	829.5	952.5	1024.8	1106.6	1060.2	1067.7
	Avg. Tekber [ppm]	236.1	322.9	600.2	846.2	1018.7	1097.4	1189.8	1165.3	1186.4
	Avg. dif. Abs. [ppm]	-35.8	-53.0	-47.3	16.7	66.1	72.6	83.2	105.1	118.7
	Avg. dif. Rel. [%]	-13.2	-14.1	-7.3	2.0	6.9	7.1	7.5	9.9	11.1
2,000 rpm	Avg. Horiba [ppm]	250.5	410.2	706.8	928.8	1070.7	1209.7	1216.9	1181.9	1179.7
	Avg. Tekber [ppm]	235.0	407.9	764.6	1079.5	1300.3	1473.3	1459.1	1415.5	1399.5
	Avg. dif. Abs. [ppm]	-15.5	-2.2	57.8	150.7	229.6	263.6	242.2	233.6	219.9
	Avg. dif. Rel. [%]	-6.2	-0.5	8.2	16.2	21.4	21.8	19.9	19.8	18.6
2,500 rpm	Avg. Horiba [ppm]	220.1	318.4	522.7	734.2	851.1	953.9	1060.1	957.1	955.4
	Avg. Tekber [ppm]	200.5	308.5	538.6	783.5	934.8	1062.6	1166.8	1059.0	1077.8
	Avg. dif. Abs. [ppm]	-19.6	-9.8	15.9	49.3	83.7	108.7	106.6	101.9	122.5
	Avg. dif. Rel. [%]	-8.9	-3.1	3.0	6.7	9.8	11.4	10.1	10.6	12.8
3,000 rpm	Avg. Horiba [ppm]	173.0	284.8	467.4	571.8	738.2	941.0	1085.1	1084.6	1053.9
	Avg. Tekber [ppm]	148.1	284.8	446.5	574.7	775.1	1046.3	1236.5	1241.7	1208.4
	Avg. dif. Abs. [ppm]	-24.9	0.0	-20.9	2.9	37.0	105.3	151.4	157.1	154.4
	Avg. dif. Rel. [%]	-14.4	0.0	-4.5	0.5	5.0	11.2	13.9	14.5	14.7

Table 5-13. Summary of Avg. concentration and differences between Horiba and Tekber equipment with EGR deactivated

As with the Static Idling Internal Load Tests for PTI, the same set of tests was conducted with the EGR disconnected, directly resulting in increased NO_x concentrations, especially for low load demand slots.

In low-demand situations, where the EGR was clearly active, a significant difference in the NO_x concentration measured by both devices was observed. Instead, the NO_x concentration was similar to the EGR-activated tests for the high load states (when load demand is 80% or higher). This is because, in the EGR-activated tests, EGR was closed or nearly closed when the load demand was high.

As was observed in the first part of the tests, a higher concentration in the exhaust gases increases the discrepancies between both measuring devices. The higher concentrations of NO_x with the EGR disconnected show that the difference observed for the low load states between both devices was higher than for the EGR-activated tests.

Results are summarized from these sets of tests in Table 5-13, with the same information previously detailed in the EGR-activated case.

Table 5-14 shows the average differences calculated (in absolute values), from every test performed at the different engine speeds and load demand states, for the Tekber equipment with respect to the Horiba equipment results when the EGR was activated.

Engine Speed	Load demand								
	20%	30%	40%	50%	60%	70%	80%	90%	100%
800 rpm	1.6	0.7	5.4	6.6	9.0	7.2	229.2	200.8	183.7
1,000 rpm	17.5	17.6	17.0	15.7	11.7	11.0	10.0	67.8	94.8
1,500 rpm	3.5	0.5	9.9	18.0	3.7	30.0	85.8	112.6	118.2
2,000 rpm	7.1	9.5	12.7	9.3	13.8	65.6	170.0	207.9	221.6
2,500 rpm	5.1	24.5	24.4	23.7	12.5	30.4	93.7	108.1	123.7
3,000 rpm	7.5	5.9	2.2	10.1	19.0	54.7	150.1	128.5	n.d.
Avg. Diff. [ppm]	7.1	9.8	11.9	13.9	11.6	33.2	123.1	137.6	148.4
Rel. Diff. [%]	9.8%	12.4%	11.1%	8.9%	5.4%	7.1%	12.6%	12.8%	13.6%

Table 5-14. Summary of Avg. absolute differences (ppm NO_x) between Tekber and Horiba equipment with EGR

The deviation between both devices is lower than 14 ppm from the load demand scenarios below 70%. The relative difference is 13.6% in the situation of 100% load demand when the NO_x concentration is the highest.

Figure 5-11 shows the average deviation in absolute and relative terms from the Tekber equipment results compared to the average NO_x concentration value

measured by the Horiba and the Tekber equipment at every load demand slot. After analyzing the data from several tests, it can be concluded that the absolute deviation increases when the load demand and the average NO_x concentration increase.

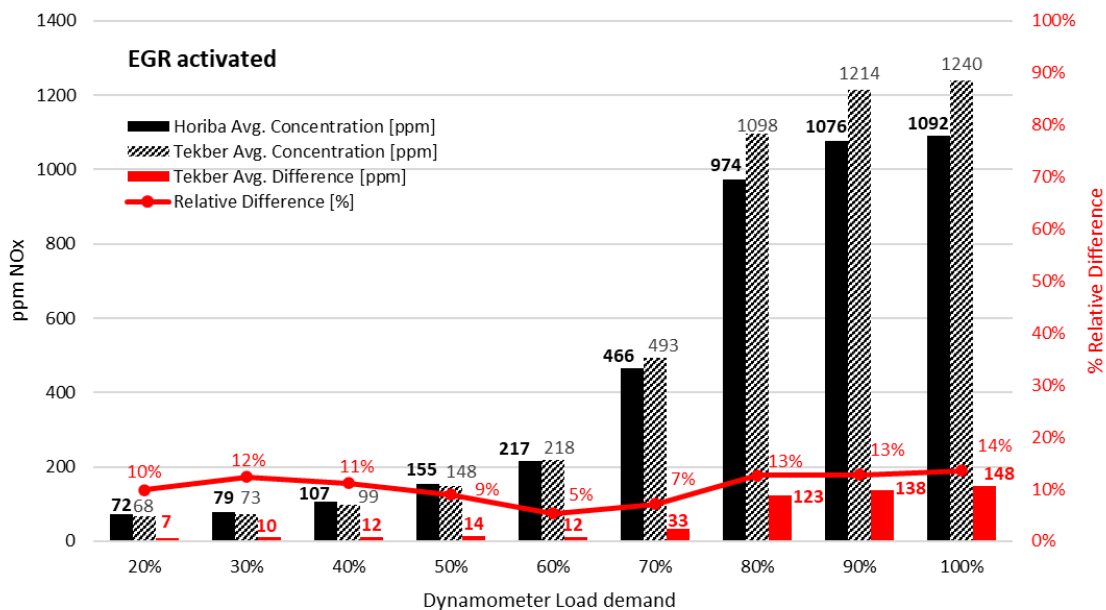


Figure 5-11. Differences between Tekber and Horiba results according to the load demand with EGR.

Below 700 ppm, the deviation between the two measures stays below 65 ppm, with an average difference value of less than 15 ppm, in absolute terms, i.e., accumulating the deviations. This translates into differences of 9% in relative terms for these sections. It should be mentioned that there are occasional measurements with larger relative differences, mainly at very low concentrations, of the order of 20-30 ppm, where a small difference in the absolute value of 5 ppm can mean a difference in relative terms of 15-20%.

At 700 ppm NO_x and above, Tekber deviations are significantly larger, with an average difference of 136 ppm in absolute terms or 13% in relative terms.

For measurements performed with EGR deactivated, the results obtained are less homogeneous, due to the absence of the "normalizing" performance of the vehicles' EGR.

In addition, the NO_x concentration values in the exhaust gas stream are clearly higher for the low-load demand zones than those measured in the tests performed with the EGR system operating.

Table 5-15 shows a summary of the average differences from every test performed at the different engine speeds and load demand states when the EGR was deactivated.

As for the EGR-connected tests, it can be observed that the absolute values of the difference between results of both types of equipment are lower from the load

demand scenarios below 70%, although the absolute values are significantly higher. That said, the relative difference is similar to the values observed when the EGR was connected. Only for the highest load demand situation, at 90% and 100%, the relative difference rises to more than 20%.

Engine Speed	Load demand								
	20%	30%	40%	50%	60%	70%	80%	90%	100%
800	2.5	143.3	175.1	73.5	16.6	36.8	124.8	553.9	575.6
1,000	5.8	10.5	19.6	64.3	98.3	98.9	124.4	131.5	114.5
1,500	35.8	53.0	47.3	16.7	66.1	72.6	83.2	105.1	118.7
2,000	15.5	2.2	57.8	150.7	229.6	263.6	242.2	233.6	219.9
2,500	19.6	9.8	15.9	49.3	83.7	108.7	106.6	101.9	122.5
3,000	24.9	0.0	20.9	2.9	37.0	105.3	151.4	157.1	154.4
Avg. Diff. [ppm]	17.4	36.5	56.1	59.6	88.5	114.3	138.8	213.9	230.2
Rel. Diff. [%]	8.7%	10.5%	10.1%	8.0%	9.8%	11.4%	12.9%	20.1%	21.9%

Table 5-15. Summary of Avg. absolute differences (ppm NO_x) between Tekber and Horiba equipment without EGR

Figure 5-12 shows for every slot of load demand a comparison between the average concentration deviations in absolute and relative terms for both devices and the average value of NO_x concentration measured by the Horiba and the Tekber equipment at this load demand slot. As mentioned, the behavior is similar to that shown in Figure 5-11, although the concentration values are higher, and because of this, the discrepancies increase too. When NO_x concentration is below 700 ppm, the deviation is less than 45 ppm, in absolute terms. This translates into differences of 9% in relative terms for these sections. As observed for the EGR-connected tests, when 700 ppm are exceeded, the discrepancies between both devices increase significantly, with an average difference of 142 ppm in absolute terms (14% rel.).

In summary, for NO_x concentrations below 700 ppm in the exhaust gas stream, the deviation of Tekber results concerning Horiba results is small, which makes the Tekber more accurate under these conditions.

As we shall observe in Chapter 8, a measurement campaign was conducted in various PTI stations in 2019, employing the proposed measurement method. Without preempting information, it is necessary to indicate that from the measurements performed during the campaign, out of 1,884 vehicles analyzed, only 17 exceeded the 700 ppm of NO_x concentration value measured during the emissions test execution (in the loaded or the unloaded stages). This means that only 0.90% of the vehicles in the analyzed sample exceeded the value of 700 ppm during the measurement.

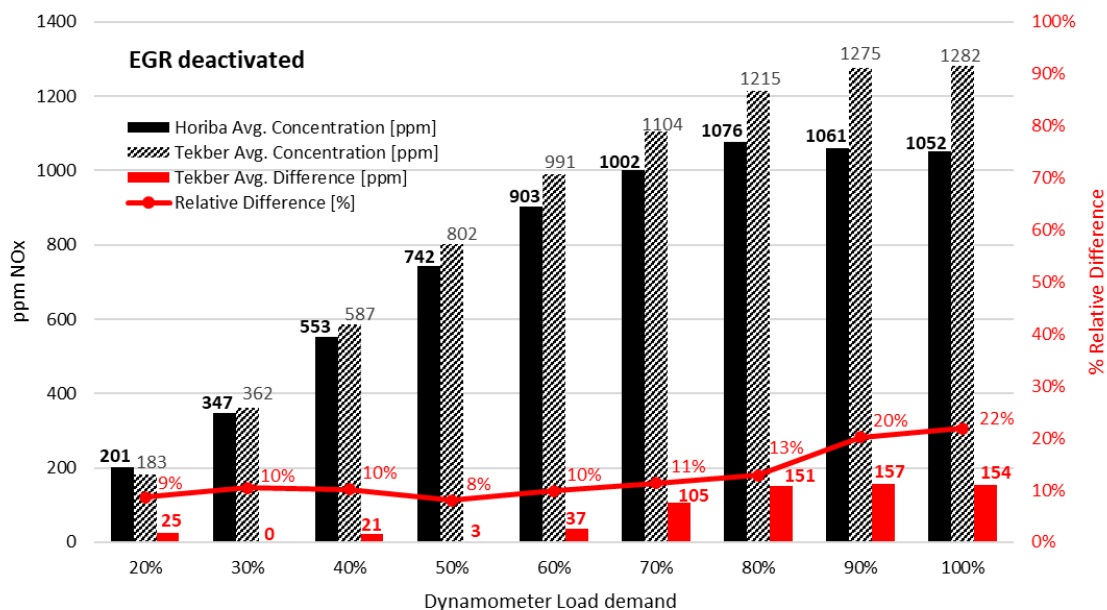


Figure 5-12. Differences between Tekber and Horiba result according to the load demand without EGR

Therefore, at least for the realization of NO_x measurement using the Static Idling Internal Load Test, the usual effective NO_x concentration measurement range is between 0-700 ppm, validating the use of the Tekber analyzer for PTI purposes.

5.4. CONCLUSIONS

An exhaustive examination of the equipment employed for measuring NO_x concentrations has been carried out in section 5.2, encompassing a description of the gas analyzer and its principal characteristics.

The equipment has been specifically designed for PTI use, thus meeting all the necessary technical and operational requirements for its application. The addition of NO_x measurement capability does not compromise its functionalities. Furthermore, this aids in the seamless integration of its use, as it is already well-incorporated into the workflow of PTI stations.

Also, the research conducted in section 5.3 aimed to assess the accuracy and suitability of NO_x measuring equipment at PTI, for which no regulatory framework has yet been established. To that end, deviations of less than 10% rel. and/or 10 ppm in absolute terms with respect to a reference were considered acceptable. The reference device selected was the Horiba equipment, designed for use in homologation processes.

By the definition of the PTI process, the methods to be used must be both fast and reliable. The equipment used must follow the same principle, adding the need to be robust and suitable to work in a wide variety of environmental conditions. It also needs to have minimal maintenance costs and times (both technical and metrological) and

require the least possible intervention on the vehicle to perform the measurement. The Tekber equipment meets these criteria, making it the chosen option for our study instead of pricier and more complex devices like PEMS or other high-maintenance laboratory-grade equipment.

From the set of tests carried out and at least **for the measurement range from 0 to 700 ppm**, which is the range found for over 99% of current vehicles (according to data from the research, see Chapter 8), can be concluded that the Tekber's **performance and accuracy can be considered acceptable for PTI use**. For instance, **average deviations recorded were 2.6 ppm or 9% rel.** (for accumulated differences) for the Static Idling Internal Load Test in low load conditions with EGR, which is the test with the most similar conditions to be found at PTI.

Of course, these differences would not be acceptable for a homologation test. However, they may be suitable for use in PTI, where the aim is not to obtain the exact emissions concentration. Instead, the aim is to have sufficient data to decide whether the vehicle is in roadworthiness condition, detect tampering and high-emitter vehicles, and verify that the anti-pollution systems are working. Regarding this matter, since the NO_x concentration levels obtained from both devices are of equal magnitude, the decision-making process will yield identical outcomes.

The technical improvement in the future would be to increase the accuracy of the measurement for the range up to 700 ppm since the trend of NO_x emissions from new vehicles is expected to be downward. This could be done by incorporating dry-basis measurement, but only as long as the economic and technical requirements are kept within a reasonable range.

In short, the tests have allowed us to verify that the method and equipment used are precise enough to check the level of NO_x emissions from a vehicle undergoing a PTI inspection, thereby determining if the EATS is operational or not.

Then, the main conclusions of this chapter are as follows:

- The gas analyzer employed in method development satisfies all the necessary requirements for its utilization in PTI.
- The accuracy of the results furnished by the equipment, particularly for concentrations below 700 ppm of NO_x, is suitable for its application in NO_x measurement for PTI.

The following chapter will analyze the results obtained by applying the proposed method in chapter four to a group of 23 vehicles, allowing an evaluation of the method's validity based on these results.

CHAPTER 6

NO_x MEASUREMENT METHOD VALIDATION

6. NO_x MEASUREMENT METHOD VALIDATION

6.1. INTRODUCTION

Following the comprehensive explanation of the entire NO_x measurement process described in Chapter 4 and after having validated the suitability of the measuring PTI-grade equipment in Chapter 5, the current chapter unveils the outcomes achieved by employing this methodology on a group of 23 vehicles.

These vehicles are representative of the vehicle fleet in Spain and the EU, making it possible to draw significant conclusions about the validity of the method from these results.

As will be seen later, one of the method's features is its ability to analyze the quality and significance of the results obtained. Additionally, one of the main advantages of this measurement method compared to other proposed methods is its high reproducibility.

Due to the importance of both of these qualities of the method, the analysis of the results obtained has been divided into three main parts:

- 1) Analysis of the quality and significance of the obtained results
- 2) Analysis of the reproducibility of the test based on the obtained results
- 3) Analysis of the obtained results

From the analysis of the obtained results, it must be determined whether the application of the method on a representative group of vehicles yields the expected outcomes. These outcomes are essential for validating the method and asserting its capability to provide accurate results.

6.2. SET OF VEHICLES TESTED FOR METHOD VALIDATION

After formulating the methodology, it was determined that the most effective approach to validate was to implement the method on a diverse set of vehicles. This collection of vehicles encompasses a wide array of characteristics and is representative of the prevalent diesel vehicles commonly found in the fleet.

In order to conduct research, design, and verify the measurement method outlined in Chapter 4, the fleet of 23 vehicles specified in Table 6-1 was utilized.

Several tests have been carried out on each vehicle to assess result consistency and guarantee replicability of the tests. The tests have been repeated consecutively on the same vehicle. Overall, the testing for each vehicle has been conducted over two separate days.

All vehicles except one are diesel-powered. The exception is vehicle No. 18, which is a petrol-powered vehicle, and has also been tested in the same way to compare the NO_x emissions of diesel engine vehicles with petrol engine vehicles. The purpose of

this comparison is to determine if the same measurement process can be used for both types of vehicles.

These vehicles come from 14 different manufacturers representative of the European market and have emission levels from Euro 3 to Euro 6, with engine sizes from 1248 cm³ to 2993 cm³, and engine power from 66 kW to 210 kW. Therefore, it is a representative selection of vehicles in the European and Spanish fleets.

Based on data provided by Eurostat⁹ in 2018 for the EU28 region, the distribution of diesel M1 vehicles by engine size was as follows: 4.98% of vehicles had engine sizes smaller than 1400 cm³, 77.4% had engine sizes ranging from 1400 cm³ to 2000 cm³, and 15.7% had engine sizes greater than 2000 cm³.

Reference Vehicle	Vehicle Manufacturer	Model	Engine Manufacturer	Engine model	Engine size (cm ³)	Engine Power (kW)	Emissions level
1	SEAT	Leon	Volkswagen	ARL	1896	110	Euro 3
2	Volvo	V50	PSA	D4204T	1997	100	Euro 4
3	Alfa Romeo	Mito	FIAT	19981000	1248	70	Euro 4
4	Audi	A4	Audi	CAG	1968	100	Euro 4
5	BMW	330D	BMW	306D3	2993	170	Euro 4
6	BMW	535d	BMW	306D5	2993	210	Euro 4
7	Peugeot	407	Peugeot	RHR	1997	100	Euro 4
8	Volkswagen	Passat	Volkswagen	BKP	1968	103	Euro 4
9	Skoda	Octavia	Volkswagen	BKD	1968	103	Euro 4
10	Audi	A5	Audi	CGKA	2698	140	Euro 5
11	Citroën	Berlingo	Citroën	9H06	1560	66	Euro 5
12	Volkswagen	Touran	Volkswagen	CFH	1968	103	Euro 5
13	Hyundai	i30	Hyundai	D4FB	1582	81	Euro 5
14	SEAT	Leon	Volkswagen	BLS	1896	77	Euro 5
15	Opel	Insignia	GMPTC	A20DTH	1956	118	Euro 5
16	Nissan	Juke	Renault	K9K	1461	81	Euro 5
17	Opel	Astra	GM	A17DTS	1686	81	Euro 5
18	Renault	Fluence	Renault	H4M D7	1598	84	Euro 6
19	Renault	Talisman	Renault	R9M E4	1598	96	Euro 6
20	Peugeot	Boxer	Peugeot	AH03	1997	96	Euro 6
21	Skoda	Superb	Volkswagen	CRL	1968	110	Euro 6
22	Kia	Sportage	Kia	D4FD	1685	85	Euro 6
23	Citroën	C4 Picasso	Citroën	BH01	1560	88	Euro 6

Table 6-1. Set of vehicles and engines used for designing the method.

⁹ <https://ec.europa.eu/eurostat/data/database>

Among the chosen vehicles, 4.3% of them have engine sizes below 1400 cm³, 82.6% have engine sizes ranging from 1400 cm³ to 2000 cm³, and 13.0% of the vehicles have engine sizes exceeding 2000 cm³.

So, according to the engine size, the sample of vehicles selected to check the hypothesis could be considered representative of the European diesel M1 vehicles fleet.

On the other hand, 13 of the 14 manufacturers are included in the group of the 20 top sellers in Spain (see Figure 6-1) according to ANFAC data [190], [191], so regarding vehicle manufacturers, the sample of vehicles could be also considered as representative of the Spanish vehicles fleet.

2019 Best-Sellers Manufacturers

New registrations of M1 vehicles in Spain along 2019 (in thousands of vehicles)

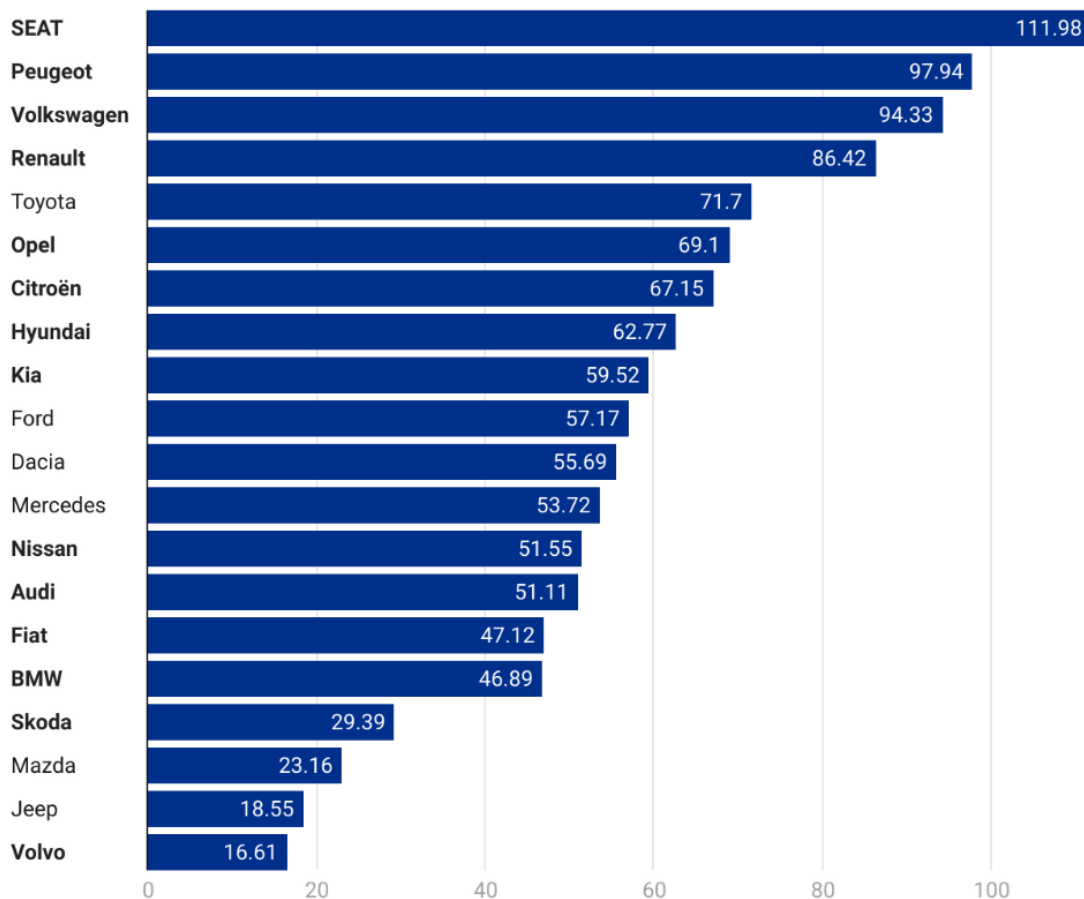


Figure 6-1. Best-Sellers Manufacturers in Spain (2019). Source of data: ANFAC [191].

Only one Euro 3 vehicle was tested because older vehicles present issues with OBD communication due to the communication protocol used. These communication problems were also detected in some Euro 4 vehicles. However, Euro 5 and Euro 6 vehicles did not exhibit any OBD communication problems during the tests.

Measurements were conducted on each vehicle across multiple instances, ensuring a sufficient number of data points for evaluating the reproducibility of the measurement procedure for each specific vehicle. Using standard statistical methods such as Standard Deviation and Coefficient of Variation, an analysis was conducted to ensure the test's robustness and consistent reproducibility across all vehicles. Instances of compromised reproducibility in specific vehicles prompted investigations into the reasons behind such deviations.

In every test and for each vehicle, an assessment was conducted regarding the strength and importance of the linear correlation between the "% engine load" value and the recorded NO_x concentration in the exhaust. To achieve this, the consistency of the relationship's behavior between these variables across all vehicles and tests was examined. Furthermore, a comparison is conducted between the outcomes derived from multiple vehicle measurements and existing data from comparable vehicles. This evaluation aims to determine whether the observed behavior of the vehicles aligns with the expectations established by regulations and literature.

The measurement of NO_x emissions through the proposed test yields a wealth of varied information. This information, once scrutinized, facilitates an assessment of the appropriateness of the measurement procedure for achieving the intended objective.

6.3. QUALITY AND SIGNIFICANCE ANALYSIS

A critical task is to assess the degree of linkage between "% engine load" and NO_x concentration across the entire set of vehicles tested. This step involves assessing the **quality** and **significance** of the correlation between the "% engine load" and NO_x concentration across all tested vehicles.

The underlying hypothesis of the measurement methodology postulates that when the engine operates under a uniform set of conditions—such as maintaining idle speed and other pertinent parameters—any alterations in power demand result in proportional variations in NO_x emissions. These emission variations are observable and quantifiable at the exhaust pipe of the vehicle.

If there are no external influences, the relationship between the values from these two variables (the "% engine load" value and the NO_x concentration in the exhaust pipe) seems to be a linear function, increasing the NO_x concentration if the "% engine load" increases. Nevertheless, the presence of external influences can impact this relationship.

To validate this relationship, the examination of R² and p-value for each vehicle within the studied set is undertaken. This analysis aims to ascertain that their trends also support the credibility of the working hypothesis.

The next sections will explain how these values are used to define the quality and significance of the relationship between the "% engine load" value and exhaust NO_x concentration at idling engine speed. Following, the main results of quality and significance from the measurement process will be explained in detail.

In a process similar to the data aggregation method defined in section 4.2.3, the data from each test is divided into four major groups, ensuring that the analysis of these groups yields detailed insights into the emissions behavior during the test.

The quality and significance analysis will be performed for the following 4 different data sets (see Figure 6-2):

- i) **Total** of measurements of the test: the complete data set is analyzed as a whole.
- ii) The **Initial** section of the test: The data corresponding to the 1st and 2nd stages are analyzed as a whole.
- iii) The **Final** section of the test: The data corresponding to the 4th and 5th stages are analyzed as a whole.
- iv) The **Acceleration** section: The data corresponding to the third section is analyzed as a whole.

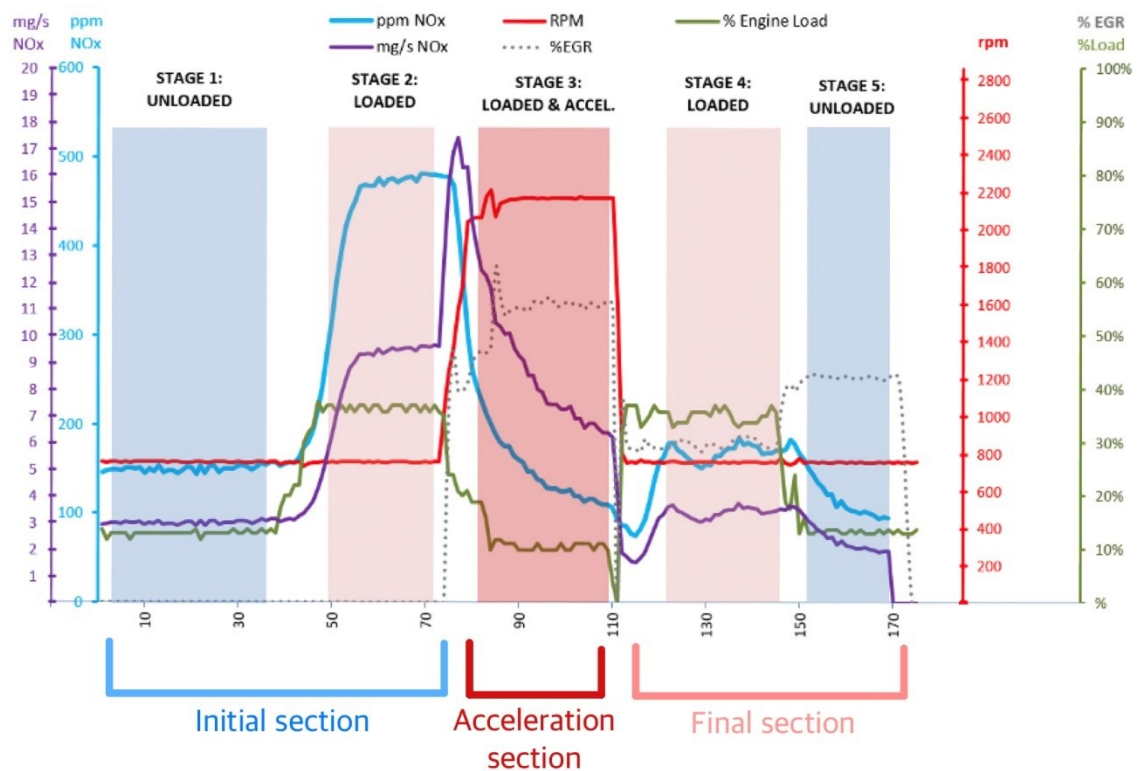


Figure 6-2. Sections for analyzing R^2 and p -value of the test.

This approach serves as a means to validate the accuracy of measurements taken during idling. It involves verifying that the test accurately represents the relationship between "% engine load" and the measured NO_x concentration, while also ensuring the collected data is of sufficient quality.

6.3.1. R² VALUE AND QUALITY

The methodology for NO_x measurement relies on the correlation between NO_x concentration in the exhaust pipe and the corresponding "% engine load" value.

Analyzing the data from the measurement of NO_x concentration in the exhaust pipe and the "% engine load" value read through the OBD system of the vehicle while the engine is idling, the regression factor (R²) can be calculated, and the quality of the relationship can be assessed.

The Linear Regression factor (coefficient of determination, R²) is calculated from the Pearson coefficient to check the quality of the model (the relationship between NO_x concentration and "% engine load" at idling). It is a coefficient that provides information about the "goodness-of-fit" of the data obtained from the measurement process to the fitted regression line calculated from them, so **the higher the Regression factor, the better the quality of the model.**

A high R² factor means that the data fit properly to the regression line calculated. Typically, this approach is employed to test a hypothesis, and in the context of this case, the results will be regarded as suggestive but not conclusive evidence of the presence of this relationship. To establish the validity and significance of this relationship, the p-value will be utilized. Meanwhile, the focus of the R² will be on assessing the strength and quality of the relationship.

For the analysis, it will be assumed as true the hypothesis of the existence of the relationship between NO_x concentration in the exhaust pipe and the "% engine load" value (although it will be checked by the p-value).

The value of R² is calculated (Equation 6-1) as the squared of the Pearson correlation coefficient:

Equation 6-1

$$R^2 = \frac{\sigma_{XY}^2}{\sigma_X^2 \sigma_Y^2}$$

σ_{XY} : *Covariance (X, Y)*

σ_X : *Standard Deviation X ("% engine load")*

σ_Y : *Standard Deviation Y (NO_x concentration)*

The behavior of the R² in the four different data groups defined (refer to Figure 6-2) is related to the way NO_x is generated and EGR and EATS work.

When the relationship is not affected by "external" circumstances (see section 4.2.1 and Figure 3-5), that means, when there are no additional variables that affect the NO_x generation from the engine and the NO_x emission in the exhaust pipe, the goodness-of-fit of the data is the best.

6.3.2. P-VALUE AND SIGNIFICANCE

A relationship between two variables, such as the relation between "% engine load" and NO_x concentration in the exhaust pipe, exhibits statistical **significance** when the probability of this relationship being random is extremely low.

The p-value is a statistical measure used to assess the likelihood of obtaining the observed results if the null hypothesis is true. In this context, the null hypothesis suggests that there is no relationship between the variables being studied. By examining the p-value, researchers can determine the significance of their findings and distinguish between outcomes that are due to random chance and those that are statistically significant.

In this context, the null hypothesis suggests that there is no observable connection between the "% engine load" parameter and the concentration of nitrogen oxides in the exhaust pipe. The p-value serves to provide the likelihood of achieving the observed measurement outcomes under the assumption that both variables are, indeed, independent of each other.

Usually, the p-value used in social research to validate the relationship between two variables is 0.05. When it is important to ensure the results, like for medical research, a more demanding value like a p-value of 0.01 is used. This value defined to validate the relationship is known as the **significance level**. In the definition of the NO_x measurement method, to ensure the results for the model studied, the significance level used was 0.01.

In this way, obtaining a p-value lower than 0.01 **suggests** that the data from the test are not consistent with the null hypothesis, because the probability of the null hypothesis is too low, and the null hypothesis can be rejected.

So, the relationship is **assumed** valid because the null hypothesis is highly implausible, although strictly the p-value method does not provide direct support for accepting a hypothesis. The low probability of "not being related" (as indicated by a small p-value) to both variables, allows us to reject the idea that "% engine load" and NO_x concentration are not related. As a result, we accept the alternative, which is that they are indeed related. So, based on the p-value, we can conclude whether the evidence supports the relationship or not, rather than outright accepting the hypothesis as true.

In this case, the use of p-value and acceptance of the hypothesis of relationship is based on the relationship previously explained from the process of generation of NO_x in the combustion chamber of diesel engines. That means, the method is not used to confirm the relationship, but the relationship is used to validate the process of measurement.

The p-value is used to quantify the significance of the model and to provide a mathematical way to check that the measured data of NO_x concentration are related to the "% engine load" and that the measurement is correct and with significance. In this way, **the lower the p-value, the higher the significance of the model**, because the lower the probability of obtaining the data if the null hypothesis is true.

Similar to the R² analysis, the p-value analysis is conducted by segregating the data from the measurement process into four distinct datasets, as outlined in Figure 6-2.

Similarly, the p-value's behavior is intricately connected to the mechanisms underlying NO_x generation and the functioning of EGR and EATS.

6.3.3. QUALITY AND SIGNIFICANCE RESULTS

Theoretically, the dataset pertaining to the Initial section consistently exhibits a higher R² value, attributed to the lack of external factors that could potentially affect the relationship. Given that the parameter of "% engine load" remains constant owing to the connected equipment and maintains a stable value, coupled with the engine speed (idling) also maintaining a consistent value over time, the concentration of NO_x is primarily contingent upon the "% engine load".

As a result, the R² value associated with this dataset, when fitted to the defined linear function, attains the highest level within the entirety of the test regimen.

Conversely, the dataset pertaining to the Acceleration section emanated from a test segment characterized by alterations in engine speed, often accompanied by the operation of EGR and conceivably the EATS. Owing to these factors, the concentration of NO_x at the exhaust pipe is not solely predicated upon the parameter of "% engine load." Instead, various additional variables exert their influence, thereby resulting in a diminished R² value between NO_x concentration in the exhaust pipe and "% engine load," which typically registers as the lowest across the entirety of the test procedure.

The dataset within the Final section can be viewed as an intermediary scenario when compared to the preceding sections (Initial and Acceleration). This is due to the consistent values exhibited by both "% engine load" and engine speed (at idling) in this phase. However, it is worth noting that EGR and EATS functionalities are usually operational during this segment of the test, intermittently spanning either the entirety or a partial duration. As a consequence, the R² value associated with this section generally attains an acceptable level of correlation, although it might not reach the same heights observed in the Initial section.

Analyzing the whole data from the test in the Total section, as the data from all the previous sections are included, the R² value reached is influenced by how much EGR and EATS affect the NO_x emissions along with the Acceleration and Final sections.

Furthermore, behavior or p-value related to the Initial, Acceleration, and Final sections is similar to R² behavior. Typically, the p-value within the initial section not only falls below the predefined significance level of 0.01, but in a majority of cases, vehicles exhibit p-values even lower than 0.0001.

Within the Acceleration section, an elevation of the p-value can be observed, commonly exceeding the predetermined significance threshold.

Within the final section, the relationship between "% engine load" and NO_x concentration becomes more complex and less straightforward compared to the Initial section. Consequently, the p-value tends to be higher in the final section than in the Initial section, but generally lower than in the Acceleration section and lower than the significance level.

From a practical standpoint, it is crucial to assess the quality of the relationship to validate the measurement process. When conducting tests on a vehicle, if the R^2 value for the Initial section is not higher than the other sections, it becomes essential to investigate whether there are any issues with the test execution or if any external factors are influencing the results. This analysis helps identify potential problems and ensures the reliability of the measurements in the context of the test setup, the initial section is generally immune to external influences that might affect the studied relationship. During vehicle idling, where the EGR and EATS systems are inactive, external factors have minimal impact on this phase. Hence, the p-value for this section is anticipated to be the lowest among all sections, accompanied by the highest R^2 value, signifying a robust correlation in the test results.

This situation can be observed in Table 6-2, from the p-value data of every vehicle in the column of the Initial section, wherein in most of the cases the p-value for the Initial section shows the lower value.

Among the conducted tests, only three vehicles deviate from this pattern, exhibiting a p-value in the Initial section that exceeds the values observed in any of the other sections.

Only two vehicles, namely Vehicle No. 5 and Vehicle No. 12, exhibit a p-value in the Initial section that surpasses the predetermined significance level. Remarkably, these two vehicles also demonstrate an anomalous rise in NO_x emissions from the Unloaded state to the Loaded state (see section 6.5). The factors attributing to this situation align with those accountable for producing exceptionally elevated p-values that surpass the predefined level of significance during the analysis.

Vehicle No. 5 is managed by an ECU configuration distinct from the rest of the vehicles, potentially leading to alterations in certain variables influencing NO_x emissions. Conversely, for Vehicle No. 12, the atypical behavior of the EGR system impacts the correlation and the resulting p-value, exhibiting consistency across all sections (Figure 6-27). For instance, it has been observed that certain vehicles from the Group VAG maintain their EGR valve consistently open during the test. Naturally, this situation impacts the NO_x emissions in the Initial section, leading to a reduction in the R^2 value when such occurrences take place.

The third vehicle with a p-value of the Initial section higher than the value from any of the other sections is vehicle No. 4. Analyzing the several tests from this vehicle, the p-value for the Initial and Final sections was always clearly lower than the significance value, so there is no doubt about the relationship between variables. However the behavior of NO_x concentration is quite similar in both sections, before and after the Acceleration section, and that makes the p-value from both sections similar too. Figure 6-3 can check how NO_x concentration is related to the "% engine load", with similar behavior in both sections.

For the rest of the vehicles, the p-value in the Initial Section is not only lower than the significance level but significantly lower than the p-value in the other 3 sections.

A comparable pattern can be noted in relation to the R^2 value. Generally, the Initial section often exhibits the highest R^2 value across a majority of vehicles, though there are a few instances where the R^2 value is greater in the Final Section.

Once more, vehicles numbered 4, 5, and 12 stand out with higher values compared to other sections: vehicles No. 4 and No. 5 in the Final section, and vehicle No. 12 in the Final Section and Acceleration Section.

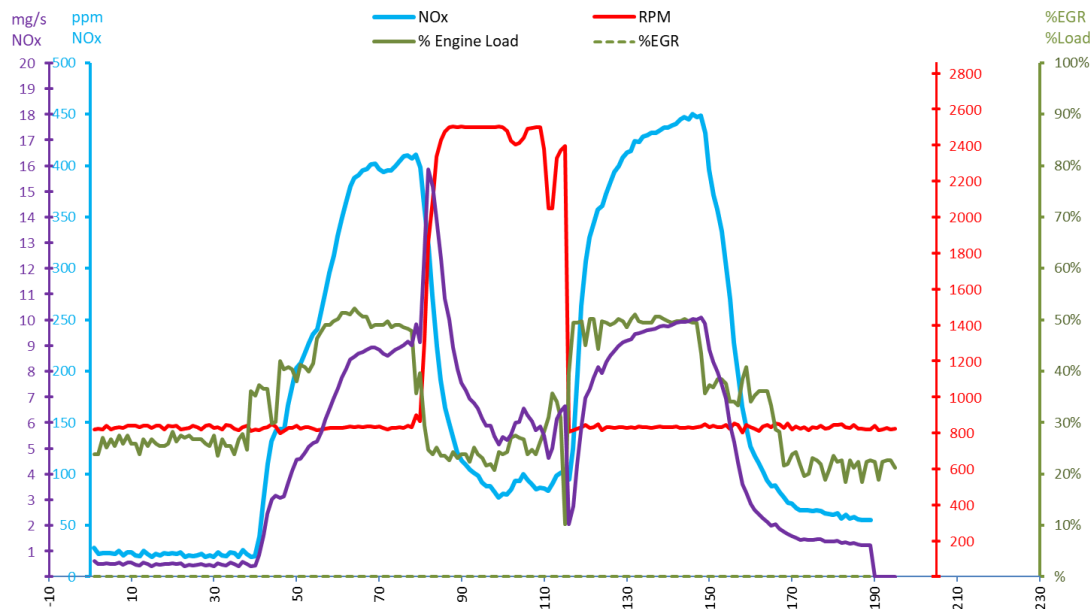


Figure 6-3. Sample of NO_x test of vehicle No. 4.

Both cases are due to the explained circumstances. Also, vehicle No. 18, the petrol one, shows an R^2 value for the Initial Section slightly lower than the Final Section. In this case, the low values for the NO_x concentration may be the cause of this unusual situation.

Lastly, in the case of Vehicle No. 23, the R^2 value in the Final Section shows a slight increase compared to the R^2 value obtained in the initial section.

In summary, the typical trend, while recognizing potential exceptions due to variations in engine conditions and NO_x emissions for each vehicle, is that the **Initial Section** tends to display a higher R^2 value and a lower p-value compared to other sections. This pattern arises because the Initial Section **reflects a scenario of NO_x emissions unaffected by external influences**.

This section is used as evidence of the relationship between NO_x concentration and **"% engine load" in the vehicle tested**. Based on the engine's operational behavior and the effectiveness of anti-pollution systems, it is possible that the values obtained in the Final Section could closely resemble or sometimes even surpass those acquired in the Initial Section.

In contrast, the Acceleration section displays a pronounced impact on the connection between NO_x concentration and "% engine load" due to fluctuations in engine speed and the influence of EGR and/or EATS systems. As a result, the p-value typically

exceeds that of other sections and sometimes even surpasses the predetermined significance level. This implies that in this section, the null hypothesis cannot be dismissed.

In simpler terms, it often suggests that there is generally no significant correlation between the measured NO_x concentration at the exhaust pipe and the "% engine load" recorded from the OBD during acceleration.

Reference Vehicle	Total Section		Initial Section		Final Section		Accel. Section	
	R ²	p-value	R ²	p-value	R ²	p-value	R ²	p-value
1	0.620	9.90E-10	0.884	7.69E-66	0.807	9.36E-19	0.227	1.75E-01
2	0.014	2.97E-01	0.907	5.26E-28	0.856	1.56E-20	0.175	1.53E-01
3	0.697	8.02E-35	0.915	1.04E-44	0.790	1.46E-10	0.269	2.19E-01
4	0.525	2.02E-24	0.567	1.38E-11	0.749	8.20E-14	0.098	5.31E-01
5	0.110	1.38E-01	0.461	4.36E-02	0.546	1.86E-09	0.380	5.30E-02
6	0.632	9.73E-07	0.852	2.65E-20	0.791	7.35E-08	0.494	2.36E-02
7	0.687	7.22E-18	0.907	4.29E-43	0.880	3.89E-17	0.427	1.59E-01
8	0.255	1.97E-01	0.920	1.25E-25	0.609	3.28E-04	0.428	1.10E-01
9	0.043	3.62E-02	0.976	2.78E-60	0.816	1.03E-18	0.480	8.73E-02
10	0.205	3.16E-04	0.887	2.95E-33	0.250	2.19E-02	0.443	1.67E-01
11	0.162	2.35E-04	0.840	3.22E-26	0.245	3.89E-02	0.249	2.76E-01
12	0.034	2.75E-01	0.094	2.51E-01	0.161	1.29E-01	0.362	3.37E-01
13	0.209	2.15E-01	0.914	1.22E-32	0.358	1.59E-02	0.217	2.65E-01
14	0.272	8.16E-03	0.905	3.86E-32	0.598	3.23E-03	0.174	3.15E-01
15	0.146	1.45E-01	0.880	5.63E-37	0.524	3.04E-05	0.482	2.02E-02
16	0.437	1.92E-04	0.857	1.82E-16	0.530	2.45E-06	0.219	2.62E-01
17	0.321	5.96E-13	0.953	6.84E-48	0.160	2.43E-01	0.158	3.70E-01
18	0.063	1.66E-01	0.350	6.31E-03	0.362	8.41E-02	0.095	2.96E-01
19	0.691	4.51E-16	0.912	2.33E-32	0.786	9.24E-06	0.313	3.12E-02
20	0.325	3.96E-08	0.798	1.10E-25	0.566	8.77E-05	0.298	1.13E-01
21	0.181	7.53E-03	0.913	8.11E-22	0.813	1.06E-18	0.315	9.12E-02
22	0.019	3.40E-01	0.927	6.13E-41	0.827	8.08E-11	0.560	1.24E-04
23	0.300	1.32E-13	0.877	7.97E-24	0.881	1.76E-17	0.323	1.02E-01

Table 6-2. Statistical analysis of results from vehicles in static sections of NO_x test.

Lastly, a similar analysis is conducted on the entire dataset encompassing the Total Section. The data within this section are influenced by the emissions behavior observed across the three previously scrutinized partial sections.

Consequently, when the data from the Acceleration Section are notably impacted, the p-value for the Total Section often surpasses the predetermined significance level.

In the context of the Total Section, the R² value generally tends to be lower than that of the Initial and Final Sections, yet higher than what is observed in the Acceleration Section.

In order to facilitate a comparative assessment of the outcomes derived from the analyzed group of vehicles, Table 6-2 incorporates the averaged values obtained from the series of measurements conducted on each individual vehicle.

It is crucial to emphasize that Table 6-2 presents the mean values resulting from the measurements conducted on each specific vehicle. Due to the typically low p-values, the average value displayed in Table 6-2 closely aligns with the highest value observed among the various tests conducted.

For example, in vehicle No. 5 the average p-value for the Initial section is $4.36 \cdot 10^{-02}$, higher than the significance level (marked in red) because there are two tests with a p-value higher than the significance level, although the rest of the tests had a p-value lower than the significance level, with values for the p-value from the order of 10^{-9} to the order of 10^{-67} .

For vehicle No. 12, most of the measurements showed a p-value in the Initial section higher than the significance level, so in this case, the average value is nearest to the usual value obtained from the measurement.

6.3.4. SUMMARY OF QUALITY AND SIGNIFICANCE

Based on the analysis of emissions from the group of vehicles presented in Table 6-1, the main features of the NO_x measurement test proposed can be detailed.

Given that the sample of vehicles is representative of both the Spanish and European fleets, the obtained results can be extrapolated to a broader context, although additional studies may be necessary to supplement the existing data and provide a more comprehensive understanding.

The examination of the quality and significance of the acquired data has been undertaken to verify whether the results of the test align with the working hypothesis. Quality and statistical Significance have been assessed using R² and p-value for analysis and testing.

The findings indicate that a **substantial percentage of vehicles exhibit an R² value exceeding 0.6 in the initial section, with all of them surpassing 0.8. Notably, this holds for 91% of diesel vehicles.** This percentage is considered acceptable for this section. Furthermore, instances of comparatively lower values have been identified, accompanied by an exploration of the underlying factors contributing to these diminished values.

Regarding the final section, it becomes evident that the attained R² values are somewhat lower. Specifically, **55% of diesel vehicles exhibit an R² value surpassing 0.6** in this section. Although this percentage is lower than that observed in the Initial Section, it is still regarded as an acceptable level of correlation.

In the Acceleration section, the R² values noticeably decrease, with none of the cases exceeding the threshold of 0.6. When considering the entire set of values, it is apparent that only 22.7% of the vehicles surpass the R² value of 0.6.

This pattern aligns with the anticipated behavior based on the measurement methodology's performance. Therefore, from the perspective of the correlation quality between the variables, it is reasonable to assert that the outcomes derived from the analyzed set of measurements serve to validate the measurement method. The results are consistent with the expected behavior, further strengthening the method's credibility.

A similar trend emerges upon examining the p-values. The data analysis reveals a substantial proportion of tested vehicles exhibiting p-values below the predetermined significance level. In cases where this doesn't occur, the underlying reasons can be identified.

In the **Initial Section**, where the relationship is most prominent due to the lack of external factors, a noteworthy observation is that **90% of the diesel vehicles** (or 93% when including gasoline vehicles) **displayed a p-value below the predetermined significance threshold of 0.01**. For the remaining cases where this threshold was not met, it becomes possible to estimate the technical factors contributing to this deviation from compliance.

Similar to the R² data, the significance values in the subsequent sections are not as strong as those in the initial section. Specifically, in the final section, a noteworthy **77% of the diesel vehicles displayed a p-value below the significance threshold**—a commendable outcome, albeit slightly lower than that achieved in the initial section. However, this percentage reduces to 68% when considering the entire dataset.

In the Acceleration section, it is important to note that only one vehicle demonstrated a p-value below the significance level, indicating a unique result compared to the other sections.

As in the case of the R² data, the significance values obtained in the rest of the sections are not as good as in the initial section. **In the final section, 77% of the diesel vehicles presented a p-value below the significance level** (which is also a very good result, although lower than that obtained in the initial section), dropping to 68% if the total data is analyzed. In the Acceleration section, only one vehicle presented a p-value below the significance level.

As explained, this behavior is to be expected given the operating basis of the measurement method, since in the Final section there may be external influences (EGR and EATS) that modify the behavior of NO_x emissions, and therefore the relationship of these with the "% engine load", this being very pronounced in the Acceleration section.

Therefore, as with the Quality of the relationship, the results obtained from the measurements confirm what was expected to be obtained in terms of Significance, so from this point of view, it is also possible to state that the **results obtained validate and confirm the proposed measurement method**.

6.4. REPRODUCIBILITY ANALYSIS

Reproducibility can be defined in different ways. In the context of research, reproducibility is the capacity of a test or experiment to be reproduced or replicated by others. However, this is not the capacity to which we will refer in this analysis. Rather, we will focus on an approach closer to that of metrology.

With this approach, reproducibility can be defined as the variation caused by the measurement system, observed when different operators measure the same part many times using the same measurement system under the same conditions.

Another possibility, closer to the subject of this thesis, is to define reproducibility as the capability of an instrument (or a method) to yield the same result in different measurements conducted under the same conditions over extended periods.

Considering that the object of measurement (the NO_x concentration) will inherently exhibit a high degree of variation, such that repeating measurements will involve changes in the object itself, a more appropriate definition of **Reproducibility** for the test could be **the ability of the test to obtain consistent results when replicating the measurement over the same subject, from a different set of data but following the same measurement method procedure.**

Reproducibility is a valuable indicator that assesses the extent of error deviation between different measurements. It assures that the test method can provide reliable and stable results, even if the exact data points may differ, enhancing the overall accuracy and credibility of the measurement process.

Metrologically, one way to analyze reproducibility is by using the method of analysis of variance. In this research, to assess the reproducibility of the measurement method, a simpler approach to this method (analysis of variance) will be employed, evaluating reproducibility as an inverse property of the dispersion of results obtained from that measurement process while maintaining the conditions under which that measurement is conducted.

To assess the reproducibility through the application of the suggested method, the outcomes derived from conducting multiple instances of the NO_x measurement test on each vehicle have been examined. This examination ensures that the attained measurements consistently exhibit the requisite level of reliability and stability, thereby substantiating the viability of employing the measurement technique.

For this analysis, the usual statistical dispersion measures have been used (Table 6-3), being the most important the Standard Deviation (SD) (see Equation 6-2) and the Coefficient of Variation (CV) (see Equation 6-3), providing information about the dispersion of the results for the NO_x concentration, NO_x flow mass emission, and the "% engine load" value, among others.

Equation 6-2

$$\sigma = \sqrt{\int_{-\infty}^{+\infty} (x - \mu)^2 f(x) dx}$$

σ : Standard Deviation (SD)

x : Set of data from measurement μ : Expected Value (Mean)

Equation 6-3

$$CV = \frac{\sigma}{\mu}$$

CV: Coefficient of Variation

σ : Standard Deviation (SD) μ : Expected Value (Mean)

The SD, also known as Relative Standard Deviation (RSD), is indeed used to measure the dispersion of a set of values. It shows how the Standard Deviation is according to the Mean value, and it is calculated as the ratio of the SD to the Mean.

The Coefficient of Variation (CV) serves as a valuable tool for comparing the spread of diverse value sets, irrespective of the actual magnitudes of these sets. In this particular context, it enables a comparison of the variability demonstrated by measurements across various vehicles, regardless of the absolute emission values presented by each vehicle.

Statistical Parameters	Idle Unloaded			Idle Loaded			TMV	
	NO _x (mg/s)	NO _x (ppm)	% Engine load	NO _x (mg/s)	NO _x (ppm)	% Engine load	NO _x (mg/s)	NO _x (ppm)
Min.	mg/s	ppm	%	mg/s	ppm	%	mg/s	ppm
Max.	mg/s	ppm	%	mg/s	ppm	%	mg/s	ppm
Mean	mg/s	ppm	%	mg/s	ppm	%	mg/s	ppm
Standard Deviation	mg/s	ppm	%	mg/s	ppm	%	mg/s	ppm
Coef. of Variation	%	%	%	%	%	%	%	%
Std. Error Mean	mg/s	ppm	%	mg/s	ppm	%	mg/s	ppm
Lower limit	mg/s	ppm	%	mg/s	ppm	%	mg/s	ppm
Upper limit	mg/s	ppm	%	mg/s	ppm	%	mg/s	ppm

Table 6-3. Statistical parameters calculated for the set of measurements for each vehicle.

The CV is a commonly employed statistical parameter to assess the reproducibility and quality of studies and experiments. Similar to the SD, a lower CV signifies reduced data dispersion, indicative of enhanced test consistency and reproducibility.

Dispersion measures quantify how much the values in a set of measurements deviate from the mean of that set. A higher level of dispersion corresponds to larger values of dispersion measures. Then, greater dispersion results in reduced test reproducibility. Hence, achieving strong reproducibility requires minimizing the dispersion parameter values obtained from the measurement processes.

Reference Vehicle	Idle Unloaded			Idle Loaded			TMV	
	SD NO _x (mg/s)	SD NO _x (ppm)	SD % Engine load	SD NO _x (mg/s)	SD NO _x (ppm)	SD % Engine load	SD NO _x (mg/s)	SD NO _x (ppm)
1	0.28	10.50	0.50	1.12	46.64	5.87	2.31	86.28
2	0.20	9.93	0.94	0.31	14.43	1.05	0.69	22.45
3	0.60	45.84	0.52	1.22	82.82	2.39	2.71	180.11
4	0.61	27.08	1.92	0.80	36.28	2.88	1.66	67.02
5	0.69	22.90	2.77	0.56	19.66	2.56	1.40	51.57
6	0.45	15.84	2.21	1.43	56.14	5.19	2.55	103.36
7	0.64	32.20	1.04	3.33	161.02	2.20	4.34	222.03
8	0.30	14.57	0.77	0.53	21.60	0.77	1.34	65.53
9	0.13	6.41	0.32	0.21	9.99	1.79	0.47	23.72
10	0.40	37.03	2.23	0.44	75.34	4.78	1.24	66.80
11	0.43	25.46	1.25	1.66	100.55	5.11	4.92	298.46
12	0.22	11.59	2.59	0.21	10.73	1.44	0.39	22.08
13	0.34	22.27	2.60	1.28	83.48	4.26	2.38	156.03
14	0.26	14.60	2.75	1.14	61.08	3.43	1.26	77.07
15	0.24	11.24	0.52	0.74	34.53	1.21	1.63	75.02
16	0.34	21.88	1.50	1.39	82.90	3.23	2.49	146.68
17	0.27	19.80	0.58	1.08	70.09	1.46	3.48	162.99
18	0.05	3.03	0.28	0.10	5.49	0.77	0.55	31.97
19	0.12	7.80	1.73	1.44	87.73	2.38	2.42	158.40
20	0.16	8.10	1.43	0.66	31.80	1.37	1.74	87.14
21	0.29	15.29	0.00	0.48	25.44	0.79	1.10	58.76
22	0.16	9.72	2.19	0.72	43.41	4.27	2.72	162.16
23	0.11	16.28	1.77	0.57	66.70	0.85	1.16	69.97

Table 6-4. Standard Deviation of the set of measurements from static NO_x test.

The average results presented in Table 6-12 were derived from multiple tests conducted on each vehicle. During these tests, the NO_x concentration (ppm), NO_x flow mass emission (mg/s), and "% engine load" for the Idle Unloaded State, Idle Loaded State, and TMV were recorded for each test instance.

Furthermore, using the same set of values obtained from diverse measurements on each vehicle, the statistical parameters displayed in Table 6-3 were calculated for every individual vehicle, employing the specified units of measurement. From these data, Table 6-4 and Table 6-5 were built, which contain, respectively, the SD and CV data for each of the analyzed vehicles.

Table 6-4 presents the Standard Deviation (SD) (Equation 6-2) for NO_x emissions and "% engine load" obtained from each vehicle. The SD offers insights into how closely the set of values aligns with the Mean value. A smaller SD indicates reduced dispersion of values around the Mean, indicative of enhanced consistency and test reproducibility. The SD shares the same unit as the Mean value under examination

and illustrates the degree of proximity between the set of measurements and the Mean calculated from the dataset.

Reference Vehicle	Idle Unloaded			Idle Loaded			TMV	
	CV NO _x (mg/s)	CV NO _x (ppm)	CV % Engine load	CV NO _x (mg/s)	CV NO _x (ppm)	CV % Engine load	CV NO _x (mg/s)	CV NO _x (ppm)
1	15.46%	13.67%	2.94%	21.10%	20.62%	17.11%	14.74%	12.91%
2	23.16%	24.66%	4.51%	18.59	19.81%	2.83%	13.31%	8.67%
3	22.41%	23.09%	2.67%	16.74%	16.73%	5.73%	15.53%	15.10%
4	33.16%	33.27%	7.95%	10.23%	10.39%	6.18%	9.14%	8.31%
5	30.36%	29.90%	11.54%	15.58%	16.13%	6.62%	13.91%	15.20%
6	12.69%	11.84%	9.14%	13.59%	13.99%	9.57%	12.23%	13.10%
7	11.30%	11.95%	3.42%	21.49%	21.36%	3.64%	15.87%	17.13%
8	11.05%	10.56%	5.12%	9.85%	8.27%	2.48%	6.37%	6.37%
9	5.00%	5.40%	1.50%	3.83%	3.95%	4.26%	2.81%	3.00%
10	8.43%	18.51%	10.43%	5.59%	20.13%	10.29%	6.61%	8.11%
11	26.07%	26.44%	6.56%	32.34%	33.13%	10.89%	35.79%	36.75%
12	13.57%	14.48%	15.01%	12.22%	13.13%	3.99%	8.11%	9.31%
13	16.64%	18.09%	11.63%	28.15%	29.99%	8.17%	23.11%	24.87%
14	9.78%	10.54%	11.14%	22.32%	22.06%	8.88%	7.52%	9.06%
15	12.64%	12.72%	3.16%	11.39%	11.51%	4.27%	6.93%	6.87%
16	17.89%	18.74%	6.82%	34.86%	35.16%	7.74%	25.16%	25.18%
17	7.28%	9.54%	3.85%	14.97%	17.31%	3.94%	13.27%	11.71%
18	59.63%	65.04%	1.27%	37.90%	37.30%	2.03%	37.12%	36.48%
19	5.13%	6.06%	11.17%	17.96%	19.96%	6.71%	10.10%	12.13%
20	6.02%	6.18%	9.79%	11.24%	10.74%	3.74%	8.80%	8.79%
21	16.68%	16.80%	0.00%	14.87%	15.09%	2.04%	13.25%	13.47%
22	7.36%	7.58%	12.53%	11.15%	11.63%	9.42%	19.02%	19.63%
23	4.35%	11.52%	8.61%	5.45%	11.14%	1.59%	4.88%	5.11%

Table 6-5. Coefficient of Variation of the set of measurements from static NO_x test.

In Table 6-5 the Coefficient of Variation (CV) (Equation 6-3) for the NO_x emissions and "% engine load" from every vehicle are shown.

Based on these statistical parameters, it can be inferred that the applied method yields consistent results across various tests conducted on the same vehicle. This consistency is evident not only for unloaded idle conditions but also for loaded idle and TMV. The consistency applies equally to both NO_x concentration and NO_x mass flow measurements. This demonstrates the robustness and reliability of the measurement method in providing consistent and accurate results across different operating conditions of the vehicle.

Following this, as an illustrative instance, the procedure employed to analyze the reproducibility of one of the study's vehicles (Vehicle No. 20 in Table 6-1) will be delineated. The same methodology has been implemented for all vehicles.

Test number	Idle Unloaded			Idle Loaded			Th. Max. Value	
	NO _x (mg/s)	NO _x (ppm)	% Engine load	NO _x (mg/s)	NO _x (ppm)	% Engine load	NO _x (mg/s)	NO _x (ppm)
1	2.67	133	16	5.94	296	39	18.29	912
2	2.27	114	16	7.55	380	35	23.04	1155
3	2.83	142	16	5.43	273	36	19.57	982
4	2.51	126	14	5.65	284	37	18.90	949
5	2.53	127	14	5.72	287	37	19.15	958
6	2.46	124	14	5.68	285	36	18.90	950
7	2.63	132	13	5.87	294	36	20.30	1018
8	2.66	133	13	5.92	297	35	20.59	1032
9	2.72	136	13	6.10	306	36	21.84	1096
10	2.84	142	15	6.04	303	36	20.61	1034

Table 6-6. Summary of results for the set of static NO_x tests for Vehicle No. 20.

Statistical Parameters	Idle Unloaded			Idle Loaded			TMV	
	NO _x (mg/s)	NO _x (ppm)	% Engine load	NO _x (mg/s)	NO _x (ppm)	% Engine load	NO _x (mg/s)	NO _x (ppm)
Min.	2.27	114	13	5	251	35	17.09	860
Max.	2.83	142	17	7.55	380	39	23.04	1155
Mean	2.59	131	14.64	5.89	296	36.55	19.77	991
Standard Deviation	0.16	8.10	1.43	0.66	31.80	1.37	1.74	87.14
Coef. of Variation	6.02%	6.18%	9.79%	11.24%	10.74%	3.74%	8.80%	8.79%
Std. Error Mean	0.05	2.44	0.43	0.21	9.59	0.41	0.55	27.56
Lower limit	2.50	126.21	13.79	5.48	277.21	35.74	18.69	937.19
Upper limit	2.69	135.79	15.48	6.30	314.79	37.35	20.85	1045.21

Table 6-7. Statistical parameters from the static NO_x tests for Vehicle No. 20.

For each vehicle, the data derived from the series of measurements conducted facilitated the creation of Table 6-6, encompassing the most pertinent outcomes.

To evaluate the consistency and reproducibility of the test, the statistical dispersion parameters are computed using the complete set of results for each vehicle. These parameters, which encompass the Standard Deviation (SD) and the Coefficient of Variation (CV), are subsequently organized into a table resembling Table 6-7 for each vehicle, accentuating their importance. These values were used to construct Table 6-4 and Table 6-5.

Moreover, separate graphs resembling NO_x concentration (Figure 6-4) and NO_x mass flow (Figure 6-5) can be generated, incorporating SD values to evaluate the reproducibility of each vehicle for both types of emissions measurements

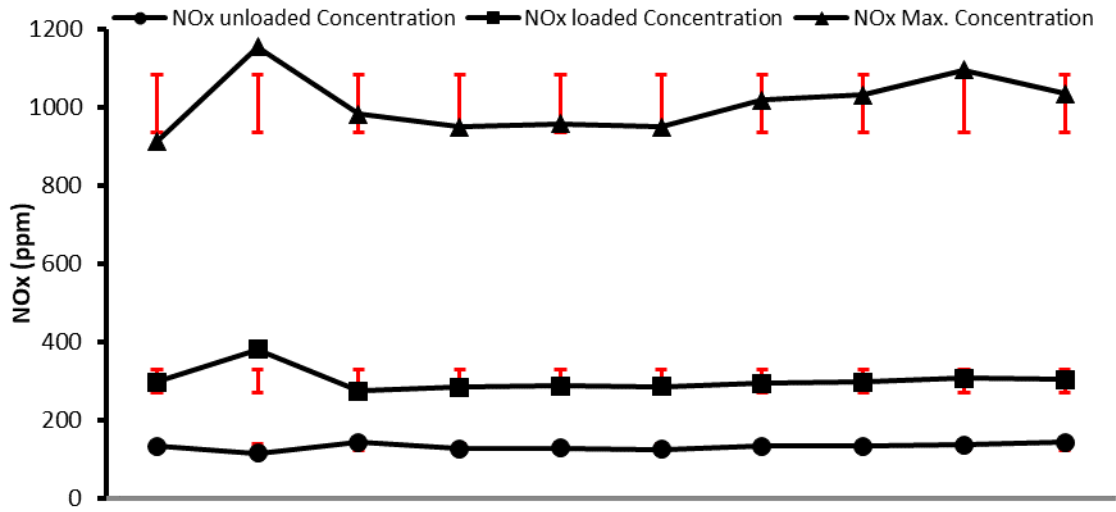


Figure 6-4. Standard Deviation (SD) of NO_x concentration measurements in vehicle No. 20.

Within both graphs, the red bars serve to illustrate the extent of the SD in relation to each measurement taken on the vehicle. The SD for both measures (unloaded and loaded states) is relatively small when compared to the actual measured value. Notably, even in the case of the TMV, which is derived through extrapolation, a significant portion of the values fall within or in close proximity to the boundaries set by the SD around the mean value of the entire dataset.

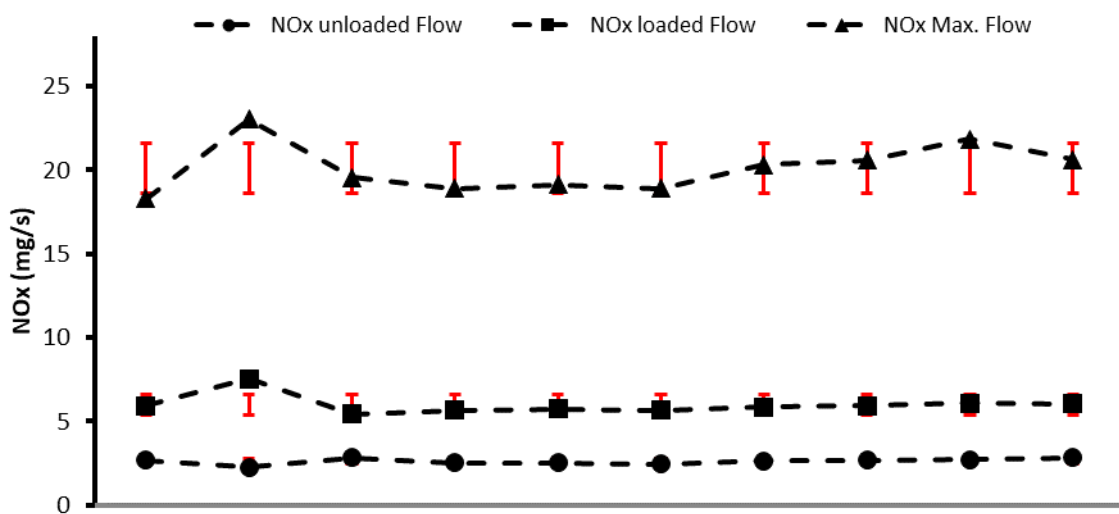


Figure 6-5. Standard Deviation for NO_x mass flow measurements in vehicle No. 20.

6.4.1. UNLOADED STATE REPRODUCIBILITY ANALYSIS

Analyzing the dispersion data for the Unloaded state makes it possible to highlight some relevant points. In the first place, from Table 6-12 data, the average value of emissions from the whole set of vehicles is 122 ppm of NO_x concentration and 2.41 mg/s of NO_x mass emission flow. Related to these values, the average value of the SD for the NO_x concentration is 18 ppm of NO_x in concentration, and 0.32 mg/s of NO_x in mass emission flow.

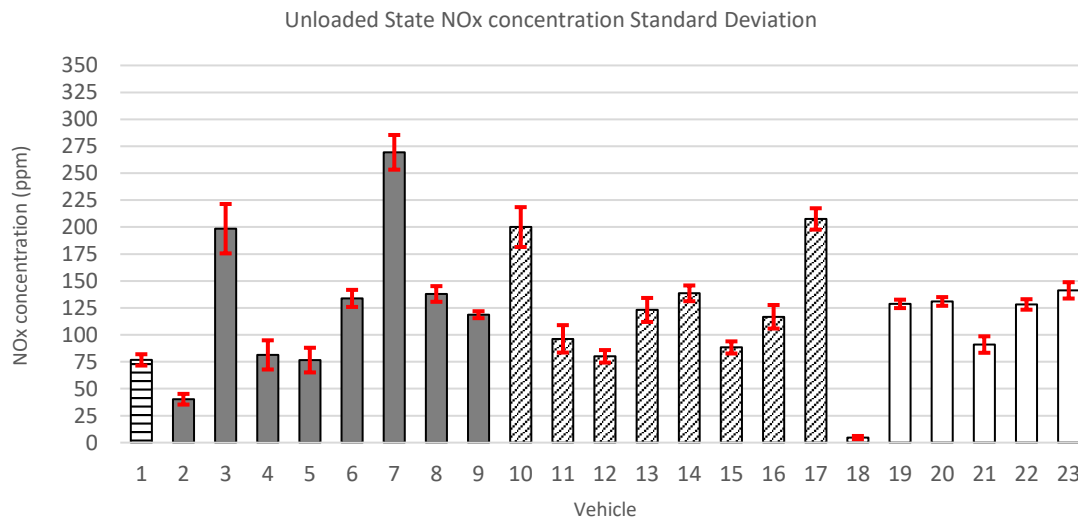


Figure 6-6. NO_x concentration and SD (red bar) for Unloaded State.

In Figure 6-6, the SD (in ppm) of the NO_x concentration at the Unloaded State (the red bar) compared to the average NO_x concentration is shown for each vehicle. It can be seen how in every case the SD is a reduced value compared with the value of the average NO_x concentration at the Unloaded State for every vehicle, being the higher value of the SD from vehicle No. 3. (46 ppm).

In Figure 6-7 the SD values are shown for a direct comparison between them. Data from vehicles are divided into Euro 4, Euro 5, and Euro 6 emission levels for a detailed analysis, and to facilitate comparison between vehicles with a similar level of emissions.

It can be checked in Figure 6-6 that most vehicles present a NO_x concentration value under 150 ppm. Euro 6 vehicles show a homogeneous NO_x concentration, while data from Euro 4 and Euro 5 vehicles present a higher heterogeneity, but with the limit of 150 ppm, only 4 times surpassed. This situation provides the idea of the high consistency and reproducibility of the results obtained from the Unloaded State measurements.

About the absolute values of SD, it can be seen in Figure 6-7 that Euro 6 vehicles show a lower avg. value of 11 ppm (without accounting the vehicle No. 18), with an upper limit of 15 ppm. Instead, Euro 5 vehicles are shown as an avg. SD value of 20.5 ppm and Euro 4 and avg. SD value of almost 22 ppm.

This implies that the data variability among Euro 6 vehicles was smaller compared to vehicles from other emission levels, with Euro 4 vehicles having a higher average standard deviation value. This does not apply to the Euro 3 vehicle, since its emissions and SD value are substantially lower than most Euro 4 vehicles.

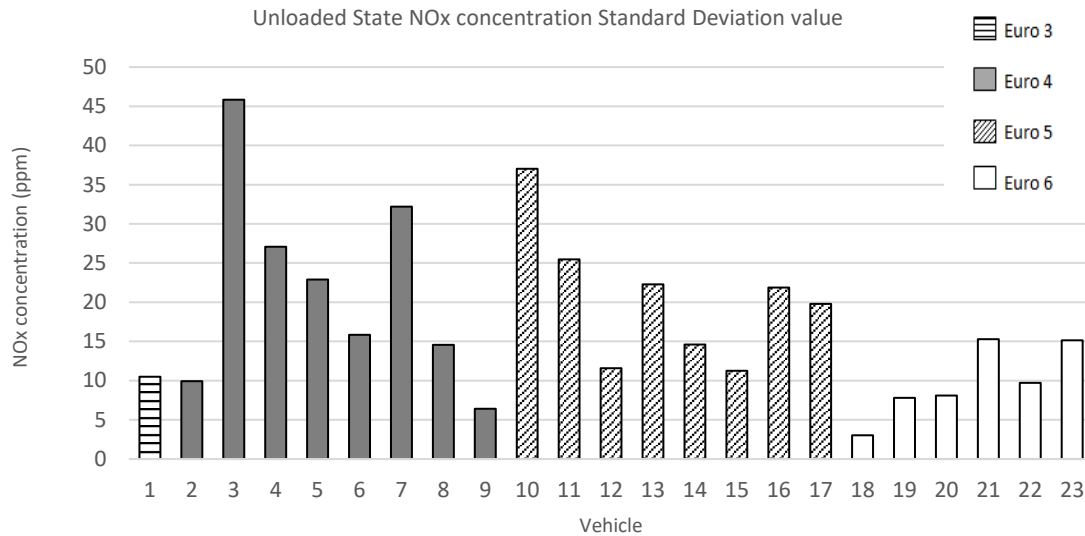


Figure 6-7. SD value for Unloaded State NO_x concentration.

It can also be seen that the three vehicles with the highest average emission values also have the highest SD values.

Vehicle No. 18 presents a special behavior. Figure 6-6 can be checked as the NO_x concentration value is substantially lower than the lowest value recorded for diesel vehicles. The same behavior is observed for the SD value, which is less than half of the lowest diesel SD value. Such low values have not been taken into account when calculating the average values of Euro 6 vehicles so that these can be compared directly with the average values of the other diesel vehicles without the influence of the values of the petrol vehicle.

Figure 6-8 presents analogous information to Figure 6-6, albeit concerning the NO_x mass emission flow during the Unloaded State. Once again, a parallel trend can be observed when analyzing mass emission flow in comparison to concentration data. However, in some instances, the standard deviation (SD) for mass emission flow appears marginally smaller in contrast to the average value. Notably, the SD value remains relatively small in relation to the average value of NO_x mass emissions for each vehicle. Noteworthy among these is vehicle No. 5, which exhibits the highest SD of 0.69 mg/s.

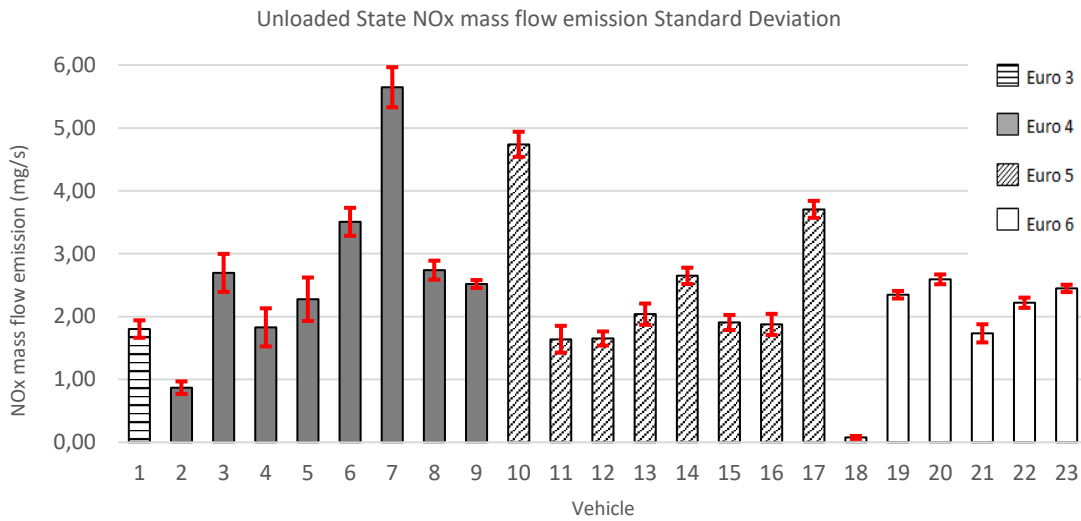


Figure 6-8. NO_x mass flow emission and SD (red bar) for Unloaded State.

In terms of mass emission flow, the collective average value for NO_x emissions across the vehicle set was 2.41 mg/s, with an average SD value of 0.32 mg/s.

Upon scrutinizing the analysis of Euro emission levels, it becomes apparent that the average NO_x mass emissions are marginally lower for Euro 6 vehicles. Specifically, the average NO_x mass emission for Euro 6 vehicles stands at 2.3 mg/s, whereas Euro 5 vehicles show an average NO_x mass emission of 2.5 mg/s, and Euro 4 vehicles exhibit an average of 2.8 mg/s. Interestingly, Euro 3 vehicles display lower NO_x mass emissions than the majority of Euro 4 vehicles. Notably, the NO_x mass emissions of vehicle No. 18 are significantly lower, multiple times less, than even the lowest recorded NO_x mass emission from a diesel vehicle.

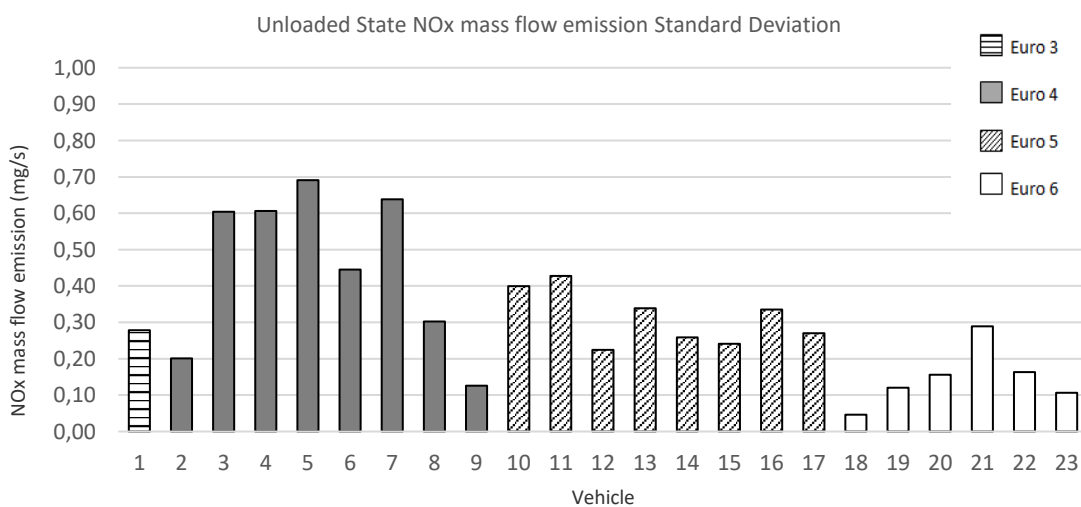


Figure 6-9. SD value for Unloaded State NO_x mass emission flow.

Regarding the standard deviation (SD) values, the pattern persists: the SD value for Euro 6 vehicles remains lower compared to the others. Specifically, the average SD value for Euro 6 vehicles (excluding vehicle No. 18) is 0.17 mg/s. In contrast, Euro 5 vehicles exhibit an average SD value of 0.31 mg/s, and Euro 4 vehicles display an average SD value of 0.5 mg/s. Notably, the SD value for Euro 3 vehicles aligns closely with the average SD value of Euro 5 vehicles.

Indeed, just as observed with the NO_x concentration data, the trend holds for the standard deviation (SD) values as well. On average, the SD values are lower for the Euro 6 vehicles.

Moreover, there is another important value to analyze when determining the reproducibility of the test: the "% engine load" value. One of the main features of the measurement method is simplicity, which allows repeating the measurement process in the same conditions easily, providing consistent results. This simplicity has to be reflected in the "% engine load" values obtained from several tests. In this way, Figure 6-10 shows the standard deviation for the "% engine load" value, where it can be seen how for the "% engine load" the SD values are even smaller than for NO_x concentration or NO_x mass emission flow when compared to the avg. value of "% engine load". The average value of SD for the "% engine load" value at Unloaded State was 1.41% engine load, the same as that avg. value of SD "% engine load" from Euro 6 vehicles.

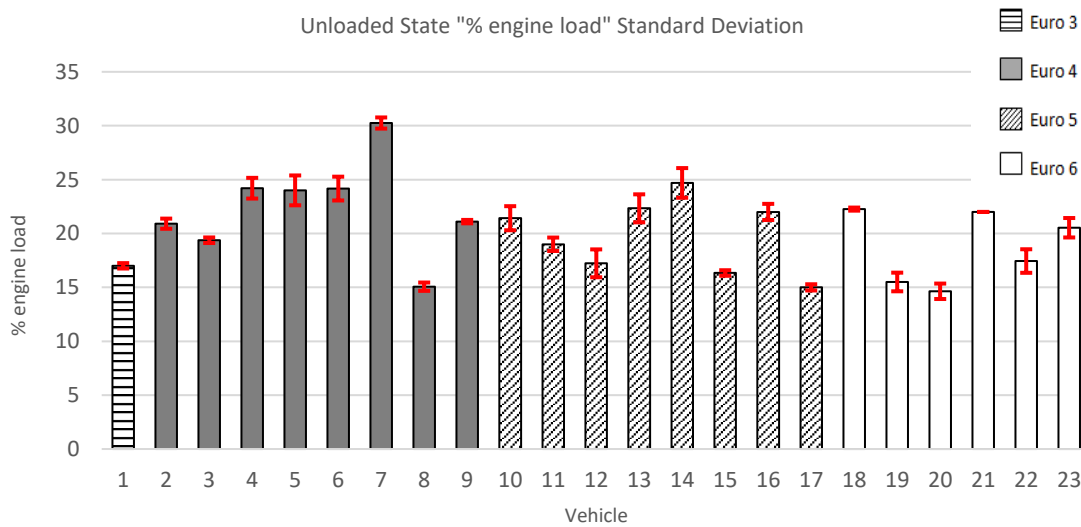


Figure 6-10. "% engine load" value and SD (red bar) for Unloaded State.

The average value of "% engine load" remains fairly consistent across all vehicles, albeit slightly lower for Euro 6 vehicles (average 18% engine load). There is a marginal increase for Euro 5 vehicles (average 20% engine load) and a slight uptick for Euro 4 vehicles (average 22% engine load). This trend of variation is illustrated in Figure 6-10 which showcases the uniformity of these values.

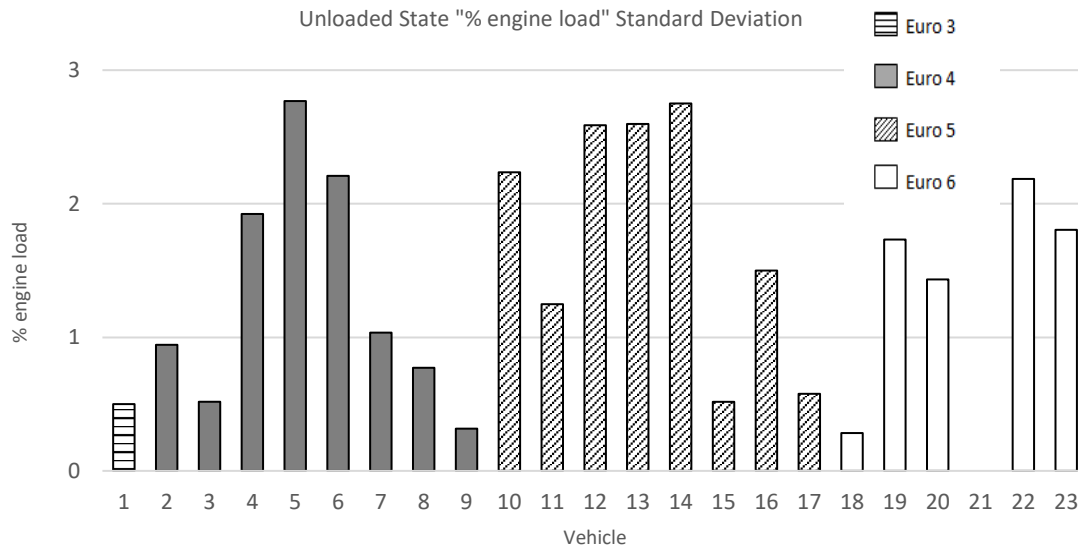


Figure 6-11. SD value for "% engine load" at Unloaded State.

Conversely, the standard deviation (SD) of "% engine load" exhibits consistently low values across all instances. This results in a relatively higher relative variability than that seen in the emission values, as depicted in Figure 6-11. Notably, the greatest SD value for "% engine load" pertains to vehicle 5 (2.7%), while the lowest is registered for vehicle 21, denoting an SD value of 0%. This indicates a lack of appreciable variation in "% engine load" data across multiple tests for this particular vehicle.

These values were obtained with an average "% engine load" during the Unloaded State at 20%, consisting of an 18% average for Euro 6 vehicles, 20% for Euro 5 vehicles, and 22% for Euro 4 vehicles.

In summary, the reduced value of the standard deviation (SD) in relation to the average values of both NO_x concentration and NO_x mass emission suggests that the measurement dispersion during the Unloaded State could be considered appropriate for the measurement purpose. Furthermore, the low dispersion of "% engine load" also indicates that the reproducibility of "% engine load" during the Unloaded State was highly satisfactory, aligning with the anticipated behavior. This favorable scenario contributes to the strong correlation between NO_x concentration and "% engine load" during the Unloaded State, as previously discussed (confirmed by a p-value lower than the significance level), forming the foundation of the measurement methodology.

This aspect regarding data dispersion can be further evaluated by employing the Coefficient of Variation (CV). This metric, also recognized as the Relative Standard Deviation (RSD), is derived by dividing the standard deviation (SD) by the Mean, thereby generating a dimensionless value that conveys the relationship between the SD and the mean (see Section 4.4). Figure 6-12 visually represents the CV values for NO_x concentration, NO_x mass emission flow, and "% engine load" for each vehicle.

Upon examining this figure, one can observe the similarity in behavior of the CV values for both NO_x metrics in the majority of vehicles, with some minor distinctions. Moreover, the CV for "% engine load" showcases even more favorable behavior.

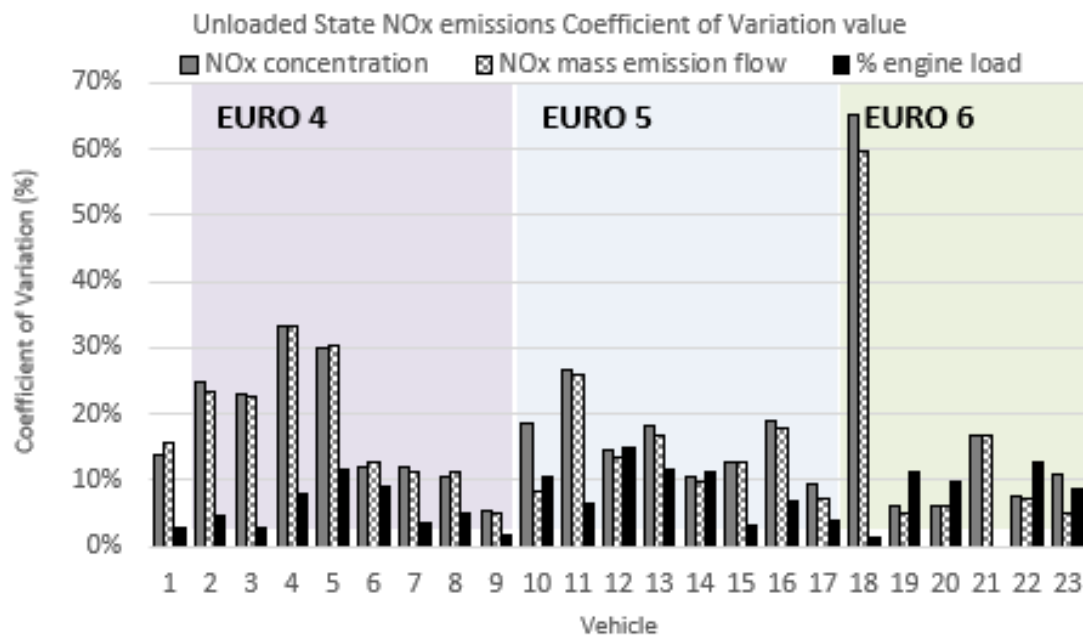


Figure 6-12. CV at Unloaded State.

The CV value for NO_x emissions in the case of vehicle No. 18 (the petrol vehicle) stands out as higher than that of the other vehicles due to the exceptionally low average NO_x concentration during the Unloaded State. Consequently, despite having the lowest SD value among the set of vehicles, the CV reaches around 60% for both types of measurements.

Excluding this unique case, a significant portion of the other vehicles exhibit CV values below 20%. Half of the vehicles in the set display a CV of approximately 10%, with an average NO_x concentration of 18% and an average NO_x mass emission flow of 16%. It is worth noting that vehicle No. 21 demonstrates a CV of zero for "% engine load", implying that there were no notable variations in the "% engine load" values during the testing phase.

For both emissions measures, the avg. value for Euro 6 vehicles was the lowest (10% for the NO_x concentration and 8% for NO_x mass emission), followed by the Euro 5 vehicles (16% for the NO_x concentration and 14% for NO_x mass emission) and the Euro 4 vehicles (19% for both NO_x concentration and mass emission).

Regarding the "% engine load", the average CV is 7%, with only 6 vehicles showing a CV higher than 10%. The avg. value was similar for the Euro 4, Euro 5, and Euro 6 vehicles, being lower for the Euro 3 vehicle. Anyway, its behavior is even better than NO_x measures. These results are consistent with the assumption that the simplicity of the measurement method allows for high reproducibility in the measurement process and provides information about the consistency and robustness of the process.

In summary, in the **Unloaded State**, the dispersion measures indicated that the reproducibility of the test was adequate for the measurement purpose, with an SD

average value NO_x concentration of 18 ppm, and an average value of NO_x mass flow emission of 0.32 mg/s. The Coefficient of Variation for both types of values is 18% and 16% respectively.

Operational conditions maintained a consistent pattern throughout the various tests, with the SD of "% engine load" at 1.4% for an average of 20% engine load. Consequently, the CV for "% engine load" stood at 7%. Similarly, the operational factor of Engine Temperature yielded a CV of 6%, alongside an average value of 80°C and an SD of 4.6°C. These values collectively affirm that operational conditions during the Unloaded State exhibit suitable reproducibility across the set of vehicles.

Indeed, the key takeaways are that NO_x emissions during the Unloaded state exhibit a CV of 17%, while operational conditions including "% engine load" and temperature maintain a CV of 7%. Both of these CV values are sufficiently low to establish the reproducibility of the measurement method under this engine condition.

To consolidate the comprehensive understanding of the Unloaded State results, Table 6-8 compiles the values pertaining to data dispersion for NO_x emissions and "% engine load" across the analyzed vehicle set.

Table 6-8. Summary of dispersion values for Unloaded State.

Reference Vehicle	Vehicle Manufacturer	Model	Avg. NO _x (mg/s)	Avg. NO _x (ppm)	SD NO _x (mg/s)	SD NO _x (ppm)	CV NO _x (mg/s)	CV NO _x (ppm)	Avg. % Engine load	SD % Engine load	CV %Engine load
1	SEAT	León	1.80	77	0.28	10.50	15%	14%	17.00	0.50	3%
2	Volvo	V50	0.87	40	0.20	9.93	23%	25%	20.91	0.94	5%
3	Alfa Romeo	Mito	2.70	199	0.60	45.84	22%	23%	19.38	0.52	3%
4	Audi	A4	1.83	81	0.61	27.08	33%	33%	24.20	1.92	8%
5	BMW	330D	2.28	77	0.69	22.90	30%	30%	24.00	2.77	12%
6	BMW	535d	3.51	134	0.45	15.84	13%	12%	24.17	2.21	9%
7	Peugeot	407	5.65	269	0.64	32.20	11%	12%	30.25	1.04	3%
8	Volkswagen	Passat	2.74	138	0.30	14.57	11%	11%	15.06	0.77	5%
9	Skoda	Octavia	2.52	119	0.13	6.41	5%	5%	21.10	0.32	1%
10	Audi	A5	4.74	200	0.40	37.03	8%	19%	21.42	2.23	10%
11	Citroën	Berlingo	1.64	96	0.43	25.46	26%	26%	19.00	1.25	7%
12	Volkswagen	Touran	1.65	80	0.22	11.59	14%	14%	17.23	2.59	15%
13	Hyundai	i30	2.04	123	0.34	22.27	17%	18%	22.33	2.60	12%
14	SEAT	León	2.65	139	0.26	14.60	10%	11%	24.69	2.75	11%
15	Opel	Insignia	1.91	88	0.24	11.24	13%	13%	16.33	0.52	3%
16	Nissan	Juke	1.88	117	0.34	21.88	18%	19%	22.00	1.50	7%
17	Opel	Astra	3.71	208	0.27	19.80	7%	10%	15.00	0.58	4%
18	Renault	Fluence	0.08	5	0.05	3.03	60%	65%	22.26	0.28	1%
19	Renault	Talisman	2.35	129	0.12	7.80	5%	6%	15.50	1.73	11%
20	Peugeot	Boxer	2.59	131	0.16	8.10	6%	6%	14.64	1.43	10%
21	Skoda	Superb	1.73	91	0.29	15.29	17%	17%	22.00	0.00	0%
22	Kia	Sportage	2.22	128	0.16	9.72	7%	8%	17.44	2.19	13%
23	Citroën	C4 Grand Picasso	2.45	141	0.11	16.28	4%	12%	20.53	1.77	9%
Average value			2.41	122	0.32	17.80	16%	18%	20.28	1.41	7%

6.4.2. LOADED STATE REPRODUCIBILITY ANALYSIS

At the Loaded State, a similar situation is found, showing the same behavior for the several parameters analyzed from the Unloaded State. From the dispersion data for the Loaded state is interesting to focus on the following relevant points. From

Table 6-12 data, that the average value of emissions from the whole set of vehicles is 308 ppm of NO_x concentration and 6.04 mg/s of NO_x mass emission flow. Related to these values, the average value of the SD for the NO_x concentration is 53 ppm of NO_x in concentration, and 0.93 mg/s of NO_x in mass emission flow.

Figure 6-13 visually presents the standard deviation (SD) of NO_x concentration at the Loaded State (indicated by the red bar), compared with the average NO_x concentration from each individual vehicle. Similar to the Unloaded State results, a consistent trend emerges where, in all instances, the SD remains at a diminished value compared to the average NO_x concentration for each respective vehicle. The highest SD value is attributed to vehicle No. 7, registering at 161 ppm.

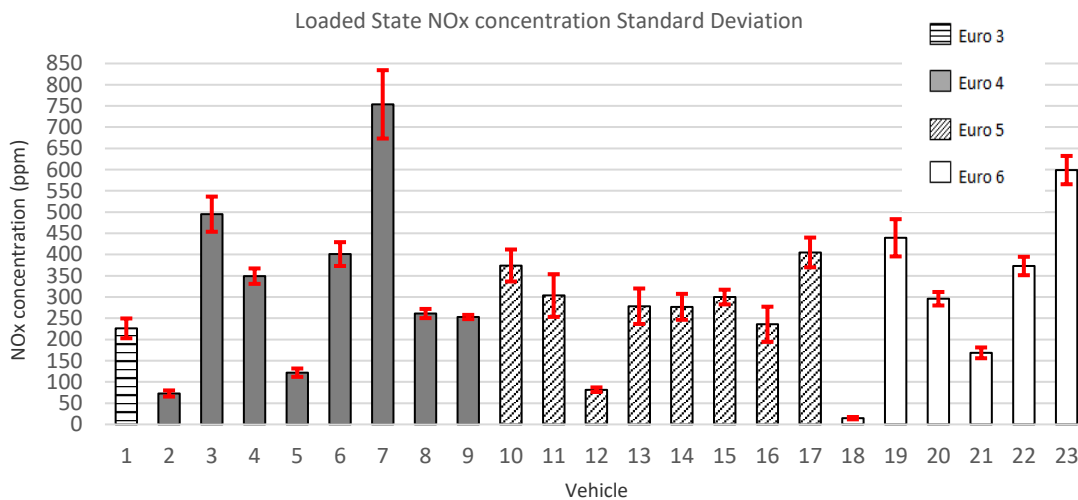


Figure 6-13. NO_x concentration and SD (red bar) for Loaded State.

This pattern strongly suggests a high level of consistency and reproducibility in the results derived from the Loaded State measurements.

In contrast to the Unloaded state, at this loading condition, the lowest average NO_x concentration is observed among the Euro 5 vehicles, with an average value of 282 ppm of NO_x concentration. Surprisingly, the Euro 3 vehicle displays an even lower NO_x concentration value than Euro 5, while the average NO_x concentration for Euro 4 vehicles (339 ppm) slightly edges below that of Euro 6 vehicles (375 ppm). It is notable that only four vehicles exhibit NO_x concentrations substantially exceeding 400 ppm, with two of these being Euro 4 vehicles and the remaining two being Euro 6 vehicles.

In terms of the standard deviation (SD) values (as depicted in Figure 6-14), an interesting contrast emerges. Euro 5 vehicles exhibit a higher average SD value in NO_x concentration, reaching 65 ppm. Conversely, both Euro 4 and Euro 6 vehicles share

the same SD value of 50 ppm for Euro 4 vehicles and 51 ppm for Euro 6 vehicles. In contrast, Euro 3 vehicles present an SD value of 46 ppm, which is lower than the average values but not the lowest among the vehicle sets.

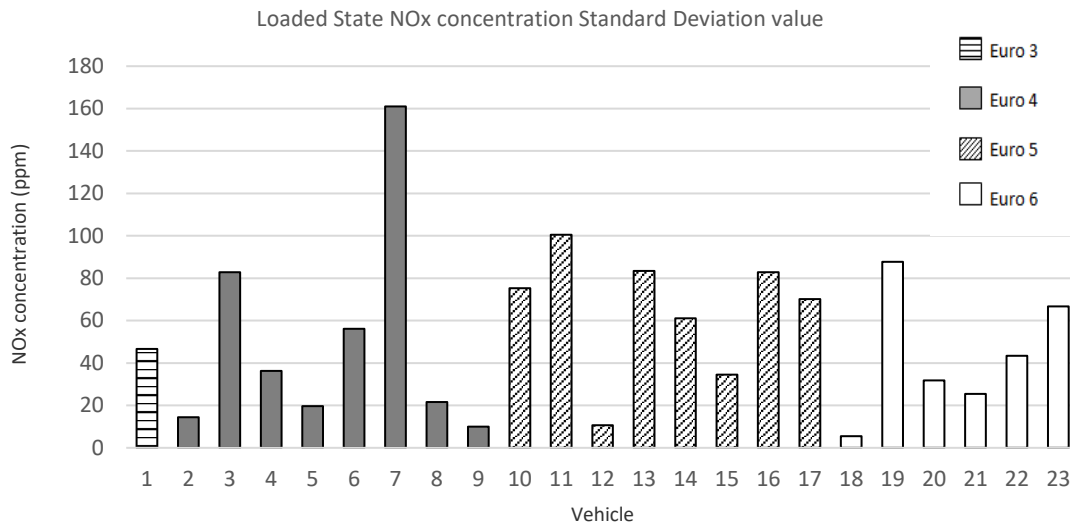


Figure 6-14. SD value for Loaded State NO_x concentration.

The SD values for the Loaded State exhibit substantial variability, showcasing that despite Euro 4 vehicles having the lowest average SD value, vehicle No. 7, a Euro 4 vehicle, records the highest SD value.

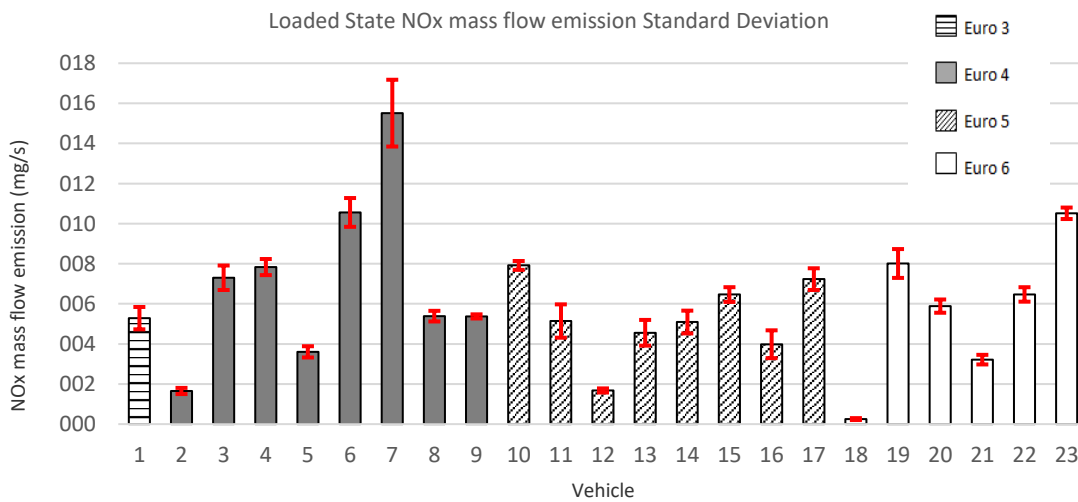


Figure 6-15. NO_x mass flow emission and SD (red bar) for Loaded State.

Figure 6-15 shows similar information with SD values compared against the average NO_x mass emission flow at the Loaded State. The general behavior mirrors the NO_x

concentration analysis, although, in some instances, the SD for mass emission flow tends to be slightly smaller compared to the concentration's SD when assessed against the average value. This parallels the pattern observed in the Unloaded State measurements as well.

In this case, vehicle No. 7 registers the highest SD value (3.33 mg/s). Regarding mass emission flow, the collective average value of NO_x emissions across the vehicle set was 6.04 mg/s, with an average SD value of 0.93 mg/s.

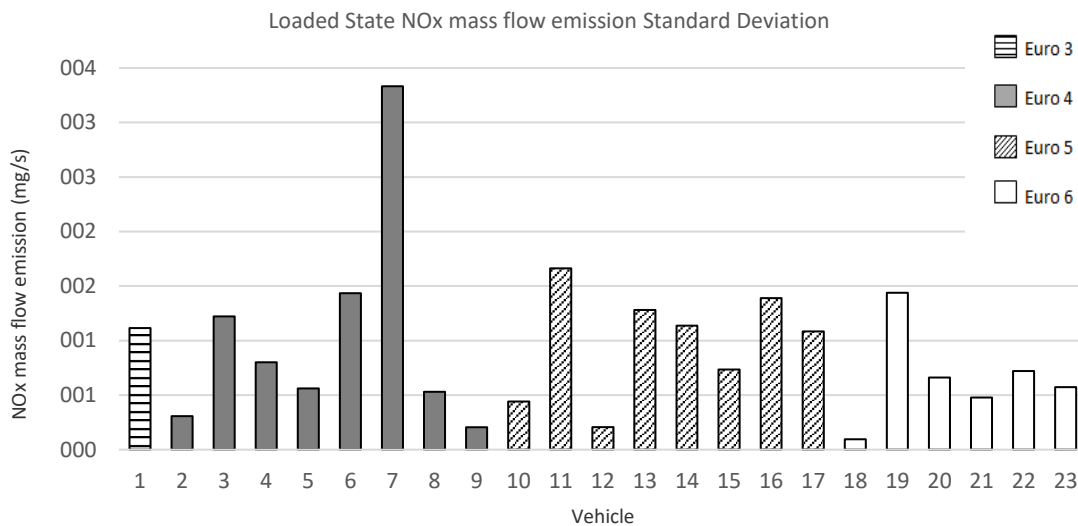


Figure 6-16. SD value for Loaded State NO_x mass emission flow.

At the Loaded State, Euro 6 vehicles present the lowest avg. SD value for NO_x mass emissions (0.77 mg/s), being higher than the avg. value for Euro 4 (1.05 mg/s) and Euro 5 (0.99 mg/s), and 1.12 mg/s of SD from the Euro 3 vehicle.

Similarly to the previous state, the analysis now shifts to the reproducibility of the test by focusing on the "% engine load" value. As previously mentioned, the measurement method's primary characteristic is its simplicity, facilitating easy replication of the test under the same conditions. The dispersion of "% engine load" values derived from multiple tests serves as an indicator of this attribute.

Figure 6-17 illustrates the SD values for the "% engine load" (indicated by the red bar). Notably, the SD behavior of "% engine load" is even smaller compared to that of NO_x concentration or NO_x mass emission flow. The average SD value for "% engine load" during the Loaded State was 2.58% engine load, with the CV for "% engine load" at 6%. These outcomes were attained with an average "% engine load" value during the Loaded State of 42%.

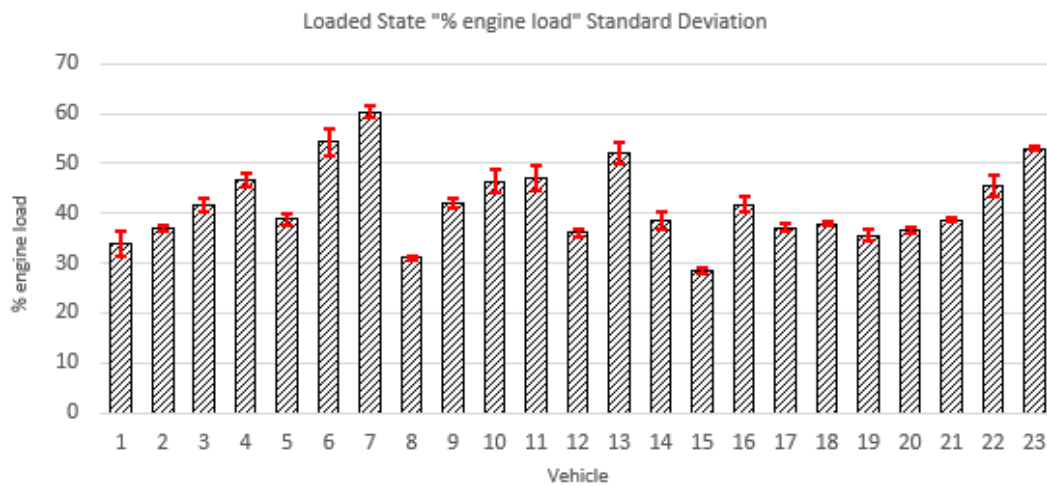


Figure 6-17. "% engine load" and SD (red bar) for Loaded State.

This implies that the reproducibility of "% engine load" during the Loaded State has been deemed satisfactory and aligns with expectations. Much like in the Unloaded State, this situation strengthens the strong relationship between NO_x concentration and "% engine load" during the Loaded State, as discussed earlier (indicated by a p-value lower than the significance level).

From the preceding values, a trend becomes apparent where the elevation in emission values from the Unloaded to the Loaded state corresponds to higher SD values. This same pattern holds true for the "% engine load" variable. To ascertain the similarity of values in both states, the CV metric is employed.

Figure 6-18 shows together with the value of CV for NO_x concentration, NO_x mass emission flow, and "% engine load" from each vehicle for the Loaded State.

By examining this figure, one can observe the similarity in behavior of the coefficient of variation (CV) for both NO_x values across most vehicles, despite minor discrepancies between them. Notably, the CV for "% engine load" exhibits an even more favorable behavior.

As previously mentioned, the CV value for NO_x emissions in the case of vehicle No. 18 (the petrol vehicle) remains elevated compared to other vehicles due to the extremely low average NO_x concentration during the Unloaded State. As a result, even though the SD value is the lowest among the set of vehicles, the CV for both types of measurements is around 60%.

As is evident, the behavior of CV in the Loaded State closely resembles that of the Unloaded State (as depicted in Figure 6-12), although the values are slightly elevated. The primary distinction is that the CV for NO_x emissions in vehicle No. 18 (the petrol vehicle) remains higher compared to other vehicles, albeit the disparity from other vehicles' CVs is not as pronounced as in the case of the Unloaded State. Again, this stems from the low NO_x emissions of vehicle No. 18. Even though the SD value is the lowest among the vehicle sets, the CV is higher for both types of measurements, approximately 37%.

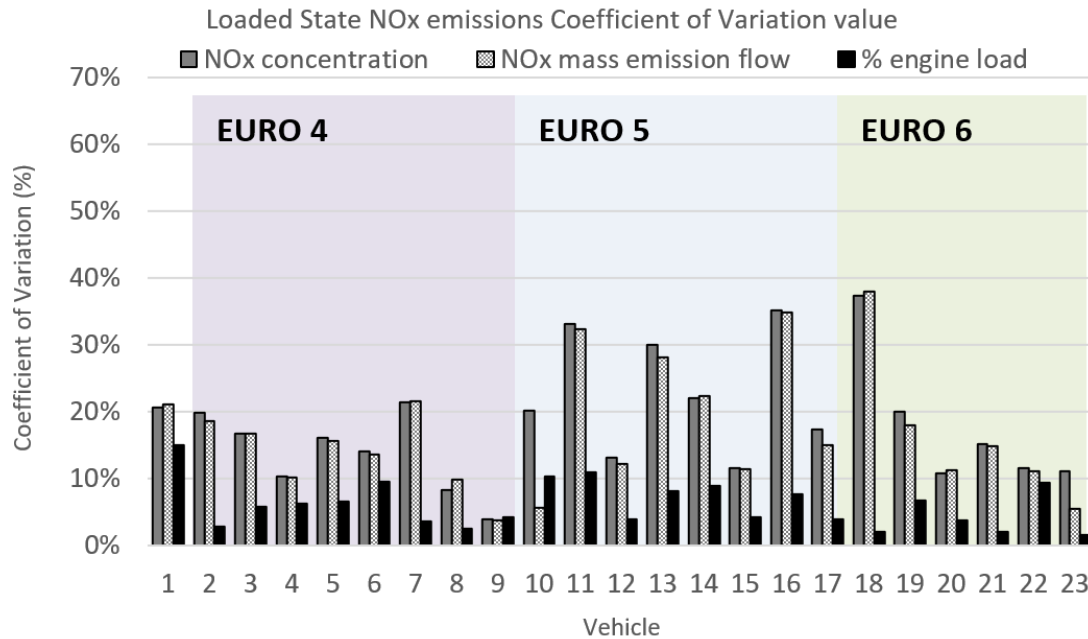


Figure 6-18. CV for variables at Loaded State.

Excluding the petrol vehicle scenario, the majority of other vehicles display a CV either below or close to 20%, with only 4 vehicles approaching or surpassing the 20% threshold of CV. The average CV value remains at 18% for NO_x concentration and 17% for NO_x mass emission flow. Remarkably, these average CV values mirror those derived from the Unloaded State measurements. This suggests that relatively speaking, **the dispersion of NO_x emission data is akin for both the Unloaded and Loaded States.**

For the "% engine load", the average CV is 6%, with only 2 vehicles showing a CV higher than 10%. Again, **these values of CV are the same as those for the Unloaded State.** Indeed, much like the Unloaded situation, the behavior of CV in the Loaded State is even more favorable than that of NO_x measures. This consistent trend aligns with the underlying assumption that the simplicity of the measurement method substantially contributes to the heightened reproducibility of the measurement process, thereby underscoring the method's reliability and robustness.

To sum up, in the Loaded State, the dispersion metrics affirm that the test's reproducibility was suitable for measurement purposes. The average value of NO_x concentration SD was 53 ppm, and the average value of NO_x mass flow emission SD stood at 0.93 mg/s. The Coefficient of Variation for both types of values was 18% for NO_x concentration and 17% for NO_x mass flow emission.

Much like the previous state, the mechanical operational conditions also exhibited consistency throughout the various tests. The SD for "% engine load" reached 2.58% for an average value of 42% engine load, translating to a CV of 6% for "% engine load." These values closely resemble those observed in the Unloaded State. With these outcomes, it can be confidently asserted that operational conditions during the Loaded State demonstrate adequate reproducibility across the set of vehicles.

Table 6-g. Summary of dispersion values for Loaded State.

Reference Vehicle	Vehicle Manufacturer	Model	Avg. NO _x (mg/s)	Avg. NO _x (ppm)	SD NO _x (mg/s)	SD NO _x (ppm)	CV NO _x (mg/s)	CV NO _x (ppm)	Avg. % Engine load	SD %Engine load	CV %Engine load
1	SEAT	León	5.29	226	1.12	46.64	21%	21%	33.89	5.06	15%
2	Volvo	V50	1.65	73	0.31	14.43	19%	20%	36.91	1.04	3%
3	Alfa Romeo	Mito	7.30	495	1.22	82.82	17%	17%	41.63	2.39	6%
4	Audi	A4	7.83	349	0.80	36.28	10%	10%	46.60	2.88	6%
5	BMW	330D	3.60	122	0.56	19.66	16%	16%	38.71	2.56	7%
6	BMW	535d	10.56	401	1.43	56.14	14%	14%	54.25	5.19	10%
7	Peugeot	407	15.51	754	3.33	161.02	21%	21%	60.38	2.20	4%
8	Volkswagen	Passat	5.39	261	0.53	21.60	10%	8%	31.06	0.77	2%
9	Skoda	Octavia	5.37	253	0.21	9.99	4%	4%	42.10	1.79	4%
10	Audi	A5	7.92	374	0.44	75.34	6%	20%	46.42	4.78	10%
11	Citroën	Berlingo	5.14	304	1.66	100.55	32%	33%	46.90	5.11	11%
12	Volkswagen	Touran	1.68	82	0.21	10.73	12%	13%	36.08	1.44	4%
13	Hyundai	i30	4.56	278	1.28	83.48	28%	30%	52.11	4.26	8%
14	SEAT	León	5.09	277	1.14	61.08	22%	22%	38.62	3.43	9%
15	Opel	Insignia	6.46	300	0.74	34.53	11%	12%	28.33	1.21	4%
16	Nissan	Juke	3.98	236	1.39	82.90	35%	35%	41.78	3.23	8%
17	Opel	Astra	7.23	405	1.08	70.09	15%	17%	37.14	1.46	4%
18	Renault	Fluence	0.25	15	0.10	5.49	38%	37%	37.87	0.77	2%
19	Renault	Talisman	8.01	440	1.44	87.73	18%	20%	35.50	2.38	7%
20	Peugeot	Boxer	5.89	296	0.66	31.80	11%	11%	36.55	1.37	4%
21	Skoda	Superb	3.22	169	0.48	25.44	15%	15%	38.57	0.79	2%
22	Kia	Sportage	6.47	373	0.72	43.41	11%	12%	45.33	4.27	9%
23	Citroën	C4 Grand Picasso	10.52	599	0.57	66.70	5%	11%	53.00	0.85	2%
Average value			6.04	307.86	0.93	53.38	17%	18%	41.73	2.58	6%

The key takeaways are that NO_x emissions during the Loaded state exhibit a CV of 17%, and engine operating conditions have a CV of 6%, both aligning with the same values obtained for the Unloaded State. These CV values are low enough to confidently assert the reproducibility of the measurement method under this engine condition.

To encapsulate this understanding, Table 6-9 provides a comprehensive overview of the values related to data dispersion during the Loaded State, covering NO_x emissions and "% engine load" across the analyzed vehicle set.

6.4.3. TMV REPRODUCIBILITY ANALYSIS

In the final set of results, the same data are scrutinized, this time focusing on the Theoretical Maximum Value (TMV) scenario. This analysis aims to examine the dispersion of emissions under the theoretical condition of 100% engine load. However, it is important to note that data dispersion for "% engine load" is not analyzed in this context, as it is consistently assumed to be 100% in the TMV situation.

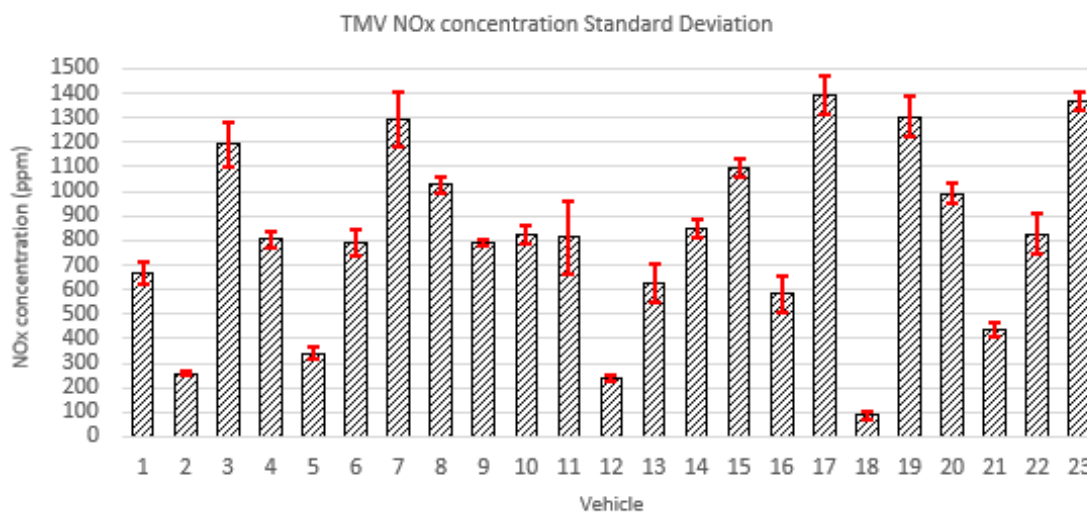


Figure 6-19. NO_x concentration and SD (red bar) for TMV.

At the TMV, the behavior for the several parameters analyzed is similar to that from the Unloaded and Loaded State. As always, there are some relevant points to focus on. In the first place, from Table 6-12 data, the average value of emissions from the whole set of vehicles is 809 ppm of NO_x concentration and 16 mg/s of NO_x mass emission flow. Related to these values, the average value of the SD for the NO_x concentration is 104 ppm of NO_x in concentration, and 1.95 mg/s of NO_x in mass emission flow.

As depicted in Figure 6-19, the standard deviation (SD) of NO_x concentration at the Theoretical Maximum Value (TMV) is represented by the red bar, contrasted against the average NO_x concentration for each individual vehicle. Much akin to the earlier states, it is evident that in all instances, the SD remains a diminished value compared

to the average NO_x concentration for each respective vehicle. The highest SD value is attributed to vehicle No. 11, recorded at 298 ppm.

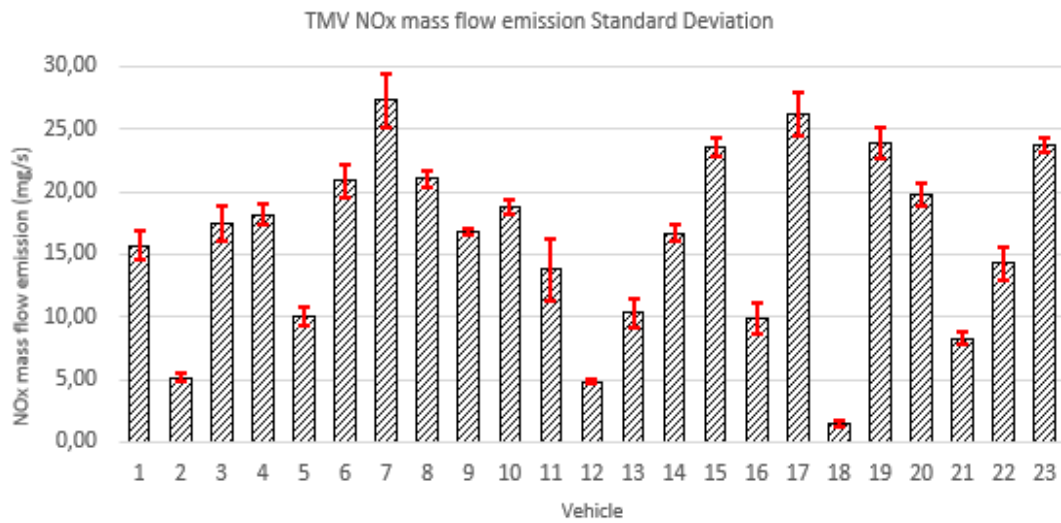


Figure 6-20. NO_x mass flow emission and SD (red bar) for TMV.

Referencing Figure 6-20, the standard deviation (SD) for the NO_x mass emission flow during the Theoretical Maximum Value (TMV) scenario is illustrated by the red bar. This representation demonstrates the similarity in behavior between the analysis of NO_x mass emission flow and NO_x concentration. Just as observed before, some instances reveal a slightly smaller SD for mass emission flow compared to concentration when evaluated against the average value. This consistency aligns with the patterns identified in the Unloaded and Loaded state measurements.

As from the NO_x concentration measures, the higher SD is for vehicle No. 11, with a value of 4.92 mg/s of NO_x. Related to mass emission flow, the average value of NO_x emission from the set of vehicles was 16 mg/s, while the average SD value was 1.95 mg/s.

The contrast in SD behavior between concentration and mass emission flow can be discerned by comparing Figure 6-21 and Figure 6-22, both of which display the SD values for each situation. By conducting this comparison, it can be observed that the behavior of both measurement types is similar, albeit with minor discrepancies based on the nature of the data analyzed. Notably, in the TMV scenario, the SD of the petrol vehicle is not the lowest for the first time, although it still remains among the smallest.

With the provided SD values, it is reasonable to deduce that for the Theoretical Maximum Value (TMV) scenario, the dispersion of the test method appears to be suitable for measurement purposes. This corresponds to the same conclusion drawn for the Unloaded and Loaded states, as the SD values in all three cases indicate that the minimal data dispersion ensures accurate reproducibility of the measurement method, particularly concerning NO_x emissions.

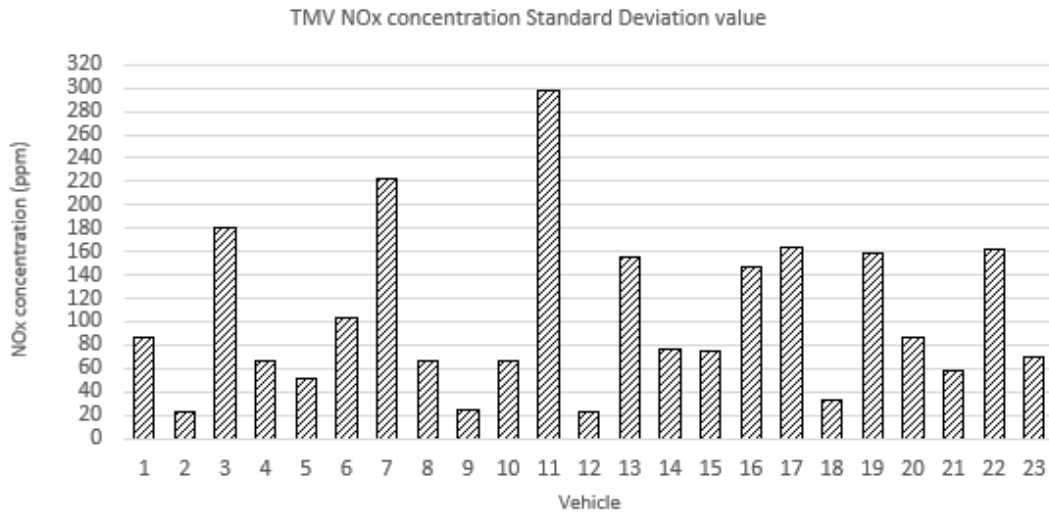


Figure 6-21. SD value for TMV NO_x concentration.

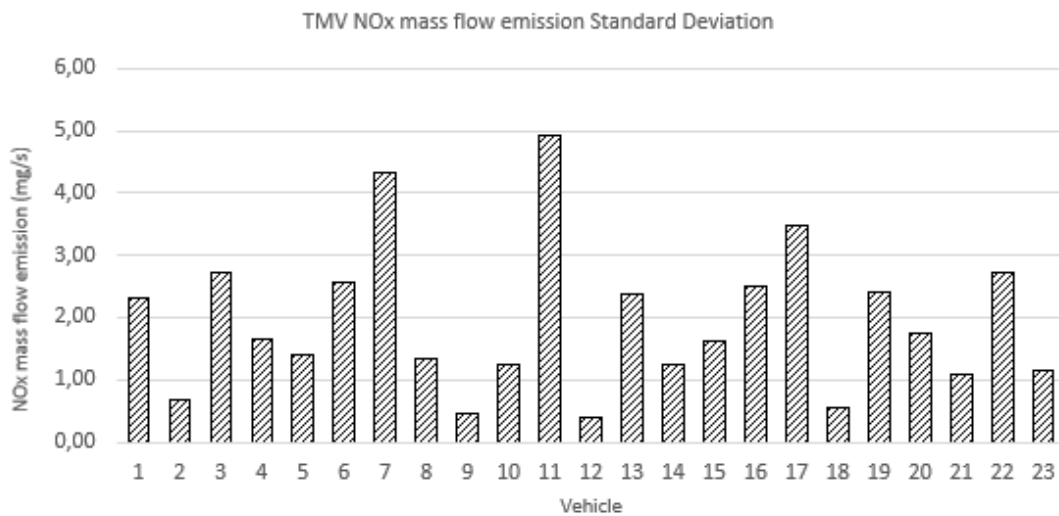


Figure 6-22. SD value for TMV NO_x mass emission flow.

Concluding the analysis of NO_x emission dispersion data, the Coefficient of Variation (CV) has been computed for the NO_x emissions during the Theoretical Maximum Value (TMV) scenario. Figure 6-23 displays the CV values for both NO_x concentration and NO_x mass emission flow. This figure serves to illustrate the akin behavior of CV for both NO_x values, despite the presence of minor differences between them.

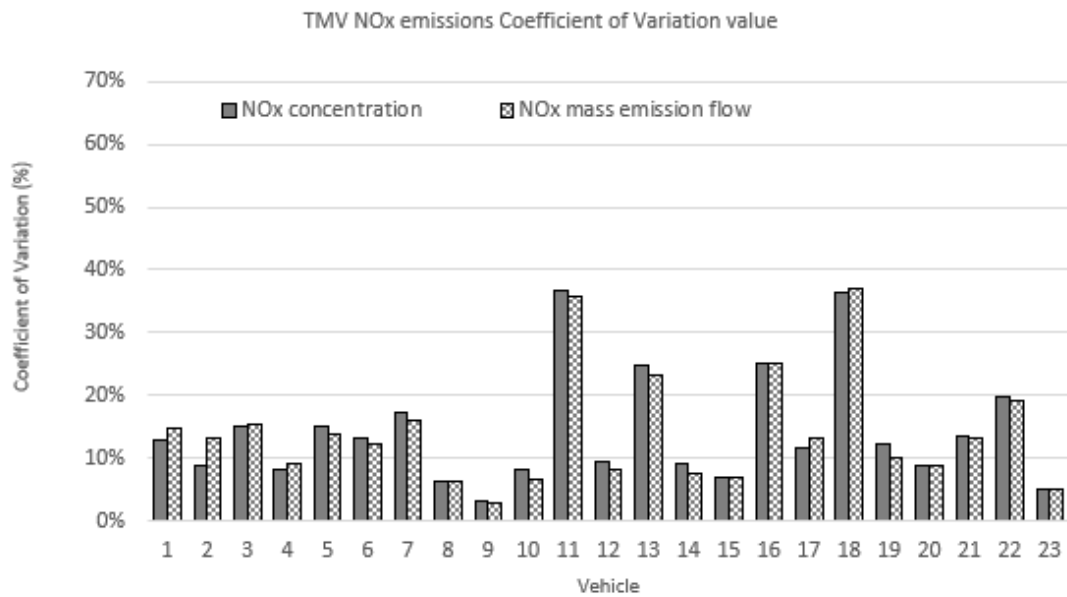


Figure 6-23. CV for variables at TMV.

As can be observed, the behavior of the CV during the TMV scenario closely resembles that of the Loaded State, although the values are marginally higher. Notably, the CV for the NO_x emissions of vehicle No. 18 (the petrol vehicle) and vehicle No. 11 surpasses that of the other vehicles. Just like in the Unloaded State, the disparity from other vehicles' CV is not as pronounced as in the case of the Loaded State.

Similar to the Loaded State, the majority of vehicles demonstrate a CV below or close to 20%, with only 4 vehicles nearing or exceeding the 20% CV value. The average CV value remains at 14% for both NO_x concentration and NO_x mass emission flow. Intriguingly, **these values not only align with but are even slightly lower than the values obtained for the average CV in both the Unloaded and Loaded States.**

So, it can be asserted that in relative terms, the dispersion of NO_x emission data during the TMV scenario is even more favorable than that of the Unloaded and Loaded States.

In summary, during the TMV scenario, the dispersion analysis indicates that the test's reproducibility was suitable for measurement purposes. The average value of NO_x concentration SD reached 104 ppm, while the average value of NO_x mass flow emission SD stood at 1.95 mg/s. The Coefficient of Variation for both types of values was 14%, indicating that this value is even more favorable than that observed for the Unloaded and Loaded states.

Reference Vehicle	Vehicle Manufacturer	Model	Avg. NO _x (mg/s)	Avg. NO _x (ppm)	SD NO _x (mg/s)	SD NO _x (ppm)	CV NO _x (mg/s)	CV NO _x (ppm)
1	SEAT	León	15.67	668	2.31	86.28	15%	13%
2	Volvo	V50	5.15	259	0.69	22.45	13%	9%
3	Alfa Romeo	Mito	17.44	1193	2.71	180.11	16%	15%
4	Audi	A4	18.20	806	1.66	67.02	9%	8%
5	BMW	330D	10.08	339	1.40	51.57	14%	15%
6	BMW	535d	20.85	789	2.55	103.36	12%	13%
7	Peugeot	407	27.31	1296	4.34	222.03	16%	17%
8	Volkswagen	Passat	21.01	1028	1.34	65.53	6%	6%
9	Skoda	Octavia	16.77	790	0.47	23.72	3%	3%
10	Audi	A5	18.82	824	1.24	66.80	7%	8%
11	Citroën	Berlingo	13.76	812	4.92	298.46	36%	37%
12	Volkswagen	Touran	4.85	237	0.39	22.08	8%	9%
13	Hyundai	i30	10.30	627	2.38	156.03	23%	25%
14	SEAT	León	16.72	851	1.26	77.07	8%	9%
15	Opel	Insignia	23.57	1093	1.63	75.02	7%	7%
16	Nissan	Juke	9.90	582	2.49	146.68	25%	25%
17	Opel	Astra	26.26	1392	3.48	162.99	13%	12%
18	Renault	Fluence	1.48	88	0.55	31.97	37%	36%
19	Renault	Talisman	23.93	1306	2.42	158.40	10%	12%
20	Peugeot	Boxer	19.77	991	1.74	87.14	9%	9%
21	Skoda	Superb	8.31	436	1.10	58.76	13%	13%
22	Kia	Sportage	14.29	826	2.72	162.16	19%	20%
23	Citroën	C4 Picasso	23.68	1368	1.16	69.97	5%	5%
Average value			16.00	808.75	1.95	104.16	14%	14%

Table 6-10. Summary of dispersion values for TMV State.

To encapsulate these findings, Table 6-10 provides a consolidated overview of the values related to data dispersion during the TMV State for the NO_x emissions across the analyzed vehicle set.

6.4.4. TEMPERATURE REPRODUCIBILITY ANALYSIS

Lastly, an additional variable to be assessed, which pertains to the test's execution and its simplicity, is the engine temperature during the test.

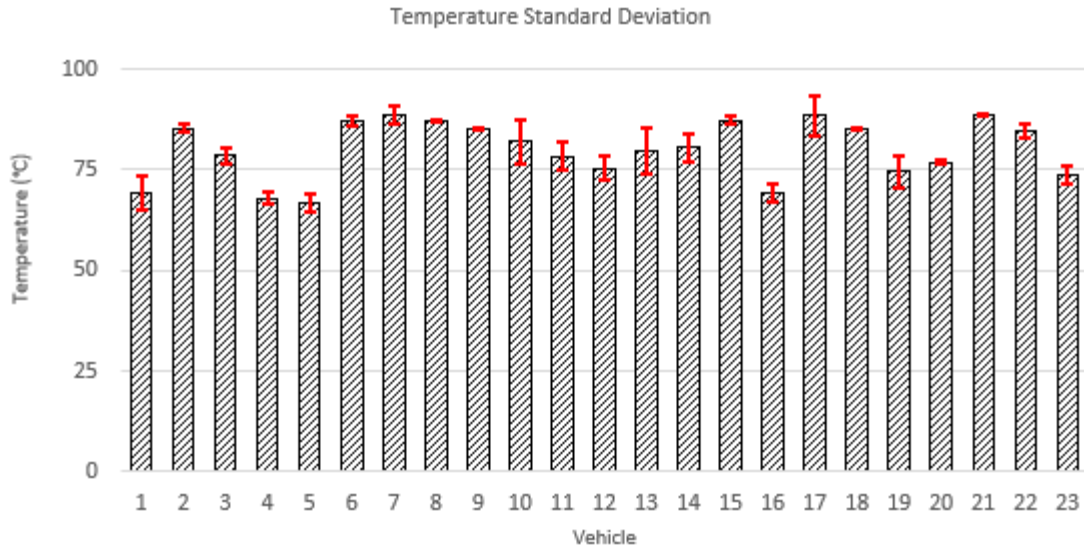


Figure 6-24. Average Temperature and SD (red bar) of Temperature along with the tests.

This value is obtained via the OBD system, and the dispersion of this data offers insights into the mechanical state of the engine at the time of the test. A measurement of engine temperature that closely aligns with the actual engine conditions indicates a higher level of consistency in the engine's operating conditions during the test.

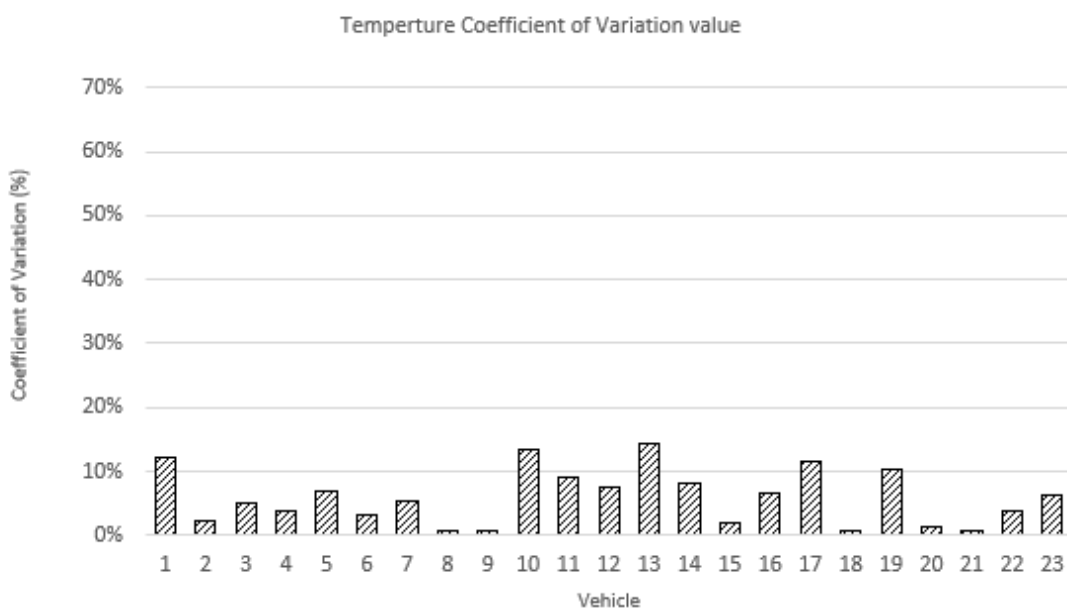


Figure 6-25. Coefficient of Variation (CV) for Temperature along with the test.

As depicted in Figure 6-24, a comparison is made between the average value and the standard deviation (SD) of Temperature in the Unloaded State. With an average temperature value of 80°C and an SD of 4.6°C, it becomes evident that the Temperature measurements were consistent across the set of measurements. This consistency underscores that similar conditions were maintained for the various tests conducted.

Reference Vehicle	Vehicle Manufacturer	Model	Avg. Temp. (°C)	SD Temp. (°C)	CV Temp. (%)
1	SEAT	León	69	8,47	12%
2	Volvo	V50	85	1,94	2%
3	Alfa Romeo	Mito	79	3,96	5%
4	Audi	A4	68	2,65	4%
5	BMW	330D	67	4,54	7%
6	BMW	535d	87	2,67	3%
7	Peugeot	407	89	4,62	5%
8	Volkswagen	Passat	87	0,62	1%
9	Skoda	Octavia	85	0,48	1%
10	Audi	A5	82	11,01	13%
11	Citroën	Berlingo	78	7,21	9%
12	Volkswagen	Touran	75	5,67	8%
13	Hyundai	i30	80	11,32	14%
14	SEAT	León	80	6,57	8%
15	Opel	Insignia	87	1,63	2%
16	Nissan	Juke	69	4,47	6%
17	Opel	Astra	88	10,29	112%
18	Renault	Fluence	85	0,50	1%
19	Renault	Talisman	75	7,77	10%
20	Peugeot	Boxer	77	1,04	1%
21	Skoda	Superb	89	0,76	1%
22	Kia	Sportage	85	3,24	4%
23	Citroën	C4 Grand Picasso	74	4,67	6%
Average value			80	4,61	6%

Table 6-11. Summary of dispersion values for engine Temperature.

This consistency can further be observed by examining the Coefficient of Variation (CV) for the Temperature values, as shown in Figure 6-25. The CV for Temperature displays a pattern akin to that of the CV for "% engine load," with most vehicles exhibiting a Temperature CV lower than 10% and an average value of 6%.

To encapsulate this understanding, Table 6-11 provides a concise summary of the values related to data dispersion for the engine Temperature across the set of vehicles.

6.4.5. SUMMARY OF THE REPRODUCIBILITY ANALYSIS

Considering the emission analysis of the vehicle group outlined in Table 6-1, which can be seen as a representative sample of vehicles from both the Spanish and European fleets, the results obtained have the potential to be extended to a wider context. Nevertheless, it is important to highlight that further studies might be required to complement the current dataset and offer a more comprehensive insight.

The analysis has focused on assessing the reproducibility of the test, aiming to confirm its viability for consistent application over time, yielding reliable results.

Regarding Reproducibility, it is worth highlighting a significant finding based on the collected data. The variable "% engine load" shows very low Coefficient of Variation (CV) values when measured in Unloaded and Loaded states. This can be a confirmation that the method used is straightforward and can be easily replicated under identical conditions, resulting in minimal variation between measurements.

This finding serves as an additional indicator that supports the initial hypothesis used for designing the test: the relationship between the NO_x concentration emissions during idling speed and the "% engine load" value applied to the vehicle. The low variation observed in the "% engine load" measurements reinforces the validity of the method and further validates the hypothesis.

In the Unloaded State, the average value of SD NO_x concentration was 18 ppm, and the average value of SD NO_x mass flow emission was 0.32 mg/s. The Coefficient of Variation for both types of values was 18% and 16% respectively. The "% engine load" SD was 1.4% for an average value of 20% engine load, which means the "% engine load" CV was 7%. Also, the Engine Temperature shows a CV of 6%, being an average value of 80°C and an SD of 4.6°C.

So, highlights will be that NO_x emissions at the Unloaded state present a CV of 17%, and engine operating conditions (% engine load and temperature) present a CV of 7%, which are both low enough to ensure reproducibility of the measurement method at this engine condition.

Analyzing the Loaded State, the average value of SD NO_x concentration was 53 ppm and the average value of SD NO_x mass flow emission was 0.93 mg/s. About CV, the average value was 18% for the NO_x concentration, and 17% for the NO_x mass emission flow. **These are the same values obtained for the average value of CV in the Unloaded State.** So, it could be said that in relative values, NO_x emission data dispersion is similar for the Unloaded and Loaded States.

For the "% engine load", the average CV was 6%, with only 2 vehicles showing a CV higher than 10%. Again, **these values of CV are the same as those for the Unloaded State.**

Consequently, the findings align with the hypothesis that the straightforwardness of the measurement technique contributes to a strong level of reproducibility in the measurement procedure. This, in turn, offers valuable insights into the reliability and resilience of the process.

Therefore, it can be observed that the SD values are elevated in the Loaded State compared to the Unloaded State, a correlation that is reasonable given the higher emission values. However, the CV values for NO_x concentration and NO_x mass flow emission were on average 17%, and CV for "% engine load" was 6%, which is the same as for the Unloaded State, so the behavior of both states is similar in terms of reproducibility. This is yet another indicator of the robustness and consistency of the measurement method.

Finally, for the TMV the average value of CV is 14% for the NO_x concentration, and again 14% for the NO_x mass emission flow. These values are not only similar but are even somewhat lower than values obtained for the average value of CV in the Unloaded and Loaded States.

The trend observed across the measurements reveals that the absolute value of the SD increases correspondingly from the Unloaded to Loaded States, and further to the TMV scenario. This behavior aligns with the increase in the absolute value of NO_x emissions, as SD tends to increase with higher emission values.

However, the CV holds a distinct characteristic, it remains consistent for all vehicles across the three states. The CV, being relative to the mean, remains independent of the absolute values of the measurements. This uniform CV value provides crucial insight into the consistency of the measurement method and the accuracy of the emission value estimation at 100% engine load. This stability across states and vehicles suggests a robust and reliable measurement process.

To conclude, the following key points highlight the reproducibility findings:

- a) **The standard Deviation** for NO_x concentration is lower in the **Unloaded State (18 ppm)** than in the **Loaded State (53 ppm)** and, naturally, the **TMV (104 ppm)**.
- b) **The standard Deviation** for NO_x mass emission flow is lower in the **Unloaded State (0.32 mg/s)** than in the **Loaded State (0.93 mg/s)** and, again, the **TMV (1.95 mg/s)**.
- c) **The standard Deviation** for "% engine load" is lower in the Unloaded State than in the Loaded State, yet remains consistently low in both states (1.4% during unloaded idle, 2.6% during loaded idle).
- d) **The coefficient of Variation remains consistent** for the **NO_x concentration and NO_x mass flow emission** in both the **Unloaded and Loaded States (16%-18%)**. This indicates uniform data dispersion for both states and types of measurements. **The TMV's CV is even lower (14%)**, further enhancing its reproducibility. These dispersion values are considered suitable for PTI measurement.
- e) **The coefficient of Variation for the "% engine load" value is 7%** for both idle states. This confirms the consistent maintenance of operational conditions during the tests.
- f) **The coefficient of Variation for the engine Temperature is 6%**, confirming the reproducibility of operational conditions during the tests.

Therefore, the results obtained in the tests performed allow us to affirm that in terms of reproducibility, the proposed NO_x measurement test presents an adequate performance for the purpose for which it is intended.

6.5. VALIDATION OF THE MEASUREMENT PROCESS FROM THE RESULTS

The main result obtained from the test is the average value of NO_x mass emissions flow and NO_x concentration in the vehicle's exhaust while idling, as well as the estimation of the TMV for both types of NO_x measure expected for the vehicle at 100% of "% engine load" at idle speed.

Reference Vehicle	Idle Unloaded			Idle Loaded			TMV	
	NO _x (mg/s)	NO _x (ppm)	% Engine load	NO _x (mg/s)	NO _x (ppm)	% Engine load	NO _x (mg/s)	NO _x (ppm)
1	0.87	40	21	1.65	73	37	5.15	259
2	1.80	77	17	5.29	226	34	15.67	668
3	2.70	199	19	7.30	495	42	17.44	1193
4	1.83	81	24	7.83	349	47	18.20	806
5	2.28	77	24	3.60	122	39	10.08	339
6	3.51	134	24	10.56	401	54	20.85	789
7	5.65	269	30	15.51	754	60	27.31	1296
8	2.74	138	15	5.39	261	31	21.01	1028
9	2.52	119	21	5.37	253	42	16.77	790
10	4.74	200	21	7.92	374	46	18.82	824
11	1.64	96	19	5.14	304	47	13.76	812
12	1.65	80	17	1.68	82	36	4.85	237
13	2.04	123	22	4.56	278	52	10.30	627
14	2.65	139	25	5.09	277	39	16.72	851
15	1.91	88	16	6.46	300	28	23.57	1093
16	1.88	117	22	3.98	236	42	9.90	582
17	3.71	208	15	7.23	405	37	26.26	1392
18	0.08	5	22	0.25	15	37	1.483	88
19	2.35	129	16	8.01	440	36	23.93	1306
20	2.59	131	15	5.89	296	37	19.77	991
21	1.73	91	22	3.22	169	39	8.31	436
22	2.22	128	17	6.47	373	45	14.29	826
23	2.45	141	21	10.52	599	53	23.68	1368

Table 6-12. NO_x emissions average values for the unloaded idle state, loaded idle states, and TMV from static NO_x test.

Furthermore, the "% engine load" values corresponding to the various load states are crucial pieces of information derived from the PTI measurement test.

The average value dataset offers practical insights into vehicle emissions during urban driving, while the TMV dataset offers a comparative metric for assessing NO_x emission levels among vehicles. This TMV dataset serves as an indicator of how a vehicle's NO_x emissions behave under load, enabling effective inter-vehicle comparisons.

The collective results from this comprehensive series of measurements conducted on vehicles indicated in Table 6-1, are displayed in Table 6-12. This table illustrates the average values derived from multiple tests conducted on each individual vehicle.

6.5.1. METHOD VALIDATION FROM LOAD STATE RESULTS

Analyzing the whole average results, the average NO_x concentration at loaded idle was 152% higher than the average NO_x concentration at unloaded idle, and the average "% engine load" value at loaded idle was 106% higher than the average "% engine load" value at unloaded idle. So, the increase of the "% engine load" value between both load states is large enough for the explained linear extrapolation (see Table 6-14).

Moreover, these findings align with the foundational hypothesis upon which the proposal is built: the connection between NO_x concentration in the exhaust pipe and the "% engine load". This relationship is observed to correspondingly increase as the "% engine load" value rises.

The same situation is observed for the **NO_x mass flow** emissions, where the average value of loaded state emissions is 150% higher than average unloaded idle emissions. Again, the increase of NO_x mass flow emissions between both load states allows the building of a linear function.

The average engine load reached loaded idle is 41.7% (in some cases it went up to 60.0%), while the average engine load at unloaded idle is 20.3%. This demonstrates how the static NO_x measurement method, devoid of supplementary equipment or simulation setups, enables the "% engine load" value to double between unloaded and loaded idle conditions. This capability facilitates the analysis and comparison of NO_x emissions in two distinct load scenarios.

	NO _x [mg/s]	NO _x [ppm]	% engine load
Unloaded	2.52	127.5	20.2%
Loaded	6.30	321.2	41.9%
TMV	16.67	841.5	100%

Table 6-13. Summary of avg. NO_x emissions from diesel vehicles.

	NO _x [mg/s]	NO _x [ppm]	% engine load
Unloaded	2.41	122.3	20.3%
Loaded	6.04	307.9	41.7%
TMV	16.00	808.7	100%

Table 6-14. Summary of avg. NO_x emissions from vehicles including the petrol one.

Excluding petrol vehicles from the averaging process yields the average values as presented in Table 6-13. The average NO_x emissions are higher in this scenario, even though the "% engine load" values remain comparable, in contrast to the inclusion of petrol vehicles, which are reflected in the average values displayed in Table 6-14.

For the petrol engine vehicle (No. 18), NO_x concentration at unloaded and loaded idle is more than 20 times smaller than the average concentration for diesel ones. This difference is even higher for the NO_x mass flow emissions and influences the average values.

However, the "% engine load" value reached is similar to diesel engine vehicles, and the value for both states, 22.0% engine load for unloaded idle and 38.0 % for loaded idle is near to the mean of the complete set of vehicles previously mentioned. These results are in line with the situation already indicated, the fact that diesel vehicles are the main NO_x emitters [5]–[7].

Based on the data examined thus far, the following key insights can be highlighted:

- There is an **average increase of 106% of the "% engine load"** value from the unloaded idle to the loaded idle for the complete set of vehicles tested.
- There is a significant increase in **NO_x concentration** from the unloaded idle to the loaded idle in all vehicles, with an **average increase of 152%**.
- There is a significant increase in **NO_x mass emission flow** from the unloaded idle to the loaded idle in all vehicles, with an **average increase of 150%**.
- Regarding emissions during unloaded idle, the estimated TMV of NO_x concentration and mass emission flow witnessed a notable surge of 563%. The average increase of "% engine load" is from the average value at unloaded idle of 20% engine load to 100%.
- **Petrol engine** vehicle shows the same levels of "% engine load" as diesel vehicles, but **NO_x concentration values are 20 times smaller** than average diesel vehicles' NO_x concentration, and the difference is even higher for the NO_x mass flow emission.

When individually analyzing the rise in NO_x concentration and mass emission, Figure 6-26 illustrates that a majority of vehicles exhibited an increase in emissions surpassing 100% (16 vehicles), with an additional 5 vehicles displaying an increase exceeding 80%. Furthermore, it is evident that the Euro emission level does not appear to correlate with either the increase in emissions or the augmentation of "% engine load".

However, two vehicles show different behavior than the others from the set, vehicles No. 5 and No. 12. Is there any explanation for this behavior?

Vehicle No. 5 presents an increase of NO_x emissions similar to the increase of "% engine load", around 60% in both parameters. It is the second most powerful vehicle of the set, and it is a Coupe vehicle. This means that it is a vehicle with a sports setup, both in terms of bodywork and suspension, as well as in terms of electronic engine management. This could affect the "% engine load" variation at idle, because if the available torque at idle is very large compared to the load increase of switching on the vehicle's equipment for the test, the engine load increase will be smaller

compared to other vehicles that, due to engine management, have less torque at idle speed.

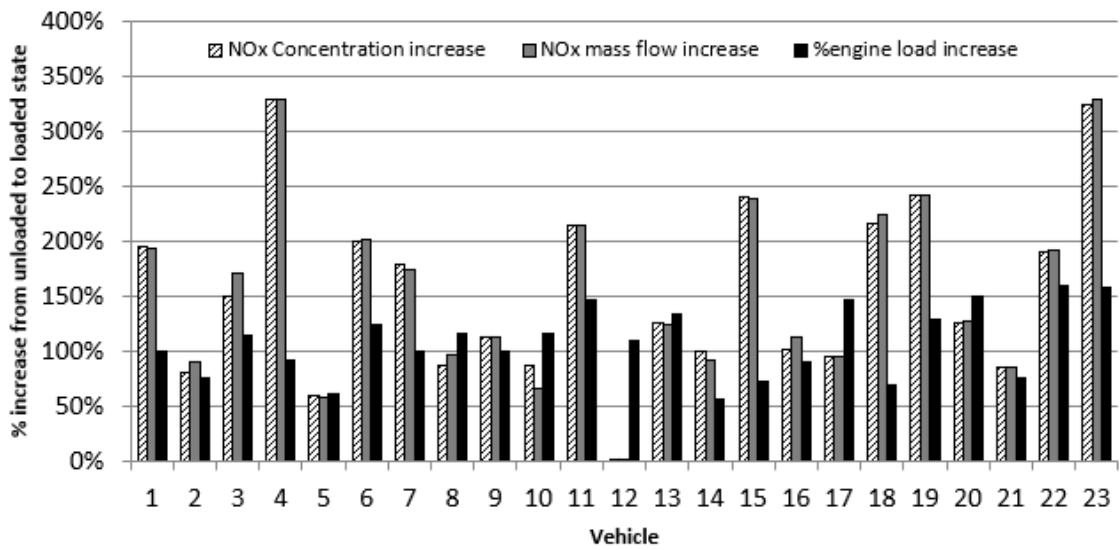


Figure 6-26. Percentage of increase of variables from unloaded to loaded state.

Anyway, this is only a hypothesis, because there is not enough information to know with certainty why the increase is so low.

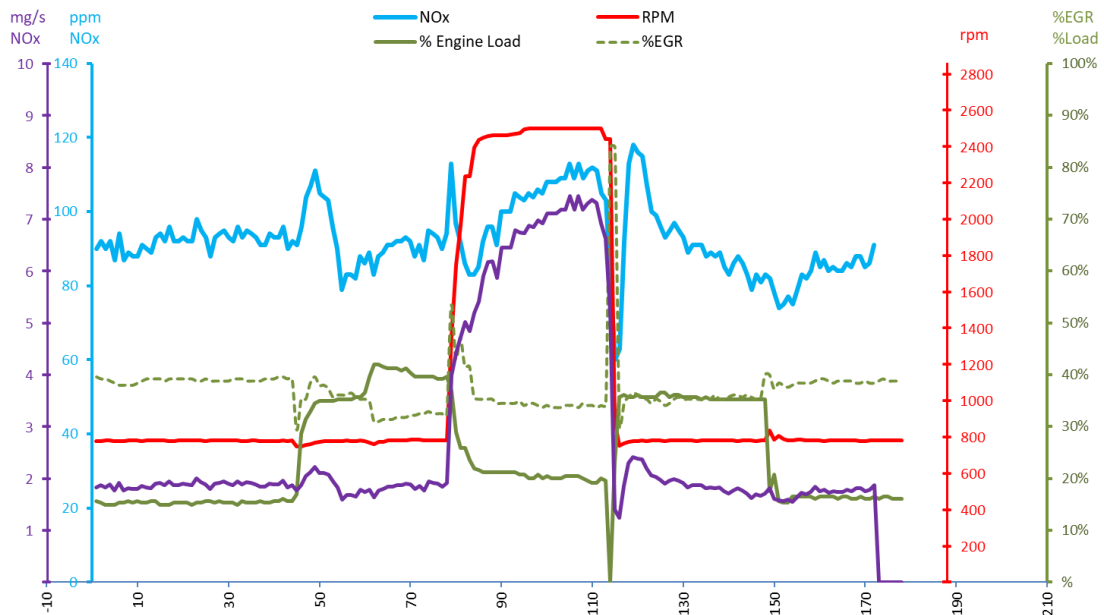


Figure 6-27. Sample of NO_x test of vehicle No. 12.

Regarding vehicle No. 12, while the increase in "% engine load" falls within the average range, the rise in NO_x concentration and mass flow emission from the unloaded to

loaded state is merely 2%. To comprehend the distinct behavior of this vehicle, it is imperative to examine the graphical representation of a specific test (Figure 6-27).

The behavior exhibited by this vehicle showcases a distinct characteristic that has subsequently been noted in other vehicles produced by the same manufacturer.

Usually, in the initial and second stages of the test (the unloaded and loaded stages before acceleration), the EGR system remains inactive. It only becomes operational when the vehicle accelerates during the third stage. Depending on the individual vehicle, the EGR system may return to its initial state or partially close after a certain duration.

However, in this specific case, as depicted in Figure 6-27, it is evident that the EGR system remains active throughout the entire test, maintaining a consistent aperture percentage with minimal fluctuations. Consequently, while the "% engine load" behavior is correctly exhibited during the test, the NO_x concentration remains relatively uniform, even during the Acceleration section. This consistent behavior of the EGR system contributes to the minimal **variation** in NO_x concentration and mass emission flow between the unloaded and loaded states for this particular vehicle.*

As was explained previously, there is a large number of variables related to NO_x emissions, and a variation of any of them could make a change in the final exhaust vehicle emissions. This case is an example of this situation, where a different behavior of one variable (in this case the EGR behavior) changes the behavior of the NO_x emissions of the vehicle, compared with the rest of the vehicles of the set.

In summary, from the unloaded idle state to the loaded idle state **the average increase of "% engine load" for the set of vehicles is 109%**, more than double, and the average increase of NO_x emissions (both concentration and mass emission flow) is 155%, being this behavior representative for the most of vehicles.

This behavior is a confirmation of the working basis hypothesis, that is, the NO_x emissions at the exhaust pipe are related to the "% engine load" value, increasing the emissions when the "% engine load" increases.

6.5.2. METHOD VALIDATION BASED ON COMPARISON WITH EUROPEAN EMISSION STANDARDS

The comprehensive dataset comprising over 200 NO_x measurements presents the opportunity for various types of analyses, which offer valuable insights into both vehicle emissions at large and the intricacies of the measurement process itself. This extensive data pool can yield meaningful findings that contribute to a broader understanding of emissions and provide in-depth insights into the measurement methodology.

The initial analysis involves a comparison between the emission test outcomes and the anticipated emissions based on the theoretical European emission standards associated with each vehicle's approval type.

Each vehicle listed in Table 6-1 holds a European Approval Type and adheres to a specific Euro emission level, which corresponds to a designated Emission Factor for

NO_x emissions – the upper limit of permissible emissions. Ordinarily, vehicles exhibit an Emission Factor that's lower than their Euro level's maximum threshold. However, for the purpose of comparison, the maximum value stipulated by the Euro emission level will be employed.

In this way, according to the Emissions Level thresholds indicated in Table 6-15, vehicles from Table 6-1 should not exceed the NO_x emissions limits shown in Figure 6-28.

In Figure 6-28 it is evident that NO_x emissions theoretically decrease as the Emission Level increases. Specifically, the maximum anticipated NO_x emissions for Euro 6 diesel vehicles are only 33% of the maximum expected NO_x emissions for Euro 4 diesel vehicles.

	EF_{NOx} [g/km]	
	DIESEL	PETROL
Euro 3	0.50	0.15
Euro 4	0.25	0.08
Euro 5	0.18	0.06
Euro 6	0.08	0.06

Table 6-15. NO_x Emissions Factors according to Emissions level

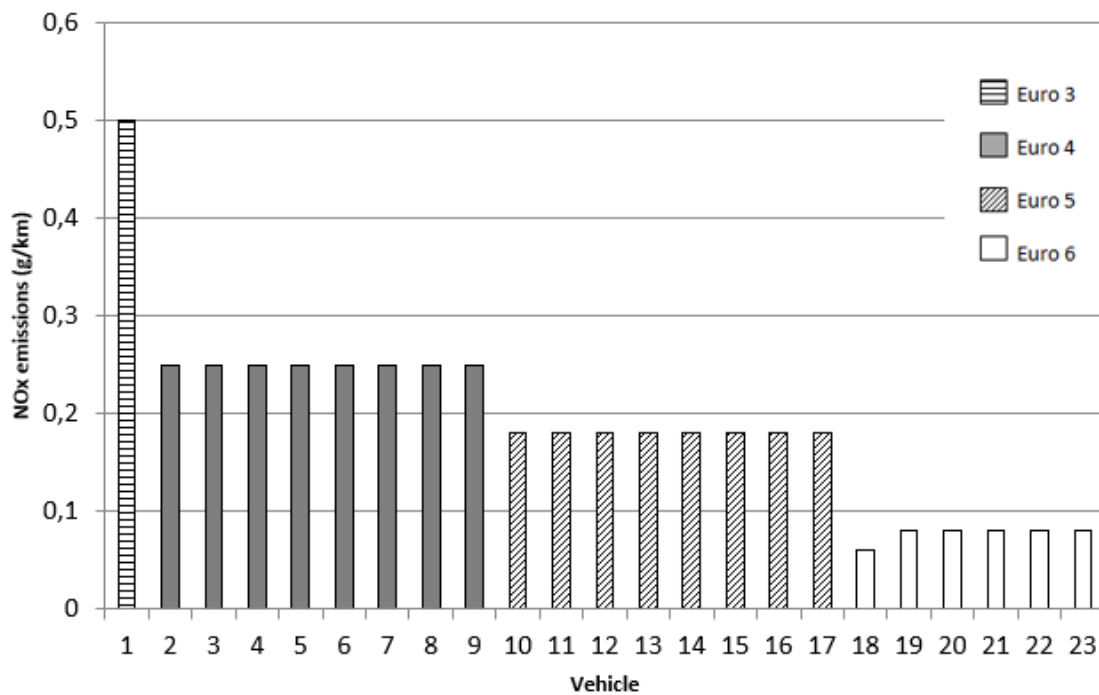


Figure 6-28. Vehicle's NO_x Emissions Factors according to Emission Level

The maximum NO_x emissions from Euro 3 vehicle is expected to be more than 6 times higher than Euro 6 diesel vehicle emissions. It is also appreciated how the NO_x emissions expected for a Euro 6 gasoline vehicle (No. 18) are 25% lower than those of a diesel vehicle with the same level of emissions.

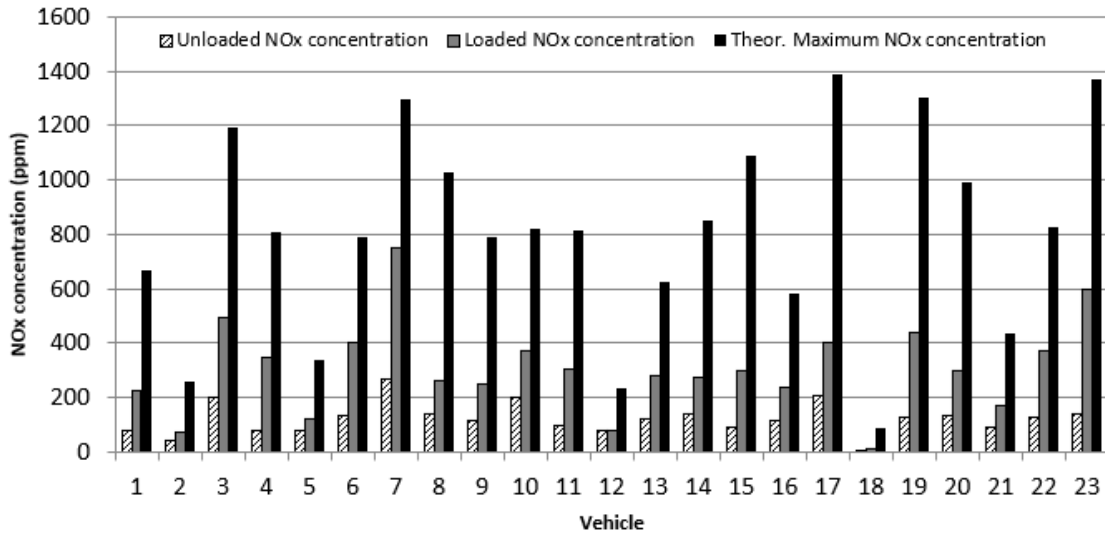


Figure 6-29. Vehicle's NO_x concentration from static measurement.

However, when the measurement results are presented in a similar graphical format, a notable disparity emerges between the actual measured NO_x emissions behavior and the theoretically projected values. If the vehicles are arranged according to their reference numbers, Figure 6-29 and Figure 6-30 depict the average concentration and mass flow emissions for each vehicle in both states (unloaded and loaded), as well as for the TMV.

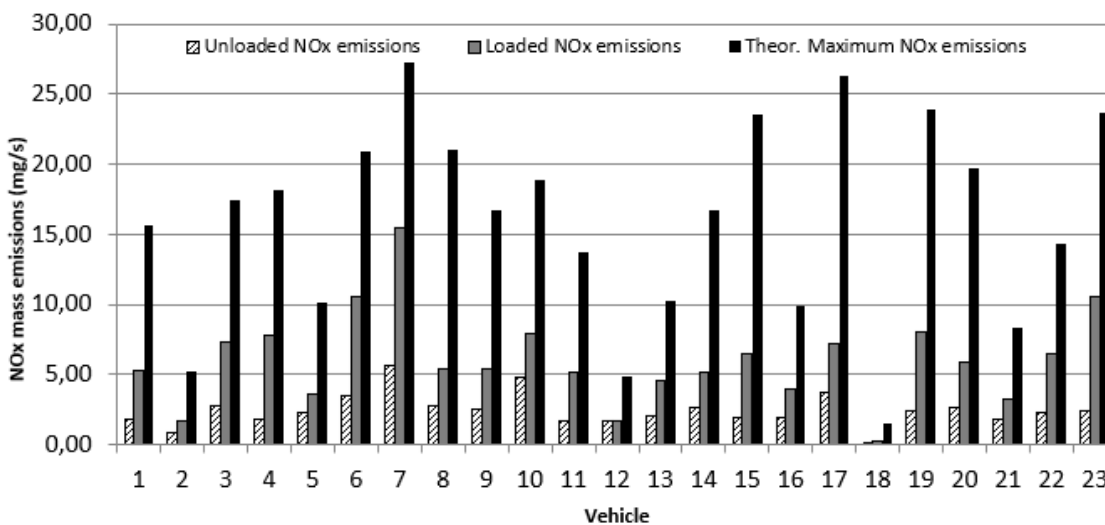


Figure 6-30. Vehicle's NO_x mass emission flow from static measurement.

In both NO_x concentration and NO_x mass emissions flow, the relative values derived from the measurement process substantially deviate from the anticipated values based on the Type Approval of the vehicles.

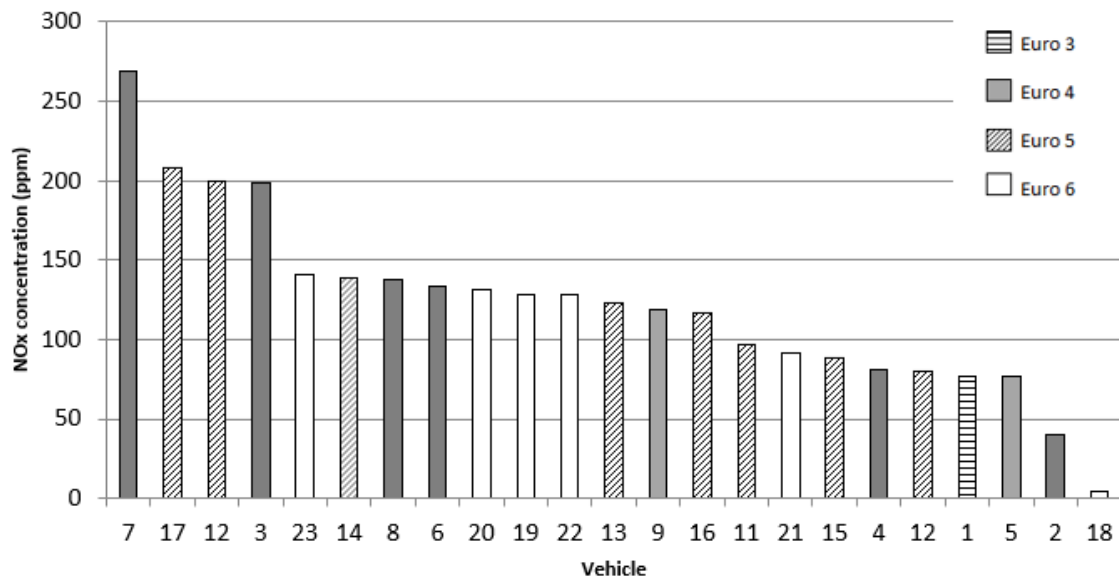


Figure 6-31. Vehicles ordered according to NO_x concentration at Unloaded state.

Initially, the anticipated emission order based on the Euro Emissions Level is not reflected in the results of the static idling measurement. This implies that the NO_x emissions observed in the measurement process do not conform to the distribution outlined by the Euro levels in Figure 6-28.

When vehicles are arranged based on the measurement results, it becomes apparent that the Euro emissions level does not accurately represent the measured emissions emanating from the vehicles.

In Figure 6-31, vehicles are ordered according to the average NO_x concentration measured at the **Unloaded state**. Clearly, the petrol vehicle shows a minimum concentration compared with the rest of the vehicles, and a great heterogeneity from the emissions of Euro 4, Euro 5, and Euro 6 vehicles can be observed.

Unexpectedly, it is noticeable that vehicle No. 1 (classified as Euro 3) does not possess the highest NO_x concentration; in fact, it is one of the lower emitters. Interestingly, some vehicles categorized as Euro 6 (theoretically representing lower pollutant levels) exhibit higher NO_x concentrations in the exhaust compared to vehicles with lower Euro levels.

Likewise, a similar scenario applies to emissions in a loaded state, where the vehicle is stationary but with certain systems active (typically the Air Conditioning and Lighting systems).

From this data, it could be interpreted that vehicles with Euro 6 emission levels, which were theoretically considered to be lower emitters and thus expected to contribute

to the reduction of NO_x concentration in cities, may not be contributing in the anticipated manner.

Three distinct vehicle groups are discernible:

1. The first group features unloaded concentrations below 100 ppm, comprising predominantly Euro 3, Euro 4, and Euro 5 vehicles. Only one Euro 6 vehicle is present within this category.

2. The second group falls within the 100 ppm to 150 ppm range of unloaded concentrations. This category is a mix of Euro 4, Euro 5, and Euro 6 vehicles.

3. The third group exhibits NO_x concentrations surpassing 150 ppm. This group comprises primarily Euro 4 and Euro 5 vehicles, with one Euro 4 vehicle recording an exceptional concentration exceeding 250 ppm.

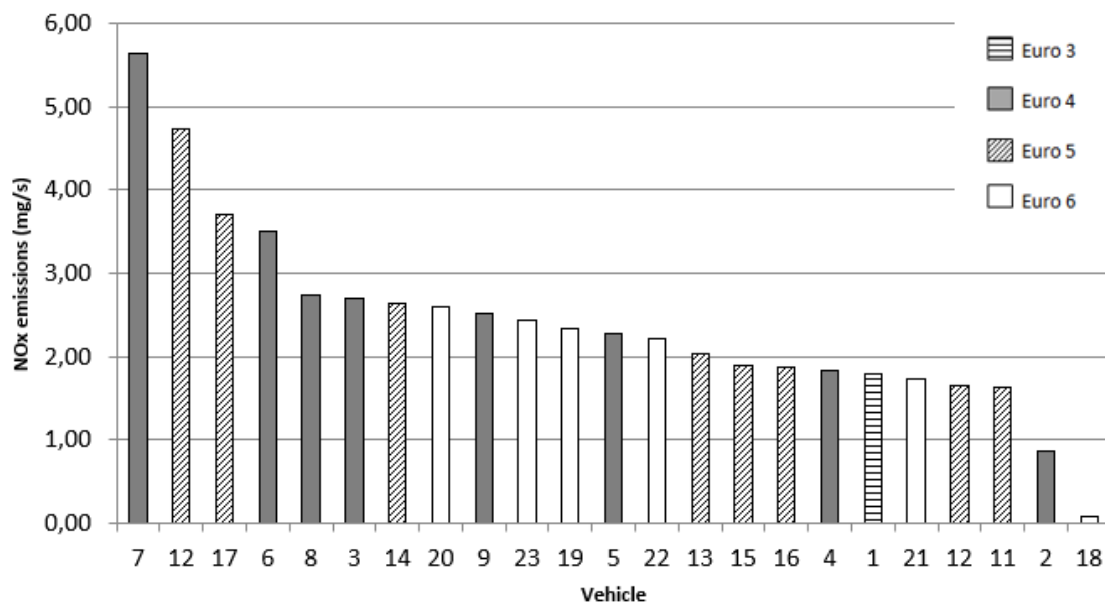


Figure 6-32. Vehicles ordered according to NO_x mass emission flow at Unloaded state.

Regarding NO_x mass emission flow at the unloaded state, the situation is quite similar to the NO_x concentration. Figure 6-32 shows the vehicles ordered according to NO_x mass emission flow, and it can be verified that the distribution of the vehicles does not correspond to the Euro emission level of the vehicles either. It can also be observed that the sequence of vehicles is not identical to that shown in Figure 6-31, owing to variations in NO_x emissions behavior and engine characteristics across the different vehicles.

This is a demonstration of the importance of determining the mass emission flow, concerning only the use of the concentration to define the vehicle's emissions.

Indeed, certain vehicles consistently display the highest and lowest emissions across both measurement categories. Vehicle 7 consistently exhibits the highest emission mass flow and concentration among all vehicles tested. In contrast, vehicle 18, which

is powered by petrol, consistently demonstrates the lowest emission mass flow and concentration.

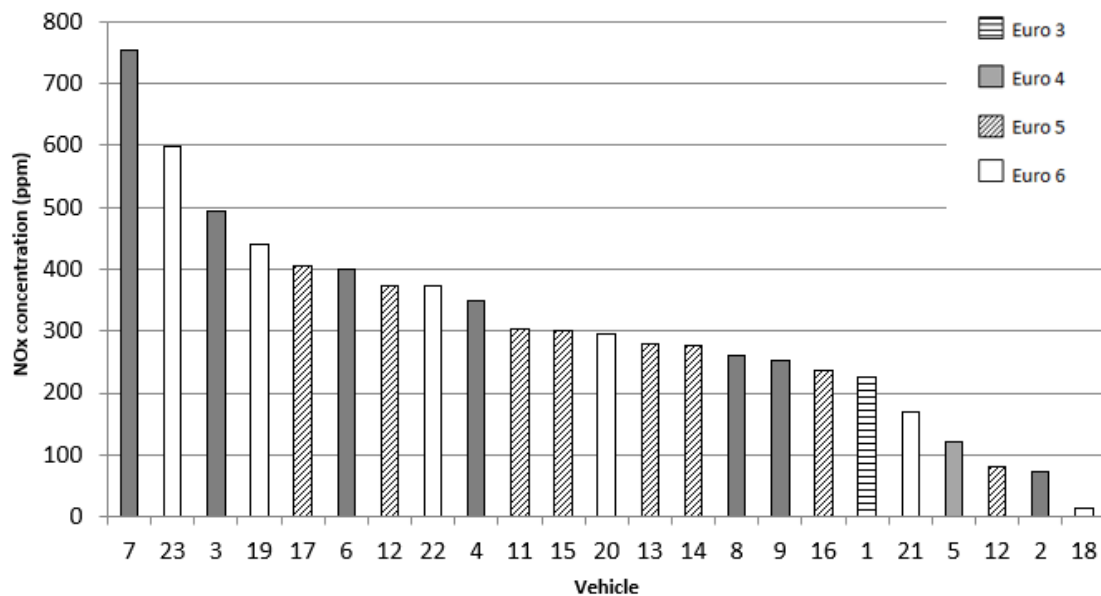


Figure 6-33. Vehicles ordered according to NO_x concentration at Loaded state.

Upon analyzing the **Loaded state**, the degree of heterogeneity becomes even more pronounced. Concentration-wise (as depicted in Figure 6-33), merely 5 vehicles exhibit concentrations below 200 ppm (as opposed to the Unloaded state where only 2 vehicles surpassed 200 ppm). Within this group, we observe a mix of Euro 4, Euro 5, and Euro 6 emission levels. Moreover, a sizable cluster of 9 vehicles registers concentrations ranging from 200 ppm to 300 ppm. This group encompasses vehicles from Euro 3, Euro 4, Euro 5, and even a Euro 6 emission level.

A group of 4 vehicles shows NO_x concentration between 300 ppm and 400 ppm with vehicles of the three Euro levels, and results for 5 vehicles were higher than 400 ppm, including two Euro 6 vehicles.

As was said for the unloaded state, it is an interesting fact that two of the four higher emitters were Euro 6 vehicles, instead, the Euro 3 vehicle was the fifth diesel vehicle with fewer NO_x emissions at this loaded state.

Upon analyzing NO_x mass emission flow (as shown in Figure 6-34), a similar situation emerges. Within the group of the four highest emitters, two Euro 6 vehicles are included. Notably, the disparity between diesel vehicles with lower emissions and those with higher emissions exceeds fivefold.

This observation holds true even when excluding the extreme cases represented by the vehicle with the lowest emissions (No. 18, the petrol vehicle) and the vehicle with the highest emissions (No. 7). Regarding the disparities in emissions, a similar pattern emerges for NO_x concentration. Variations exceeding 600% are observed between Vehicle 2 and Vehicle 23 in terms of emissions.

Similar to the unloaded measurements, vehicle number 7 consistently exhibits the highest mass emission flow and concentration among the vehicle group. On the other hand, vehicle number 18 (the petrol one) consistently displays the lowest mass emission flow and concentration.

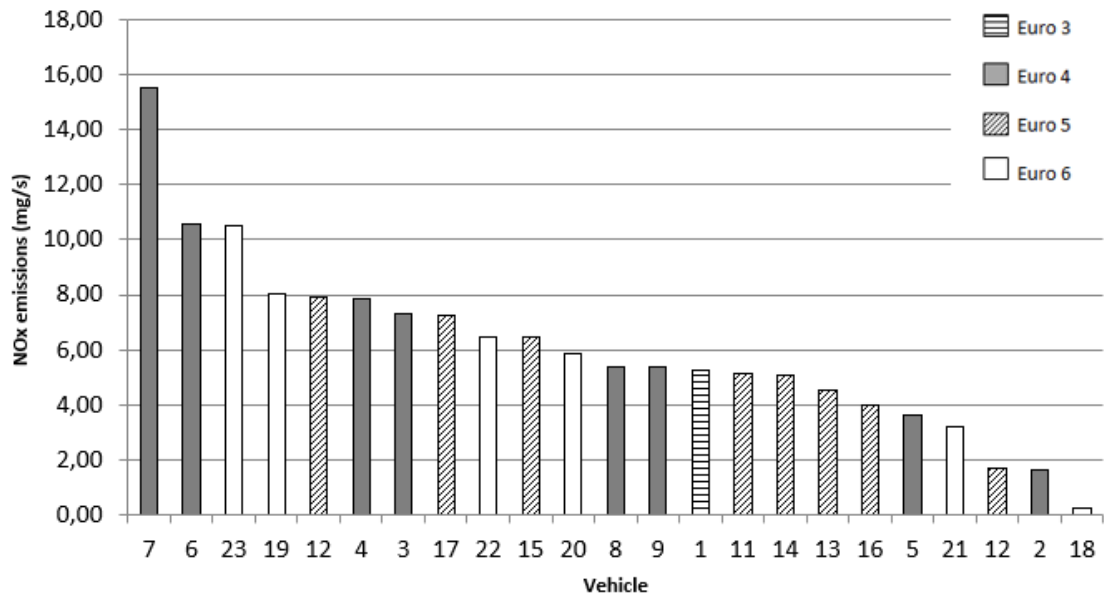


Figure 6-34. Vehicles ordered according to NO_x mass emission flow at Loaded state.

Finally, in the analysis of the emissions from the **TMV**, the situation is quite similar. Vehicle No. 18 stands out as the one with the lowest concentration and mass emission flow. Its values for both measurement types are over three times lower than those of the diesel vehicles exhibiting the lowest emissions (see Figure 6-35).

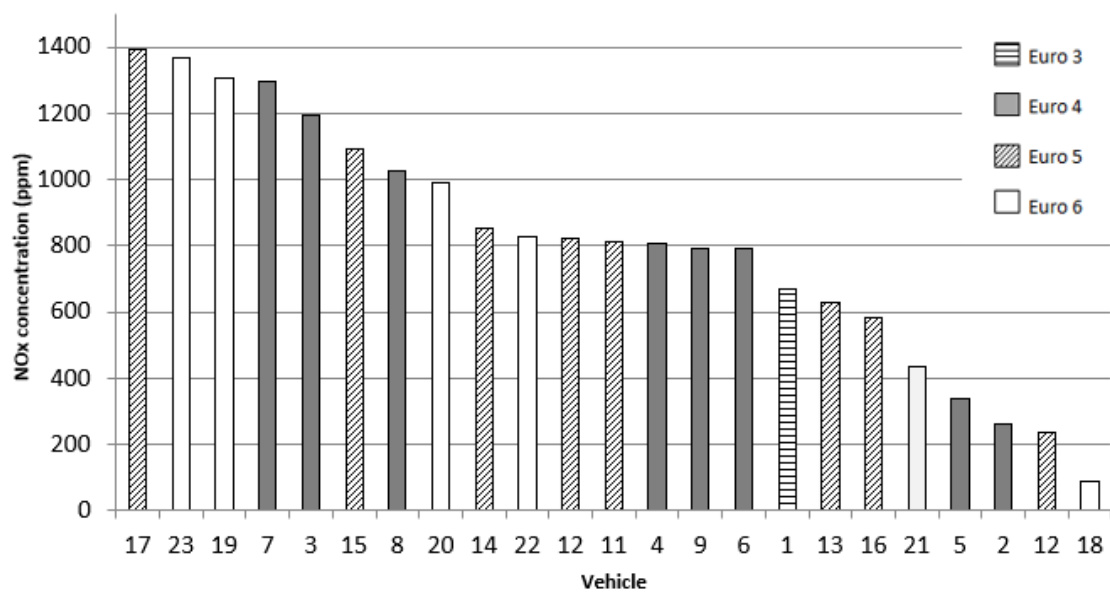


Figure 6-35. Vehicles ordered according to NO_x concentration: TMV.

Upon analyzing the NO_x concentration data, the vehicles can be categorized into three distinct groups: 8 vehicles present a concentration lower than 700 ppm (including 1 Euro 6 vehicle, and the Euro 3 vehicle), 7 vehicles present a concentration around 800 ppm (including 1 Euro 6 vehicle), and finally, a group of 8 vehicles with a concentration equal or higher than 1000 ppm (including 3 Euro 6 vehicles).

In this concentration analysis, it is notable that the highest emissions are not attributed to vehicle No. 7 (even though its value was close to the highest). Instead, vehicle No. 17 claims this distinction, marking the sole instance where this occurs. Throughout the rest of the analysis, vehicle No. 7 consistently emerges as the vehicle with the highest concentration and mass emission flow.

Finally, for the TMV of mass emission flow (Figure 6-36), it can be found a group of 7 vehicles with NO_x emissions lower or equal to 10 mg/s. The second group of 11 vehicles presents NO_x emissions higher than 10 mg/s and lightly higher than 20 mg/s. At least, a group of 5 vehicles, formed by two Euro 6 vehicles, two Euro 5 vehicles, and one Euro 4 vehicle show emissions higher than 23 mg/s.

Thus, drawn from the test results, a significant inference about vehicle emissions becomes evident: Euro 6 vehicles exhibit emissions levels that are not as low as anticipated. Surprisingly, some Euro 6 vehicles find themselves categorized as higher emitters within the vehicle set under the test conditions. Conversely, the older vehicle (Vehicle No. 1, Euro 3), which theoretically should have higher emissions, consistently resides within the group of lower emitters among the analyzed vehicles.

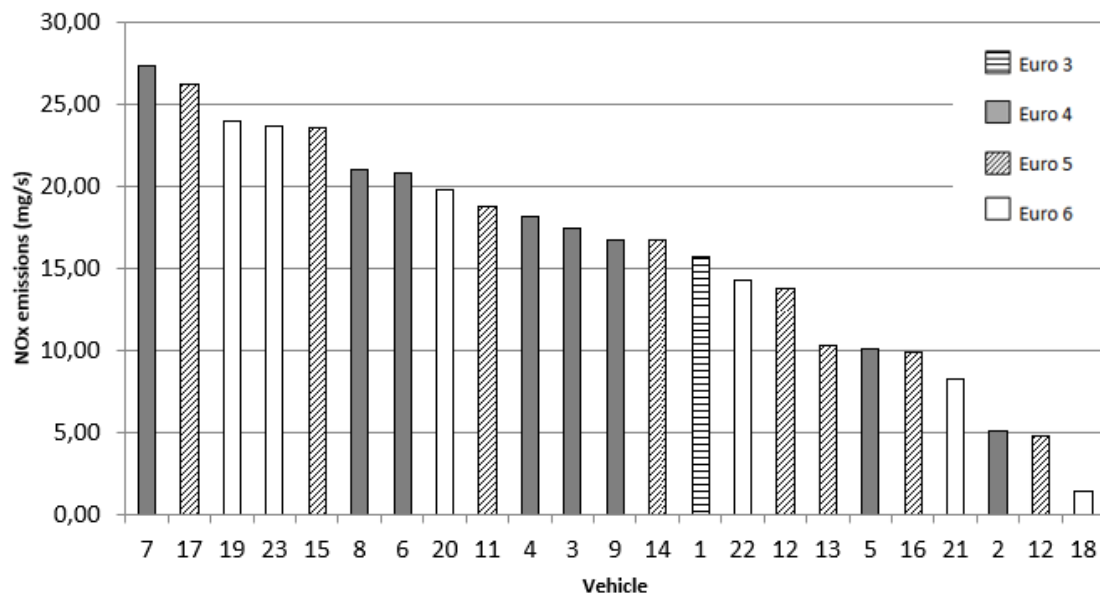


Figure 6-36. Vehicles ordered according to NO_x mass emission flow: TMV.

Excluding petrol vehicles, it is notable that NO_x emissions and concentration experience an increase of up to sevenfold, ranging from the minimum to maximum values. This substantial discrepancy between the lowest and highest emissions is indicative of a significant variation within the studied set of vehicles.

Instead, "% engine load" values from the 23 vehicles, and for the Unloaded and Loaded states, present an increase of approx. 100% from the lower to the higher value in each of both states. As can be seen from Figure 6-37 and Figure 6-38, there is no relationship between the Euro level and the value of "% engine load" registered in the test.

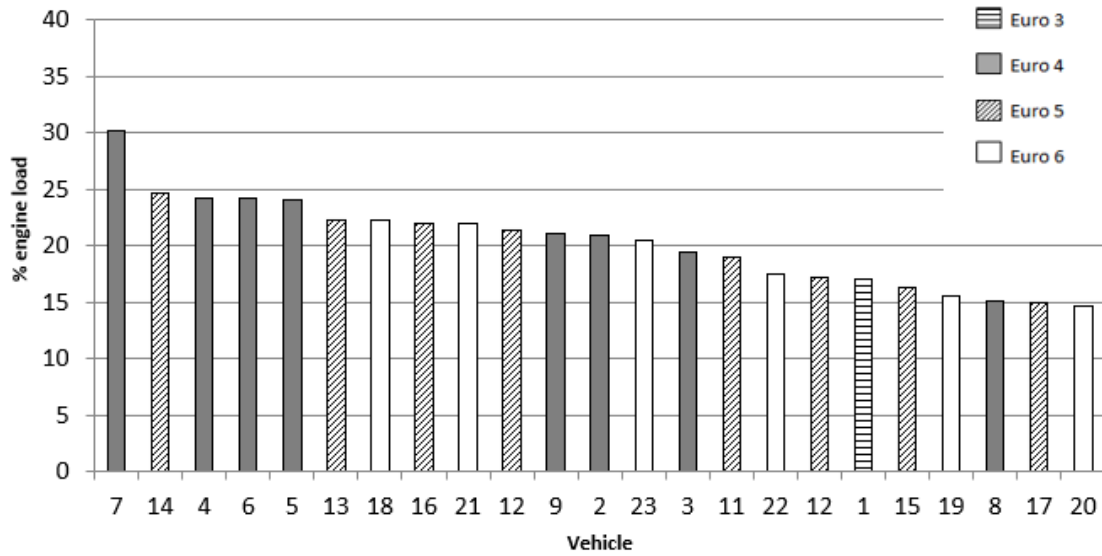


Figure 6-37. Vehicles are ordered according to the average "% engine load" values for the Unloaded state.

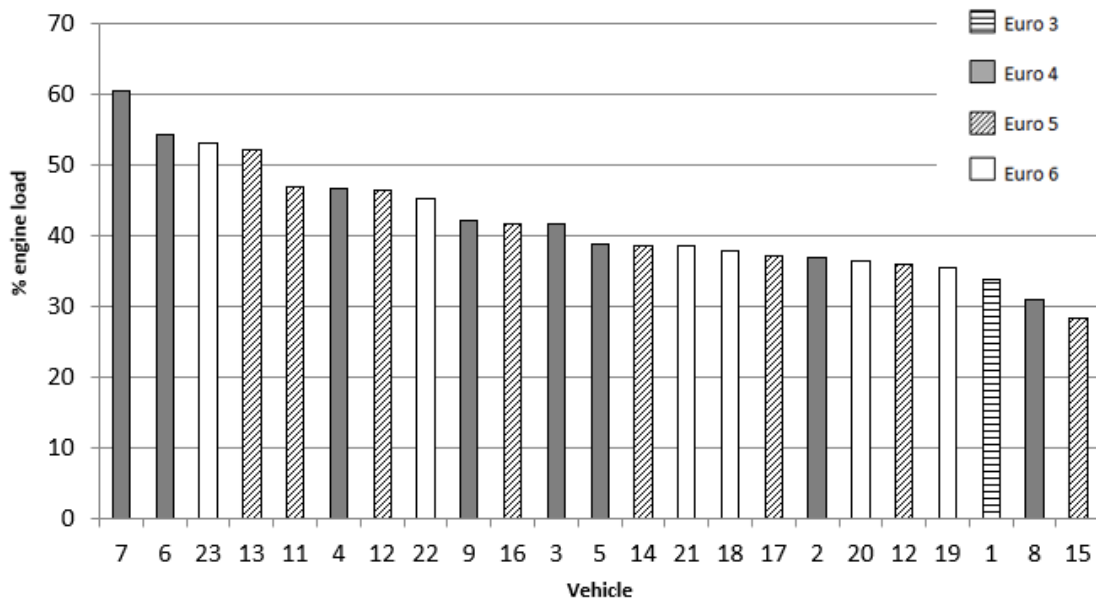


Figure 6-38. Vehicles are ordered according to the average "% engine load" values for the Loaded state.

A noteworthy observation is that vehicle No. 7 also exhibits the highest "% engine load" value. In essence, the vehicle displaying notably elevated average "% engine load" values, both when unloaded and loaded, is the same vehicle showing the highest NO_x emissions in both conditions.

Based on the data examined thus far, the following key insights can be highlighted:

- **The petrol engine** vehicle shows the same levels of "% engine load" as diesel vehicles, but **NO_x concentration values are 20 times smaller** than average diesel vehicles' NO_x concentration, and the difference is even higher for the NO_x mass flow emission.
- Vehicle No. 7 stands out as it exhibits the highest NO_x concentration and mass emission flow among the analyzed vehicles. Furthermore, this same vehicle also boasts the highest "% engine load" value within the vehicle set under examination.
- A discernible correlation between the Euro emission level and the measured NO_x emissions is not readily apparent.

Furthermore, it has been verified that the Euro emissions level is not correlated with the NO_x emissions recorded during the test. This observation is consistent with findings in the scientific literature that demonstrate how vehicle emissions behave during real-world driving [27], [30]–[35].

6.5.3. SUMMARY OF VALIDATION OF THE MEASUREMENT PROCESS

Based on the analysis of emissions from the group of vehicles presented in Table 6-1, the main features of the NO_x measurement test proposed can be detailed.

Given that the sample of vehicles is representative of both the Spanish and European fleets, the obtained results can be extrapolated to a broader context. However, it is worth noting that additional studies may be necessary to supplement the existing data and provide a more comprehensive understanding. Thus, for instance, in Chapter 8, the results of a measurement campaign conducted at various ITV stations using the proposed method will be analyzed.

From the data in section 6.5, can be found the following key points based on the available data:

- 1) Results from the tests are according to the expected from the working hypothesis.
- 2) NO_x emissions measured and estimated from the measurement method are compared with the expected results from Approval-Type.

Regarding the initial point, within the complete dataset derived from the tests, it was observed that the average **NO_x concentration** during loaded idle conditions was approximately **152% higher** than the average NO_x concentration at unloaded idle. The average **NO_x mass flow** emissions at loaded idle were **150% higher** than the average NO_x mass flow emissions at unloaded idle, and the average **"% engine load"** value at loaded idle was **106% higher** than the average "% engine load" value at unloaded idle.

This indicates that the substantial rise in the "percentage engine load" value derived from the measurement method between the two load states is sufficiently substantial (exceeding 100%) to result in a notable escalation in both NO_x concentration and NO_x mass flow (surpassing 150%) within the exhaust pipe as the transition occurs from the unloaded to the loaded state. This data serves as the foundation for extrapolating to the theoretical maximum value (TMV) through linear extrapolation.

It is important to note that every measurement process is subject to the occurrence of errors in the measurements or uncertainties in the obtained results. The proposed NO_x measurement process is no exception.

As a result, the results obtained throughout the process, at various levels (measured values, estimated values, averaged values, extrapolated values), are subject to uncertainties that depend on the measurement equipment used and the actual measurement and data processing process. These uncertainties can be determined and are reflected in Table 6-16.

Variable	Units	Instantaneous	Average	Extrapolation
NO _x concentration	ppm	±4% rel. ppm	$s(\bar{q}) \gg \pm 4\%$ rel. ppm	$s_{y,x} \gg \pm 8\%$ rel. ppm
NO _x mass flow	mg/s	±8% mg/s	$s(\bar{q}) \gg \pm 4\%$ rel. mg/s	$s_{y,x} \gg \pm 8\%$ rel. mg/s
% Engine load	%	±1%	$s(\bar{q}) \gg \pm 2\%$ rel. %	--
Engine speed	rpm	±1% rpm	$s(\bar{q}) \gg \pm 2\%$ rel. rpm	--
% EGR aperture	%	±1%	$s(\bar{q}) \gg \pm 2\%$ rel. %	--
Engine Temperature	°C	±1% °C	$s(\bar{q}) \gg \pm 2\%$ rel. °C	--

Table 6-16. Standard uncertainty for measures and type of data.

More detailed information about the uncertainties in the measurement process can be found in the Appendices Chapter, Section 11.3.

These outcomes are consistent with the underlying hypothesis upon which the proposal was built. Thus, it can be deduced from these findings that the methodology has been substantiated and validated.

Regarding the second point, upon contrasting the attained results with the projected outcomes based on Approval-Type thresholds, it becomes evident that **there is not a distinct correlation between the Euro emission level and the NO_x emission test results.**

The NO_x emission results, encompassing both unloaded and loaded conditions across all vehicles, reveal a lack of connection between the Emission Factor threshold established by the respective Euro emission level and the observed NO_x emission values for the vehicles.

Both in NO_x concentration and NO_x mass emissions flow, the relative order of vehicles from values obtained in the measurement process is significantly different from the expected order according to the Type Approval of the vehicles (see Figure 6-28), as can be checked in Section 6.5.

Hence, this section underscores that the emission values are not consistently the lowest in Euro 6 vehicles. In certain instances, Euro 6 vehicles exhibit higher emissions, while at times, it is the Euro 4 vehicles that demonstrate the lowest levels of emissions.

With the exception of the Euro 6 gasoline vehicle consistently displaying the lowest emissions, the remaining vehicles exhibit significant heterogeneity in their emission levels. A discernible pattern correlating with the respective Euro level is notably absent among these vehicles.

This outcome was anticipated as a result of the test. It is evident from the scientific literature that actual NO_x emissions from vehicles often diverge from the levels prescribed by their corresponding Approval-Type standards. This very situation, as highlighted in the introduction, is one of the contributing factors that has led to the prevailing issue concerning NO_x emissions.

As a result, given that the measurement outcomes align with the anticipated patterns, substantiated by extensive scientific literature, it is plausible to infer that the results indeed represent the authentic emissions of the vehicles. Consequently, the test holds reliability in facilitating a comparative assessment of emission levels among different vehicles. Thus, the culmination of these findings supports the conclusion that the methodology has been validated.

6.6. CONCLUSIONS

This Chapter has presented the results obtained from applying the measurement method to the set of 23 vehicles proposed, which is considered representative of the Spanish (and EU) vehicle fleet.

Variations of "% engine load" and NO_x emissions (both in terms of concentration and mass flow) from the unloaded state to the loaded state are as expected. Additionally, TMV values align with the anticipated data.

Furthermore, the relationship between the two variables (NO_x concentration in exhaust and "% engine load") is also justified in terms of both quality and significance, as indicated by the obtained values of R² and p-value. This aspect can also be regarded as a validation of the method.

The reproducibility of the test has also been demonstrated to be appropriate for the intended purpose, as evidenced by the SD and CV values obtained from the over 250 measurements conducted on the vehicle set.

These results align with the expected outcomes based on the working hypothesis established during the design of the measurement method, thus serving as a validation of the method.

Furthermore, the behavior of the obtained results compared to theoretical emissions from Approval-Type homologation, aligns with expectations as per the available scientific literature.

Consequently, the main conclusion of this Chapter is that the results corroborate the anticipated outcomes based on the initial working hypothesis, thereby validating the feasibility and utility of the measurement method.

In the following Chapter, the representativeness of the results obtained through NO_x measurement in PTI will be examined. To achieve this, measurements have been conducted to ascertain the actual on-road emissions of several vehicles and to compare them with the results obtained from measuring NO_x emissions during PTI.

CHAPTER 7

URBAN ON-ROAD MEASUREMENTS

7. URBAN ON-ROAD MEASUREMENTS

7.1. INTRODUCTION

Once the significance, accuracy, reliability, and reproducibility of the proposal for NO_x measurement have been checked, the next step has to be to compare the results from the idling NO_x measurement test to real urban circulation NO_x emissions. This comparison aims to assess representativeness, determining whether there exists any correlation between the measurement test results and real-world emissions.

A notable aspect of measuring NO_x during idling is that it offers genuine insights into the NO_x emissions of vehicles amidst urban traffic. This assessment provides emission data while the vehicle is stationary yet the engine is operational, mirroring scenarios encountered during city driving, and this situation can apply for a significant portion of travel time in cases of traffic congestion [108]. In normal conditions, it is realistic to assume a stopped time in urban traffic between 24% and 34% of the time, increasing to 40%-50% of the time when traffic density increases and traffic average speed decreases [50], [140], [166].

However, going beyond the significance of this particular emission data (which is valuable in its own right), it becomes intriguing to ascertain whether the test outcomes offer insights (or can be inferred) into the broader performance of the vehicle concerning NO_x emissions within actual urban traffic conditions. This prompts the question of whether the results accurately represent the genuine NO_x emissions of vehicles in real-world urban environments.

For this objective, the equipment utilized for measuring NO_x emissions during static testing has been employed to gauge NO_x emissions while the vehicle replicates urban driving scenarios.

Given the challenges and complexities associated with conducting controlled assessments in actual city traffic, a racetrack has been employed to replicate the conditions of urban driving. This approach ensures uniform conditions for all vehicles undergoing testing, facilitating a comprehensive comparison of results while mitigating safety concerns.

A total of eight vehicles were subjected to testing under six distinct driving conditions and two different equipment load scenarios. These assessments were conducted at the International Karting Circuit located within *Motorland Aragón*. The outcomes from these evaluations were subsequently juxtaposed with results from conventional static measurement tests performed on the same set of vehicles.

Assessing whether a connection exists between emissions during idling and actual urban emissions would assist in validating the effectiveness of this approach. To achieve this, it is necessary to juxtapose the outcomes of idling tests with genuine on-road NO_x emissions, thereby determining the proximity or disparity between vehicle emissions under idling conditions and real-world conditions, and potentially identifying any correlations between the two.

To facilitate this comparison, obtaining accurate on-road NO_x emissions data for different vehicles is imperative. This data serves as a benchmark against which the results obtained from the NO_x measurement test for these identical vehicles can be evaluated.

While a substantial body of scientific literature exists on real NO_x emissions [31], [34], [192], [193], the preferred approach for comparing on-road NO_x emissions with idling NO_x measurement outcomes involves conducting direct on-road measurements of the vehicles. To ensure a meaningful and consistent comparison between these measurements, it is advisable to employ the same measuring equipment for both scenarios. This choice offers a more optimal and accurate means of evaluating the relationship between on-road and idling NO_x emissions.

Typically, in on-road assessments of real driving emissions, such as those outlined in RDE (Real Driving Emissions) regulation tests, three distinct scenarios are examined to reflect varied driving conditions: urban, rural, and motorway driving [11], [103], [104]. In a similar fashion, for the purposes of this study, on-road tests are conducted across tracks that encompass segments corresponding to these three circulation types [33]. Although the test conducted does not strictly adhere to the RDE regulations, the logical framework of distinguishing between different driving conditions can still be effectively applied.

NO_x emissions are harmful to human health, particularly in urban settings [2], [12], [18] where people face heightened exposure to pollutants. Most of the NO_x emissions originate from the traffic road [5], [128], with diesel-powered vehicles being a notable contributor [6], [7], [194]. This impact is particularly pronounced within cities, where other significant sources of NO_x emissions, such as energy generation, are typically absent. Given these considerations, while understanding real NO_x emissions across all driving conditions is crucial if a choice must be made among the three scenarios, the focus should primarily be on urban emissions, the most vital aspect to address.

Hence, the decision was made to concentrate our analysis on assessing NO_x emissions during urban driving conditions.

The main characteristics of this driving situation are a (theoretical) maximum speed of 50 km/h, and frequent stops and start due to traffic lights, traffic signs, and urban traffic congestion itself.

After the decision to assess NO_x emissions in urban driving conditions, two options emerged for conducting these measurements: performing tests in an actual urban environment or simulating an urban environment for testing purposes.

Both alternatives come with their respective advantages and disadvantages. Real urban measurements offer the advantage of faithfully replicating genuine traffic conditions, but they are limited in repeatability due to the variability of traffic situations. Additionally, safety concerns pertaining to road conditions pose a challenge. Conversely, simulated urban environment measurements address these drawbacks by enabling repeated tests under consistent conditions. Safety is better ensured within a closed circuit designed to minimize accident risks.

On the flip side, the main drawback of simulated urban environment measurements is their inability to perfectly mimic actual urban driving conditions. To mitigate this limitation, a series of tests were devised to encompass a wide array of potential urban traffic scenarios.

To facilitate a comparison between idling measurement test results and real on-road NO_x emissions, a total of eight vehicles underwent multiple rounds of testing. These assessments were conducted on a closed racetrack, featuring six distinct tests that aimed to emulate diverse urban traffic conditions. The vehicles underwent these tests under two different load conditions to capture emissions data across a comprehensive spectrum of situations.

Subsequently, data from both sources were juxtaposed to analyze the correlation between idling NO_x measurement test outcomes and real on-road NO_x emissions.

7.2. DESIGNING VALIDATION OF IDLING NO_x MEASUREMENT TEST THROUGH URBAN ON-ROAD MEASUREMENTS

7.2.1. DESCRIPTION OF VEHICLES

The chosen vehicles for the study were typical models commonly found in the European market. Among the selected vehicles, there were six equipped with diesel engines and one with a petrol engine (see Table 7-1). These vehicles spanned emission levels ranging from Euro 4 to Euro 6 standards. Moreover, the engine specifications, including power and size, fell within the typical range of the average vehicle fleet in the EU-28 region, with an average power of 98 kW and an engine size of 1580 cm³ [194].

Vehicles 1 and 2 were identical models, differing only in their Exhaust Gas Recirculation (EGR) system operating conditions. The first vehicle had its EGR disconnected, while the second had its EGR functioning properly. The remaining vehicles were in prime condition, devoid of any mechanical or electrical issues.

VEHICLE No.	CAR MANUFACTURER	MODEL	EMISSIONS LEVEL	ENGINE SIZE [cm ³]	POWER [kW]	ENGINE MODEL
1	VOLVO	V50	EURO 4	1997	100	D4204T(*)
2	VOLVO	V50	EURO 4	1997	100	D4204T
3	NISSAN	JUKE	EURO 5	1461	81	K9K
4	VW	TOURAN	EURO 5	1968	103	CFH
5	OPEL	ASTRA	EURO 5	1686	81	A17DTS
6	CITROËN	C4	EURO 6	1560	88	BH01
7	KIA	SPORTAGE	EURO 6	1685	85	D4FD
8	RENAULT	FLUENCE	EURO 6	1598	84	H4M D7

(*) EGR not operative

Table 7-1. Vehicles selected for on-road urban circulation test.



Figure 7-1. Vehicles No. 1-2 (right), No. 6 (middle), and No. 7 (left) on the first test day.



Figure 7-2. Vehicles No. 5 (right), No. 3 (middle right), No. 4 (middle left), and No. 8 (left)

These specific vehicles were part of the larger collection of 23 vehicles utilized in establishing the methodology (as detailed in Chapter 5). This approach ensured the availability of an extensive array of measurements conducted through the static NO_x measurement method for each of these vehicles.

7.2.2. DESCRIPTION OF CIRCUIT AND TEST CONDITIONS

The tests were carried out in the International Karting Circuit of Motorland Aragón placed in Alcañiz (Aragón, Spain). It is a racetrack with Level A homologation by CIK-FIA for international events. The short variant was used, with its main characteristics outlined in Table 7-2. The design of this variant is visually depicted in Figure 7-3.

The technical prerequisites to simulate urban circulation conditions and to conduct multiple tests under optimum conditions of safety and reproducibility are perfect in this infrastructure. This facility, originally intended for competitive events and safety driving instruction, provides an ideal environment for these purposes.

CIRCUIT CHARACTERISTICS	
LENGTH (<i>d</i>)	1600 m
WIDTH	10 m
ALTITUDE	371 m
AVG. SLOPE	2.9 %

Table 7-2. Characteristics of the test racetrack

The decision to opt for the Karting Circuit over the Road Racing Circuit was based on specific advantages for simulating urban traffic scenarios. The Karting Circuit's shorter length proves more suitable for emulating urban circulation compared to the larger speed-oriented racetrack, where longer straight sections are present (notably, a 1726 km straight section in the Road Racing Circuit). Urban traffic is typically characterized by short distances, frequent speed fluctuations, as well as frequent stops and starts due to traffic and signals. Moreover, it commonly involves speeds below 50 km/h.

The layout of the Karting Circuit naturally facilitates the maintenance of speeds below 50 km/h, while the multitude of curves introduces consistent variations in vehicle speed and acceleration. These elements collectively contribute to a more faithful simulation of urban driving conditions, enhancing the accuracy of the tests conducted.

Moreover, the variations of slope along with the track guarantee power demand when the road is uphill, and undemanding areas when it is downhill, so that both situations are balanced, thus simulating an average real traffic situation.

Even the altitude of the circuit was considered as an ideal option to get representative data, balanced between sea level situation and high-altitude cities. There are cities at sea level along the coast and cities with altitudes exceeding 1100 meters in the mountainous regions.



Figure 7-3. Racetrack short variant (grey) design.

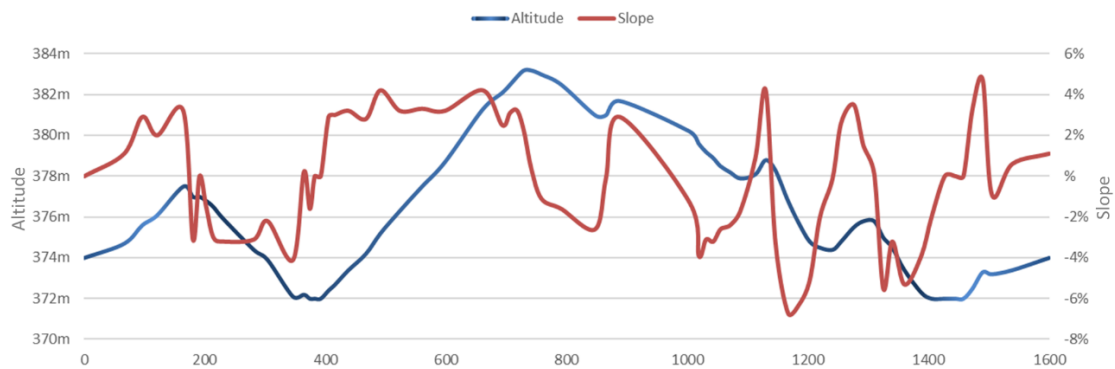


Figure 7-4. Altitude and slope of the racetrack.

The testing procedures spanned two consecutive days, during which the environmental conditions were deemed favorable. Notably, the atmospheric pressure on the first day was lower compared to the second day during the test duration, albeit displaying a greater degree of uniformity. Temperature fluctuations were observed as well, with the first day ranging between 21°C and 29°C, and the second day experiencing temperatures between 19°C and 30°C.

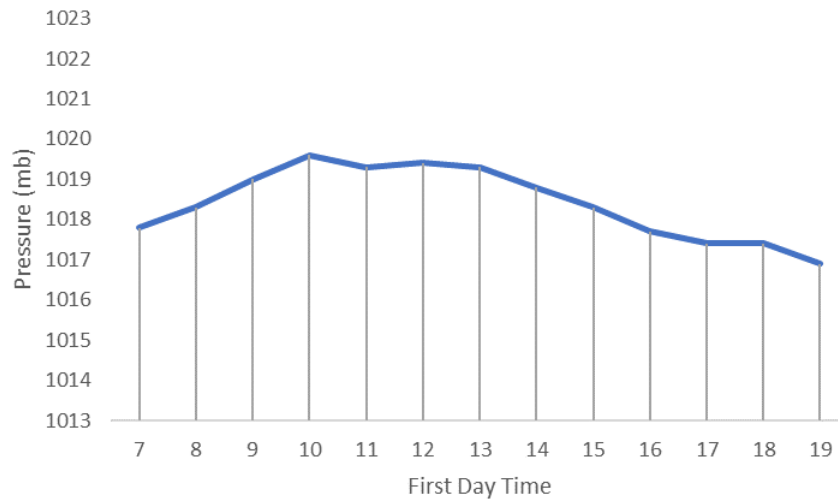


Figure 7-5. Pressure first test day.

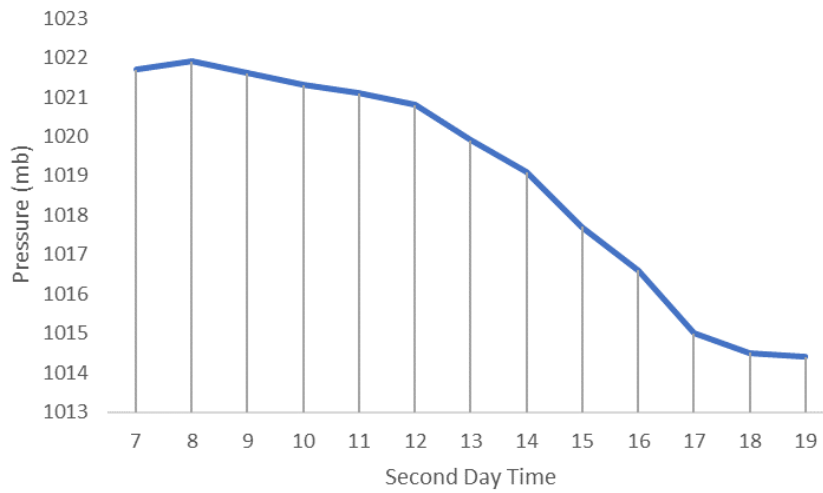


Figure 7-6. Pressure second test day.

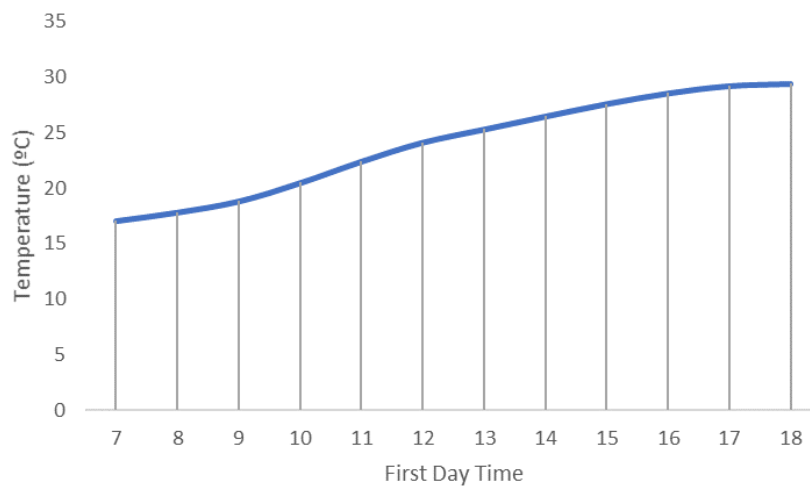


Figure 7-7. Temperature first test day.

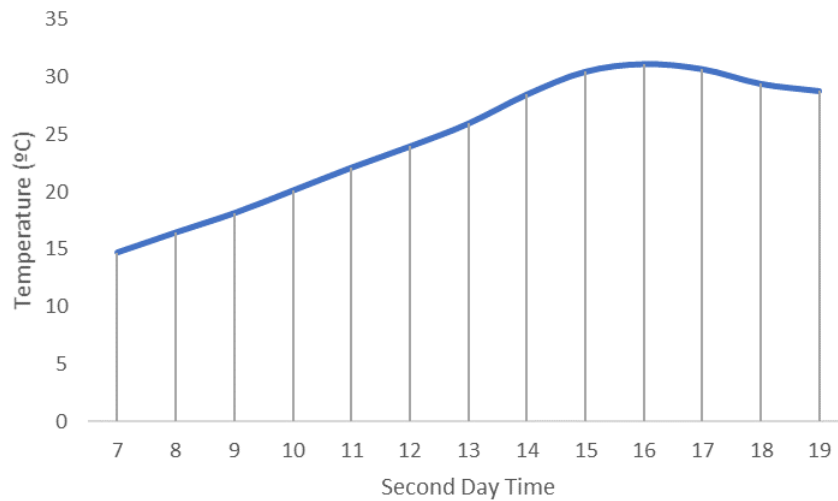


Figure 7-8. Temperature second test day.

7.2.3. DESCRIPTION OF EQUIPMENT FOR THE ON-ROAD TEST

For a better comparison of results from both tests, the equipment used to read NO_x emissions and OBD data in the on-road test was the same used to carry out the static idling NO_x measurement test.

Technical characteristics of the equipment were described in Chapter 5. Specific software, described in the Appendices (section 11.1), was used to register from the gas analyzer and the OBD system the same relevant data as for the NO_x idling test.

Every day, previously to the tests, the equipment was calibrated with the same certified standard gas cylinder (see appendix), to guarantee corrections of measurements. After every test day, the equipment was calibrated again to check the degradation of the reading signal. On the first day of the tests, the calibration results at the end of the day were 2100 ppm, and on the second day of the tests, the calibration results at the end of the day were 2030 ppm. That means degradation of 4.8% and 1.3% respectively according to the calibration reference value (2003 ppm).

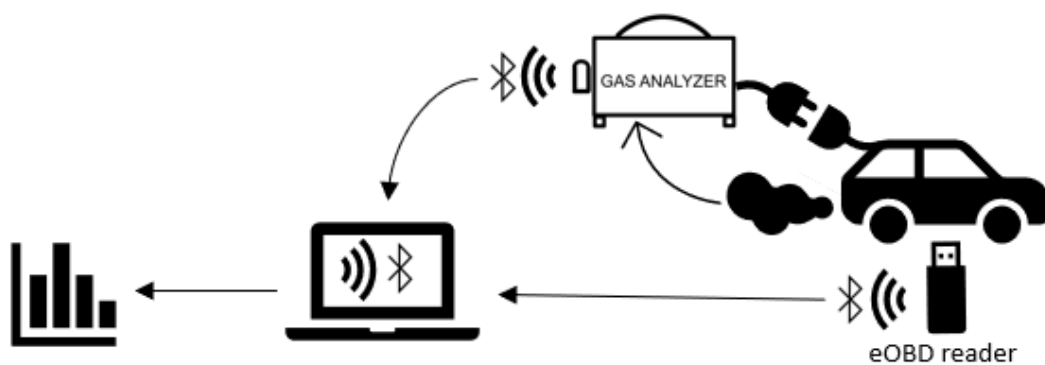


Figure 7-9. Scheme of equipment connected to the vehicle for the on-road test.

The measurement equipment is composed of the Gas Analyzer described in Chapter 5, accompanied by a blowpipe that is affixed to it. This blowpipe is carefully inserted into the vehicle's exhaust pipe, secured in place to prevent unintended detachment, and serves the purpose of transporting gases to the analyzer (see Figure 7-10). A computer is employed in conjunction with the setup, executing the software developed by the analyzer's manufacturer. Additionally, the equipment concurrently carries out the reading of engine operating parameters through the On-Board Diagnostics (OBD) connector of the vehicle, further enhancing the scope of data acquisition.

The OBD reader and the Gas Analyzer are connected by Bluetooth® technology to the Gas Analyzer computer (Figure 7-9). This connection enables the recording of various operational parameters of the vehicle, including metrics such as "% engine load", engine speed, vehicle speed, % EGR aperture (if available), and engine temperature.



Figure 7-10. Measurement equipment installed into the trunk of vehicle No. 1.

The gas analyzer is onboard into the trunk of the vehicle, and the electrical supply is from the vehicle through a 12V-220V AC converter. This supply increases the load demand but is a constant demand over time, and equal for every vehicle.

7.2.4. DESCRIPTION OF THE TESTS

A total of six distinct tests were conducted for each vehicle, with the details outlined in Table 7-3. Each of these tests was repeated twice: the initial instance involved conducting the test without any additional equipment connected, while the second iteration involved connecting both the A/C (air conditioning) system and the lighting system. This setup was employed to elevate the engine's load demand. As a result, this approach facilitated the analysis of two distinct load demand scenarios or situations for each test.

The test design seeks to reproduce specific conditions in urban circulation and to cover, with the whole set of tests, most of the situations that a vehicle can find in normal urban traffic.

Each test begins and ends with the vehicle standing on the finish line and is developed according to the indications in Table 7-3.

During each test, two persons were present inside the vehicle. The first person assumed the role of the driver, responsible for operating the vehicle, while the second supervised the proper execution of the test and diligently recorded the pertinent data.

The tests were carried out sequentially, from the 1st to the 6th test without any equipment connected. Subsequently, the same sequence of tests was repeated, from the 1st to the 6th, this time with the equipment connected. The entire set of tests for each vehicle lasted approximately one hour.

Prior to commencing the test sequence, an examination of the engine temperature and the mechanical condition of the vehicles was conducted to ensure that each vehicle was in an optimal state for testing. Additionally, a minimum break of at least 2 minutes was observed between each of the tests to ensure the stability of all vehicle systems at the beginning of each test.

Test #1 replicates a typical urban traffic scenario characterized by continuous movement without coming to a complete stop. The procedure involves gradually accelerating the vehicle's speed up to 50 km/h through gear shifts spanning from 1st to 3rd gear. Once the desired speed of 50 km/h is attained, it is maintained throughout the duration of the test. The specific gear engaged for each section of the test is systematically defined to ensure uniformity across all vehicles and tests, thereby guaranteeing consistent and comparable results (see Figure 7-11).

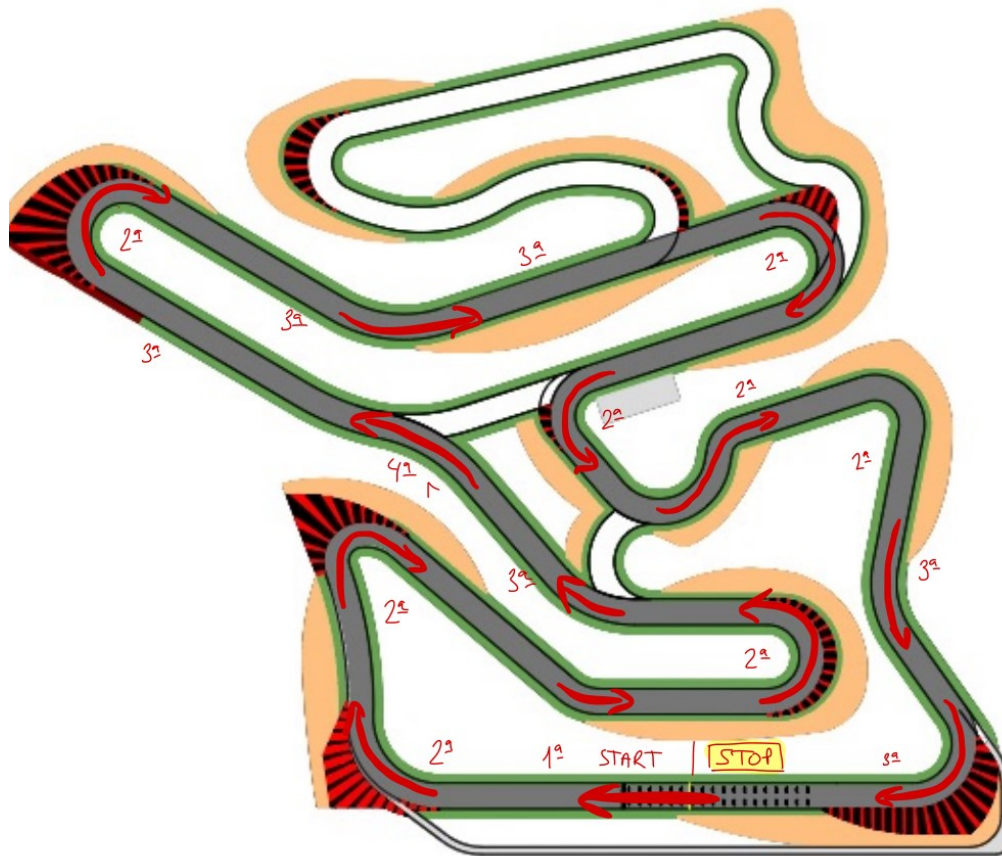


Figure 7-11. Gear shifting distribution in Test#1.

Test #2 emulates a standard urban driving scenario similar to Test #1, with the inclusion of predetermined and fixed stops. These stops are designed to replicate the halts commonly encountered in urban traffic, followed by the subsequent acceleration upon resuming movement. Crucially, these stops occur at specified, predefined locations, ensuring that all vehicles cover the identical distance between each stop and execute these maneuvers at consistent speeds. This meticulous approach guarantees uniformity in testing conditions across all vehicles, enabling meaningful comparisons of results (see Figure 7-12).

Test #3 closely resembles Test #1 in terms of continuous motion without any interruptions on the track. The vehicle's speed is carefully sustained at 50 km/h, mirroring urban traffic conditions. However, a distinctive feature of Test #3 is that once the vehicle attains a speed of 50 km/h and achieves the third gear, this gear position remains constant throughout the duration of the test. There are no subsequent gear changes made, and the vehicle maintains a consistent speed without further adjustments until the conclusion of the run.

Test #4 and #5 are similar to Test #3, with the only difference of the gear selected, the 4th gear for test #4, and the 5th gear for test #5.

Finally, Test #6 is similar to Test #5, the only difference the vehicle speed must be the maximum possible speed (higher than 50 km/h).

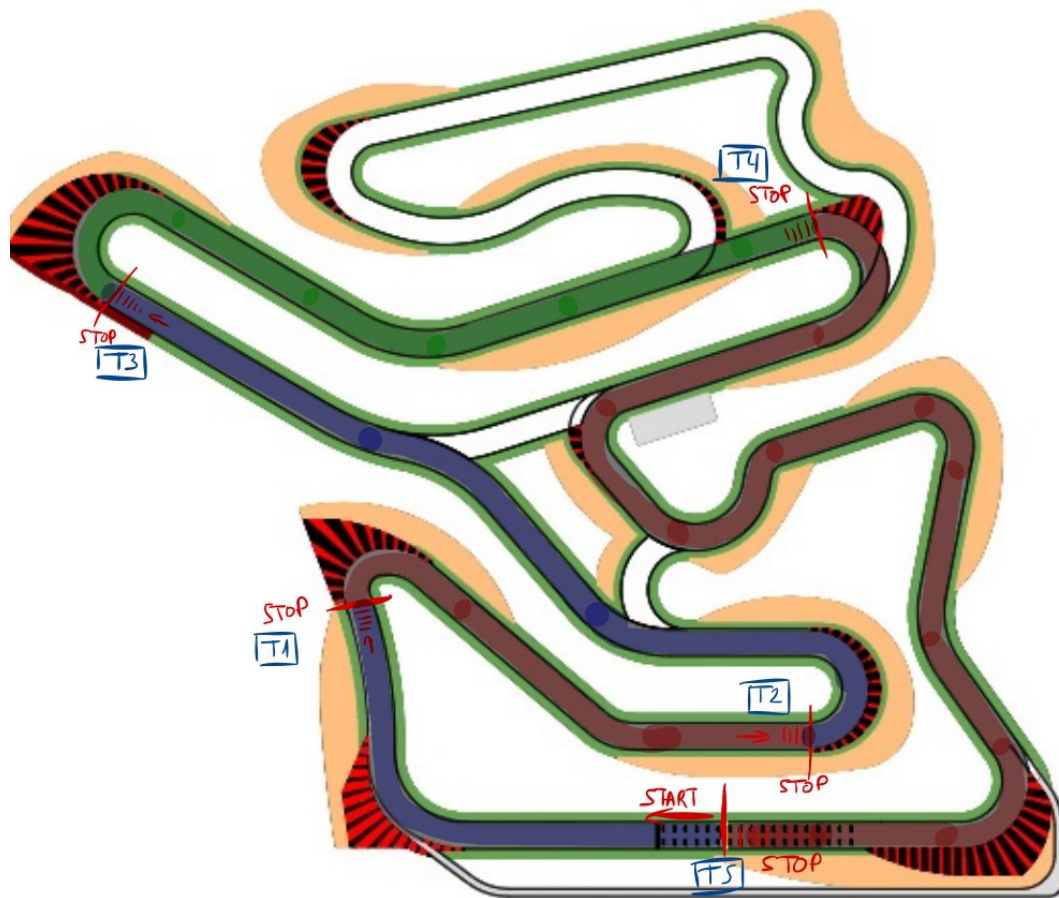


Figure 7-12. Stops distribution in Test#2.

This set of tests covers most of the situations a vehicle can find in urban circulation, from frequent start-stop situations to driving at 50 km/h with the 5th gear engaged.

Concurrently with the execution of each test, data is recorded at a frequency of 1 Hz. This includes the measurement of NO_x concentration at the exhaust pipe using the gas analyzer, while simultaneously capturing engine speed, "% engine load", and vehicle speed through the vehicle's On-Board Diagnostics (OBD) system.

# TEST	SPEED	GEAR ENGAGED	DESCRIPTION
1	50 km/h	1/2/3	Start from a standstill, until reaching 50 km/h, maintaining this speed until the circuit is completed. The gear engaged according to the definition of the test (see Figure 7-11).
2	0-50 km/h	1/2/3	Start from a standstill, trying to reach 50 km/h, stopping the vehicle at the end of the sections defined in the test. Stop the vehicle by reducing gears. The gear engaged as defined in the test (see Figure 7-12).
3	50 km/h	3	Start from a standstill, until reaching 50 km/h circulating in 3rd gear, maintaining this speed and gear until the circuit is completed.
4	50 km/h	4	Start from a standstill, until reaching 50 km/h circulating in 4th gear, maintaining this speed and gear until the circuit is completed.
5	50 km/h	5	Start from a standstill, until reaching 50 km/h circulating in 5th gear, maintaining this speed and gear until the circuit is completed.
6	>50 km/h	5	Start from a standstill, until reaching the highest possible speed greater than 50 km/h circulating in 5th gear, maintaining the maximum possible speed and 5th gear until the circuit is completed.

Table 7-3. Summary of On-Road tests characteristics.

7.3. ASSESSMENT OF RESULTS FROM ON-ROAD TESTS

As was explained previously, from the NO_x concentration in ppm measured with the gas analyzer, it is possible to calculate the value of NO_x emission mass flow (g/s).

$$x_i = \text{NO}_x \text{ concentration (ppm)} \quad \rightarrow \quad \dot{m}_i = \text{NO}_x \text{ emission mass flow (g/s)}$$

Once the instantaneous NO_x concentration and the NO_x mass emission per second of the vehicle along with the test are known, the NO_x Total Mass Emission, M_{Total} (g), can be calculated (Equation 7-1) for the whole test, that is, for each complete lap of the circuit when performing each of the tests.

Equation 7-1

$$M_{Total} = \sum_{i=0}^t \dot{m}_i \quad (g \text{ NO}_x)$$

Finally, the NO_x Emission Factor (EF_{NO_x}) in g/km can be calculated (Equation 7-2) for every test and vehicle, through the value "d" of the racetrack length in kilometers (1.6 km, Table 7-2). In this way, it is possible to compare results from the test to the Emission Factor threshold of the corresponding Euro emission level (see Table 1-4) of every vehicle.

Equation 7-2

$$EF_{NO_x} = \frac{M_{Total}}{d} \quad (g/km)$$

In the first analysis, for every test and load condition, the NO_x Emission Factor EF_{NO_x} is calculated and compared to the corresponding NO_x emission threshold that applies to each vehicle depending on its emission level.

The quantity of NO_x emissions varies for each vehicle across different tests, and even within the same vehicle, these emissions fluctuate based on the load demand, which is influenced by whether additional equipment is connected or disconnected.

	EF_{NO_x} [g/km]	
	DIESEL	PETROL
Euro 4	0.25	0.08
Euro 5	0.18	0.06
Euro 6	0.08	0.06

Table 7-4. NO_x emission Factor thresholds for M1 passenger cars.

Beyond evaluating NO_x emissions, the analysis also encompassed the calculation of average values for "% engine load," shedding light on its performance. The idling NO_x measurement method relies on establishing a connection between NO_x concentration and "% engine load" during idle conditions, a relationship that was verified under controlled circumstances. However, exploring the link between NO_x emissions and "% engine load" in actual on-road circulation is of particular interest.

In real-world scenarios, an array of variables, extending beyond engine load, exert influence over NO_x emissions. Therefore, investigating this relationship within the context of various factors is crucial for a comprehensive understanding.

Findings obtained from measurements conducted on-road were examined and juxtaposed with the EF_{NO_x} value relevant to the Euro emission standard of the vehicles. Using concentration values obtained during the testing process, the mass flow of NO_x emissions (measured in g/s) was estimated, ultimately leading to the determination of EF_{NO_x} (Equation 7-2) for each individual vehicle and test scenario.

The graphs presented in Figure 7-13 through Figure 7-20 illustrate the outcomes of the six distinct on-road tests conducted for each vehicle. The **light gray bar shows the unloaded EF_{NO_x}** (without any equipment connected) calculated from the test, and **the dark gray bar shows the loaded EF_{NO_x}** (with the Air Conditioning system and lightning system connected). The **continuous black line is the average "% engine load" for the unloaded test**, and the **dashed black line is the average "% engine load" for the loaded test**. Finally, the **red line shows the homologation EF_{NO_x} threshold value** (according to Table 7-4). On the left vertical axis, the EF_{NO_x} value in g/km is indicated, while the right vertical axis represents the "% engine load" value. The horizontal axis displays each of the six conducted tests. The various tests are defined in Table 7-3.

In an initial observation, it becomes evident that the pattern of "% engine load" behavior is consistent across all vehicles, despite variations in the actual values. Specifically, the "% engine load" during the first three tests displays a noteworthy resemblance between each test, with values notably lower than those observed during tests #4, #5, and #6.

An additional noteworthy observation is that a significant majority of the calculated EF_{NO_x} values surpass the emission level threshold for each vehicle, often exceeding it by a substantial margin. Intriguingly, this elevation of emissions above the threshold is comparatively more subdued for the Euro 4 vehicles, despite their threshold being set at a higher level, as opposed to the Euro 5 and Euro 6 vehicles.

7.3.1. ASSESSMENT OF VEHICLE EMISSIONS IN THE SET OF TESTS

In the first place, emissions from vehicles No. 1 (Figure 7-13) and No. 2 (Figure 7-14) are analyzed. This pertains to the same vehicle; however, there is a variation in the operational state of the EGR system.

While Vehicle No. 1 lacks a functioning EGR system, Vehicle No. 2 possesses a fully operational EGR system. The vehicle in question is classified as Euro 4, with the NO_x emission level threshold specified in Table 7-4.

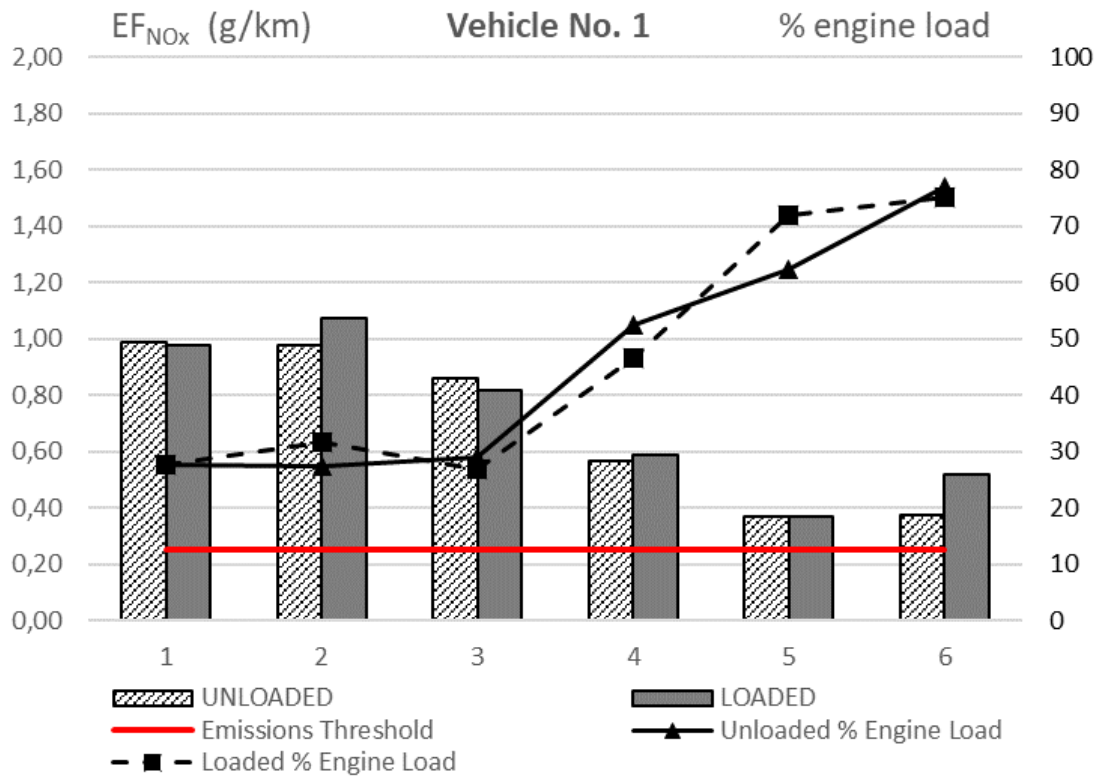


Figure 7-13. Vehicle No. 1 on-road test results.

As evident, the average “% engine load” values for every test in both vehicles are quite similar. There is not a significant difference between the unloaded and the loaded state, as far as the behavior of the engine load is concerned. Tests #1 to #3 show a similar average “% engine load” of around 30%, and test #4 to #6 shows a growth very similar in both cases until they reach more than 70% average engine load in test # 6.

The “% engine load” is quite similar in both vehicles, but the EF_{NOx} case is different because although the engine load behavior is similar, the values show important differences. For the tests from #1 to #3, the EF_{NOx} was greater for vehicle No. 1. For tests #1 and #2, the increase is about 20% and even higher for test #3, with an increase greater than 100% for loaded tests. This is supposed to be a consequence of the EGR disconnected situation, which makes NO_x emissions higher in the range of engines used in urban conditions in vehicle No. 1.

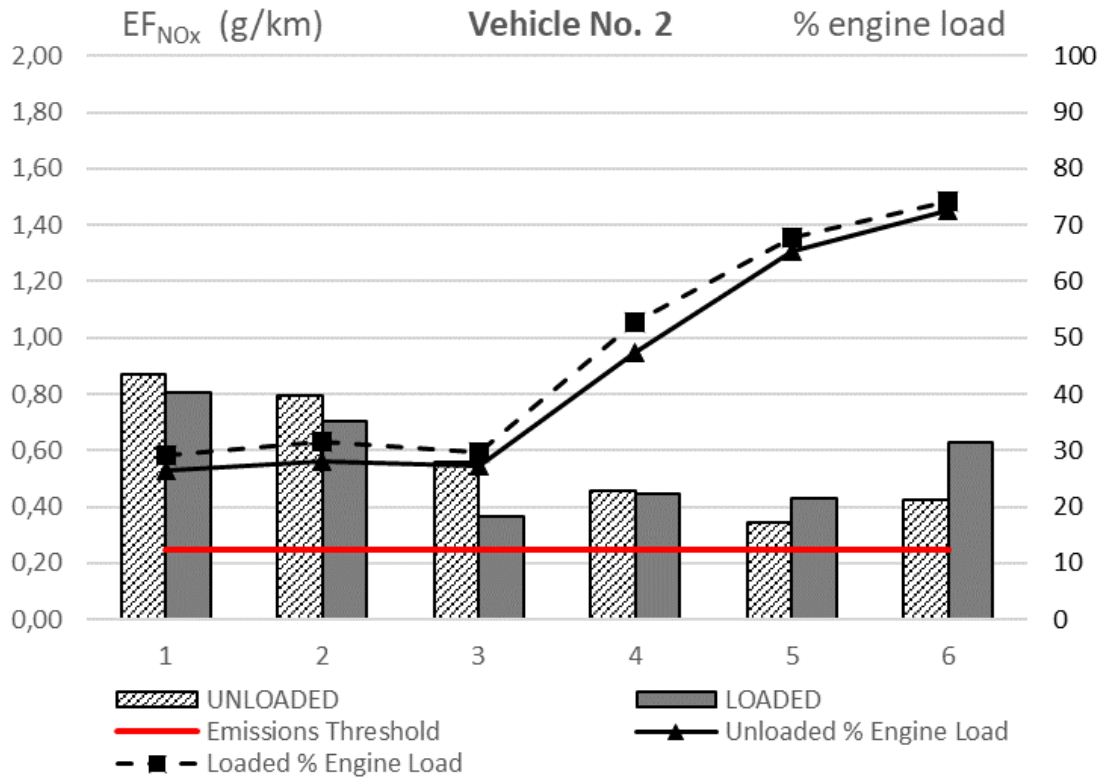


Figure 7-14. Vehicle No. 2 on-road test results.

It can also be observed in Figure 7-14 that the EF_{NO_x} is lower for loaded tests in vehicle No. 2, despite the higher "% engine load" values. Conversely, for vehicle No. 1, EF_{NO_x} is directly correlated with the "% engine load" value (as shown in Figure 7-13): higher "% engine load" values result in higher EF_{NO_x} levels.

In vehicle No. 1 the EGR is inactive, so it can't reduce the NO_x emissions, while in vehicle No. 2 the EGR is working, reducing the NO_x emissions although the "% engine load" was higher.

This situation is a validation of the utility of the EGR system in urban circulation, with an important reduction of NO_x emissions.

Instead, for tests #4 to #6, EF_{NO_x} values are close for both vehicles and in some cases, the emissions from vehicle No. 2 are higher. An interesting point to analyze is that NO_x emissions from tests #4 to #6 are lower than emissions from tests #1 to #3, even for vehicle No. 1 with the disconnected EGR, so this situation is not caused by the EGR action. That means that, for this vehicle, in real driving not only "% engine load", % EGR, or vehicle speed are variables involved in the NO_x emissions. As was previously said, a high number of variables can affect the vehicle's NO_x emissions in real driving. Opting for the idling state is a preferable approach to reduce the number of variables involved and simplify NO_x measurements.

Especially for tests #5 and #6, the engine's operating conditions are not at their optimum point (the engine speed is too low relative to the vehicle speed, due to the

gear ratio). This could explain the lower NO_x emissions instead of the expected higher "% engine load," assuming the same behavior was exhibited by other vehicles. However, for the remaining diesel vehicles, the EF_{NO_x} values for tests #4 to #6 are similar or higher than those for the preceding three tests. Consequently, we must conclude that there are additional variables influencing the NO_x emissions of this particular vehicle (possibly related to the ECU's mapping).

Summarizing, from the Figures of the set of tests carried out over vehicles No. 1 and No. 2, it can be observed that the behavior of emission factors and "% engine load" are similar in both cases, with a **variation of absolute values of EF_{NO_x} that can be explained by the operating situation of the EGR valve in every vehicle.**

Vehicles No. 3 (Figure 7-15), No. 4 (Figure 7-16), and No. 5 (Figure 7-17) are Euro 5 vehicles, so their EF_{NO_x} threshold from homologation is lower than vehicles No. 1 and No. 2, according to Table 7-4.

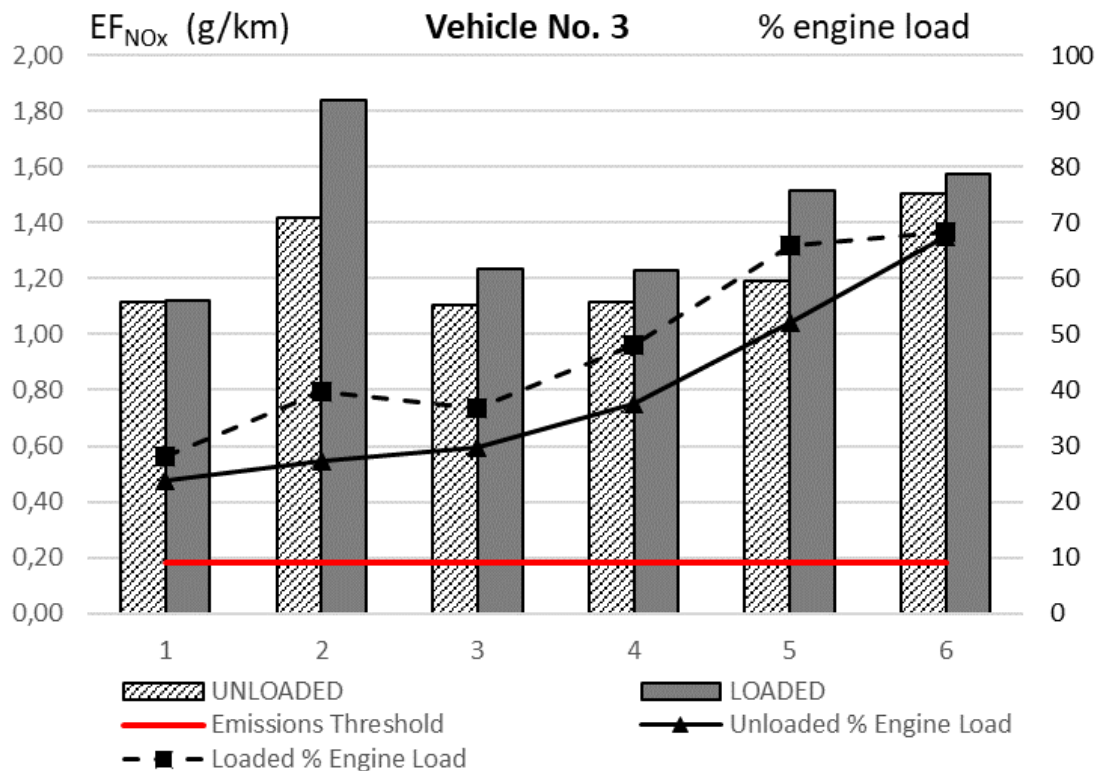


Figure 7-15. Vehicle No. 3 on-road test results.

In these three vehicles, the average "% engine load" behaves in a manner comparable to what was observed in the earlier vehicles. Tests #1 through #3 exhibit lower and comparable "% engine load" values ranging from 20% to 40%, with a slight uptick in engine load observed in test #2 under loaded conditions for each vehicle. The final three tests (from test #4 to test #6) display a progressive rise in "% engine load" from the value of test #3, culminating in its highest value in test #6.

In a more pronounced manner compared to the preceding vehicles, the EF_{NO_x} for these particular vehicles exceeds the homologation threshold by several multiples. Interestingly, in most instances, the EF_{NO_x} under loaded conditions surpasses that observed under unloaded conditions.

In these three vehicles, the emission factors from test #2 (and the engine load for the loaded tests) were greater than emission factors from tests #1 and #3 for both states (probably by the stop-start conditions of circulation in this test) unloaded and loaded. Regarding vehicles No. 3 and No. 5, the emissions observed during loaded test #2 were notably higher in comparison to the unloaded test. In the case of vehicle No. 4 during test #1 under loaded conditions, despite having the lowest EF_{NO_x} among these three vehicles, the emission factor value was threefold higher than the Euro 5 threshold. Instead, the highest EF_{NO_x} was reached during test #2 for vehicle No. 5, where the value of EF_{NO_x} in the loaded test exceeded the Euro 5 threshold by over tenfold.

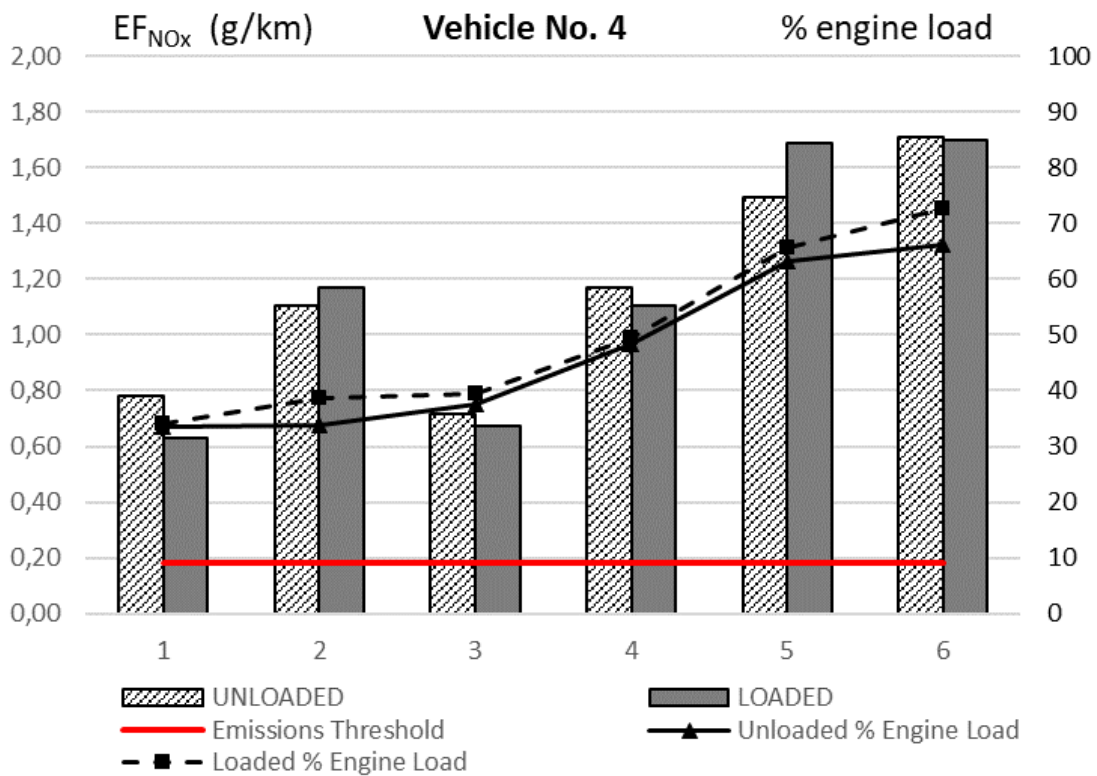


Figure 7-16. Vehicle No. 4 on-road test results.

Emission factors and average "% engine load" increase from test #4 to test #6 from the value of both variables in test #3. For the "% engine load", it increases similarly to vehicles No. 1 and No. 2, albeit with a less pronounced increase. For the emission factors, the behavior is different from Vehicle No.1 and No. 2, because in this case emission factors increase, from the value of test #3 to maximum values around 1.7 g/km. Emission factors for test #4 are higher (vehicle No. 4), similar (vehicle No. 3), or even slightly lower (vehicle No. 5) than for test #3. In these three vehicles, and for the

three last tests, is observed an increase in the value of the "% engine load" and an increase in the value of the emission factor.

Even though there are variations in emission levels and "% engine load" values, it can be concluded that the behavior of the three Euro 5 vehicles is consistent among them. The differences primarily lie in the specific emissions and achieved load values.

Finally, Euro 6 vehicles have the lowest Emission Factor threshold, specifically 0,08 g/km for diesel engine vehicles, and 0.06 g/km for petrol engine vehicles (see Table 7-4).

In this case, the behavior of the two diesel Euro 6 vehicles, vehicle No. 6 (Figure 7-18) and vehicle No. 7 (Figure 7-19) is different between them.

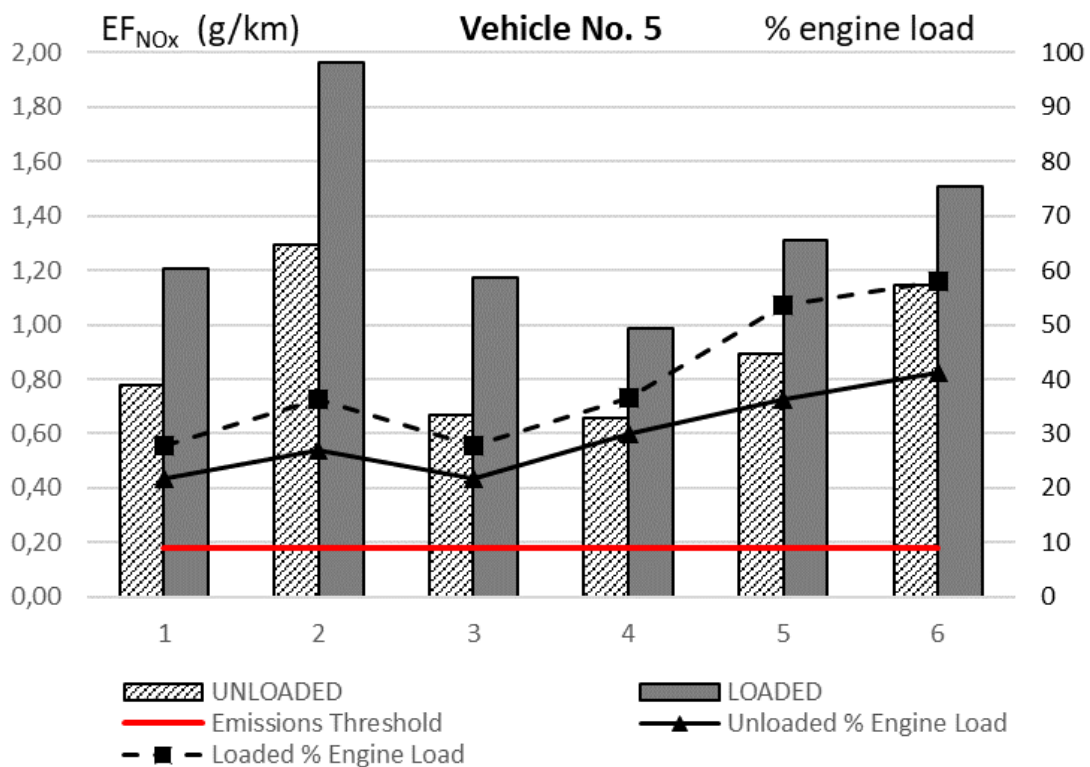


Figure 7-17. Vehicle No. 5 on-road test results.

While the engine load patterns exhibit similarity in both vehicles, featuring higher engine load values in tests #4 to #6 compared to the initial three tests, it is noteworthy that in vehicle No. 7, the engine load value during the loaded situation in test #4 is slightly lower than that of test #3. Despite this general increase in load values, the behavior of NO_x emissions diverges significantly.

In the case of vehicle No. 6, the outcomes of the initial three tests for both unloaded and loaded conditions mirror the observations made for vehicles No. 3, 4, and 5: the emission factor in test #2 is notably greater than that of tests #1 and #3.

On the other hand, for vehicle No. 7 the EF_{NOx} from the first three tests shows decreasing values for the unloaded situation and similar values for the loaded situation.

In both cases, however, the emission factor values obtained are higher than the Emission Factor limit defined by the Euro 6 level (0.08 mg/km). Indeed, the smallest recorded value is 3.6 times higher than the threshold set in the emission standards. Moreover, the remaining scenarios surpass this limit even more significantly, with the loaded situation of test #2 for vehicle No. 6 exceeding it by a substantial 13 times.

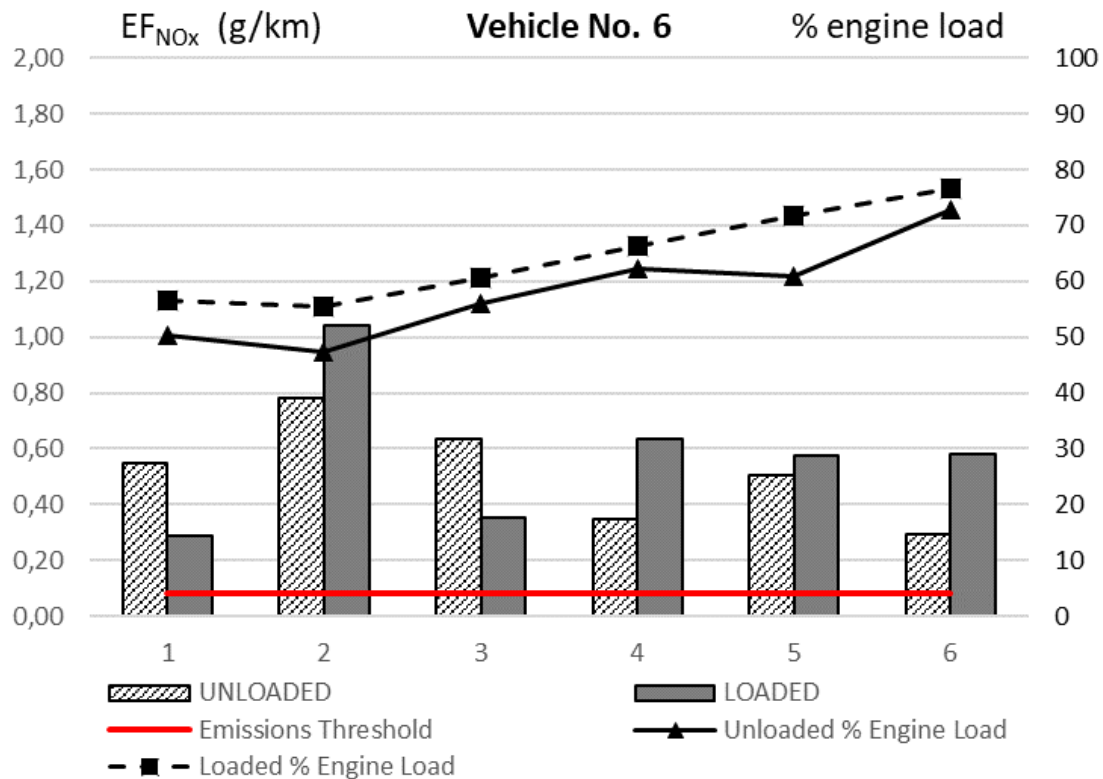


Figure 7-18. Vehicle No. 6 on-road test results.

The emissions behavior in tests #4, #5, and #6 also show different behavior between both vehicles. Vehicle No. 6 presents lower emission values than those recorded in the initial tests for the unloaded situation, while for the loaded situation similar emissions are observed for all three tests, with values higher than those recorded for test #3 but lower than those of test #2 (and in all cases higher than the unloaded situation).

Conversely, in vehicle No. 7, a distinct trend emerges where emissions during tests #4, #5, and #6 notably surpass those observed in the initial tests. Notably, in test #4, emissions for the loaded scenario are comparatively lower than the unloaded counterpart (paralleling the pattern in the first three tests). However, during the last two tests, emissions were indeed higher in the loaded condition.

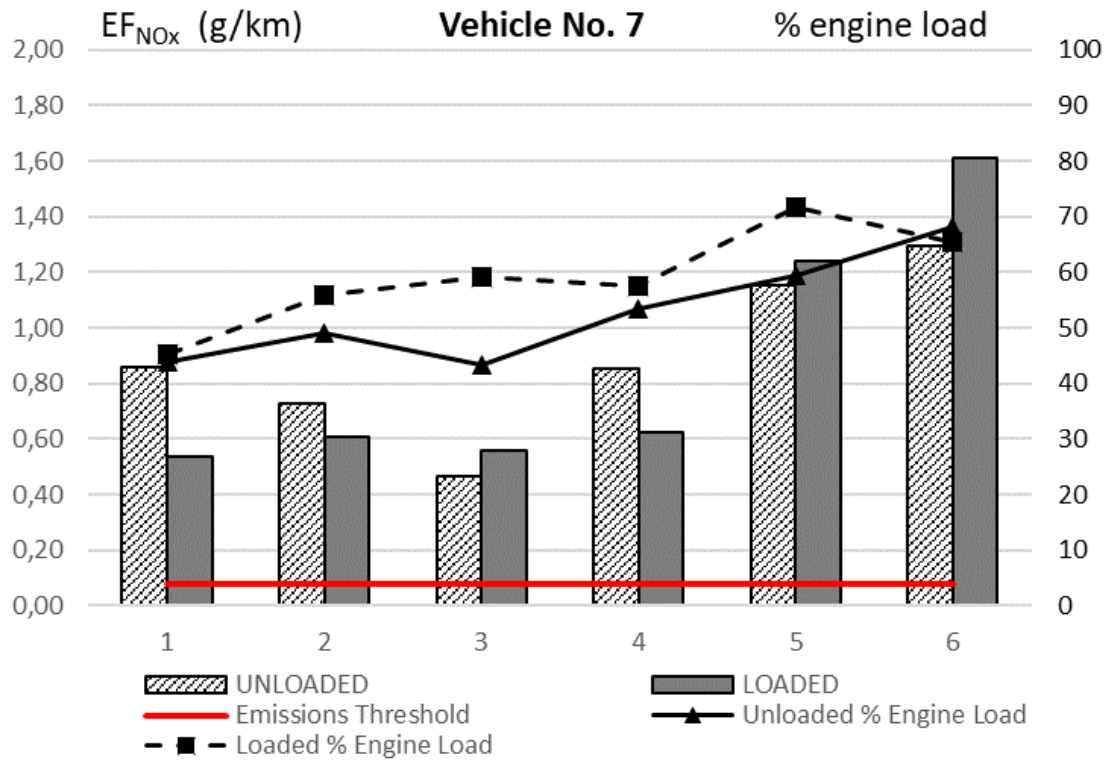


Figure 7-19. Vehicle No. 7 on-road test results.

In contrast to the consistent emission patterns observed in the Euro 5 vehicles across various tests, it is apparent that the two Euro 6 vehicles display unique emission characteristics in each test, along with markedly different emission behaviors across the tests. Nonetheless, it is important to highlight that the "% engine load" behavior remains comparable in both Euro 6 vehicles, encompassing both similar patterns and values.

This underscores the idea that attempting to generalize the NO_x emission behavior of a vehicle is a complex task, given the significant influence that multiple variables can exert on these emissions. The intricate interplay of these variables highlights the challenge of accurately predicting or categorizing a vehicle's NO_x emission traits.

Finally, regarding gasoline vehicle No. 8 (Figure 7-20), it has similar behavior in the "% engine load" values to the diesel vehicles. It can be seen how the "% engine load" values for the first three tests are similar for the unloaded situation (between 36% and 42%), with a significant increase in the engine load for the loaded situation in test #2 up to 51% (due to the continuous stopping and starting of the vehicle). For tests, #4, #5, and #6 the engine load values gradually increase in each test, until a maximum value of 74%.

Conversely, the Emission Factor values present a considerable contrast not only with Euro 6 diesel vehicles but also with the remaining analyzed diesel vehicles, exhibiting substantially lower values compared to those observed in these vehicle categories.

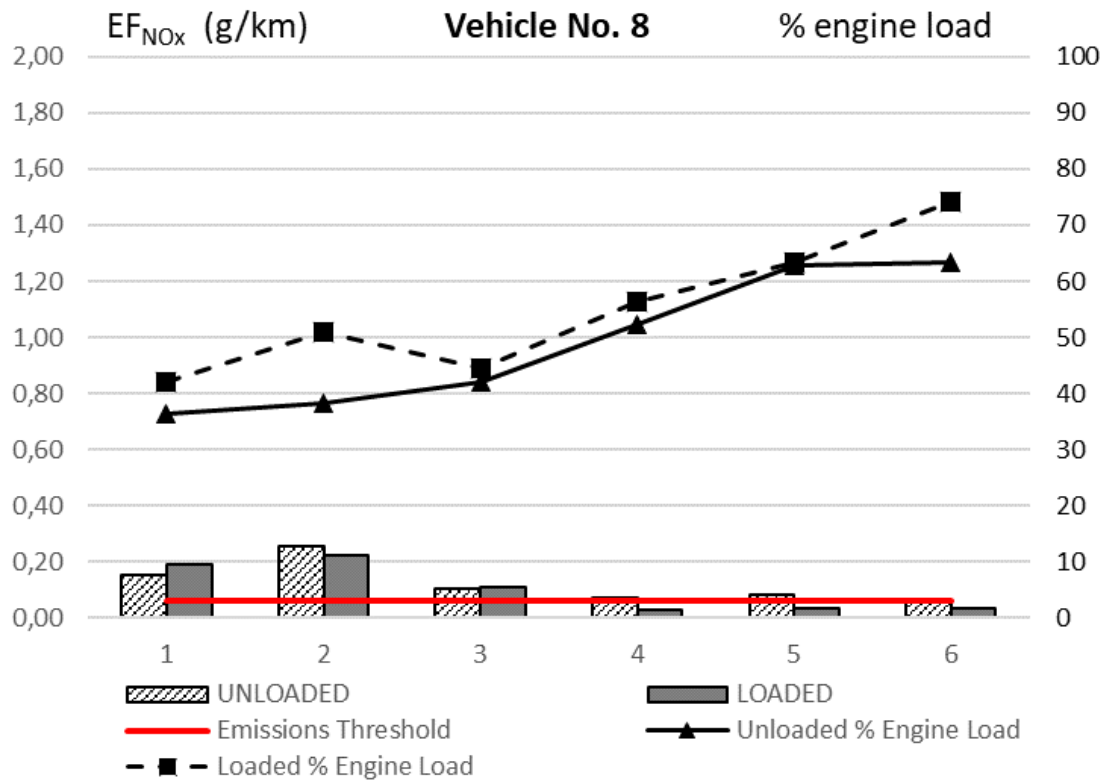


Figure 7-20. Vehicle No. 8 on-road test results.

Firstly, the emission limit according to the emission level is somewhat lower than that of diesel vehicles, being set at 0.06 mg/km for gasoline vehicles, according to the EF values (Table 7-4).

Despite surpassing the limit established by the Euro 6 standards in the initial three tests, with the highest recorded value reaching 4.6 times the set limit, this maximum value remains lower in absolute terms than the minimum value observed among any of the diesel vehicles across all test scenarios. Notably, akin to the majority of diesel vehicles, the peak emissions during the first three tests were registered in test #2.

In the final three tests, even as engine load values rise, the Emission Factors derived from emissions indicate a gradual reduction in NO_x emissions, eventually approaching and falling below the limit established by the Euro 6 standards. To sum up, the graphical representation illustrates consistently minimal emission factors for the gasoline vehicle in all instances, even surpassing the limit value. Notably, this vehicle stands out as the only one to exhibit such an exceptional outcome.

7.3.2. ASSESSMENT OF VEHICLE EMISSIONS IN TEST #1

After thoroughly examining the performance of each vehicle across the comprehensive tests, it becomes intriguing to conduct a direct comparison and analysis of the emissions measured and the engine load required among the different

vehicles in each test. This comparison aims to ascertain whether the emission levels serve as a defining factor for the emissions exhibited by the vehicles during operation.

To achieve this objective, the forthcoming graphs will juxtapose the NO_x Emission Factor against the average "% engine load" value for each vehicle across the various test scenarios. Additionally, a direct comparison will be made with the emission factor limits stipulated by the respective Euro emission levels for the vehicles participating in the tests. This comparative analysis aims to shed light on the relationship between emission factors, engine load, and the predetermined emission limits for the different vehicles under examination.

The **light gray bar shows the unloaded EF_{NO_x}** (without any equipment connected) calculated from the test, and **the dark gray bar shows the loaded EF_{NO_x}** (with the Air Conditioning system and lightning system connected). The **continuous black line is the average "% engine load" for the unloaded test**, and the **dashed black line is the average "% engine load" for the loaded test**. Finally, the **continuous colored horizontal lines show the homologation EF_{NO_x} threshold value**, according to Table 7-4, for the different emission levels (purple for the diesel euro 4, blue for the diesel euro 5, green for the diesel euro 6, and red for the petrol euro 6). The left vertical axis indicates the EF_{NO_x} value in g/km, while the right vertical axis represents the "% engine load" value. The horizontal axis displays each of the tested vehicles (as per Table 7-1). The various tests are outlined in detail in Table 7-3.

To begin, the behavior of the vehicles is examined during the execution of test #1, which involves starting from a stationary position and traversing the prescribed route while adhering to the designated gear shifts, all while maintaining a speed of 50 km/h. This test endeavors to replicate typical and optimal urban traffic scenarios, with the exception of the customary stops encountered in real traffic situations.

Figure 7-21, which compares the data obtained from all the vehicles, shows several significant circumstances.

Initially, it's noteworthy that the two Euro 4 vehicles do not exhibit the highest emission levels.

The two Euro 4 vehicles, vehicles No. 1 and No. 2 show very similar engine load values when testing, both in the unloaded and loaded situation. In other words, both vehicles have been subjected to very similar demands during the test.

It can be seen how the EF_{NO_x} of vehicle No. 1 in the unloaded and loaded situations are very similar. The engine demand in both situations has been very similar, and since the EGR does not act (it is deactivated), the emissions with the same engine demand are similar.

The emission value obtained is 3.9 times higher than the maximum limit defined in the Euro 4 emission level to which the vehicle belongs (see* Multiplier factor for average NO_x emissions exceeding the Euro level limit, Table 7-5). Considering the EF_{NO_x} limit specified by the manufacturer in the vehicle's homologation for this particular model (0.164 g/km NO_x), rather than adhering to the Euro 4 level limit, it becomes evident that the vehicle's emissions in urban traffic exceed the indicated homologation limit by a factor of 6.

In the case of vehicle No. 2, the first difference concerning vehicle No. 1 is the EF_{NOx} value during the test, which is lower (approximately 20% less).

Another difference is seen in the engine demand. Although the load values are similar in level, in this case the engine demand in the loaded situation is clearly higher than the engine demand in the unloaded situation. However, the EF_{NOx} for the loaded situation is lower than for the unloaded situation and lower than the EF_{NOx} of vehicle No. 1. This situation can be attributed to the effective functioning of the EGR. In this scenario, the EGR operates efficiently and succeeds in curbing the vehicle's emissions, even as the engine's operational requirements escalate.

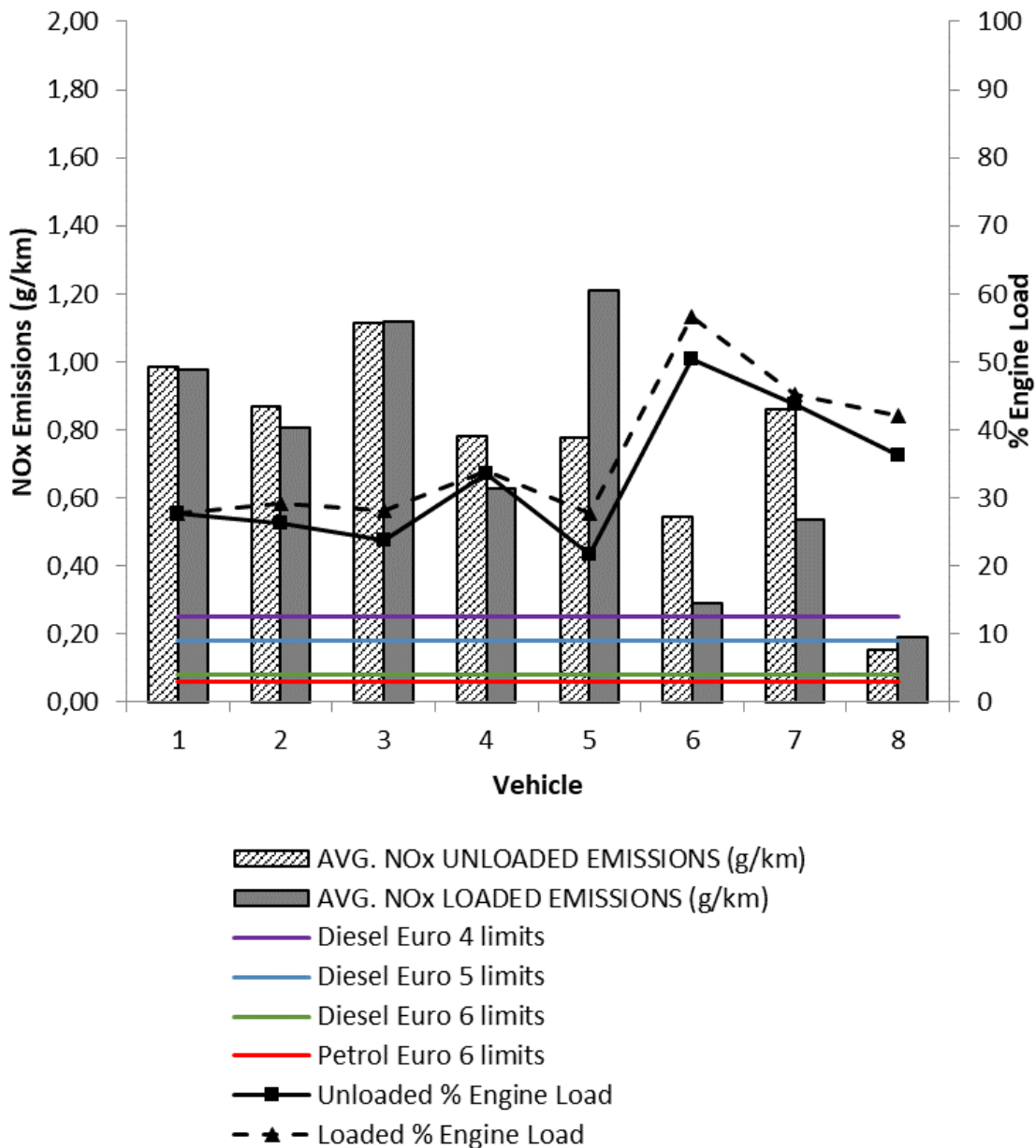


Figure 7-21. NO_x emissions and "% engine load" from the set of vehicles in test #1.

When analyzing the Euro 5 vehicles, a great heterogeneity in behavior becomes evident across the three vehicles subjected to analysis.

Vehicles No. 3 and No. 5 exhibit engine load values that align with those observed in the Euro 4 vehicles. Conversely, Vehicle No. 4 stands out with engine load values that are approximately 20% higher compared to the other two Euro 5 vehicles and the Euro 4 vehicles.

In terms of emission factors, vehicle No. 3 has the highest EF_{NO_x} for the unloaded situation of all the vehicles analyzed (the same value for the loaded situation). In turn, vehicle No. 5 has the highest EF_{NO_x} for the loaded situation of all the vehicles analyzed. On the other hand, vehicle No. 4 has lower EF_{NO_x} values than the Euro 4 vehicles.

Therefore, it finds a great variability in NO_x emissions for vehicles of this emission level, with two of them having the highest NO_x emission values. The EF_{NO_x} of vehicle No. 3 in the unloaded situation, the highest of all vehicles, is more than 6 times higher than the limit defined by the Euro 5 level (* Multiplier factor for average NO_x emissions exceeding the Euro level limit. Table 7-5). For the loaded situation, vehicle No. 5 presents the highest EF_{NO_x} value of the comparison, being 6.7 times higher than the Euro 5 limit.

The Euro 6 diesel vehicles also exhibit noteworthy disparities between them. While both vehicles feature notably elevated average engine load values in comparison to the other vehicles tested, their emissions behavior demonstrates variations in relation to engine demand.

Surprisingly, despite registering the highest engine demand levels, these vehicles do not record the highest emissions due to the superior efficiency of their onboard EATS, which effectively mitigates NO_x emissions more effectively than the systems in the Euro 5 vehicles. However, substantial discrepancies exist between the two Euro 6 vehicles in terms of EF_{NO_x} , evident in both unloaded and loaded scenarios. Specifically, Vehicle No. 7 stands out with significantly higher emission factors in both situations.

VEHICLE	EURO LEVEL	FACTOR EMISSION LIMIT (g/km)	UNLOADED			LOADED		
			AVG. ENGINE LOAD (%)	AVG. NO_x EMISSIONS (g/km)	*EURO LEVEL LIMIT MULT. FACTOR	AVG. ENGINE LOAD (%)	AVG. NO_x LOADED EMISSIONS (g/km)	*EURO LEVEL LIMIT MULT. FACTOR
1	4	0.25	28	0.99	3.9	28	0.98	3.9
2	4	0.25	26	0.87	3.5	29	0.81	3.2
3	5	0.18	24	1.12	6.2	28	1.12	6.2
4	5	0.18	34	0.78	4.3	34	0.63	3.5
5	5	0.18	22	0.78	4.3	28	1.21	6.7
6	6	0.08	50	0.55	6.8	57	0.29	3.6
7	6	0.08	44	0.86	10.7	45	0.54	6.7
8	6	0.06	36	0.15	2.5	42	0.19	3.2

* Multiplier factor for average NO_x emissions exceeding the Euro level limit.

Table 7-5. Summary of avg. results from Test #1.

In any case, both vehicles significantly surpass the limits stipulated by the Euro 6 emission standards (Figure 7-21). The lowest emission factor recorded is 3.6 times greater than the limit, while in the most extreme case (unloaded condition of vehicle No. 7), the emission factor reaches a staggering 10.7 times the limit prescribed by the Euro 6 emission standards.

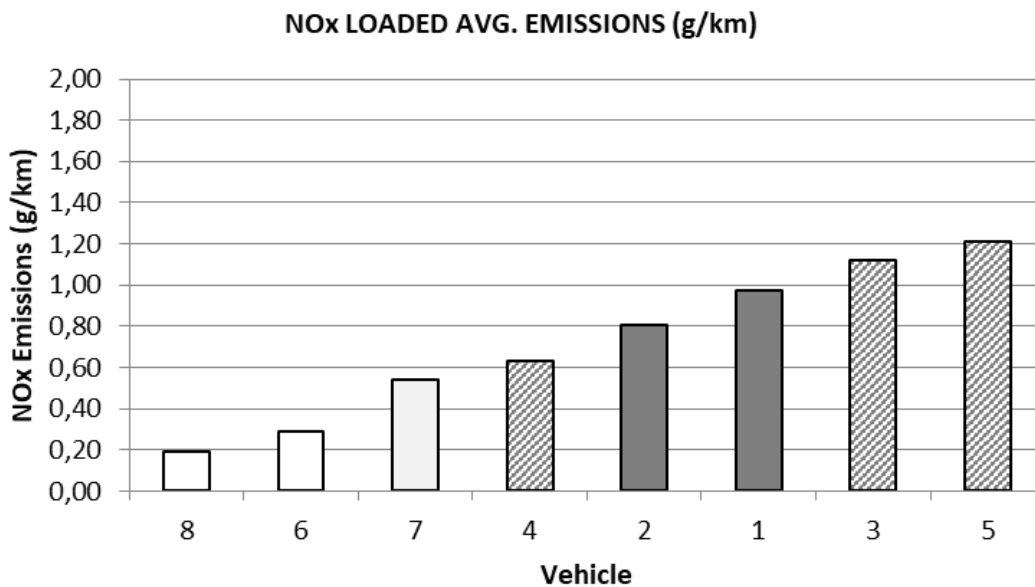
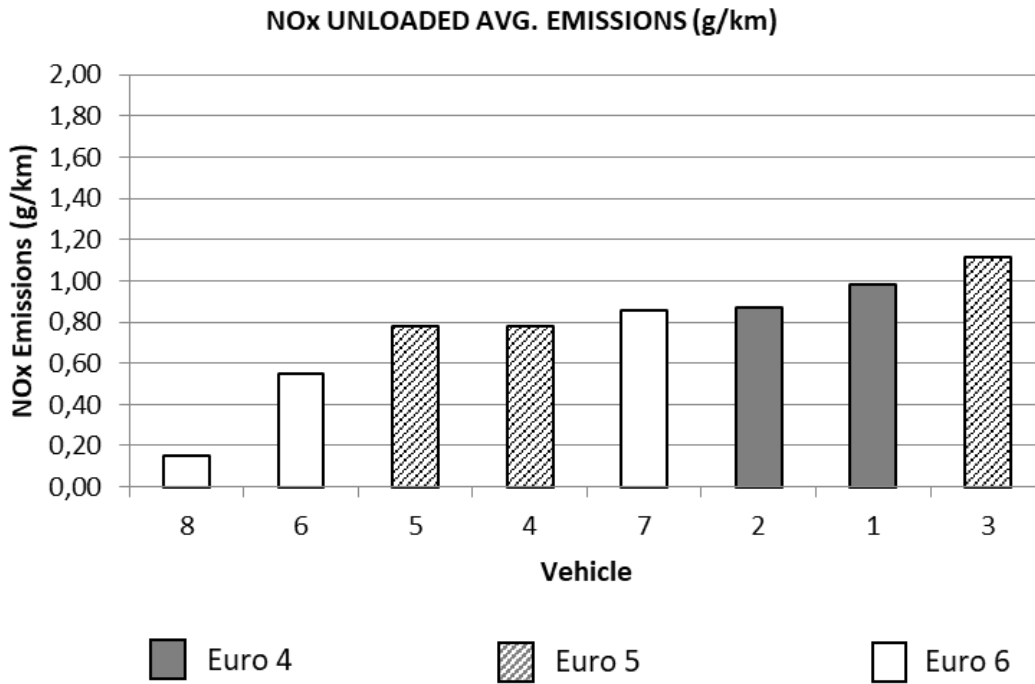


Figure 7-22. Vehicles ordered according to EF_{NOx} for unloaded (up) and loaded (down) test #1.

Lastly, the gasoline vehicle exhibits engine demand levels that are slightly lower than those observed in the other two Euro 6 vehicles, yet still higher than those recorded

for the remaining vehicles. With these engine load demand values, the emission factor measured in both situations (unloaded and loaded) is the lowest of all the vehicles analyzed.

Despite this, they are well above the limit set by the Euro 6 emission level, both for gasoline and diesel vehicles. The EF_{NOx} measured is 3.2 times higher than its emission limit. However, it is the only vehicle with emissions below the limit set for Euro 4 and Euro 5 vehicles.

To conclude the analysis of test #1, the vehicles are ordered according to the results obtained both with unloaded and loaded scenarios, as can be seen in Figure 7-22.

It can also be seen that the behavior of the vehicles is not the same in the unloaded and loaded situations, since the order of the vehicles in both situations also changes. Among the vehicles, specifically No. 8, No. 6, and No. 4, these are the sole instances where the ranking remains consistent in both situations based on the recorded emissions.

However, in the context of the Euro 5 vehicles, the relative order between them is not even sustained across both situations. For instance, vehicle No. 5 transitions from having the lowest emissions among the three in the unloaded scenario to becoming the one with the highest emissions in the loaded scenario.

The same analysis conducted using the results obtained from measurements in Test #1 has been carried out for the other 5 tests performed. For the sake of clarity in the presentation, the obtained results will be summarized in the following section.

The comprehensive analysis of each individual test is located in the appendices chapter, Section 11.4, at the end of this document.

7.3.3. DISCUSSION OF VEHICLE EMISSIONS ASSESSMENT IN ON-ROAD TESTS

In summary, in this initial part of the analysis of the on-road test results, some conclusions can be drawn:

- EF_{NOx} from each diesel vehicle tested under urban driving conditions consistently exceeds the corresponding homologation thresholds several times, regardless of the specific situation or condition.
- The actual emission factor values of the vehicles do not align with the reductions stipulated by the emission limits established in the type-approval procedures. Notably, the emissions from Euro 4 vehicles are occasionally lower than the observed values in Euro 5 and even Euro 6 vehicles (with the exception of gasoline vehicles). Consequently, relying solely on the emission level as an indicator is not a dependable method for determining the emission level of a vehicle. This situation agrees with most of the literature, and other studies of real on-road NO_x emissions [27], [123], [124], where real NO_x emissions do not correspond to the thresholds set by the homologation process.
- EF_{NOx} from the gasoline engine vehicle is notably lower than that of the diesel vehicles, despite the "% engine load" values being similar.

- Diesel Euro 4 vehicles are, together with Euro 6 gasoline vehicles, those that exceed the emission limit value corresponding to their homologation in the smallest proportion.
- The values obtained for vehicles No. 1 and No. 2 confirm the hypothesis that the performance of the EGR produces a reduction in NO_x emissions in vehicles, being a valid tool to mitigate such emissions.
- The performance of vehicle No. 1 in on-road driving validates the hypothesis proposed during the design of the measurement method: when external factors that affect emissions are absent (in this instance, the EGR is deactivated), NO_x emissions exhibit a pattern that aligns with a direct correlation between emissions and the "% engine load" experienced by the vehicle. In Figure 7-13, and Figure 7-14, Table 7-5, it can be seen how the increase of engine load between test #1 and test #2 generates an increase of EF_{NO_x} . In contrast, vehicle No. 2 (with the EGR operative) shows the same situation in test #2 an increase of engine load but a decrease of EF_{NO_x} .

This outcome was anticipated, aligning with the extensive body of scientific literature that has been highlighting for several years the notable disparity between the real-world operational emissions of vehicles and the thresholds established by the Euro emission standards in their type approvals.

The congruence between the test results using the measurement equipment and the highlighted situation from previous research findings, confirms the successful design and execution of the urban circulation simulation. This agreement validates the measurement equipment's appropriateness for assessing NO_x emissions, thereby enhancing the overall validity of the measurement method.

In summary, it can be concluded that results from on-road measurements are correct and represent the real behavior of these vehicles in urban driving conditions. Additionally, it is apparent that the emission level alone is not a dependable indicator for determining the true emission levels of vehicles.

The performance of these measurements also provides the relevant research with first-hand information on the actual emissions of vehicles in urban traffic, information of great importance for the validation of the method.

7.4. COMPARISON OF ON-ROAD EMISSIONS AND PTI NO_x MEASUREMENT

The PTI test for NO_x emissions offers direct insight into the immediate NO_x emissions produced by a vehicle when it is stationary, replicating scenarios encountered during actual urban driving. This is particularly pertinent given that stationary periods constitute a substantial portion of the total travel time within urban traffic conditions.

Nevertheless, even though the test results could be perceived as indicative of actual NO_x emissions, it is imperative to refrain from directly assuming this information as a representation of the vehicle's emissions during operation. This is due to the alteration that any change in the variables influencing NO_x emissions could bring about.

Through the implementation of on-road tests illustrated in Table 7-3, a thorough comprehension of the correlation between NO_x emissions and actual urban driving

scenarios has been sought. The objective is to juxtapose the real emissions of vehicles with the emissions measured during the PTI test, in order to evaluate its degree of representativeness.

Since the measurement was conducted using the same gas analyzer equipment utilized in the static measurement method, any contrasts between the outcomes of both test types remain unaffected by disparities in the NO_x sensor or equipment attributes.

Every vehicle that participated in the on-road test was also part of the larger pool of 23 vehicles utilized in the formulation of the static method (see Chapters 4 and 6). Specifically, from the roster of vehicles outlined in Table 7-6, the vehicles subjected to on-road tests are those indicated in bold.

Hence, the logical approach is to compare the static test results with the entirety of on-road tests rather than singling out just one. Combining the on-road test outcomes, which mirror real-world conditions in their diversity, offers a more meaningful and comprehensive basis for comparison, aligning with the dynamics and complexities of actual driving scenarios.

The first assessment is **to compare the Loaded State value** from the PTI test to the **average real emission value** of the vehicles in the on-road measurements. This would serve to check whether the PTI measurement result can be an indicator of the actual on-road average emissions.

Another aspect to analyze is **the comparison of the TMV with the maximum peak values** obtained from the on-road measurements. Specifically, it has been compared with **the highest and the lowest maximum values** recorded in the set of tests.

Using this approach, the disparity between the TMV and the real peak values is quantified to ascertain whether a correlation exists or if the measured value can serve as an indicator of actual peak emissions.

Essentially, these assessments allow for an evaluation of whether the results obtained from the PTI measurement accurately represent the urban emissions of the vehicles under scrutiny. This endeavor offers a broader perspective on the method's efficacy in reflecting real-world urban emissions.

Table 7-6 displays the vehicles subjected to on-road measurements, along with their characteristics and identification within the group of 23 vehicles analyzed in Chapter 5. The average outcomes obtained from these vehicles during this phase of the research are presented in Table 7-7.

For the comparison of the on-road results with the static PTI test outcomes, it is not possible to use the Emission Factor (EF_{NO_x}) values from section 7.3, since they represent the emissions per kilometer traveled, and from the PTI test this information is not available.

Instead, alternative data will be employed for the purpose of comparison. The NO_x Emission Mass Flow (expressed in g/s) values, derived from the concentrations measured by the Gas Analyzer, will serve as the basis for this comparison. These values have been selected for comparison as they are accessible both from the outcomes of static measurements and from the on-road measurements.

Reference Vehicle	Vehicle Manufacturer	Model	Engine Manufacturer	Engine model	Engine size (cm ³)	Engine Power (kW)	Emissions level
2	Volvo	V50	PSA	D4204T	1997	100	Euro 4
12	Volkswagen	Touran	Volkswagen	CFH	1968	103	Euro 5
16	Nissan	Juke	Renault	K9K	1461	81	Euro 5
17	Opel	Astra	GM	A17DTS	1686	81	Euro 5
18	Renault	Fluence	Renault	H4M D7	1598	84	Euro 6
22	Kia	Sportage	Kia	D4FD	1685	85	Euro 6
23	Citroën	C4 Picasso	Citroën	BH01	1560	88	Euro 6

Table 7-6. Set of vehicles and engines used for designing the method, Chapter 6.

Reference Vehicle	Idle Unloaded			Idle Loaded			TMV	
	NO _x (mg/s)	NO _x (ppm)	% Engine load	NO _x (mg/s)	NO _x (ppm)	% Engine load	NO _x (mg/s)	NO _x (ppm)
2	1.80	77	17	5.29	226	34	15.67	668
12	1.65	80	17	1.68	82	36	4.85	237
16	1.88	117	22	3.98	236	42	9.90	582
17	3.71	208	15	7.23	405	37	26.26	1392
18	0.08	5	22	0.25	15	37	1.483	88
22	2.22	128	17	6.47	373	45	14.29	826
23	2.45	141	21	10.52	599	53	23.68	1368

Table 7-7. NO_x emissions average values for the unloaded idle state, loaded idle states, and TMV from static NO_x test.

The comparison system will involve establishing a range of emission values for each vehicle in two distinct scenarios, based on the data collected from the racetrack measurements:

- Range of maximum emissions
- Range of average emissions

Once each range has been established, the connection between the values acquired during the static measurement test, particularly the loaded emission values, and the TMV is scrutinized for every vehicle.

The emission value ranges for each vehicle are computed from the data obtained during each conducted test, encompassing both the average and maximum NO_x emission values for the vehicle throughout each test.

The maximum emission value of each vehicle corresponds to the highest NO_x emission value measured during the course of the in-circuit test (see Figure 7-23).

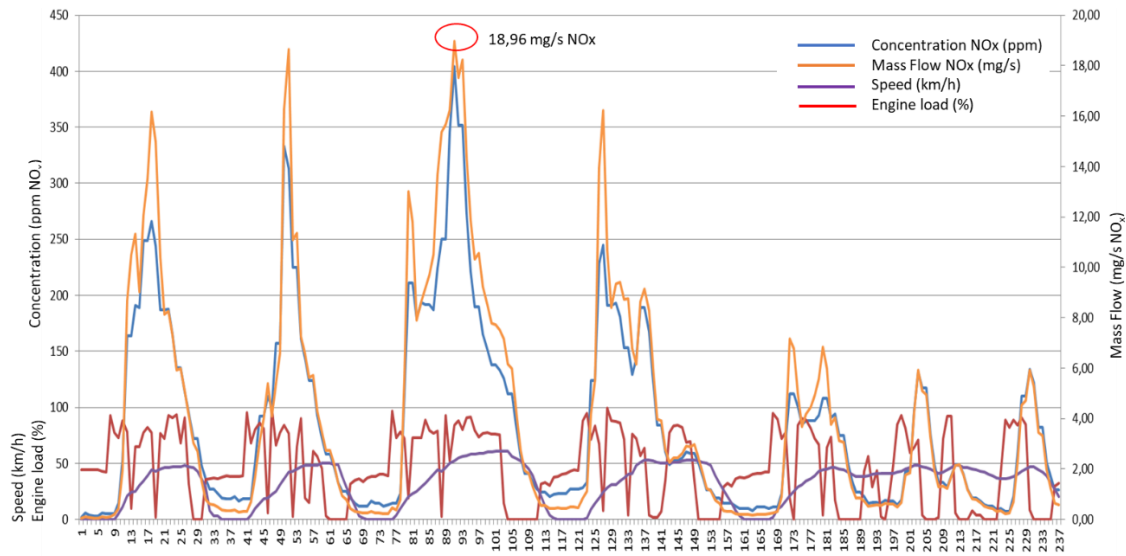


Figure 7-23. Selection of Max. NO_x mass flow value from the test.

The range of maximum values for each vehicle will encompass the spectrum of emission values that exceed the lowest maximum value recorded while remaining lower than the highest maximum value recorded.

To ascertain the range of average values for each vehicle, a similar approach is adopted. This range will encompass emission values surpassing the lowest average value while remaining below the highest average value registered for that specific vehicle.

7.4.1. COMPARISON OF RESULTS FROM VEHICLE No. 1

Starting with the analysis of vehicle No. 1, the values obtained from the different on-road measurements performed are summarized in Table 7-8.

This table shows the average, maximum, and minimum values of the NO_x concentration measured during each of the tests, as well as the "% engine load" values to which the vehicle was subjected, the engine speed, and the NO_x emissions mass flow.

These data are used to determine the total mass of NO_x emitted by the vehicle in each test and, to know the distance traveled and the EF_{NOx} emission factor for each test.

The test group on the left side of Table 7-8 comprises the outcomes of the 6 measurements conducted with added loads within the vehicle (loaded state), while the test group on the right side illustrates the results of the 6 measurements carried out without any supplementary loads attached (unloaded state).

To establish the maximum emission range for the vehicle, the row labeled "Max. NO_x Mass Flow [g/s]" in Table 7-13 should be referred to. Within this row, the highest NO_x emission values (peak emissions) recorded for the vehicle in each of the conducted tests can be found (as depicted in Figure 7-33).

Test	#	Loaded						Unloaded					
		1	2	3	4	5	6	1	2	3	4	5	6
Duration of measure	[s]	192	298	183	177	171	181	198	291	182	170	189	167
Avg. Concentration	[ppm]	141	123	132	134	104	141	135	116	144	127	98	108
Max. Concentration	[ppm]	414	398	411	320	321	435	512	348	416	417	433	401
Min. Concentration	[ppm]	22	28	24	23	16	28	12	20	14	16	15	16
Avg. engine load	[%]	28	32	27	47	72	75	28	27	29	53	62	77
Max. engine load	[%]	90.2	89.4	81.2	100	100	100	81.2	79.6	75.7	100	100	100
Min. engine load	[%]	0	0	0	0	0	0	0	0	0	0	0	0
Avg. Speed	[km/h]	42.1	36.6	43.9	45.9	47.0	47.2	41.9	34.3	42.9	46.0	45.5	47.9
Avg. Engine Speed	[rpm]	2242	1558	1948	1424	1175	1148	2181	1499	1915	1464	1082	1155
Max. Engine Speed	[rpm]	3452	3178	3058	3060	3168	3709	3175	2749	2779	3078	3300	3406
Min. Engine Speed	[rpm]	809	778	811	834	779	839	797	718	774	768	784	774
Avg. NO _x Mass Flow	[g/s]	0.008	0.006	0.007	0.005	0.003	0.005	0.008	0.005	0.008	0.005	0.003	0.004
Max. NO _x Mass Flow	[g/s]	0.033	0.031	0.023	0.024	0.019	0.029	0.042	0.023	0.024	0.028	0.029	0.026
Min. NO _x Mass Flow	[g/s]	0.001	0.001	0.001	0.001	0.000	0.001	0.001	0.000	0.001	0.001	0.000	0.000
Total emissions NO _x	[g]	1.561	1.718	1.311	0.943	0.591	0.833	1.577	1.561	1.377	0.906	0.592	0.599
Distance	[m]	1600	1600	1600	1600	1600	1600	1600	1600	1600	1600	1600	1600
Emission Factor EF _{NO_x}	[g/kml]	0.98	1.07	0.82	0.59	0.37	0.52	0.99	0.98	0.86	0.57	0.37	0.37

Table 7-8. Summary of vehicle No. 1 results from on-road tests.

The highest value recorded (highlighted in gray and bold) for this vehicle was 0.042 g/s of NO_x emitted by the vehicle when performing test #1 in an unloaded condition.

The lowest of the maximum values (highlighted in gray and bold), that is, the test where the lowest maximum peak emissions were reached, was when test #5 was conducted under loaded conditions. In this test, the highest recorded value of emitted NO_x was 0.019 g/s. Consequently, for this particular vehicle, the range of maximum NO_x Mass Flow emissions can be defined as ranging between 0.019 g/s and 0.042 g/s.

To define the average emission range, the same procedure should be followed. In this case, Table 7-13 is referred to, specifically focusing on the row indicating the values of "Avg. NO_x Mass Flow [g/s]." Within this row, averages of the NO_x emission values measured during each of the tests are recorded. The highest average value recorded for this vehicle (highlighted in gray and bold) was 0.008 g/s of NO_x emitted by the vehicle over the 192 s of test #1 in the loaded condition.

#	UNLOADED			LOADED			TMV	
	NO _x [mg/s]	NO _x [ppm]	% engine load	NO _x [mg/s]	NO _x [ppm]	% engine load	NO _x [mg/s]	% engine load
1	0.54	24.47	28	2.05	86.53	40	22.06	100
2	0.84	39.49	22	1.25	55.64	33	9.43	100
3	0.87	41.24	20	1.45	64.94	35	12.07	100
4	0.97	46.41	19	2.17	97.77	33	18.96	100
5	0.99	47.52	19	1.37	61.60	33	18.56	100
6	1.09	48.76	26	2.55	108.08	37	11.53	100
7	1.27	58.02	25	2.72	117.17	37	11.35	100
8	1.78	82.91	23	2.90	127.77	37	14.28	100
9	1.98	92.92	22	2.96	131.29	36	15.32	100
10	2.21	104.52	21	2.98	132.68	36	17.54	100
11	2.36	111.30	21	2.94	134.03	34	14.94	100
12	1.79	84.97	20	3.11	138.75	36	15.56	100
13	1.86	87.78	20	2.45	109.44	33	14.75	100
14	1.79	84.81	20	2.37	105.90	33	16.93	100
15	1.71	80.70	20	2.45	109.54	33	17.67	100

Table 7-9. Summary of Static NO_x test on Vehicle No. 1

The lowest of the average values (highlighted in gray and bold), which corresponds to test #5 in the unloaded condition, yielded an average emission value of 0.003 g/s of NO_x emitted over the 189-second duration of the test. Therefore, for this particular vehicle, it can be established that the range of average NO_x Mass Flow emissions spans between 0.003 g/s and 0.008 g/s.

Using these emission ranges, a comparison will be drawn against the outcomes of the vehicle's NO_x measurement test during the PTI, as illustrated in Table 7-9.

Indeed, by graphing the range of average emissions and incorporating the values acquired from the measurements specified in Table 7-9 for the Loaded state, a comparison can be made between the NO_x emissions value of the vehicle gauged at idle with a load (measured during the PTI test). This comparison would illustrate the emissions of the vehicle while stationary at a traffic light with the air conditioning activated and the lights on, juxtaposed with the range of average emissions when the vehicle is being driven in actual urban conditions.

As depicted in Figure 7-24, for this specific vehicle, the measurements obtained from the loaded PTI test align closely with the lower boundary of the range of actual average emission values recorded in urban traffic conditions. On average, the PTI test values stand 24% below the minimum limit of the vehicle's average emission range. Consequently, in this instance, it could be contemplated that these PTI test results **furnish valid insights for approximating vehicle emissions** during operation.

Additionally, a comparison can be conducted between the range of average emissions and the TMV values derived from the PTI test measurement, as shown in

Figure 7-25. It is important to recall that the TMV value signifies the estimated NO_x emissions of an idling vehicle if it were subjected to a "% engine load" of 100%.

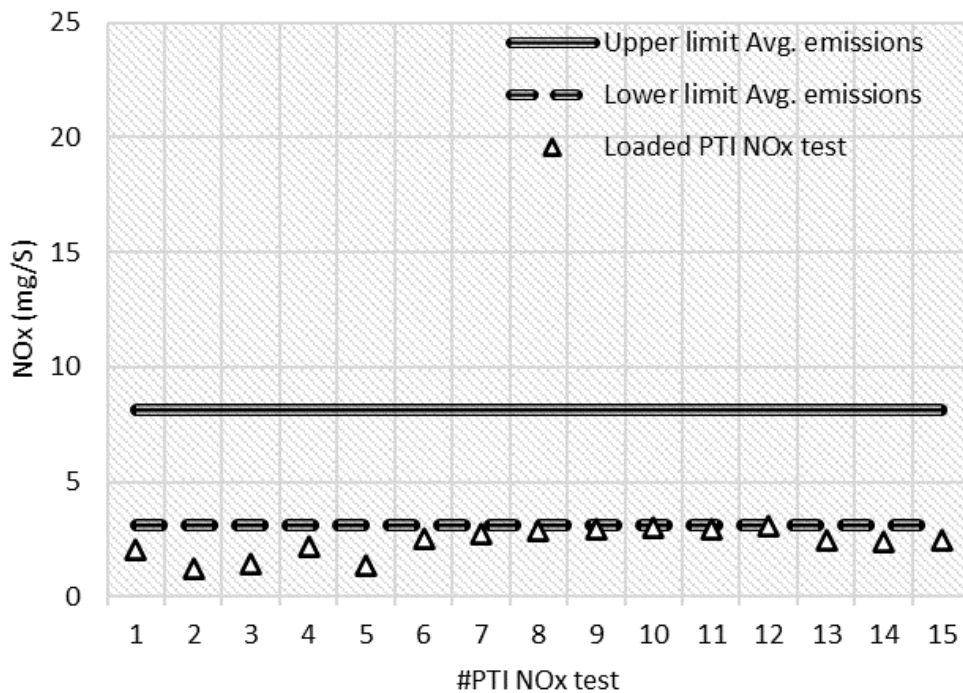


Figure 7-24. Range of Avg. On-road emissions and Loaded PTI test result for Vehicle No. 1.

In this case, it can be seen that the TMV values exceed in all cases the defined range of **average** emissions, so this data would be higher than the average emissions of the vehicle in urban circulation.

Finally, the TMV values are compared with the range of maximum emissions recorded for the vehicle in the on-road measurements to check if the TMV can be an indicator of these values, as shown in Figure 7-26.

In this scenario, it is confirmed that the TMV values closely align with, and in some instances even match, the range of maximum emissions for the vehicle. Furthermore, it is evident that the TMV values acquired never surpass the upper limit of the vehicle's maximum emissions range in any case.

Hence, the TMV values derived **can be deemed as an indicator of the actual maximum emissions** exhibited by the vehicle during urban circulation. Furthermore, it is established that the **genuine maximum emissions** of the vehicle are **never surpassed by the TMV**. Consequently, a decision to reject a vehicle during inspection based on these TMV values would ensure that the rejection is grounded in values that genuinely reflect the vehicle's emissions behavior in real-world conditions.

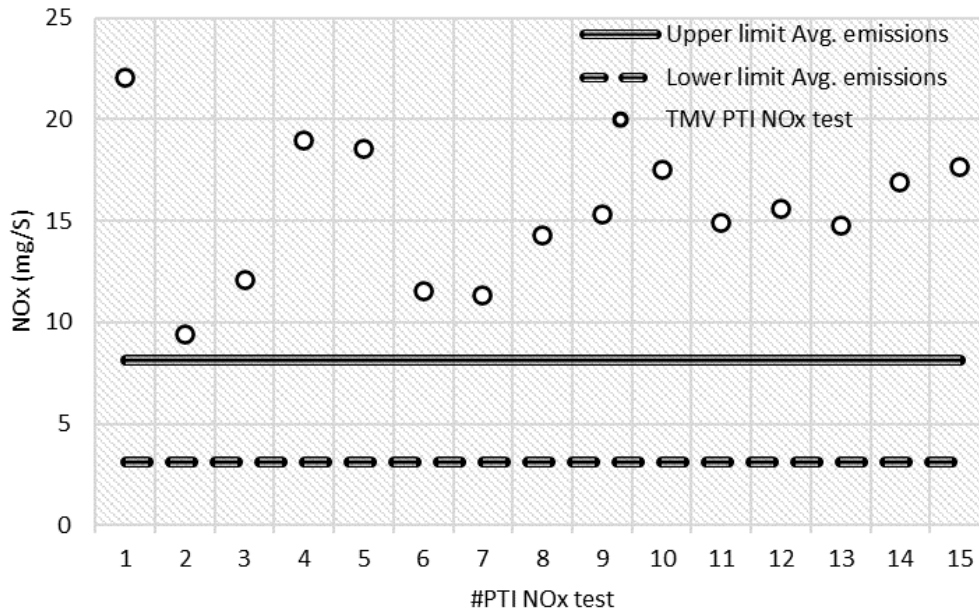


Figure 7-25. Range of Avg. On-road emissions and TMV PTI test results for Vehicle No. 1.

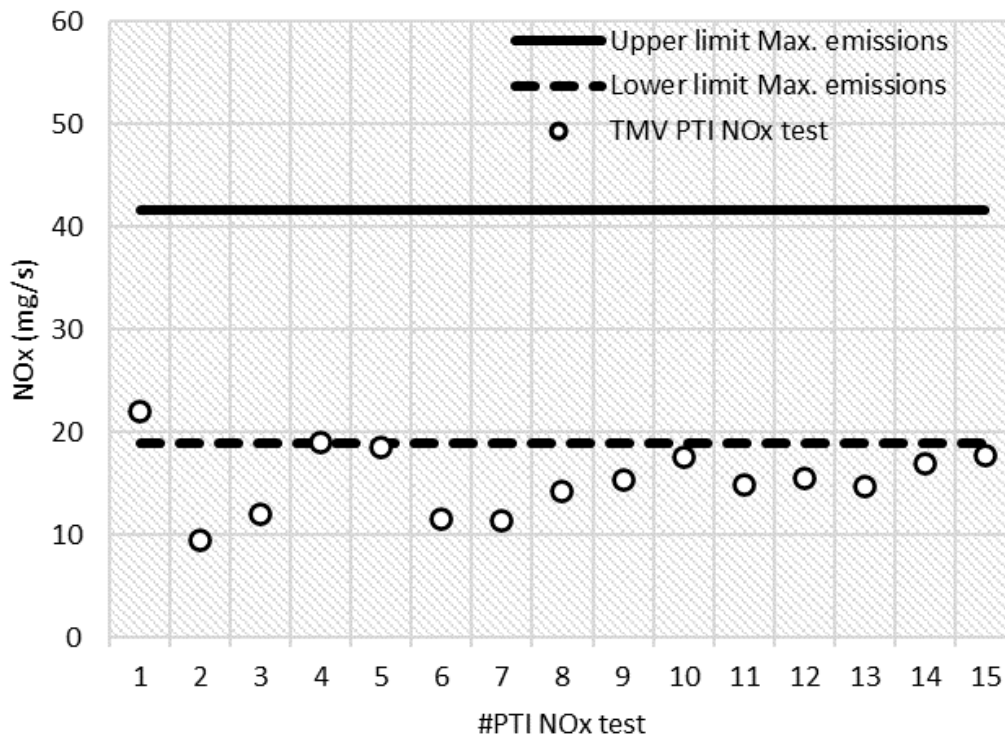


Figure 7-26. Range of Max. On-road emissions and TMV PTI test results for Vehicle No. 1.

Subsequently, identical analysis will be conducted for the remaining 7 vehicles under study. Initially, the results obtained from the tests will be condensed to establish the

ranges of average and maximum values. Subsequently, the data acquired from the static tests performed on the vehicles will be collected, and these values will be juxtaposed against the ranges established through actual emissions encountered during operation.

The same analysis conducted using the results obtained from measurements in Vehicle No. 1 has been carried out for the other vehicles analyzed. For the sake of clarity in the presentation, the obtained results will be summarized in the following section.

The comprehensive analysis of each individual vehicle is located in the appendices, in section 11.5 at the end of this document.

7.4.2. DISCUSSION FROM THE COMPARISON OF RESULTS TO THE PTI PROPOSAL

The average NO_x emissions values of the vehicles, obtained from all the diesel vehicles analyzed, are shown in Table 7-10 after excluding the data from the gasoline vehicle (which has significantly lower emissions than the rest of the vehicles analyzed and can distort the average emissions), indicate that the range of average emissions of the diesel vehicles assessed is between 2.24 mg/s NO_x and 16.37 mg/s NO_x, which has been graphically represented in Figure 7-27.

Considering the distinct average ranges for each vehicle, as indicated in Table 7-10 under the "Range width" column and depicted graphically in Figure 7-27 as "Interval", it appears suitable to establish a comprehensive average emissions range.

Vehicle No.	Average Emissions				Max. Emissions			
	Min. g/s NO _x	Max. g/s NO _x	Range width g/s NO _x	Increase %	Min. g/s NO _x	Max. g/s NO _x	Range width g/s NO _x	Increase %
1	0.00313	0.00813	0.00500	260%	0.01890	0.04155	0.02265	220%
2	0.00292	0.00705	0.00413	242%	0.01636	0.04386	0.02750	268%
3	0.00900	0.01486	0.00585	165%	0.02823	0.04658	0.01835	165%
4	0.00515	0.01637	0.01122	318%	0.02140	0.04850	0.02710	227%
5	0.00541	0.01233	0.00692	228%	0.02220	0.04175	0.01955	188%
6	0.00224	0.00634	0.00410	283%	0.01045	0.03051	0.02006	292%
7	0.00405	0.01462	0.01057	361%	0.01896	0.06620	0.04724	349%
Avg. Value	0.00456	0.01139	0.00683	265%	0.01950	0.04556	0.02606	244%
Min. Value	0.00224	0.00634	0.00410	165%	0.01045	0.03051	0.01835	165%
Max. Value	0.00900	0.01637	0.01122	361%	0.02823	0.06620	0.04724	349%

Table 7-10. Summary of Range values for Average emissions and Max. emissions.

This broader range, encapsulating all diesel vehicles, can be defined as spanning from the highest value among all the average ranges (representing the upper limit) to the lowest value among all the average ranges (representing the lower limit).

Hence, this range encompasses the individual ranges of all the examined diesel vehicles. With an amplitude exceeding 14 mg/s NO_x, it surpasses even the widest range observed among the analyzed vehicles (11.22 mg/s NO_x, Vehicle No. 4).

Considering that the vehicles used are typical models from popular manufacturers, equipped with widely used engines, it is reasonable to **consider them as representative of the general behavior** observed in a significant portion of the Spanish and European diesel vehicle fleets. Consequently, it is plausible to assume that the overall fleet's real emissions would be distributed around or in proximity to these established values.

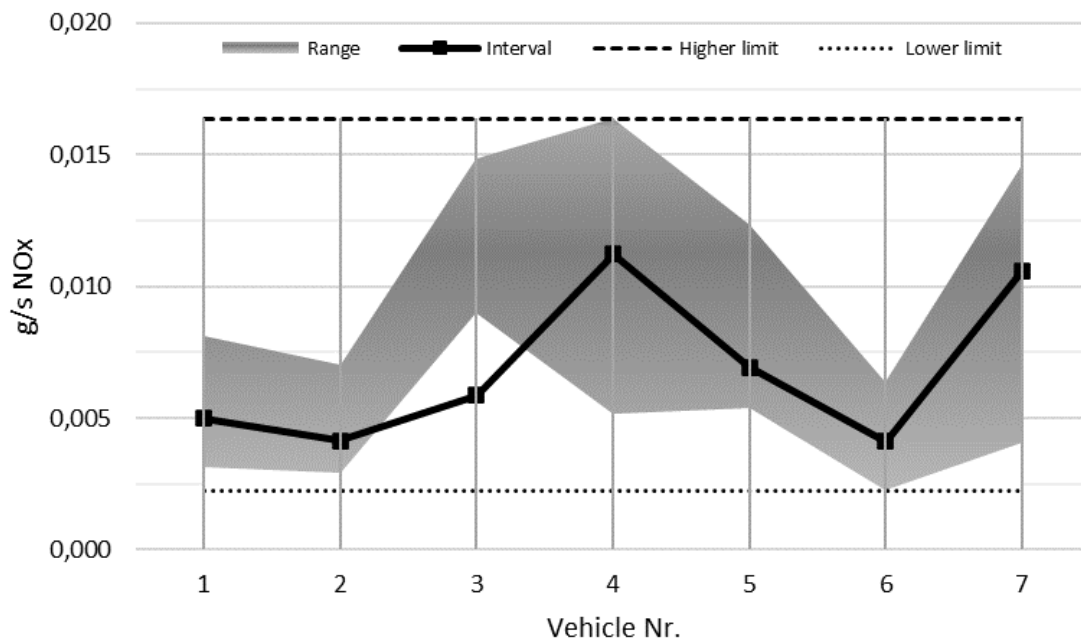


Figure 7-27. The plot of the Range of average emissions from diesel vehicles.

Upon scrutinizing the average outcomes derived from the conducted static tests, as outlined in Table 7-7, it becomes evident that 90% of the diesel vehicles investigated in these tests exhibited NO_x emission values under loaded conditions that fell within the range depicted in Figure 7-27. Fundamentally, this measurement approach meticulously assesses operational states during which vehicles emit within the scope of their average emissions under actual urban traffic circumstances.

In summary, the emission values recorded during the static PTI test for diesel vehicles in the loaded state align with a range of values that closely resemble the actual average emissions range of diesel vehicles when operating in urban conditions, as previously defined.

This data holds significant importance as it underscores the significance of the insights offered by the suggested test: in addition to representing the actual emissions value of the vehicle when it is idling (under loaded conditions), **the emissions value obtained in the loaded state can be assumed to be in the range of the actual average emissions of the vehicle in urban circulation.**

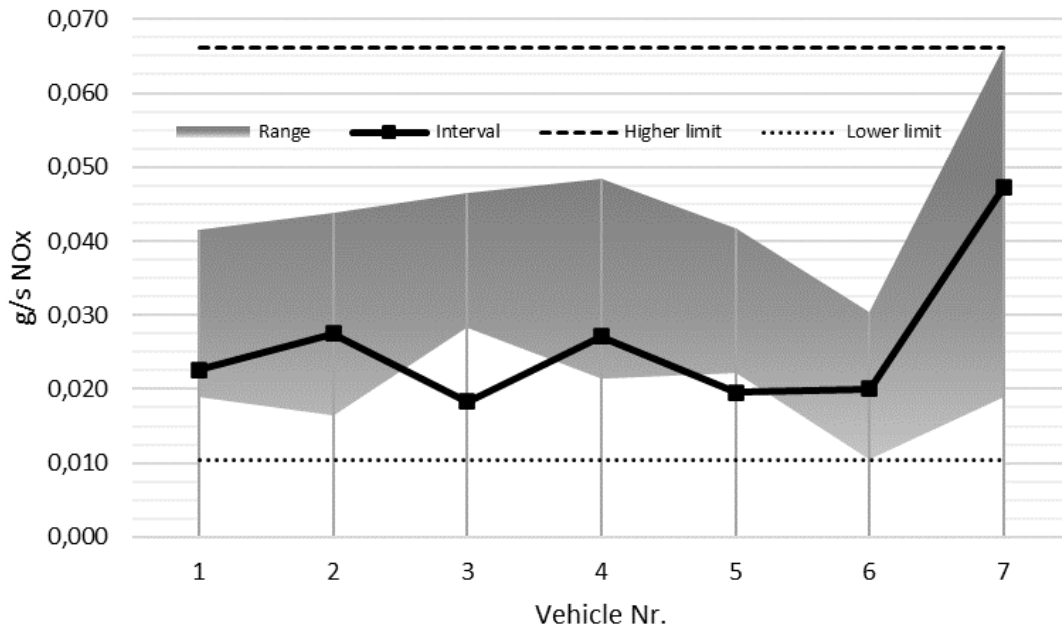


Figure 7-28. The plot of Range of Max. emissions from diesel vehicles.

Similarly, an examination is conducted on the maximum NO_x emission values exhibited by the vehicles, as detailed in Table 7-10, and determined by peak point values, as indicated in Figure 7-23. The range encompassing the maximum emissions demonstrated by the vehicles under study is delimited between 10.45 mg/s NO_x and 66.20 mg/s NO_x (Figure 7-28).

This range of maximum emissions encompasses the ranges of all diesel vehicles analyzed. It has a range of 55.75 mg/s NO_x, which is higher than the widest range of the analyzed vehicles (47.24 mg/s NO_x, Vehicle No. 7).

Similar to the average emission range, the span of each vehicle's range is visualized in Figure 7-28, where the "Interval" value for each vehicle represents the respective range amplitude data.

It has been verified, throughout section 7.4, that **the TMV values** provided by the static measurement test in PTI **never exceed the actual maximum value emitted by the vehicle in urban traffic.**

This section also shows that 82% of the vehicles analyzed in Table 7-7 have TMV values that fall within this range.

The correspondence or proximity of these TMV values to the actual peak emission values of vehicles is of great importance since knowing with certainty the peak emissions of vehicles can also be used to make estimations of actual emissions, given that the greatest amount of NO_x is emitted by a vehicle occur in high emission episodes of short duration, such as those seen in Figure 7-23 [192].

In summary, the most important aspects to point out from the comparison are:

- 1) The measurements conducted on vehicles in real-world circulation confirm that despite the variations observed in emissions across different vehicles, urban driving conditions yield average emissions that can be encompassed within a defined emissions range or interval.
- 2) The NO_x measurement test implemented for PTI generates multiple emission values as a result. Among them, the **idle NO_x emissions value in the loaded state** (with connected equipment) falls within a range of values comparable to the average emissions range observed in genuine urban traffic scenarios. Consequently, this parameter can be regarded as an **indicator of a vehicle's average emissions during urban driving**.
- 3) The **TMV** obtained from the NO_x measurement in PTI **never surpasses the highest value recorded during actual urban vehicle circulation**. This holds special significance as the TMV is proposed as a parameter to establish a rejection threshold during inspections. Ensuring that the TMV never surpasses the vehicle's genuine maximum emissions provides the guarantee that a vehicle will not be subject to rejection during inspections due to emission levels higher than its authentic on-road performance.
- 4) The **TMV** yielded by the static test yields emission values within a range akin to the spectrum of peak vehicle emissions witnessed in actual urban traffic scenarios. Consequently, it can be regarded as an **indicator of a vehicle's maximum or peak emissions during urban driving**.

Hence, it can be deduced that the suggested NO_x measurement approach in PTI holds validity as its outcomes can be confidently correlated with the actual emissions of vehicles during urban driving, a context where NO_x emissions pose greater health risks to individuals.

7.5. CONCLUSIONS

In this chapter, a comprehensive analysis has been conducted on the results obtained from measuring NO_x emissions of a set of vehicles under real urban driving conditions. The measurements have been carried out using the same equipment employed for the development and emission measurement in the PTI test. This ensures the ability to compare the results from both types of measurements, eliminating potential discrepancies in the outcomes due to the equipment used.

On one hand, the obtained results have been compared with the values corresponding to the vehicles based on their approval type emission levels. From the comparison with the homologation limits, the following observations can be made:

- EF_{NO_x} values of each diesel vehicle tested under urban driving conditions consistently surpass the corresponding homologation thresholds by a considerable margin, regardless of the specific situation or condition.
- EF_{NO_x} value of the gasoline engine vehicle is notably lower than that of the diesel ones, even though the "% engine load" values are similar. The EF_{NO_x} value of the gasoline engine vehicle also exceeds the respective homologation thresholds.

- The actual emission factor values of the vehicles do not align with the reduction in emission limits stipulated in the type-approval procedures.

The comparison of the obtained results with the approval type limits reveals a significant disparity in the real NO_x emissions of these vehicles concerning homologation data. Relying solely on the corresponding Euro level to predict their emissions behavior does not seem to be the most reliable approach for accurately identifying vehicles with the highest emissions.

This outcome was expected, aligning with the extensive body of scientific literature that has been underscoring the significant gap between the real-world operational emissions of vehicles and the thresholds established by the Euro emission standards in their type approvals for several years.

Consequently, it can be inferred that the results obtained from on-road measurements are accurate and correspond to the actual emissions of the vehicles, thereby validating the conclusions drawn from them.

On the other hand, the obtained results have been compared with the outcomes derived from applying the proposed PTI measurement method to these vehicles.

The main conclusions drawn from comparing the results obtained from on-road measurements with the results obtained from measurements using the proposed PTI method are:

- In addition to representing the actual emissions value of the vehicle when it is idling (under loaded conditions), **the emissions value obtained from the PTI test in the loaded state can be assumed to be in the range of the actual average emissions of the vehicle in urban circulation.** Therefore, it can be considered an indicator of the average emissions of the vehicle during urban traffic.
- The **TMV** results provided by the static measurement test in PTI **never exceed the actual maximum value emitted by the vehicle in urban traffic.** That guarantees that a vehicle will not be rejected in inspection for an emissions value higher than what it will emit when driving.
- The **TMV** results from the static PTI test yield emission values within a range akin to the spectrum of peak vehicle emissions witnessed in actual urban traffic scenarios. Consequently, it can be regarded as an **indicator of a vehicle's maximum or peak emissions during urban driving.**

To conclude the validation process of the proposed method, the next chapter will outline and elaborate on a measurement campaign.

CHAPTER 8

NO_x MEASUREMENT CAMPAIGN IN PTI

8. NO_x MEASUREMENT CAMPAIGN IN PTI

8.1. INTRODUCTION

The only remaining step to validate the proposed measurement method is its practical application. This involves conducting measurements using the method at PTI stations, which includes testing it within the actual inspection process. To achieve this, a NO_x measurement campaign was conducted at PTI.

During this campaign, the proposed method was implemented on a daily basis for vehicles passing through the stations. These vehicles were part of the regular inspection flow and were not specially prepared for the test. The selection of vehicles was random and encompassed Euro 4, Euro 5, and Euro 6 diesel vehicles that were undergoing inspection at the participating stations.

The objective of developing this measurement campaign is to determine:

- 1) Whether the method can be applied feasibly within the PTI context without disrupting the inspection process or substantially extending the inspection duration for vehicles.
- 2) Whether the method's application remains simple. While a researcher well-versed in the method can execute measurements with attention to detail and handle any challenges that arise, transferring the measurement setup to a different PTI station and imparting basic training on equipment usage and the measurement protocol to the staff tasked with measurements necessitates robust, reliable, and user-friendly equipment and procedures. This ensures consistent measurements are obtained, devoid of operational or procedural impediments.
- 3) Whether the previously established conditions of quality and significance between the variables are maintained, as well as whether the behavior of the engine load value remains as expected across the set of measurements.
- 4) It is crucial to ascertain whether the emission values derived from the NO_x measurement process, conducted on a substantial sample size of vehicles, exhibit comparable patterns to those attained during the initial method validation tests. In addition, it should be checked whether the characteristics and behavior of emissions observed in the vehicles used for the definition of the method are maintained.
- 5) The feasibility of establishing a valid and practical emission threshold, grounded in the static measurement method, needs to be investigated. This threshold should adeptly discern and exclude vehicles exhibiting excessive emissions from regular use while circumventing the unnecessary rejection of properly maintained and fully functional vehicles. This endeavor requires a substantial statistical dataset of measurements to ensure the meaningful derivation of such a threshold.

These are ambitious goals pursued through an extensive measurement campaign. The campaign's substantial scale ensures that the statistical significance of the sample utilized enables an assessment of its subsequent applicability on a broader scale.

8.2. DEVELOPMENT OF THE NO_x MEASUREMENT CAMPAIGN

Pursuing these objectives, a NO_x measurement campaign was conducted across five PTI stations operated by GRUPO ITEVELESA. The campaign involved equipping these stations with the instrumentation detailed in Chapter 5. This setup facilitated the execution of measurements, as outlined in the method, on a random selection of in-service vehicles that traverse these stations on a daily basis.

8.2.1. LOCATIONS INVOLVED IN THE MEASUREMENT CAMPAIGN

GRUPO ITEVELESA is a reference company in the field of vehicle technical inspection in Spain. Dedicated since its foundation in 1982 to the PTI, it currently has more than 70 operating stations spread over 10 Autonomous Communities, with 155 inspection lines. Annually, GRUPO ITEVELESA inspects approximately 2.3 million vehicles of all types.



Figure 8-1. Location of PTI stations from the measurement campaign.

The PTI stations involved in this measurement process were the following:

- 1- ITV 5001 Malpica-Zaragoza (Aragón)¹⁰
- 2- ITV 2831 Las Rozas (Madrid)
- 3- ITV 0825, Sant Fruitós de Bages, Barcelona (Cataluña)
- 4- ITV 3908 Laredo & ITV 3906 Reinoso (Cantabria)

These stations vary in terms of their geographical locations, station sizes, prevalent vehicle types, demographic features of their respective areas, and more. Consequently, the sample of vehicles subjected to analysis in the measurement campaign offers a more comprehensive representation of the entire fleet of vehicles. The selection of these stations has also been influenced by the average daily inspection count they undertake, ensuring an ample volume of vehicles for inspection.

Figure 8-1 displays the distribution of PTI stations across the Spanish territory. It can be observed that these stations are situated in 4 out of the 10 regions where GRUPO IVEVELESA operates, which are highlighted in dark gray within the same figure.

In terms of size, PTI stations identified as 3 and 4 have three inspection lines. Stations 1 and 2 are larger and are located in towns with larger populations, with seven inspection lines each.



Figure 8-2. PTI stations involved in the measurement campaign: ITV 5001 (left upper), ITV 2831 (right upper), ITV 0825 (left down), ITV 3908 (middle down), ITV 3906 (right down).

These stations inspect all types of vehicles, including category M1 and N1 vehicles, which will be the object of the measurement campaign.

Neither the equipment nor the training of the personnel of the selected stations has been an element to be taken into account when selecting them, since they have

¹⁰ PTI station where the measurement method has been developed

similar equipment and personnel to the rest of the stations of the group, and to the stations of other operators.

8.2.2. VEHICLES INVOLVED IN THE MEASUREMENT CAMPAIGN

In total, excluding the measurements taken from the 23 vehicles used to establish the method (which were measured on average more than 10 times each), a total of 1882 vehicles have been measured. This sample size holds considerable significance as it represents a substantial portion of the Spanish vehicle fleet.

Specifically, concerning the Spanish fleet of diesel vehicles of category M1 or N1, with Euro 4, Euro 5, and Euro 6 emission levels, the statistical values of the sample have a Confidence Level of 95% and an Error Rate of 2.3% (Figure 8-3), taking into account that the Spanish fleet of Euro 4, Euro 5 and Euro 6 diesel vehicles of category M1 and N1 is of approximately 8.5 million vehicles ¹¹.



Figure 8-3. Statistical values of the sample size.

Of the whole vehicles measured, 32% are Euro 6 vehicles, 61% are Euro 5 vehicles, and 6% are Euro 4 vehicles. Figure 8-4 shows the number of vehicles from every Emission Level that has been measured according to the proposed method in the campaign.

Figure 8-5 illustrates the vehicle manufacturers involved in the measurement campaign. These manufacturers are arranged in descending order based on the number of vehicles from each brand that has been measured, as indicated on the left axis of the graph. The highest number of vehicles analyzed belongs to VOLKSWAGEN, with a total of 220 vehicles assessed. The subsequent nine manufacturers had between 100 and 150 vehicles subjected to examination.

¹¹ According to Eurostat data.

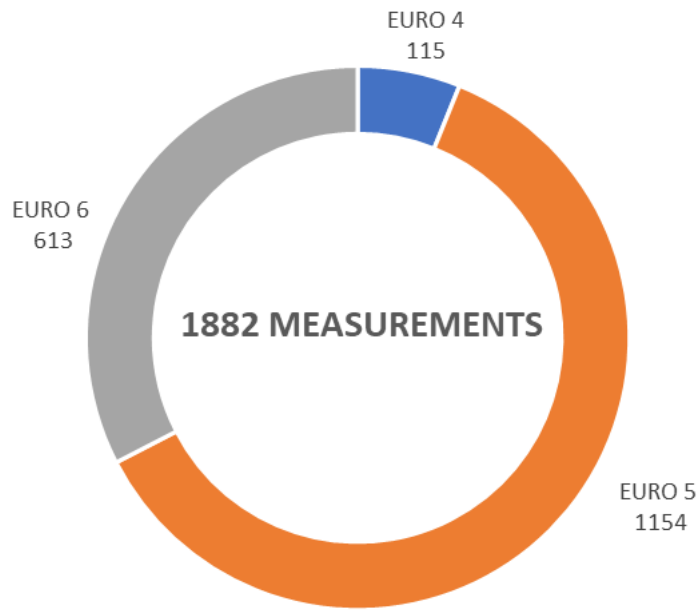


Figure 8-4. Distribution of tested vehicles according to emissions Euro level.

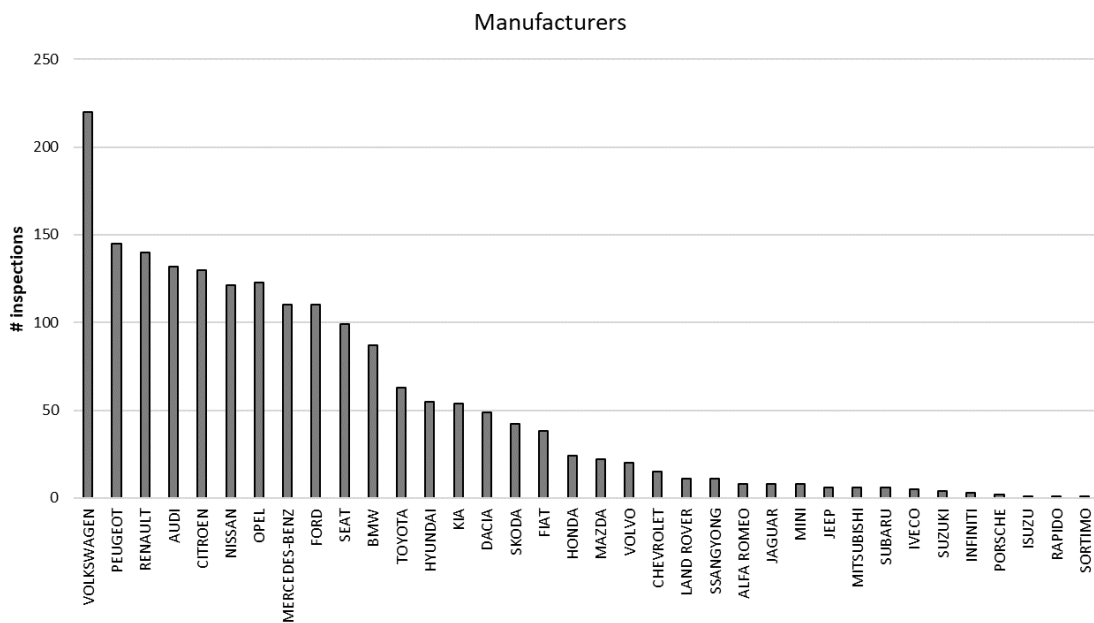


Figure 8-5. Distribution of tested vehicles according to manufacturers.

The vehicle selection was carried out through a random process, implying that the likelihood of selecting vehicles for analysis from various manufacturers solely depends on the proportion of vehicles registered by each brand within the vehicle fleet that has undergone PTI at these stations.

Figure 6-1 illustrates the prominent manufacturers ranked by M1 sales in Spain during 2019 [191]. This graph demonstrates that the manufacturers listed at the upper part of

the chart of vehicles analyzed align (although not necessarily in exact order) with the manufacturers that have the highest vehicle sales in Spain.

Concerning the difference in the order of sales of the manufacturers and the vehicles analyzed, it should be noted that Figure 6-1 shows the number of M1 vehicles registered without discriminating by fuel type, while the vehicles in Figure 8-5 show diesel vehicles exclusively, which are the ones analyzed in the measurement campaign.

In addition to the vehicle manufacturer, there are other distinguishing characteristics among the vehicles that have been analyzed.

One of the primary attributes of the vehicles is their engine displacement. Measurements have been conducted on vehicles with various engine sizes, although a significant proportion of the measured vehicles fall within the engine size range of 1400-1600 cm³, accounting for 47.8% of the total measured vehicles. Another notable engine size category is 1800-2000 cm³, encompassing 28.5% of the measured vehicles, as depicted in Figure 8-6.

The assortment of diverse cylinder capacities was chosen entirely at random, ensuring that the proportions align with the representation of vehicle fleet characteristics in Spain concerning cylinder capacity. The same principle applies to other vehicle attributes analyzed, where their distribution among the set of vehicles is solely influenced by the fleet's composition, rather than being guided by specific vehicle selection criteria.

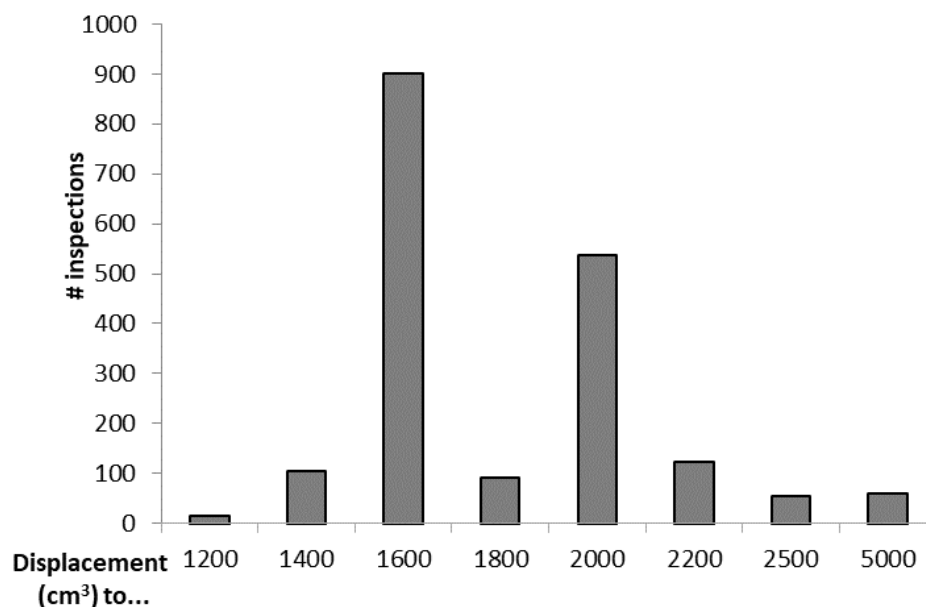


Figure 8-6. Vehicles measured according to Engine Displacement (cm³)

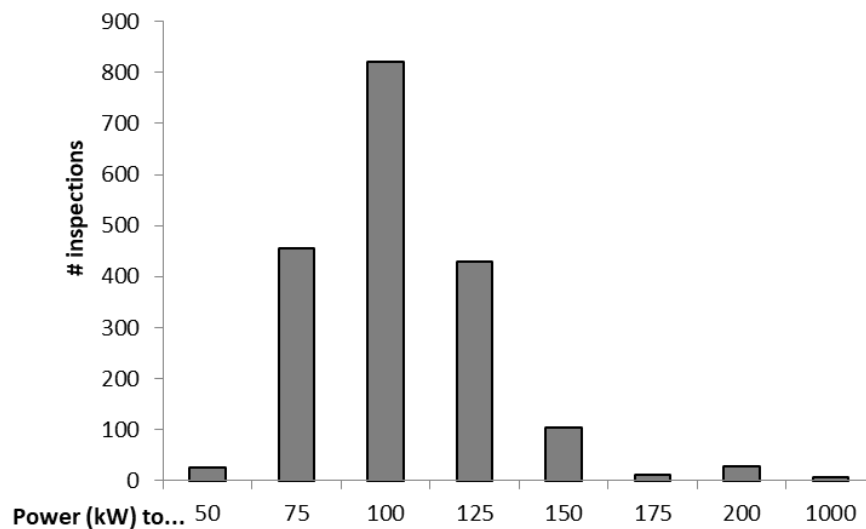


Figure 8-7. Vehicles measured according to Engine Power (kW).

With respect to engine power, as can be seen in Figure 8-7, 43% of the vehicles (821 vehicles) had power ratings between 75 kW and 100 kW, 24% of the vehicles (455 vehicles) were between 50 kW and 75 kW, and 23% (430 vehicles) were between 100 kW and 125 kW.

In terms of mileage traveled (Figure 8-8), only 3.4% would have traveled less than 25,000 km. This is because the first periodic inspection for an M1 category vehicle is four years after registration, so it is usual for vehicles to have traveled long distances in that time.

Category N1 vehicles, which have to pass their first inspection two years after registration, are generally used for professional delivery, so the distances traveled in the first years are usually high.

The same applies to category M1 public service vehicles (cab, rental with driver, VTC, etc.), which, although they pass their first inspection two years after registration, have high mileage due to their intensive use.

The majority of the vehicles inspected had a mileage between 100,000 km and 150,000 km, 25% of the vehicles (470 vehicles). 22% of the vehicles (419 vehicles) had a mileage between 50,000 km and 100,000 km.

As the mileage passes 150,000 km, the proportion of vehicles decreases, with only 2% of vehicles with more than 300,000 km traveled.

Regarding the age distribution of the vehicles, Figure 8-9 shows the distribution. The majority of vehicles, constituting the highest percentage, fall within the age range of up to 4 years. It is important to note that a significant portion of these vehicles are likely undergoing their initial inspection.

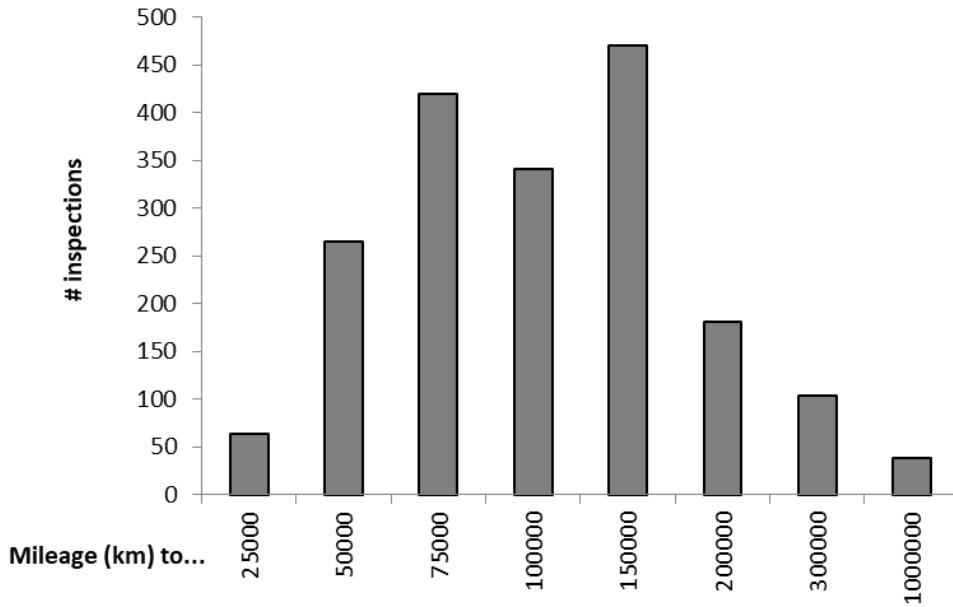


Figure 8-8. Vehicles measured according to Mileage (km).

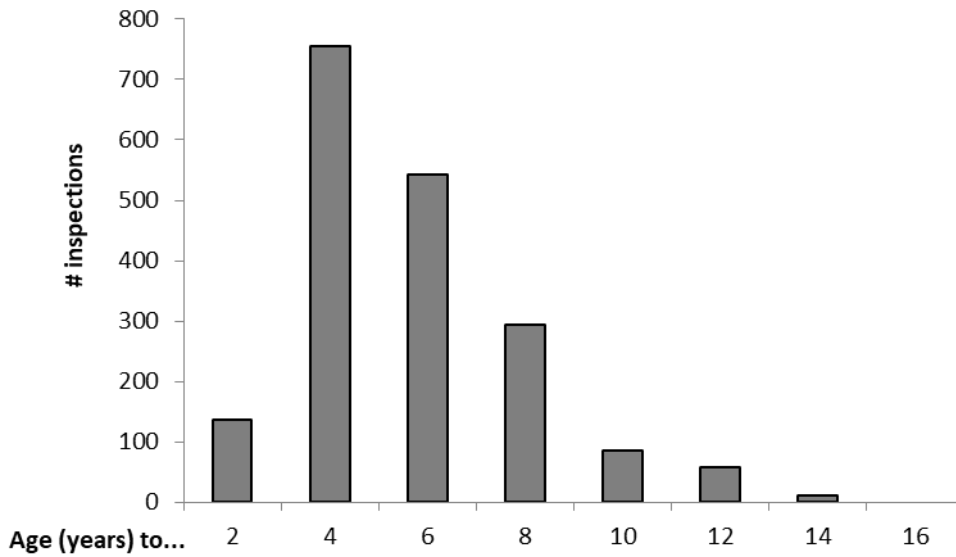


Figure 8-9. Vehicles measured according to Age (years).

These vehicles account for 40% of the total number of vehicles inspected (756 vehicles).

Since we are measuring emissions on vehicles that are at least Euro 4 compliant or newer, the age in years will be constrained by the implementation of the Euro 4 standards (Table 8-1). As a result, considering that the measurement campaign was carried out continuously from 2019 to 2020 (with interruptions due to COVID-19), the maximum age of the vehicles is limited to a maximum of 14 years.

			<1305 kg		1305-3500 kg	
	M1 diesel	M1 petrol	N1 diesel	N1 petrol	N1 diesel	N1 petrol
Euro 1	Jul.-1992	Jul.-1992	Oct.-1994	Oct.-1994	Oct.-1994	Oct.-1994
Euro 2	Jan.-1996	Jan.-1996	Jan.-1998	Jan.-1998	Jan.-1998	Jan.-1998
Euro 3	Jan.-2000	Jan.-2000	Jan.-2000	Jan.-2000	Jan.-2001	Jan.-2001
Euro 4	Jan.-2005	Jan.-2005	Jan.-2005	Jan.-2005	Jan.-2006	Jan.-2006
Euro 5	Sep.-2009	Sep.-2009	Sep.-2010	Sep.-2010	Sep.-2010	Sep.-2010
Euro 6	Sep.-2014	Sep.-2014	Sep.-2015		Sep.-2015	

Table 8-1. Date of entry into force Euro Emission Levels by vehicle category

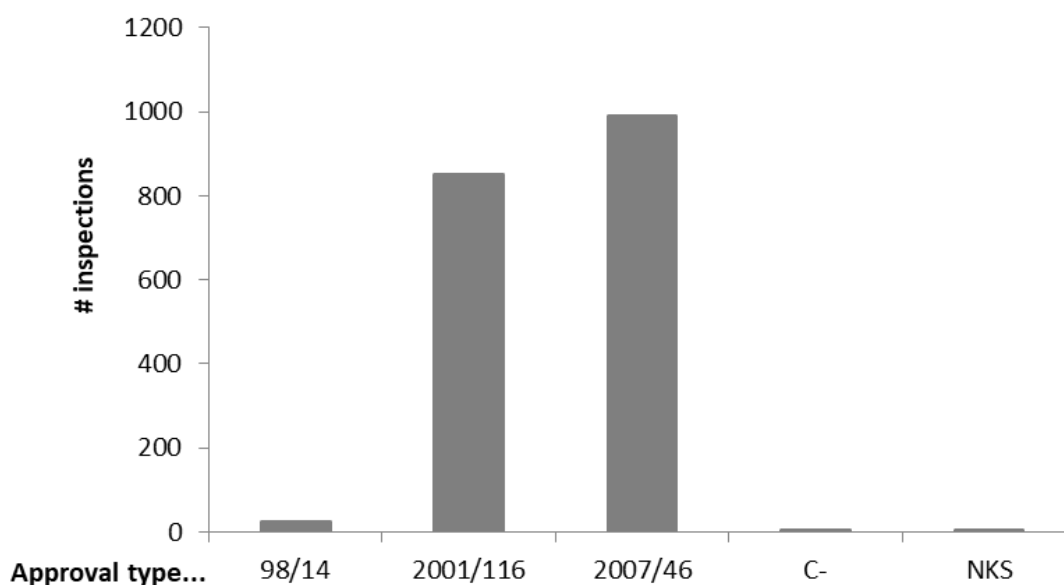


Figure 8-10. Vehicles measured according to Approval Type.

In any case, most of the vehicles are up to 8 years old, with 92% of the vehicles analyzed, a total of 1,728 vehicles, being within this age range.

Regarding the type approval status of the vehicles, and in direct correlation with the earlier observation about the vehicles' age, it becomes apparent that the type approvals of the analyzed vehicles (Figure 8-10) are primarily concentrated within two directives. These directives have succeeded each other as the prevailing type of approval regulations since the implementation of the Euro 4 emissions standard.

Approximately 45% of the vehicles are approved in accordance with Directive 2006/116/EC, while around 53% are approved in line with Directive 2007/46/EC. The oldest vehicles hold approvals under Directive 98/14/EC. Six vehicles possess short series type approval (NKS), and an additional six vehicles hold Spanish type approval (Type C).

8.2.3. EQUIPMENT INVOLVED IN THE MEASUREMENT CAMPAIGN

The necessary technical equipment to be installed at the chosen stations for the measurement campaign is straightforward and minimal, facilitating swift and efficient adaptation.

The previously described NO_x measurement equipment is already integrated into the equipment used across all stations, as GRUPO ITEVELESA routinely employs the TEKBER CENTRALAUTO Gas Analyzer model SPEKTRA 3011 in their facilities.



Figure 8-11. Gas Analyzer TEKBER CENTRALAUTO SPEKTRA 3011.

The sole modification from the original equipment involves the addition of a NO_x sensor, which is integrated alongside the existing O₂ sensor within the equipment. This

adjustment to the equipment incurs minimal financial expense, albeit necessitating the equipment to be sent to its manufacturer for the required modifications to accommodate the new sensor installation.

Likewise, the software application installed in the computer that governs the gas analyzer is modified (modification provided by the equipment manufacturer), installing the new version that incorporates the NO_x measurement phase, which can be activated or deactivated, to perform or not the measurement test.

A detailed description of the software used for the measurement has been included in Chapter 11 Appendices (section 11.1).

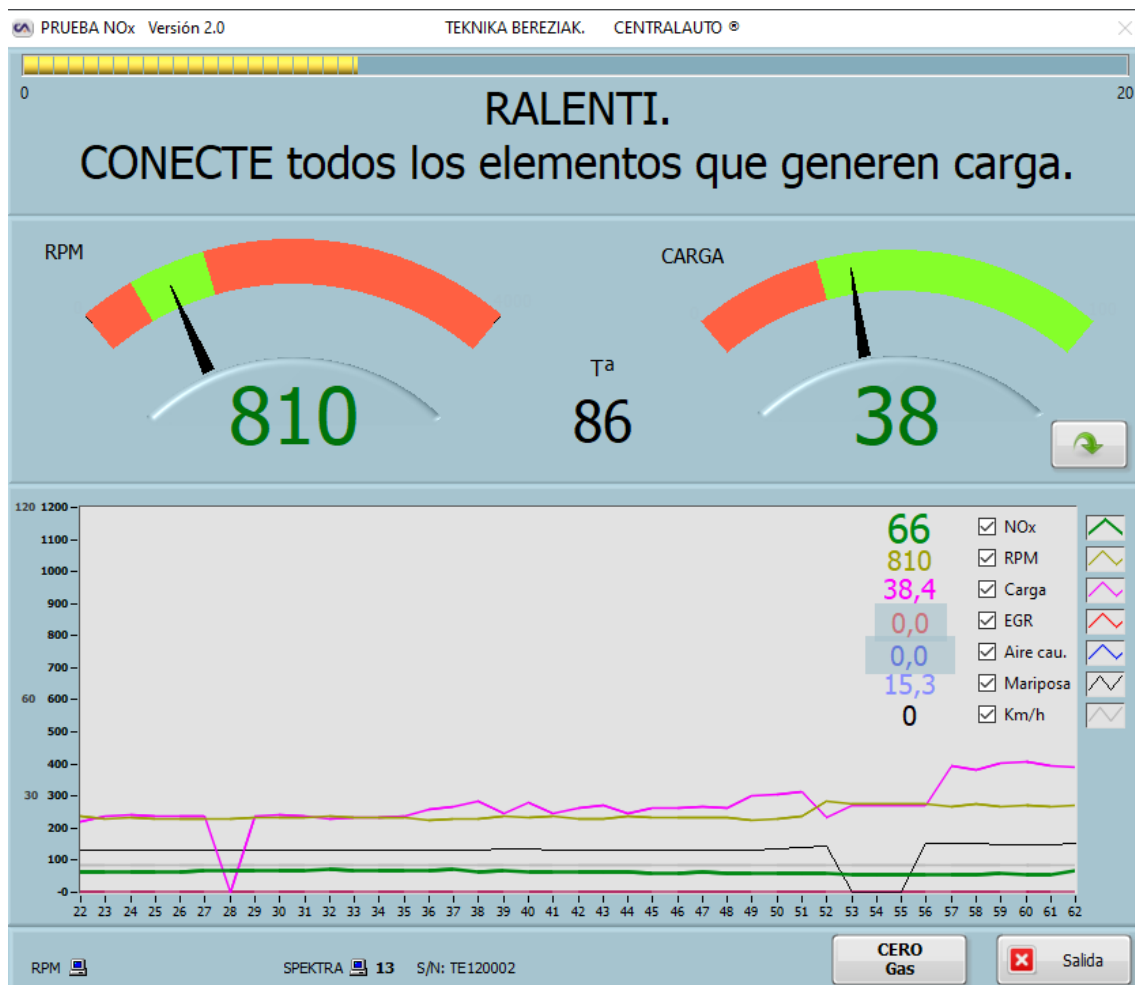


Figure 8-12. TEKBER software for NO_x measurement for the proposed method.

Once the equipment has been adjusted by incorporating the NO_x sensor and the computer application has been updated to integrate the NO_x measurement functionality, all the essential components are now in place to conduct the measurements.

Regarding metrological control, the specifications for this control concerning PTI equipment are not presently established at a regulatory level. This aspect remains to be developed and defined.

Even though a standardized protocol is not presently established, the stations have been provided with a gas cylinder conforming to a standard. The technical specifications of the gas cylinder are detailed in the appendix chapter.

The start-up of the equipment once modified does not differ from the normal start-up, so the staff responsible for the equipment at each station can proceed normally with the equipment, installing it in the inspection line chosen to carry out the measurements.

The new software application intercalates the NO_x measurement between the two emission control tests currently performed at the PTI stations: the OBD control and the opacity measurement.

The software capitalizes on the situation where the device remains connected after the OBD control test. This continuity allows for the execution of the NO_x measurement test, as it requires the measurement of parameters such as "% engine load," engine RPM, engine temperature, and EGR opening.

Upon the completion of the NO_x measurement, the application seamlessly transitions to conducting the opacity test, utilizing the OBD reader once again for engine RPM measurement.

This approach ensures minimal interference stemming from the NO_x measurement. As a result, the average time increase introduced by the NO_x measurement process during the inspection stands at 2.5 minutes.

The outcome of the NO_x measurement is stored within the computer system in the form of a set of files, which are then subjected to analysis to extract the measurement results.

Regarding the training of personnel for conducting the measurements, it is important to highlight that the process is exceedingly straightforward.

On all occasions, the estimated training duration necessary to effectively carry out the tests, considering potential challenges that might arise during the process, has been around one hour.

Given the experience and training level of the inspection personnel, this duration is sufficient to comprehensively grasp the essential training required for conducting the tests. The tests can be executed in two different manners:

- The inspector, after preparing the measuring equipment, provides the vehicle driver with the requisite instructions for appropriately connecting and disconnecting the equipment from the vehicle at the designated intervals.
- The inspector, following equipment setup, takes the place of the vehicle driver and manages the activation and deactivation of the vehicle's equipment at suitable junctures.

The test's straightforward nature enables the software to conduct measurements autonomously, devoid of the inspector's intervention. The software automatically updates the test conditions and transitions to the subsequent measurement phase based on the information it receives from the vehicle.

For instance, upon completing Stage 1 of the Unloaded state measurement at idling speed, the software presents a prompt instructing the activation of the equipment (Figure 8-12). Once it identifies that the "% engine load" value has reached an appropriate threshold for initiating Stage 2, the measurement commences automatically without the need for inspector intervention.

This allows the inspector to be inside the vehicle replacing the driver, since he does not have to manipulate the computer or perform other inspection functions in parallel while the equipment is performing the NO_x measurement, thus saving time in the process.

8.3. FEASIBILITY, QUALITY, SIGNIFICANCE, AND BEHAVIOR OF THE MEASUREMENT CAMPAIGN

8.3.1. PERFORMANCE AND FEASIBILITY OF THE TEST FROM THE MEASUREMENT CAMPAIGN

Upon the installation of the equipment and the completion of personnel training, NO_x measurements were carried out on vehicles undergoing the mandatory periodic inspection at the station.

The selection of vehicles for testing was made randomly from among those vehicles that presented themselves for inspection and met all of the criteria listed below:

- M1 or N1 category vehicles¹²
- Vehicles using diesel fuel (compression-ignition engines)
- Vehicles with Euro 4 emission level with accessible OBD port, vehicles with Euro 5 emission level, or vehicles with Euro 6 emission level.

It is evident that there are no limitations concerning the type of vehicle transmission (such as 4x4, automatic or manual transmission, non-disconnectable traction control, etc.).

Every week, the files resulting from the diverse measurements conducted were forwarded to the doctoral student responsible for overseeing and analyzing the data generated from the NO_x measurement procedures. This arrangement was necessitated by the somewhat intricate nature of the data processing and analysis process.

The Centralauto application generates, from the measurement of every vehicle, a set of 7 files with raw data. Some of these files can be opened with Notepad or similar applications, but the other files can't be read directly.

¹² M1 vehicles refer to passenger cars, while N1 vehicles pertain to LDV.

The name of the files is generated from the information introduced when the measurement begins so that all the files of the same measurement are identifiable. In Figure 8-13, the number 002629341 is the number of inspections carried out, and this data is entered in an initial data entry window. Employing the inspection number enables subsequent vehicle identification, facilitating the retrieval of essential technical data as needed.

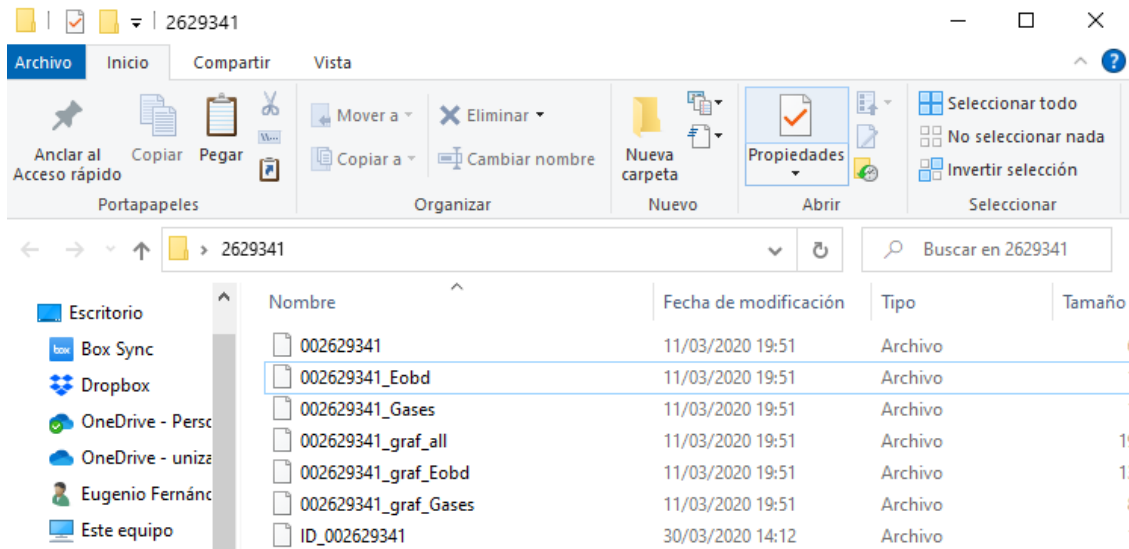


Figure 8-13. Example of files from NO_x measurement.

Files named in the format [****_Eobd] and [*****_Gases] can be opened with the Notepad application and include a summary of information compiled through the OBD and the Gas Analyzer.

With a proprietary application from Centralauto (the equipment manufacturer), the information contained in the other files can be extracted, converting it into a *.txt file that can be read by other applications.

Lastly, an Excel file equipped with various macros has been developed to facilitate the swift import of essential information. This file amalgamates data from each inspection, allowing for comprehensive analysis. Through the Excel file, the entire test graph is generated from inspection data. It undertakes analysis to determine values in the unloaded, loaded states, and TMV for both NO_x concentration and NO_x mass emission flow. Additionally, it conducts p-value and R² analyses to assess the quality

and significance of the correlation between measured NO_x concentration and the "% engine load" to which the vehicle is exposed.

Furthermore, the Excel file furnishes a condensed overview of the most pivotal measurement data, subsequently transferring this data, along with measurement data from all vehicles tested during the measurement campaign, into a single file.



Figure 8-14. Screenshots from Excel file used for NO_x data analysis.

In this way, a database is obtained with all the fundamental data of all the measurements performed, which allows the analysis explained in section 8.4.

All this information treatment process can be automated and included in the software programming of the equipment so that if the process is implemented in the future in the inspection process, the equipment itself could directly provide the final data resulting from the inspection.

The approximate duration of the measurement campaign was one year, from March 2019 to March 2020.

Unfortunately, the situation generated by the COVID-19 pandemic put an early end to the campaign, since in March 2020 a confinement of the population was decreed, which paralyzed the activity at the PTI stations.

Upon resumption of operations, the campaign was finalized, as the primary focus was to ensure the smooth reestablishment of station activities. Therefore, all available organizational resources were directed towards this objective.

In any case, the size of this measurement campaign is the largest ever carried out to date in terms of PTI measurements. As far as we are aware, only a study recently carried out by 3DATX [152], which involved approx. 600 vehicles, come close in the number of vehicles analyzed.

Up to the moment of completion, the measurement campaign was carried out without notable incidents, and any problems being reported by any of the stations involved in the campaign in terms of:

- Operation of the measuring equipment
- Operation of the measurement software
- Incidents in the inspection caused by the NO_x measurement.

It should also be noted that the NO_x measurement process was transparent to the users and that they did not raise any objections to the measurements. Rather, there was interest on the part of the users, who asked questions about the measurements that were being taken.

Undoubtedly, this was contributed to by the fact that the test performed for NO_x measurement is very non-invasive, so it does not generate rejection by vehicle owners.

As indicated in section 0, the development of this measurement campaign has several objectives, two of them being to demonstrate that:

- 1) It is feasible to apply the measurement method in PTI
- 2) The method is simple to apply

Regarding point 1), it is noteworthy that following over 1880 measurements, no issues have been reported regarding the application of the proposed method. This holds true both from a technical standpoint and in terms of user experience. Inspection durations have not witnessed any substantial extension beyond the additional time required for measurement execution. Furthermore, no complications impacting other aspects of the inspection process have arisen as a result.

Concerning point 2), the inspectors of the various stations involved in the measurement quickly began to perform the measurements, without requiring extra training, and without reporting problems in the execution of the test.

Therefore, it can be stated that both objectives have been fully achieved with the development of the measurement campaign. This does not prevent the method can being further investigated and evolved to reduce as much as possible the execution times, and even make it simpler if possible.

In conclusion, it has been firmly established that the suggested NO_x measurement method can be seamlessly integrated into the PTI inspection system without imposing any adverse impact on the inspection process or inspection durations, except for the additional time necessitated by the measurement test itself.

8.3.2. QUALITY AND SIGNIFICANCE OF THE MEASUREMENT CAMPAIGN

Another objective that was mentioned in the introduction, which was intended to be fulfilled through the execution of the measurement campaign, was to verify whether the conditions of quality and significance observed in the measurements conducted up to that point (refer to Chapter 6) were being maintained.

The proposed measurement method is based on the relationship between the concentration of NO_x emissions measured at the tailpipe outlet and the load on the engine, recorded by the "% engine load" value.

As explained in Chapter 4, two mathematical tools are used to check the significance and quality of this relationship:

- a) The Regression Factor (R^2) of the relationship is calculated to determine the quality of the relationship. The higher its value, the higher the quality of the relationship between the variables
- b) The p-value of the relationship is calculated to determine the significance of the relationship, that is, to verify that the probability that the relationship is random is low enough to reject the hypothesis. The lower the calculated value, the lower the probability that the relationship is random, and therefore the higher the significance. For the calculations, a p-value of 0.01 is defined for the analysis

These two values are calculated for each measurement performed so that an indicator of the quality and significance of the measurement (that means if the values meet expectations) can be obtained so that it is possible to analyze if there is any behavior out of the expected for each measurement.

As a reminder of the analysis process, the data from each measurement were grouped and calculated for each of the following sections, indicated in Figure 6-2:

- a) Initial
- b) Final
- c) Acceleration
- d) Total (all three of the above)

In summary, the most significant and meaningful values for analysis are in the Initial and Final phases, despite calculations being done for all four situations.

In the Initial phase, it is usually observed the most favorable values in both cases due to minimal external interference, aligning with the working hypothesis that predicts a strong relationship between variables. The Final phase, while typically not as favorable as the Unloaded phase, still presents generally acceptable values affected by EATS and EGR system performance.

In contrast, the Acceleration phase often yields low R^2 values and p-values exceeding the limit, attributed to external factors such as engine speed, EGR operation, and EATS performance. The total data phase falls between these extremes, but like the Acceleration phase, it is not suitable for assessing the relationship due to potential external influences.

Therefore, it is crucial to focus on the Initial and Final phases to validate the expected correlation between NO_x concentration and "% engine load".

Then, the values obtained in the measurement campaign are analyzed below, starting with the analysis of the quality values of the relationship, the Regression Factor (R^2).

To begin with, upon compiling the R^2 values attained from all vehicles measured in the initial section, the pattern depicted in the figure below Figure 8-15 becomes evident.

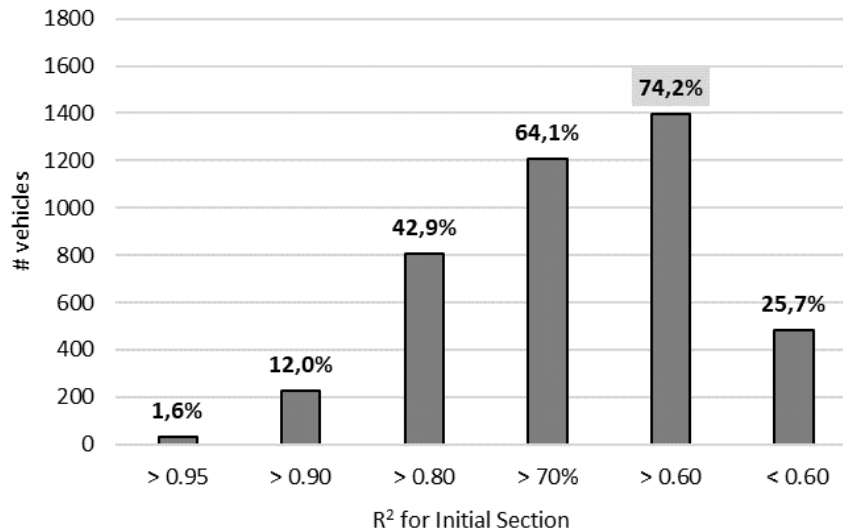


Figure 8-15. Distribution of Regression Factor values for the Initial Section.

The graph shows that 74.2% of the inspected vehicles present, for the initial section, an R^2 value greater than 0.60, the minimum value considered adequate for the quality of the relationship, according to the hypothesis.

Therefore, although 75% of all inspections are correct according to the criterion proposed, there are 25% of inspections that do not comply with the hypothesis proposed for the initial section, which is where it should theoretically behave more similarly to the theoretical approach. In principle, this value should be considered excessive, so it is necessary to analyze if there is any cause for this situation.

This proportion of 25.7% corresponds to a total of 483 vehicles. Upon scrutinizing the vehicles exhibiting this pattern, their distribution by the manufacturer is as follows:

- a) Group VAG: 198 vehicles
- b) Group Renault: 46 vehicles
- c) Group PSA: 39 vehicles
- d) Group BMW: 32 vehicles
- e) Group Toyota: 36 vehicles
- f) Group Daimler-Benz: 23 vehicles

This distribution already offers insights into the potential causes behind a portion of the inspections that do not align with the hypothesis.

During the measurements, it has been observed that vehicles from the VAG group exhibit distinct behavior compared to others regarding the usage of the Exhaust Gas

Recirculation (EGR) system. Typically, the EGR remains inactive in the initial section and is activated during the acceleration phase, with varying degrees of operation throughout the final section (varies among vehicles). However, VAG group vehicles maintain continuous EGR activation, even during the initial section.

This situation was already pointed out since in the group of vehicles used for the validation of the method there was a vehicle that presented this behavior. An example of this situation can be seen in Figure 6-27, where it can be seen that the EGR is active throughout the test.

This is therefore not a problem of the measurement method, but a particularity of the operation of these vehicles.

Once these vehicles have been discarded, there are 176 other vehicles that have an R^2 value below the desired value of 0.60. These represent 9.35% of the vehicles analyzed.

It would be necessary to analyze on a case-by-case basis whether there are more vehicles exhibiting unusual EGR system behavior, as seen in the case of the VAG Group, or if it could be a vehicle-specific issue, which might indicate some type of malfunction.

If the analysis is further refined to examine vehicles with an R^2 value below 0.6, and a more stringent threshold, for example, an R^2 value of 0.2, is applied, it is revealed that there are 179 vehicles, accounting for 9.51% of the total, with an R^2 value below 0.2. This indicates a very poor quality in the relationship between variables.

Again, analyzing these vehicles, 90 of them belong to the VAG group, leaving 89 vehicles from other manufacturers with very low R^2 values. This represents 4.7% of the total number of vehicles analyzed.

In the tests performed on the set of vehicles used to define the method, with respect to the average R^2 value obtained (the average is used because several measurements were performed on these vehicles to also assess reproducibility) in the Initial section, four of the 23 vehicles had an R^2 value lower than 0.60, i.e. 17% of the vehicles (see Table 4-19). Therefore, the percentage of vehicles that did not reach this value was lower than that observed in the measurement campaign.

One of the vehicles that presented a value lower than 0.60 belonged to the VAG group and presented the behavior indicated above, so we have located the cause of the low value observed.

After discounting this vehicle, the percentage of vehicles that do not comply with the minimum value indicated is 13%. Therefore, it is verified that the percentage, in both groups, of vehicles (once those of the VAG group are identified) that do not reach the $R^2 \geq 0.60$ value is similar, 13% for the initial group, and 9.35% for the measurement campaign group.

Once the Initial section has been analyzed, which is the most representative to check the quality of the relationship between the variables, the behavior of the rest of the sections is checked, which, as previously stated, will have worse performance than the Initial Section.

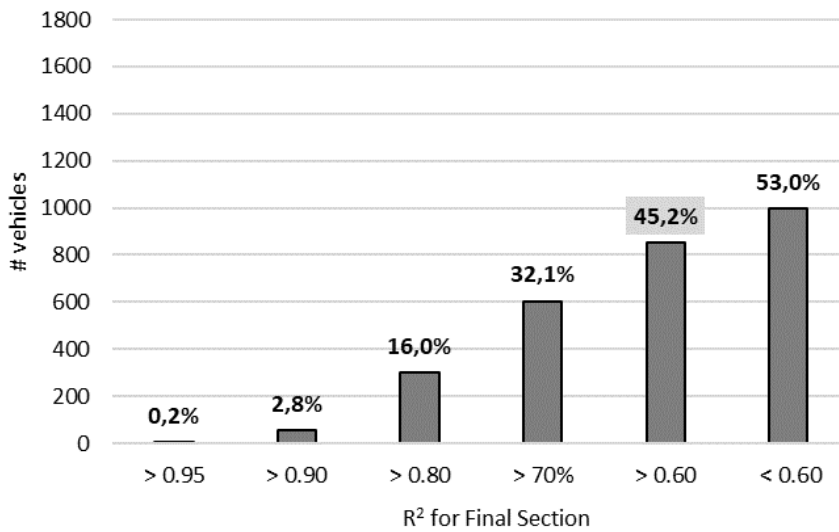


Figure 8-16. Distribution of Regression Factor values for the Final Section.

The R² values for the Final section, which can be seen in Figure 8-16, as stated in the hypothesis, already show a worse behavior than the Initial Section. In this case, only 45% of the vehicles present in this section have an R² value greater than 0.60. As indicated above, in this section it is common for the EGR or EATS to be active (at least in part), which influences the relationship between the variables and causes the R² value to be lower.

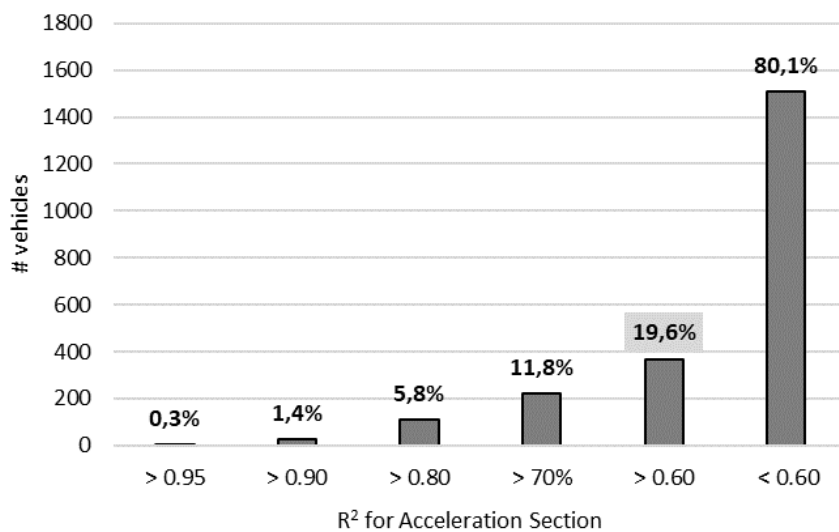


Figure 8-17. Distribution of Regression Factor values for the Acceleration Section.

In the group of 23 vehicles used for the definition of the method, it is observed that 52% of the vehicles reached an R^2 value greater than 0.60 in the Final section. Therefore, again the percentages are similar in both groups of vehicles.

In the Acceleration section (see Figure 8-17), as indicated, the relationship between variables is very altered, due to the operating conditions of the section. Therefore, 80% of the measurements are below the value of $R^2 = 0.60$. In the initial set of 23 vehicles, this percentage was 100%.

Finally, Figure 8-18 shows the set of all the sections, called the Total section, where, as indicated, the relationship between variables is very altered, and 88.3% of the measurements are below the R^2 value of 0.60. In the initial set of 23 vehicles used for the test design, this percentage was 78%.

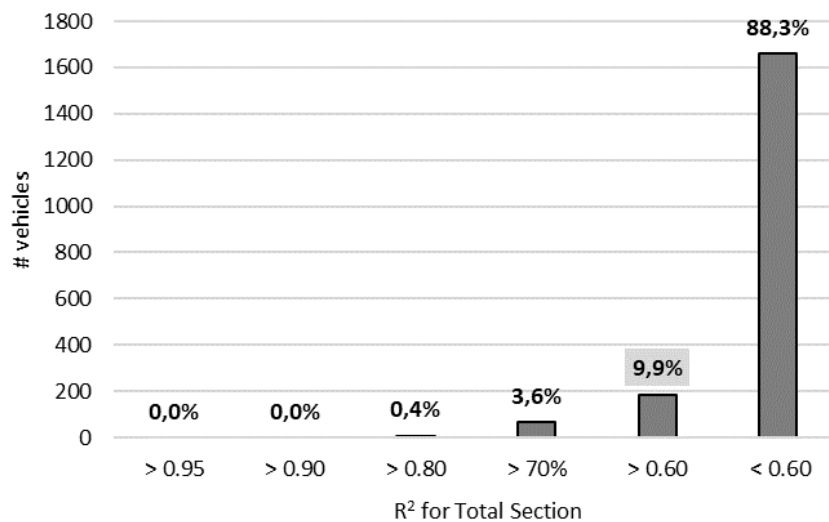


Figure 8-18. Distribution of Regression Factor values for the Final Section.

Next, the behavior of the significance of the measurements will be analyzed, i.e., the p-value that each of the sections presents for the set of measurements will be checked.

Figure 8-19 shows the distribution of the p-value for the vehicles in the Initial Section. It can be seen that in this section 93.6% of the vehicles present a value lower than the p-value: 0.01. For those measurements in which this occurs, the null hypothesis can be discarded and, therefore, it is considered that the relationship between the two variables is not random, but that there is indeed a relationship between them.

The 6.4% of the vehicles exceeding the p-value represents 120 vehicles of the total. Of these 120 vehicles, 69 are vehicles of the VAG group, so the explanation for these vehicles of the measured value is the situation already mentioned in the operation of the EGR system.

Once these vehicles have been discounted, it can be seen that only 2.7% of the vehicles present, in the Initial section, values greater than the defined p-value.

It would be necessary to analyze one by one the vehicles in which this occurs, to try to detect the cause, which could be the same as that of the vehicles of the VAG group, or have some kind of technical problem.

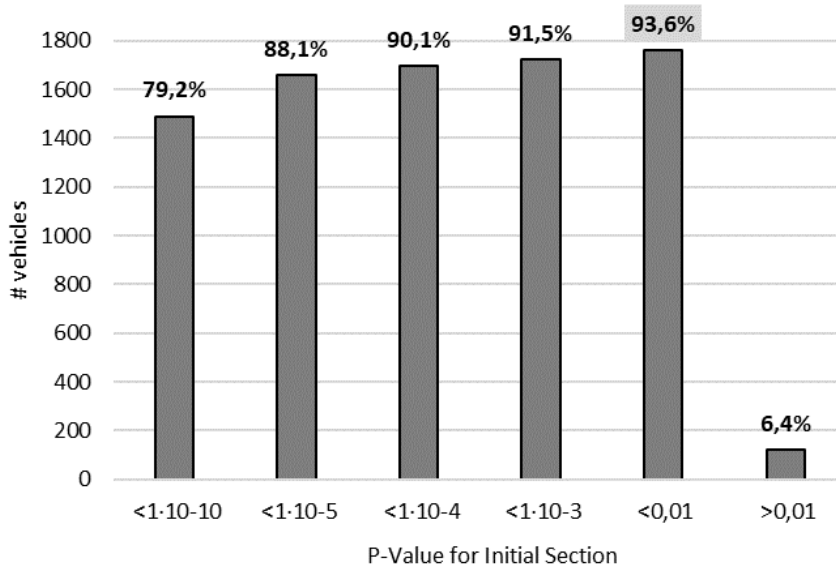


Figure 8-19. Distribution of p-value for the Initial Section.

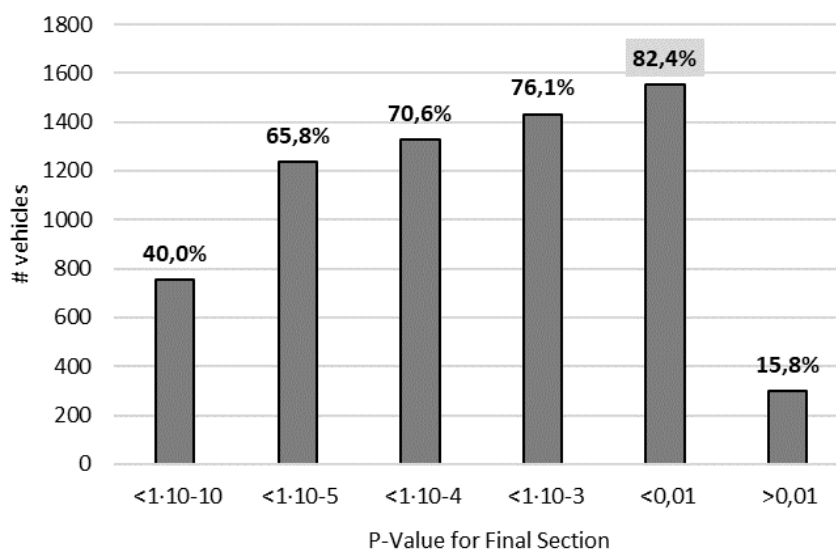


Figure 8-20. Distribution of p-value for the Final Section.

However, more important than the percentage of vehicles that do not comply is the fact that, of the vehicles that have a p-value less than 0.01, 80% of the vehicles have a p-value less than $1 \cdot 10^{-10}$. That is, it is not only found to be smaller, but it has very small values.

The fact that the p-value is so small implies that the significance is very high.. Therefore, 80% of the measurements show a really small value, which allows us to affirm with great certainty the significance of the relationship, and therefore to confirm for a very representative number of vehicles the validity of the hypothesis on which the measurement method is based.

Figure 8-20 shows the distribution of the p-values obtained in the final section, where it is also found that a very important percentage of the vehicles present a p-value below 0.01. Specifically, 82.4% of the vehicles present in the final section have this characteristic, considering this value very high, in terms of ratifying the relationship between both variables also in the final section.

From the vehicles that present a p-value higher than 0.01 (297 vehicles), 53 are vehicles of the VAG group, so the percentage of vehicles that do not meet the criterion, once these are discounted, is 13%.

As indicated, in this section the EATS and EGR systems are generally operating, so it is to be expected that the number of vehicles presenting a p-value > 0.01 in this section will be higher than in the Initial section. In any case, the result obtained in this part of the measurement is considered more than acceptable.

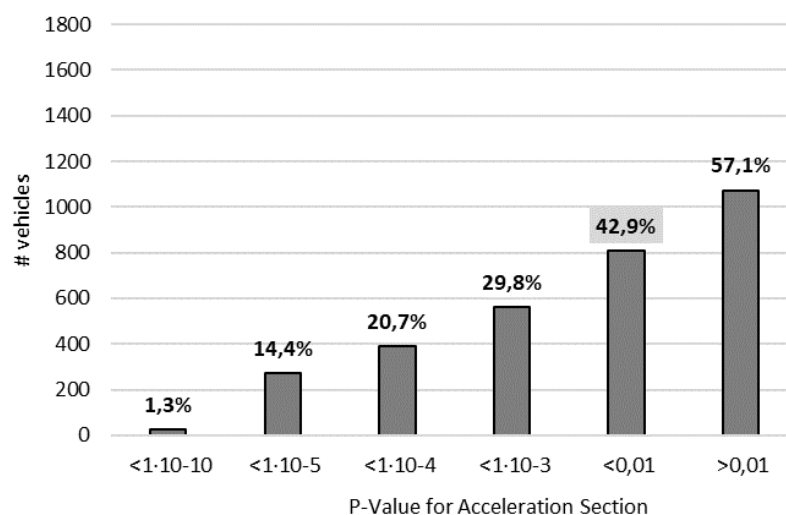


Figure 8-21. Distribution of p-value for the Acceleration Section.

In the Acceleration section, as expected, the percentage of vehicles with p-values > 0.01 is very high. More than half of the vehicles, specifically 57.1% of the vehicles inspected present these high values (see Figure 8-21).

Perhaps more surprising is the high number of vehicles with values below 0.01 in the total measurement. Specifically, Figure 8-22 shows that 75.7% of the vehicles present for the total section have a p-value < 0.01.

In comparison, in the set of 23 vehicles used for the definition of the method, the percentage of vehicles presenting these values was 60.8%.

Summarizing, it can be concluded that the behavior of the p-value obtained in the measurements of the campaign coincides with, and even improves, the data obtained from the initial selection of 23 vehicles, being able to affirm that from these data the existing relationship between the NO_x concentration measured at the exhaust pipe outlet of the vehicles and the value of "% engine load" to which they are subjected, even in conditions such as those of the Final section in which the EATS and EGR systems are acting, can be verified.

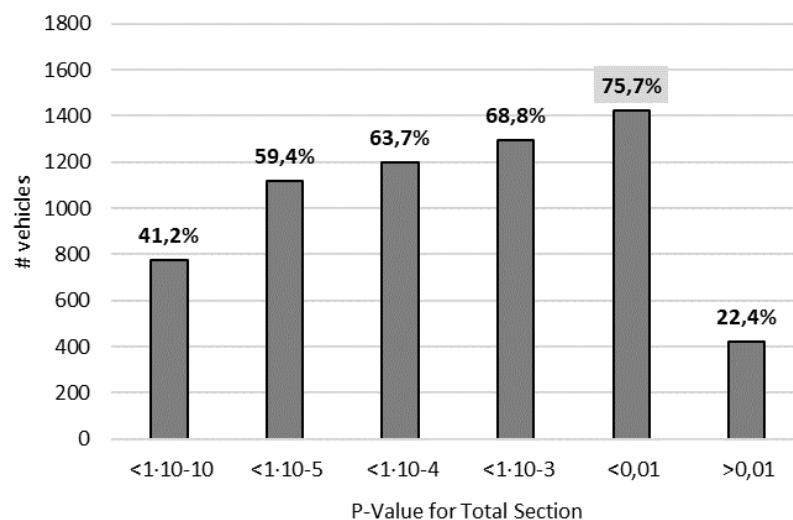


Figure 8-22. Distribution of p-value for the Total Section.

8.3.3. ENGINE LOAD BEHAVIOR FROM THE MEASUREMENT CAMPAIGN

Another important aspect to consider in the measurement campaign, and which is interesting to compare with what was observed in the first part of the research, is the behavior of the "% engine load", i.e., the load to which the vehicles can be subjected when performing the proposed test.

The measurement method relies on attaining two distinct load states while the vehicle is idling. These states must exhibit a noticeable difference in NO_x concentration in the exhaust. This significant difference allows for the establishment of a meaningful

relationship between the two variables, enabling the extrapolation of emissions values at 100% engine load.

In Chapter 4, where the initial process of defining the method is described, the difference in the "% engine load" values between the Unloaded state and the Loaded state was analyzed, seeing that it was sufficient to be able to apply the method correctly.

In fact, from the set of 23 vehicles analyzed, it was obtained that the average value of "% engine load" in the Unloaded state was 20.3%, while for the Loaded state, the average value of "% engine load" reached was 41.7%.

Simplified, the method showed that without needing additional external tools, and by relying on the vehicle's internal usage, the "% engine load" value was effectively doubled on average. This corresponds to a clear 105% increase in the engine load.

When examining the data collected during the measurement campaign, a crucial aspect to validate is whether the trend observed in all vehicles regarding the rise in "% engine load" between the unloaded and loaded states is consistent with what was observed in Chapter 6. This involves confirming whether there is an approximate 100% increase in "% engine load" as expected.

To verify this, the average "% engine load" value experienced by the vehicles during the test is computed based on all the measurements conducted.

From observations, one of the factors that can impact the "% engine load" value an engine undergoes is its size. Therefore, how the engine load behaves relative to the engine's cubic capacity was examined. Figure 8-23 shows the evolution of the "% engine load" value for the Unloaded and Loaded states, as a function of engine size.

Analyzing the average "% engine load" values for various engine sizes of the vehicles measured during the campaign, it is concluded that the average "% engine load" in the Unloaded state is 20.3%. This is consistent with the value obtained for the initial set of vehicles.

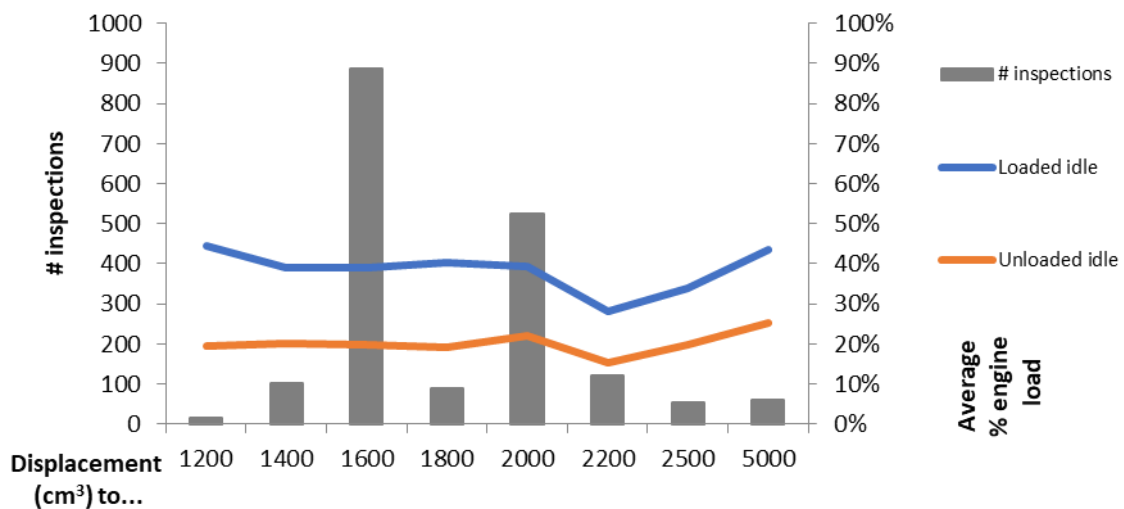


Figure 8-23. Avg. value of "% engine load" according to Displacement (cm³).

This represents the average value across the entire set of measurements, and for the majority of cases, the measured values closely align with this average, particularly in relation to engine size.

Specifically, for engine sizes up to 1600 cm³, the average value obtained is 19.83%. For engines up to 2000 cm³, there is a slight increase, which is important since this engine size is the second most frequent in the vehicle sample. Also for engines larger than 2500 cm³, there is an increase over the average value, up to a value of 25%.

But in general, it can be stated that most of the vehicles have an average value of "% engine load" in the Unloaded state of 20%.

For the Loaded state, a similar pattern emerges. The average "% engine load" value for the entire set of vehicles is approximately 38.5%, although it may not precisely match this value for every individual vehicle.

Figure 8-23 illustrates that the pattern of "% engine load" for the Loaded state mirrors that of the Unloaded state, albeit with higher values across the board.

For engine sizes up to 1600 cm³, the average value obtained is 38.9%. For engines up to 2000 cm³, there is a slight increase to 39.5%, which is important since this engine size is the second most frequent in the vehicle sample. Also for engines larger than 2500 cm³, there is an increase over the average value, up to a value of 43.4%. The value obtained of 28.2% for vehicles with engines up to 2200 cm³, which is an important group with 120 units measured, is what brings the overall average value to 38.5%.

Table 8-2 shows the average values of "% engine load" for the Loaded and Unloaded states for both sets of vehicles. From these data, it can be affirmed that the behavior of both groups of vehicles is similar, and therefore the same behavior of the load demands on the engines is maintained in a larger group of vehicles.

	Unloaded	Loaded
Set of 23 vehicles	20.3%	41.7%
Set of 1882 vehicles	20.3%	38.5%

Table 8-2. Comparison Avg. values of "% engine load" from sets of vehicles

Furthermore, apart from examining the load value in each state, it is also valuable to compare the increase in load from the Unloaded state to the Loaded state.

Among the group of 23 vehicles, the average elevation in "% engine load" from the Unloaded state to the Loaded state registers at 105%, effectively doubling the engine's load demand.

Figure 8-24 shows the average increase, as a function of engine size, of the measured vehicles.

In this scenario, there is an observable trend where the augmentation in "% engine load" tends to diminish as the engine size grows. The calculated weighted average arrives at 98%, a value akin to that derived from the group of 23 vehicles. To put it differently, transitioning from the Unloaded state to the Loaded state essentially doubles the engine load on the whole.

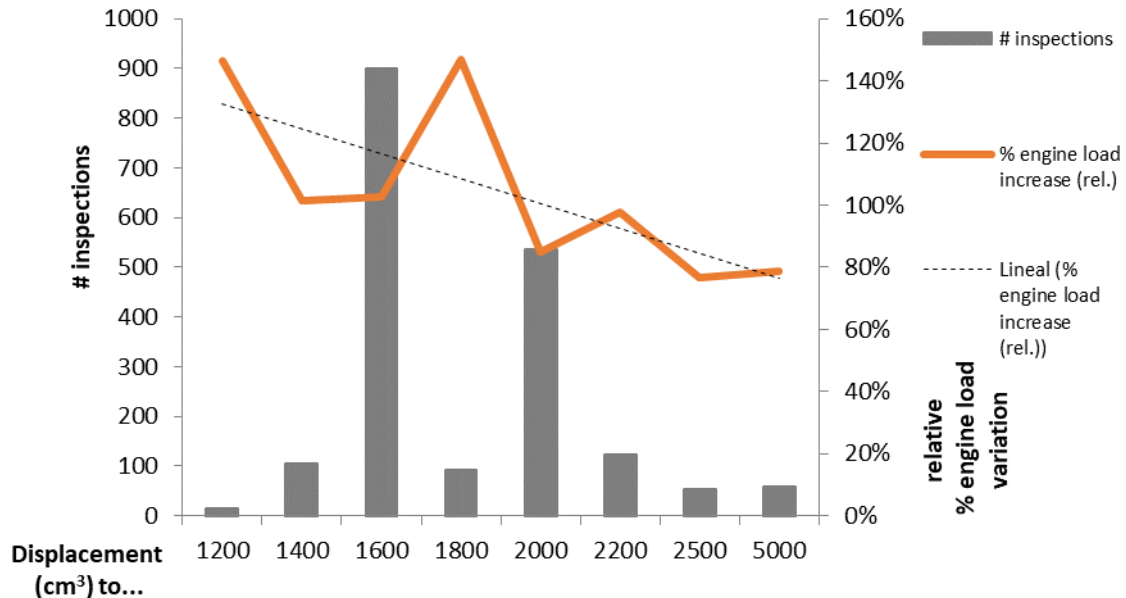


Figure 8-24. Avg. increase of "% engine load" from Unloaded to Loaded state.

A detailed analysis of the data shows that for the largest group of vehicles (engines from 1400 cm³ to 1600 cm³), the average increase is 103%. For the next largest group, engines between 1800 cm³ and 2000 cm³, the increased value is 85%. It is the combination of the average values of these two groups, which account for 76% of the vehicles, that defines the average value of the whole.

In conclusion, after closely examining the behavior of "% engine load" in both Unloaded and Loaded states, as well as the fluctuations between these states, we can confidently affirm that the results obtained from the measurement campaign align with the observations made during the formulation of the method. In essence, the utilization of the **vehicle's internal consumption during idling effectively facilitates the generation of two distinct load states, with one being twice as much as the other.**

8.4. RESULTS FROM THE MEASUREMENT CAMPAIGN

A comprehensive count of 1882 vehicles underwent emissions measurements throughout the NO_x measurement campaign, yielding a substantial volume of data that necessitates meticulous processing and analysis to derive significant conclusions.

In this section, the results obtained from the set of measurement processes conducted on the vehicles will be analyzed, in order to determine whether the results exhibit similar or comparable behavior to those obtained from the set of vehicles used

in defining the method. This will thus verify whether the objective set forth in the introduction of the chapter has been achieved.

8.4.1. NO_x EMISSION AVERAGE VALUES

The main outcome of the measurement campaign entails obtaining the test outcomes for each vehicle. This encompasses the average NO_x emission values measured during the Unloaded and Loaded states at idling speed. Furthermore, the TMV is estimated through extrapolation, representing the projected emissions of the vehicle under the scenario of idling speed while exposed to 100% of the "% engine load."

These results are provided in two different forms:

- In NO_x concentration values (ppm) as measured directly by the Gas Analyzer
- In mass flow values of NO_x emitted (mg/s) estimated from the measured concentration, engine speed, and engine size.

In addition to the emission values obtained from a vehicle's measurement, the average "% engine load" value for both the Unloaded and Loaded states is also documented (with a value of 100% for TMV). Consequently, each vehicle's inspection results yield a tabulated outcome akin to the format illustrated in Table 8-3.

	NO _x [mg/s]	NO _x [ppm]	% engine load
Unloaded	2.72	136	13%
Loaded	6.10	306	36%
TMV	21.84	1096	100%

Table 8-3. Example of results of a static NO_x measurement at PTI.

Hence, the test outcome is not represented by a solitary numerical figure but rather consists of a compilation of six distinct values that collectively constitute the measurement result.

	NO _x [mg/s]	NO _x [ppm]
Unloaded	1.99	107
Loaded	3.71	198
TMV	11.82	626

Table 8-4. Summary of average results of the measurement campaign.

Based on this data, the overall average values for all the measurements were computed, and the outcomes are presented in Table 8-4. The average values of "% engine load" are not included here, because they were analyzed in depth in section 8.3.3.

Figure 8-25 shows the graphical representation of these values, on the one hand, the average values of NO_x Mass Flow emissions in mg/s, and on the other hand the average values of NO_x concentration emissions in ppm.

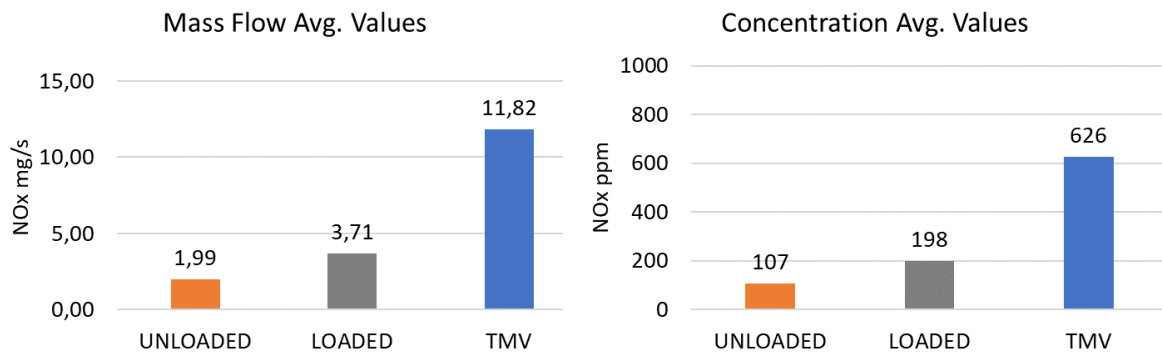


Figure 8-25. Summary of avg. results: NO_x Mass Flow (left) and NO_x Concentration (right).

It is evident that the average values exhibit similar trends in both scenarios, and the proportions are also closely comparable. For both Mass Flow emissions values and concentration emissions values, the TMV value is approximately 3.15 times the Loaded state emissions value, with the Loaded state emissions being roughly 85% higher than those in the Unloaded state.

Assessing the result of the average emissions according to the Euro emission level of the vehicles (Figure 8-26), several noteworthy circumstances can be detected.

When analyzing the emissions data in concentration (ppm), it can be seen that the average emissions of Euro 5 vehicles are the highest of the three groups, being the lowest those corresponding to Euro 6 vehicles, which present average values around 10% lower than the values of Euro 4 vehicles. This situation occurs for the three values analyzed: emissions in the Unloaded state, in the Loaded state, and TMV.

On the other hand, when analyzing the Mass Flow emissions (mg/s), it can be seen that the emissions measured in the unloaded and loaded state are similar between Euro 4 and Euro 5, with values for Euro 6 vehicles around 20% lower, while the TMV is higher for Euro 4 than for Euro 5. In all cases, the values obtained for Euro 6 vehicles are the lowest.

Analyzing the same data (average emission values), but separately according to the level of emissions of the various vehicles, a similar behavior to that observed for the data as a whole can be found.

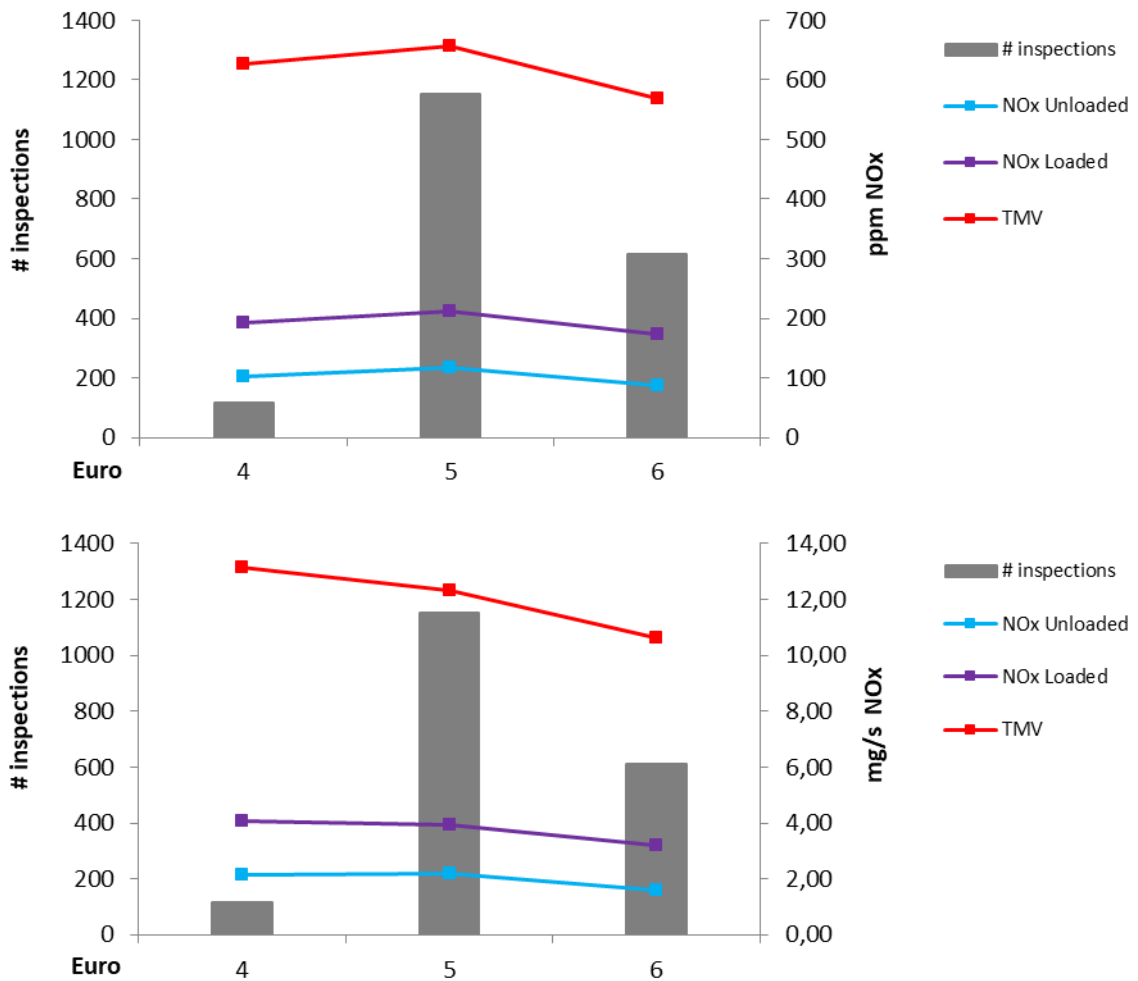


Figure 8-26. NO_x emissions from Euro level: Mass Flow (down) and Concentration (up).

Starting with the values obtained for Euro 4 vehicles (see Figure 8-27), it is found that for Euro 4 vehicles the TMV values obtained are approximately 3.25 times higher than the values obtained in the Loaded state, both in concentration (ppm) and mass flow (mg/s). This ratio is similar to but slightly higher than, that observed for the complete vehicle dataset.

	NO _x [mg/s]	NO _x [ppm]
Unloaded	2.15	103
Loaded	4.05	192
TMV	13.14	628

Table 8-5. Summary of average results of measurement campaign for Euro 4 vehicles.

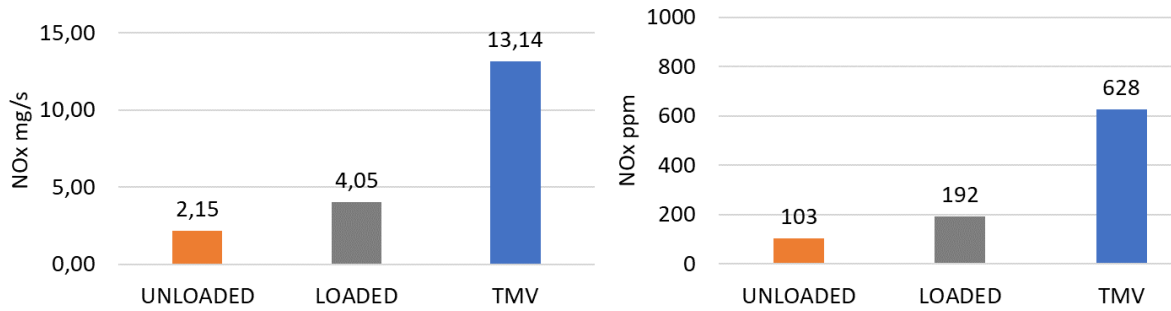


Figure 8-27. Euro 4 avg. results: NO_x Mass Flow (left) and NO_x Concentration (right).

Similarly, the emissions measured in the Loaded state are roughly 87% greater than those in the Unloaded state, encompassing both types of measurements (concentration and mass flow). This pattern closely mirrors the overall measurements, albeit with slightly elevated values.

Concerning Euro 5 vehicles, the TMV values acquired are roughly 3.10 times higher than the values derived from the Loaded state, spanning both concentration (ppm) and mass flow (mg/s). This trend aligns with the overarching observations for the entire vehicle group.

	NO _x [mg/s]	NO _x [ppm]
Unloaded	2.19	118
Loaded	3.93	211
TMV	12.33	656

Table 8-6. Summary of average results of measurement campaign for Euro 5 vehicles

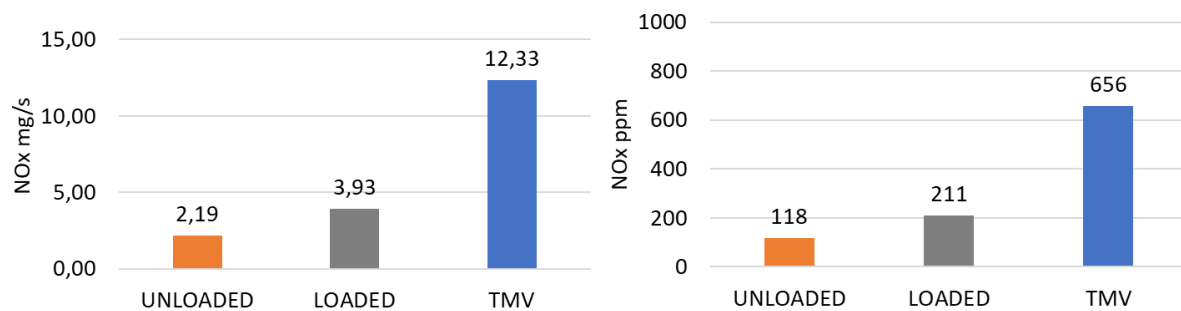


Figure 8-28. Euro 5 avg. results: NO_x Mass Flow (left) and NO_x Concentration (right).

Likewise, the emissions measured in the Loaded state are approximately 79% higher than those in the Unloaded state, in both types of measurements (concentration and mass flow). This situation is similar to that observed in the set of measurements seen before, although presenting a smaller increase than that observed in the previous cases.

Concerning Euro 6 vehicles, the TMV values obtained are 3.3 times higher than the values obtained in the Loaded state in mass flow (mg/s) and 3.9 times higher if measured in concentration. Therefore, it is found that in Euro 6 vehicles the difference between the TMV and the value in the Loaded state is greater than in the other cases, being especially striking when the concentration (ppm) is taken into account.

Conversely, emissions measured in the Loaded state are approximately 69% greater than those in the Unloaded state when examined in terms of concentration, and 100% higher when assessed in mass flow. This scenario displays the most distinct variance from the observations in the previously discussed set of measurements.

	NO _x [mg/s]	NO _x [ppm]
Unloaded	1.60	87
Loaded	3.21	147
TMV	10.61	569

Table 8-7. Summary of average results of measurement campaign for Euro 6 vehicles.

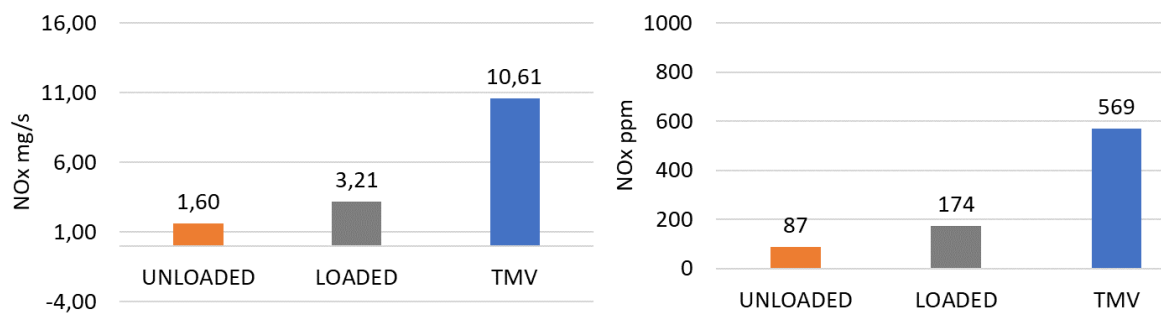


Figure 8-29. Euro 5 avg. results: NO_x Mass Flow (left) and NO_x Concentration (right).

Hence, the data analysis reveals that the relative disparities between emissions in the Unloaded, Loaded, and TMV states exhibit similarity for both Euro 4 and Euro 5 vehicles in relation to the overall values. Moreover, Euro 6 vehicles showcase greater relative discrepancies between the various states where TMV measurements or estimations are conducted.

From the measurements made on the group of 23 vehicles with which the method was designed, but excluding the gasoline vehicle to compare exclusively the emissions of diesel vehicles, the average results shown in Table 8-8 were obtained:

The average results obtained from the initial method design group, compared to the campaign values shown in Table 8-4, present higher emission values, both in concentration and Mass Flow.

	NO _x [mg/s]	NO _x [ppm]
Unloaded	2.52	127
Loaded	6.30	321
TMV	16.67	841

Table 8-8. Summary NO_x emissions from the initial group of 22 diesel vehicles.

On average, values were 22% higher for the Unloaded state, 66% higher for the Loaded state, and 37.5% higher for TMV.

The difference in sample size undoubtedly affects the average values, and the population sample of the measurement campaign developed in PTI should be considered more representative. In any case, the values obtained for both groups of vehicles are of the same order of magnitude.

When analyzing the behavior or difference in emissions between the various states Unloaded → Loaded → TMV, it is evident that in the outcomes of the 23-vehicle group, a more pronounced disparity between emissions in the Unloaded and Loaded states existed compared to the outcomes from the PTI campaign.

As indicated above, from the values measured in the campaign, the average difference in emissions between the two states is an 85% increase in the Loaded state, both for emissions in concentration and in Mass Flow.

On the other hand, in the initial group of vehicles, this increase reaches 150% for both types of emissions.

When comparing the difference between the TMV and the Loaded state, the opposite situation occurs. The difference between the two values is greater in the data collected in the PTI campaign. In this case, the average increase from the Loaded state to the TMV value is on average 3.15 times; in contrast, for the initial design group, the average increase is 2.64 times.

Consequently, in both groups, a more substantial relative increment is observable when contrasting the Loaded value with the TMV than when comparing the Unloaded value with the Loaded value. Nonetheless, the extent of this increase differs for each of the two groups.

8.4.2. COMPARISON OF THE METHOD'S RESULTS TO ON-ROAD EMISSIONS

In Chapter 7 it was determined, based on the on-road measurements carried out, that the range of average emissions for urban circulation of the set of diesel vehicles formed by the Euro 4, Euro 5, and Euro 6 emission levels was defined **between 2.24 mg/s and 16.37 mg/s of NO_x**.

Looking at the average emissions data obtained from the measurement campaign on 1882 vehicles, which are summarized in Table 8-4, and the average emissions data obtained from the group of 22 diesel vehicles used for the method definition, which are summarized in Table 8-8, it is found that both groups of measurements present values in the Loaded state that are within the range of average emissions in urban circulation defined in Chapter 7.

Moreover, the TMV values are within the range defined for maximum emissions in urban circulation, which was defined **between 10.45 mg/s NO_x and 66.20 mg/s NO_x** from the data obtained in the measurements, as can also be seen in Chapter 7.

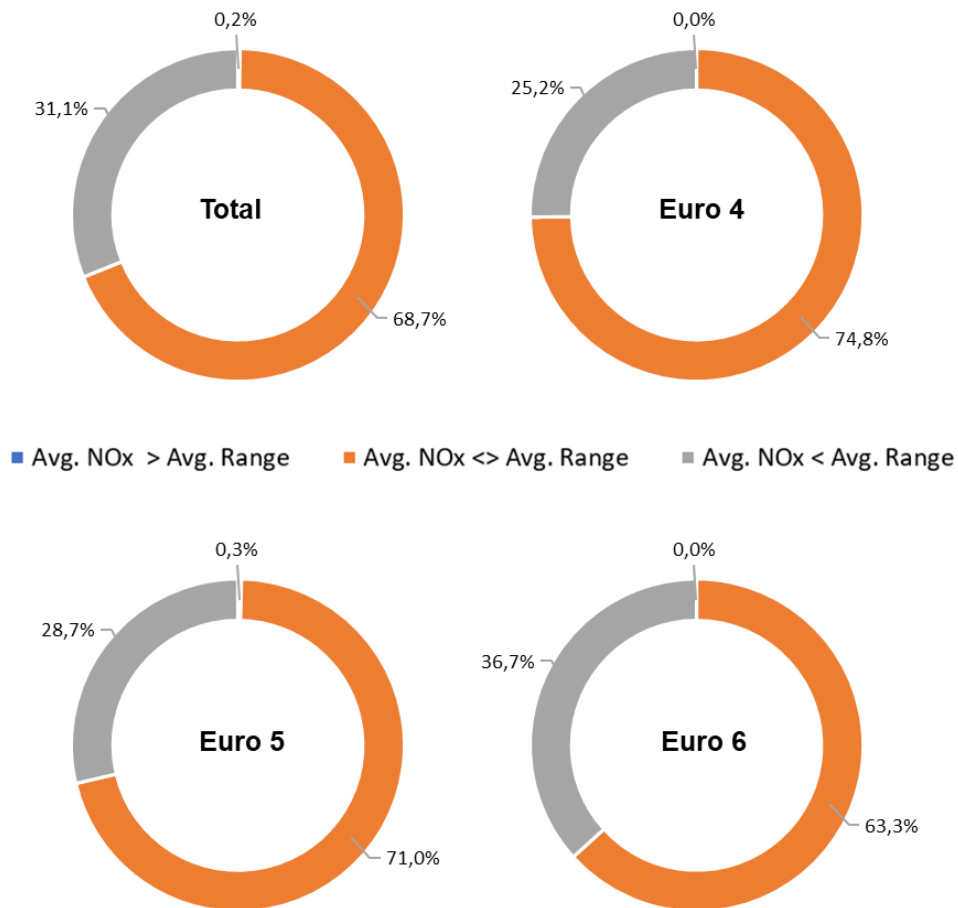


Figure 8-30. Distribution of NO_x Loaded Emissions to On-Road Avg. Range.

The TMV values obtained in the measurement campaign at PTI are also within the average emission range, specifically 1444 vehicles (76.7% of the vehicles), with 391 vehicles (20.8% of the vehicles) presenting a TMV higher than the upper limit of the average emission range, and only 47 vehicles (2.5% of the vehicles) presenting a TMV lower than the lower limit of the average emission range.

In addition to the average values, it is also possible to analyze individual vehicle emissions by comparing them to the average emission ranges defined in Chapter 7.

Out of the total of 1,882 measurements conducted on vehicles utilized throughout the daily measurement campaign, the distribution of emissions based on the average on-road emissions range is illustrated in Figure 8-30. The orange color indicates the number of vehicles whose emissions showed values within the emissions range, the gray color indicates the number of vehicles with emissions below the emissions range, and the blue color indicates the number of vehicles with emissions above the emissions range.

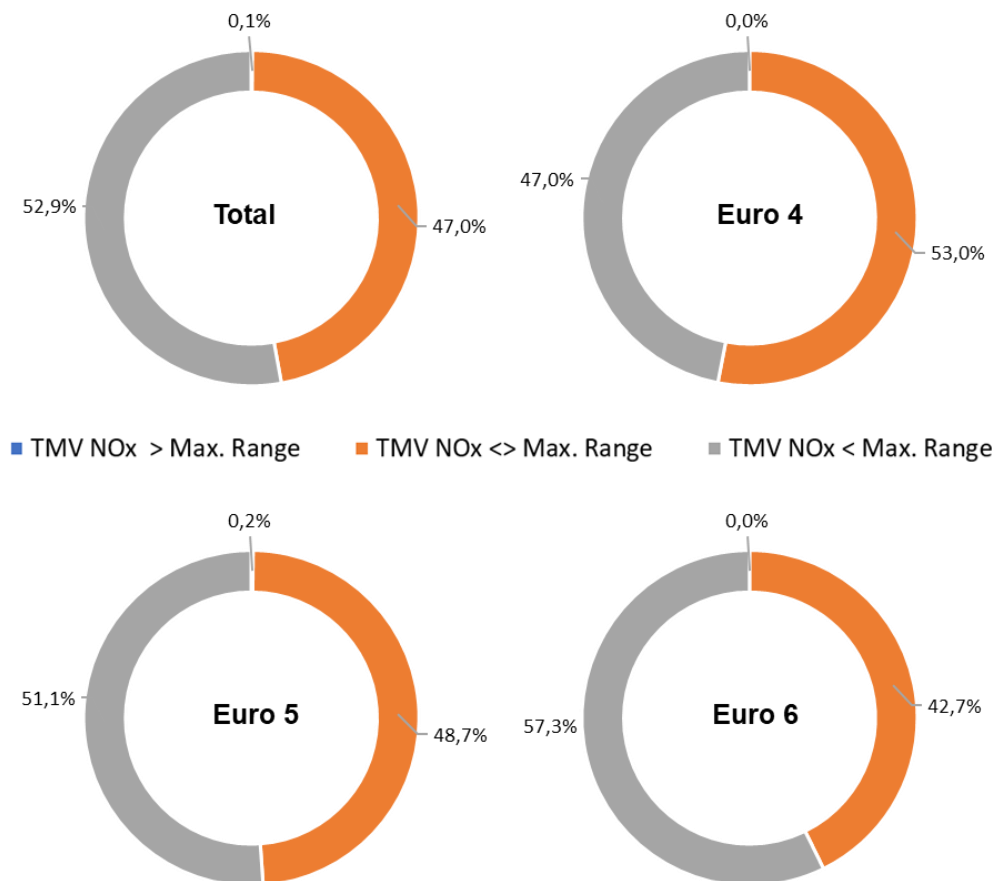


Figure 8-31. Distribution of NO_x TMV Emissions to On-Road Max. Range.

The specific figures are as follows:

- 1293 vehicles (68.7% of the total vehicles) showed values within the range of average emissions in urban traffic
- 585 vehicles (31.1% of the total number of vehicles) showed values below the range of average emissions in urban traffic
- 4 vehicles (0.2% of the total number of vehicles) showed values higher than the range.

The distribution by Euro levels provides a similar result to the total distribution of inspections, with a majority percentage of vehicles within the average emissions range. This percentage varies from 63.3% of euro 6 vehicles to 74.8% of euro 4 vehicles.

It is also noteworthy that the PTI test result indicates that there are no values that will be above what the vehicle actually emits on average in urban traffic (only four Euro 5 vehicles exceeded the upper limit).

The same analysis can be performed on the range of maximum emissions (see Figure 8-31), comparing the TMV values obtained with the maximum emissions in urban traffic.

When analyzing the set of TMV values, it can be seen that:

- 885 vehicles (47.0% of the total number of vehicles) showed values within the range of maximum emissions in urban traffic
- 995 vehicles (52.9% of the total number of vehicles) showed values lower than the range of maximum emissions in urban traffic
- 2 vehicles (0.1% of the total number of vehicles) showed values higher than the range of maximum emissions in urban traffic

It is evident that the count of vehicles with TMV emissions falling within the range of maximum on-road emissions has diminished compared to the percentage of average emissions. However, this count remains close to 50%.

Merely 2 vehicles (belonging to the Euro 5 emission level) exhibited TMV values surpassing the upper limit of the Max. Emissions Range. This pattern remains consistent across all Euro levels, with comparable percentages of similar magnitude.

Therefore, it can be concluded that the emission results obtained in the measurement campaign confirm what had already been seen with the group of vehicles used for the definition of the method: **the emission value in the Loaded state provides reliable and reasonably accurate information on the actual average emissions in urban traffic of the vehicles, and the TMV value provides information on the maximum emissions.**

8.4.3. COMPARISON OF THE METHOD'S RESULTS TO OTHER STUDIES

As a final means of confirming the validity of the method based on the outcomes of the measurement campaign, a comparison is made between the obtained results and those from other conducted measurement campaigns that employed different equipment and measurement approaches. This is done to ensure the comparability and similarity of the achieved results.

Among the diverse array of measurement techniques available, the ones that yield the highest quantity of measurements are the measurement campaigns executed using Remote Sensing Devices (RSDs), as elaborated upon in Chapter 2. This approach involves conducting campaigns where thousands of vehicle measurements are taken at designated locations.

In recent years, perhaps the most relevant are those carried out in several European capitals by the ICCT [123]–[127]. Within these measurement campaigns, emissions emanating from a substantial quantity of vehicles have been assessed amidst the context of urban traffic conditions.

Utilizing the gathered data, approximations are derived for the genuine average emissions exhibited by the vehicle fleet. These estimations subsequently contribute to a Europe-wide emissions database known as CONOX [121], [122], which is constructed using measurements acquired from RSD campaigns.

If the outcomes obtained through the measurement campaign align with the data furnished by these RSD measurements, it would serve as an additional confirmation of the credibility of the acquired measurements.

Certainly, it is important to note that while the numerical values may not align precisely, due to the significant variability in conditions affecting engine and emissions after-treatment systems during RSD measurements, the extensive quantity of measurements ensures that the observed patterns among various vehicle types remain entirely comparable (in terms of behavior) to the outcomes of the PTI measurements.

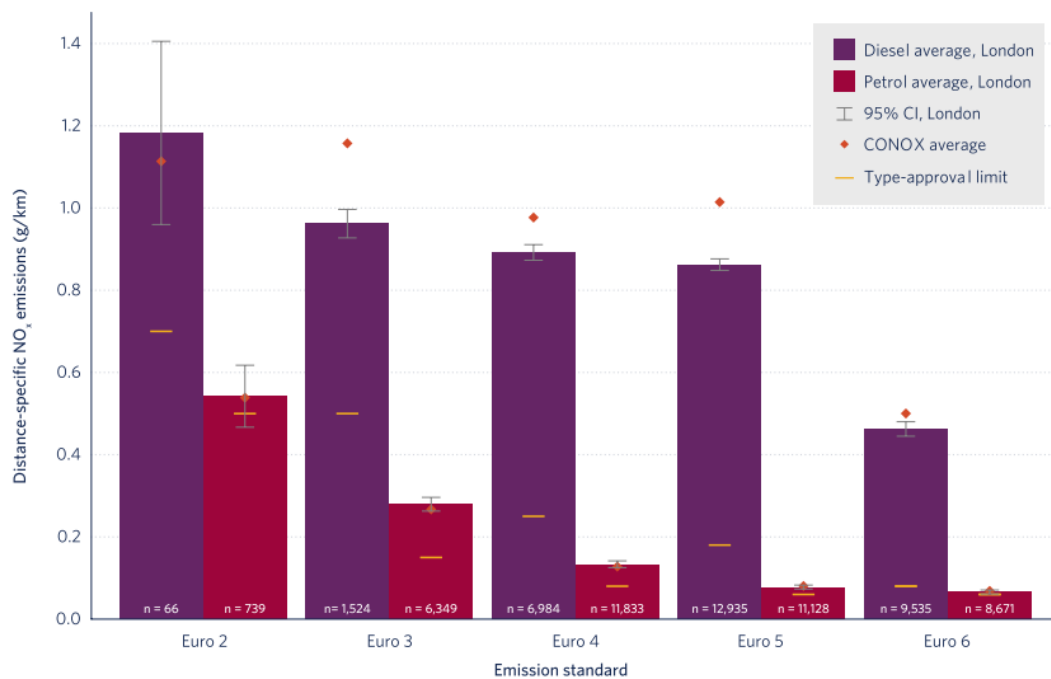


Figure 8-32. Results from RSD measurements in London. Source: TRUE, 2018. [124]

The measurement campaigns used for comparison were conducted in the following cities, with the results published in the years indicated: London 2018, Paris 2019, Zurich 2019, Krakow 2020, and Brussels 2021.

In all the measurements, common elements are observed, with perhaps the most significant being that the average Emission Factors obtained in all the measurement campaigns are, in all cases, significantly higher than the maximum limits defined by the corresponding Euro levels.

As an illustration, consider Figure 8-32, which centers on diesel emissions. This figure displays the average outcomes of the measurements conducted in London. It is evident from the figure that the Emission Factors for Euro 3, Euro 4, and Euro 5 exhibit remarkable similarity, while Euro 6 demonstrates a substantial reduction in comparison to Euro 5. The yellow line represents in all cases the maximum limit by type approval.

Hence, in the context of London, it becomes evident that while emissions have been on a downward trend, with Euro 6 showcasing a notable decline, a comparative analysis of the measured emissions against the maximum permissible limit set by the type approval reveals a concerning pattern. With each progression to a new Euro level, the scenario worsens. This is due to the measured emissions displaying an increasingly substantial percentage difference in relation to the permitted emissions limit.

This shift progresses from a disparity of less than twofold in Euro 2 to an excess of 500% in the case of Euro 6.

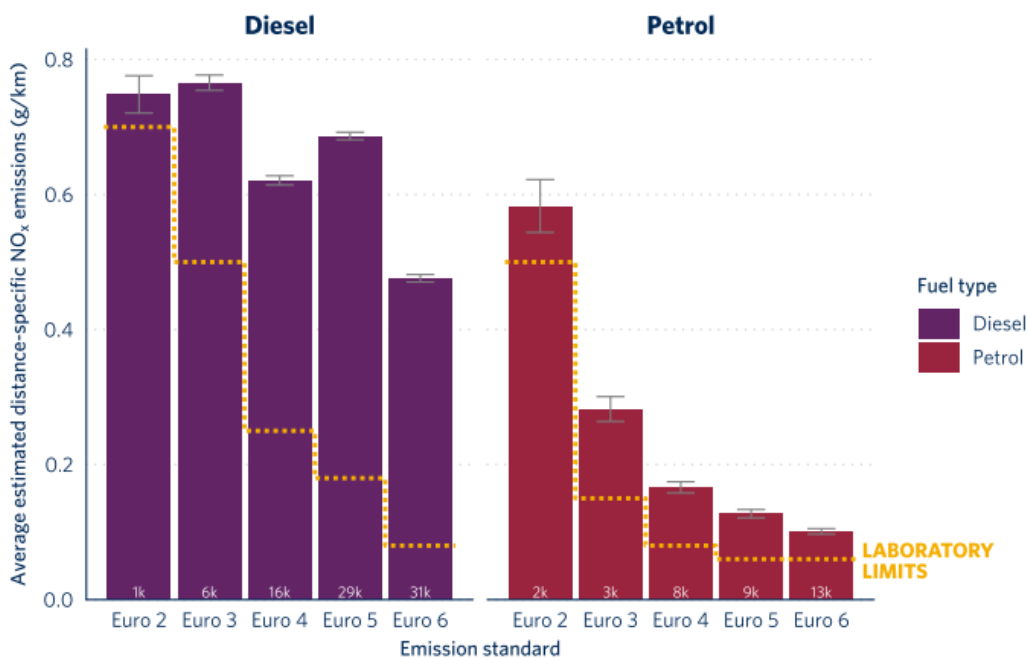


Figure 8-33. Results from RSD measurements in Paris. Source: TRUE, 2019. [123]

A comparable scenario is observable in Figure 8-33, which illustrates the emissions measured during the measurement campaign conducted in Paris. In this context, it is noticeable that the measured Emission Factors are generally less than those observed in the London campaign. However, this trend differs for Euro 6 vehicles, which exhibit similar values.

While the absolute values are reduced, the trend remains consistent. The Emission Factors of Euro 4 and Euro 5 are lower than those of Euro 2 and Euro 3, and the average Emission Factor of Euro 6 is clearly lower than that of Euro 5.

Nevertheless, the emission factors still remain several times greater than the values established by homologation standards, exacerbating this circumstance, particularly in the context of diesel vehicles. This holds true even as the overall emissions diminish.

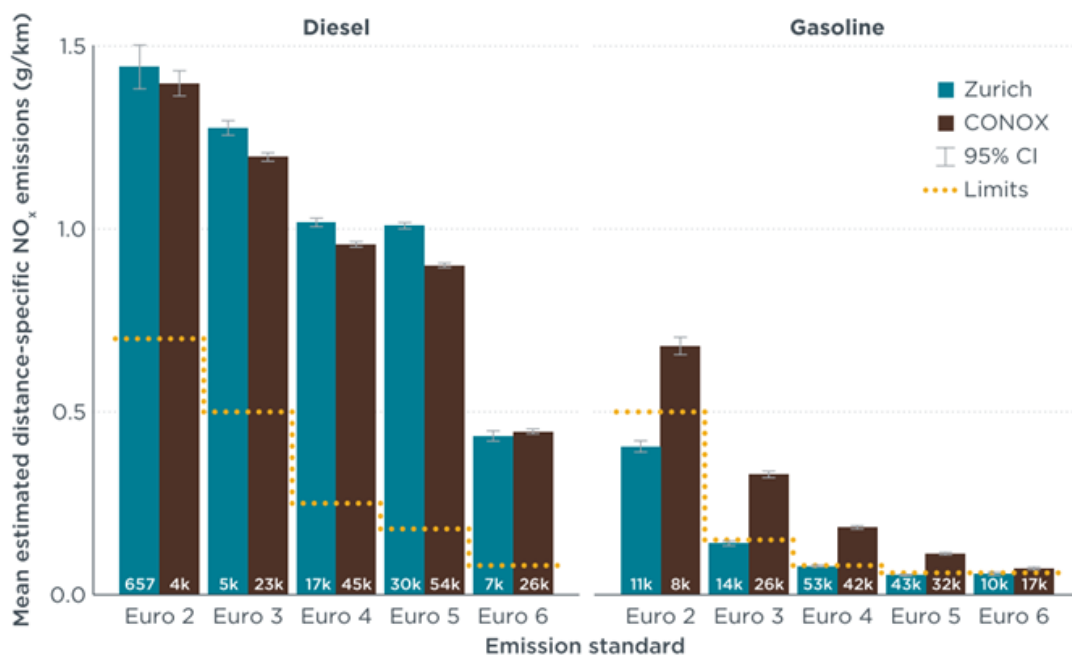


Figure 8-34. 2019 Zurich Remote Sensing Campaign avg. results. Source: The ICCT [127].

The pattern persists in the Zurich measurements depicted in Figure 8-34. In this instance, the obtained net values are more akin to those witnessed in the London assessments.

The notable distinction lies in the inclusion of vehicles adhering to the Euro 6d-Temp emissions standard, which exhibits a conspicuous discrepancy in emissions. There is a significant reduction evident, although it remains in close proximity to the maximum values permitted by homologation standards, although still surpassing them.

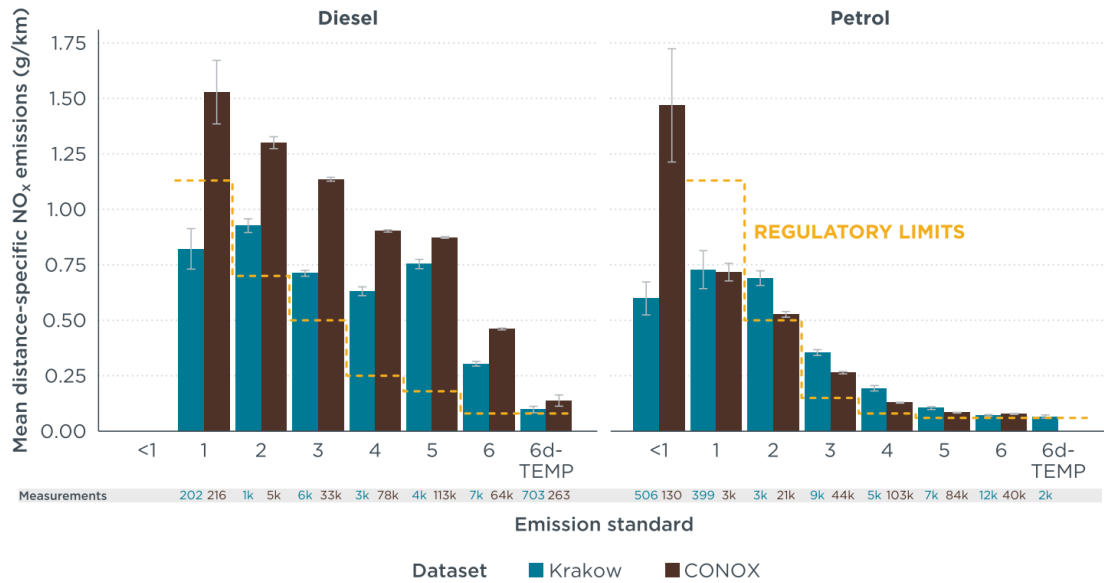


Figure 8-35. 2020 Krakow Remote Sensing Campaign avg. results. Source: The ICCT [126].

Illustrated in Figure 8-35, the emissions trends observed in Krakow mirror those seen in Zurich, with comparable emission values. The recurrent pattern continues, encompassing a reduction in the Euro 6 category and a distinct decline in emissions emanating from vehicles aligned with the Euro 6d-temp standard.

Concluding with the measurements undertaken in Brussels, showcased in Figure 8-36, the identical behavior evident in prior cities reemerges, characterized by Emission Factors closely resembling those observed in Zurich and Krakow.

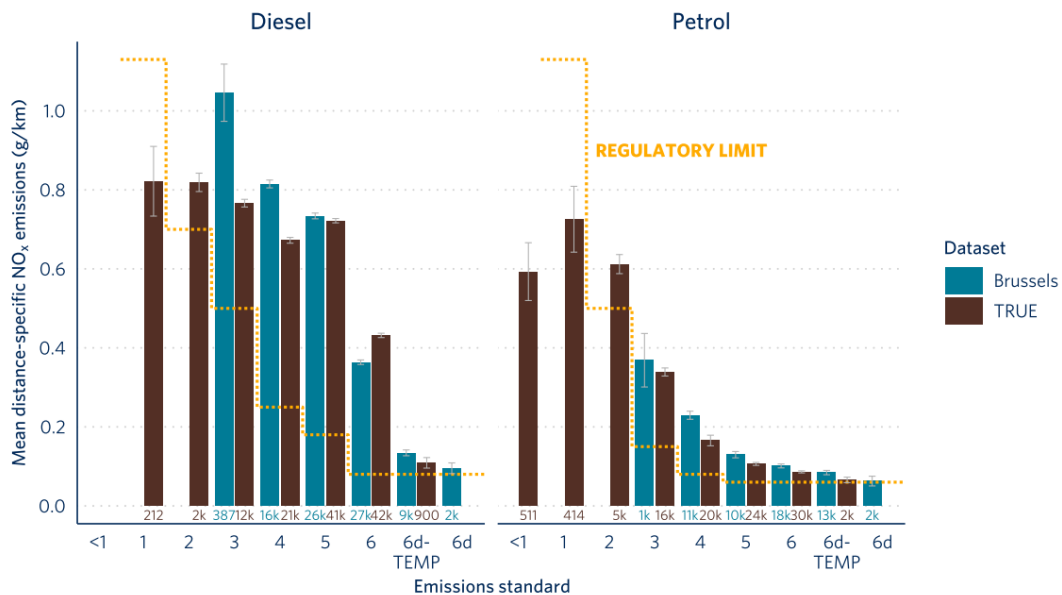


Figure 8-36. 2021 Brussels Remote Sensing Campaign avg. results. Source: The ICCT [125].

Consequently, it is only in the most recent measurement campaigns where vehicles adhering to Euro 6d-Temp d and Euro 6d standards have been incorporated that a marked reduction in Euro 6-level emissions becomes noticeable. These emissions trends approach the values specified by homologation standards, although they have not fallen below the homologation limit in any instance.

Furthermore, it is intriguing to observe that, across all scenarios, the emissions from Euro 4 and Euro 5 vehicles are notably similar to each other. In certain cases, Euro 5 vehicles even exhibit higher emissions than their Euro 4 counterparts, and these levels do not significantly differ from Euro 3 emissions.

In contrast, Euro 6 vehicles do exhibit a discernible reduction in comparison to Euro 5, as previously noted. However, as highlighted earlier, their emissions remain well above the permissible limits.

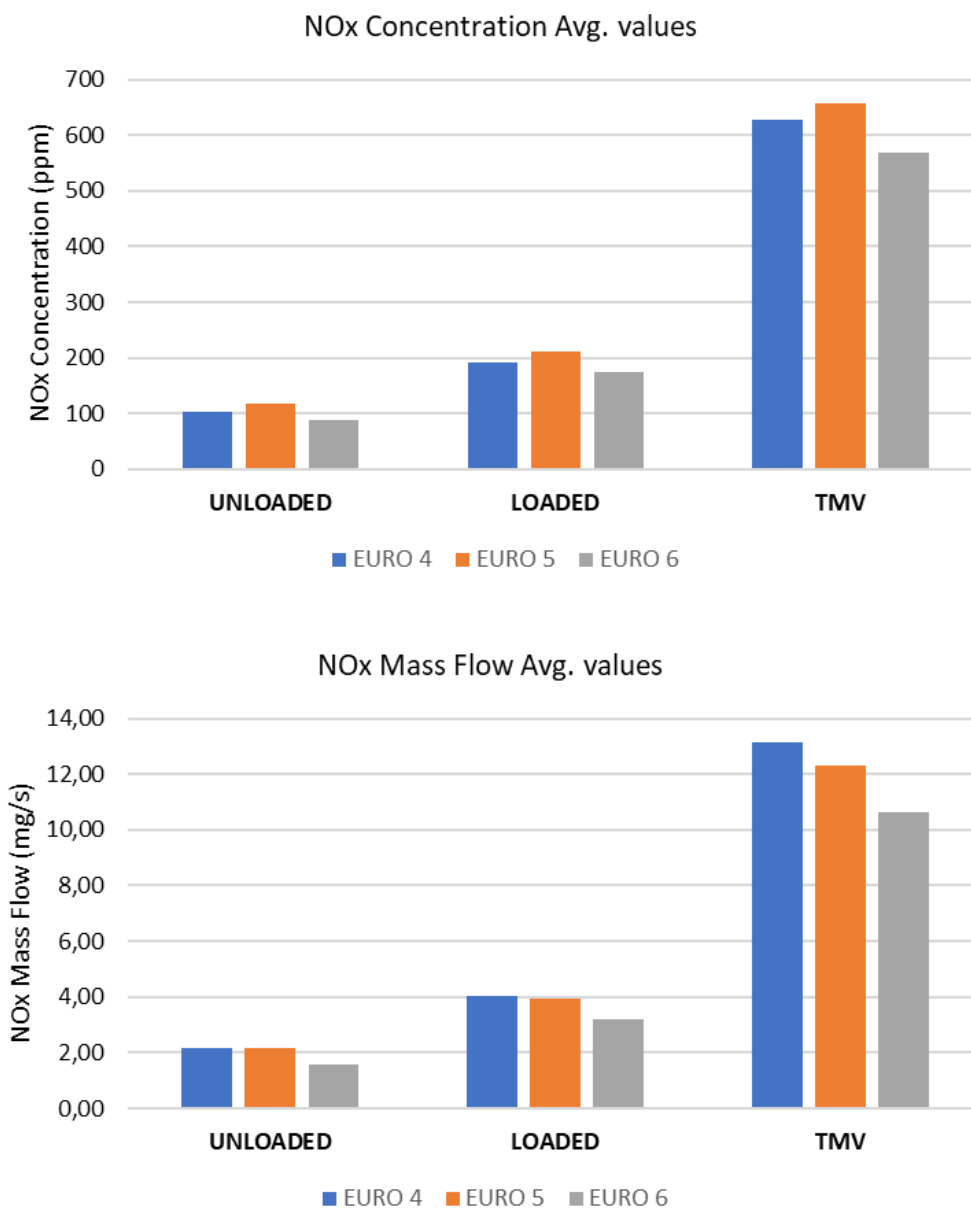


Figure 8-37. Summary of NO_x emissions from PTI campaign, Concentration (up), and Mass Flow (down).

The findings stemming from the PTI measurement campaign exhibit an analogous trend in the recorded average values, consistent with the patterns observed in the preceding instances of RSD measurements. Notably, emissions from Euro 4 and Euro 5 vehicles mirror each other closely. It is important to note that no data is available for earlier vehicles since the method requires OBD, rendering it inapplicable to older vehicles. Meanwhile, Euro 6 vehicles already manifest a noticeable reduction in emissions when juxtaposed with Euro 5 counterparts.

In this particular case, measurements for Euro 6d-temp or Euro 6d vehicles are absent, given that the campaign was executed before the implementation of inspection requirements for these vehicles, owing to their date of registration.

Hence, it is confirmed that the emission value patterns recorded, encompassing both NO_x concentration and NO_x Mass Emission Flow, align closely with those derived from comprehensive remote measurement campaigns (RSDs). This consistent behavior is evident across the three load states assessed within the proposed test: Unloaded state, Loaded state, and TMV.

This congruence in behavior serves as an additional validation of the accuracy of the measurement method's results. The fact that these results mirror those obtained from other extensively employed measurement techniques found in scientific literature further strengthens their reliability and credibility.

8.5. NO_x THRESHOLDS DETERMINATION FOR PTI

As stated in the introduction of this chapter, the last objective aimed to be achieved through the execution of this measurement campaign was the determination of a rejection threshold to be applied in the PTI inspection process.

One of the most challenging aspects to establish in the NO_x measurement process when implemented in PTI is identifying the grounds for rejection. These reasons render a vehicle unable to operate until the underlying issue behind the rejection is rectified.

Given the economic and even legal implications of such a rejection, the determination of the cause and the rejection criteria is a fundamental aspect when defining a PTI inspection test.

So far, among the various proposals that have been made for NO_x measurement in PTI, no clear criterion has been defined to apply, largely due to the difficulty of determining what should be the emissions of a vehicle at a particular operating point, for all the causes widely discussed throughout the previous sections.

PTI rejections grounded in numerical outcomes derived from a measurement process can be categorized into two types:

- a) Rejection due to failure to meet a minimum value.
- b) Rejection due to surpassing a maximum value.

The former usually originate from tests where the effectiveness of a system is evaluated, such as, for example, the braking effectiveness test. If the result shows that minimum effectiveness is not reached, the vehicle is rejected.

The latter is typical in emission tests (gaseous, noise,...). If the vehicle is found to have emissions above a limit value, the vehicle is rejected.

The NO_x measurement, given the nature of the intended test, should adhere to the second group's rejection criterion (where the analysis pertains to the vehicle's emissions rather than the system's effectiveness).

Hence, it becomes imperative to ascertain an emissions threshold and a measurement threshold. If the emissions value surpasses this point, in accordance with the predetermined criteria, the vehicle is subject to rejection. This rejection prompts the need to address potential inadequacies leading to the emissions value that resulted in the rejection.

As discussed in section 8.4.1 above, the proposed NO_x measurement test result provides six numerical values, corresponding to three different points of engine operation during the test, which can be used to define a rejection limit suitable for inspection use.

Consequently, it becomes essential to establish the value or values beyond which it is evident that the vehicle must not be permitted to operate due to an underlying issue (malfunction, tampering, etc.) leading to excessive NO_x emissions.

This value should be set sufficiently high to avoid unwarranted rejections of vehicles in proper condition. However, it should not be overly high to the extent that it fails to serve its purpose. Striking a balance is crucial, as an excessively high value might result in vehicles emitting beyond acceptable limits due to technical reasons, yet passing the test since they fall short of the threshold.

When considering the absence of comprehensive vehicle emissions data and the intricacies involved in accurately estimating NO_x emissions at specific instances (except for simplified scenarios like idling), the complexity of the matter becomes apparent.

While not suggesting that this is the definitive approach, but rather offering a potential solution, the following outlines a proposal for establishing a rejection threshold for the PTI measurement test under examination in this thesis, grounded in the data acquired from the conducted measurement campaign.

The initial stage in formulating a rejection threshold involves identifying the vehicles that should be subject to rejection.

One initial response would be to target vehicles with malfunctioning or improperly functioning engines, EATS, and/or EGR systems, owing to wear and tear, breakdowns, or tampering.

However, the proposed method lacks a direct mechanism or systematic approach for detecting such failures and/or manipulations. Given that the method solely measures emissions, it becomes essential to deduce from the obtained measurements whether the diverse systems are operating as intended or not.

The challenge with this approach lies in the fact that to identify from the measurement data whether the systems are functioning properly, a prior understanding of the emissions data that would be generated under proper system operation is required, along with **reference values for each vehicle**. Regrettably, this information is presently unavailable.

While it is possible that vehicle manufacturers might provide such information in the future for this method or a similar one to be employed in this manner, currently, this limitation impedes the use of this method or any other reliant solely on emissions measurement to definitively ascertain vehicle anomalies without the presence of a reference value for comparison against measurement results.

Having ruled out the option of setting individual limits for each vehicle based on proper operation, the next approach is to establish a universal value that is sufficiently high to not be exceeded by any properly functioning vehicle.

Once again, the challenge of inadequate information surfaces, as there isn't enough comprehensive data available on all vehicles in circulation to preemptively determine such a generic value.

It is clear that defining such a generic limit cannot be done arbitrarily but must be based on a solid foundation that allows the process to be effective in terms of detecting vehicles that emit excessively while guaranteeing that the probability of rejecting a vehicle in good condition is reduced to the minimum possible.

One possible solution, which is proposed below, is based on data provided by the European Commission itself when analyzing the NO_x emissions problem. In a 2012 report, called "ROADWORTHINESS PACKAGE, COMMISSION STAFF WORKING PAPER, IMPACT ASSESSMENT" version SWD(2012) 206 final [53], is stated that:

*"Vehicle defects also increase emissions (e.g. CO, HC, NO, and CO₂) by some 1.2% and 5.7%, depending on the vehicle and fuel type. A large fraction of total emissions is due to a minority of vehicles with malfunctioning emission control systems. **5% of the vehicle fleet causes 25% of all pollutant emissions and 20% of vehicles cause 60 % of pollutant emissions.**"*

This sentence implicitly defines what the rejection limit should be in a pollutant emissions test: 5% of the vehicles with the highest emissions should be rejected since they are responsible for 25% of all pollutant emissions.

Hence, if it becomes feasible to identify the emission threshold that designates any vehicle surpassing it as belonging to the top 5% of vehicles with the highest emissions, a valid rejection threshold will have been established for implementation.

According to data from Mincotur¹³ (Spanish Ministry of Industry, Commerce and Tourism) the rejection level for the PTI emissions test in 2021 was 7.23% for M1 vehicles and 6.98% for N1 vehicles. Therefore, setting a limit that rejects 5% of the inspected vehicles seems to be aligned with the rejection level of the current emissions test.

¹³ <https://industria.gob.es/Calidad-Industrial/vehiculos/Paginas/inspeccion-tecnica-vehiculos.aspx>

Similarly, the statement from the European Commission introduces an additional secondary rejection threshold, noting that 20% of vehicles contribute to 60% of emissions. Hence, by pinpointing the threshold that designates 20% of vehicles and consequently identifying the vehicles within that category, opens up the possibility of implementing strategies to mitigate 60% of overall pollutant emissions.

Once it has been defined at a theoretical level which data will be used to define the proposed emission limit, the path to be followed to determine which value is sought must be explored.

For this purpose, the tool explained in this section will be used: the data obtained from the measurement campaign conducted on a set of vehicles that has a sample size large enough for this set of measurements to be significant (see Figure 8-3).

Indeed, the comprehensive dataset is not solely characterized by the mean values of the measurement outcomes. Various statistical measures can be computed to offer insights into the data distribution and characteristics.

Since the test provides two types of results (emissions in concentration [ppm] and emissions in Mass Flow [mg/s]), it is necessary to calculate the statistics for both types of results.

The most interesting data for this purpose, besides the average values, are the Standard Deviation (SD) and Coefficient of Variation (CV) values, which provide information about the dispersion of the data collected in the measurement campaign. The Maximum (Max.), Minimum (Min.), and Standard Error data are also collected.

	UNLOADED	LOADED	TMV	units
MEASURES	1882	1882	1882	#
AVERAGE	107	198	626	ppm NO _x
SD	68	134	445	ppm NO _x
CV	64.05%	67.47%	71.13%	%
STD. ERROR	2	3	10	ppm NO _x
MAX. VALUE	934	990	5179	ppm NO _x
MIN. VALUE	0,05	0,10	8,10	ppm NO _x

Table 8-9. NO_x Concentration results campaign summary with statistical.

Upon analyzing the dataset obtained from the measurement campaign, it becomes apparent that the data distribution aligns with a common pattern: it exhibits characteristics resembling a Normal Distribution, often referred to as a Gaussian Bell curve.

	UNLOADED	LOADED	TMV	units
MEASURES	1882	1882	1882	#
AVERAGE	1,99	3,71	11,82	mg/s NO _x
SD	1,39	2,62	8,67	mg/s NO _x
CV	69,95%	70,84%	73,35%	%
STD. ERROR	0,03	0,06	0,20	mg/s NO _x
MAX. VALUE	22,39	39,10	107,55	mg/s NO _x
MIN. VALUE	0,00	0,00	0,17	mg/s NO _x

Table 8-10. NO_x Mass Flow results campaign summary with statistical.

This possesses significant advantages when dealing with the data, given our understanding of this distribution. To begin, the density function's graph is centered around the mean (μ), which is essentially the average value of the data, a value already available from the measurements. Moreover, this plot exhibits a symmetrical pattern with respect to the mean value.

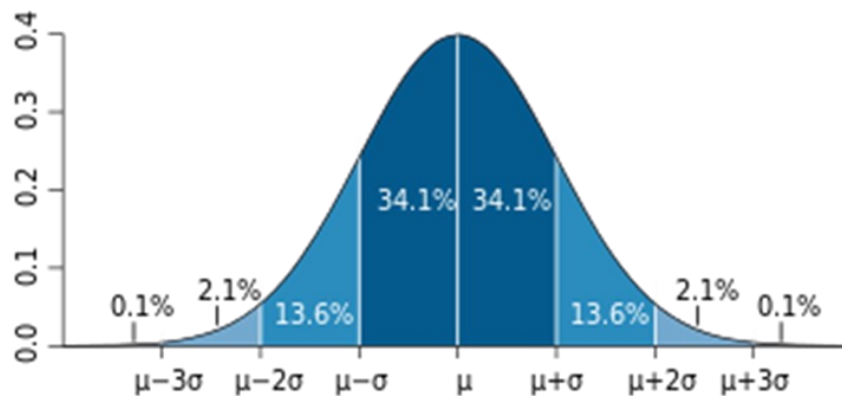


Figure 8-38. The plot of Normal Distribution (a bell-shaped curve). Source: Wikipedia.

In addition, the width of the Gaussian bell is known, since it is defined by the SD (σ) value of the data set.

Lastly, the quantity of data contained within various segments of the distribution can be determined. These segments are established by adding the standard deviation (σ) to the mean (μ), and this can be done one or multiple times.

Thus, it is known that in the section of data centered on the value μ , and ranging from the value $\mu-\sigma$ to the value $\mu+\sigma$, **68.2%** of the total data forming the distribution are found (see Figure 8-38). If the interval is defined by the values $\mu-2\sigma$ to $\mu+2\sigma$, **95.4%** of the total data of the distribution are found within it. If the interval is extended to be defined by

the values $\mu-3\sigma$ to $\mu+3\sigma$, **99.6%** of the total data of the distribution is included in the interval.

As the interval is expanded by adding additional multiples of the sigma value, more data points from the distribution's tails are encompassed. However, with each successive increase in σ , a smaller portion of data is added. In this way, the number of standard deviations (σ) determines the extent of data included in the distribution, reflecting the level of information precision in the dataset (greater σ values include fewer data gaps and result in more reliable conclusions).

Whether the data follow this Normal Distribution can be used to define the emission limit for the proposed static test.

To precisely identify the top 5% of most polluting vehicles, the process involves locating the highest emission value within the distribution (typically situated at the right end of the distribution curve). Subsequently, the emission value immediately to the left of this highest point corresponds to the threshold for the top 5% of measured values. This particular value would then serve as the cutoff point for determining which vehicles exceed the emissions limit.

Based on Figure 8-39, it is evident that by setting a limit at the $\mu+2\sigma$ value on the far right, approximately 2.2% of the total data within the distribution will fall to the right of this limit.

In the context of value distribution, like the measurements recorded in the loaded state, placing the limit at $\mu+2\sigma$ will symbolize the emission value that is exceeded by the uppermost 2.2% of vehicles exhibiting the highest emissions within the distribution. Conversely, if the limit is established at $\mu+\sigma$, it will denote that the emission level is surpassed by approximately 15.8% of the vehicles showcasing the greatest emissions within the distribution.

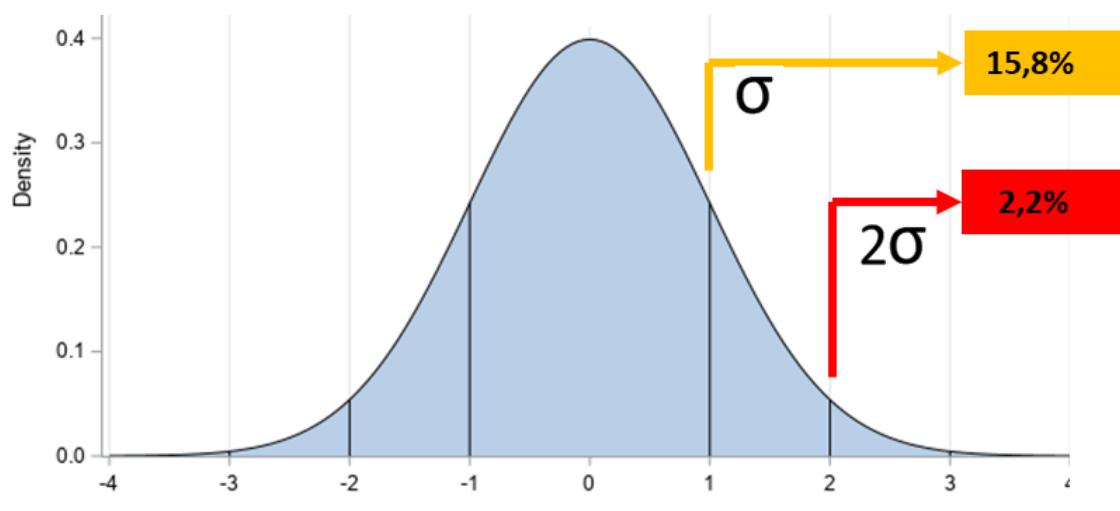


Figure 8-39. Definition of Thresholds from Normal Distribution. Source: sas.com, modified by the author.

While the European Commission document suggested desirable limits of 5% and 20% for vehicles, it is analytically more precise to directly establish the limits based on σ values. As a result, the emission test's recommended limit will be determined by the $\mu+2\sigma$ value for rejecting vehicles, and the $\mu+\sigma$ value for signaling a warning to the owner, prompting them to inspect their vehicle.

It is therefore a more conservative limit than the one proposed by the European Commission document, but it can be a good starting point, to be adjusted more strictly if necessary.

The upcoming graphs will display the density function and frequency distribution of the measured values corresponding to the Unloaded, Loaded, and TMV states, presented in both concentration (ppm) and Mass Flow (mg/s) formats. Additionally, the 2σ value will be marked on the density function to provide a visual representation of the proportion of vehicles that would be subjected to rejection if the 2σ value is used as the limit.

Consequently, after establishing the criterion employed to establish the proposed emissions limit and visually demonstrating the count of vehicles that would be subjected to rejection by implementing this criterion in each of the method's outcomes, the values designated as the limit, derived from the outcomes attained in the measurement campaign, will be presented.

Table 8-9 and Table 8-10 show the average values (μ) and the main statistics including the Standard Distribution (σ) of the data collected in the measurement campaign.

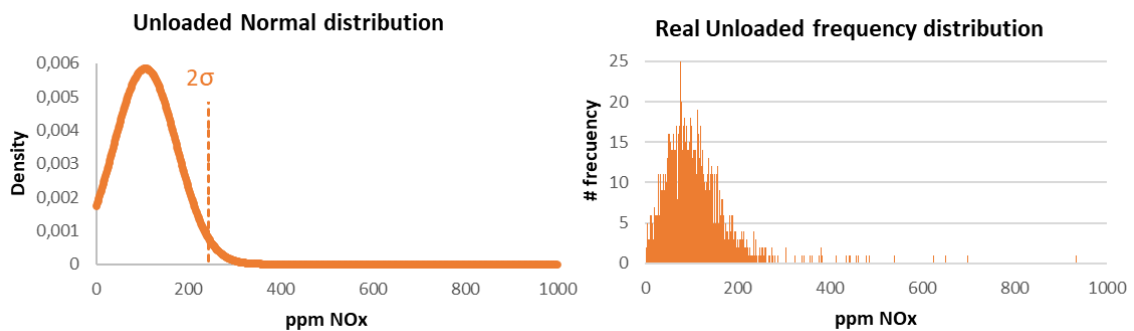


Figure 8-40. Normal distribution and frequency distribution for Unloaded concentration results.

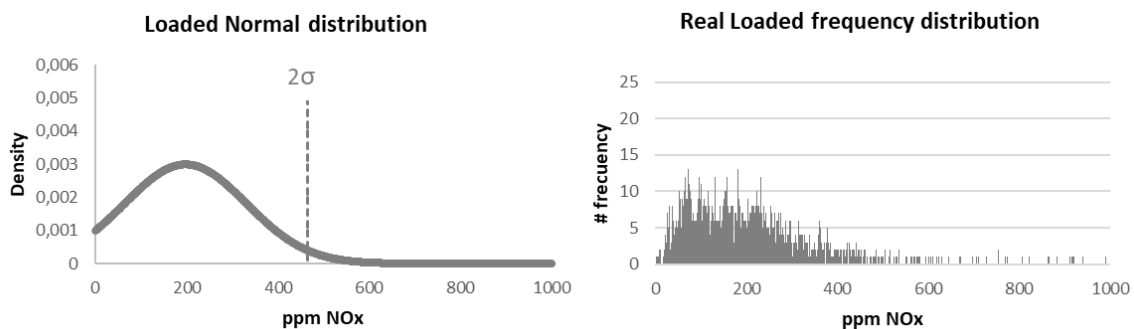


Figure 8-41. Normal distribution and frequency distribution for Loaded concentration results.

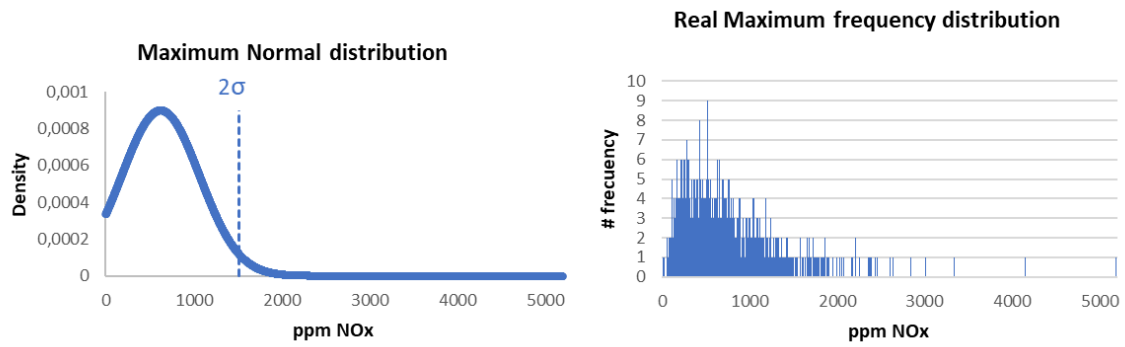


Figure 8-42. Normal distribution and frequency distribution for TMV concentration results.

	AVERAGE (μ)	SD (σ)	THRESHOLD 1 σ	THRESHOLD 2 σ	units
UNLOADED	107	68	175	244	ppm NO _x
LOADED	198	134	332	465	ppm NO _x
TMV	626	445	1071	1517	ppm NO _x

Table 8-11. Results statistical and Threshold definition in concentration.

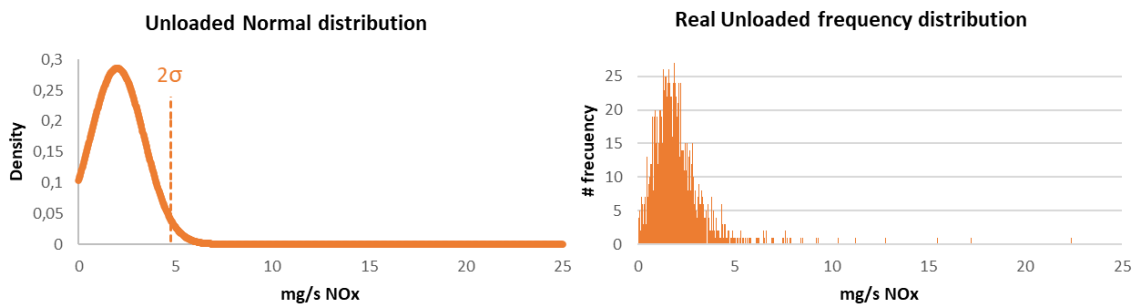


Figure 8-43. Normal distribution and frequency distribution for Unloaded Mass Flow results.

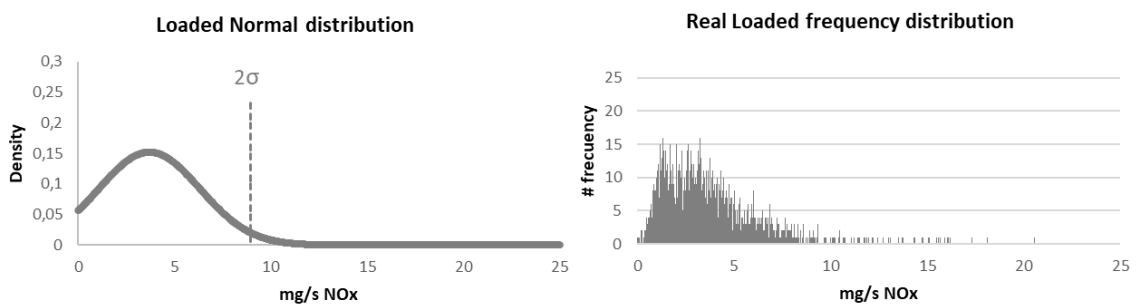


Figure 8-44. Normal distribution and frequency distribution for Loaded Mass Flow results.

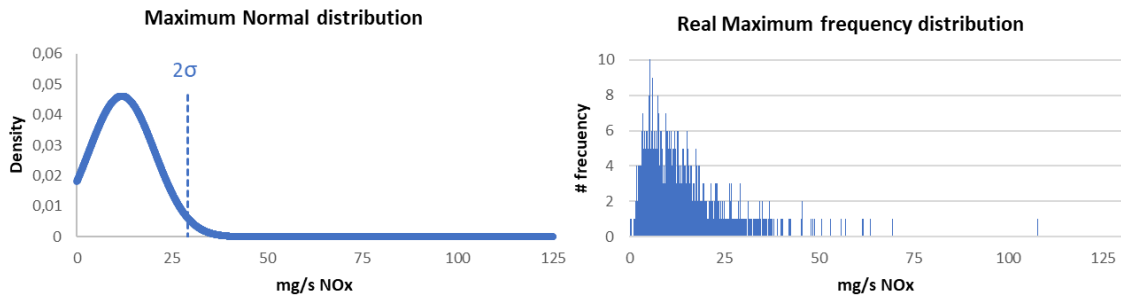


Figure 8-45. Normal distribution and frequency distribution for TMV Mass Flow results.

	AVERAGE (μ)	SD (σ)	THRESHOLD 1 σ	THRESHOLD 2 σ	units
UNLOADED	1.99	1.39	3.39	4.78	mg/s NO _x
LOADED	3.71	2.62	6.33	8.96	mg/s NO _x
TMV	11.82	8.67	20.49	29.16	mg/s NO _x

Table 8-12. Results statistical and Threshold definition in mass flow.

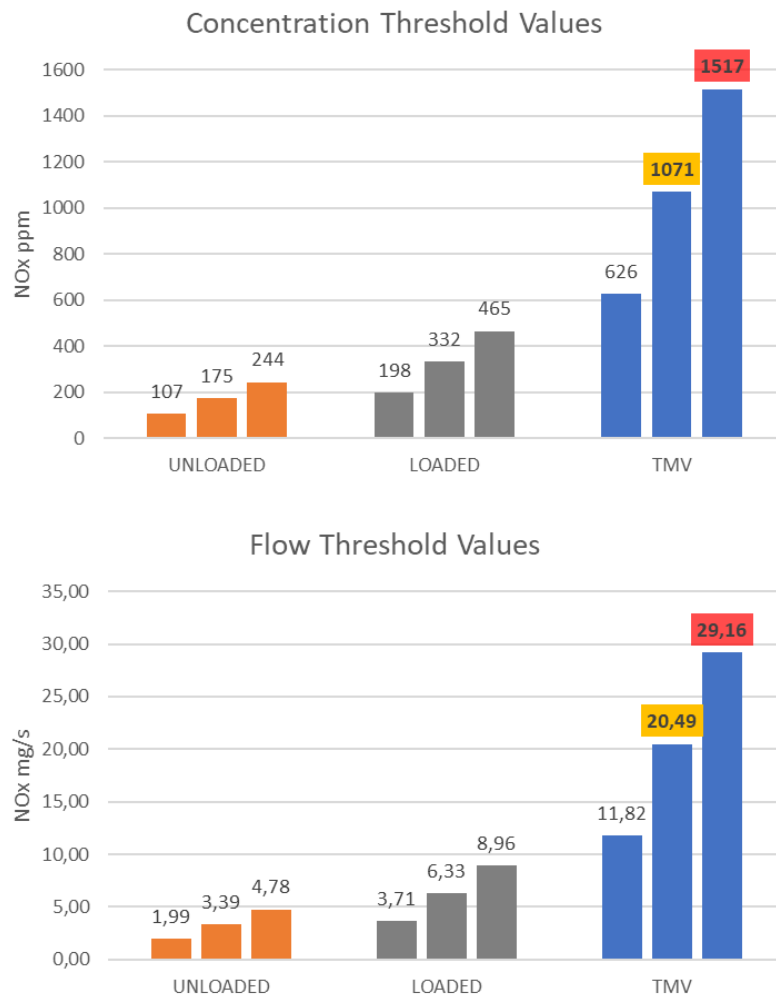


Figure 8-46. Thresholds for NO_x emissions in Concentration (up) and Mass Flow (down).

Using this data, the subsequent tables are formulated to deduce the emission thresholds grounded on the registered concentration (Table 8-11) and derived from the registered Mass Flow (Table 8-12).

The threshold values are established according to the TMV measurement, as it appears reasonable that the higher values determine the maximum emissions.

Furthermore, as mentioned earlier, the TMV value is the most suitable for comparing NO_x emissions between vehicles, regardless of their technical characteristics (such as displacement, power, etc.).

Nonetheless, data for both the LOADED and UNLOADED states are accessible, allowing for the option of defining the limit based on either state, contingent on the requirements.

The graphical representation of these values can be seen in Figure 8-46, which shows together the behavior of the defined limits concerning the average value obtained for each load state.

Hence, if the decision is made to opt for rejection criteria based on the measured concentration, the limit values determined with the aforementioned criteria would be **1071 ppm** for the initial threshold, prompting the user to address exceptionally high NO_x emissions by checking the vehicle, and **1517 ppm** for the secondary threshold, leading to inspection rejection and rendering the vehicle inoperable until the identified issue is resolved.

Conversely, if opting to set the rejection threshold according to mass flow emissions, the limit values derived from the aforementioned criteria would amount to **20.49 mg/s** for the initial limit. At this point, the user is notified about their vehicle's remarkably high NO_x emissions, prompting a recommended vehicle inspection. Subsequently, the second limit is established at **29.16 mg/s**, leading to a rejection within the inspection procedure and rendering the vehicle ineligible until the identified issue is rectified.

Besides reducing emissions through the removal of detected vehicles from circulation, implementing the system could have a potential deterrent effect, leading to the elimination of certain vehicle manipulations (such as EGR and SCR overrides) due to the possibility of rejection during a PTI inspection. This, in turn, would also contribute to an overall reduction in emissions.

	Concentration [ppm]	Mass Flow [mg/s]
THRESHOLD 1 σ (WARNING)	1000	20
THRESHOLD 2 σ (REJECTION)	1500	29

Table 8-13. Final Thresholds proposed for TMV value in the PTI test.

Since the exact limits defined with this method are not round numbers, and the limits thus defined are conservative compared to what was proposed by the European Commission in its document, a downward rounding of these limits is proposed, to finally leave them with the values indicated in Table 8-13.

It is interesting to check graphically, with respect to the distribution of the results of the set of measurements carried out in the campaign, where the limit of rejection is located (Figure 8-47).

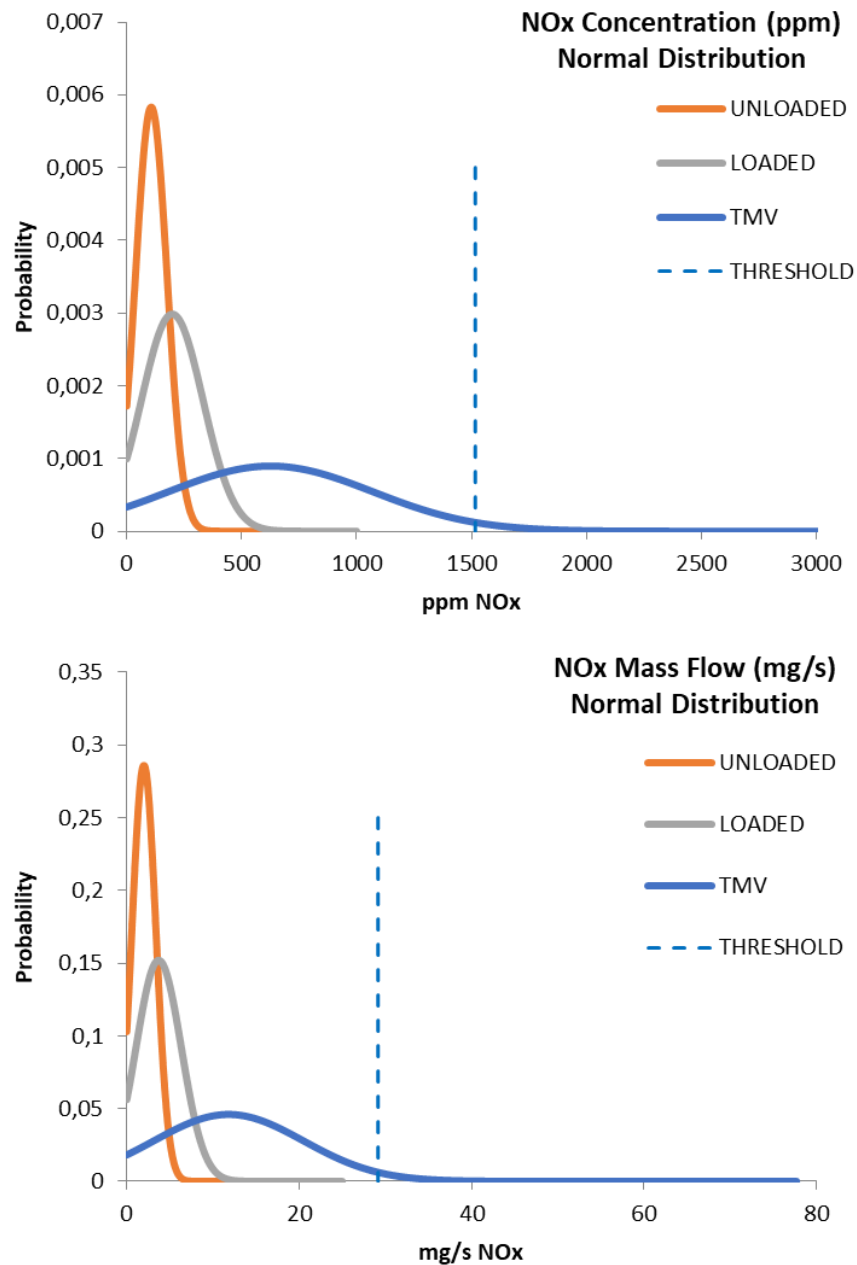


Figure 8-47. Threshold compared with the distribution of emissions in Concentration (up) and Mass Flow (down).

Applying the rejection limit values defined in Table 8-13 to the measurements made in the campaign carried out, based on the concentration limit, 76 vehicles would have been rejected, **4.03%** of the vehicles inspected, and based on the Mass Flow limit, 99 vehicles would have been rejected, **4.67%** of the total number of vehicles.

On the other hand, applying the warning limit set in Table 8-13, a total of 146 vehicles (apart from the 99 vehicles that exceed the rejection limit and would be directly rejected) would have been warned considering the mass flow limit, and 237 vehicles (apart from the 76 vehicles that exceed the rejection limit) if the concentration limit is considered.

Thus, applying both limits, **13.0%** of the most polluting vehicles would be detected by the mass flow limit, and **16.6%** of the vehicles with the highest emissions would be detected by the concentration limit.

In summary, from the set of measurements carried out, an emission limit of 1500 ppm concentration of NO_x in the exhaust gases, or a mass emission of 29 mg/s of NO_x has been defined and proposed, to detect and reject approximately 5% of the vehicles with the highest emissions.

Coincidentally, this emission limit of 1500 ppm NO_x is the same that is applied in China according to the GB 3847-2018, but applying the lung-down test [96].

8.6. CONCLUSIONS

Across this chapter, diverse facets linked to the measurement campaign conducted on vehicles passing through five stations of GRUPO ITEVELESA in Spain have been examined.

This measurement campaign, the most extensive of its kind thus far, encompassed the inspection of 1882 vehicles. The primary aim was to ascertain the validity of the NO_x measurement method within PTI, assess the dependability of its outcomes, and determine its feasibility for implementation within the PTI process.

For this purpose, five objectives were set to be met by the measurement campaign, with the following results:

- 1) The method is feasible to apply in the PTI.

Ensuring the seamless integration of the measurement method within the PTI process, without disrupting ongoing inspections or significantly extending vehicle inspection duration, holds paramount importance. Based on the description of the campaign, it has been established, following more than 1880 measurements, that no issues have arisen concerning its implementation. This holds true both from a technical perspective and in the eyes of the service users.

The introduction of the measurement method has not led to any substantial extension of inspection times beyond the additional time required for conducting the measurement. Moreover, there have been no adverse effects on other aspects of the inspection process.

Furthermore, the campaign has underscored the method's robustness and consistency in terms of the outcomes it produces. This is evident through a comparison of the obtained results with both the results from the design phase and those stemming from other measurement methodologies.

2) The method is simple to apply.

The method has successfully demonstrated its adherence to the principle of being easily applicable. The personnel responsible for conducting the measurement campaign underwent training lasting approximately 1 hour, after which they were fully equipped to execute the required measurements for the campaign without encountering significant issues.

The collective expertise of the personnel in the realm of vehicle inspection, combined with the method's straightforward application process and utilization of equipment familiar to the personnel, contributes to streamlining the method's execution. As previously noted, the method's simplicity is to such an extent that it can be performed either by the inspector directly or even by the vehicle owner, following instructions provided by the inspector, while the inspector attends to other inspection duties.

Additionally, the software employed for implementing the method further contributes to its user-friendliness and ease of application.

3) The conditions of quality and significance between the variables are maintained, and the behavior of the engine load value remains as expected.

It has been verified that the quality and significance behavior of both groups of vehicles (the initial set of 23 vehicles and the set of vehicles from the measurement campaign) is similar.

Regarding the quality of the relationship between the variables (NO_x concentration and "% engine load"), it is observed that the percentage of vehicles exhibiting R² values greater than 0.60 is similar for different load conditions. Therefore, the quality behavior is similar and is thus maintained in the larger group of vehicles.

It is also noted that the causes preventing certain vehicles from achieving R² values above 0.60 are similar.

Regarding significance, from the results obtained, it can be concluded that the behavior of the p-values obtained in the measurements of the campaign aligns with, and in some cases surpasses, the data obtained from the initial selection of 23 vehicles. It can be affirmed that from this data, the existing relationship between the NO_x concentration measured at the exhaust pipe outlet of the vehicles and the "% engine load" to which they are subjected can be verified, even under conditions such as those in the final section where the EATS and EGR systems are in operation.

Furthermore, concerning the observed behavior of the "% engine load" variation in different load states for the set of vehicles in the measurement campaign, compared to the initial set of 23 vehicles, it can be stated that the results obtained confirm the behavior observed during the development of the measurement method. The utilization of the vehicle's internal consumption during idling effectively facilitates the generation of two distinct load states, with one being twice as high as the other.

- 4) The behavior of the results and the characteristics of the test from the campaign exhibit similarity to the outcomes as outlined in the method's specifications.

The outcomes garnered from the measurement campaign have undergone a comprehensive analysis, including an intricate juxtaposition with the results acquired during the method's conceptualization phase. This meticulous evaluation has affirmed the congruity between the projected behaviors and the actual observed behaviors, thus validating the conclusions drawn during the method's development.

The results from both measurement sets exhibit alignment. Essentially, the characteristics observed within the initial measurement subset, which initially validated the method's effectiveness, persist as the scope broadens to encompass a representative cross-section of the Spanish vehicle fleet.

The subtle divergences noted can be attributed to the variations in sample sizes of vehicles. As a consequence, the values stemming from the measurement campaign hold greater accuracy in comparison, owing to the substantially larger sample's increased statistical significance.

- 5) It is possible to define a valid and realistic emission threshold.

An exposition has been provided regarding the establishment of a potential rejection threshold intended for implementation during inspections. This threshold has been formulated using the devised measurement method.

It is worth noting that alternative limits could be suggested, grounded in different criteria. These alternative limits might prove to be equally, or even more, efficacious in achieving the ultimate objective: contributing to the reduction of NO_x emissions. However, the limit proposed here is rooted in the establishment of a threshold derived through mathematical methodologies. It aligns with the expectations articulated by the European Commission and maintains consistency with the prevailing rate of rejection observed within the context of the existing emissions test during PTI.

The suggested limit, formulated through the static measurement method, will facilitate the exclusion of vehicles emitting higher levels of pollutants from circulation. Importantly, this limit ensures that vehicles in excellent maintenance and operational condition will not be erroneously rejected.

Hence, with the substantiated demonstration that the method seamlessly integrates into PTI without hindering the process or unduly extending inspection times, the simplicity in applying the measurement process (a fundamental prerequisite for PTI implementation), the validation of results obtained from the extensive measurement campaign spanning over 1880 vehicles, which corroborate the conclusions derived during the method's definition phase, and the feasibility of establishing a rejection threshold for method application during inspection – it is unequivocal that the campaign's objectives have been successfully achieved.

Consequently, the method's attributes have been thoroughly validated, rendering it suitable for implementation within the context of PTI.

In the following chapter, an exposition will be given on how the measurement campaign, in addition to enabling the validation of the proposed method, provides additional pertinent information regarding the behavior of vehicle fleet emissions. Furthermore, a comparison will be made between the results obtained from this campaign and the results of other NO_x measurement campaigns conducted using different methods.

CHAPTER 9

ADDITIONAL VERIFICATION MEASURES OF THE PROPOSED PTI TEST

9. ADDITIONAL VERIFICATION MEASURES OF THE PROPOSED PTI TEST

9.1. INTRODUCTION

This Chapter will encompass relevant information pertaining to the data obtained in the measurement process during the campaign, as elucidated in the previous Chapter.

Firstly, additional information derived from the measurement results will be elaborated upon. The proposed measurement process provides copious data that, when analyzed, can be utilized to draw pertinent conclusions. As previously indicated, this method furnishes valuable information that can be employed in formulating fleet management and environmental protection policies.

In addition to the relationship between the variables used in the method definition, other potential correlations between different variables and the measured NO_x emissions have been analyzed. The goal of this comparison is to ascertain whether other variables, in addition to the engine load ("% engine load"), can be used to analyze vehicle emissions.

Following this, during the validation of the suggested method, a crucial aspect is to juxtapose the performance and outcomes derived from applying this method with those acquired through an alternative method proposed for NO_x measurement in PTI. This Chapter encompasses a thorough comparative examination, contrasting the outcomes of the proposed test with those of a power bench NO_x measurement method.

In the final section, we will show how the data from the measurement process can be used to analyze the emissions during a specific urban route, using a straightforward modeling approach that we applied to three vehicles as an example.

Therefore, this Chapter demonstrates the variety and utility of the information derived from the application of the proposed NO_x measurement method in PTI.

9.2. CORRELATION ANALYSIS BETWEEN VARIABLES BASED ON THE MEASUREMENT CAMPAIGN

Undoubtedly, conducting a measurement campaign of the extensive scope witnessed in the analysis yields a wealth of information. While certain information directly pertains to the study's focus, a substantial portion, although not immediately applicable or within the study's primary goals, can prove highly significant. Consequently, it is crucial to disseminate such information, as it may hold value beyond the intended scope of the research.

This section will delve into the observed patterns of NO_x emissions when employing the proposed measurement method. We will examine how the obtained results correlate with various vehicle variables, offering valuable insights for fleet management and the formulation of sustainable mobility and environmental

preservation policies. The data for analysis, coupled with emissions data, comprises available vehicle information recorded during inspections.

The behavior of the set of measurements will be analyzed, without distinguishing by emission level, since the general behavior usually coincides with the specific behavior of the emission levels. If in any case there is a different behavior of any of the Euro levels analyzed, it will be indicated at that point.

Correlation between Vehicle Engine Size and Test NO_x Emissions

Initially, a comparison is drawn between the measured emissions and engine size. Figure 9-1 reveals a lack of discernible correlation between engine displacement and vehicle emissions, reflecting a highly heterogeneous pattern in this aspect.

This observation persists when dissecting the data by Euro levels, as no definitive connection between engine size and vehicle NO_x emissions can be established from these findings.

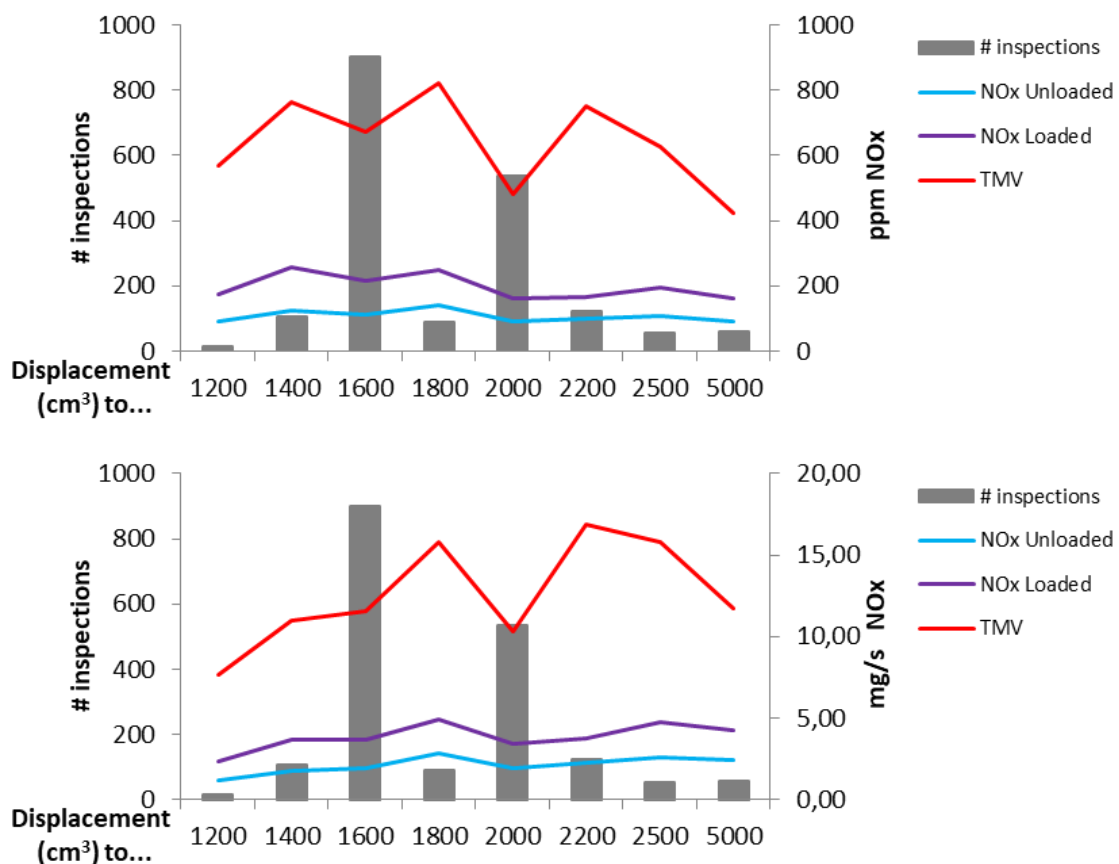


Figure 9-1. NO_x emissions to Displacement, in Concentration (up) and Mass Flow (down).

Correlation between Vehicle Weight and Test NO_x Emissions

Continuing the analysis, the focus shifts to the relationship between NO_x emissions and vehicle weight. Figure 9-2 portrays the absence of a discernible connection between vehicle weight and NO_x emissions. An interesting observation is the contrasting trend depending on whether concentration or Mass Flow is examined, indicating a lack of uniformity in behavior.

Despite the differentiation between concentration and Mass Flow, the potential linear function that could approximate TMV emissions, regardless of the measure type, exhibits an R² value below 0.60—deemed unsatisfactory.

This pattern remains consistent across different Euro levels, leading to the conclusion that establishing a definitive relationship between vehicle weight and NO_x emissions remains unfeasible.

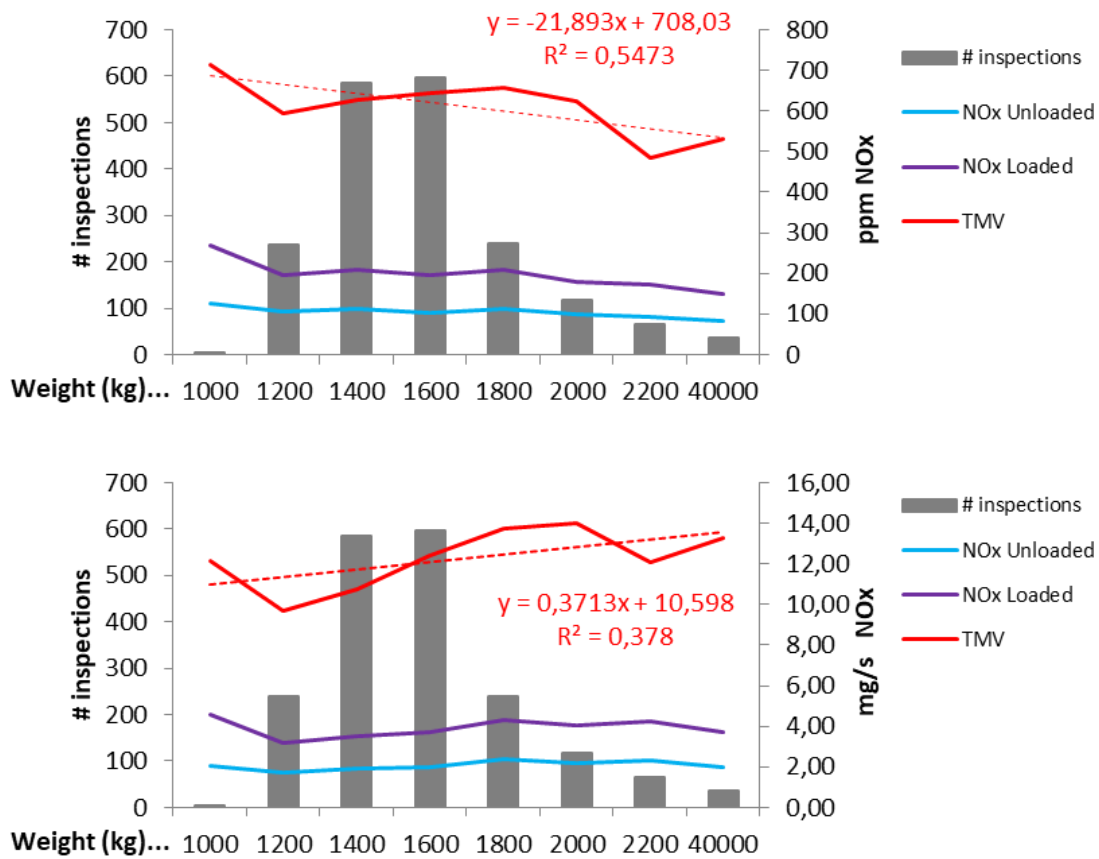


Figure 9-2. NO_x emissions to Weight, in Concentration (up) and Mass Flow (down).

Correlation between Vehicle MMA and Test NO_x Emissions

Another vehicle characteristic to analyze is the load capacity, specifically the Maximum Mass Admissible (MMA), which represents the maximum combined mass of the vehicle and its load. In essence, it encapsulates the sum of the vehicle's empty mass and the maximum load it can legally carry (including passengers and cargo).

As depicted in Figure 9-3, no direct correlation emerges suggesting that higher MMAs, indicative of greater load capacity, result in elevated emissions. Although Mass Flow analysis seemingly points towards this trend, the low R² value obtained underpins the inability to conclusively establish this connection.

Upon scrutinizing different Euro levels, the outcomes remain consistent, affirming the overarching trend witnessed across all vehicles.

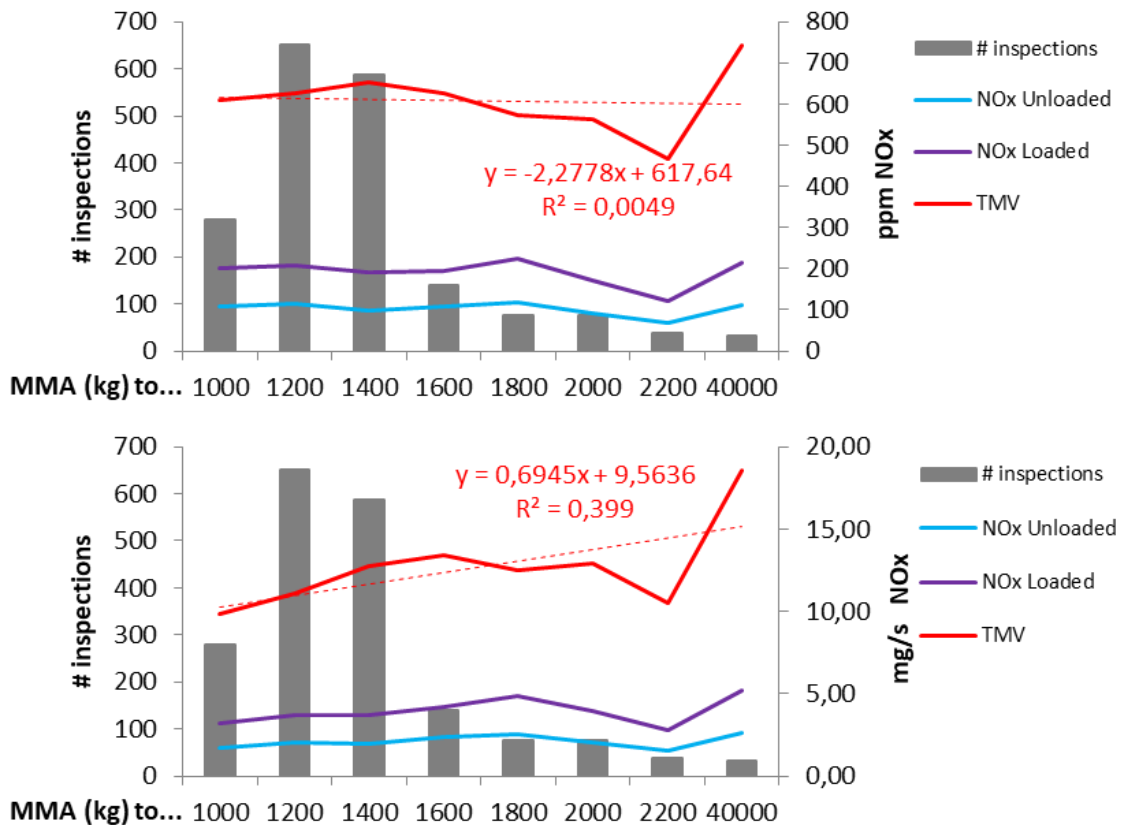


Figure 9-3. NO_x emissions to MMA, in Concentration (up) and Mass Flow (down).

Correlation between Vehicle engine Power and Test NO_x Emissions

Regarding engine power (see Figure 9-4), a noteworthy relationship seems to emerge within the data set, particularly when evaluating emissions through NO_x concentration. In this instance, emissions (TMV) exhibit a declining trend as engine power rises. The R² value of the interplay between the two variables registers at 0.7, indicating an acceptable level of correlation.

Conversely, when dissecting the data concerning Mass Flow emissions, no discernible connection emerges. Given the disparities in values between the two measurement approaches, drawing concrete conclusions becomes challenging without further information.

One might speculate that vehicles with higher available power might reach lower "% engine load" values during testing, translating to lower emissions. However, this

hypothesis remains unsubstantiated when Mass Flow emissions are under consideration.

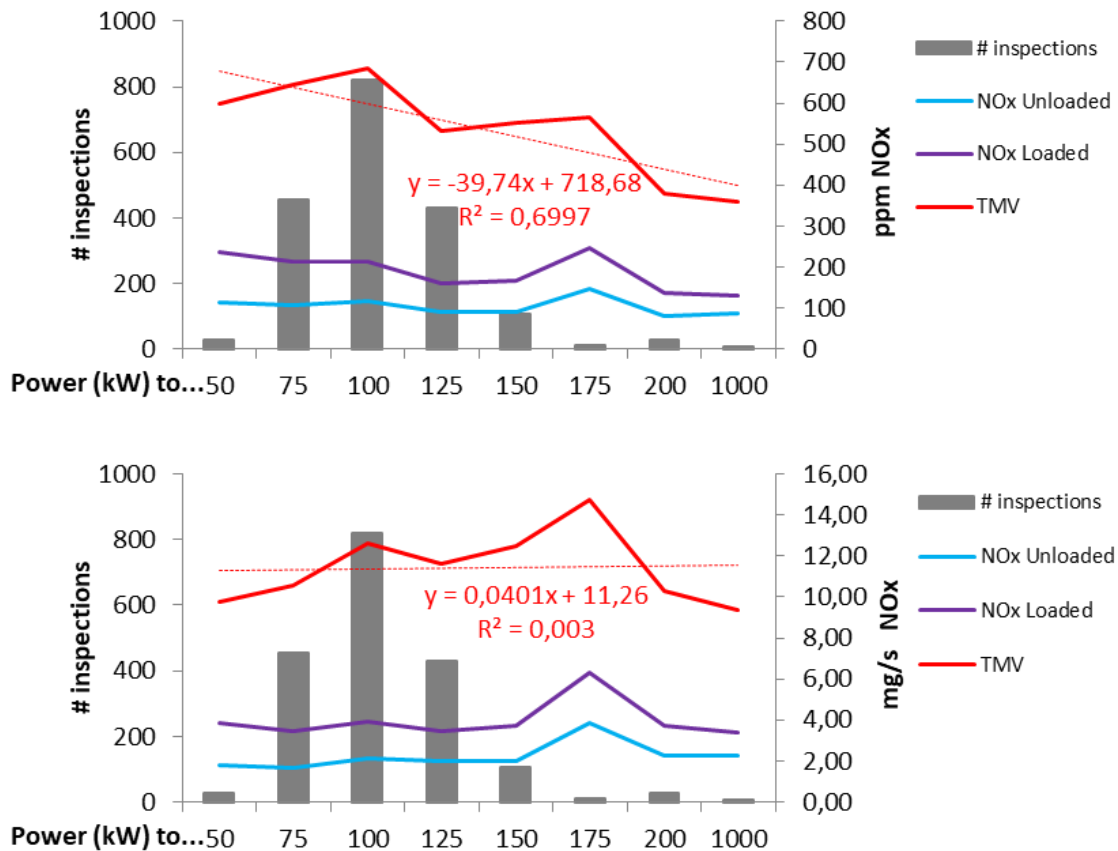


Figure 9-4. NO_x emissions to Power, in Concentration (up) and Mass Flow (down).

Correlation between Vehicle Opacity and Test NO_x Emissions

Currently, diesel vehicles undergo a pollutant emissions test wherein the opacity of exhaust gases is measured as they exit the vehicle's exhaust pipe. During this opacity test at PTI, the measured value is juxtaposed against the corresponding limit set by the manufacturer in the vehicle's homologation. If this manufacturer-specific data is not available, a generic limit stipulated by applicable regulations is employed.

Upon scrutinizing the measured NO_x emissions against opacity values recorded during inspections, and as required by homologation, no discernible relationship emerges.

Correlation between Vehicle Mileage, Age and Test NO_x Emissions

Furthermore, another potential factor influencing NO_x emissions could be the age of the vehicle, coupled with wear and tear, potentially estimated by the total number of kilometers driven.

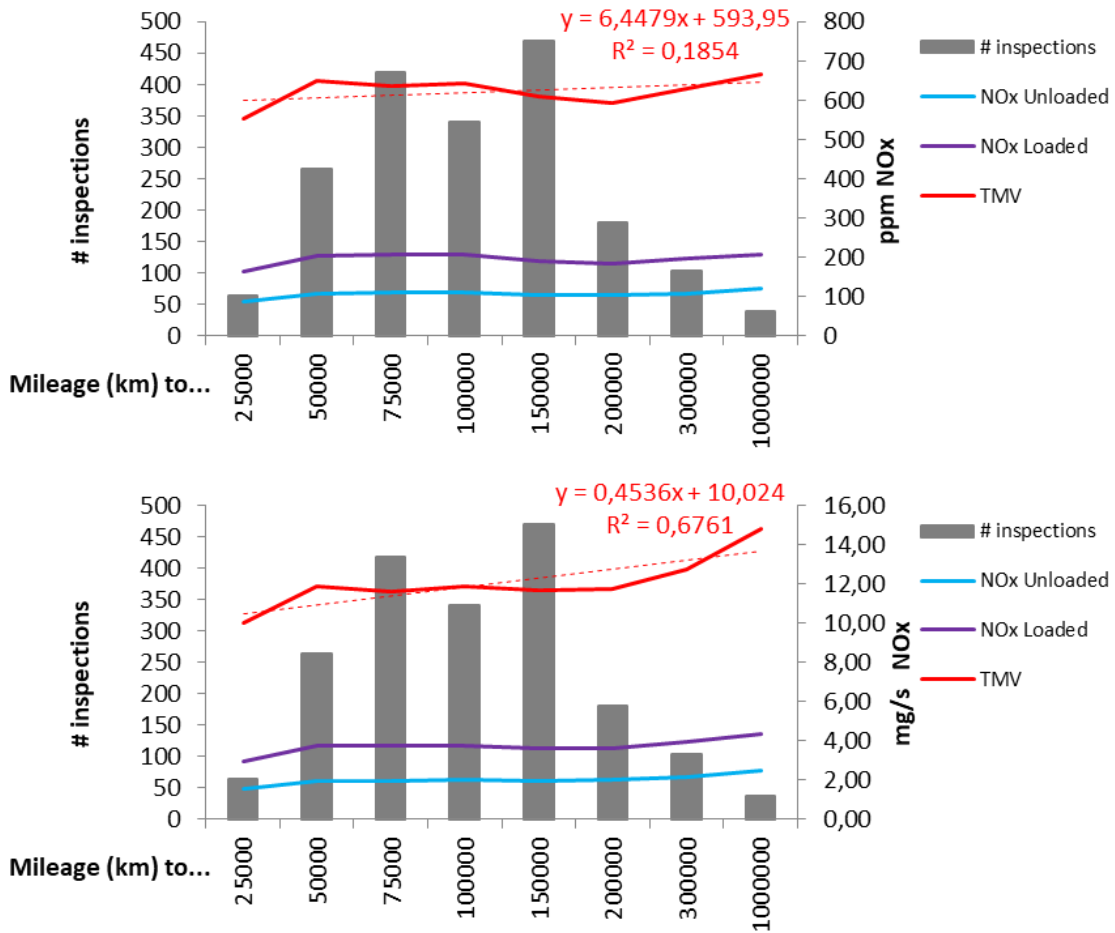


Figure 9-5. NO_x emissions to Mileage, in Concentration (up) and Mass Flow (down).

Upon analyzing the results in relation to the mileage of the examined vehicles, Figure 9-5 visually displays the close alignment of the trend line with the obtained measurement data.

Although the graph seems to suggest a strong approximation, the R² value for the relationship, especially when considering concentration-based emissions, remains quite low.

Interestingly, in terms of Mass Flow-based emissions, the calculated R² value does assume an acceptable level, potentially implying a feasible relationship. This observation harmonizes with existing scientific literature indicating that emissions might indeed increase as mileage accumulates or as vehicles age [66].

A comparable situation emerges when contrasting emissions with the age of vehicles (at the time of inspection) in years (Figure 9-6). However, in this case, the R² value never attains an acceptable level.

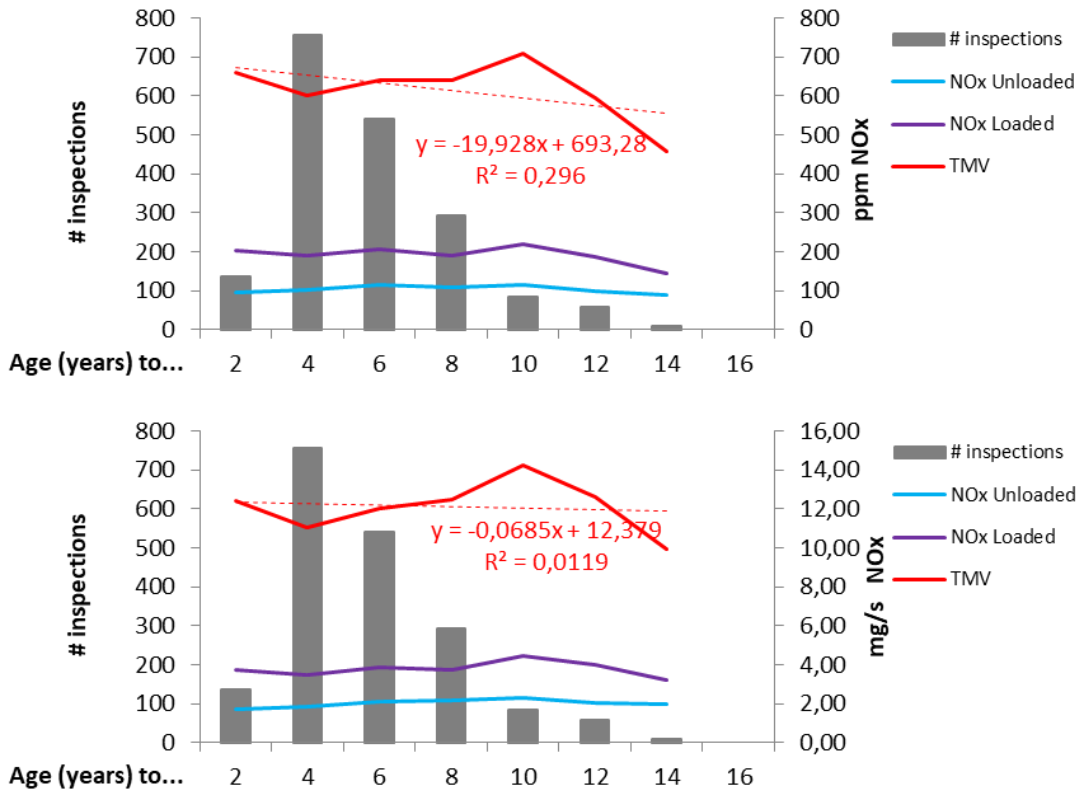


Figure 9-6. NO_x emissions to Age, in Concentration (up) and Mass Flow (down).

Correlation between Vehicle CO₂ Approval-type Emissions and Test NO_x Emissions

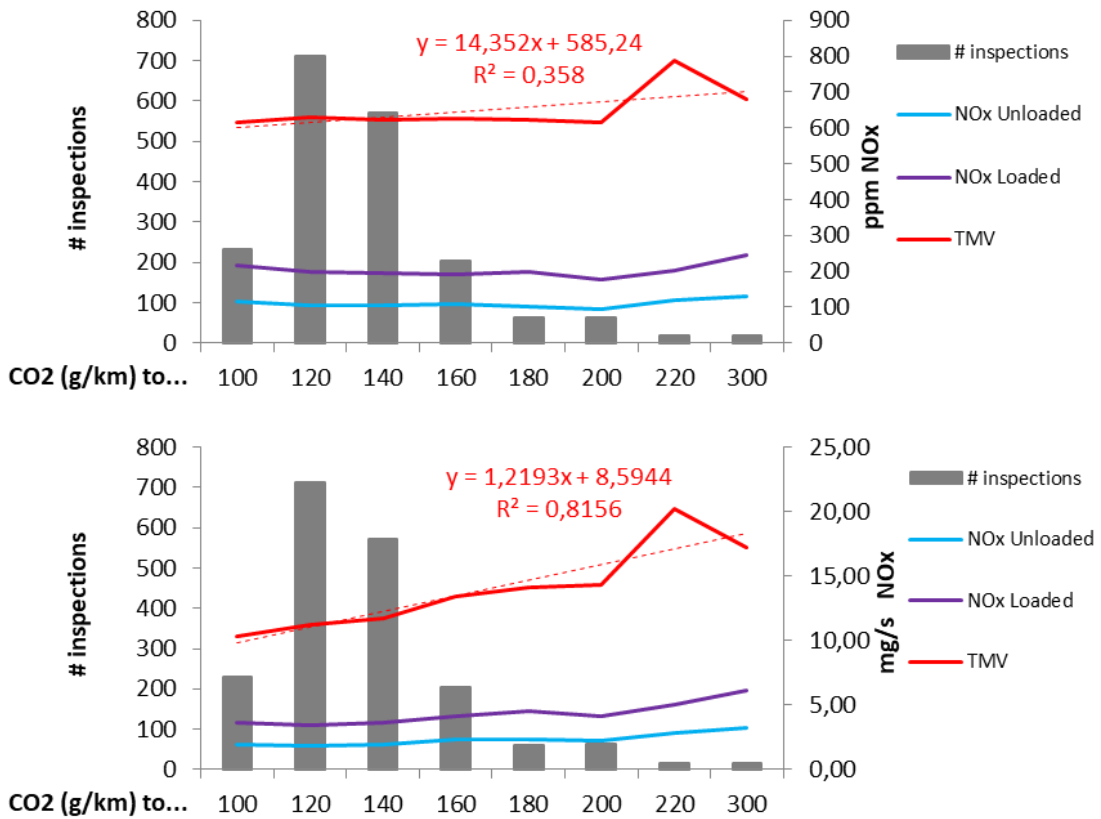


Figure 9-7. NO_x emissions to CO₂ emissions, in Concentration (up) and Mass Flow (down).

CO₂ emissions are also a very important vehicle characteristic and are an indicator used to classify vehicles in terms of their polluting capacity. CO₂ is also generated in the combustion process, so it is worth asking whether there is any relationship between a vehicle's CO₂ emissions (the combined data provided from the Approval-Type of the vehicle) and NO_x emissions.

Concerning the concentration-based measure of NO_x emissions, a noticeable lack of correlation between the two variables is evident, indicated by an R² value below 0.4. In observing the associated graph, it becomes apparent that the average NO_x emissions remain relatively constant across a broad spectrum of CO₂ emissions.

In contrast, when exploring the relationship through the Mass Flow perspective, an observable inclination towards increased NO_x emissions corresponding to higher CO₂ emissions is noticeable. This relationship garners an R² value of 0.81, signifying an acceptable level of relationship quality. Consequently, **this correlation implies that vehicles with elevated CO₂ emissions tend to exhibit higher NO_x emissions.** However, this connection warrants further investigation to gain a more comprehensive understanding.

Correlation between Vehicle Approval-type and Test NO_x Emissions

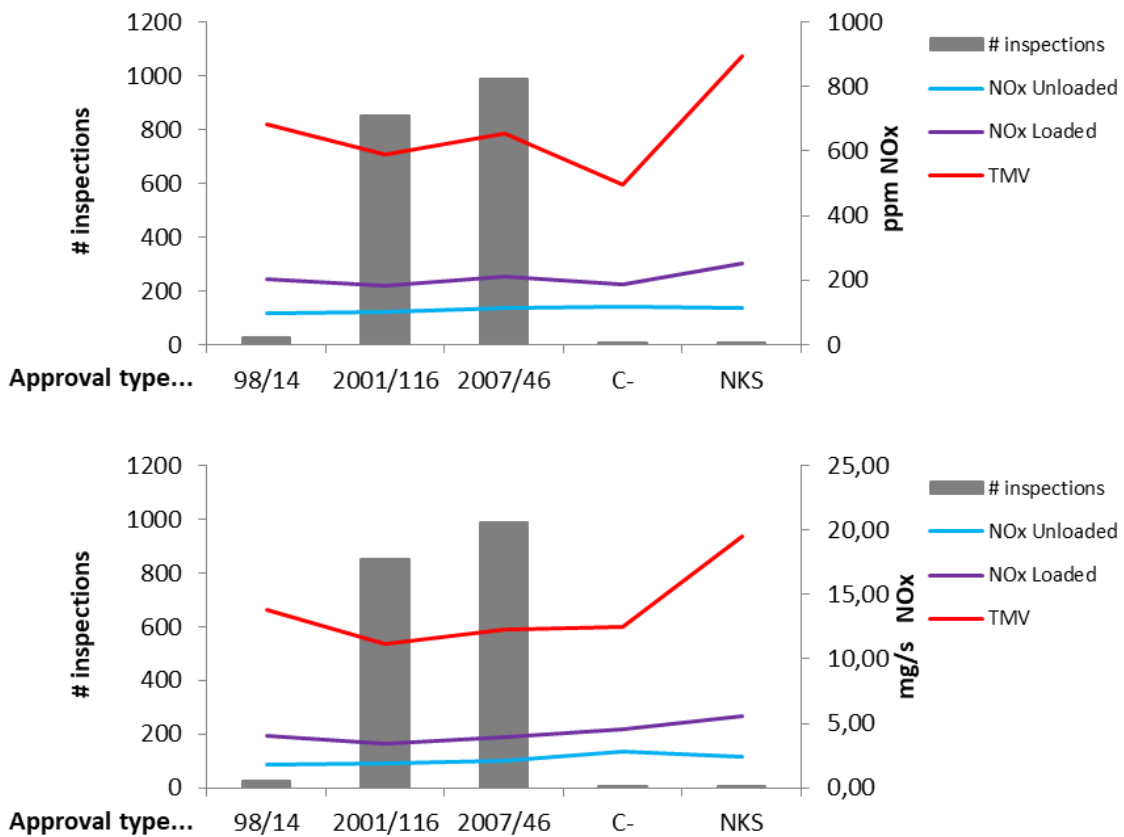


Figure 9-8. NO_x emissions to Approval type, in Concentration (up) and Mass Flow (down).

Lastly, another distinctive aspect to consider is the directive under which vehicles are homologated. As the focus here encompasses Euro 4, Euro 5, and Euro 6 vehicles, the available homologation directives that these vehicles can conform to are inherently restricted.

Yet again, it seems that the vehicle type-approval directive does not exhibit a direct linear correlation with the vehicle's NO_x emissions. Up to this point, none of the scrutinized vehicle characteristics appear to display a clear-cut relationship with NO_x emissions. This holds true even when a relationship is observable when investigating one type of emissions (e.g., emissions in concentration); the quality of this connection may not be replicated when studying the other type.

Correlation between Vehicle Ratio Power/MOM and Test NO_x Emissions

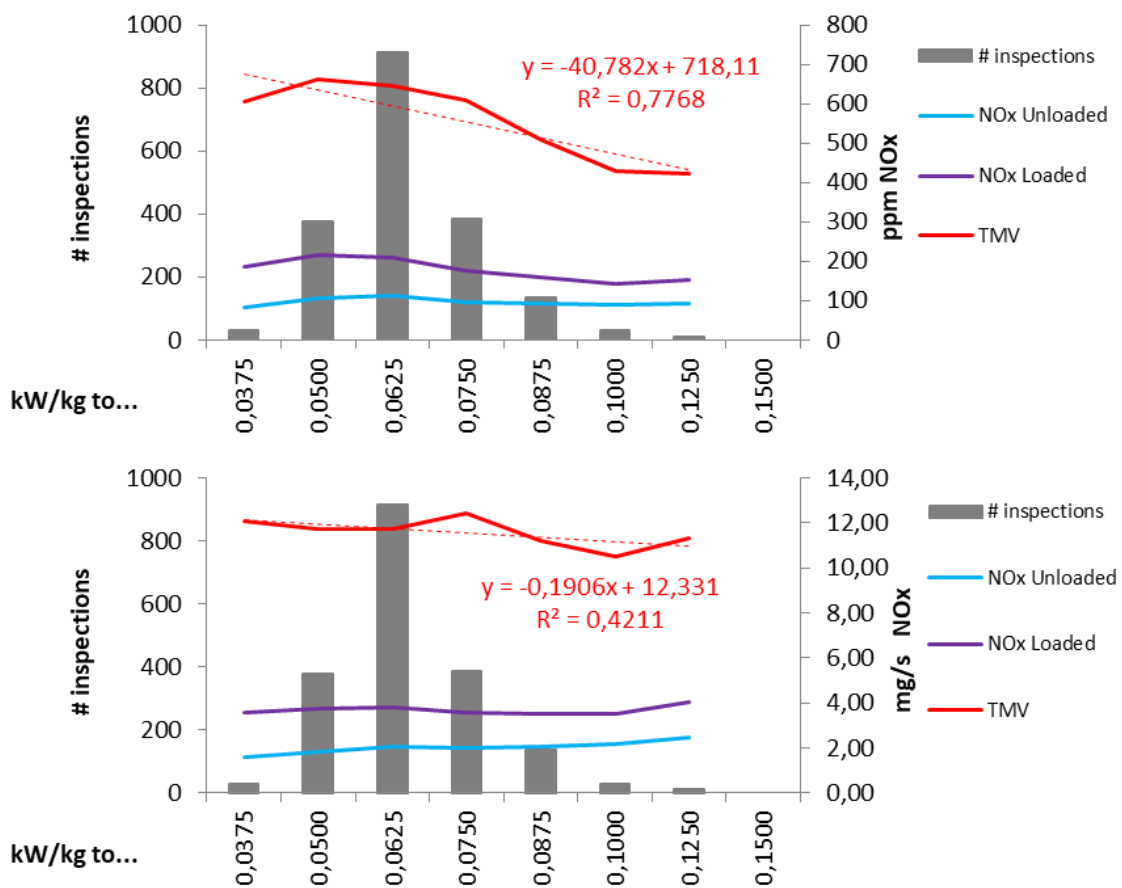


Figure 9-9. NO_x emissions to ratio Power/MOM (kW/kg), in Concentration (up) and Mass Flow (down).

Further exploration could encompass analyzing the relationship between NO_x emissions and not just one vehicle characteristic, but rather a combination of two characteristics. For instance, one common pairing for assessing a vehicle's dynamic behavior is the Power/MOM (mass in running order) ratio, expressed in kW/kg. In essence, this metric denotes the amount of power in kilowatts that the engine

generates per kilogram of vehicle mass. A higher ratio signifies that the vehicle's dynamic performance is more robust.

Should the NO_x emissions be evaluated as a function of the Power/MOM ratios of the examined vehicles, the ensuing diagram would emerge.

From the graph, it becomes apparent that a discernible relationship is present. Upon scrutinizing the concentration analysis, an R² value of 0.78 is calculated—a value that indicates the quality of the relationship might indeed exist. Conversely, in the mass flow analysis, the R² coefficient dips to 0.42, suggesting a weaker association.

Nevertheless, this pattern suggests that some form of numerical relationship, potentially not strictly causal, could potentially link NO_x emissions and a correlation among vehicle characteristics.

Because NO_x emissions are influenced by the engine, we examined various ratios that relate engine properties (like displacement and power) to other vehicle features (such as unladen masses and maximum masses). Two ratios explored were the Power/MMA ratio (kW/kg) and the Displacement/Power ratio (cm³/kW). The Power/MMA ratio behaved similarly to the Power/MOM ratio, which is logical since they involve the same variables but with differing mass data magnitudes (smaller for MOM and larger for MMA).

Correlation between Vehicle ratio Displacement/MOM and Test NO_x Emissions

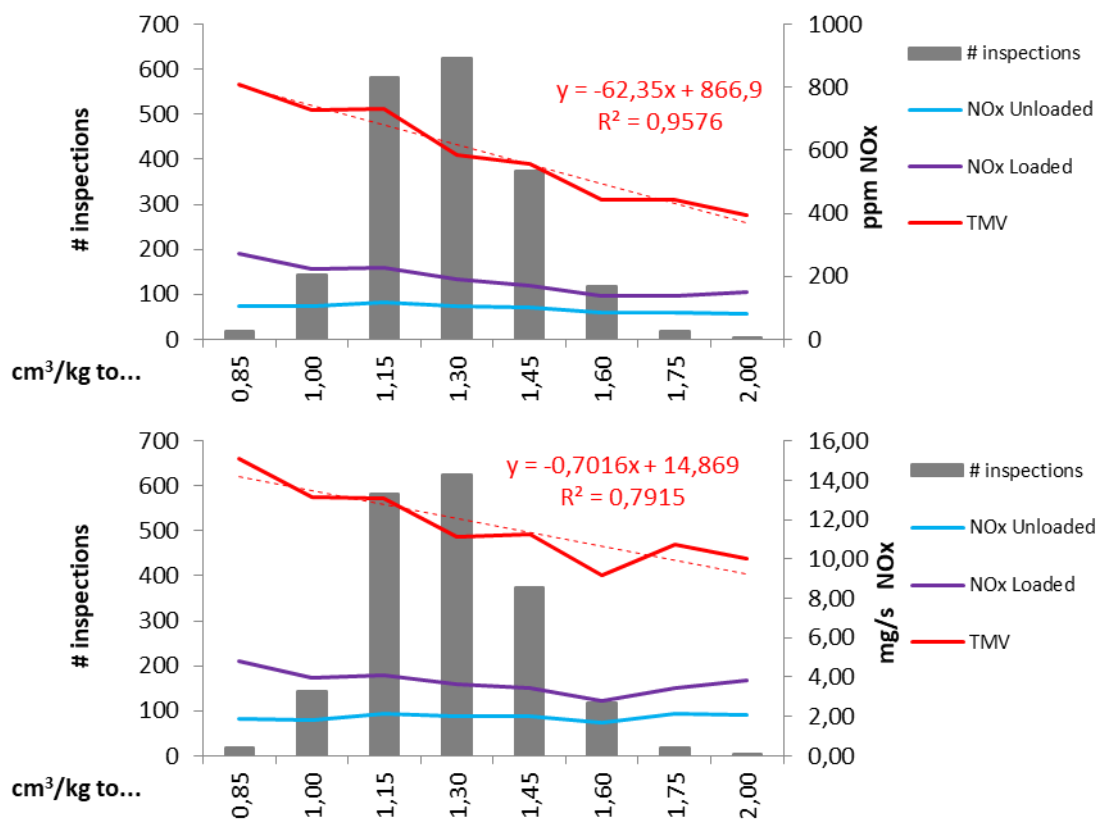


Figure 9-10. NO_x emissions to ratio Displacement/MOM (cm³/kg), in Concentration (up) and Mass Flow (down).

The Displacement/Power ratio had weaker performance and didn't seem to have a clear relationship with NO_x emissions. On the other hand, we identified a ratio that exhibited a numerical connection with NO_x emissions: the displacement/MOM ratio (cm³/kg). This ratio gauges the engine's size in relation to the vehicle's unladen mass. The findings indicated that **vehicles with larger displacement engines relative to their weight tend to have lower average NO_x emissions.**

While the analysis shows potential numerical relationships between these variables, it is essential to understand that these findings might not confirm a direct cause-and-effect link between them. To establish a more concrete cause-and-effect relationship, further extensive research is necessary. This could involve considering additional factors like emission control mechanisms, driving conditions, and fuel quality to comprehensively understand the dynamics affecting NO_x emissions.

Correlation between Test Season and Test NO_x Emissions

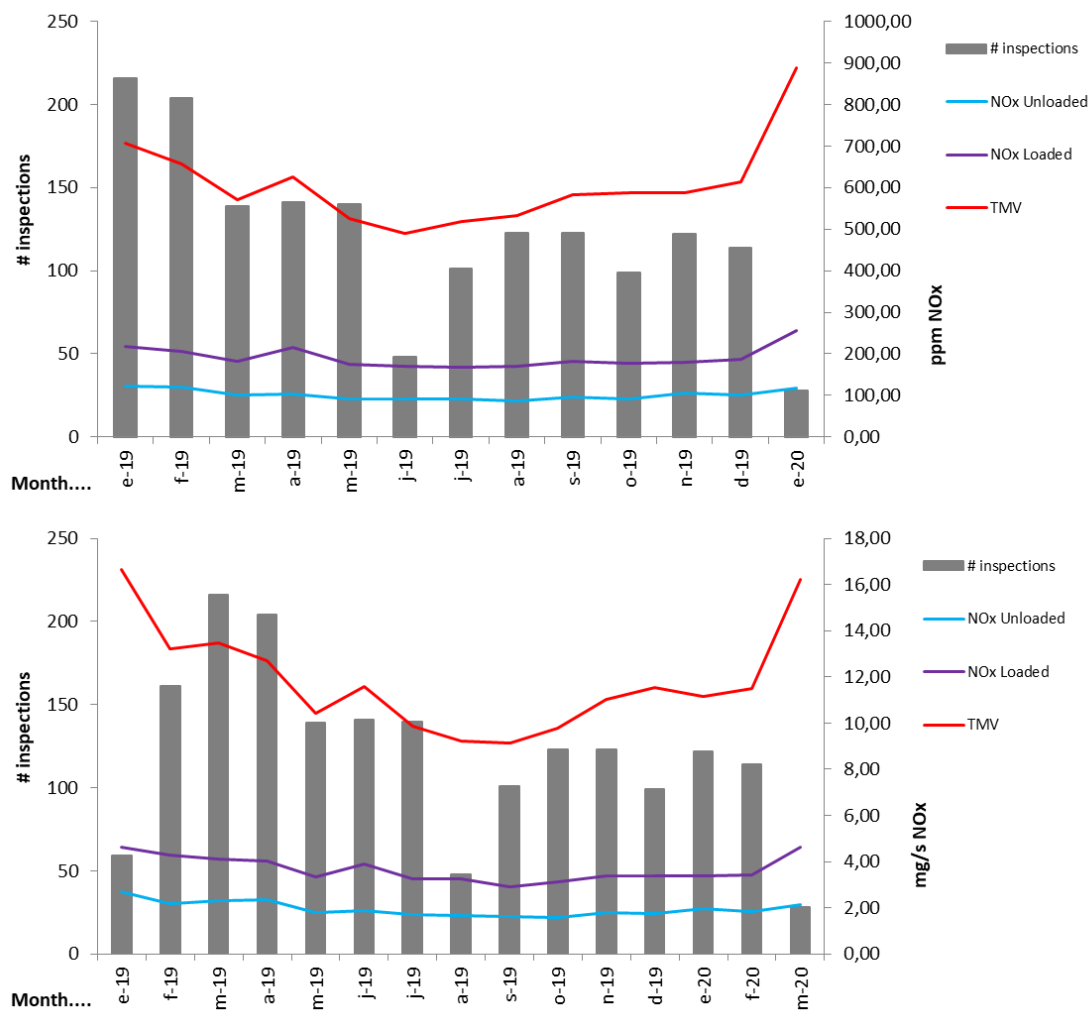


Figure 9-11. NO_x emissions evolution along the year 2019-20, in Concentration (up) and Mass Flow (down).

Finally, considering the extensive duration of the measurement campaign spanning over a year, we analyzed the evolution of emissions over different seasons to

determine if environmental conditions could impact emissions and if there's any seasonal pattern in emissions.

Given that the sample of vehicles was randomly selected and is considered homogeneous, one would expect that average emissions remain relatively stable throughout the year unless some external factors come into play.

According to Figure 9-11, which represents the data, it is evident that during the central months of the year, specifically between March and September (spring and summer), average emissions are lower compared to the other months, which correspond to autumn and winter. Notably, emissions are at their lowest average in June and reach their highest value in January.

While these findings are promising and suggestive of potential seasonality in NO_x emissions from vehicles, it is important to note that a more extensive and longer-term dataset would be needed to solidify the existence of such a seasonal pattern.

Correlation between Vehicle Manufacturer and Test NO_x Emissions

Finally, an interesting situation detected as a result of the measurement campaign is the behavior of emission values by vehicle manufacturers, and more specifically by industrial groups that bring together several manufacturers.

The purpose of these large industrial groups is to improve economic flows by creating synergies between the various brands or manufacturers included in the groups.

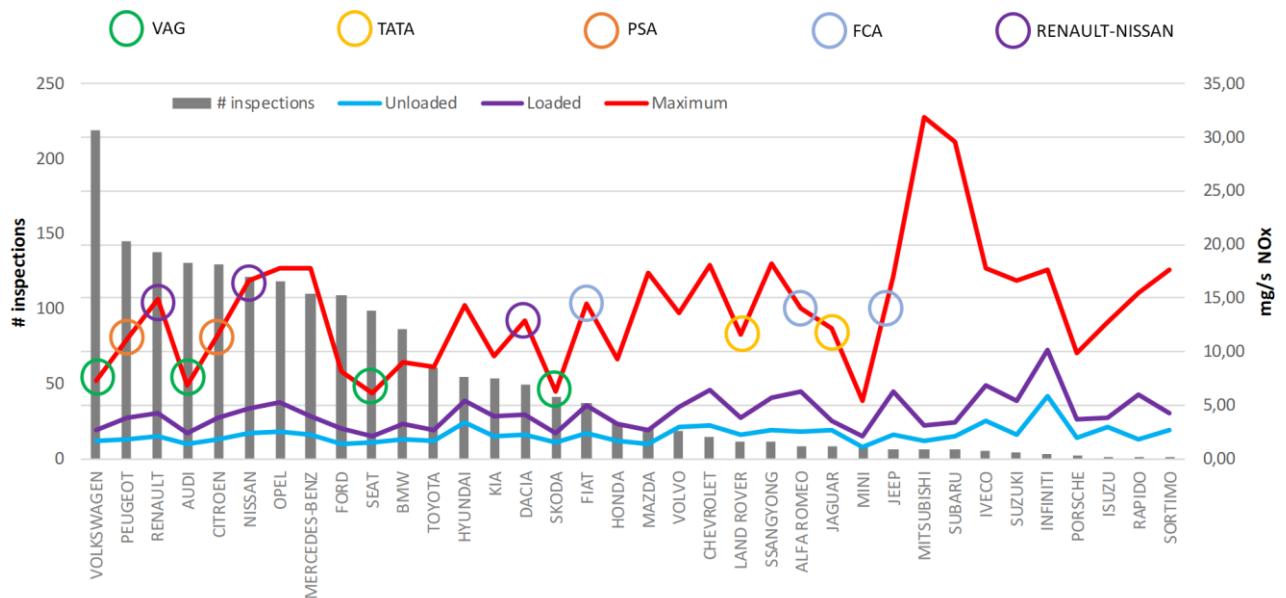


Figure 9-12. Manufacturers avg. NO_x emission.

It is quite common for vehicles of different brands in the same industrial group to share technical components, such as chassis, suspensions, engines, and other systems.

It seems logical to think that emission mitigation technologies, the EATS, would also be shared among the various brands of the same group, just as engines are shared.

If this were to happen, it would be expected that the vehicles of these brands, which are sharing engines and possibly emission mitigation technologies, would have similar emission values.

To check whether this is the case, the average emissions per manufacturer have been compared, the result being Figure 9-12, sorted by the number of inspections for each manufacturer.

The graph has been annotated with circles around manufacturers that are part of the same industrial group, using matching colors for manufacturers within each group. This has been done to facilitate quick visual identification.

Upon reviewing the graph, it becomes evident that manufacturers belonging to a common industrial group exhibit comparable average emission values.

Starting with the VAG group, which likely holds one of the highest combined sales volumes, a consistent pattern emerges. The average emissions for the brands Volkswagen, Audi, SEAT, and Skoda, measured using the TMV value, consistently fall within a narrow range of approximately 7 ± 0.5 mg/s.

A similar trend is observable with the PSA group (Peugeot and Citroën), noting that Opel was not yet part of the PSA group during the time of measurements. The average emissions for the TMV value in this case cluster within the range of 11.5 ± 0.25 mg/s.

This trend extends to other automotive conglomerates as well. The Renault-Nissan group, including Dacia, the FCA group (Fiat, Alfa Romeo, Jeep), and the TATA group, all exhibit similar emission values among their respective brands, maintaining the same order of magnitude.

Thus, the measurement method employed validates the hypothesis that manufacturers belonging to the same group and sharing technological platforms tend to showcase similar emission levels.

This observation further strengthens the credibility and utility of the method for accurately determining NO_x emission levels in vehicles.

In summary, as seen in Table 9-1, if we use the R² value obtained from the relationship between variables as an indicator of the relationship between them, it can generally be stated that NO_x emissions do not appear to be related to any of the variables commonly used to classify vehicle characteristics.

From the results obtained in the measurement campaign, it can be inferred that the NO_x emissions of vehicles do not seem to be related to either the engine size, weight, or carrying capacity of the vehicle. Neither the age nor the mileage of the vehicles seems to be useful data for determining *a priori* the NO_x emissions of a vehicle.

The behavior of some variables, such as CO₂ emissions, or the seasonality of emissions (i.e., the time of year when the measurement is taken), shows some indication that there could be a relationship between these variables. However, with

the available data, it is not possible to reach any definitive conclusion. More measurements would be needed to obtain conclusive results.

Variable analyzed	Unit	NO _x emissions	
		Concentration (ppm)	Mass Flow (mg/s)
		R ²	R ²
Weight	kg	0.5473	0.3780
MMA	kg	0.0049	0.3990
Power	kW	0.6997	0.0030
Mileage	km	0.1854	0.6761
Age	year	0.2960	0.0119
CO ₂ emissions	g/km	0.3580	0.8156
Ratio Power/MOM	kW/kg	0.7768	0.4211
Ratio Displacement/MOM	cm ³ /kg	0.9576	0.7915

Table 9-1. Correlation between variables and NO_x emissions.

In the specific case of CO₂ emissions, it may be interesting to verify the existence of a relationship between these variables, since until now, the level of CO₂ emissions indicated in vehicle homologation has been used as an index or indicator to determine how "clean" or polluting a vehicle is. Being able to confirm that the same conclusions drawn from CO₂ emissions can be applied to NO_x emissions (even though both emissions are not initially related) would be highly significant.

Of the analyzed relationships, there is only one that presents R² values (in both NO_x emission measurements) that would suggest a possible relationship between the variables. This is the Displacement/MOM Ratio (cm³/kg), which shows an R² value above 0.79 for both NO_x emission measurements, indicating a relationship between them.

The Displacement/MOM Ratio (cm³/kg) provides information about the engine size relative to the vehicle's weight, indicating that as the ratio increases, NO_x emissions decrease. In other words, the larger the engine size for a given vehicle weight, the lower the NO_x emissions.

This behavior appears consistent with the mechanism of NO_x formation in engines. With equal vehicle weight, a larger engine will be subjected to a lower relative load (lower "% engine load") to perform the same work, resulting in lower NO_x generation.

In any case, this potential relationship would require a more detailed analysis and a larger number of measurements to confirm the observed behavior.

9.3. COMPARATIVE ANALYSIS WITH MEASUREMENT AT POWER BENCH

Throughout the course of this research, a consistent theme has emerged where the act of conducting measurements at idle has generated noteworthy debate in various forums. Despite the comprehensive justification provided throughout the thesis, establishing idle as the optimal operating point for NO_x measurement in PTI, it is deemed pertinent to address this topic within this Chapter as well. This inclusion serves to reinforce the central message and underscore the rationale behind the choice of idling as the preferred measurement scenario.

Just to recap, the aim is to conduct measurements at a specific condition that generates outcomes reflective of real-world scenarios. This endeavor seeks to estimate a vehicle's emissions under real on-road driving conditions. By utilizing the test results, the objective is to distinguish vehicles that are likely to exhibit elevated emissions in practical, real-world settings. This strategic approach ensures that the test outcomes are not only precise within controlled circumstances but also have the capacity to identify vehicles with potentially higher emissions during genuine operating conditions.

Measurement cycle description

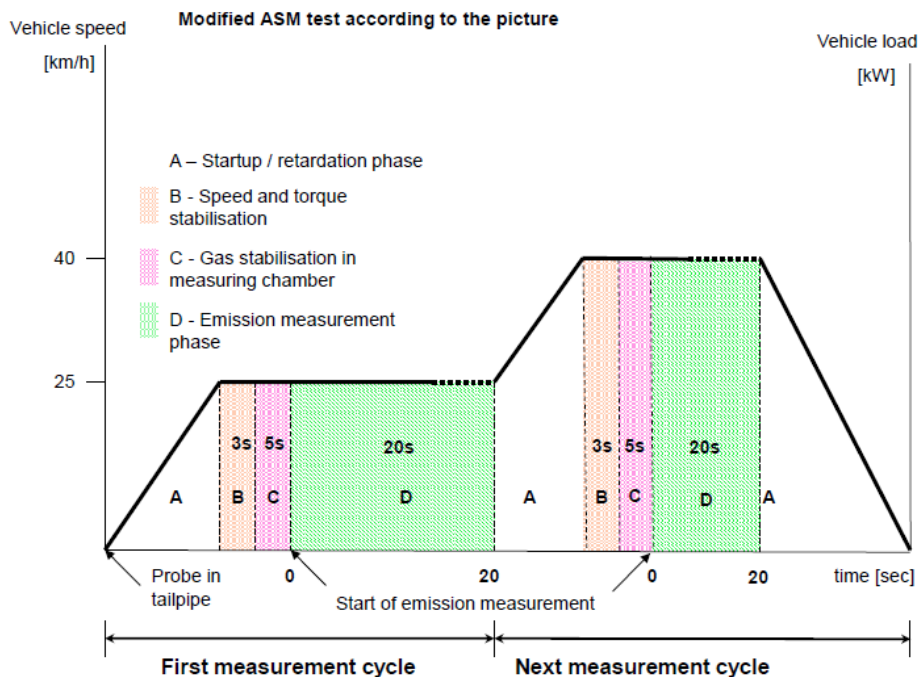


Figure 9-13. ASM2040 representation. Source: ACTIA.

Nonetheless, a decade of experience has unequivocally demonstrated that there is no single test, particularly referring to a solitary measurement point, that can furnish genuinely representative insights into real vehicle emissions. This holds true even within the context of type approval procedures. Notably, Real Driving Emissions (RDE) measurements conducted using Portable Emission Measurement Systems (PEMS)

have also revealed their need for further enhancement and refinement to bolster their representativeness. This observation pertains not only to comprehensive vehicle emissions but also extends to urban emissions, where NO_x emissions, notably detrimental, hold prominence.

However, the common approach typically involves measuring emissions, including NO_x, by subjecting the vehicle to a simulated cycle on a dynamometer (roller bench). This simulation effectively mimics the vehicle's movement, thereby emulating the emissions that the vehicle would produce during real-world operation.

An example of this approach is the ASM cycle, such as the ASM cycle 2040 (Figure 9-13) or the ASM 2050 (Figure 9-15). These cycles are purposefully crafted to replicate driving scenarios within urban settings and were explained in Chapter 2.

This approach is geared towards capturing emissions characteristics akin to those exhibited by the vehicle during real-world urban driving conditions.

Once the static idling test for NO_x measuring has been deeply analyzed, the quality of the relationship between NO_x concentration and "% engine load" when the engine is idling has been checked, the reproducibility of the test has been verified, and the significance and representativity of the results have been demonstrated, the proposed measurement process has been compared to this common approach for NO_x measurement with power bench.

The comparison process uses the ASM 2050 cycle, which is shown in Figure 9-15. In this testing method, the vehicle is placed on a dynamometer bench. It then goes through a series of steps: it starts by accelerating from 0 km/h to 20 km/h, stays at that speed for a while, accelerates again to 50 km/h, and finally slows down until it stops. This procedure assesses how the vehicle behaves under controlled and consistent conditions, simulating real-world driving situations.

To compare the two measurement procedures, vehicle number 13 from Table 5-1 was selected from the initial set used for defining the static test. First, this vehicle underwent testing on a power bench, following the ASM 2050 cycle guidelines provided by the equipment's instructions. Then, the same vehicle was tested using the proposed static idling method under identical mechanical and environmental conditions. Both tests were conducted consecutively on the same day and at the same location.

The comparison of the two methods involved three different types of tests, each performed multiple times on the same vehicle to determine the consistency of the measurements. These tests were conducted one after the other, following the details outlined in the subsequent tables. All testing steps were conducted without interruption, adhering to the specified sequence as indicated in the provided tables.

9.3.1 DESCRIPTION AND RESULTS OF THE TESTS

Test number 1: the vehicle was tested in the simulation power bench according to the ASM 2050 cycle test. OBD data and exhaust gas composition **were read with the ASM 2050 cycle equipment.**

The "% engine load" value was not recorded because the equipment did not provide this capability. As a result, only the NO_x concentration and vehicle speed were captured during the test. The load requirement and traction executed are depicted by the purple and red lines, respectively, in Figure 9-14. These lines serve to assess the comparability of conditions across the tests, instead "% engine load".

Test number	20 km/h		50 km/h	
	NO _x (ppm)	Speed (km/h)	NO _x (ppm)	Speed (km/h)
1	174.19	23.14	354.06	46.89
2	258.28	22.59	276.2	49.56
3	127.45	22.55	193.34	47.86
4	528.12	23.61	422.57	48.06
5	194.65	22.37	234.7	46.96
6	535.57	22.74	451.73	48.91
7	237.03	22.13	267.94	48.01

Table 9-2. Average values from NO_x (ASM 2050) Test No. 1.

The mean values derived from the tests, achieved when the vehicle speed stabilizes, are presented in Table 9-2. Additionally, the key statistical parameters for this collection of tests are outlined in Table 9-3.

In the section of data from 20 km/h, speed was in every case over the expected value, being the average value 13.65% higher than 20 km/h. Instead, in the section of data from 50 km/h, speed was in every case below the expected value, being the average value 3.92% lower than 50 km/h.

Statistical Parameters	20 km/h		50 km/h	
	NO _x (ppm)	Speed (km/h)	NO _x (ppm)	Speed (km/h)
Min.	127	22.13	193	46.89
Max.	536	23.61	452	49.56
Average	294	22.73	314	48.04
Standard Deviation	168.15	0.50	97.26	0.97
Coef. of Variation	57.27%	2.19%	30.94%	2.01%

Table 9-3. Statistical values from NO_x (ASM 2050) Test No. 1.

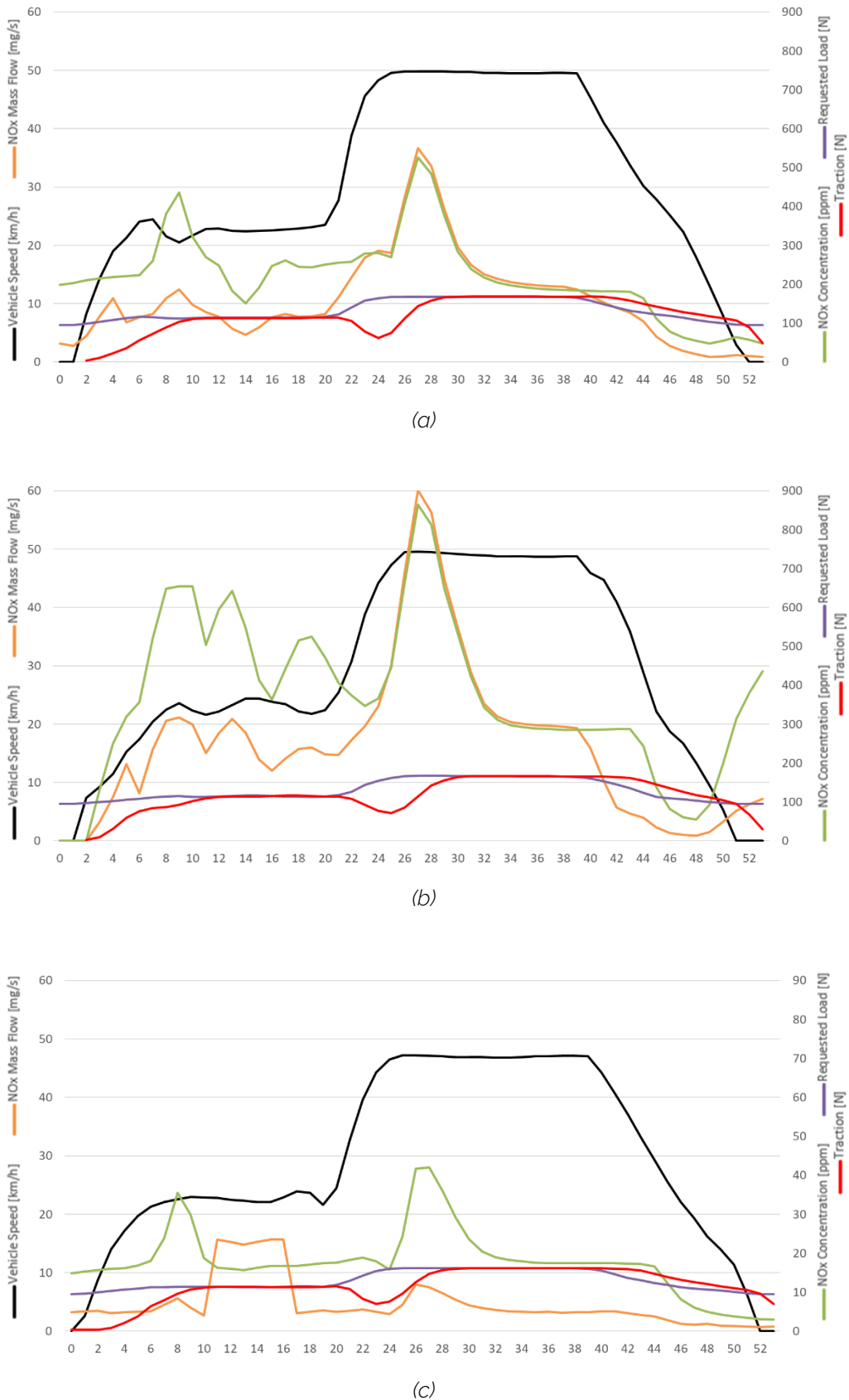


Figure 9-14. Data plots of NO_x measurements (ASM 2050) in Test Nr. 1.

The speed data displayed in both segments exhibit a low standard deviation and coefficient of variation, indicating that the speed behavior remained consistent across

the various tests in both sections. However, the NO_x concentration in both sections demonstrates a high standard deviation and coefficient of variation, suggesting that the test results exhibit substantial dispersion and variability.

Figure 9-14 illustrates that while the load and traction requirements are similar for each test, and the speed trends show a comparable pattern, there are significant differences in the emissions of NO_x between the tests. These disparities are clearly evident from the data presented in Table 9-3.

It is evident that despite maintaining similar test conditions across all cases, there is a distinct divergence in emissions behavior among the tests, resulting in significantly varying concentrations and mass flow values. Consequently, using these measurement outcomes to predict real-world emissions from the vehicle and comparing them with emissions from another vehicle measured using the same procedure might pose challenges in terms of justification. The discrepancies in the emissions behavior make such comparisons and estimations complex.

Test number 2: the vehicle was tested in the simulation power bench according to the ASM 2050 cycle test. However, in this test, the **OBD data and exhaust gas composition were read with the equipment used to develop the static method** (Tekber Centralauto equipment). In this case, as data were registered through the idling test equipment, the "% engine load" value was registered.

The values obtained from the test are shown in Table 9-4, reflecting the main statistical values from this set of tests in Table 9-5.

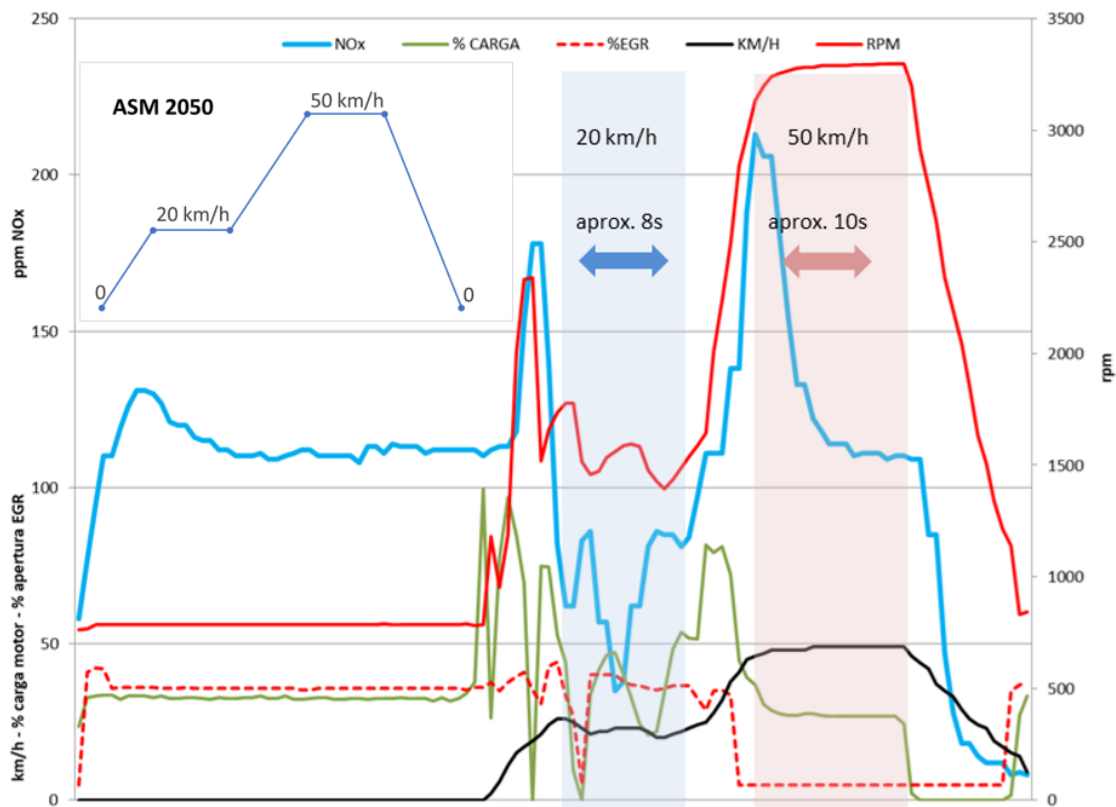


Figure 9-15. Test Nr. 2 (ASM 2050) complete test graphical representation.

As was previously explained, the NO_x concentration and "% engine load" values are related, but additional variable variations such as the engine speed can affect the NO_x emissions. Then, the quality and significance of the relationship between NO_x concentration and "% engine load" can be affected.

Test number	20 km/h			50 km/h		
	NO _x (ppm)	% Engine load	Speed (km/h)	NO _x (ppm)	% Engine load	Speed (km/h)
1	84.39	37.12	22.53	127.06	27.25	48.59
2	163.67	30.31	21.82	135.83	27.09	48.00
3	68.08	32.62	22.79	132.71	27.25	48.59
4	131.16	38.08	22.05	144.33	27.7	46.90

Table 9-4. Average values from NO_x (ASM 2050) Test No. 2.

Statistical Parameters	20 km/h			50 km/h		
	NO _x (ppm)	% Engine load	Speed (km/h)	NO _x (ppm)	% Engine load	Speed (km/h)
Min.	68	30	17.00	127	27	45.00
Max.	164	38	26.00	144	28	49.00
Average	112	35	22.30	135	27	48.02
Standard Deviation	43.70	3.69	0.44	7.21	0.26	1.00
Coef. of Variation	39.08%	10.67%	1.97%	5.34%	0.96%	2.08%

Table 9-5. Statistical values from NO_x (ASM 2050) Test No. 2.

Similarly during Test No. 1, achieving precise vehicle speed adjustment posed challenges. Within the 20 km/h data segment, it was consistently observed that the average vehicle speed exceeded the anticipated value, with an average deviation of 11.49% higher than the targeted 20 km/h. Conversely, within the 50 km/h data segment, the speed consistently fell below the expected value, with an average deviation of 3.96% lower than the intended 50 km/h.

However, despite these challenges, it is noteworthy that the vehicle speed values exhibited similarity between both Test No. 1 and Test No. 2. This congruence implies that the testing procedure was likely executed correctly, despite the difficulties encountered in accurately adjusting the vehicle speed.

Nevertheless, in this second test, the parameter "% engine load" was successfully recorded, adding further insights to the test results. In the 20 km/h segment, the average "% engine load" exhibited minimal variation, with an even lower dispersion observed in the 50 km/h segment. Conversely, the NO_x concentration demonstrated

a higher degree of variability in the 20 km/h segment, while displaying more favorable trends in the 50 km/h segment.

In addition, when examining the correlation and significance between "% engine load" and NO_x concentration using the data from Test No. 2, the results presented in Table 9-6 indicate that the calculated p-value generally exceeds the significance threshold (highlighted in red). This suggests that, for the conditions of the ASM 2050 test, the relationship significance between "% engine load" and NO_x concentration is low.

Test number	20 km/h		50 km/h	
	R ²	p-value	R ²	p-value
1	0.12	0.21	0.78	1.08E-05
2	0.14	0.16	0.045	0.41
3	0.39	0.03	0.22	0.04
4	0.01	0.67	0.25	0.04

Table 9-6. R² and p-value from NO_x (ASM 2050) Test Nr. 2.

The recorded data from this test also provides insights into the behavior of the EGR system. It is apparent that the EGR valve closes when the vehicle reaches a speed of 50 km/h. This observation implies that, for this particular vehicle, conducting a measurement solely on a roller bench at 50 km/h would not be sufficient to accurately assess the proper functioning of the EGR system.

This is due to the fact that the operational characteristics of the EGR system (and other emissions after-treatment systems) are not known beforehand. As a result, it is impossible to determine from the test alone whether the EGR system's operation is correct or not, since there is no baseline understanding of whether it should or should not be active at that speed.

This is a prevalent issue in emissions measurement. While it is feasible to confirm proper functionality, it remains challenging to discern the root cause if the system is not working as expected. It could be due to a malfunction, tampering, or alterations in the ECU programming. Moreover, determining whether the system is adhering to the manufacturer's original design is also unattainable in such cases.

Furthermore, upon examining Figure 9-15, it becomes apparent that the NO_x concentration measured during vehicle idling is comparable to the NO_x concentration measured during the 50 km/h section. This suggests that the substantial investment in equipment and resources required to conduct this measurement test might not be practical for routine PTI usage. While such equipment is certainly valuable for research objectives aimed at understanding NO_x emission behavior, it appears redundant for PTI purposes, as the same NO_x concentration observed at 50 km/h can also be captured during idling speed measurements.

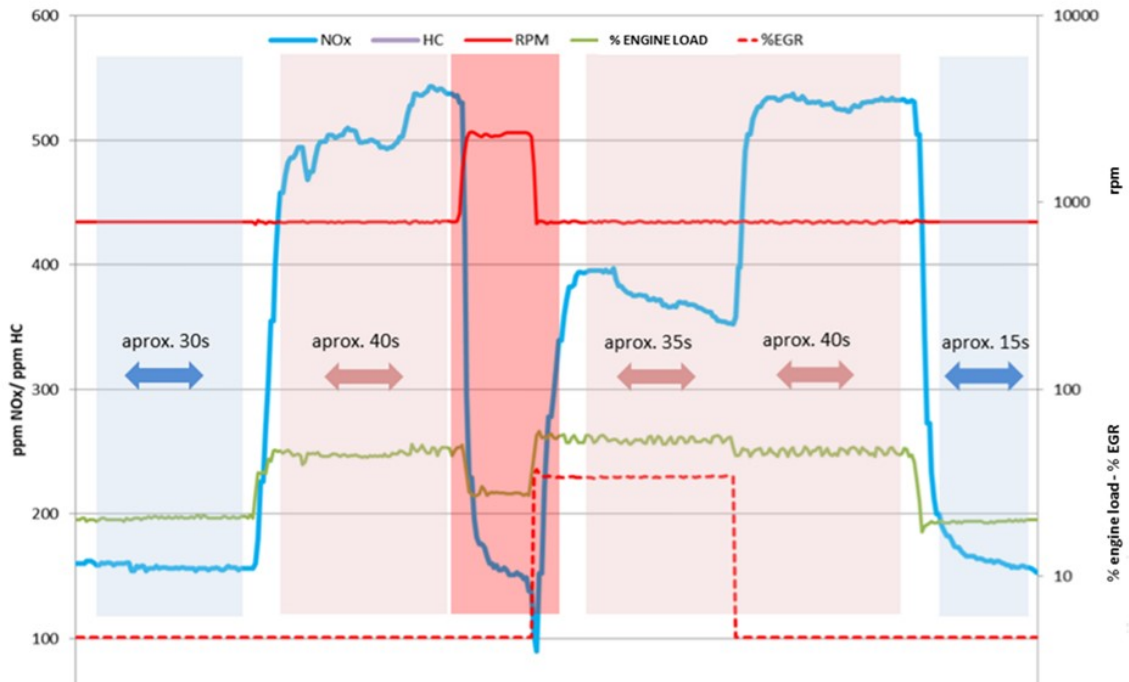


Figure 9-16. Static idling NO_x measurement test.

Test number 3: the vehicle was tested according to the proposed static idling test. OBD data and exhaust gas composition were read with static method equipment. As always with the idling test, the “% engine load” was registered.

The values obtained from the test are shown in Table 9-7, the main statistical values from this set of the test are reflected in Table 9-8.

Finally, the relationship between “% engine load” and NO_x concentration was analyzed through the R² and the p-value, to know the quality and significance of the relationship between data of both variables. Values obtained are shown in Table 9-9.

Test number	Unloaded idle		Loaded idle	
	NO _x (ppm)	% Engine load	NO _x (ppm)	% Engine load
1	179.62	22.19	536.49	49.20
2	159.33	20.00	471.92	48.41
3	154.50	19.72	418.99	51.66

Table 9-7. Average values from NO_x static Test Nr. 3.

Statistical Parameters	Unloaded idle		Loaded idle	
	NO _x (ppm)	% Engine load	NO _x (ppm)	% Engine load
Min.	154.50	19.72	418.99	48.41
Max.	179.62	22.19	536.49	51.66
Average	164.48	20.64	475.80	49.76
Standard Deviation	13.33	1.35	58.85	1.69
Coef. of Variation	8.10%	6.55%	12.37%	3.40%

Table 9-8. Statistical values from NO_x static Test Nr. 3.

Test number	Unloaded idle		Loaded idle	
	R ²	p-value	R ²	p-value
1	0.92	3.53E-70	0.92	6.58E-78
2	0.95	5.52E-97	0.46	5.22E-27
3	0.78	1.16E-46	0.07	1.00E-06

Table 9-9. R² and p-value from NO_x static Test Nr. 3.

9.3.2. DISCUSSION OF THE RESULTS

Tests Number 1 and Number 2 followed a consistent procedure: the vehicle was positioned on the chassis dyno, secured, and subjected to preconditions. A trained driver then conducted the test in accordance with the ASM 2050 cycle. Notably, the additional time needed for setup on the simulation bench was not factored into the test evaluation.

The sole distinction between Test Number 1 and Test Number 2 lay in the measurement equipment used; the tests were otherwise executed in an identical manner.

Figure 9-15 depicts the visual representation of data gathered during Test Number 2. In theory, data from Test Number 1 should resemble that of Test Number 2. However, the chassis dyno equipment did not capture readings for % engine load and % EGR in Test Number 1, rendering it impossible to create a graphical representation. Figure 9-14, features graphical depictions of the data recorded during Test Number 1.

Lastly, the static method proposed in this thesis was applied to the vehicle in Test number 3, according to instructions from Chapter 4. Figure 9-16 shows a graphical representation of data from one of these tests.

According to registered data from the three tests, we can state the following:

1. For the ASM 2050 cycle, it is difficult to repeat the test with the same result.

As can be seen in Figure 9-15, and data acquired from the test, in the 20 km/h section the engine speed is not homogeneous. The same behavior was observed from “%

engine load", % EGR and NO_x concentration. This suggests that NO_x emissions from this data section may not be very representative, due to the variation of so many variables. Besides this, it is hard for the driver to maintain a constant speed of 20 km/h, and it is even harder to reproduce the test several times with the same conditions of rpm and "% engine load" (refer to measurement error analysis).

In both data segments (20 km/h and 50 km/h), it is worth noting that the time frame employed to calculate the average NO_x emissions might be relatively brief, potentially affecting the attainment of a comprehensive average value (given the measurement frequency of 1 Hz). Importantly, it should be emphasized that test procedures are dictated by the capabilities of the testing equipment, which in turn guides the trained driver on the vehicle's operational protocols.

2. For the ASM 2050 cycle test, the Standard Deviation and Coefficient of Variation are higher than for the static cycle test.

Specifically, in Test Number 1, for both sections (20 km/h and 50 km/h) the Standard Deviation and Coefficient of Variation of the NO_x concentration are remarkable. As is shown in Table 9-2, at 20 km/h the highest NO_x concentration is 4 times greater than the lowest, and at 50 km/h more than 2.3 times greater. The SD at 20 km/h is 168.15 ppm, while at 50 km/h it is 97.26 ppm, and the corresponding CV is 57.97% and 30.94%.

For Test number 2, the SD is significantly lower than for Test number 1, but the CV at 20 km/h is 39.08%. This indicates that the dispersion of data is high. On the contrary, these dispersion metrics are better for the static test than for the dynamic one. The unloaded idle presents an SD of 13.33 ppm and a CV of 8.10%, while for the loaded idle the SD was 58.85 ppm and CV was 12.37%, similar values in both situations. In short, the static test shows lower dispersion, that is, better reproducibility.

3. For the ASM 2050 cycle test (equally for Test number 1 and Test number 2), the highest NO_x emissions are indistinctly reached at the 20 km/h or 50 km/h section, while for the static cycle test highest NO_x emissions are always reached at the loaded state.

The difficulty of repeating the ASM 2050 cycle test in the same conditions means that the "% engine load" presents high variability and consequently, NO_x emissions are variable too. Instead, the simplicity of the static test allows us to achieve a similar "% engine load" at unloaded and loaded states, and consequently, similar NO_x emissions are reached from several tests: always the higher NO_x emissions are reached at the loaded state.

4. There are important differences between NO_x emissions values from Test Number 1 and Test Number 2. Although the test was developed in the same way, the average NO_x emissions from Test Number 1 were more than 2 times greater than those from Test Number 2. This could be attributed to the difference between the NO_x sensors of both types of equipment. However, the behavior in both Tests is different too, so not only the different NO_x sensors can explain the differences. In the same way, results from Test Number 2 and Test Number 3 show great differences, although the gas analyzer was the same. The NO_x concentration for the static idling Test Number 3 was higher than for dynamic Test Number 2.

5. In Test number 2, the "% engine load" is higher for the 20 km/h section than for the 50 km/h section. Instead, NO_x emissions are higher (on average) for the 50 km/h than for the 20 km/h section.

This seems to indicate that in this type of test, data from NO_x emissions are not correlated to "% engine load". Calculating the significance of the model in Test 2 with the p-value, as was explained before, seven of the eight p-values calculated were higher than the significance level (Table 9-6), so the null hypothesis cannot be rejected for both situations.

We can observe that when the vehicle accelerates to 50 km/h, both engine speed and "% engine load" exhibit a higher level of homogeneity compared to the 20 km/h section, and % EGR is nearly closed. It could be assumed that NO_x emissions are more representative in this section. However, in this scenario, where rpm, "% engine load," and % EGR exhibit consistent behavior, NO_x emissions decrease from their maximum value to the same concentration as at idle speed. Consequently, it becomes challenging to establish a correlation between NO_x emissions and "% engine load" in this particular section.

6. The "% engine load" reached from the static test is significantly higher than for the dynamic test with a chassis dyno.

In Test Number 2 the higher engine load was 38.08% at 20 km/h. Instead, in Test number 3 the higher engine load was 51.66% at loaded idle, being the average engine load at loaded idle being 49.76%.

The highest engine load in Test number 3 generates also the highest NO_x emissions, individually for every test, and on average. Instead, in Test number 2 sometimes the highest engine load does not correspond to the highest NO_x emissions. This occurs individually for some of the tests and with the average value. The average NO_x concentration for loaded idle was 475.80 ppm, while for the dynamic test, the higher average NO_x emissions read were 314.36 ppm at 50 km/h in Test number 1, and 134.98 ppm at 50 k/h in Test number 2.

So, the NO_x concentration measured with the static test is higher than the NO_x concentration read with the ASM 50-20 dynamic test (in this vehicle).

7. It is easier to reproduce the static test than the ASM 2050 dynamic test.

In this way, it is possible to make the static test repeatedly with similar results, and the duration of each step of the test can be deliberately extended to obtain a stable and adequate set of data to calculate the average NO_x emissions easily.

For Tests, number 1 and number 2, the extension of the section to calculate average emissions was approx. 20 s for 20 km/h and 50 km/h respectively (indicated by the equipment to the driver), but the time of steady values of emissions is lower.

In Test Number 3, the duration of any of the measurement steps exceeds 30 seconds. If not required, they could be shorter (typically, 20 seconds is sufficient for accurate results). However, if necessary, they can be extended to achieve the correct average NO_x emissions because the simplicity of the method allows for it.

This is because, as could be seen in Figure 9-16, the behavior of "% engine load", engine speed, and % EGR is much more stable in the static test than those shown in the dynamic one (Figure 9-15). Consequently, NO_x emissions are more stable, and therefore, it is easier to get a representative and accurate average NO_x emissions value.

To finish, as was explained previously, a vehicle is a complex combination of interacting systems regulated by the ECU (Engine Control Unit), and the real on-road NO_x emission from the vehicle at the exhaust pipe depends on a large number of variables. Results from Tests number 1 and number 2 show how the measurement of emissions when the vehicle is in circulation cannot be related to a single variable (as could be the "% engine load"), and to correctly understand the results it is necessary to know how each of the variables intervenes to modify the final NO_x concentration value.

On the other hand, for static measurements, only "% engine load" is required to easily control NO_x emissions.

In summary, the main differences between both methods are that the reproducibility, significance, and results in the dispersion of the static test are significantly better than those for the dynamic one. Moreover, the "% engine load" reached and the NO_x concentration read with the static test are higher, and yet the time, equipment, and staff training requirements are lower than for the dynamic test.

Ultimately, the key distinctions arising from the comparison are summarized and presented in Table 9-10.

	ASM 2050 DYNAMIC TEST	IDLING STATIC TEST
EQUIPMENT	COMPLEX	SIMPLE
PROCEDURE	COMPLEX	SIMPLE
% ENGINE LOAD	LOW	MEDIUM
REPRODUCIBILITY	LOW	HIGH
MEASUREMENT DISPERSION	HIGH	LOW
REL. % ENGINE LOAD - NO _x	LOW	HIGH

Table 9-10. Main differences between dynamic and static tests.

9.4. MODELING AND ANALYSIS OF NO_x EMISSIONS IN URBAN CIRCULATION

Throughout the thesis, a recurring theme has been the assertion that the insights offered by the measurement method can serve as a valuable tool for comprehending the emissions produced by an entire fleet of vehicles. This information holds the potential to shape environmental policies and strategies, among other applications. This underscores the significant importance of integrating a NO_x measurement component into the framework of PTI.

While this document does not delve deeply into highly advanced modeling methods, it is worth demonstrating through an example how even a basic and straightforward system can yield valuable insights. With dependable data from this measurement method as a foundation, it becomes feasible to generate meaningful information. This information can then be employed to evaluate the NO_x emissions of a vehicle fleet, leading to valuable conclusions that prove instrumental in crafting and implementing effective environmental and health protection policies.

To illustrate the practical significance of understanding actual vehicle emissions at idling speed through the proposed test, let us proceed to compare the projected emissions of three vehicles examined in the measurement campaign. We will envision these vehicles following an identical urban route under equivalent conditions.

To make the estimation, a typical journey in an urban environment in a big city (in this case Madrid) has been chosen. It is a 6 km, 18-minute journey in the center of Madrid, specifically from the Santiago Bernabeu Stadium to the Spanish High-Speed Train (AVE) station at Puerta de Atocha.

The route is shown in Figure 9-17, revealing that despite being an urban course, it predominantly traverses broad main avenues featuring extended straight segments. The specific day and time of the route (Monday at 11:40 a.m.) are indicated, along with the anticipated traffic congestion along the route. It is worth noting that this route typically experiences substantial traffic volume.

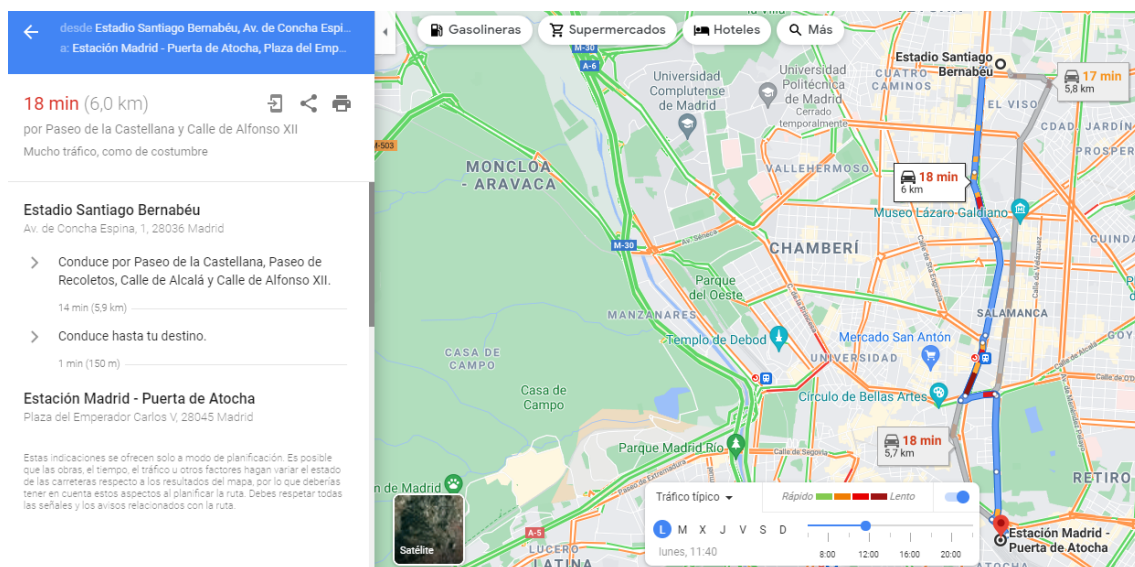


Figure 9-17. Sample of a typical urban trip in Madrid center. Source: Google Maps.

With the information about the time that a vehicle is stopped according to the type of route and the traffic congestion in which it circulates, it is possible to estimate the time that a vehicle will be stopped while performing the route proposed for comparison. For this calculation, the description of 12 typical traffic conditions used by ARTEMIS and defined in 1997 with onboard measurements will be used [108], [195].

From the data in Figure 9-17, it can be determined that 5% of the trip can be considered fast (free-flow urban driving), 80% of the trip can be considered normal (low steady speed), 10% of the trip occurs in slow traffic conditions, and 5% of the trip occurs in very slow traffic conditions (high stop duration). In Table 9-11, the shaded and bolded data indicates the percentage of time the vehicle remains stationary under each of these four traffic conditions.

Classes of driving conditions and their description				Percentage of total mileage (%)	Running speed (km/h)	Average speed (km/h)	Stop duration (%)	Stop rate (stop/km)
1	congested urban	high stop duration		3.7	25.9	10.2	60.8	3.9
2				5.9	23.6	15.9	32.7	3.0
3		low steady speeds		2.4	16.5	13.2	19.5	3.4
4	free-flow urban			5.1	28.0	26.1	6.7	0.97
5		unsteady speeds		12.2	35.6	32.3	9.1	0.98
6	secondary roads	unsteady speeds		10.8	52.2	48.8	6.6	0.41
7				8.8	45.5	43.8	3.7	0.39
8		steady speeds		7.2	65.0	64.0	1.5	0.15
9	main roads	unsteady speeds		11.8	75.0	72.5	3.3	0.15
10				6.2	86.1	85.7	0.4	0.04
11	motorways	unsteady speeds		10.4	115.6	114.9	0.7	0.03
12				15.6	123.8	123.7	0.1	0.01

Table 9-11. European Driving Conditions. Source: André, 1997 [195].

Driving condition	Trip (%)	Stop duration (%)	Trip time (min.)	Stop time (min.)	Stop time (s)
Free-flow	5%	6.7%	0.9	0.1	4
Low steady speeds	80%	19.5%	14.4	2.8	168
Low unsteady speeds	10%	32.7%	1.8	0.6	35
High stop duration	5%	60.8%	0.9	0.5	33
Total	100%		18.0	4.0	240

Table 9-12. Stop timing in the sample trip.

Using these percentage values and considering the overall expected duration of the journey, it becomes feasible to approximate the duration during which a vehicle will be stationary with the engine idling over the course of this trip (Table 9-12). This

estimation indicates that the vehicle remains at a standstill for approximately 22% of the total travel duration, a figure that aligns well with estimations from similar studies.

With this idling duration established, and **armed with the genuine emission data acquired from the proposed test while the vehicle is idling**, it becomes possible to generate a practical assessment of the total emissions produced by the vehicle during its idle periods. By having access to the vehicular traffic flow for a specific journey, it is conceivable to formulate an estimation of the emissions that might be anticipated for that trip.

Conducting this procedure with multiple vehicles allows us to ascertain, for a specific journey, which vehicle is likely to exhibit greater emissions during idling periods. In essence, it helps us identify which vehicle will contribute more emissions while stationary during an urban trip.

To achieve this objective, the example below estimates the emissions of three vehicles with similar engines that will undertake the same trip under identical conditions. The data have been obtained using the procedure proposed in this thesis during the measurement campaign conducted on real vehicles passing through the PTI stations daily, as detailed in Chapter 8.

The first vehicle (Vehicle 1) analyzed is a Ford Focus C-Max registered on 30/12/2010, with a **1560 cm³** engine and Euro 4 emissions level.

The second vehicle (Vehicle 2) analyzed is a Peugeot Partner registered on 08/07/2016, with a **1560 cm³** engine and Euro 5 emission level.

Finally, the third vehicle (Vehicle 3) analyzed is a Citroën Berlingo registered on 03/26/2018, with a **1560 cm³** engine and Euro 6 emission level.

Table 9-13 presents a comprehensive compilation of results obtained from these vehicles through the implementation of the proposed method. Using the data acquired from these measurements (Test results column), the NO_x emissions for each vehicle are computed for the duration it remains stationary at idling speed during the journey (Trip Stop emissions column). This calculation is performed for two scenarios: firstly, when the vehicles operate with all equipment disconnected (Unloaded), and secondly, when they operate with the test equipment connected (Loaded).

Finally, by taking into account the trip's distance (6 km), the total theoretical emissions of each vehicle are calculated according to their Euro standard emission factor (EF_{NO_x}) (Trip emissions according to EF_{NO_x} column).

A Euro 4 vehicle has an emission factor (EF_{NO_x}) of a maximum of 0.25 g of NO_x per kilometer driven (Table 9-14), so on a 6 km trip like the one in the example, NO_x emissions should be, according to this emission factor 1,500 mg of NO_x.

However, it is evident that emissions while the vehicle is idling at a standstill already reach 1,468 mg of NO_x emitted (i.e., without considering the emissions of the vehicle in motion, the theoretical maximum emissions according to the vehicle type approval is already reached).

		Test results			Trip Stop emissions	Trip emissions according to EF _{NOx}
		NO _x ppm	NO _x mg/s	% engine load	NO _x mg	NO _x mg
Vehicle 1	Unloaded	116	1.88	14	451.66	
	Loaded	377	6.11	43	1467.90	1500
	TMV	1004	16.22	100		
Vehicle 2	Unloaded	103	1.65	24	396.41	
	Loaded	431	7.23	59	1736.98	1080
	TMV	1027	17.16	100		
Vehicle 3	Unloaded	95	1.59	17	381.99	
	Loaded	241	4.06	41	975.40	480
	TMV	673	11.47	100		

Table 9-13. Results of PTI test and estimation of sample trip emissions.

Emission Standard	Emission Thresholds (g/km)				
	CO	HC	HC+NO _x	NO _x	PM
Diesel (M1)					
Euro 1	2.72	--	0.97	--	0.14
Euro 2	1	--	0.7	--	0.08
Euro 3	0.64	--	0.56	0.5	0.05
Euro 4	0.5	--	0.3	0.25	0.025
Euro 5	0.5	--	0.23	0.18	0.005
Euro 6	0.5	--	0.17	0.08	0.005
Gasoline (M1)					
Euro 1	2.72	--	0.97	--	--
Euro 2	2.2	--	0.5	--	--
Euro 3	2.3	0.2	--	0.15	--
Euro 4	1	0.1	--	0.08	--
Euro 5	1	0.1	--	0.06	0.005
Euro 6	1	0.1	--	0.06	0.005

Table 9-14. Emission thresholds for passenger cars (M1) in the EU.

In the case of the Euro 5 vehicle, the corresponding emission factor is 0.18 g of NO_x emitted per kilometer traveled, which means that in the 6 km trip analyzed, emissions should be 1,080 mg of NO_x. The vehicle's emissions while it has been stopped on this route already exceed by 60% the emissions that it should theoretically have over the entire route, reaching 1,737 mg of NO_x emitted. Indeed, by the time this vehicle came

to a stop, it had produced NO_x emissions exceeding the maximum expected for a Euro 4 vehicle. In the case of the Euro 6 vehicle, its emission factor is 0.08 g of NO_x emitted per kilometer driven. This means that the vehicle should emit a total of 480 mg of NO_x during the 6 km trip. The vehicle's emissions while stopped during the trip represent an increase of more than 100% for this value, reaching 975 mg of NO_x emitted.

Figure 9-18 shows the graphical representation of these results, together with the result (TMV) of the measurement in PTI with the proposed method.

In this figure the gray dashed column represents the theoretical emissions from their Euro standard EF_{NO_x} , the dark gray column represents the estimated emissions of NO_x while the vehicle remains stationary at idling speed during the journey with equipment connected (loaded emission), and the light gray columns represent the estimated emissions of NO_x while the vehicle remains stationary at idling speed during the journey with equipment disconnected (unloaded emission).

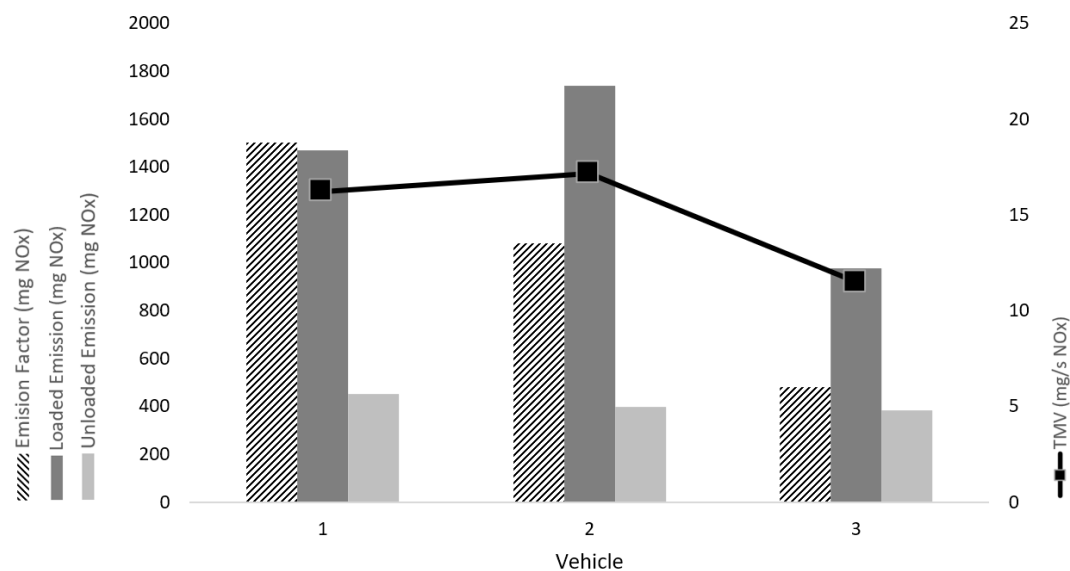


Figure 9-18. Plot results of sample trip.

From these data, it can be seen that the Euro 6 vehicle (vehicle 3) has significantly lower emissions than the other two vehicles, although it has a greater relative difference between the real emissions and the theoretical emissions that correspond to it.

It can be seen how, theoretically, the emissions of the Euro 6 vehicle (vehicle 3) should be one-third of the emissions of the Euro 4 vehicle (vehicle 1). However, in reality, when both vehicles make the same trip, we can see that the emissions of vehicle 3 are 33% lower than those of vehicle 1, i.e. the reduction in emissions (at least in the idling situation) is half of what was expected.

It can also be seen that the final test results between Euro 4 and Euro 5 vehicles are similar, although slightly higher for the Euro 5 vehicle, and the mass of NO_x emitted by both vehicles in the loaded state (the typical summer traffic situation) shows a

difference according to the data obtained in the loaded measurement (Loaded), with higher emissions from vehicle 2, as indicated by the test result.

Additionally, it is noteworthy that when vehicles are operating without the equipment activated, their emissions are comparable while stationary and idling. The distinctions between them arise when the equipment is engaged, specifically when the "% engine load" rises.

In summary, we see that all vehicles have higher emissions than expected from their Emission Factor, and we see that vehicles with more stringent emission standards have a larger (relative) difference between the estimated emissions from the test and the theoretical emission.

In contrast, in vehicles with less stringent emission standards, because there are not as many emission reduction systems, there is less of a difference between idle and running emissions.

Although it may seem "unfair" to measure the most modern vehicles in this situation where their anti-pollution systems are not working, the reality is that when vehicles are running, these "unfair" emissions are the ones that contribute to pollution in cities, with the effects explained in Chapter 1.

This basic yet missing information, absent from existing NO_x measurement methods in PTI, can serve as a crucial resource for modeling emissions across the entire vehicle fleet. With the right modeling tools, it can help establish effective policies and mechanisms for systematically reducing NO_x concentrations in urban environments using real and reliable data.

9.5. CONCLUSIONS

Throughout this Chapter, it has been demonstrated how the information gathered from the NO_x measurement campaign allows for additional analyses beyond the mere validation of the proposed method.

From these analyses, it has been observed that apart from the "% engine load", there are no straightforward vehicle variables that appear to have a direct relationship with NO_x emissions. However, certain ratios between variables may potentially have some connection to NO_x emissions, although a more comprehensive analysis and a greater number of measurements would be needed to confirm this.

Furthermore, the proposed measurement procedure has been compared with the NO_x measurement method ASM, based on a power bench, that also has been considered for use in PTI. A thorough analysis has been conducted to compare the results of applying both tests on the same vehicle. The results obtained clearly indicate that the method proposed in this study exhibits superior characteristics in various aspects, making it more suitable for use in PTI.

Finally, the results obtained from the measurement campaign have been applied in a practical example to demonstrate that the obtained results have additional utility, serving as an indicator of vehicle urban emission levels.

All the elements presented in this Chapter constitute pieces of information that thoroughly confirm the validity and usefulness of the proposed measurement process, rendering it suitable for implementation within the context of PTI.

Having examined all aspects of the proposed measurement method, the following Chapter will provide a brief summary of the information presented thus far. This will be followed by an assessment of whether the objectives outlined in the first Chapter of the thesis have been met. Finally, the Chapter will conclude with the final conclusions drawn from the study.

CHAPTER 10

CONCLUSIONS

10. CONCLUSIONS

10.1. INTRODUCTION

In this concluding chapter, after a brief summary of the methodology, its validation, and its empirical verification within the context of PTI, an overview of the practicality of the proposed implementation will be provided.

Simultaneously, a retrospective evaluation of the initially established research objectives will be conducted to determine their achievement. Additionally, the overall impact of the efforts made throughout the thesis will be explained. Following this assessment, a list of potential directions for future research endeavors arising from this study will be presented, ultimately leading to the closure with a review of the visibility of the research.

10.2. SUMMARY

Since the final objective of this Thesis was to define a valid and suitable NO_x measurement method to be used in PTI, a series of steps, described throughout the different chapters of the present document, had to be followed until the method was fully validated.

In the initial **Chapter 1**, the motivation for undertaking the thesis has been presented, aiming to find a tool that contributes to solving the identified issue posed by NO_x emissions. Additionally, the objectives to be addressed in the thesis development have been outlined.

Up to this point, the *State of the Art* has been investigated in **Chapter 2**. This demonstrates that despite the wide array of methods and systems employed for NO_x measurement across different domains, there currently exists no universally accepted or utilized method that facilitates a swift, straightforward, and dependable NO_x measurement suitable for PTI. Such a method should be readily implementable on a large scale for a diverse range of vehicles. The chapter encompasses a list of diverse methods employed for NO_x measurement, some applied within PTI, while others are used for homologation or various research purposes. It also features a description of the most prevalent technologies for NO_x measurement, along with a compilation of the latest advancements in NO_x measurement proposed during the doctoral student's research journey.

In **Chapter 3**, the method has been theoretically formulated by ensuring that the technical prerequisites that a measurement designed for implementation in PTI needs to fulfill. A working hypothesis has been established, enabling the technical substantiation of the method. The process of NO_x generation in combustion engines has been detailed, including how the characteristics of this process have been used to define and develop the measurement method. Finally, the main characteristics and advantages of this measurement method have been indicated.

Chapter 4 describes and elaborates on the method, providing detailed information on both the measurement process and the handling of data obtained during the measurement. With the content of this chapter, the measurement method can be replicated. Additionally, the results obtained from the measurement process are explained, along with the tools for assessing the quality and significance of the relationship between the key variables linked by the measurement method: NO_x concentration in the exhaust and the "% engine load" value.

The equipment used for NO_x measurement has also great importance, and the validity of the measurement method may depend on the suitability, capability, and accuracy of the equipment used. Therefore, in **Chapter 5** the suitability of the equipment used has been assessed, comparing its performance and results with measuring equipment intended for use in technical laboratories. Several tests have been carried out to verify if the equipment is valid and suitable for the purpose for which it has been intended, the measurement of NO_x in PTI. Throughout the chapter it has been demonstrated that the equipment used meets the requirements for equipment suitable for use in PTI, and also provides measurements with a level of certainty and precision appropriate for its intended use, taking laboratory equipment as a reference. A peer-reviewed paper was published with the complete information of the tested equipment [180].

Chapter 6 verified and validated the method, tested its underlying hypothesis, and demonstrated its reliability and trustworthiness through sufficient reproducibility and measurement precision. The method has been extensively described and validated through testing on a dataset of 23 vehicles, with numerous measurements conducted. Based on the results obtained, the validity of the method in terms of significance, accuracy, and reproducibility has been verified. A summary of this chapter and chapter 4 was published in a peer-reviewed paper [175].

Once a measurement method is established as valid, technically justified, and suitable for the intended purpose, ensuring it provides reliable, accurate, and precise measurements, the next step is to assess whether the results obtained when applying the method correlate with the actual emissions of vehicles during urban driving conditions. **Chapter 7** describes the process of conducting emissions measurements on a group of vehicles in urban driving conditions. The obtained results have been compared to the theoretical emission limits of the vehicles based on their emission level, as well as to the results obtained from the proposed measurement method. These findings demonstrate that the PTI measurement results offer valuable, representative, and valid information regarding both the average and maximum emissions of vehicles during urban driving.

Thus, the last step remaining to validate the proposed measurement method was to apply it, and therefore to carry out measurements with it at PTI stations, including the test in the inspection process itself. For this purpose, a NO_x measurement campaign has been carried out in PTI, applying the proposed method on vehicles passing through the stations daily, i.e., on vehicles that come daily to be inspected, not on vehicles prepared *ad hoc*. The vehicles have been randomly selected among the Euro 4, Euro 5, and Euro 6 diesel vehicles attending the stations involved in the measurement campaign. The results of this measurement campaign are detailed in **Chapter 8**.

The measurement method and the measurement campaign generate such a large amount of data that not only allows for the validation of the method but also provides additional information that can be utilized in formulating fleet management and environmental protection policies. **Chapter 9** analyzes the relationship between various variables measurable from the analyzed vehicle set and NO_x emissions. It also compares the results obtained from the method with another measurement method based on the use of a dynamometer bench to analyze the differences between the two. Finally, emissions from three vehicles on a route are modeled based on the measurement results to demonstrate the utility of the obtained information.

Throughout these chapters, a method for measuring NO_x has been defined, technically justified, and validated through experimental results. This method can be rapidly, simply, and economically implemented in PTI to monitor NO_x emissions from the entire fleet of diesel passenger cars and LDVs, thereby identifying vehicles with higher emissions. This provides a tool, namely appropriate information, to formulate policies aimed at mitigating the consequences of population exposure to NO_x emissions from vehicles.

10.3. CONCLUSIONS

This section conducts a review of the objectives outlined in Chapter 1 to ascertain their successful achievement. Should any objectives remain unmet, we will analyze the factors that hindered their realization.

After verifying the attainment of these results, a discussion is undertaken regarding the outcomes achieved and the fulfillment of the initially formulated hypotheses.

Objective #1: Definition of a NO_x measurement procedure.

The first objective was to define a new measurement procedure, which should meet the requirements for its implementation in the PTI process in technical and economic terms.

It is evident that the research has made significant progress toward achieving the first objective outlined in the thesis. The proposed method has indeed introduced a novel approach that was previously unexplored.

Based on the principles of NO_x generation in compression engines, the method has been designed to establish a correlation between an easily accessible engine operating parameter, obtainable through the OBD system, and NO_x emissions during a static idle test.

Through meticulous examination of the development and application of the method, the research has successfully demonstrated the method's suitability for integration into the PTI process, both in terms of its economic viability (minimal equipment costs) and its technical alignment with necessary requirements. Additionally, the method is applicable across M1 and N1 category vehicles, as evidenced by the extensive analysis and measurement campaign explained in Chapter 8.

While the method's application to heavier vehicle categories (M2, M3, N2, N3, etc.) holds promise in theory, the research acknowledges the need for further investigation. The core challenge lies in achieving a substantial engine load increase while the vehicle's engine is idling, particularly in vehicles with larger engines such as trucks and buses.

Although this aspect requires deeper exploration, it can be affirmed that the first objective has been largely met, while recognizing the necessity for continued research to address the unique challenges posed by heavy vehicles.

Objective #2: Representativeness of the results

The research has convincingly demonstrated the achievement of the second objective, which aimed to ensure that results obtained through the new measurement method are indeed representative of the genuine NO_x emissions from vehicles.

Throughout the thesis, comprehensive validation has been conducted to confirm that the values derived from NO_x measurements using this method align with the average NO_x emission values exhibited by vehicles during urban driving conditions (as seen in the loaded state), according to the results from Chapter 7. This has been verified both for the set of 23 vehicles used in the method validation and in the measurements conducted during the PTI campaign.

Furthermore, the significance of measuring emissions at idle, while the vehicle is stationary during urban driving, has been extensively justified in relation to the representativeness of the proposed measurement.

Finally, the maximum value attained (TMV) through this method falls within the range of maximum emissions produced by vehicles during urban driving. This demonstrates that TMV is a valid indicator of vehicle NO_x emissions level. Its application enables the comparison of emission levels between different vehicles.

Therefore, it can be confidently asserted that the objective of obtaining representative results from the tests has been fully accomplished.

Objective #3: Compliance with PTI requirements

The research has conclusively addressed the third objective of aligning equipment and staff requirements with PTI prerequisites, both from technical and economic standpoints.

The employed equipment, which is already utilized for CO measurement in inspections, fulfills all PTI stipulations, substantiating its technical and economic compatibility. Furthermore, the equipment's suitability for NO_x measurement has been substantiated in Chapter 5, where its performance was compared to that of a reference gas analyzer used in research and homologation laboratories.

In regard to personnel requirements, the method's straightforwardness and simplicity have been extensively confirmed. Staff members do not need to undergo complex training, and the method's execution and subsequent daily implementation in the

inspection process do not demand excessive time, as has been demonstrated in Chapter 8.

Furthermore, as an additional advantage, the safety levels for both vehicles, equipment, and personnel reach the same standards as the rest of the tests in the inspection process.

In this light, it is clear that the third objective has been fully met.

Objective #4: Comparison with other methods

The research has undeniably fulfilled the fourth objective, which centered on attaining at least the same level of representativeness and accuracy in NO_x measurement results as other methods, while concurrently maintaining equal or lower requirements for the measurement process.

Through meticulous comparison with alternative methods proposed for NO_x measurement in PTI, as can be checked in Chapter 9, it was conclusively demonstrated that the results obtained via the proposed method surpassed not only equal representation but actually exhibited superior representativeness. This superiority stemmed from addressing and rectifying the shortcomings identified in the compared method.

Furthermore, the proposed method's requirements in terms of equipment (both cost and complexity) and the measurement process (including complexity and time demands) were notably more favorable when contrasted with competing methods. The research also validated the measurement equipment's appropriate accuracy by juxtaposing it with more intricate and costly equipment.

Discussion

Thus, it is evident that the four objectives specified in Chapter 1 have been successfully attained over the duration of this research endeavor. In light of these accomplishments, it is a well-founded conclusion that the research has successfully reached its culmination.

The conducted research is inherently groundbreaking due to its distinctive focus on the context of PTI. While a wealth of scientific literature exists regarding NO_x emissions from compression engines, the novelty of this research lies in its dedicated exploration of measuring these emissions within the framework of PTI, and the theoretical approach used for the analysis of the NO_x emissions.

Prior to this endeavor, a conspicuous gap existed in scholarly investigations directed specifically at the measurement of such emissions from the vantage point of PTI protocols.

The present moment finds NO_x measurement within the context of PTI under active deliberation by the European Commission. This deliberation centers on the potential inclusion of NO_x measurement as a component of the periodic inspection framework.

Consequently, this research is unfolding contemporaneously with the decision-making process conducted by the relevant authority on this matter. Given this temporal alignment, it becomes apparent that there exists minimal pre-existing groundwork upon which to anchor the investigation. As a result, the research is chiefly reliant on the advancements achieved organically throughout its course, serving as the primary foundation for its findings and implications.

Conversely, this concurrent scenario has engendered a circumstance where the ongoing progression of the research has been contemporaneously accessible to stakeholders engaged in the decision-making process. Consequently, there exists the potential for the present research to exert a tangible influence in real-time on the ultimate determination pertaining to the incorporation of NO_x measurement within the framework of PTI.

The current proposal for Euro 7 [196] being handled by the European Commission (still in draft form) sets specific objectives: a) to reduce the complexity of the current Euro emission standards, b) to provide updated limits for all relevant pollutants (including NO_x), and c) to improve the control of real vehicle emissions.

The implementation of the measurement method outlined in this thesis holds the potential to contribute significantly toward the attainment of these three objectives. Despite forthcoming EU legislation aiming to phase out combustion engine vehicles by 2035, it is crucial to recognize that the challenge of NO_x emissions won't automatically resolve with the removal of pollutant vehicles by that timeline.

The proposed measurement method is pertinent because it addresses existing vehicles' emissions, ensuring ongoing compliance with environmental and health protection goals, even beyond the phase-out of combustion engine vehicles.

Indeed, the prohibition on registering new vehicles does not lead to the instantaneous disappearance of existing vehicles, as these vehicles will persistently remain in circulation and emit pollutants throughout their operational lifespan until they are eventually replaced by vehicles employing alternative technologies.

This process of replacement is unlikely to transpire swiftly and will extend over a prolonged duration.

Conversely, alternatives to the outright ban on combustion engine vehicles are already surfacing. Among these alternatives is the utilization of e-fuels produced through the hydrogenation of CO₂ captured from the atmosphere. This approach would enable the ongoing sale and operation of vehicles equipped with combustion engines. However, this alternative will effectively extend the lifespan of such vehicles, resulting in continued emissions of pollutants like NO_x—despite their CO₂—neutral status.

An additional potential alternative involves the adoption of combustion engines fueled by hydrogen. While this technology has not seen widespread adoption due to its limited performance benefits in comparison to conventional internal combustion engines and the challenges associated with hydrogen acquisition and utilization, it could experience a resurgence in relevance.

This resurgence could occur in a scenario where the accessibility and feasibility of utilizing hydrogen as a fuel—particularly for fuel cells—become more convenient and economically viable, rendering hydrogen-driven combustion engines an attractive and feasible technological choice.

Within this paradigm, the key pollutant emissions requiring mitigation are NO_x emissions, similar to other combustion-based vehicles. Thus, addressing NO_x emissions necessitates the implementation of the same EATS as applied to traditional combustion vehicles [197].

Certain perspectives advocate for broader societal decarbonization strategies encompassing a spectrum of technologies, rather than exclusively prioritizing electrification. They assert that dismissing combustion engine technology might not be prudent due to potential environmental advantages. In a comprehensive "cradle-to-grave" assessment, combustion engines could exhibit lower CO₂ emissions and fewer critical raw material supply challenges compared to electric vehicles, contingent on the existing European energy blend and national contexts [198]. Consequently, it becomes crucial to meticulously consider and scientifically analyze the extension of the presence of these vehicles within a broader context of sustainability and environmental impact.

Consequently, it is reasonable to anticipate that the prevalence of combustion vehicles emitting NO_x will persist steadily and prominently for a minimum of the forthcoming two decades, if not extending beyond that timeframe. This projection pertains exclusively to the European Union, as it is conceivable that in other global regions, the longevity of these vehicles emitting NO_x will extend even further.

Hence, the regulation of NO_x emissions from combustion vehicles via the PTI can emerge as an immensely crucial instrument for an extended duration, surpassing initial perceptions.

The thesis has effectively substantiated that the proposed method, from a technical standpoint, satisfies the two fundamental prerequisites for its practical application:

1. The measurement outcomes are dependable and accurately depict real vehicle NO_x emissions.
2. The method's attributes render it highly suitable for integration within the framework of PTI: fast, simple, and inexpensive as well as effective.

The integration of NO_x measurement into the PTI process, whether employing this method or an alternative, would constitute a highly promising development. Such a step holds the potential for substantial and enduring positive implications, particularly in safeguarding public health over the medium and long term.

Should this research have exerted any form of influence in contributing to the realization of this objective, it would represent the foremost accomplishment of the research's overarching purpose.

10.4. PERSPECTIVES

The research is not meant to be a concluded endeavor but rather an inaugural stride within a broader line of investigation. The objective is to expedite the implementation of enhancements in the vehicle technical inspection process, augmenting its effectiveness and bolstering its role in safeguarding the environment and public health.

Moreover, the aspiration is to optimize the inspection's efficiency by minimizing the expenditure of resources, including time and equipment.

The subsequent avenue of research that naturally emanates from this work involves exploring the feasibility of integrating NO_x measurement using the proposed method with Particle Number (PN) measurement. This would be facilitated through idling measurement procedures recently proposed in Belgium and Germany. By combining these measurements, it aims to create a more comprehensive assessment of emissions during the inspection process.

In essence, this research serves as the foundation for a continuous quest to refine and improve vehicle inspection practices, striving for the highest standards of environmental protection and operational efficiency.

Indeed, there is a promising avenue for research in exploring the alignment between PN (Particle Number) measurement processes and the idling conditions posed by the proposed NO_x measurement method. The synchronization of these measurements, both conducted while the engine is idling, opens up the potential for a consolidated test. Such an integrated approach would offer substantial time savings by combining the assessment of both NO_x and PN emissions into a single procedure.

The prospect of harmonizing NO_x and PN measurements within a single test holds immense significance. This innovation can considerably reduce the testing time while concurrently enhancing the detection of vehicles with elevated PN and NO_x emissions during the periodic technical inspection. This dual measurement approach could stand as a pivotal tool in diminishing pollutant emissions within urban environments, thereby alleviating the detrimental impacts on public health outlined in Chapter 1.

To fully realize the potential of this concept, further investigation and in-depth research are essential to ascertain its feasibility, accuracy, and practical implementation.

On a different note, if CITA's proposition to the Commission for the endorsement of this measurement method moves forward and attains approval at the EU level, several subsequent actions would become imperative. Prior to the method's implementation, a more extensive series of measurements would need to be conducted. This effort aims to establish meticulously adjusted and definitive rejection thresholds. These limits might vary based on distinct emission levels, reflecting the diverse emission characteristics of various vehicles.

Furthermore, a comprehensive evaluation of alternative measurement equipment's suitability would be essential. The rationale behind this approach is to avoid reliance on a solitary piece of equipment, ensuring a range of viable options for implementation.

Proposing feasible and well-defined timelines for execution would be another critical step. These timelines must account for both regulatory bodies' readiness and the operational capacities of inspection facilities.

It is important to acknowledge that while the method's fundamental design is tailored for scrutinizing NO_x emissions from compression (Diesel) engines—leveraging theoretical principles grounded in their operating attributes—promising results have also been achieved when applying the method to vehicles equipped with internal combustion engines (gasoline). However, a more extensive assessment of the method's suitability for gasoline engines would be indispensable, paving the way for its potential application in this vehicle category as well.

In conclusion, there is a critical need to explore the adaptation of the proposed method for heavy-duty vehicles (trucks and buses), as these vehicles significantly contribute to overall NO_x emissions in urban settings.

The method, as currently structured, may not be directly transferable to these vehicles due to potentially insufficient fluctuations in power demand on their engines. However, a dedicated investigation into methods for eliciting higher power demands from the engines of these heavy-duty vehicles could illuminate the path toward applying the same measurement concept. This could involve devising strategies to achieve two distinct levels of power demand while the engine is idling, thereby extending the applicability of the method to heavy-duty vehicles. This research avenue holds the potential to enhance emissions control and measurement strategies for this substantial source of urban pollution.

Indeed, this research lays the groundwork for a plethora of future studies of significant relevance and importance, all intricately linked to societal well-being and health. Several avenues for further investigation emerge:

- **Health and Economic Impacts:** Delve into the potential repercussions of implementing this or alternative NO_x (and PN) measurement methods within periodic technical inspections. This could encompass quantifying the anticipated reduction in environmentally linked diseases and mortality, as well as assessing the economic impact of diminished atmospheric pollutants—ultimately leading to savings within the healthcare system.
- **Economic Implications:** Analyze the economic repercussions associated with the method's implementation in PTI. This could encompass evaluating changes in repair frequencies, and their economic implications on repair workshops, spare parts manufacturing, new vehicle sales, and the second-hand vehicle market.
- **Effectiveness of Emission Restrictions:** Quantify the effectiveness of emission restriction measures, such as the establishment of Low Emission Zones, through a comparison of emissions measured during PTI for vehicles permitted within these zones (e.g., residents and delivery vehicles) with recorded pollutant levels employing environmental measurement equipment within these zones.
- **Comprehensive Cost-Benefit Analysis:** Undertake a comprehensive Cost-Benefit Analysis (CBA) of the proposed or analogous measures. Such an

analysis could encapsulate the multifaceted dimensions of health improvements, economic gains, and enhanced environmental outcomes.

The research's impact extends beyond its immediate scope, fostering the prospect of substantial exploration, influencing policy decisions, and amplifying efforts to fortify public health, economic stability, and environmental sustainability.

10.5. INFLUENCE AND VISIBILITY

While the thesis development represents an academic endeavor, the author's direct involvement in the PTI field has facilitated the dissemination of the research findings to relevant stakeholders responsible for devising and integrating novel procedures.

This dissemination has extended to various platforms within the institutional realm, encompassing both national and European spheres, through which the newly developed method has been shared.

In the first place, in November 2017, the method was introduced to personnel from the Spanish Ministry of Industry at the PTI facility operated by GRUPO ITEVELESA in Las Rozas, Madrid.

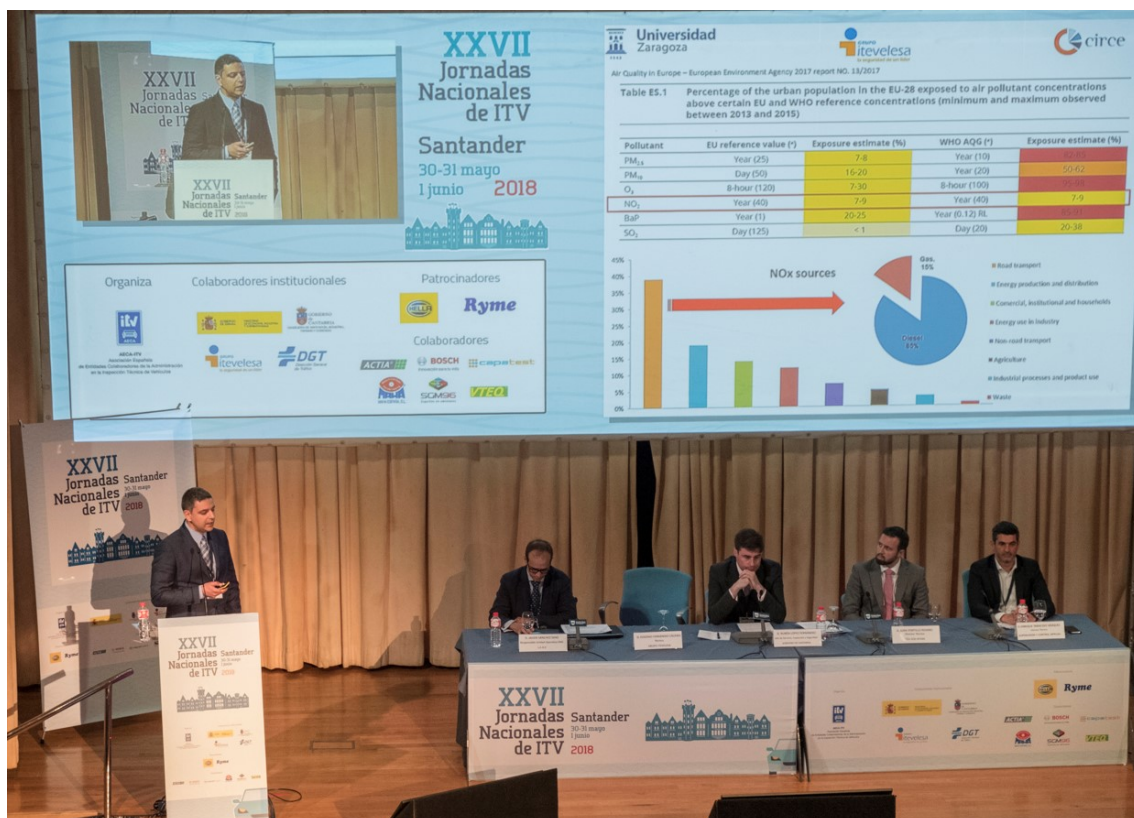


Figure 10-1. Presentation of measurement proposal in the XXVII Jornadas Nacionales de ITV (Santander, 2018).

In May 2018, the methodology was publicly unveiled at the *XXVII Jornadas Nacionales de ITV* held in Santander (Figure 10-1).

This presentation highlighted the prevailing challenges concerning NO_x emissions while elucidating the underlying principles and potential of the suggested measurement approach.

Next year, in October 2019 during the *XXVIII Jornadas Nacionales de ITV* held in Zaragoza (Figure 10-2), the advancements achieved in method development were showcased.



Figure 10-2. Presentation of measurement proposal in the *XXVIII Jornadas Nacionales de ITV* (Zaragoza, 2019).

This presentation involved detailing the outcomes derived from measurements conducted on vehicles in operation, with a subsequent comparison against the results generated by the proposed procedure.

On an international scale, the inaugural introduction of the method took place at the *13th SDEWES Conference* held in Palermo in October.

In March 2019, the author of this thesis actively engaged in the 15th meeting of Working Group 2 under CITA (International Motor Vehicle Inspection Committee), or RAG Europe. During this participation, the author delivered a presentation to the working group, detailing the progress made in developing the measurement method.

Exactly a year later, in March 2020, the outcomes stemming from the measurement campaign that implemented the suggested method were shared with the same Working Group 2 of CITA. This presentation offered insights into the findings of the campaign.

In order to formulate CITA's standpoint on the issue of NO_x measurement in PTI, a dedicated working subgroup was established. This subgroup's mandate was to assess the available options for NO_x measurement in the context of PTI and subsequently articulate CITA's organizational stance on this matter.

Thanks to the previously mentioned presentations, the author of this thesis was granted the opportunity to engage in this working group. Collaborating alongside accomplished experts hailing from various sectors related to PTI, this group encompassed professionals representing PTI service providers across multiple European nations, manufacturers of PTI equipment, public institutions, and entities indirectly involved such as technical gas suppliers.

Within this collaborative working group, a comprehensive examination of 7 distinct methodologies for NO_x measurement in PTI took place across multiple meetings spanning a year and a half. The culmination of these efforts culminated in a report termed a Position Paper by CITA [199]. This document highlights the method advocated in this thesis as the most fitting among those scrutinized within the document. Consequently, this method **was deemed suitable for prompt integration into the PTI process at the European level.**

Undoubtedly, the affirmation made within CITA's POSITION PAPER carries substantial significance, given the entity's stature and authority. The recognition of the proposed method's validity and practical feasibility, as demonstrated through its real-world implementation potential, holds particular weight. CITA embraced the conclusion of the working group and formally incorporated it into their own standpoint. This pivotal endorsement was presented on April 6, 2022, during the CITA Hybrid meeting held in Nitra, Slovakia.

In 2020, the method was further introduced in a meeting with a Policy Officer at the European Commission, Dr. Vicente Franco. This presentation provided an avenue to communicate the method's intricacies and potential. Additionally, in October 2021, the method received exposure from members of the Joint Research Centre (JRC).

Furthermore, the method detailed in this research underwent an independent evaluation by Carlos III University. This assessment was carried out within a report commissioned by AECA-ITV, a report that explored various alternatives for measuring NO_x and PM within the PTI context.

The report, formally unveiled on April 20, 2022, during the MOTORTEC 2022 Fair held in Madrid, provided a favorable evaluation of the outcomes achieved through the application of this method. The report compared its findings to those derived from other more "conventional" methods, such as roller bench measurements. Notably, the report emphasized the method's advantages as elucidated throughout the thesis in terms of its suitability for integration into the PTI process [150]. This assessment drew attention to the conclusion that a static measurement approach with a load stands out as the most preferable and effective choice for conducting NO_x measurements within the PTI context.

In a parallel effort unrelated to this research, GOCA Vlaanderen in Belgium undertook an independent assessment involving various methods for NO_x measurement in PTI. This evaluation, culminating in a report presented in August 2022 [149], encompassed

the methods extensively scrutinized, akin to the one advocated in this thesis, yielding favorable outcomes. It is noteworthy that GOCA Vlaanderen, an organization with substantial expertise in the evaluation and implementation of inspection methods within the context of PTI, had already been responsible for evaluating and incorporating PN (Particle Number) measurement procedures in Belgium in 2022.

Until recently, the widely held belief was that roller bench measurements represented the pinnacle of technical precision for evaluating a vehicle's real-world NO_x emissions. However, a significant body of scientific literature has surfaced to challenge this perspective. This is particularly evident in the contrasting results observed between the NEDC (New European Driving Cycle) and WLTP (Worldwide Harmonized Light Vehicles Test Procedure) cycles—both considered highly sophisticated and meticulously conducted—and the actual emission levels exhibited by vehicles in real-world conditions.

The emergence of methodologies such as the one delineated in this research, alongside others that are likely to emerge based on vehicle-derived data, has illuminated the inadequacies of a PTI measurement system reliant on roller bench technology. Apart from being economically unsustainable and resource-intensive (in terms of time and personnel), roller bench-based measurements are shown to be less representative than alternative measurement methods.

In terms of identifying tampering or malfunctions related to NO_x emissions in vehicles, there is no conclusive evidence supporting the superiority of roller bench measurements or demonstrating any inherent advantages over alternative methods.

A study conducted in Germany [147] arrived at the conclusion that utilizing a dynamometer bench is more sensitive in identifying instances of tampering or malfunctions, suggesting a numerical measure for the sensitivity ratio of the method relative to the emission disparity between a manipulated vehicle and an unmanipulated one.

However, this comparison encounters a fundamental issue. In the context of PTI, it is not known in advance whether a vehicle has been tampered with. Consequently, lacking a pre-established reference value for comparison, it becomes impossible to definitively deduce from the test result alone whether a vehicle has been manipulated. This challenge arises due to the substantial variability exhibited by NO_x emissions in response to alterations in the test's boundary conditions.

Certainly, this challenge remains applicable to any measurement technique. However, the method elucidated in this research, as expounded throughout the thesis, possesses a notable advantage in significantly mitigating the variables capable of influencing measurement outcomes. Consequently, this method diminishes the inherent variability in measurement results.

In summary, the NO_x measurement method examined and proposed in this thesis, while requiring further refinement for effective application, has exerted substantial influence both at the national and European levels. It has introduced a fresh perspective to NO_x measurement within the context of PTI, despite the intrinsic constraints associated with its execution.

Finally, it should be noted that the research has generated relevant documentation that contributes to its visibility. Among these, the researcher's publication of two peer-reviewed papers is included. One of them was published in 2021, describing the proposed method for measuring NO_x in PTI [175], and another was published in 2022, assessing the suitability of the equipment used for NO_x measurement in PTI [180]. These documents are included in this thesis as direct deliverables generated by the research.

Additionally, the documents referenced earlier in this section (mainly the CITA Position Paper [199], as well as the Carlos III University report [150], and the GOCA Vlaanderen report [149]) also contribute to the visibility of the proposed method.

To conclude, the visibility provided by the dissemination of information regarding the development of the proposed method in the various forums mentioned has led the author to be invited as a speaker at various events, always in their capacity as an expert in combustion vehicle emissions and their control through the PTI.



Figure 10-3. Participation in Split Session during the 2023 CITA International Conference (Rotterdam, 2023)

Among the most recent events, we can highlight the author's participation as a speaker in a series of Split Sessions held during the 2023 CITA International Conference, which took place in Rotterdam from June 6th to 8th, 2023 (Figure 10-3).

Additionally, the author also participated in the conference "Vehicle Inspection and Society: Beyond Technology" which was jointly hosted by CITA with the Spanish Presidency of the Council of the European Union and held in Brussels on September 26, 2023 (Figure 10-4).



Figure 10-4. Participation in the conference "Vehicle Inspection and Society: Beyond Technology" (Brussels, 2023).

CHAPTER 11

APPENDICES

11. APPENDICES

This Chapter includes significant information that was not integrated to maintain clarity and argumentation. This also includes elaboration on measurement results from previous Chapters, which we found more suitable for inclusion here to manage the extensive information effectively.

11.1. MEASUREMENT SOFTWARE DESCRIPTION

The gas analyzer equipment was extensively described in Chapter 5. In conjunction with the gas analyzer, a crucial component of the measurement equipment is the software employed for recording the data collected by the gas analyzer and the OBD system. This software plays a vital role in effectively capturing and managing the measurements, ensuring seamless synchronization between the gas analyzer's data and the engine operating values from the OBD system. It facilitates comprehensive data storage, analysis, and further processing for accurate and reliable results.

During the research, two distinct software packages provided by the gas analyzer manufacturer were utilized.

In the first part of the research, generic acquisition data software was used. This software records and shows, in a continuous way, the time evolution from the variables read through the gas analyzer and the OBD system. The performance of stages of the test have to be performed and controlled by the researcher.

Once the test finishes, a file is generated with all the data recorded. From this file, the software can visualize the data measurement and generate a *.xls file with the whole data from the test, in an easy way to be analyzed.

Figure 11-1 shows a sample from a typical measurement, with the five stages of the measurement process visible. The information shown on the screen is:

- 1) Graphical variables evolution
- 2) Legend of variables shown
- 3) Data from measurement
- 4) *.xls file exportation button

The dotted purple line shows the value of "% engine load", the light green line shows the value of NO_x concentration, and the thin yellow line represents the engine speed value. Variable visualization can be activated or deactivated to make easy the visualization of the test.

At first, this software was deemed suitable for research purposes, and it was initially used to analyze a set of 23 vehicles to define and assess the measurement method. Furthermore, due to its specific characteristics, it was employed to conduct the on-road measurements detailed in Chapter 7.

However, once the decision was made to increase the number of measurements and develop measurements in several PTI stations, it became evident that this type of software was not the best choice.

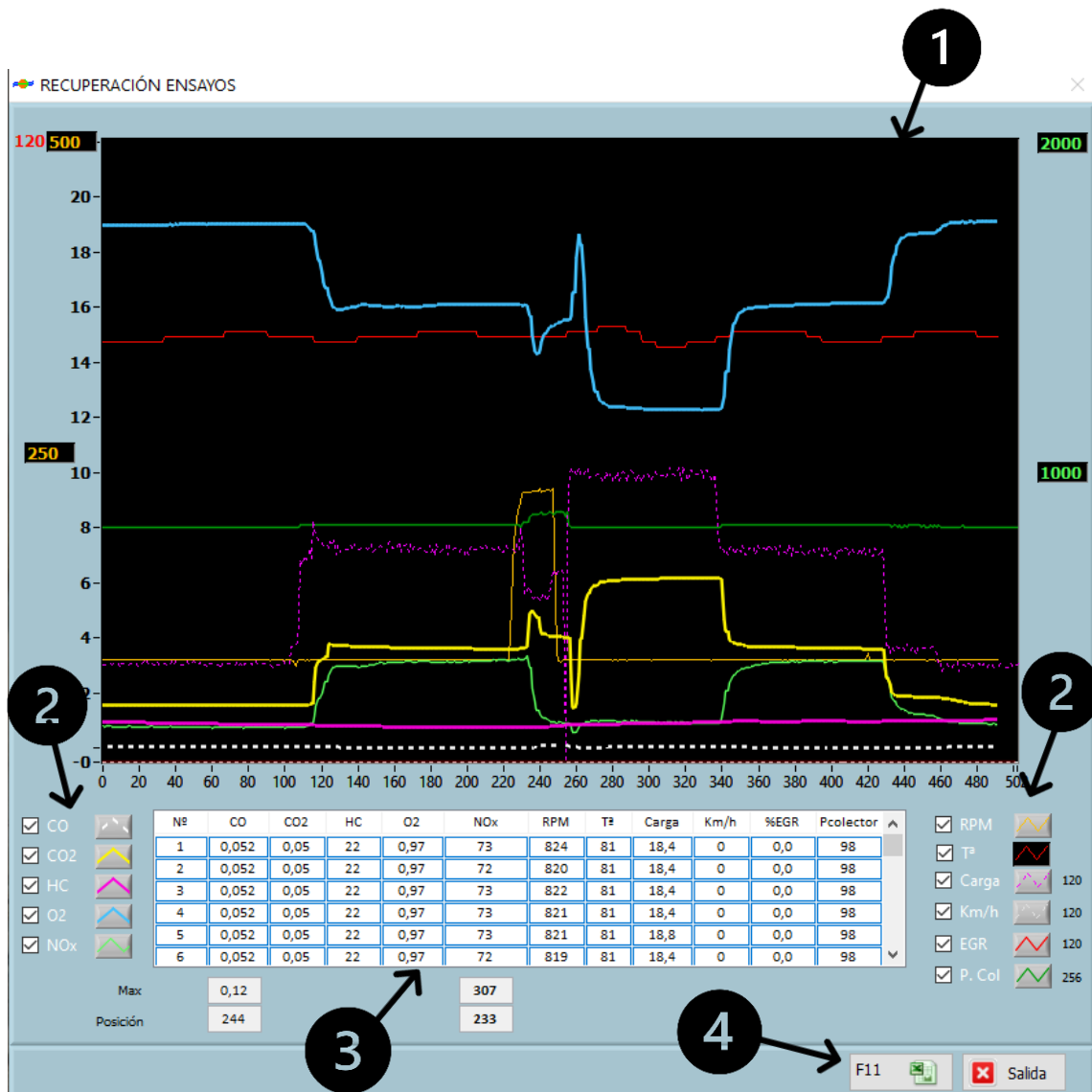


Figure 11-1. Generic acquisition software showing results from a measurement.

To achieve this objective, the measuring equipment manufacturer developed new software that adhered to the prescribed process guidelines. This software was designed to automate the various steps of the measurement procedure and provide clear instructions to the operator conducting the test. The aim was to make the test accessible to personnel with minimal training and no direct involvement in the research process. By employing this user-friendly software, the measurement process was standardized, ensuring consistency across all tests and minimizing potential errors associated with human intervention during the measurements.

To incorporate NO_x measurement into the regular inspection process, and to minimize any additional time required for the test, the new software used was integrated with the existing PTI software. As the initial steps of the NO_x test (vehicle condition verification and preconditioning) align with those of the current opacity test applied to diesel vehicles, this integration proved to be highly effective. By merging the new

software with the pre-existing PTI software, the execution of the test involved only a minimal increase in the overall inspection time. This approach ensured a smooth and efficient integration of NO_x measurement into the standard inspection procedures, without causing any significant disruptions to the PTI process.

According to Spanish regulation, the current Euro 5 and Euro 6 diesel vehicle emission test is divided into two different phases:

- 1) OBD test
- 2) Opacity test

The vehicle's verification and preconditioning are carried out prior to the OBD test. As a result, by the time the OBD test concludes, the vehicle is already prepared, and the OBD reader is linked to the vehicle. With this in mind, the NO_x measurement software has been developed to conduct the NO_x test after the OBD test has concluded and before proceeding with the opacity test. Once the NO_x measurement is finished, the software automatically continues with the opacity test, also using the OBD reader to measure engine speed and temperature (data required for the opacity test), although it could be possible to use another tachometer. In this way, the time requirements for the test performance are the lowest.

To maintain the accuracy and reliability of the NO_x measurement test, a strategic decision was made to conduct it right after the OBD test and before the opacity test. This sequencing was chosen to prevent the accelerations necessary for the opacity measurement from potentially impacting the performance of the vehicle's EATS. By avoiding any alterations to the expected behavior of the vehicle during the NO_x test, the measurements remained unaffected by external factors, ensuring consistent and dependable results. This approach ensured that each test was conducted under the most appropriate conditions, enhancing the overall quality and validity of the NO_x measurement process.

As a result, the NO_x measurement has been integrated into the current emissions test. All the required tests, including NO_x measurement, are now conducted without any disruptions or interruptions, ensuring a smooth and efficient process. This integration eliminates the need for additional setup or discontinuity in the testing sequence, minimizing any interference in the normal operation of the testing station. Moreover, this approach confirms that **the NO_x measurement process easily fits within the current emission measurement system** for diesel vehicles in the PTI process.

The manufacturer of the measurement equipment (TEKBER) developed the software based on the guidelines provided by the doctoral student and in accordance with the method outlined in Chapter 4. This was done after designing the method and incorporating it into the software used for PTI emissions tests.

As a result of the measurement process, the software provides the average values of NO_x concentration, "% engine load", engine speed, and engine temperature among others for each of the five stages of the measurement process.

The software provides this information through the screen when the NO_x measurement is finished (Figure 11-7) and before starting the opacity test. Moreover, the software generates a set of files with the information from the NO_x measurement, enabling the analysis of the acquired information.

On one hand, average values of the set of variables analyzed for each of the five stages are provided. On the other hand, the complete set of data registered for all the variables involved is provided in the set of files and can be analyzed, to get a complete overview of the measurement.

Currently, the software supplied by the equipment manufacturer provides the complete measurement information but does not analyze the information. It is necessary to externally process the information for deep calculations and information analysis.

The gas analyzer software provides valuable information that allows for the Aggregation and Extrapolation process. While the current version of the measurement software does not include this aggregation process, there is a possibility of integrating it in the future to enable rapid data analysis.

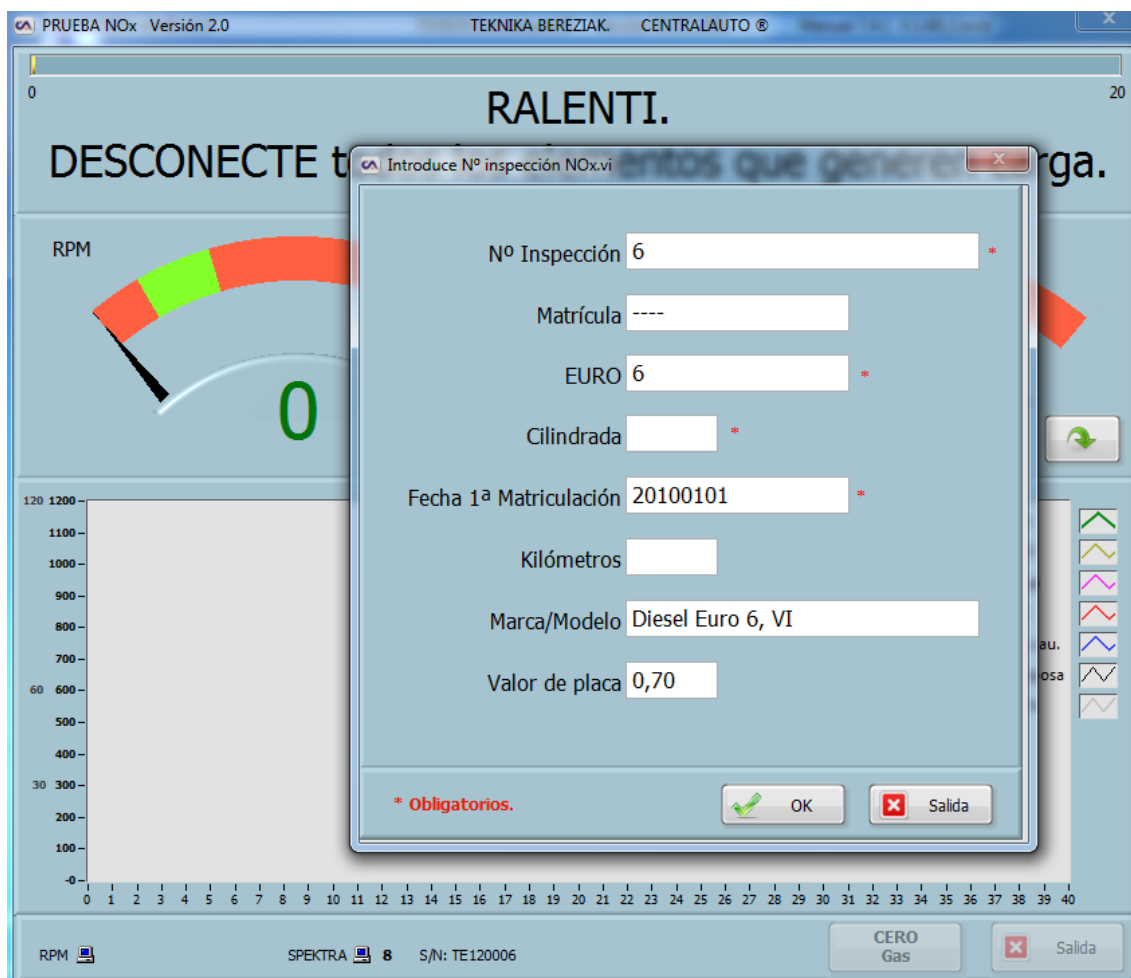


Figure 11-2. Vehicle data introduction screen previous to NO_x measurement.

About the execution of the test, the measurement process is guided by the software, guaranteeing that the measurement process is equally performed for all the vehicles.

Before starting the test, some information about the vehicle has to be introduced (see Figure 11-2), being this information important for the subsequent analysis of the data. In this way, the plate number, Euro emissions level, engine size, first registration date, mileage from the odometer, and model of the vehicle are registered.

Once the information is introduced, the "OK" button must be clicked to continue and start with the first of the five stages: the Unloaded Idle stage.

For each of the five stages of the measurement process, a measurement screen with common elements is displayed to guide the PTI worker in operating the vehicle correctly to perform the measurement. On the screen, the software provides essential information to guide the worker through the entire measurement process (refer to Figure 11-3). This information remains consistent throughout all stages and plays a crucial role in ensuring precise measurements. It includes the following:

- 1) Upper area with simple instructions on how to operate
- 2) Upper test time measurement bar
- 3) Left gauge indicator: engine rotation speed value
- 4) Right gauge indicator: "% engine load" value
- 5) Central engine temperature indicator
- 6) Lower real-time graph of the evolution of various variables throughout the measurement, with a legend of the active variables in the measurement process

During each measurement phase, the software displays the engine rotation speed indicator, which shows the current reading and the valid range (green area) for that specific phase. This visual display allows for easy and quick verification of the engine's conditions during the measurement. Similarly, the "% engine load" indicator also shows the instantaneous reading and its valid range. Both of these values are obtained through the OBD system, ensuring accurate and reliable data for the measurements.

Once the vehicle registers accurate values for engine speed and "% engine load", the software initiates the data collection process for the variables involved to calculate the average value for each stage. The upper test time measurement bar begins to fill up. The predetermined time for each stage is set to 20 seconds, although this duration can be adjusted if needed. During the data collection process, the software continuously checks for the completion of the time bar. Once the bar is full, a sufficient number of values have been gathered to calculate the average for that stage, and the software proceeds to the next measurement phase.

However, if at any point during the measurement in a stage, the engine speed or "% engine load" displays values that fall outside the expected range indicated by the respective indicators, the data collection for the average calculation is halted. The upper time measurement bar resets and the measurement phase starts again from the beginning. The software waits for suitable measurement conditions before restarting, and the defined 20 seconds of data collection needs to be completed again once the appropriate conditions are met. This ensures that accurate and reliable data are collected for the average calculation.

Figure 11-3 shows the screen for the first unloaded part of the test when the engine speed is idle, and the "% engine load" reflects the lower possible situation. For 20

seconds this situation is maintained, for a stable NO_x concentration measurement in the exhaust pipe.

In this first stage, the engine speed must be idling, and all equipment must be disconnected. The idling engine speed indicator is typically positioned within the range of low engine speeds, typically between 600 rpm and 1000 rpm, and the "% engine load" indicator is usually set around a low value, commonly around 20%. In the upper area of the screen, a message indicates that all equipment must be disconnected and the engine must be idling (see Figure 11-3).

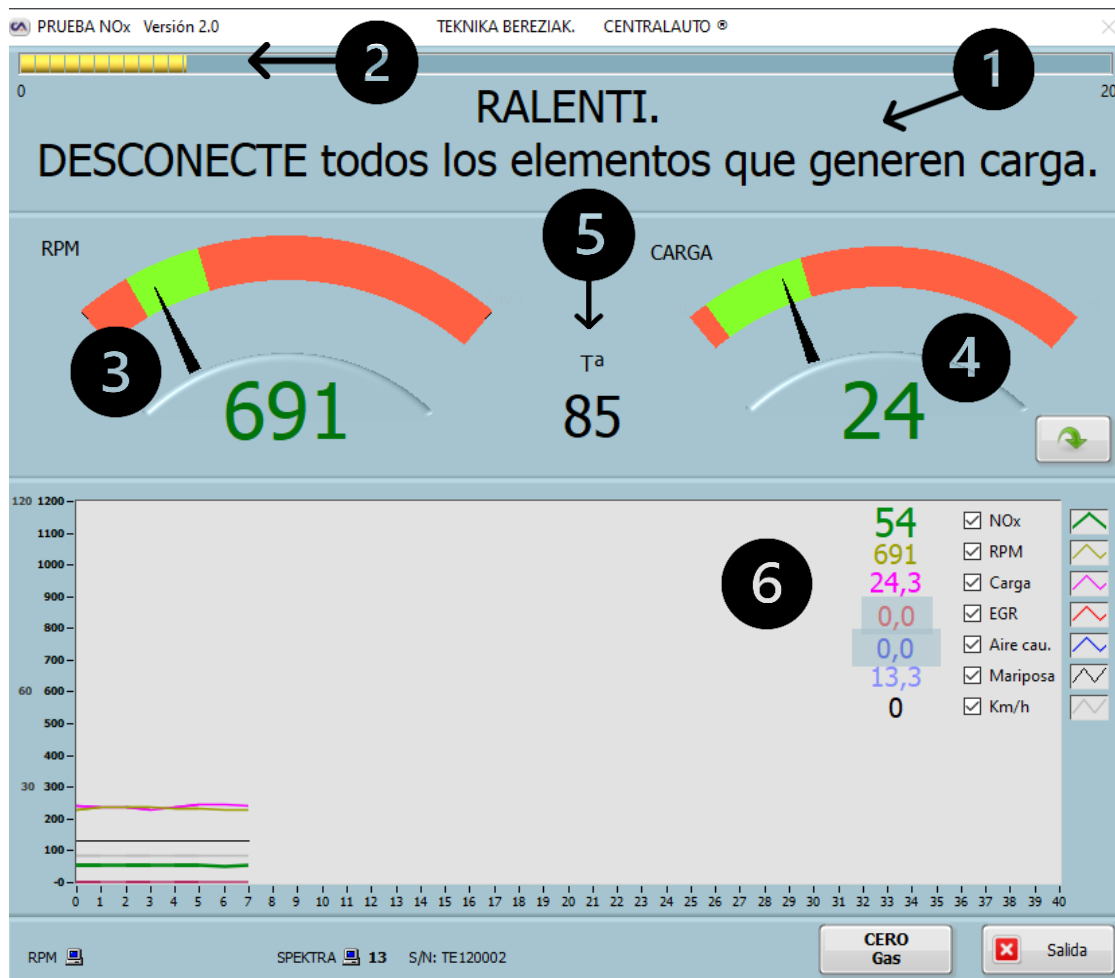


Figure 11-3. Measurement screen for Unloaded stage.

After successfully completing the 20-second measurement duration, signified by the filling of the yellow upper bar, the first stage concludes, and the equipment is prepared to proceed to the second stage. At this point, the message displayed in the upper area of the screen changes, indicating that the equipment needs to be connected (as shown in Figure 11-4) while ensuring the engine is set to idle. This equipment will be connected in this order: the Air Conditioning system, the lighting and signaling system, and the rear window heating system.

The engine speed indicator will remain positioned around the same low engine speed as in the first stage. However, the "% engine load" indicator will now be placed around

a higher value, typically around double the value observed during the first stage. The green area in the "% engine load" indicator will visually represent the expected level or target "% engine load" value for this particular stage.

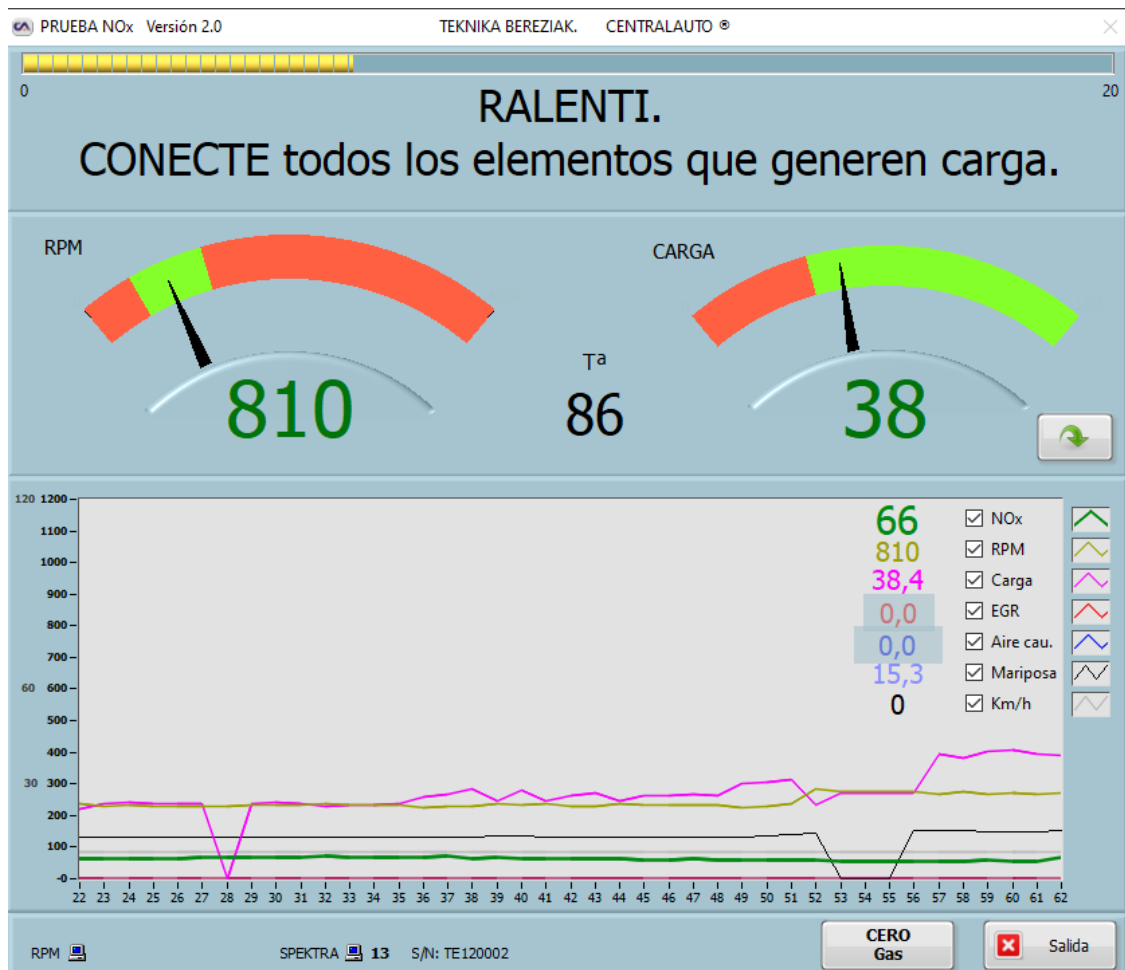


Figure 11-4. Measurement screen for Loaded stage.

After completing the second stage, the third stage begins, and a message appears in the upper area of the screen instructing the user to accelerate the engine (as shown in Figure 11-5). During this stage, the engine needs to be accelerated to a target speed of 2500 ± 500 rpm, while the equipment remains connected and measures data for 20 seconds. In this particular stage, the "% engine load" becomes less relevant, and the primary focus is on accelerating the engine. The purpose of this stage is to "wake up" certain components like the EGR and EATS if they are available. By achieving the specified engine speed, these components can be activated and prepared for further stages.

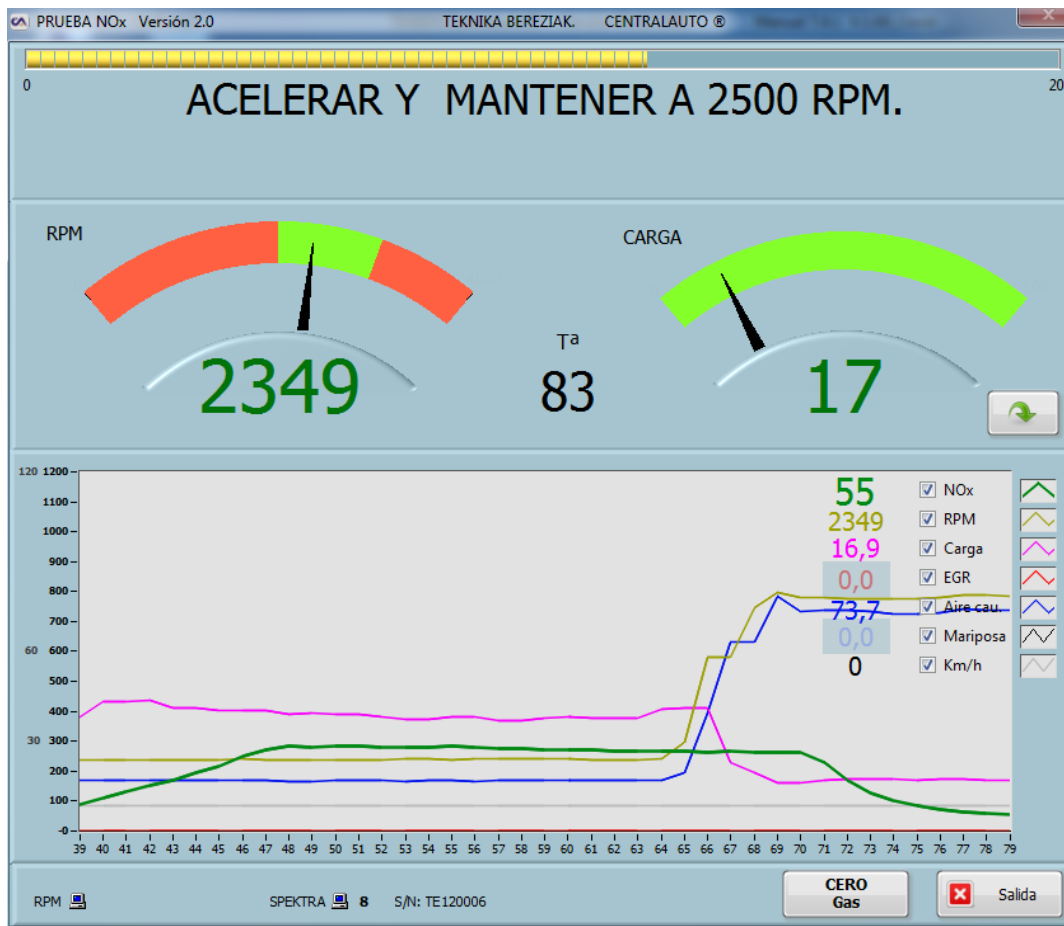


Figure 11-5. Measurement screen for Acceleration stage.

After completing the third stage, the software switches back to the screens shown in Figure 11-4, where the engine speed must return to idling while the equipment remains connected. This situation is the same as in the second stage, and the engine speed is set to idle while all equipment remains connected.

In the fifth and final stage, all the equipment must be disconnected, and the engine returns to idling conditions, just like in the first stage (refer to Figure 11-3).

Upon the conclusion of this fifth stage, the system notifies the user that the test has been completed, as depicted in Figure 11-6.



Figure 11-6. Measurement finishing screen.

Following this, the NO_x measurement test presents the averaged values acquired from all five stages (Figure 11-7). At this point, the equipment is primed to advance to the opacity test, thus marking the culmination of the comprehensive emissions testing procedure. Under standard conditions devoid of any complications during the test, the entire NO_x measurement procedure takes approximately 2 minutes. This time frame encompasses the sequence from data input to result presentation. It is important to note that this duration must be factored in alongside the typical OBD and opacity test durations.

The software's display (Figure 11-7) of the average NO_x measurement values obtained from the five stages provides a simplified representation of the emissions behavior obtained by analyzing the entire set of data measured at each of the stages (see Figure 4-4).

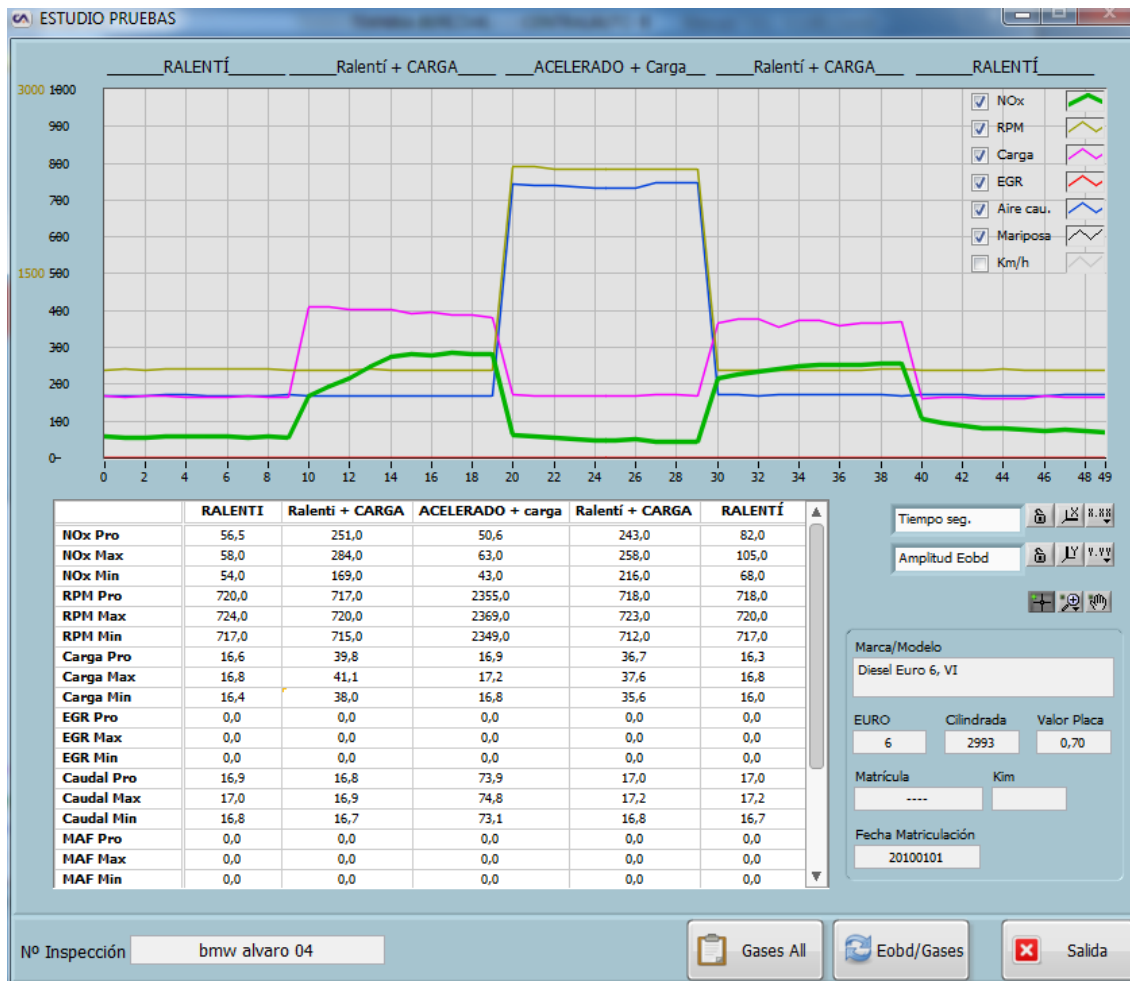


Figure 11-7. Measurement results screen.

11.2. MEASUREMENT WITH CAPELEC GAS ANALYZER

In the Chapter 5 conclusions, one of the advantages highlighted for the proposed method is that it is not dependent on a specific measuring device.

Indeed, provided that the requisite technical specifications are met, encompassing the measurement of NO_x concentration in ppm, engine speed measurement, and "% engine load" measurement, any appropriate equipment can perform the test cycle and estimate the TMV of NO_x emissions.

While dedicated equipment equipped with specialized software is more efficient, it is possible for any NO_x measurement equipment to potentially conduct the suggested test.

To assess this concept, a Gas Analyzer from CAPELEC, specifically the CAP3010+S model, was employed to measure NO_x emissions in accordance with the static idling NO_x test.



Figure 11-8. CAPELEC Gas Analyzer model CAP3010+S

This particular equipment is of a generic nature and is tailored for use in PTI and workshops. Its primary focus lies in measuring CO, CO₂, HC, and O₂ levels. The measurement of CO, CO₂, and HC employs Non-Dispersive Infrared (NDIR) technology.

The equipment has an option for a NO_x measurement kit (with an electrochemical sensor for NO_x) and allows the calculation of the CO corrected and the Lambda value.

Working together with the Gas Analyzer, a CAPELEC interface EOBD CAP 4250+S was used to measure "% engine value" and engine speed from the vehicle in an easy way.

The measurement procedure adhered to the steps delineated in Chapter 4, with the sole variation being the use of different measurement equipment, data recording software, and a distinct file format for storing the results. Despite these disparities, the fundamental process remained unchanged.

The emissions pattern of NO_x from vehicles closely resembled the behavior observed during the test with the Centralauto equipment. Furthermore, the outcomes of the test aligned with the results obtained during the research phase.

Due to the absence of dedicated software tailored to the proposed NO_x measurement test method, the measurement was carried out in a continuous manner by manipulating the vehicle's equipment to meet the test criteria outlined in Chapter 4.

This measurement approach is straightforward and robust, enabling research-driven test execution even without specialized software. While having dedicated software streamlines the process and is crucial for practical use in PTI, the method's simplicity allows for research-based testing without such software.



Figure 11-g. CAPELEC interface EOBD CAP 4250+S

**GOODNESS TO FIT ANALYSIS (R2)
SIGNIFICANCE ANALYSIS (P-VALUE)**

datos.entrada position	from	2	145	100	2
	to	90	235	130	235
MANUALLY					
		initial	final	accelerated	total
a		32,0466	28,7620	-43,6179	23,2981
average NOx		361,7865	305,0000	196,1935	312,7863
average % engine load		26,6978	23,5462	16,7968	23,8705
b		-493,7861	-372,2355	928,8333	-243,3515
x (% engine load)		100	100	100	100
y(NOx)=a·x+b		2711	2504	-3433	2086
Coefficient of determination R²		0,8476	0,8877	0,1501	0,7337
Coefficient of Pearson		0,9206	0,9422	-0,3875	0,8565
P-value		2,6713E-37	4,9441E-44	3,1277E-02	1,3610E-68
Freedom degree		1	1	1	1
Number of measurements		89	91	31	234
Significance's level		0,01	0,01	0,01	0,01
Significance of the model		OK	OK	FAIL	OK

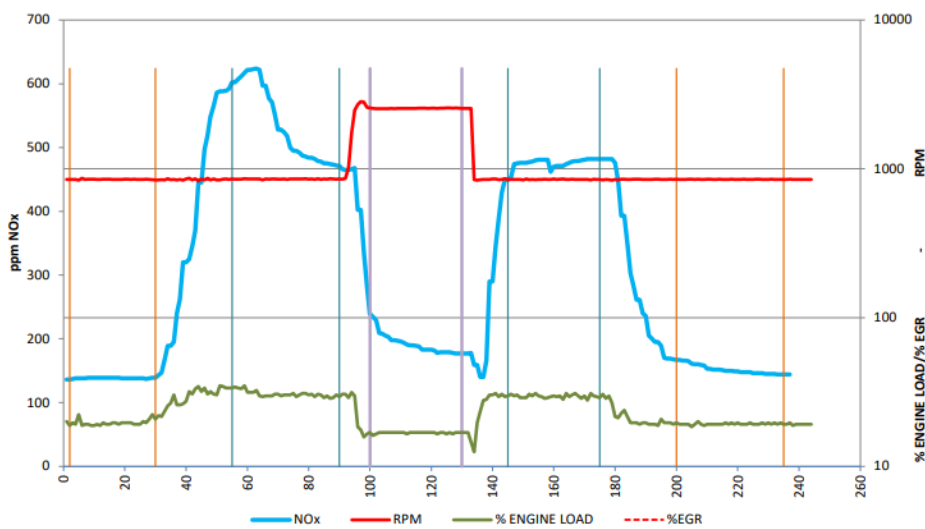


Figure 11-10. The plot of results and Quality and significance analysis for NO_x measurement with CAPELEC equipment.

Figure 11-10 presents a graphical representation of the outcomes from a single test, displaying NO_x concentration (ppm NO_x), "% engine load", and engine speed (rpm). Notably, the patterns of these variables mirror the explanation provided for the test conducted using the Centralauto equipment. This observation signifies that the emissions behavior remains consistent regardless of the specific measurement equipment employed.

Additionally, a Quality and Significance analysis can be conducted. In terms of Quality, the R² value for both the Initial and Final sections is reasonably good, with 0.84 for the initial section and 0.88 for the final section. Even in the Total section, the R² value is considered more than acceptable, standing at 0.73. However, in the Acceleration Section, as expected, the R² shows a lower value, indicating poorer performance.

Regarding the Significance, it can be observed that the p-value is lower than the significance level. The p-value is so low for the initial, final, and total sections that it approaches zero. Having such low values is an important indication of the existence of the relationship between the two variables.

This measurement serves as an example of a typical scenario where the "% engine load" value in the final section closely resembles that of the initial section. However, it is noticeable that the NO_x concentration measured in the final section is lower than in the initial section, likely attributed to the influence of the EATS and possibly the EGR (although the system did not record data on its operation).

In the Acceleration section, as is always the case, there is a sharp decrease in NO_x concentration due to the increase in engine speed. In both the initial and final sections, the variation in NO_x concentration is clearly seen as the "% engine load" value changes.

Of course, results include the extrapolation to obtain the TMV, for the Initial Section, the Final Section, and the Total Section (see Figure 11-11).

The method's versatility is highlighted by the fact that it is not tied to any particular equipment manufacturer; suitable equipment can be sourced from a variety of manufacturers.

Furthermore, while there are some disparities in the treatment of data, stemming from differences in the characteristics of the data file generated by different manufacturers, the overall output from the test remains consistent. In essence, the test's outcomes and results remain unchanged, regardless of the equipment used for conducting the test.

	TOTAL AVERAGE		INITIAL AVERAGE		FINAL AVERAGE	
	NOx (ppm)	% engine load	NOx (ppm)	% engine load	NOx (ppm)	% engine load
UNLOADED averaged	146	19	138	20	153	19
LOADED averaged	508	30	541	31	474	30
MAX. Theoric	1734	100	1761	100	1551	100
y(NOx)=a·x+b	1734		1761		1551	
Coefficiente R ²	0,9849		0,9831		0,9883	

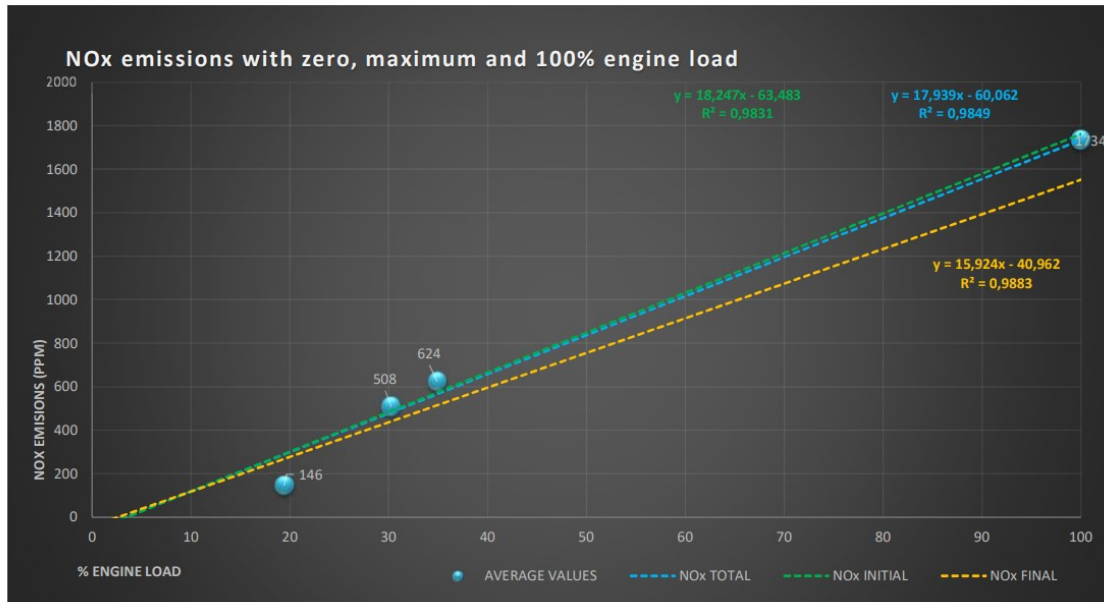


Figure 11-11. Final results and extrapolation of TMV for NO_x measurement with CAPELEC equipment.

This example effectively demonstrates that the entire measurement method can be adapted for use with alternative equipment, thus not being restricted to the specific equipment utilized during the research's development. This adaptability contributes significantly to the practicality of implementing this NO_x measurement method within the framework of PTI.

11.3. MEASUREMENT ERROR ANALYSIS

As was indicated in Chapter 6 (section 6.5.3), every measurement process is susceptible to the occurrence of errors, and the proposed method is no exception.

Consequently, it is imperative to ascertain the uncertainties associated with the measurement process to ensure the provision of accurate results.

Next, an analysis of the errors associated with each of the steps and outcomes of the proposed measurement process is conducted, ultimately yielding the uncertainties of the values provided as results after the measurement process.

11.3.1. DEFINITIONS

The *Measurement Error* is the difference between the NO_x concentration measured value from the equipment and the true value.

As the measurement error impacts the dependent variable (NO_x concentration) within the relationship, a rise in this error leads to a reduction in the R² value compared to what would result from an error-free scenario. However, it does not render the measurement itself invalid.

75% of vehicles tested in the research showed an R² value for the Initial section higher than 0.6, and this can be considered as an indicator that the errors introduced, although they can be significant, are not so great that they invalidate the measurement process. The measurement error is composed of partial errors, which belong to one of the following two groups (see Figure 11-12): Systematic error, and Random error. The overall error will be the sum of these partial errors.

Systematic error. This pertains to the errors experienced during the measurement process, which can be classified as either inherent to the system or the measuring instrument itself, stemming from the measurement procedure itself, human intervention, or environmental conditions. These errors are consistently present whenever the measurement procedure is conducted under identical conditions and circumstances.

As such, they can be considered predictable, except in cases of significant human mistakes or gross errors.

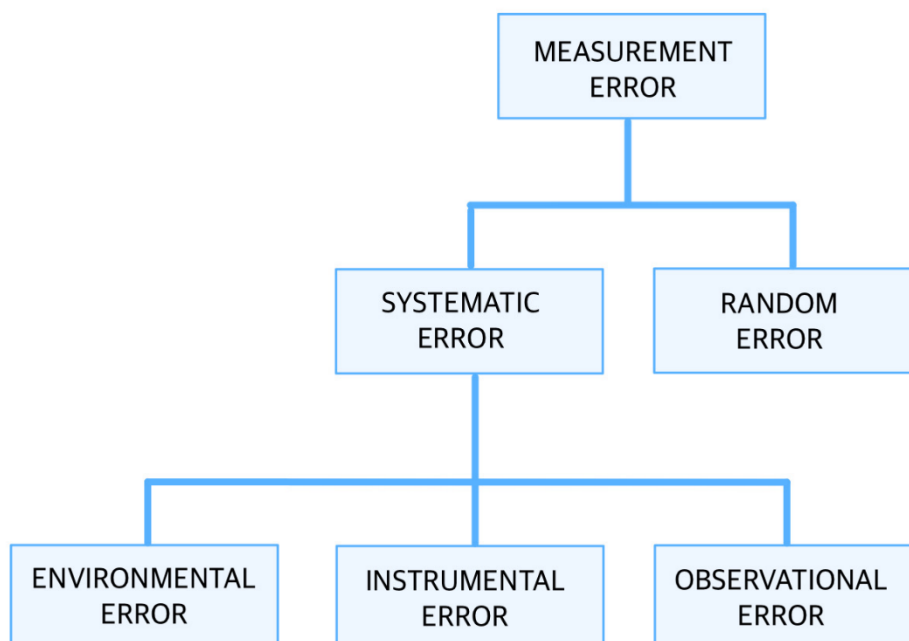


Figure 11-12. Distribution of measurement error.

Human mistakes that are included in systematic errors are those that have some probability of occurrence due to the nature of the measurement process itself.

For instance, in a measurement process that involves complex operations to be carried out by the observer, there is a higher likelihood of mistakes occurring depending on the experience and skills of the person conducting the measurements. Even though these specific errors may not be predictable in terms of when or how they occur, they are still categorized as systematic errors because they are a result of the measurement process itself.

The term *Accuracy* refers to the **deviation of systematic errors**, which means, the **size of the systematic error**. In a formal definition, it is the difference between a measured value and a reference value (see Figure 11-13), traceable to a national standard, and describes the correctness of a result [105]. Indeed, the greater the accuracy of a measured value, the closer that value is to the true value. Accuracy can be established through a single measurement.

Among the Systematic errors, the following may be found:

Instrumental errors are inherent to the measuring equipment, or due to a misuse of the measuring equipment.

From the first ones, we can find the errors due to the NO_x measurement equipment itself, detailed in Table 6-3. Even though the NO_x measurement equipment exhibits a slightly higher error compared to the equipment used for CO measurement, this error value is still considered acceptable for PTI purposes. This is because the errors are within the same order of magnitude, and the CO error is deemed appropriate for PTI application.

Among the second type of errors, examples include incorrect zeroing of the equipment or gross errors resulting from human mistakes. *Gross errors* are inherent in measurements and are due to errors by human observers in the measurement process. Automating the measurement process to the greatest extent feasible, minimizing human intervention, and enabling measurement equipment to directly produce results without relying on human observers significantly diminish the occurrence of this error.

A primary objective of this test proposal is to mitigate measurement error by streamlining the process. In comparison to other methods, like the power bench measurement that demands substantial human involvement for conducting NO_x measurement, this approach holds the advantage of minimizing such errors.

Environmental errors. The appearance of these errors in the measurement, due to environmental conditions, is common to those of other measurement processes. Ambient temperature, relative humidity, atmospheric pressure, etc., can affect the measurement result.

The use of a climatized location with standardized conditions would be one way to reduce these errors, but its use is misplaced in PTI, for the reasons of simplicity and cost savings explained previously. This type of facility is required and used for NEDC and WLTP tests in the homologation process, but is not adequate for PTI inspection, because it is high time and resource-demanding.

Another possibility would be the application of **correction factors** depending on the **environmental conditions**. Future research would be necessary to correctly define if these correction factors can be an adequate solution.

Observational error. They are errors **produced in the reading of the measurement result**. Automating this process through a software application greatly reduces this error throughout the measurement process.

Random error. Random errors stem from unpredictable factors that are beyond control and have the potential to impact measurements. These errors often exhibit variability from one measurement to another, even when the conditions and measurement scenario remain constant. They are inherently unpredictable in nature. This type of error can manifest even after systematic human and equipment errors have been rectified. Expanding the number of measurements conducted can mitigate the occurrence of random errors.

The *Precision* of measurement is the size of the random errors in the measurement. In a formal definition, this is the degree to which repeated measurements under unchanged conditions show the same results (see Figure 11-13). Usually, this value is associated with the Standard Deviation [105]. To evaluate *Precision*, repeated measures are required; they cannot be determined with only one measure.

So, the concepts of precision and accuracy of measurement are connected through these two types of error in the measurement process: systematic error is linked to accuracy and random error is linked to precision and is used to define the quality of the measurement process. Obtaining a correct measurement is necessary for the good behavior of both skills.

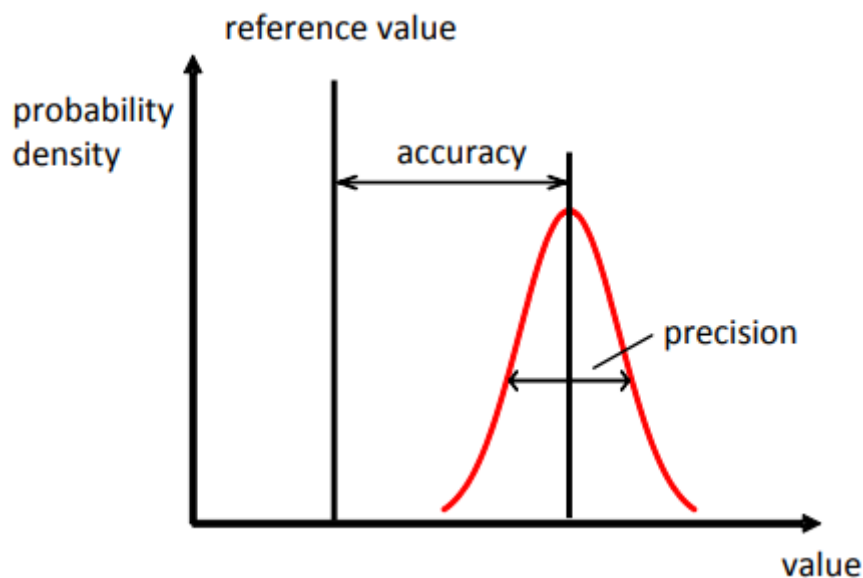


Figure 11-13. Formal representation of accuracy and precision (Source: UN GTR 15) [105]

However, an easier way to understand the meaning of both terms can be seen in the sample in Figure 11-13: high precision in the measurement is not enough if there is low accuracy. Random errors are unpredictable, so although they have great importance for the measurement process, it is through accuracy (that means, reducing systematic error) that the measurement process can be modified to reduce the measurement error.

Nonetheless, the combination of a good performance of both parameters is the most desirable situation for a measurement process, as can be seen in Figure 11-14.

When delving into the assessment of how uncertainty propagates through the measurement process, various forms of measurement and different types of errors need to be determined. The guidance outlined in the JCGM 100:2008 document has been employed as a point of reference for gauging and articulating measurement uncertainty.

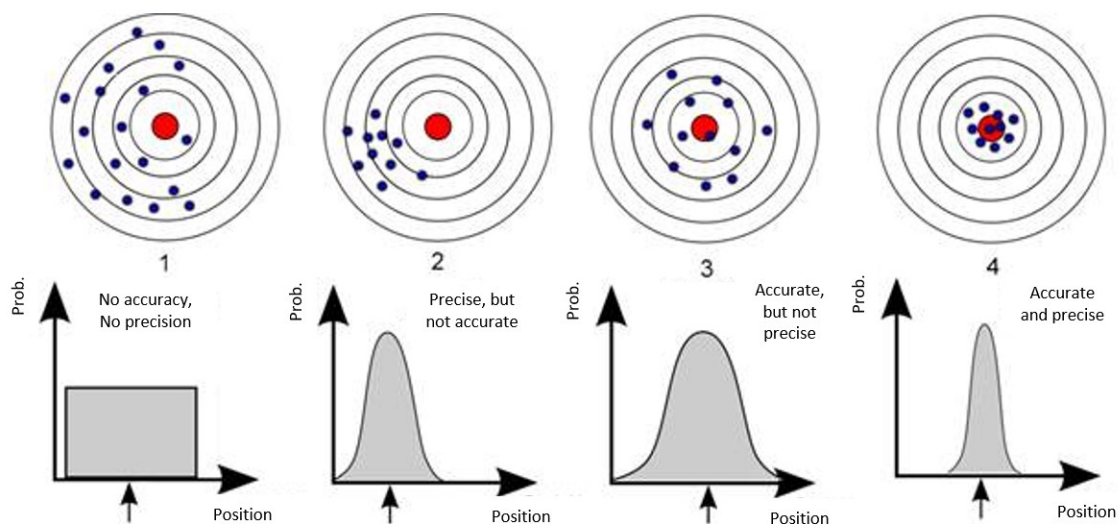


Figure 11-14. Difference between accuracy and precision in the measurement process.

In the subsequent content, the terms "error" and "uncertainty" will be used interchangeably, although in strict terms they are distinct. The formal definition of measurement uncertainty refers to the parameter linked to the measurement result that describes the spread of values that could reasonably be associated with the measured quantity [200].

11.3.2. ERROR ANALYSIS FOR NO_x EMISSIONS MEASUREMENT

The primary objective of the measurement process is to obtain the **instantaneous NO_x concentration** using the equipment described in Chapter 4, which comes with a **systematic error (associated standard uncertainty) of $\pm 4\%$ rel.**, as per the manufacturer's specifications. Additionally, there may be errors caused by environmental conditions, and the possibility of random errors arising, which would be added to the systematic error.

To put it differently: The aim of this analysis is not to establish the precise accuracy required for equipment in PTI applications. However, since the systematic error in measuring NO_x concentration using this equipment aligns with the systematic error in measuring CO, it can be concluded that both, the process and the equipment are suitable for PTI measurements. This similarity in measurement uncertainty underscores their adequacy for PTI purposes.

In addition to monitoring NO_x concentration, the OBD system records multiple values. Due to the unavailability of information about the uncertainty linked to this measurement process (as it is specific to each vehicle and inaccessible), the resolution of each variable can be treated as a systematic error inherent to the measurement process. To account for this, a conservative approach was taken, attributing a minimum of ±1% relative error to each variable. The outcomes of the measurements validated the accuracy of these assigned systematic error values. They were not surpassed in situations where other forms of errors were not present. Next, systematic errors associated with the measured variables are shown in Table 11-1.

Variable	Units	Error	Resolution
NO _x concentration	ppm	±4% ppm	1 ppm
% Engine load	%	±1%	1 %
Engine speed	rpm	±1% rpm	1 rpm
% EGR aperture	%	±1%	1 %
Engine Temperature	°C	±1% °C	±1°C

Table 11-1. Data registered and associated error in instantaneous measurement.

11.3.3. ERROR ANALYSIS FOR MEASUREMENT RESULTS AVERAGING

In the measurement procedure, the average value of the several variables for each of the five stages into which the measurement cycle is divided is calculated. This **average value** comes from a 20-second sample size for each stage of the measurement process, with a frequency of acquisition of 1 Hz. This implies that a collection of 20 measurements is utilized to compute the average outcome, which serves as the representative value for the measurement in each of the four stages employed for calculating the vehicle's NO_x emissions.

According to the JCGM 100:2008 guide and the EA-4/02 M:2013 document [201] for the evaluation of measurement uncertainty in calibrations, from the evaluation Type A of the standard uncertainty for a set of values with more than 10 values, the estimated value of the magnitude is the average from the measured values (Equation 11-1), and the uncertainty associated to this estimated value is the experimental SD (Standard Deviation) to the mean from the sample data (Equation 11-2).

Equation 11-1

$$\bar{q} = \frac{1}{n} \sum_{j=1}^n q_j$$

Equation 11-2

$$u(\bar{q}) = s(\bar{q})$$

Equation 11-3

$$s(\bar{q}) = \sqrt{\frac{s^2(q)}{n}}$$

Equation 11-4

$$s^2(q) = \frac{1}{n-1} \sum_{j=1}^n (q_j - \bar{q})^2$$

Employing the average value to present measurement results, as opposed to relying solely on instantaneous values, can aid in mitigating the potential impact of random errors that might have arisen in certain individual measurements. This approach is typically considered the "best estimate of the expectation or expected value of a quantity" in situations where independent observations have been collected under consistent measurement conditions [200].

The experimental data collected during the various stages of the test were utilized to calculate the standard deviation (SD) associated with the values employed in computing the average NO_x concentration for each of the four stages used in the measurement test to determine the NO_x emissions.

By evaluating the outcomes derived from the measurement process and juxtaposing the standard deviation (SD) with the mean value computed for each stage, it was determined that the standard uncertainty associated with the data concerning NO_x concentration remained consistently at 4% or below. In other words, **the error in NO_x concentration** measurements from the dataset utilized to establish the average NO_x emissions of the vehicle was either **equal to or less than 4%**, mirroring the systematic error of the gas analyzer. This correspondence was observed under stable conditions in the variables' behavior.

In cases of vehicles exhibiting fluctuations in variable values, the standard deviation (SD) value increases due to the wider dispersal of data caused by numerous factors altering behavior. These factors include the vehicle's inherent operation (external factors like exhaust after-treatment system performance) as well as the presence of diverse error sources such as environmental or random errors.

The same situation applies to the other recorded variables. When the variables exhibited consistent behavior, the observed uncertainty closely matched the systematic error associated with the variable. In sections where the variables showed variability, the standard deviation (SD) value increases, yet the systematic error can still be defined as per Table 11-1.

In summary, when computing the average values for each segment within the divided measurement cycle, each of the measured variables can be observed in two scenarios:

1) In certain instances, the uncertainty associated with the average value is either equivalent to or even lower than the anticipated systematic error. This occurs when the sole source of uncertainty impacting the outcome is the previously mentioned systematic error of the measuring equipment.

2) At times, when greater variability is observed in the studied variables or when random or environmental uncertainties come into play, the uncertainty associated with the average value surpasses the anticipated systematic error.

In any case, the expression of the average value for the analyzed variable is expressed as: $\bar{q} \pm u(\bar{q})$ (calculated from Equation 11-1 and Equation 11-2).

Using the collection of average NO_x concentration values and their respective uncertainties for both Unloaded and Loaded states, it is possible to establish a linear regression equation. This equation captures the correlation between the "% engine load" and NO_x concentration during idling, offering an estimation of the anticipated NO_x concentration at idling under a 100% "engine load."

This projected NO_x concentration value during idling at a 100% "engine load" carries an associated uncertainty, calculable from the linear relationship function.

For this, Least Squares Fit can be used to determine the uncertainty of the results of the value y obtained from the linear function according to Equation 11-5.

Equation 11-5

$$y = mx + b$$

It is possible to construct a confidence interval from the function using the t -distribution with $(n-2)$ degrees of freedom (as there are 2 regression parameters). This allows us to obtain a 95% confidence interval for both the slope and intercept by calculating the value of $t_{\alpha/2, n-2}$ for $\alpha=0.05$. This linear function [4] is suitable for use in uncertainty propagation for the model (Equation 10.6) [5]. Consequently, the confidence interval for a calculated y value based on an x_p value can be defined by the following equation:

Equation 11-6

$$y(x_p) = (\hat{m}x_p + \hat{b}) \pm t_{\alpha/2, n-2} s_{y,x} \sqrt{\frac{1}{n} + \frac{(x_p - \bar{x})^2}{SS_{xx}}}$$

and it is also possible to calculate the Standard Deviation of $y(x)$:

Equation 11-7

$$s_{y,x} = \sqrt{\left(\frac{1}{n-2}\right) \sum_{i=1}^n (y_i - \bar{y})^2}$$

This equation provides the **standard error value for the y variable** when it is calculated from the linear function for a specific x value, with \bar{y} calculated using Equation 10.1.

A summary of the errors from the measurement process is shown in Table 11-2.

Variable	Units	Average
NO _x concentration	ppm	$s(\bar{q}) \gg \pm 4\%$ rel. ppm
NO _x mass flow	mg/s	$s(\bar{q}) \gg \pm 4\%$ rel. mg/s
% Engine load	%	$s(\bar{q}) \gg \pm 2\%$ rel. %
Engine speed	rpm	$s(\bar{q}) \gg \pm 2\%$ rel. rpm
% EGR aperture	%	$s(\bar{q}) \gg \pm 2\%$ rel. %
Engine Temperature	°C	$s(\bar{q}) \gg \pm 2\%$ rel. °C

Table 11-2. Data registered and associated errors in the average measurement process.

11.3.4. ERROR ANALYSIS FOR THE EXTRAPOLATION PROCESS

Thus, the uncertainty for the NO_x concentration at idling under a 100% engine load can be determined through the linear function derived from the average concentration data collected throughout the static cycle. This uncertainty is contingent upon the degree of data dispersion observed in the measurements.

Using the recorded data from the test, the mass flow of NO_x is computed and incorporated into the final outcomes. Just as the uncertainty propagation is assessed for the NO_x concentration and the other variables engaged in the measurement process, a similar evaluation is necessary to determine the uncertainty associated with these calculated NO_x mass flow emission values.

The value of mass emission flow is calculated from the NO_x concentration and the exhaust gas flow rate, using several values to estimate it. In addition to estimating its value, it is necessary to calculate the uncertainty associated with the calculated value of the mass flow of NO_x emission. The value of the mass flow of NO_x emissions can be calculated according to Equation 11-8.

Equation 11-8

$$f(X_1, X_2, \dots, X_N) = m_i = C \cdot \frac{rpm \cdot P \cdot \alpha_i}{T}$$

m_i : NO_x mass emission flow (mg/s)

C: constant value, depending on engine size and NO_x molar mass

rpm: engine speed (rpm), variable

P: Atmospheric Pressure (mb), variable

α_i : NO_x concentration (ppm NO_x), variable

T: Exhaust Gas Temperature (°C), variable

According to the JCGM 100:2008 and the EA-4/02 M:2013, when a value y can be calculated as a function of another variable uncorrelated between them, the uncertainty associated with the calculated value y can be defined as:

Equation 11-9

$$u^2(y) = \sum_{i=1}^n u_i^2(y)$$

Being $u_i(y)$ the contribution to the final uncertainty from the uncertainty associated with the several input values. This quantity is calculated following (Eq. 4-12) as the product of the sensitivity coefficient and the associated uncertainties of the input variables.

Equation 11-10

$$u_i(y) = c_i u(x_i)$$

c_i is called the sensitivity coefficient associated with every input value used to calculate the y value, and $u(x_i)$ is the uncertainty from any of the input variables. It depends on the input and is the partial derivative of the function concerning the input variable analyzed.

Equation 11-11

$$c_i = \frac{\partial f}{\partial x_i} = \left. \frac{\partial f}{\partial X_i} \right|_{X_1=x_1..X_N=x_N}$$

This sensitivity coefficient provides information about the influence on the final result uncertainty from the variations in the input values of the function.

From the function defined in Equation 11-8, the partial derivative concerning every input variable is the following:

Equation 11-12

$$c_{rpm} = \frac{\partial(m_i)}{\partial(rpm)} = \frac{C \cdot P \cdot \alpha_i}{T}$$

Equation 11-13

$$c_P = \frac{\partial(m_i)}{\partial(P)} = \frac{C \cdot rpm \cdot \alpha_i}{T}$$

Equation 11-14

$$c_{\alpha_i} = \frac{\partial(m_i)}{\partial(\alpha_i)} = \frac{C \cdot rpm \cdot P}{T}$$

Equation 11-15

$$c_T = \frac{\partial(m_i)}{\partial(T)} = \frac{-C \cdot rpm \cdot P \cdot \alpha_i}{T^2}$$

The uncertainty analysis (also called uncertainty budget) for the NO_x mass emission flow has to include all the possible sources of uncertainty, with the associated uncertainties of measure.

To recap the outcomes of the uncertainty assessment performed in accordance with Equation 11-9, it is advisable to present a comprehensive table containing pertinent data for computation. This table should encompass all sources of uncertainty, their estimated values, corresponding uncertainties, sensitivity coefficients, and the contributions of each source to the final result.

The value for every source is provided by the measurement procedure, and the Sensitivity coefficients are defined by Equation 11-12, Equation 11-13, Equation 11-14, and Equation 11-15.

Variable	Units	Extrapolation
NO _x concentration	ppm	$s_{y,x} \gg \pm 8\%$ rel. ppm
NO _x mass flow	mg/s	$s_{y,x} \gg \pm 8\%$ rel. mg/s
% Engine load	%	--
Engine speed	rpm	--
% EGR aperture	%	--
Engine Temperature	°C	--

Table 11-3. Data registered and associated errors in the extrapolation measurement process.

11.3.5. ERROR ANALYSIS FOR THE NO_x MASS FLOW ESTIMATION

The Standard uncertainty values for NO_x concentration and rpm are defined in Table 11-1. However, the remaining values (pressure and temperature) possess distinct uncertainties that require specific definitions.

Atmospheric pressure is a parameter that can impact the computation of exhaust gas flow and consequently the NO_x mass flow. In the estimation process, a uniform value

of 1 atmosphere (1013 mb) has been consistently applied as the atmospheric pressure. However, for the measurements conducted in Zaragoza during the study period, the atmospheric pressure displayed variations. The maximum pressure recorded was 1005 mb, the minimum pressure was 959 mb, and the average pressure was 987 mb.

Employing the fixed value of 1 atmosphere (1013 mb) instead of the direct atmospheric pressure introduces a **systematic uncertainty equivalent to 2.6% relative** to the actual atmospheric pressure value. This particular uncertainty contributes to the ultimate uncertainty in the NO_x mass emission flow, which will be utilized. The alterations in the Pressure value utilized for calculating the NO_x mass flow lead to differences in the average emissions for the Unloaded and Loaded states. Consequently, using the precise atmospheric pressure value rather than the generic 1013 mb value results in distinct final NO_x mass flow emission outcomes.

Source	Units	Estimate value	Source standard uncertainty	Sensitivity coefficient	Contribution to standard uncertainty
X_i		x_i	$u(x_i)$	c_i	$u_i(y)$
rpm	<i>rpm</i>	$x(\text{rpm})$	$u(\text{rpm})$	C_{rpm}	$u(\text{rpm}) \cdot C_{rpm}$
P	<i>mb</i>	$x(P)$	$u(P)$	C_P	$u(P) \cdot C_P$
α_i	<i>ppm NO_x</i>	$x(\alpha_i)$	$u(\alpha_i)$	C_{α_i}	$u(\alpha_i) \cdot C_{\alpha_i}$
T	<i>°C</i>	$x(T)$	$u(T)$	C_T	$u(T) \cdot C_T$
m_i	<i>mg/s NO_x</i>	$C \cdot \frac{\text{rpm} \cdot P \cdot \alpha_i}{T}$			$\sqrt{\sum_{i=1}^n u_i^2(y)}$

Table 11-4. Uncertainty for measures and type of data.

Upon analyzing the data, it can be determined that the contribution of this method to the overall uncertainty in mass emission flow is sufficiently low. Thus, it is reasonable to conclude that a higher level of accuracy is not imperative for accounting for uncertainty in mass emission flow variations. Nevertheless, there exists a technical possibility to enhance accuracy by measuring air pressure throughout the test, thereby reducing the uncertainty associated with this variable.

Similarly, instead of directly measuring the exhaust gas temperature, the estimation of exhaust gas flow and NO_x mass flow values involved utilizing the engine temperature value obtained from the OBD system.

In order to characterize the potential uncertainty associated with employing this estimated exhaust gas temperature instead of actual measurement, a series of exhaust gas temperature measurements were conducted at the vehicle's exhaust pipe. These measurements were taken concurrently with the NO_x testing of the vehicle. This approach aimed to establish the variance between the present exhaust gas temperature and the OBD temperature value being utilized. It allowed for a clearer understanding of the disparities between the two values.

Based on these measurements, it was observed that the exhaust gas temperature at the outlet pipe exhibited significant variations across various vehicles. In certain instances, this temperature coincided with the operational temperature of the engine, while in other instances, it exceeded that temperature. The recorded measurements ranged from a minimum of 75°C to a maximum of 120°C.

Based on these figures, it can be established that there exists a level of **uncertainty related to temperature** when utilizing the temperature data obtained from the OBD system as opposed to the actual current temperature of the exhaust gas pipe. This **uncertainty is calculated to be 3.8% relative to the engine temperature**, with all temperatures considered in degrees Kelvin (K).

This systematic error was deemed to fall within an acceptable range, considering the precision needed for the test. Its impact on the overall uncertainty was subsequently computed.

Considering all the information presented earlier, along with the uncertainties connected to the variables engaged in estimating the **NO_x mass flow** rate, it has been determined that the **standard level of uncertainty** linked to this value typically falls within the **range of 7-8% relative** to the estimated NO_x mass flow value (mg/s). While the exact uncertainty can differ for each vehicle and measurement, it is reasonable to establish a typical uncertainty of around 8% relative to the value.

After consulting the manufacturer of the equipment, it has been determined that it is technically feasible to obtain real-time measurements of the atmospheric pressure during the moment of testing, as well as the temperature of the exhaust gases within the measuring chamber where the NO_x sensor assesses the concentration of this compound from the exhaust gases. These potential enhancements could be integrated into the equipment in the future, leading to enhanced result accuracy. Such improvements would involve implementing software modifications, thus incurring a relatively low-cost impact on the equipment.

To gauge the extent of the reduction in uncertainty that would arise from the adoption of these direct readings, as opposed to the estimations employed in the current study, it is essential to determine the fresh uncertainty values associated with the measurement of both variables.

As of the time of composing this thesis, precise details regarding the uncertainty of these data are unavailable. Upon the successful implementation of the equipment modifications enabling the direct measurement of both atmospheric pressure and exhaust gas temperature within the measuring chamber, the experimental determination of uncertainties would become possible. It is important to note that given these measurements would be taken internally by the gas analyzer systems, a reasonable assumption is that they inherently possess a low level of uncertainty. This assumption is crucial to maintain the accuracy of the conducted measurements.

Assuming a reduction in the uncertainties of both variables to 1%, compared to the current values of 2.6% for Pressure and 3.8% for Temperature, leads to a reduction of approximately 1.5% in the overall uncertainty associated with the final NO_x mass flow value when compared to the value calculated with the existing uncertainties.

While enhancing the precision of measurements and reducing uncertainties is certainly desirable, it is evident that the estimations employed for both variables do not introduce a significant increase in the associated uncertainty. Instead, they have facilitated a simplified approach to conducting measurements.

Additionally, another source of uncertainty introduced when calculating the NO_x mass flow from the measured concentration is due to the molar weight used for the calculation.

In the process of estimating the mass flow, the assumption was made that the entirety of NO_x measured by the sensor corresponds to NO₂. This approach was taken due to the fact that the utilized equipment lacks distinct sensors for separate NO and NO₂ measurements.

However, in instances where equipment provides measurements for both compounds individually, this particular error can be rectified by incorporating the concentrations of both compounds and subsequently calculating the precise mass for either of them. This refinement serves to enhance the accuracy of the outcomes.

Absolutely, the integration of distinct sensors for both NO and NO₂ measurements could indeed be viewed as a valuable enhancement for future equipment iterations. This improvement would effectively enhance the accuracy of calculating emitted NO_x mass, without introducing complexity or excessive costs, all while preserving the benefits of the NO_x measurement procedure.

It is worth noting that the current level of uncertainty is deemed satisfactory for the intended method's purpose, highlighting the feasibility and reliability of the approach at hand.

Just as the average NO_x concentration value was computed using the instantaneous estimated NO_x mass flow data during the measurement procedure, the calculated value for the magnitude at each test stage is obtained by averaging the measured values (Equation 11-1). The associated uncertainty for this calculated value is determined by the experimental standard deviation (SD) relative to the mean of the sampled data (

Equation 11-2). This approach provides a method to quantify and account for the variability in the measured data, ensuring a more accurate representation of the overall measurements.

Based on the outcomes derived from the measurement process, it is noteworthy that the standard deviation (SD) of the NO_x mass flow data for each stage closely resembles the SD results obtained for NO_x concentration, both hovering around 4% relative to the SD. This trend allows us to establish that across the various stages of the measurement procedure, the **standard uncertainty associated with the average NO_x mass flow** values can be reasonably set at **4% relative** to the value. This determination reinforces the reliability of the methodology and its consistency in handling uncertainties.

Indeed, when an elevation in the variability of NO_x concentration values is observed, it correlates with a corresponding increase in the variability of NO_x mass flow values. This mutual trend confirms that, on a general basis, the uncertainty associated with the averaging of NO_x mass flow values mirrors the uncertainty associated with

averaging NO_x concentration values. This consistency highlights the interconnectedness of these measurements and the uniformity in their uncertainty patterns.

11.3.6. SUMMARY OF ERROR ANALYSIS

Conclusively, similar to the approach taken for NO_x concentration, the collection of average NO_x mass flow values for both Unloaded and Loaded states enables the creation of a linear regression function as detailed in Chapter 4. This linear regression function, as outlined in Equation 11-5, delineates the correlation between "% engine load" and NO_x mass flow emissions during idling conditions. This function can serve as a means to predict the anticipated NO_x mass flow emission value at idling when the "% engine load" is at 100%.

This estimated value of NO_x mass flow emission at idling when "% engine load" is 100% has also associated uncertainty, which can be calculated from the linear relation function, with Equation 11-7.

Table 6-16 compiles and summarizes the standard uncertainties originating from multiple registered variables, juxtaposed with the mean value observed through the measurements undertaken in the current study.

11.4. ASSESSMENT OF VEHICLE EMISSIONS FROM ON-ROAD TESTS

In order to facilitate a clear presentation of the results obtained from on-road measurements in Chapter 7 (Section 7.3.2), only the results for Test #1 have been elaborated upon in that section.

Below, the results obtained from the execution of Tests #2, #3, #4, #5, and #6 are compiled and delineated.

11.4.1. ASSESSMENT OF VEHICLE EMISSIONS IN TEST #2

For test #2 (see Figure 11-15), the observed behaviors are broadly repeated, although some vehicles show significant increases in the level of emissions measured.

It is crucial to recall that the primary distinction between this test and test #1 is the introduction of vehicle stops, simulating scenarios such as traffic lights or slow-moving traffic, followed by subsequent vehicle restarts, as delineated in Figure 7-12 and Table 7-3.

Consequently, vehicles No. 1 and No. 2 undergo a marginal uptick in engine demand values compared to test #1. However, this minor alteration does not yield a substantial impact on their emissions performance.

For vehicle No. 1 there is a slight increase in the emission factor for the loaded situation, and for vehicle No. 2 there is a slight decrease in the emission factor for both situations. In any case, the differences are small, so it is possible to state that the behavior of both vehicles, in terms of engine load and NO_x emissions, is similar for test

#1 and test #2. The EF_{NOx} for the most favorable case (i.e. lower emissions) is 2.8 times higher than the limit allowed according to the Euro 4 emission level (see Table 11-5 for the summary of data results from test #2).

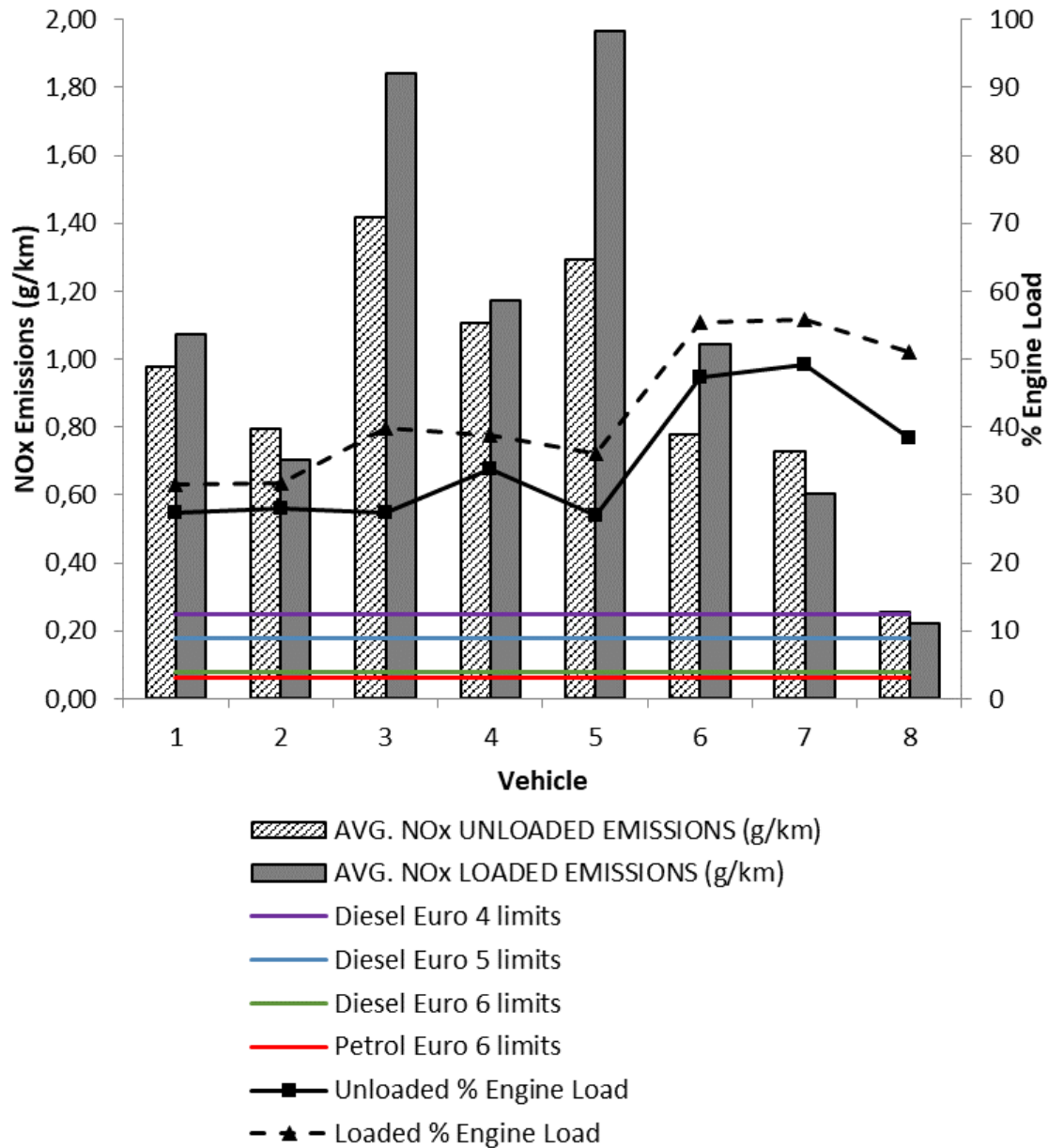


Figure 11-15. NO_x emissions and "% engine load" from the set of vehicles in test #2.

For the Euro 5 vehicles, significant changes are observed in test #1. The engine demand values for the unloaded situation are similar to those recorded in test #1, but for the loaded situation, there is an appreciable increase in each of the three vehicles. Vehicle No. 3 has an increase of 42% for the "% engine load" value in the loaded situation, a 15% increase for vehicle No. 4, and a 28% increase for vehicle No. 5.

Conversely, the EF_{NO_x} values also experienced a notably substantial rise, mirroring the pattern observed in test #1, yet attaining considerably elevated EF_{NO_x} values across all three scenarios.

Similar to test #1, the emissions from vehicle No. 5 under the loaded condition are the highest among all the tests, with vehicle No. 3 closely following its emissions value. The main difference is: the EF_{NO_x} is 1.97 g/km for vehicle No. 5, instead of the value of 1.21 g/km obtained in test #1. This means an increase of 63% concerning test #1, due to the stops and starts to which the vehicle was subjected in the test. Compared to the Euro 5 level, the emission factor of vehicle No. 5 has exceeded the limit value by 10.9 times.

In the case of vehicle No. 3, the measured increase in EF_{NO_x} is also 62% over the value recorded for the situation loaded in test #1.

Vehicle No. 4, which, much like in test #1, demonstrated the lowest emissions among the Euro 5 vehicles during the test, exhibited an EF_{NO_x} value of 1.11 g/km under the unloaded condition. This signifies a notable 42% elevation compared to the emissions value from test #1, resulting in an exceeding of the Euro 5 limit value by a factor of 6.1.

Hence, it is evident that the Euro 5 vehicle group has exhibited a behavior akin to that of test #1, distinguished by a notable rise in the recorded engine load (particularly in the loaded scenario) and a substantial escalation in emissions generated. Notably, this increase in emissions far exceeds the proportionate rise in engine load.

Regarding the Euro 6 vehicles, variability in their performance persists. The outcomes across various driving tests clearly indicate that the installed EATS in each vehicle exhibit distinct behaviors, lacking a consistent pattern in the results.

VEHICLE	EURO LEVEL	FACTOR EMISSION LIMIT (g/km)	UNLOADED			LOADED		
			AVG. ENGINE LOAD (%)	AVG. NO _x EMISSIONS (g/km)	*EURO LEVEL LIMIT MULT. FACTOR	AVG. ENGINE LOAD (%)	AVG. NO _x LOADED EMISSIONS (g/km)	*EURO LEVEL LIMIT MULT. FACTOR
1	4	0.25	27	0.98	3.9	32	1.07	4.3
2	4	0.25	28	0.80	3.2	32	0.70	2.8
3	5	0.18	27	1.42	7.9	40	1.84	10.2
4	5	0.18	34	1.11	6.1	39	1.17	6.5
5	5	0.18	27	1.29	7.2	36	1.97	10.9
6	6	0.08	47	0.78	9.8	55	1.04	13.0
7	6	0.08	49	0.73	9.1	56	0.60	7.6
8	6	0.06	38	0.26	4.3	51	0.22	3.7

* Multiplier factor for average NO_x emissions exceeding the Euro level limit.

Table 11-5. Summary of avg. results from Test #2

When comparing the average "% engine load" values to which these vehicles were subjected, it becomes evident that the values are of a similar magnitude in both tests. However, a slightly more notable discrepancy can be observed in the engine demand of vehicle No. 7 during test #2. In this case, there is a 24% rise in "% engine load" under

the loaded condition and an 8% increase in the unloaded situation. On the other hand, the "% engine load" values for vehicle No. 6 closely resemble those recorded in test #1.

In terms of NO_x emissions, vehicle No. 6 demonstrates an escalation in both measured scenarios, with a more noticeable rise observed in the emission factor for the unloaded condition. In this case, an EF_{NO_x} of 1.04 g/km has been documented, marking the highest among the Euro 6 vehicles. This signifies a substantial increase of 360% over the emissions recorded in test #1 under the same situation. Remarkably, this value surpasses the limit established by the Euro 6 standards by a staggering 13-fold.

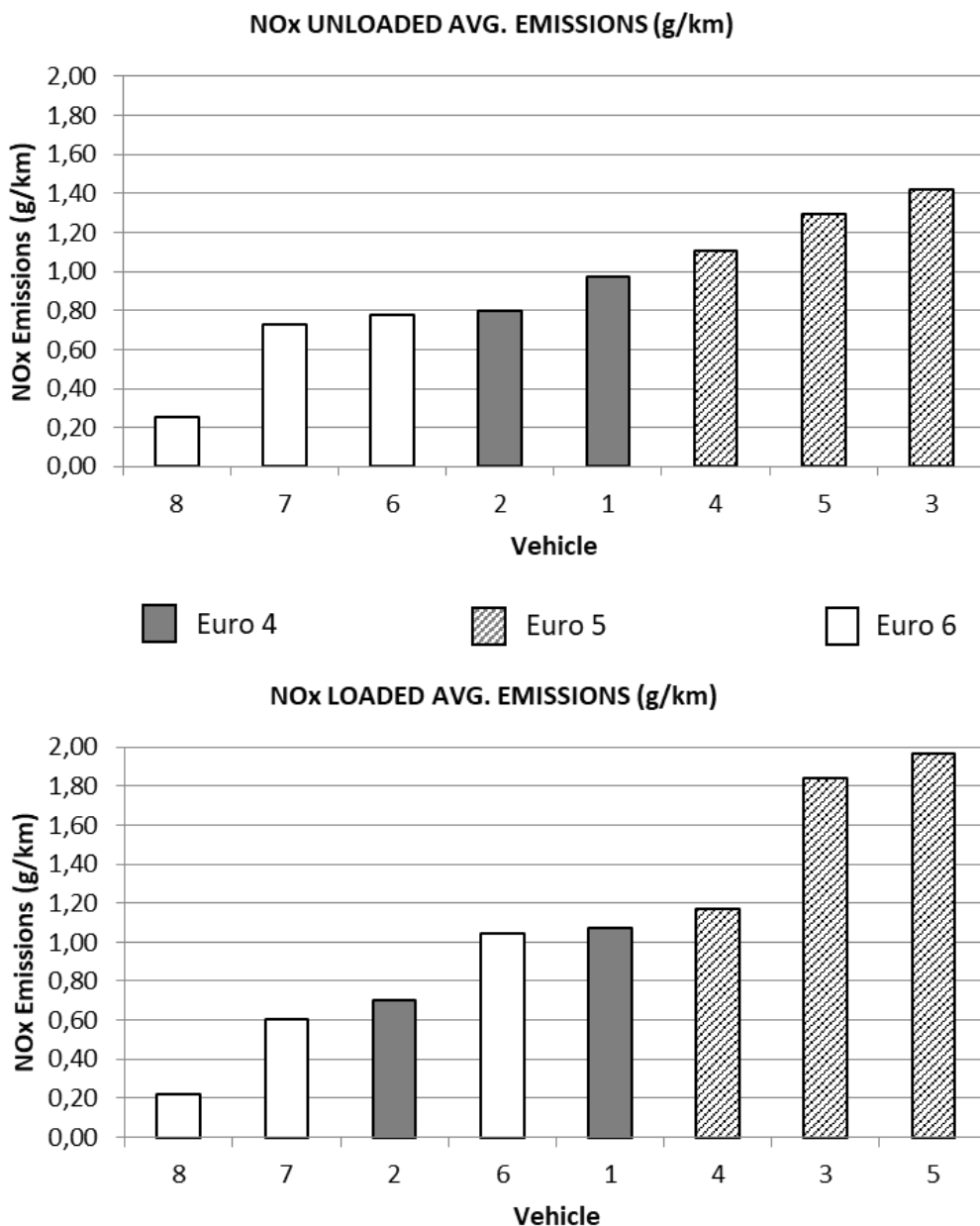


Figure 11-16. Vehicles ordered according to EF_{NO_x} for unloaded (up) and loaded (down) test #2.

Vehicle No. 7 instead presents a slight decrease in the emission factor for the unloaded situation with a decrease of 16% to a value of 0.73 g/km and an increase of the emission factor for the loaded situation to a value of 0.60 g/km (i.e. an increase of 11%). In the least unfavorable case, the recorded emission factor exceeds the Euro 6 limit by 7.6 times.

It is also evident in these vehicles that the fluctuations in the engine load they experienced do not align with the fluctuations observed in the recorded emission factor. This discrepancy can be attributed to the distinct performance of the EATS within each vehicle.

Finally, when analyzing the behavior of vehicle No. 8 in test #2, in terms of the average engine load to which it has been subjected, it can be seen that in the unloaded situation, the engine load value is similar, and for the loaded situation there has been an increase of 21%.

Concerning the emission factors, a notable increase of 73% has been observed for the unloaded situation, resulting in a value of 0.26 g/km. Conversely, for the loaded situation, the recorded value remains comparable to that of test #1. In the case of the unloaded situation, the measured emission factor surpasses the Euro 6 limit by a factor of 4.3.

The values measured in this test represent the highest recorded values for vehicle No. 8 throughout the entire series of tests (see Figure 7-20).

To conclude the analysis of test #2, the vehicles are ordered according to the results obtained both with and without fuel consumption, as can be seen in Figure 11-16.

Furthermore, it's evident that the vehicles do not exhibit consistent behavior between the unloaded and loaded scenarios, as the ranking of vehicles changes in both situations. Only vehicles No. 8, No. 7, No. 1, and No. 4 maintain the same positions in both situations when sorted by recorded emissions.

Regarding the Euro 5 vehicles, the relative order among them is not even preserved in both situations. Specifically, vehicles No. 5 and No. 3 switch positions between the unloaded and loaded conditions.

11.4.2. ASSESSMENT OF VEHICLE EMISSIONS IN TEST #3

Concerning the outcomes from test #3 (Figure 11-17), detailed in Table 7-3, a notable observation is that the patterns of "% engine load" and emission factors across the different vehicles in this test mirror those obtained in test #1. However, some variations are apparent in the actual recorded values, with instances of increases and decreases among the vehicles.

The primary distinction between the two tests lies in the utilization of the vehicle's gearbox. In test #1, the gears were sequentially engaged in a predetermined order, encompassing the 1st, 2nd, and 3rd gears. Conversely, in test #3, once the 3rd gear is engaged, it remains constant for the entire duration of the test, while maintaining a consistent speed of 50 km/h.

Consequently, variations in the powertrain of the vehicle result in discrepancies in the achieved engine load values. These differences in "% engine load," compounded by the inherent variability of the test due to other emissions-affecting variables, can impact the performance of the EATS. This system is controlled by the ECU, which responds to diverse parameters such as engine speed, vehicle speed, engine load, engaged gear, system temperatures, and more. These variations contribute to differences in the recorded values.

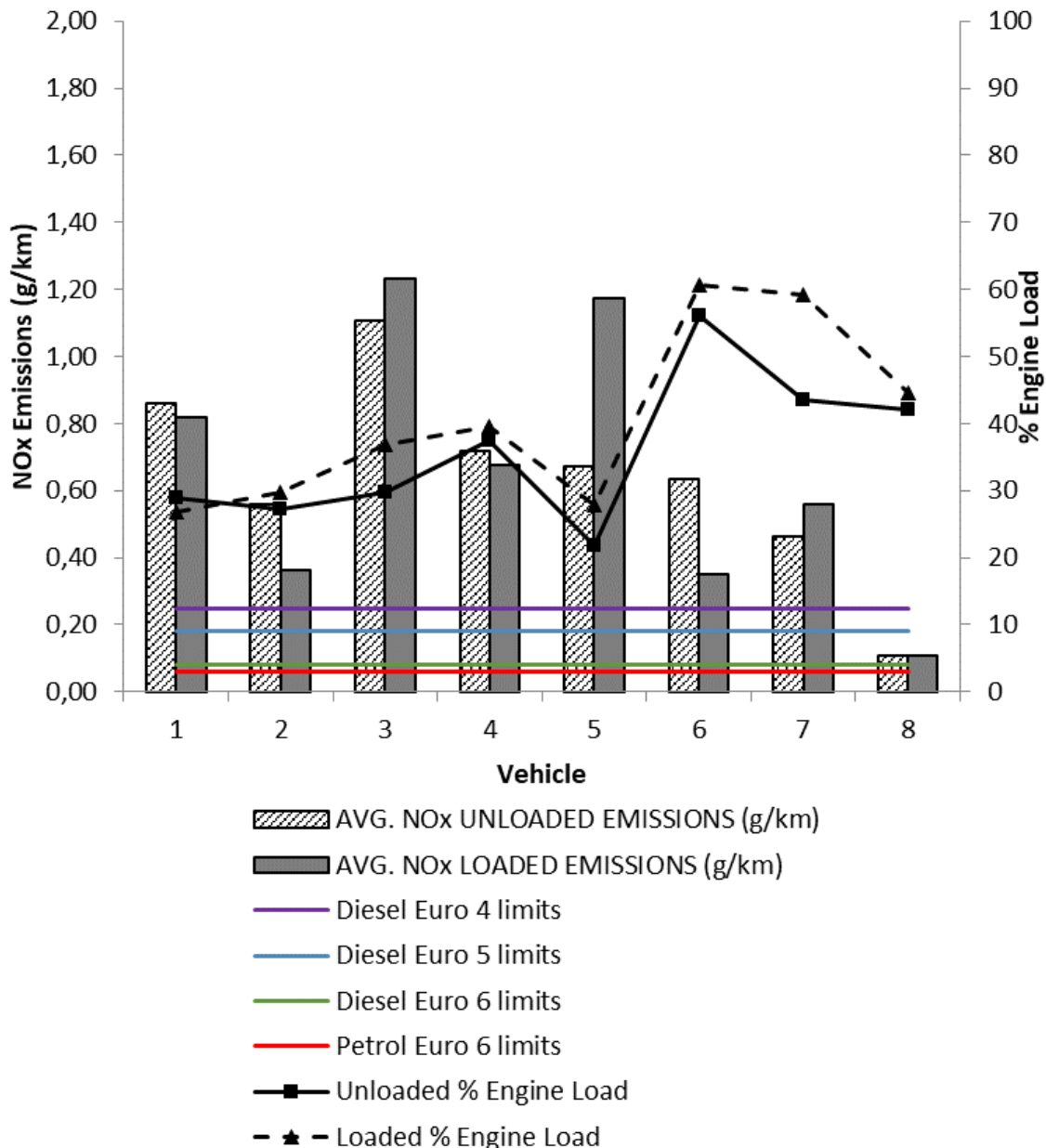


Figure 11-17. NO_x emissions and "% engine load" from the set of vehicles in test #3.

Nevertheless, as previously mentioned, the overall behavior observed across all vehicles remains consistent with the findings from test #1.

Euro 4 vehicles present values of "% engine load" similar to those obtained in test #1. On the other hand, the emission factor obtained for both vehicles and in both situations, is lower than those measured in test #1, with a more pronounced decrease for vehicle No. 2, which presents a 55% decrease in EF_{NOx} in the loaded situation. For the unloaded situation, the recorded decrease in EF_{NOx} is 35%. For vehicle No. 1, the average decrease in EF_{NOx} in both situations is 15%.

As in test #1, vehicle No. 2 (with EGR on) has lower emissions than vehicle No. 1, even more noticeably than in test #1. The emission factor of vehicle No. 1 in the unloaded situation is 1.5 times higher than for vehicle No. 2, and for the loaded situation, the difference is even higher, up to 2.3 times higher.

Euro 5 vehicles reproduce in test #3 the behavior observed in test #1 in a very similar way, including the values obtained for emission factors and "% engine load".

Regarding engine load, the most significant is a slight increase in the "% engine load" values for vehicle #3, with increases of around 27% in both situations. For the rest of the vehicles, the values measured in test #3 of "% engine load" are very similar to those of test #1.

Regarding the emission factors, vehicles No. 4 and No. 5 reproduce the results obtained in test #1, with very small variations. Vehicle No. 3 presents a 10% increase in the emissions of test #1 in the loaded situation. The same result was obtained for the unloaded situation.

VEHICLE	EURO LEVEL	FACTOR EMISSION LIMIT (g/km)	UNLOADED			LOADED		
			AVG. ENGINE LOAD (%)	AVG. NO _x EMISSIONS (g/km)	*EURO LEVEL LIMIT MULT. FACTOR	AVG. ENGINE LOAD (%)	AVG. NO _x LOADED EMISSIONS (g/km)	*EURO LEVEL LIMIT MULT. FACTOR
1	4	0.25	29	0.86	3.4	27	0.82	3.3
2	4	0.25	27	0.56	2.2	30	0.36	1.5
3	5	0.18	30	1.11	6.1	37	1.23	6.8
4	5	0.18	37	0.72	4.0	39	0.68	3.8
5	5	0.18	22	0.67	3.7	28	1.17	6.5
6	6	0.08	56	0.64	8.0	61	0.35	4.4
7	6	0.08	43	0.46	5.8	59	0.56	7.0
8	6	0.06	42	0.11	1.8	45	0.11	1.8

* Multiplier factor for average NO_x emissions exceeding the Euro level limit.

Table 11-6. Summary of avg. results from Test #3

Therefore, it is possible to state that the results of tests #1 and #3 are similar for the Euro 5 vehicles analyzed.

As for the Euro 6 vehicles, the heterogeneity in their behavior is still noticeable. Vehicle No. 6 presents an average increase of 18% in both load situations to the results of test #1, while the engine load increase is on average 10%.

On the other hand, vehicle No. 7 shows a significant decrease of 45% in the EF_{NOx} values in the unloaded situation, while the engine load value for the unloaded situation is unchanged.

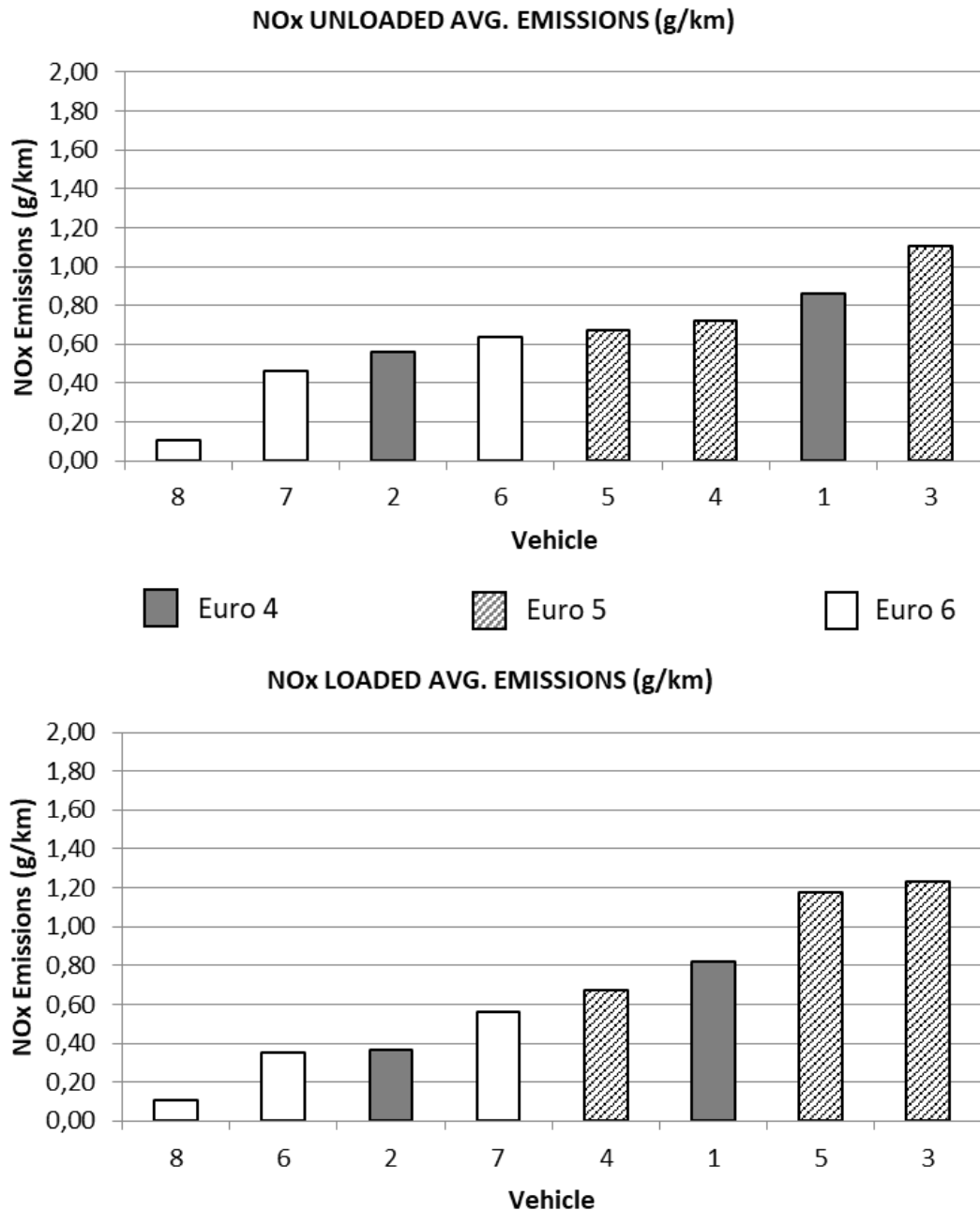


Figure 11-18. Vehicles ordered according to EF_{NOx} for unloaded (up) and loaded (down) test #3.

In contrast, the EF_{NOx} for the loaded situation is practically the same, while the engine load value for the loaded situation has undergone a 31% increase in value.

Once again, it can be seen that the operation of the EATS commanded by the ECU has great importance on the final emissions of the vehicle, without being able to establish a homogeneous criterion of operation based on the level of emissions.

Finally, vehicle No. 8 presents engine load values of the same order as in test #1, and the emission factors obtained present a decrease that, although not very large in absolute values (it is reduced from 0.18 g/km to 0.11 g/km for the loaded situation), represent a significant reduction of 26% for the unloaded situation and 42% for the loaded situation.

In a broad summary of the analysis of test #3, the emission factor trends and engine load values for all vehicles appear comparable to those observed in test #1, albeit with some variations in the values. Consequently, a similar scenario arises: all vehicles significantly surpass the NO_x emission factor limits outlined in their respective emission standards. Among these vehicles, vehicle No. 8 stands out with the least emissions, surpassing the emission limit by the smallest margin (roughly twice the limit).

To conclude the analysis of test #3, the vehicles are ordered according to the results obtained both in the unloaded and loaded situations, as can be seen in Figure 11-18.

For diesel Euro 5 and Euro 6 vehicles, the relative order between them in both situations is not maintained, since vehicles No. 4, No. 5, No. 6, and No. 7 interchange their positions between unloaded and loaded situations.

Additionally, it is evident that the vehicles do not exhibit consistent behavior between the unloaded and loaded scenarios in test #3 as well, as the ranking of vehicles changes in both situations. Only vehicles No. 8, No. 2, and No. 3 maintain the same relative positions in both situations when sorted according to the recorded emissions.

11.4.3. ASSESSMENT OF VEHICLE EMISSIONS IN TEST #4

The final three tests (test #4, #5, and #6) exhibit a resemblance to test #3, differing in the utilization of higher gear ratios to maintain a speed of 50 km/h (or potentially even higher speeds in the case of test #6). Consequently, the outcomes of tests #4, #5, and #6 will be juxtaposed with the results obtained from test #3 for comparative analysis.

Consequently, the operational circumstances under which the vehicles were tested, although possibly not ideal for urban traffic due to the utilization of relatively "long" gears, simulate scenarios that could realistically arise. These situations might be intentionally chosen by certain drivers for a variety of reasons, such as aiming to lower fuel consumption.

Specifically for test #4 (Figure 11-19), in general, the behavior of the "% engine load" shows a significant increase in the engine load values in both situations, with the only exception of vehicle No. 7 in the loaded situation.

Summarizing, the two Euro 4 vehicles show the following behavior:

- 1) Vehicle No. 1 shows a decrease in the emission factor in both situations of approximately 30%

- 2) Vehicle No. 2 shows a decrease in the unloaded situation of 17% and an increase of 22% for the loaded situation.

Euro 5 vehicles show a disparate performance among them:

- 1) Vehicle No. 3 has the same emission factors for both situations.
- 2) Vehicle No. 4 presents respectively an increase of 62.5% and 61.7% of the emission factor for the unloaded and loaded situations, the most significant variation of this test.
- 3) Vehicle No. 5 presents the same emission factor for the unloaded situation and a decrease of 16% for the loaded situation.

Euro 6 vehicles continue to maintain the heterogeneity seen in previous tests. Concerning the values of test #3:

- 1) Vehicle No. 6 decreases the EF_{NO_x} for the unloaded situation and increases it for the loaded situation.
- 2) Vehicle No. 7 increased the EF_{NO_x} in both situations, significantly for the unloaded situation, and more slightly for the unloaded one.
- 3) Vehicle No. 8 decreases emissions in both situations, remaining for the loaded situation so low that it is below the emission level limit.

So, the behavior of the emission factors and engine load values of all vehicles are in line with those obtained in test #3, although there are differences in the values. Of course, the same situation can be observed: all vehicles (except vehicle No. 8) exceed the NO_x factor emission limits defined in their corresponding emission levels in a very outstanding way. Vehicle No. 8 is the one with the lowest emissions of all vehicles, and the only one that does not exceed the emission limit set (for the loaded situation).

VEHICLE	EURO LEVEL	FACTOR EMISSION LIMIT (g/km)	UNLOADED			LOADED		
			AVG. ENGINE LOAD (%)	AVG. NO_x EMISSIONS (g/km)	*EURO LEVEL LIMIT MULT. FACTOR	AVG. ENGINE LOAD (%)	AVG. NO_x EMISSIONS (g/km)	*EURO LEVEL LIMIT MULT. FACTOR
1	4	0,25	53	0,57	2,3	47	0,59	2,4
2	4	0,25	47	0,46	1,8	53	0,44	1,8
3	5	0,18	38	1,12	6,2	48	1,23	6,8
4	5	0,18	48	1,17	6,5	49	1,10	6,1
5	5	0,18	30	0,66	3,6	37	0,98	5,5
6	6	0,08	62	0,35	4,3	66	0,64	8,0
7	6	0,08	53	0,85	10,7	57	0,63	7,8
8	6	0,06	52	0,07	1,2	56	0,03	0,5

* Multiplier factor for average NO_x emissions exceeding the Euro level limit.

Table 11-7. Summary of avg. results from Test #4

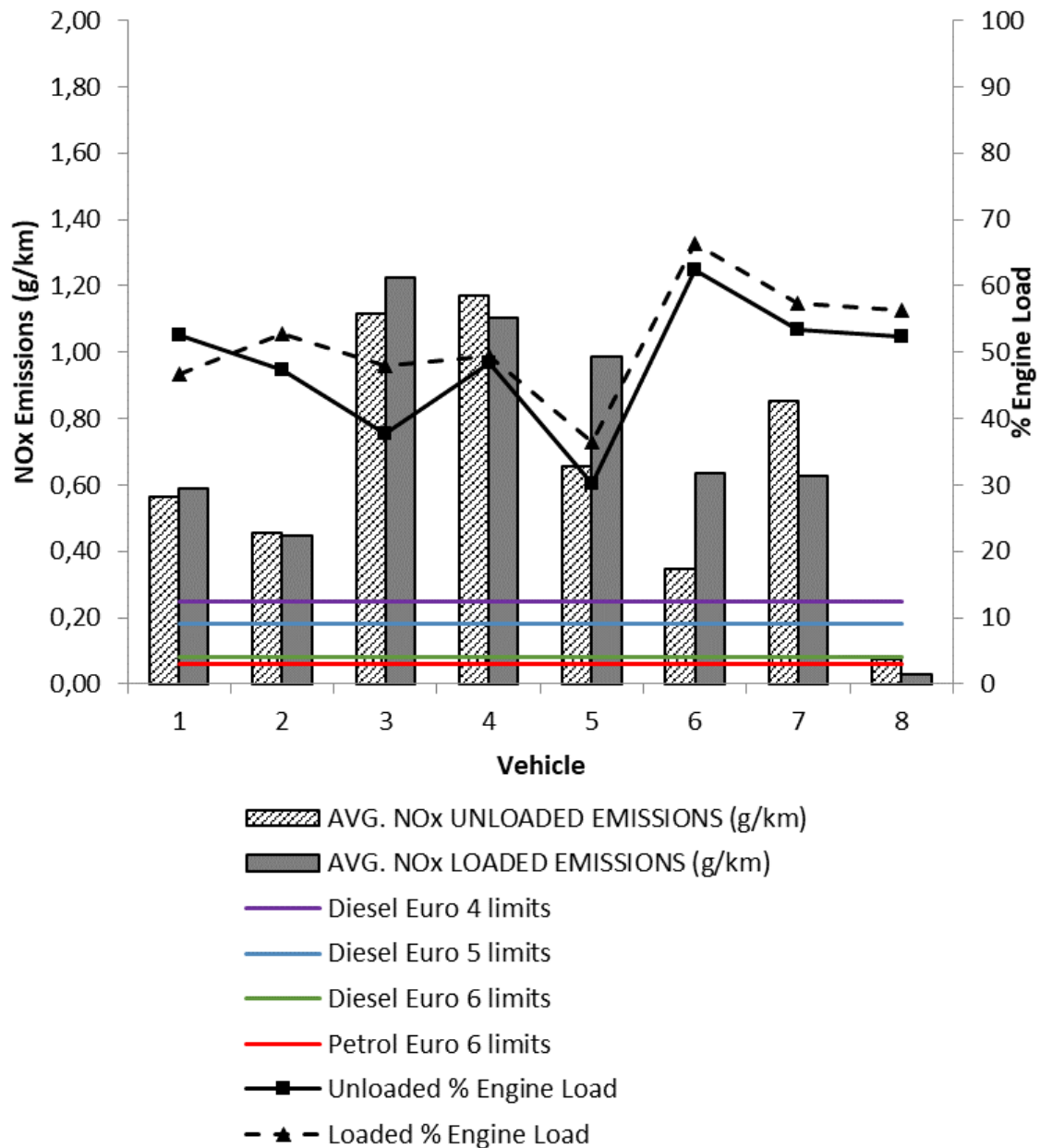


Figure 11-19. NO_x emissions and "% engine load" from the set of vehicles in test #4.

To conclude the analysis of test #4, the vehicles are ordered according to the results obtained both in unloaded and loaded situations, as can be seen in Figure 11-20.

It can also be seen that the behavior of the vehicles is not the same in the unloaded and loaded situations, since the order of the vehicles in both situations also changes. Vehicle No. 8 is the only one maintaining the same position in both situations when ordered according to the recorded emissions.

In the case of the Euro 5 and Euro 6 vehicles, the relative order between them in both situations is not even maintained, since vehicles No. 3 and No. 4, and vehicles No. 6 and No. 7, interchange their positions between unloaded and loaded situations.

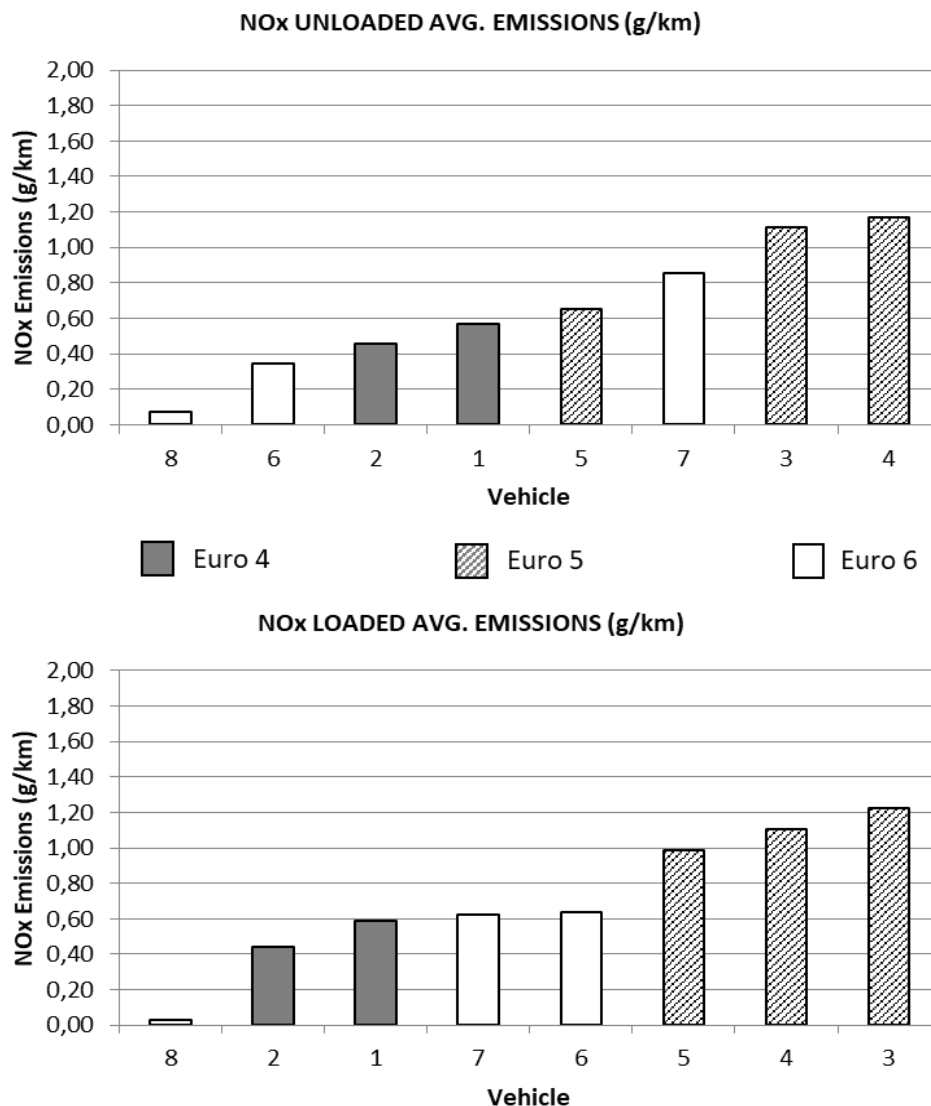


Figure 11-20. Vehicles ordered according to EF_{NO_x} for unloaded (up) and loaded (down) test #4.

11.4.4. ASSESSMENT OF VEHICLE EMISSIONS IN TEST #5 AND TEST #6

For test #5 (see Figure 11-21) and for test #6 (see Figure 11-23) the conditions are similar to those in test #4, but with even higher values observed. This applies to both the "% engine load" and EF_{NO_x} for diesel vehicles.

Throughout both tests, vehicle No. 8 exhibits values that closely resemble those of test #4, remaining either close to or below the limit value established by the Euro 6 emission standard (see Table 11-8).

When vehicles in Test #5 are ordered according to the results obtained both in unloaded and loaded situations, the situation is similar to previous tests, as can be seen in Figure 11-22.

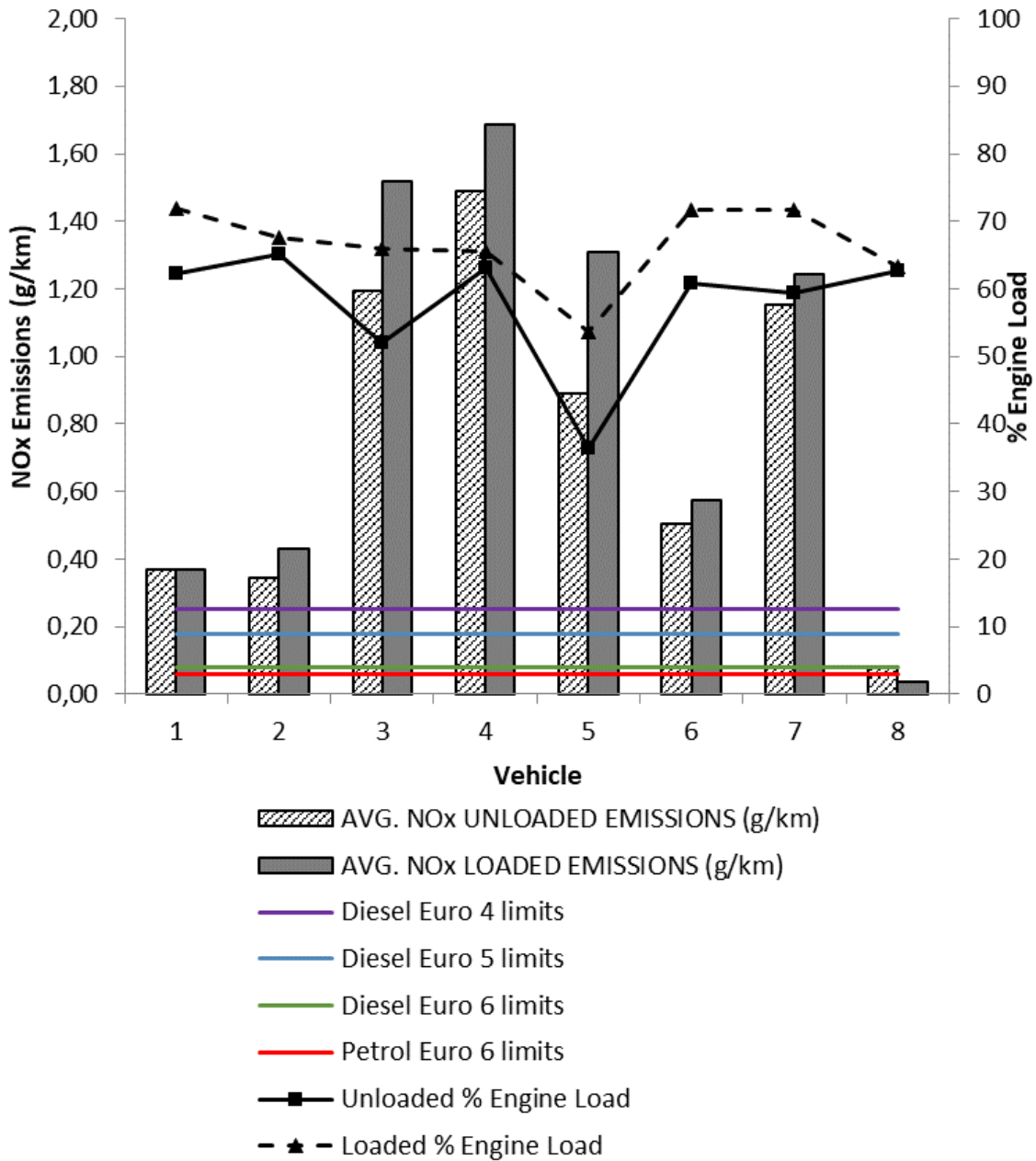


Figure 11-21. NO_x emissions and "% engine load" from the set of vehicles in test #5.

Consistently, it is evident that the vehicles do not exhibit consistent behavior between the unloaded and loaded scenarios in tests #5 and #6 as well, as the ranking of vehicles changes in both situations. Only vehicles No. 8, No. 6, No. 3, and No. 4 maintain the same positions in both situations when sorted according to the recorded emissions.

As in the previous cases, a summary of the results from Test #5 in comparison to the emission level limits can be found in Table 11-8. Similarly, the results from Test #6 are available in Table 11-9.

Finally, when the vehicles in Test #6 are ordered according to the results obtained both in unloaded and loaded situations, the same situation of previous tests can be observed, as is shown in Figure 11-24.

For diesel Euro 4, Euro 5, and Euro 6 vehicles, the order between them in both situations is not maintained, with several changes in the order of vehicles according to EF_{NOx} between unloaded and loaded situations.

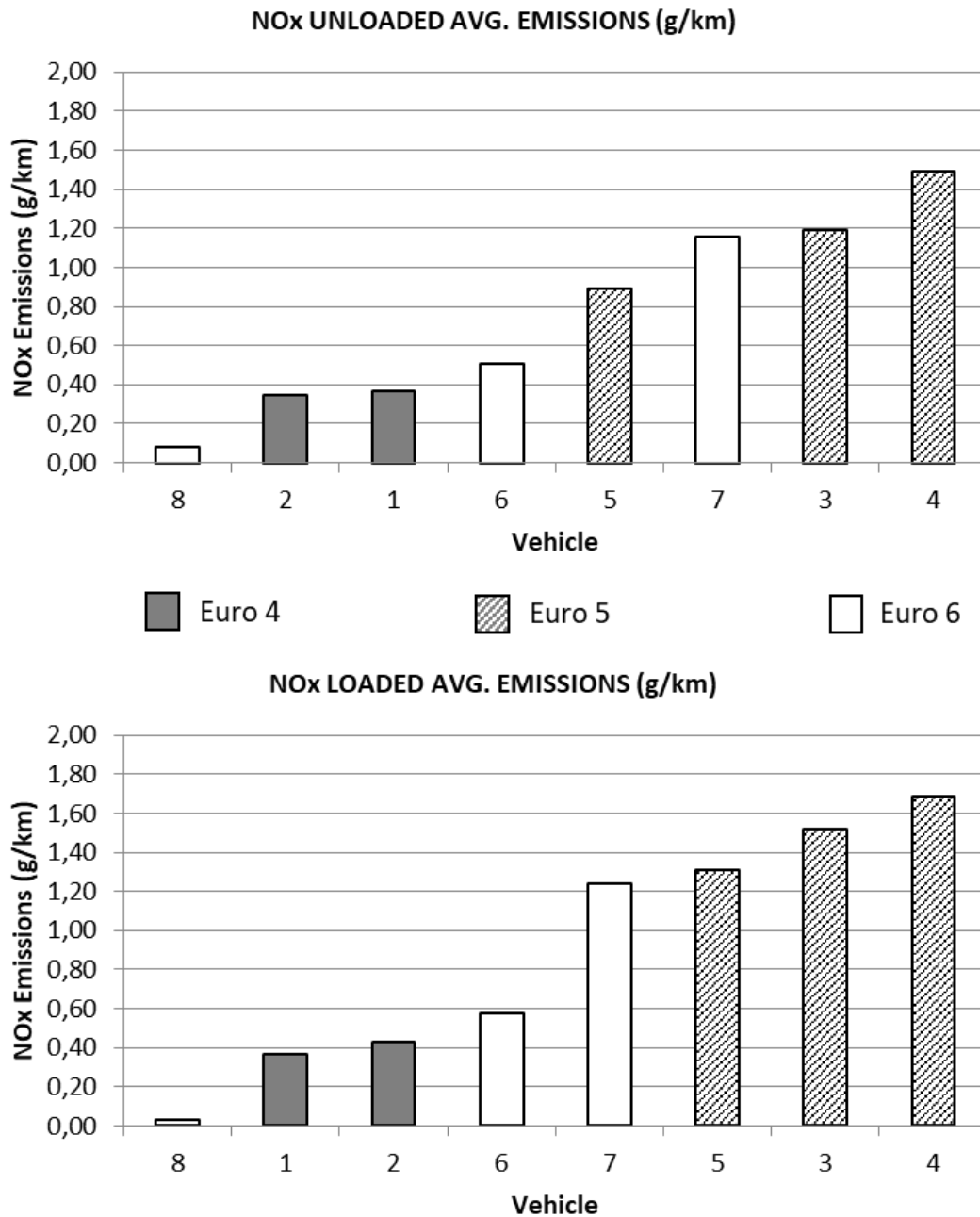


Figure 11-22. Vehicles ordered according to EF_{NOx} for unloaded (up) and loaded (down) test #5.

VEHICLE	EURO LEVEL	FACTOR EMISSION LIMIT (g/km)	UNLOADED			LOADED		
			AVG. ENGINE LOAD (%)	AVG. NO _x EMISSIONS (g/km)	*EURO LEVEL LIMIT MULT. FACTOR	AVG. ENGINE LOAD (%)	AVG. NO _x EMISSIONS (g/km)	*EURO LEVEL LIMIT MULT. FACTOR
1	4	0.25	62	0.37	1.5	72	0.37	1.5
2	4	0.25	65	0.34	1.4	68	0.43	1.7
3	5	0.18	52	1.19	6.6	66	1.52	8.4
4	5	0.18	63	1.49	8.3	66	1.69	9.4
5	5	0.18	36	0.89	5.0	54	1.31	7.3
6	6	0.08	61	0.50	6.3	72	0.57	7.2
7	6	0.08	59	1.15	14.4	72	1.24	15.5
8	6	0.06	63	0.08	1.4	63	0.03	0.6

* Multiplier factor for average NO_x emissions exceeding the Euro level limit.

Table 11-8. Summary of avg. results from Test #5.

VEHICLE	EURO LEVEL	FACTOR EMISSION LIMIT (g/km)	UNLOADED			LOADED		
			AVG. ENGINE LOAD (%)	AVG. NO _x EMISSIONS (g/km)	*EURO LEVEL LIMIT MULT. FACTOR	AVG. ENGINE LOAD (%)	AVG. NO _x EMISSIONS (g/km)	*EURO LEVEL LIMIT MULT. FACTOR
1	4	0.25	77	0.37	1.5	75	0.52	2.1
2	4	0.25	73	0.43	1.7	74	0.63	2.5
3	5	0.18	68	1.50	8.4	68	1.57	8.7
4	5	0.18	66	1.71	9.5	72	1.70	9.4
5	5	0.18	41	1.15	6.4	58	1.51	8.4
6	6	0.08	73	0.29	3.7	77	0.58	7.3
7	6	0.08	68	1.29	16.2	66	1.61	20.1
8	6	0.06	63	0.06	0.9	74	0.03	0.5

* Multiplier factor for average NO_x emissions exceeding the Euro level limit.

Table 11-9. Summary of avg. results from Test #6.

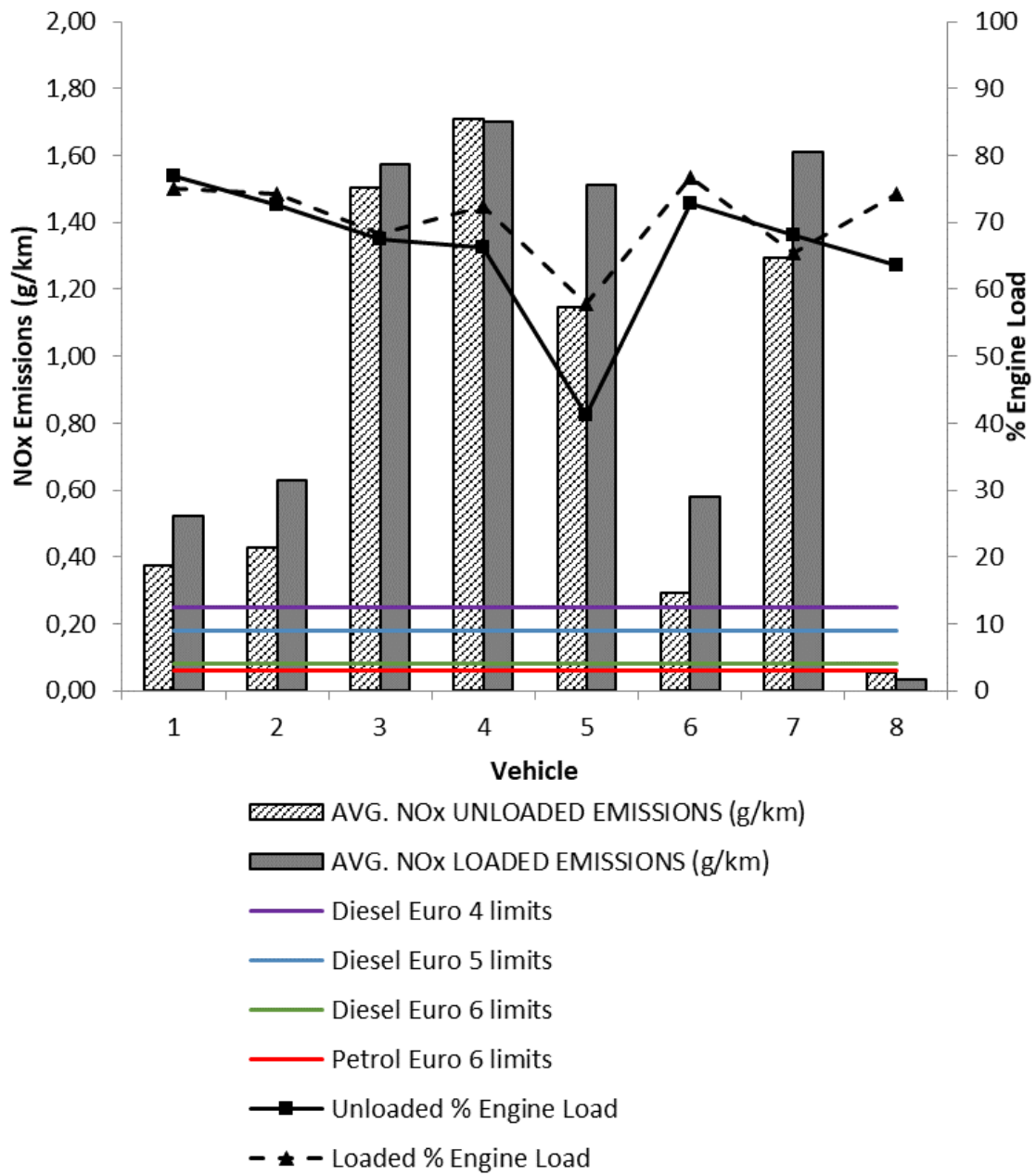


Figure 11-23. NO_x emissions and "% engine load" from the set of vehicles in test #6.

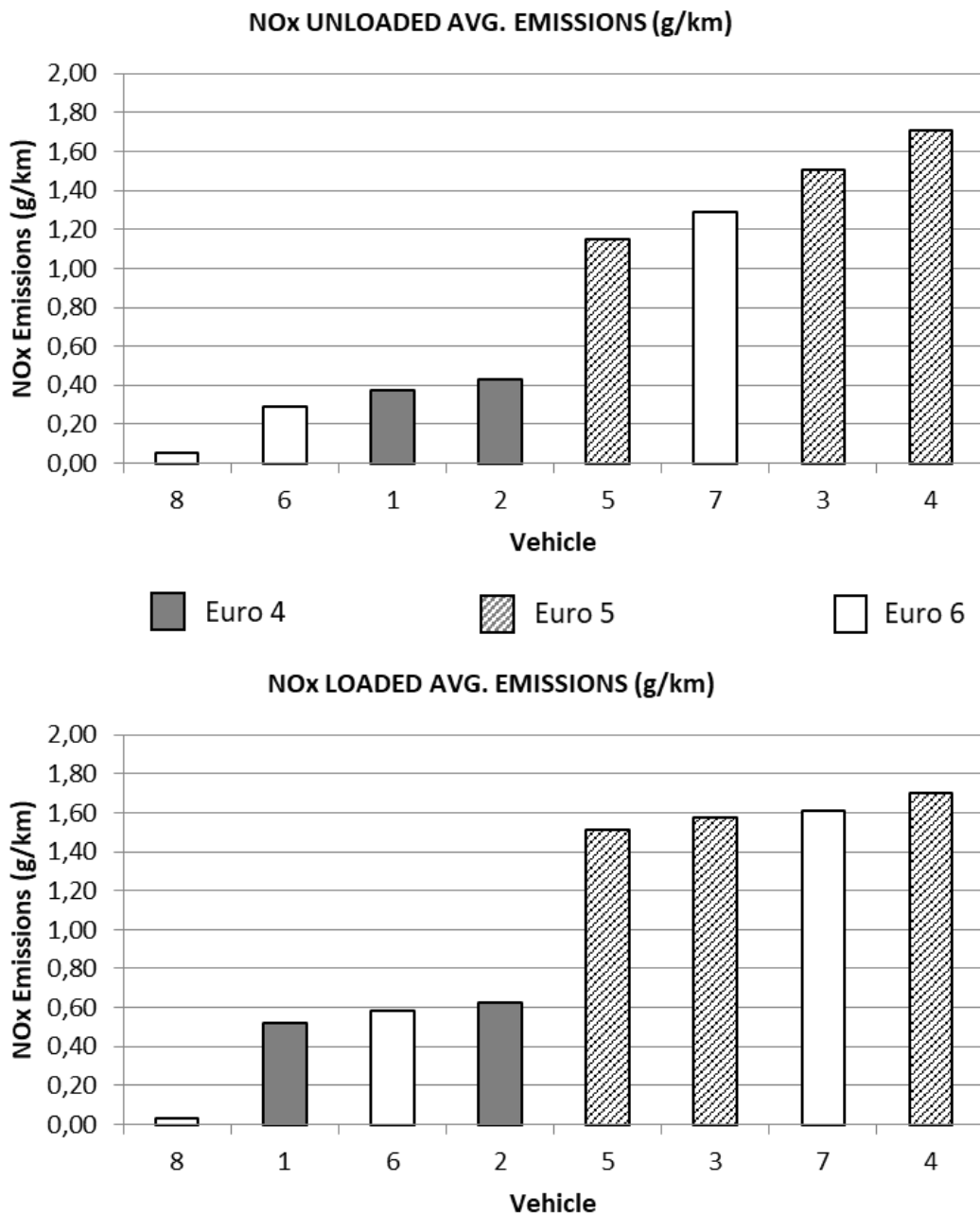


Figure 11-24. Vehicles ordered according to EF_{NO_x} for unloaded (up) and loaded (down) test #6.

11.5. COMPARISON OF ON-ROAD EMISSIONS AND PTI RESULTS

To facilitate a clear presentation of the results obtained from on-road measurements in Chapter 7 (Section 7.4.1), only the results for Vehicle No. 1 have been elaborated upon therein.

Subsequently, the results obtained from the tests conducted on Vehicles No. 2, No. 3, No. 4, No. 5, No. 6, No. 7, and No. 8 are compiled and delineated below.

11.5.1. COMPARISON OF RESULTS FROM VEHICLE No. 2

Data measured in the tests on the vehicle are collected, and the values obtained from the different measurements are used to build Table 11-10.

Similar to the preceding vehicle, this table presents the mean, maximum, and minimum NO_x concentration values recorded in each test, alongside the corresponding "% engine load" values, engine speed, and NO_x emissions mass flow.

Test	#	Loaded						Unloaded					
		1	2	3	4	5	6	1	2	3	4	5	6
Duration of measure	[s]	183	279	157	187	175	162	198	269	186	171	188	166
Avg. Concentration	[ppm]	112	77	72	91	112	154	121	99	92	110	96	109
Max. Concentration	[ppm]	390	363	290	310	367	499	569	380	418	399	367	427
Min. Concentration	[ppm]	20	1	7	10	17	42	10	11	7	8	11	22
Avg. engine load	[%]	29	32	30	53	68	74	26	28	27	47	65	73
Max. engine load	[%]	83.9	85.9	84.3	100	100	100	98.4	72.9	83.5	99.2	100	100
Min. engine load	[%]	0	0	0	0	0	0	0	0	0	0	0	0
Avg. Speed	[km/h]	43.7	34.7	42.6	44.2	46.2	48.5	40.0	35.1	42.9	44.1	43.1	47.4
Avg. Engine Speed	[rpm]	2376	1606	1875	1403	1166	1270	2182	1604	1890	1399	1069	1233
Max. Engine Speed	[rpm]	3307	2947	2323	3102	3181	4439	3252	2790	2804	2910	3561	3393
Min. Engine Speed	[rpm]	815	679	837	840	758	791	709	718	793	818	748	766
Avg. NO _x Mass Flow	[g/s]	0.007	0.004	0.004	0.004	0.004	0.006	0.007	0.005	0.005	0.004	0.003	0.004
Max. NO _x Mass Flow	[g/s]	0.022	0.020	0.016	0.025	0.031	0.044	0.035	0.021	0.030	0.025	0.029	0.029
Min. NO _x Mass Flow	[g/s]	0.001	0.000	0.000	0.000	0.000	0.001	0.001	0.000	0.000	0.000	0.000	0.000
Total emissions NO _x	[g]	1.291	1.124	0.583	0.712	0.689	1.006	1.388	1.273	0.893	0.730	0.549	0.683
Distance	[m]	1600	1600	1600	1600	1600	1600	1600	1600	1600	1600	1600	1600
Emission Factor EF _{NOx}	[g/km]	0.81	0.70	0.36	0.44	0.43	0.63	0.87	0.80	0.56	0.46	0.34	0.43

Table 11-10. Summary of vehicle No. 2 results from on-road tests.

For both the maximum and average NO_x emission values, the highest and lowest values in each category have been highlighted in bold and shaded in gray. These marked values will serve as the basis for establishing the range of maximum emissions and the range of average emissions.

To ascertain the range of maximum emissions, the values within the "Max. NO_x Mass Flow" row should be referred to. Similarly, for establishing the range of average emissions, the values within the "Avg. NO_x Mass Flow" rows should be considered.

From the values recorded in the measurements, the following two ranges are therefore defined:

- Maximum emission range for vehicle No. 2: between 0.016 g/s and 0.044 g/s
- Average emissions range for vehicle No. 2: between 0.003 g/s and 0.007 g/s

Once both ranges have been defined, the values obtained in various tests with the PTI measurement method on the vehicle (Table 11-11) is used to compare the behavior of the values from the static test with the emission values from the on-road measurements.

Figure 11-25 shows that the values measured during the loaded PTI test are close to, and even almost within the range of the average emissions of the vehicle.

This situation is very similar to that shown in the case of vehicle No. 1. In this case, the values resulting from the PTI measurement are on average 44% lower than the average emission range entry threshold.

#	UNLOADED			LOADED			TMV	
	NO _x [mg/s]	NO _x [ppm]	% engine load	NO _x [mg/s]	NO _x [ppm]	% engine load	NO _x [mg/s]	% engine load
1	1.01	48.50	20	1.73	78.05	36	6.15	100
2	0.93	44.45	20	1.63	73.55	35	5.72	100
3	0.78	37.55	20	1.31	59.30	36	5.45	100
4	1.64	77.85	22	4.65	208.75	38	15.29	100
5	0.98	46.60	21	2.18	98.00	38	6.30	100
6	0.93	44.50	21	2.05	92.15	38	6.36	100
7	0.76	36.10	21	1.68	75.85	37	5.16	100
8	0.73	34.85	21	1.56	70.20	37	4.68	100
9	0.63	30.00	20	1.26	56.90	36	4.56	100
10	0.70	33.70	20	1.42	63.95	35	5.89	100
11	1.23	59.10	20	1.91	87.20	38	6.03	100
12	1.05	50.50	20	1.82	82.85	37	5.74	100
13	0.72	34.45	20	1.46	66.50	37	4.99	100
14	0.73	35.10	19	1.39	63.00	37	4.27	100
15	0.60	28.80	19	1.22	55.30	36	4.14	100

Table 11-11. Summary of Static NO_x test on Vehicle No. 2.

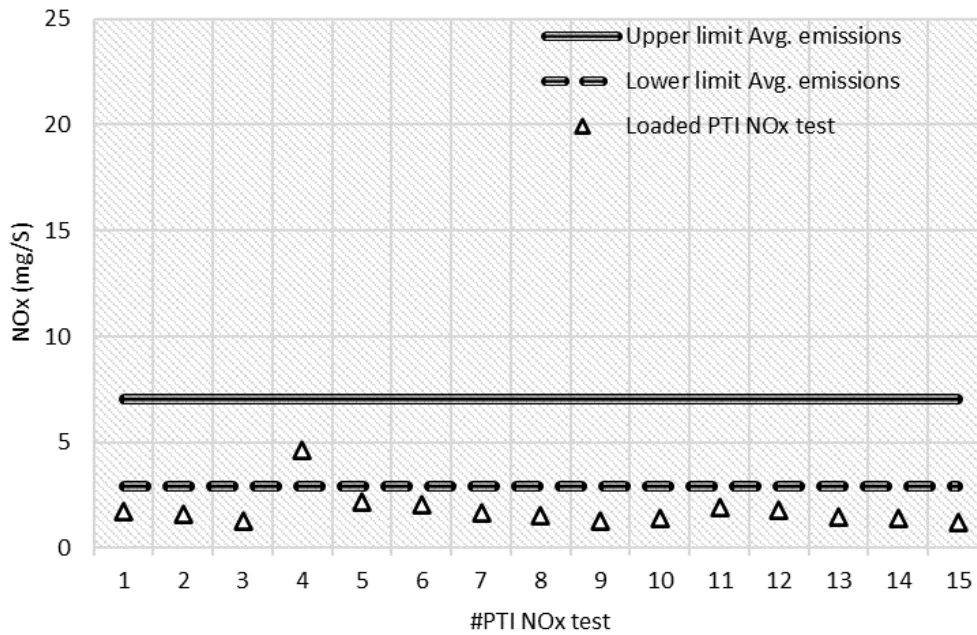


Figure 11-25. Range of Avg. On-road emissions and Loaded PTI test result for Vehicle No. 2.

If the TMV values are used for comparison with the average vehicle emissions range, we find the situation shown in Figure 11-26.

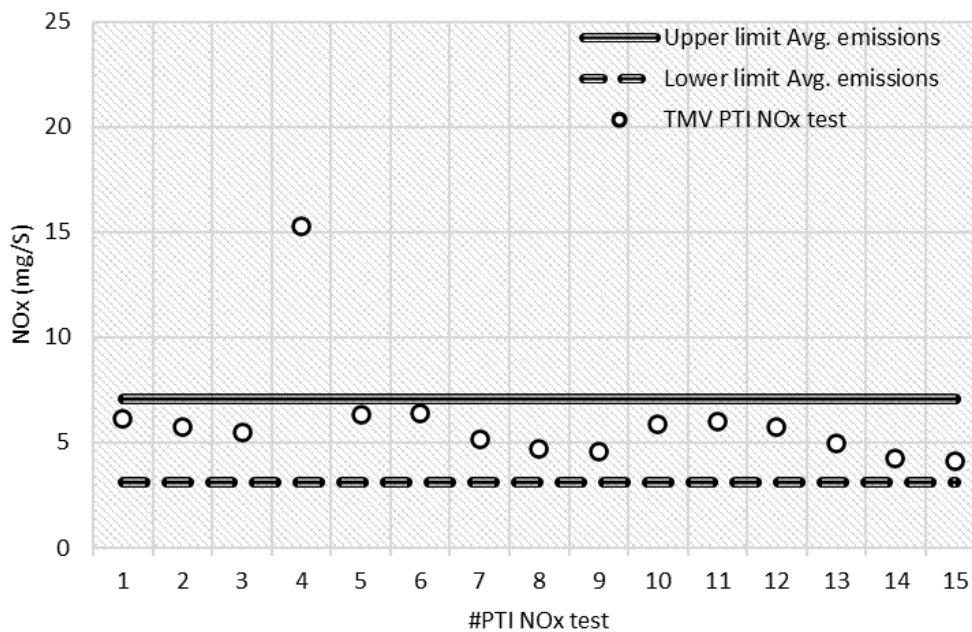


Figure 11-26. Range of Avg. On-road emissions and TMV PTI test results for Vehicle No. 2.

In the case of this particular vehicle, the values derived from the static measurement align well with the average emission range of the vehicle. Consequently, for this scenario, the outcome of the static test during the PTI serves as an indicative value for estimating the emissions the vehicle will produce in urban traffic conditions.

In contrast, the same comparison for vehicle No. 1 in Figure 7-25 (which is the same vehicle but with the EGR deactivated) indicated that the TMV values of that vehicle were well above the average emission range. Apparently, this would be caused by the absence of EGR operation.

Lastly, when juxtaposing the TMV values with the vehicle's range of maximum emissions, it is evident that in every instance, the values obtained from the static PTI test do not surpass the upper limit of this emissions range.

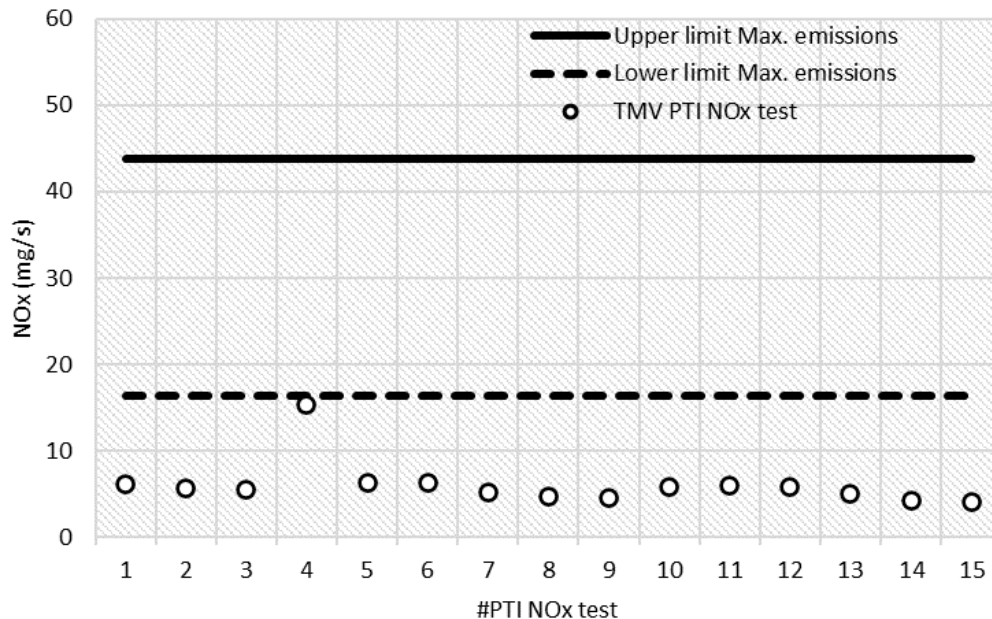


Figure 11-27. Range of Max. On-road emissions and TMV PTI test results for Vehicle No. 2.

This situation resembles what was observed for vehicle No. 1, which displayed a comparable range of maximum emissions and a similar trend in TMV values (although higher in that case). In both instances, the TMV values consistently remain below the upper limit of the range. This assurance underscores that the value measured during the PTI never surpasses the actual emissions of the vehicle, thereby averting any misrepresentation that could lead to a possible inspection rejection based on that value.

11.5.2. COMPARISON OF RESULTS FROM VEHICLE No. 3

Employing the identical methodology as in prior cases, the data acquired from the tests conducted on the vehicle is aggregated, resulting in the construction of Table 11-12.

In this table, the values defining the ranges of maximum emissions and average emissions of the vehicle have been marked in bold and shaded in gray, with values included in the Max. NO_x Mass Flow row and Avg. NO_x Mass Flow row respectively.

Test	#	Loaded						Unloaded					
		1	2	3	4	5	6	1	2	3	4	5	6
Duration of measure	[s]	172	297	158	184	189	197	189	252	161	162	174	162
Avg. Concentration	[ppm]	229	315	289	344	543	510	208	254	257	338	436	552
Max. Concentration	[ppm]	726	781	931	868	949	931	926	730	713	936	845	952
Min. Concentration	[ppm]	39	73	39	45	84	104	22	38	23	48	70	107
Avg. engine load	[%]	28	40	37	48	66	68	24	27	30	38	52	68
Max. engine load	[%]	88.2	99.6	99.2	100	99.6	100	85.5	98.4	95.7	100	100	100
Min. engine load	[%]	0	0	0	0	0	0	0	0	0	0	0	0
Avg. Speed	[km/h]	45.0	39.1	48.4	45.9	43.7	47.6	43.5	37.0	47.7	47.8	46.0	48.5
Avg. Engine Speed	[rpm]	2387	1410	2125	1465	1172	1208	2238	1601	2089	1573	1225	1315
Max. Engine Speed	[rpm]	3143	2612	2682	2532	2374	2716	3208	2543	2670	2439	2355	2458
Min. Engine Speed	[rpm]	845	825	847	816	830	827	778	770	798	800	780	786
Avg. NO _x Mass Flow	[g/s]	0.011	0.010	0.012	0.011	0.013	0.013	0.009	0.009	0.011	0.011	0.011	0.015
Max. NO _x Mass Flow	[g/s]	0.035	0.034	0.045	0.037	0.033	0.031	0.047	0.030	0.032	0.036	0.028	0.034
Min. NO _x Mass Flow	[g/s]	0.001	0.001	0.001	0.001	0.002	0.002	0.001	0.001	0.000	0.001	0.002	0.003
Total emissions NO _x	[g]	1.792	2.944	1.971	1.962	2.427	2.516	1.784	2.269	1.769	1.786	1.909	2.407
Distance	[m]	1600	1600	1600	1600	1600	1600	1600	1600	1600	1600	1600	1600
Emission Factor EF _{NO_x}	[g/km]	1.12	1.84	1.23	1.23	1.52	1.57	1.12	1.42	1.11	1.12	1.19	1.50

Table 11-12. Summary of vehicle No. 3 results from on-road tests.

#	UNLOADED			LOADED			TMV	
	NO _x [mg/s]	NO _x [ppm]	% engine load	NO _x [mg/s]	NO _x [ppm]	% engine load	NO _x [mg/s]	% engine load
1	2.16	137.14	21	5.77	344.00	45	17.86	100
2	2.31	147.45	19	6.81	407.54	45	14.98	100
3	2.18	128.20	25	4.94	292.58	45	22.37	100
4	2.04	128.43	22	5.08	301.45	44	14.12	100
5	2.12	133.72	21	5.19	308.83	44	13.91	100
6	2.13	134.89	21	5.74	342.56	45	13.63	100
7	1.59	92.60	24	2.03	118.31	39	10.24	100
8	1.57	98.97	21	2.76	163.07	37	9.89	100
9	1.57	98.86	21	2.84	168.34	38	10.65	100
10	1.48	93.99	21	2.75	164.01	39	8.63	100

Table 11-13. Summary of Static NO_x test on Vehicle No. 3

From the values included in the table, the following ranges are defined:

- Maximum emissions range for vehicle No. 3: between 0.028 and 0.047 g/s
- Average emissions range for vehicle No. 3: between 0.009 and 0.015 g/s

Subsequently, by utilizing the values extracted from the different static tests executed during the method definition (Table 11-13), a comparison is established between the outcomes of these tests and the authentic emissions generated by the vehicle in real-world operation.

To facilitate this comparison, Figure 11-28 is generated. This graph plots the vehicle's average emission range alongside the emission values recorded in the loaded state of the PTI test.

As observed in earlier instances, the emission values recorded during the PTI test are below the average emission range of the vehicle during urban traffic. Certain measurements are in close proximity to the minimum value of the range, while others exhibit more substantial disparities. On average, the values measured in the static load test for this vehicle are approximately 50% of the minimum value within the average emission range.

Subsequently, the TMV values are contrasted with the vehicle's average emission range. As depicted in Figure 11-29, a majority of the TMV values fall within the range of average measurements. Therefore, in this vehicle's case, the outcome of the static measurement conducted during the PTI test furnishes a value (TMV) that offers precise information about the NO_x emissions exhibited by the vehicle during urban traffic.

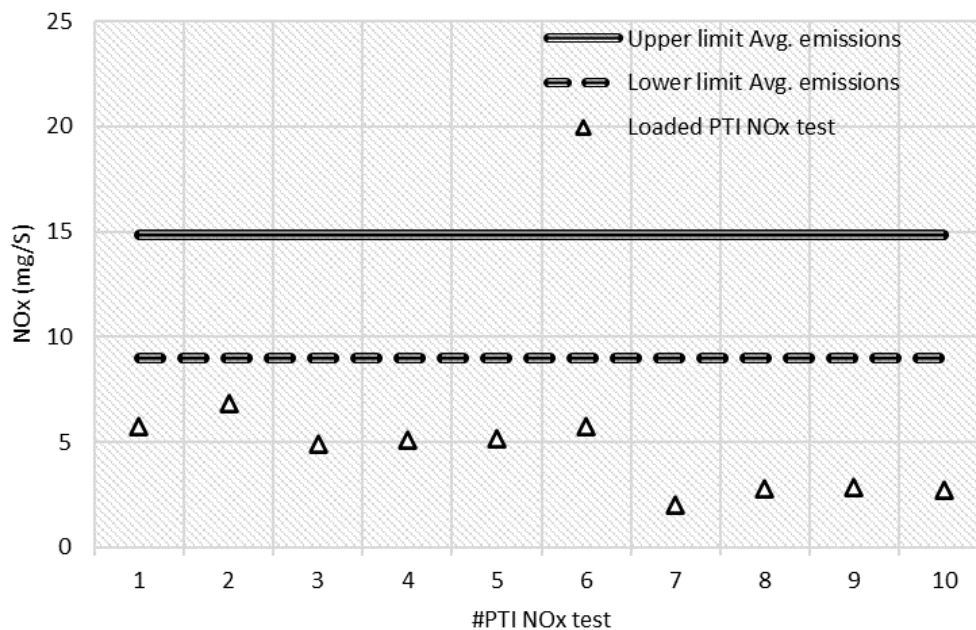


Figure 11-28. Range of Avg. On-road emissions and Loaded PTI test result for Vehicle No. 3.

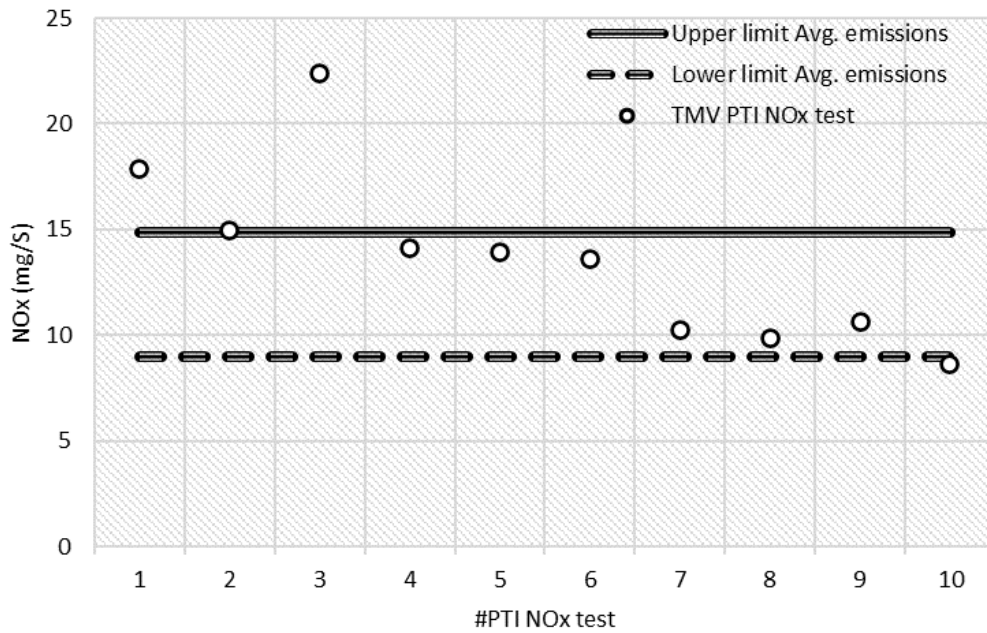


Figure 11-29. Range of Avg. On-road emissions and TMV PTI test results for Vehicle No. 3.

Lastly, upon juxtaposing the TMV values with the vehicle's range of maximum emissions, it is evident that the values derived from the static PTI test do not surpass the upper limit of this emissions range as well.

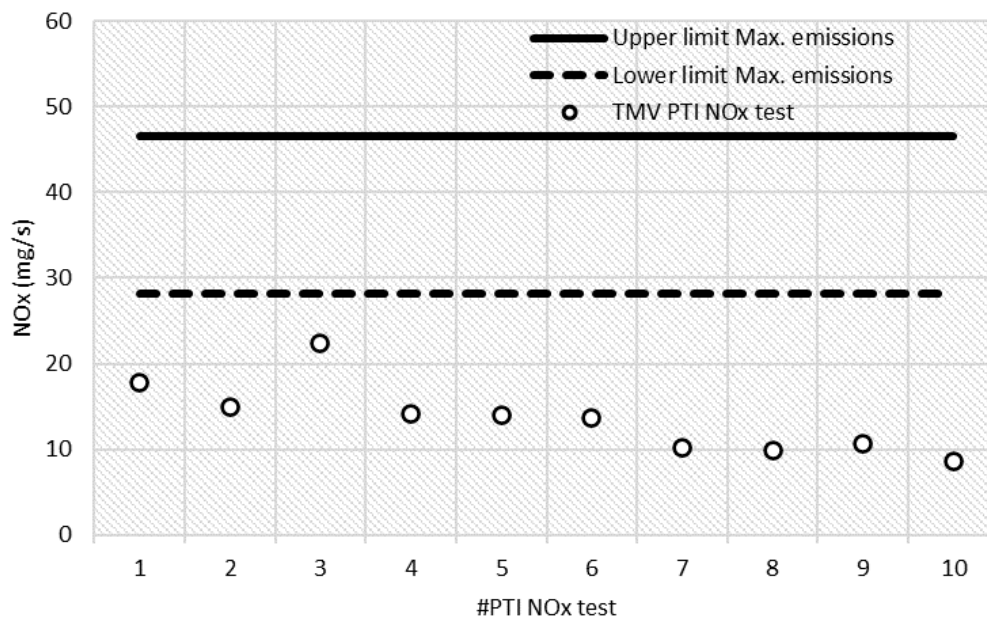


Figure 11-30. Range of Max. On-road emissions and TMV PTI test results for Vehicle No. 3.

It is noticeable that the TMV values, predominantly falling within the average emissions range, consistently remain below the maximum value of the maximum emissions range. This assurance underscores the feasibility of utilizing this measure for inspection purposes.

11.5.3. COMPARISON OF RESULTS FROM VEHICLE No. 4

From the values included in the Table 11-14, the following ranges are defined:

- Maximum emissions range for vehicle No. 4: between 0.021 and 0.049 g/s
- Average emission range for vehicle No. 4: between 0.005 and 0.016 g/s

Subsequently, utilizing the values extracted from the diverse static tests conducted during the method's formulation (Table 11-15), the outcomes of these tests are juxtaposed against the actual emissions generated by the vehicle in operational scenarios.

As a result, Figure 11-31 is formulated. This graph presents the emission values acquired from the static measurements of the PTI test over the average emission range of vehicle No. 4.

Test	#	Loaded						Unloaded					
		1	2	3	4	5	6	1	2	3	4	5	6
Duration of measure	[s]	195	276	172	186	187	174	192	256	183	185	176	167
Avg. Concentration	[ppm]	102	164	136	284	562	604	134	165	144	306	514	589
Max. Concentration	[ppm]	426	669	816	1273	1280	1349	760	505	883	1272	1248	1382
Min. Concentration	[ppm]	13	32	16	23	37	99	8	20	6	35	59	79
Avg. engine load	[%]	34	39	39	49	66	72	34	34	37	48	63	66
Max. engine load	[%]	94.5	89.4	94.5	99.6	100	100	96.5	85.9	94.9	99.6	100	100
Min. engine load	[%]	0	0	0	0	0	0	0	0	0	0	0	0
Avg. Speed	[km/h]	40.4	36.2	44.1	43.1	42.1	43.8	40.1	35.7	42.1	42.5	43.7	45.6
Avg. Engine Speed	[rpm]	2049	1454	1782	1251	1002	1037	2051	1515	1699	1254	1055	1107
Max. Engine Speed	[rpm]	2926	2566	2167	2475	2102	2352	2888	2634	2220	2430	2400	2653
Min. Engine Speed	[rpm]	752	747	778	762	762	746	778	778	778	778	780	734
Avg. NO _x Mass Flow	[g/s]	0.005	0.007	0.006	0.009	0.014	0.016	0.007	0.007	0.006	0.010	0.014	0.016
Max. NO _x Mass Flow	[g/s]	0.021	0.030	0.037	0.045	0.037	0.045	0.028	0.024	0.037	0.044	0.034	0.049
Min. NO _x Mass Flow	[g/s]	0.001	0.001	0.001	0.001	0.001	0.002	0.000	0.001	0.000	0.001	0.001	0.001
Total emissions NO _x	[g]	1.004	1.874	1.081	1.767	2.697	2.719	1.252	1.768	1.148	1.870	2.386	2.734
Distance	[m]	1600	1600	1600	1600	1600	1600	1600	1600	1600	1600	1600	1600
Emission Factor EF _{NO_x}	[g/km]	0.63	1.17	0.68	1.10	1.69	1.70	0.78	1.11	0.72	1.17	1.49	1.71

Table 11-14. Summary of vehicle No. 4 results from the on-road test.

#	UNLOADED			LOADED			TMV	
	NO _x [mg/s]	NO _x [ppm]	% engine load	NO _x [mg/s]	NO _x [ppm]	% engine load	NO _x [mg/s]	% engine load
1	2.69	134.76	15	3.48	173.99	36	26.55	100
2	2.74	137.70	14	3.87	194.36	37	24.63	100
3	2.78	144.23	15	4.22	212.97	39	14.80	100
4	2.84	142.95	14	4.04	203.62	38	15.46	100
5	2.78	140.30	14	4.27	216.27	39	13.93	100
6	1.37	63.46	21	1.44	67.09	35	10.01	100
7	1.55	74.06	19	1.67	79.88	37	11.28	100
8	1.69	81.82	17	1.73	84.23	34	12.75	100
9	1.74	85.21	16	1.75	85.71	33	12.93	100
10	1.79	87.08	16	1.91	93.40	37	12.35	100
11	1.84	89.86	15	1.90	93.37	34	14.34	100
12	1.81	88.90	15	1.90	93.55	35	14.06	100
13	1.77	86.49	15	1.92	93.79	35	13.44	100
14	1.81	88.36	15	1.92	94.46	37	13.12	100
15	1.84	89.88	15	2.02	99.68	37	13.00	100

Table 11-15. Summary of Static NO_x test on Vehicle No. 4.

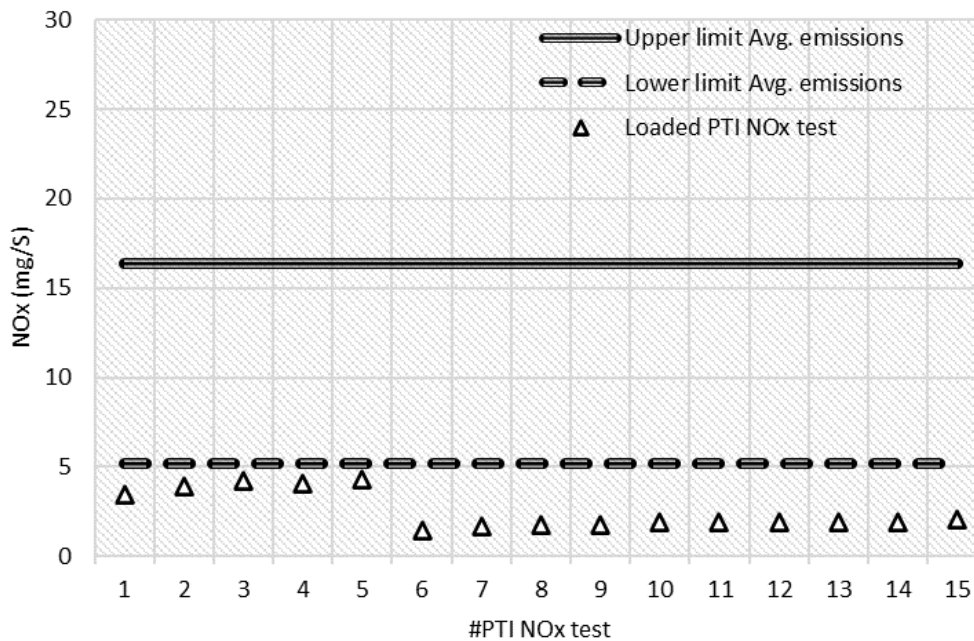


Figure 11-31. Range of Avg. On-road emissions and Loaded PTI test result for Vehicle No. 4.

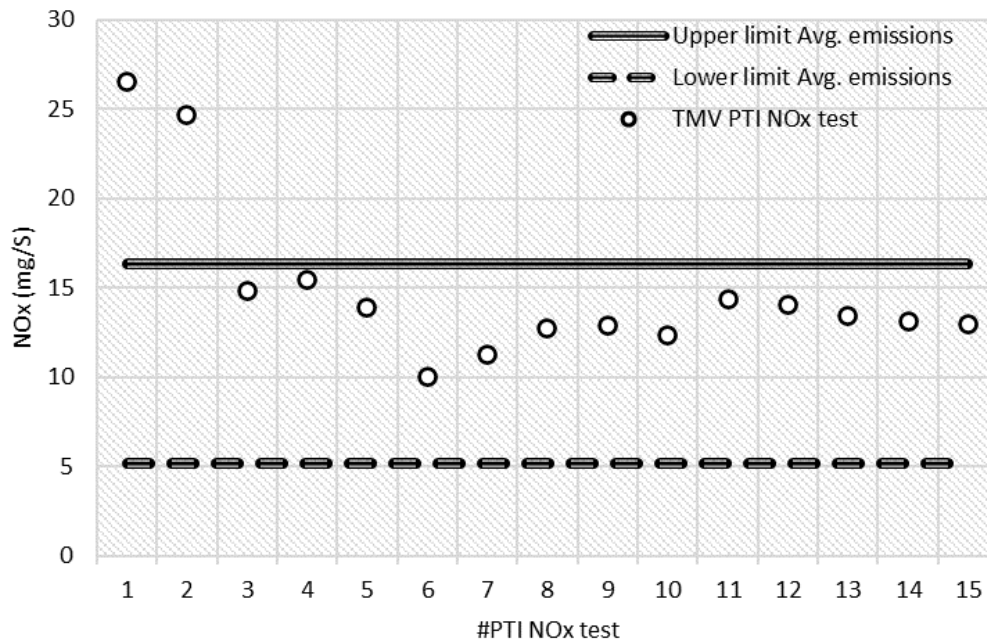


Figure 11-32. Range of Avg. On-road emissions and TMV PTI test results for Vehicle No. 4.

Similar to prior instances, these emission values remain below the range of average vehicle emissions in actual urban traffic conditions. Some values closely align, while others display more pronounced deviations. On average, the values derived from the static load test for this particular vehicle equate to approximately 50% of the minimum value within the average emission range.

The next step is the comparison of the TMV values with the average emission range of the vehicle. In Figure 11-32, a recurring trend is observed wherein a significant portion of the TMV values aligns within the range of average measurements. Consequently, for this particular vehicle, the outcome of the static measurement conducted during the PTI test yields a value (TMV) that offers accurate insights into the vehicle's NO_x emissions during urban traffic.

Conclusively, the TMV values are juxtaposed against the vehicle's maximum emission range to ascertain whether the values garnered from the static PTI test surpass the upper limit of said range.

Figure 11-33 illustrates that the TMV values within the average emissions range remain beneath the minimum threshold of the maximum emissions range. Two measurements that exceeded the average range are still within the scope of the maximum emissions range. In all instances, the upper limit of the maximum emissions is never exceeded, thereby guaranteeing the effectiveness of the measurement for inspection purposes.

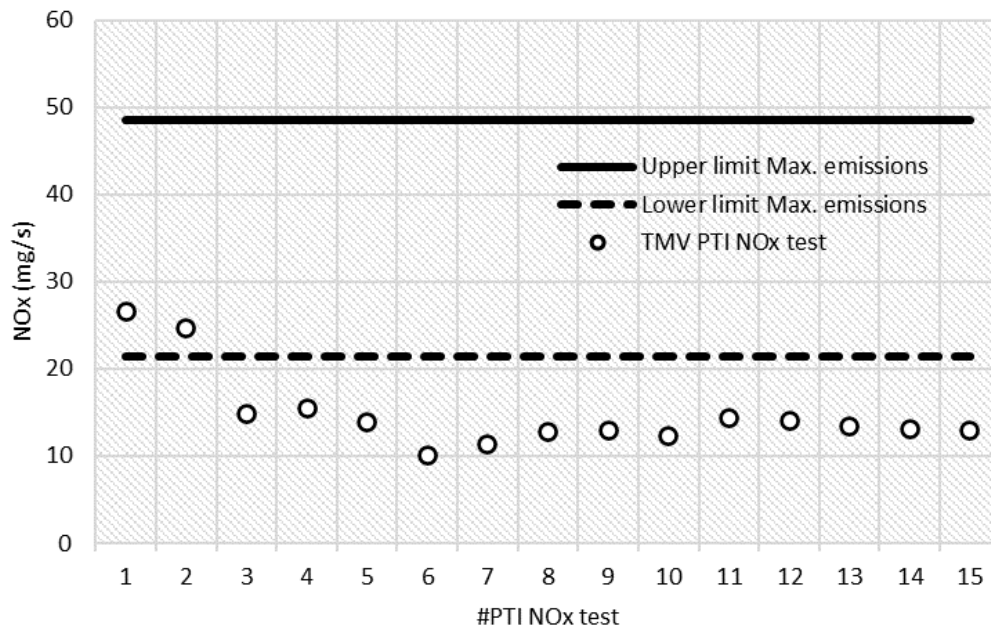


Figure 11-33. Range of Max. On-road emissions and TMV PTI test results for Vehicle No. 4.

11.5.4. COMPARISON OF RESULTS FROM VEHICLE No. 5

Following the pattern established in previous instances, the initial step for comparing the outcomes of vehicle No. 5 involves the compilation of all measured data from the diverse tests conducted on the circuit. Through the analysis and manipulation of this accumulated data, Table 11-16 is built.

From the values included in the table, the following ranges are defined:

- Maximum emissions range for vehicle No. 5: between 0.022 and 0.042 g/s
- Average emissions range for vehicle No. 5: between 0.005 and 0.012 g/s

Subsequently, by utilizing the values derived from the different static tests executed during the method's formulation (Table 11-17), a comparison is established between the outcomes of these tests and the actual emissions encountered during the vehicle's operational use.

Using these values, Figure 11-34 is generated. This visual representation illustrates the average emission range of Vehicle No. 5 juxtaposed with the values acquired during the loaded state while executing the NO_x measurement PTI test.

Test	#	Loaded						Unloaded					
		1	2	3	4	5	6	1	2	3	4	5	6
Duration of measure	[s]	266	360	195	195	207	196	192	315	186	194	212	216
Avg. Concentration	[ppm]	248	299	259	276	470	555	133	191	147	176	317	414
Max. Concentration	[ppm]	774	782	744	843	1159	1148	560	995	608	640	1293	1348
Min. Concentration	[ppm]	58	27	29	39	80	109	8	17	13	17	42	53
Avg. engine load	[%]	28	36	28	37	54	58	22	27	22	30	36	41
Max. engine load	[%]	90.6	100	100	95.3	97.6	100	100	100	80.8	100	92.5	100
Min. engine load	[%]	0	0	0	0	0	0	0	0	0	0	0	0
Avg. Speed	[km/h]	42.8	35.6	43.3	43.3	41.2	42.5	43.3	38.0	44.1	43.9	40.4	40.8
Avg. Engine Speed	[rpm]	1757	1308	1708	1310	1022	1058	2191	1363	1757	1334	1007	989
Max. Engine Speed	[rpm]	2959	2213	2066	2076	2172	2258	3052	2258	2134	2272	2088	1936
Min. Engine Speed	[rpm]	816	779	815	800	688	676	798	778	818	772	637	657
Avg. NO _x Mass Flow	[g/s]	0.009	0.009	0.010	0.008	0.010	0.012	0.006	0.007	0.006	0.005	0.007	0.008
Max. NO _x Mass Flow	[g/s]	0.029	0.030	0.029	0.027	0.027	0.030	0.028	0.042	0.024	0.022	0.034	0.027
Min. NO _x Mass Flow	[g/s]	0.001	0.000	0.001	0.001	0.002	0.002	0.000	0.000	0.000	0.000	0.001	0.001
Total emissions NO _x	[g]	1.934	3.145	1.878	1.576	2.093	2.416	1.245	2.070	1.072	1.049	1.428	1.834
Distance	[m]	1600	1600	1600	1600	1600	1600	1600	1600	1600	1600	1600	1600
Emission Factor EF _{NO_x}	[g/km]	1.21	1.97	1.17	0.98	1.31	1.51	0.78	1.29	0.67	0.66	0.89	1.15

Table 11-16. Summary of vehicle No. 5 results from the on-road test.

#	UNLOADED			LOADED			TMV	
	NO _x [mg/s]	NO _x [ppm]	% engine load	NO _x [mg/s]	NO _x [ppm]	% engine load	NO _x [mg/s]	% engine load
1	1.98	102.27	13	6.38	329.46	34	25.35	100
2	2.22	121.13	12	6.60	357.95	33	32.34	100
3	2.38	133.02	12	4.27	238.34	21	26.11	100
4	2.60	146.83	13	7.88	443.80	35	25.06	100
5	2.65	149.53	14	7.75	438.61	36	18.02	100
6	3.29	169.92	14	8.42	338.98	27	24.82	100
7	3.07	161.35	15	5.29	278.05	34	20.35	100
8	3.36	187.60	15	6.42	357.10	38	22.40	100
9	3.37	189.90	14	6.81	385.40	37	24.31	100
10	3.46	195.75	15	7.20	408.40	37	24.93	100
11	3.57	202.65	15	7.41	420.55	38	25.49	100
12	3.75	213.55	15	7.97	454.80	39	26.61	100
13	3.88	220.85	15	7.78	442.60	38	27.01	100

Table 11-17. Summary of Static NO_x test on Vehicle No. 5.

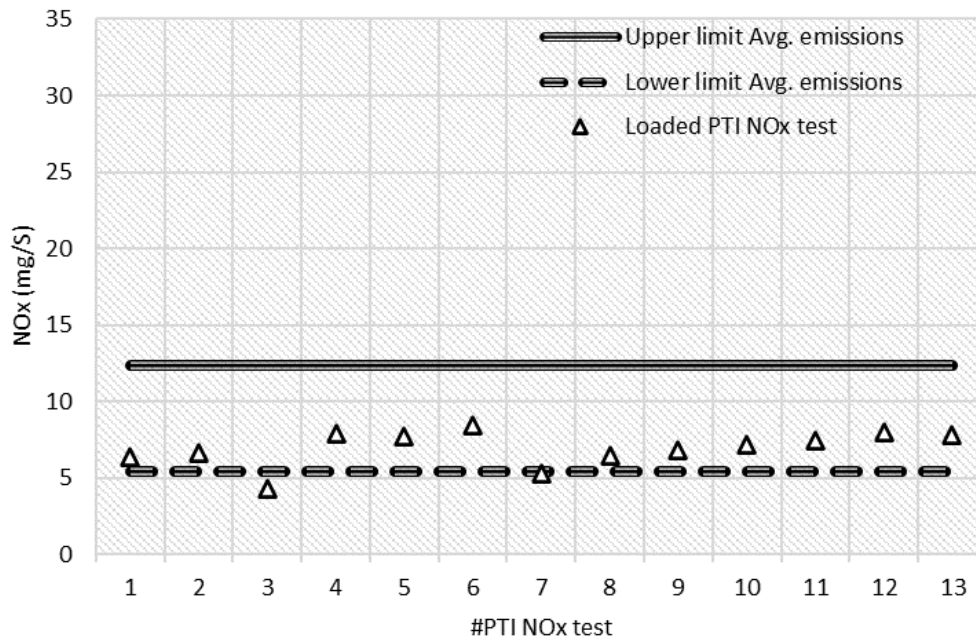


Figure 11-34. Range of Avg. On-road emissions and Loaded PTI test result for Vehicle No. 5.

In this instance, a notable trend emerges where the majority of the values obtained from the PTI test align within the range of average emissions encountered by the vehicle during genuine urban circulation. Consequently, we can infer that, for this particular vehicle, the outcome of the idling load measurement provides accurate insights into its performance when operating in an urban setting.

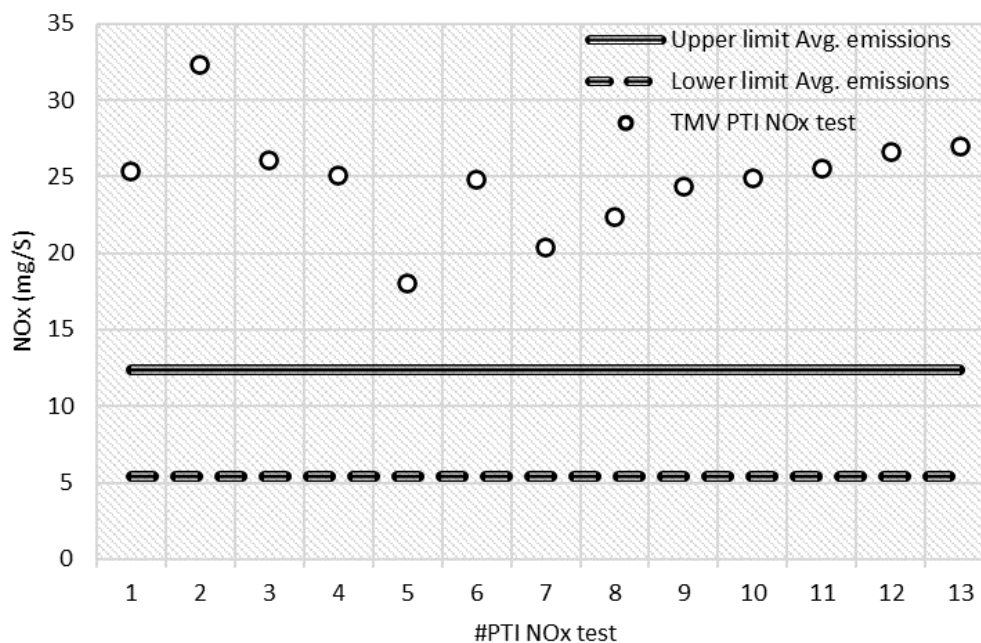


Figure 11-35. Range of Avg. On-road emissions and TMV PTI test results for Vehicle No. 5.

Next, the evaluation of the TMV values against the vehicle's average emission range is undertaken. Figure 11-35 illustrates that all TMV values surpass the scope of average measurements.

To conclude the vehicle analysis, the TMV values are juxtaposed against the vehicle's maximum emission range to verify if the measured values surpass the upper limit of this range. Such an occurrence would be detrimental to the measurement's accuracy.

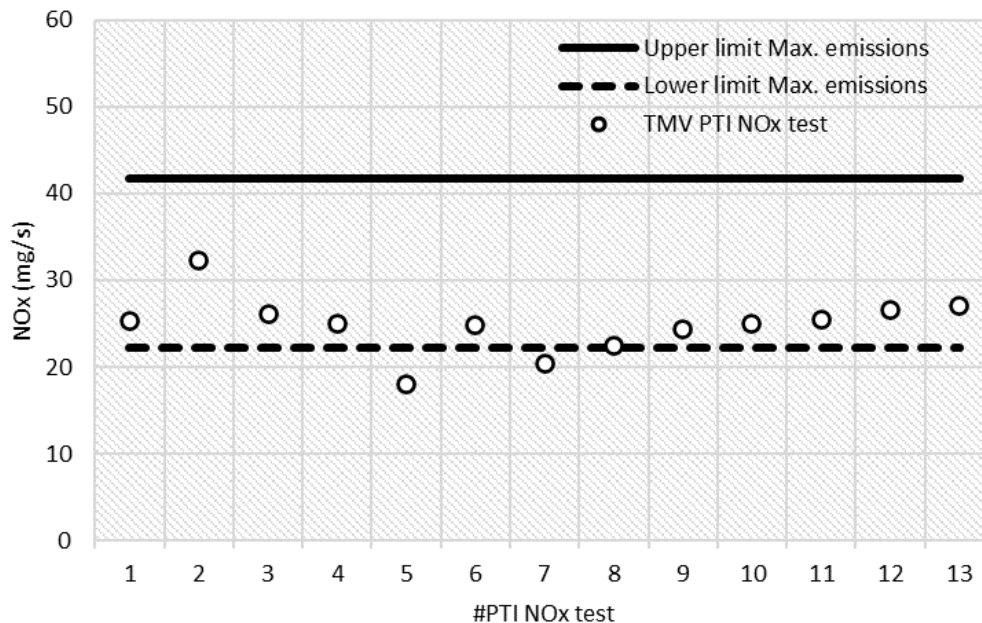


Figure 11-36. Range of Max. On-road emissions and TMV PTI test results for Vehicle No. 5.

Evident from Figure 11-36 is that nearly all values fall within the range of maximum emissions, or closely align with the lower limit. In no instance does any value exceed the upper limit of the range. Consequently, for this specific scenario, the TMV value derived from the PTI measurement offers a value that lies within the range of the vehicle's maximum emissions during urban traffic.

11.5.5. COMPARISON OF RESULTS FROM VEHICLE No. 6

Proceeding with the analysis of the Euro 6 vehicles, the identical process will be followed. Initially, the data collected during the circuit measurements will be utilized to construct Table 11-18.

From this table, ranges of vehicle emissions in driving conditions are defined: the range of maximum emissions and average emissions. As always, both ranges are shaded and in bold in Table 11-18.

Test	#	Loaded						Unloaded					
		1	2	3	4	5	6	1	2	3	4	5	6
Duration of measure	[s]	125	263	195	191	170	205	183	269	189	200	224	140
Avg. Concentration	[ppm]	61	189	86	197	223	219	130	131	156	112	170	101
Max. Concentration	[ppm]	405	634	526	764	641	506	919	479	576	485	602	451
Min. Concentration	[ppm]	5	17	1	20	17	18	4	22	19	12	22	6
Avg. engine load	[%]	57	55	61	66	72	77	50	47	56	62	61	73
Max. engine load	[%]	99.2	100	100	100	100	100	98.8	100	100	100	100	100
Min. engine load	[%]	0	0	0	0	0	0	0	0	0	0	0	0
Avg. Speed	[km/h]	41.4	36.1	40.8	40.1	40.2	38.0	42.2	36.2	42.4	40.1	39.8	40.9
Avg. Engine Speed	[rpm]	1894	1533	1586	1189	1095	990	1971	1536	1622	1133	988	1054
Max. Engine Speed	[rpm]	2864	2813	2522	2283	2908	2745	2724	2944	2497	2808	2874	2358
Min. Engine Speed	[rpm]	797	780	816	760	612	642	740	726	746	740	672	647
Avg. NO _x Mass Flow	[g/s]	0.002	0.006	0.003	0.005	0.005	0.005	0.005	0.005	0.005	0.003	0.004	0.002
Max. NO _x Mass Flow	[g/s]	0.017	0.023	0.018	0.024	0.024	0.020	0.031	0.018	0.022	0.014	0.018	0.010
Min. NO _x Mass Flow	[g/s]	0.000	0.000	0.000	0.000	0.000	0.000	0.000	0.000	0.000	0.000	0.000	0.000
Total emissions NO _x	[g]	0.280	1.668	0.561	1.018	0.918	0.931	0.874	1.248	1.018	0.554	0.806	0.329
Distance	[m]	970	1600	1600	1600	1600	1600	1600	1600	1600	1600	1600	1120
Emission Factor EF _{NO_x}	[g/km]	0.29	1.04	0.35	0.64	0.57	0.58	0.55	0.78	0.64	0.35	0.50	0.29

Table 11-18. Summary of vehicle No. 6 results from the on-road test.

#	UNLOADED			LOADED			TMV	
	NO _x [mg/s]	NO _x [ppm]	% engine load	NO _x [mg/s]	NO _x [ppm]	% engine load	NO _x [mg/s]	% engine load
1	2.32	134.74	17	9.55	562.54	51	21.77	100
2	2.59	149.88	19	10.35	602.18	52	23.43	100
3	2.49	142.55	21	10.13	583.81	53	24.48	100
4	2.50	142.04	22	10.33	590.25	53	22.68	100
5	2.44	139.51	21	10.50	602.44	53	24.54	100
6	2.43	138.33	18	10.21	584.05	52	23.14	100
7	2.59	147.87	22	10.32	592.94	53	23.15	100
8	2.32	132.26	21	10.43	598.20	53	23.55	100
9	2.50	143.89	20	10.88	626.23	53	24.63	100
10	2.68	156.91	21	11.90	699.73	53	26.77	100
11	2.68	157.65	22	11.91	705.80	54	25.88	100
12	2.74	160.38	21	12.04	707.58	53	26.28	100
13	2.20	130.40	22	8.68	513.54	54	19.25	100
14	2.24	131.73	22	8.75	518.27	54	18.69	100
15	1.83	107.03	22	8.40	492.26	54	18.31	100

Table 11-19. Summary of Static NO_x test on Vehicle No. 6.

From the values included in the table, the following ranges are defined:

- Maximum emissions range for vehicle No. 6: between 0.010 and 0.031 g/s
- Average emissions range for vehicle No. 6: between 0.002 and 0.006 g/s

Subsequently, by utilizing the data extracted from the diverse static measurements conducted during the method's establishment (Table 11-19), the outcomes of these tests are contrasted against the real-world emissions of the operational vehicle.

With these values Figure 11-37 is constructed, showing the average emission range of Vehicle No. 5 and the values obtained in the loaded state when performing the NO_x measurement PTI test.

This particular instance marks the sole case among the 8 vehicles analyzed where the value in the loaded state of the NO_x emissions test in PTI exceeds the average emission range of the vehicle during urban circulation. The most evident explanation for this phenomenon is that during the PTI test, the EATS systems were not activated by the ECU, making their presence irrelevant to the results of the static measurements.

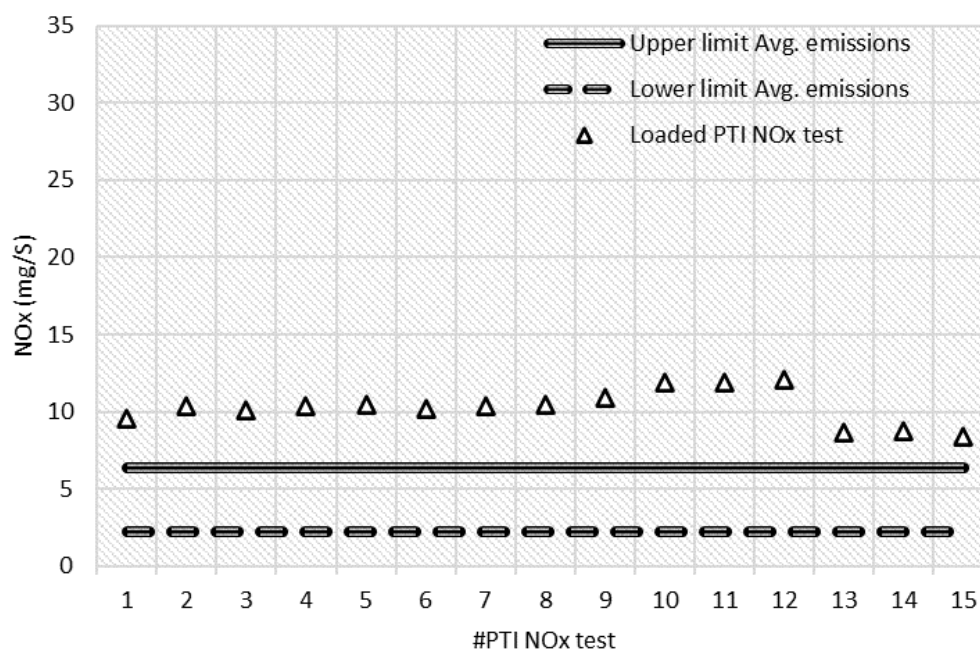


Figure 11-37. Range of Avg. On-road emissions and Loaded PTI test result for Vehicle No. 6.

During operation, the functioning of the EATS systems leads to a reduction in the average NO_x emissions of the vehicle compared to the emissions observed when the vehicle is stationary and idling.

Since the values at load already exceed the maximum value of the average emission range, when we compare the TMV values obtained with the average emission range of the vehicle, evidently the difference between these values concerning the upper limit of the range is very noticeable, as shown in Figure 11-38.

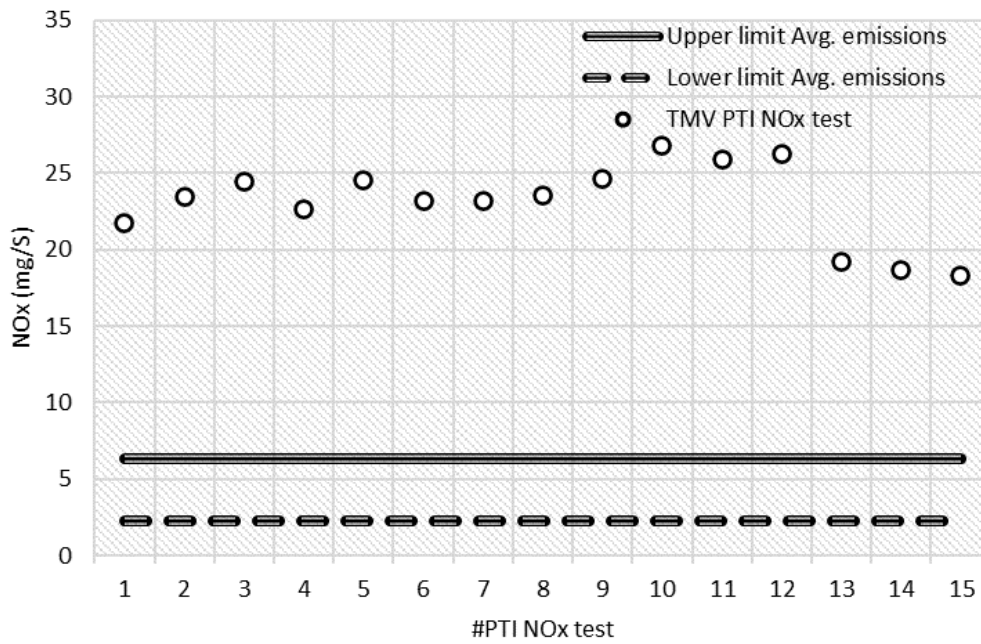


Figure 11-38. Range of Avg. On-road emissions and TMV PTI test results for Vehicle No. 6.

In any case, when comparing the TMV values with the range of maximum emissions of the vehicle, it is verified that the TMV values are completely within this range, without exceeding the upper limit on any occasion, which guarantees the suitability of the static measurement.

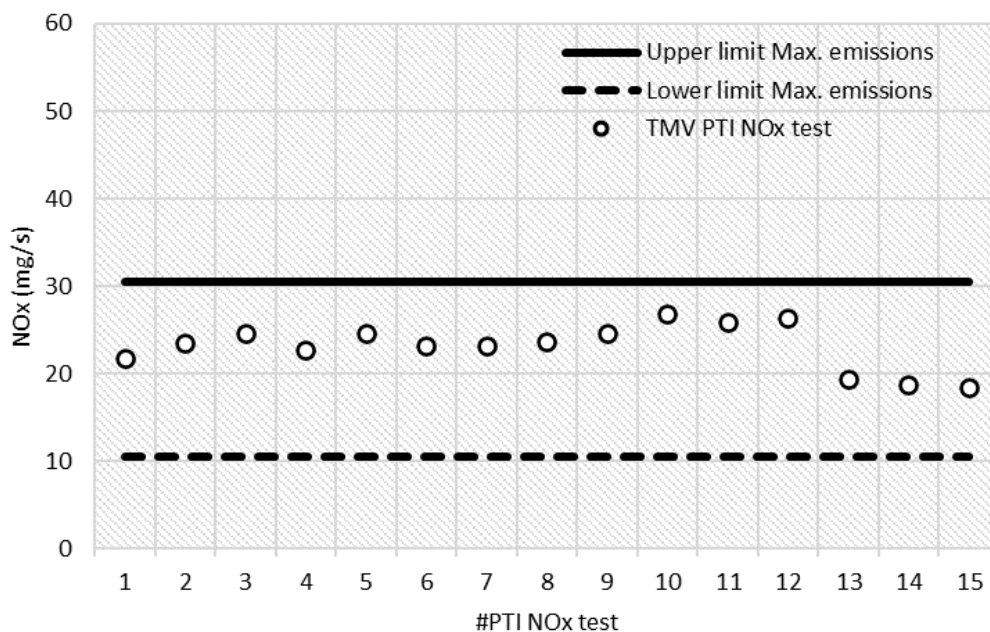


Figure 11-39. Range of Max. On-road emissions and TMV PTI test results for Vehicle No. 6.

Given the results, for this vehicle, the loaded emissions value from the test is not an indicator of the vehicle's emissions level, but the TMV value obtained in the test is a clear indicator of the maximum emissions that the vehicle will produce in urban traffic.

11.5.6. COMPARISON OF RESULTS FROM VEHICLE No. 7

For the upcoming Euro 6 vehicle, the methodology employed in all the preceding instances is reiterated. In order to juxtapose the on-road emissions recorded with the values derived from the proposed static test, the initial step involves creating Table 11-20. This table will encapsulate the key vehicle data gathered throughout the different tests.

As always, the limit values defining the ranges of maximum and average emissions are shaded and in bold to facilitate their identification.

Of the values included in the table, the following ranges are defined:

- Maximum emission range for vehicle No. 7: between 0.019 and 0.066 g/s
- Average emissions range for vehicle No. 7: between 0.004 and 0.015 g/s

Test	#	Loaded						Unloaded					
		1	2	3	4	5	6	1	2	3	4	5	6
Duration of measure	[s]	182	237	170	171	156	176	181	252	183	179	171	167
Avg. Concentration	[ppm]	94	84	110	161	470	522	162	118	90	196	400	430
Max. Concentration	[ppm]	539	404	806	775	1509	1598	725	926	603	841	1444	1459
Min. Concentration	[ppm]	10	2	4	6	2	19	16	9	4	6	2	4
Avg. engine load	[%]	45	56	59	57	72	66	44	49	43	53	59	68
Max. engine load	[%]	99.6	99.6	99.6	99.6	99.2	100	99.6	99.2	93.7	99.6	99.6	100
Min. engine load	[%]	0	0	0	0	0	0	0	0	0.1	0	0	0
Avg. Speed	[km/h]	43.1	37.3	45.7	46.3	46.0	45.8	42.8	37.4	44.0	44.2	45.3	48.1
Avg. Engine Speed	[rpm]	2338	1821	1998	1527	1222	1219	2261	1759	1873	1508	1187	1258
Max. Engine Speed	[rpm]	3333	3028	3916	2876	3532	3742	3332	3171	2971	4020	3143	3090
Min. Engine Speed	[rpm]	786	788	786	786	787	787	788	786	788	788	788	788
Avg. NO _x Mass Flow	[g/s]	0.005	0.004	0.005	0.006	0.013	0.015	0.008	0.006	0.004	0.008	0.011	0.012
Max. NO _x Mass Flow	[g/s]	0.028	0.019	0.041	0.030	0.047	0.053	0.034	0.043	0.035	0.066	0.045	0.051
Min. NO _x Mass Flow	[g/s]	0.000	0.000	0.000	0.000	0.000	0.000	0.000	0.000	0.000	0.000	0.000	0.000
Total emissions NO _x	[g]	0.860	0.967	0.893	1.001	1.987	2.573	1.376	1.164	0.742	1.363	1.846	2.067
Distance	[m]	1600	1600	1600	1600	1600	1600	1600	1600	1600	1600	1600	1600
Emission Factor EF _{NOx}	[g/km]	0.54	0.60	0.56	0.63	1.24	1.61	0.86	0.73	0.46	0.85	1.15	1.29

Table 11-20. Summary of vehicle No. 7 results from the on-road test.

#	UNLOADED			LOADED			TMV	
	NO _x [mg/s]	NO _x [ppm]	% engine load	NO _x [mg/s]	NO _x [ppm]	% engine load	NO _x [mg/s]	% engine load
1	1.89	107.60	14	5.39	306.94	46	16.02	100
2	2.19	124.80	19	5.60	318.81	47	12.92	100
3	2.14	122.83	17	6.23	356.52	47	12.95	100
4	2.14	123.55	14	6.63	382.23	47	14.50	100
5	2.71	156.12	21	6.86	394.20	47	15.85	100
6	2.56	148.48	21	7.22	419.00	48	17.17	100
7	2.41	140.18	19	7.33	426.49	48	12.49	100
8	2.42	140.46	19	5.89	342.42	42	10.04	100
9	2.21	128.23	19	6.93	403.34	48	11.69	100

Table 11-21. Summary of Static NO_x test on Vehicle No. 7.

With this information, it is now possible to generate Figure 11-40 showing the position of the loaded idle emission values measured during the static PTI test in relation to the emission ranges of the vehicle.

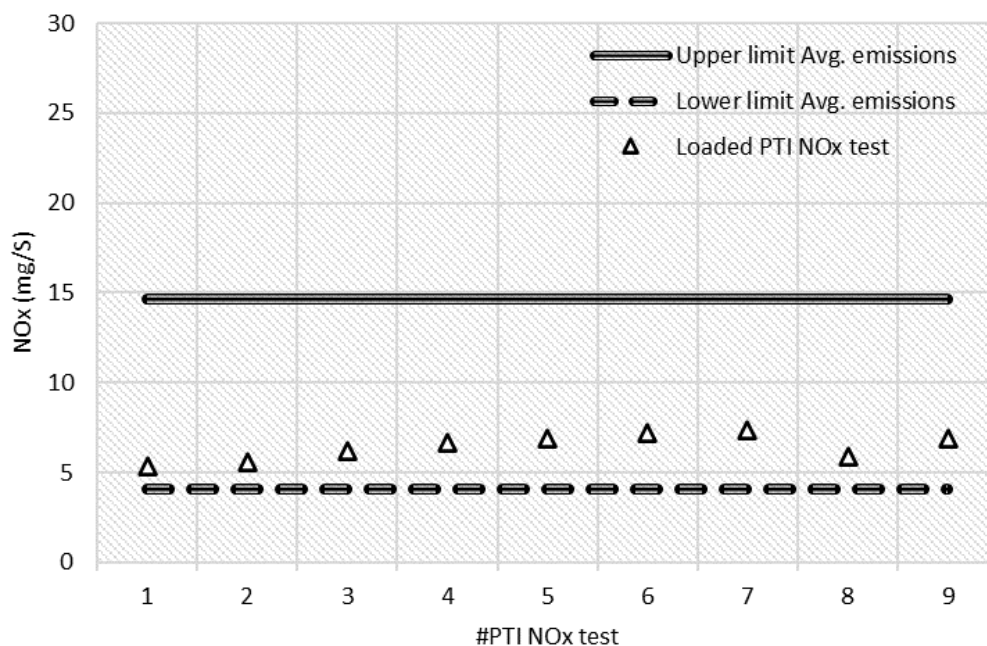


Figure 11-40. Range of Avg. On-road emissions and Loaded PTI test result for Vehicle No. 7.

In this scenario, it becomes evident that the emission values recorded during idling under load in the static PTI test all fall within the predetermined range of average emissions for the vehicle in urban traffic. Consequently, the outcome of the static measurement test would serve as an excellent indicator of the vehicle's average emissions in urban traffic conditions.

Upon contrasting the TMV values obtained with the average emission range, it becomes apparent that numerous of these values remain within the specified range. Moreover, those that surpass the upper limit value do so by a marginal margin.

Finally, the vehicle analysis compares the TMV values with the vehicle's range of maximum emissions, checking whether or not the measured values exceed the upper limit of this range, which would be counterproductive for the quality of the measurement.

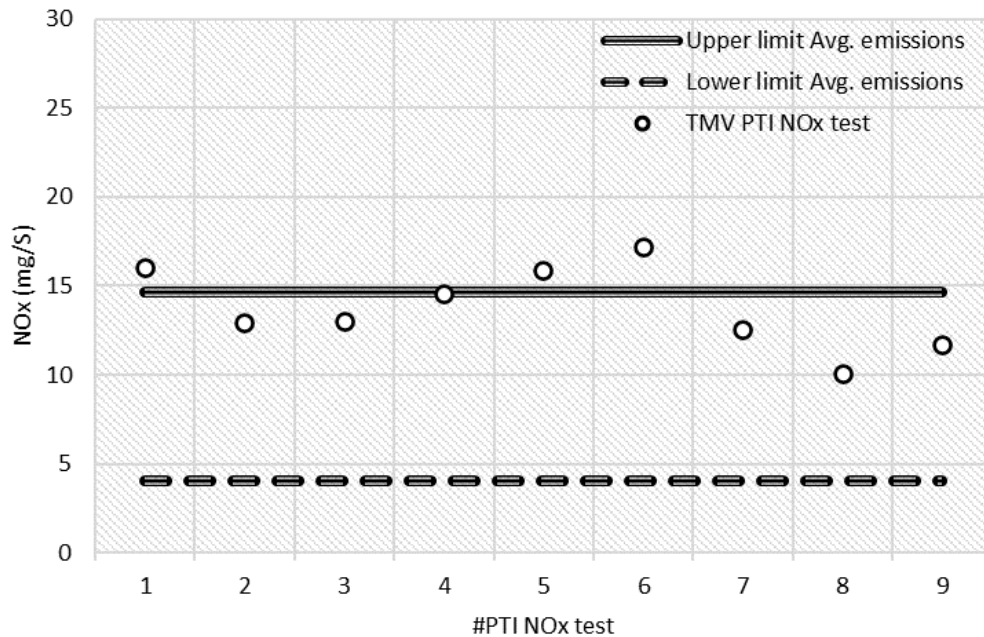


Figure 11-41. Range of Avg. On-road emissions and TMV PTI test results for Vehicle No. 7.

In this case, as anticipated from Figure 11-41, the TMV values only marginally approach the lower boundary of the maximum emissions range (Figure 11-42). Consequently, similar to the other vehicles, the upper threshold of the vehicle's maximum emissions range is never breached. This implies that the test does not yield any false negatives. In other words, the emissions indicated by the test align with the emissions the vehicle would emit in urban traffic conditions.

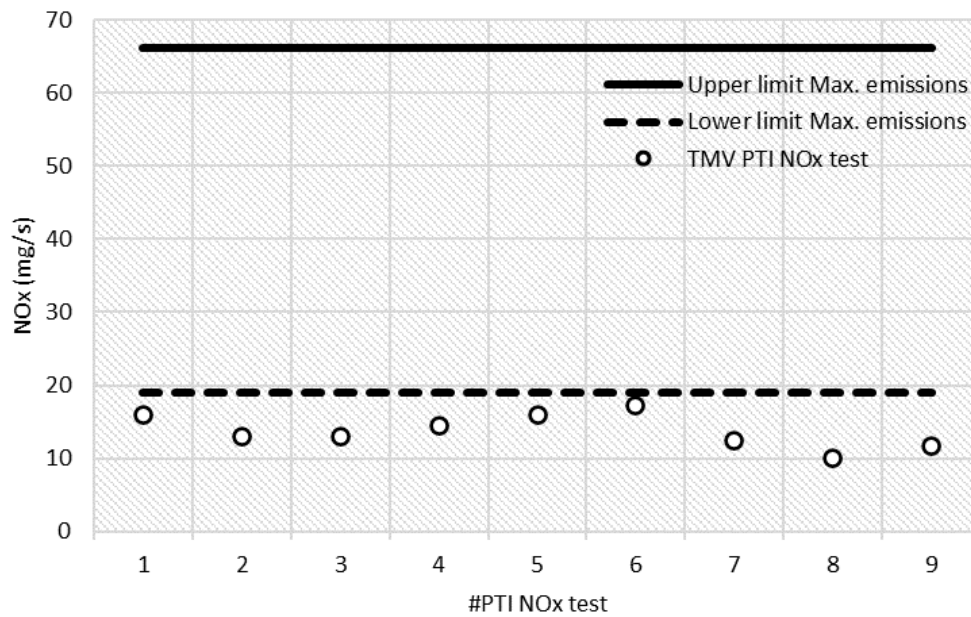


Figure 11-42. Range of Max. On-road emissions and TMV PTI test results for Vehicle No. 7.

11.5.7. COMPARISON OF RESULTS FROM VEHICLE No. 8

Lastly, the performance of Vehicle No. 8, which stands as the sole gasoline-fueled vehicle in the group under investigation, is examined.

The process once again follows the same steps. From the dataset of on-road measurements, Table 11-22 is compiled. This table encapsulates the key vehicle data during the execution of various tests on the circuit designed to simulate urban traffic conditions. As customary, the limit values delineating the ranges of maximum and average emissions are shaded and highlighted in bold to aid their recognition.

From the values included in the table, the following ranges are defined:

- Maximum emissions range for vehicle No. 8: between 0.003 and 0.020 g/s
- Average emission range for vehicle No. 8: between 0.0002 and 0.002 g/s

Utilizing this data, in conjunction with the measurements obtained from the vehicle using the proposed PTI measurement method, as outlined in Table 11-23, it becomes feasible to create Figure 11-43.

This figure offers a comparative view of the values measured under loaded conditions in the static test, relative to the range of average emissions exhibited by the vehicle in urban traffic scenarios. This figure shows that most of the values measured in the static test are located in the average emissions range or very close to it.

Hence, concerning this specific vehicle, it can be asserted that the value acquired from the idling measurement under loaded conditions furnishes trustworthy insights into the actual emissions of the vehicle during urban traffic operations. Therefore, in this instance as well, the results of the static test would serve as a reliable indicator to employ.

Test	#	Loaded						Unloaded					
		1	2	3	4	5	6	1	2	3	4	5	6
Duration of measure	[s]	170	263	175	167	180	166	171	278	168	161	160	166
Avg. Concentration	[ppm]	31	33	21	7	10	9	24	35	21	15	23	13
Max. Concentration	[ppm]	359	455	267	67	121	152	191	266	152	137	205	216
Min. Concentration	[ppm]	0.1	0.1	0.1	0.1	0.1	0.1	1	1	1	1	1	0.1
Avg. engine load	[%]	42	51	45	56	63	74	36	38	42	52	63	63
Max. engine load	[%]	100	100	100	100	100	100	100	100	100	100	100	100
Min. engine load	[%]	0	0	0	0	0	0	0	0	0	0	0	0
Avg. Speed	[km/h]	46.4	36.0	44.4	48.0	46.6	49.4	46.3	37.6	48.9	49.7	49.7	50.0
Avg. Engine Speed	[rpm]	2973	1927	2364	2037	1529	1647	2983	1818	2532	2145	1649	1634
Max. Engine Speed	[rpm]	4128	3543	3045	3171	3184	3146	4022	4114	3267	3936	4222	4072
Min. Engine Speed	[rpm]	806	775	979	790	796	891	795	683	692	701	697	694
Avg. NO _x Mass Flow	[g/s]	0.002	0.001	0.001	0.0002	0.000	0.000	0.001	0.001	0.001	0.001	0.001	0.001
Max. NO _x Mass Flow	[g/s]	0.018	0.020	0.012	0.003	0.004	0.005	0.011	0.013	0.008	0.010	0.009	0.009
Min. NO _x Mass Flow	[g/s]	0.000	0.000	0.000	0.000	0.000	0.000	0.000	0.000	0.000	0.000	0.000	0.000
Total emissions NO _x	[g]	0.308	0.355	0.172	0.047	0.055	0.052	0.244	0.410	0.170	0.117	0.133	0.089
Distance	[m]	1600	1600	1600	1600	1600	1600	1600	1600	1600	1600	1600	1600
Emission Factor EF _{NO_x}	[g/km]	0.19	0.22	0.11	0.03	0.03	0.03	0.15	0.26	0.11	0.07	0.08	0.06

Table 11-22. Summary of vehicle No. 8 results from the on-road test.

#	UNLOADED			LOADED			TMV	
	NO _x [mg/s]	NO _x [ppm]	% engine load	NO _x [mg/s]	NO _x [ppm]	% engine load	NO _x [mg/s]	% engine load
1	0,07	4,74	22	0,32	19,18	38	1,41	100
2	0,02	1,51	22	0,08	4,73	39	0,56	100
3	0,39	24,57	21	1,48	89,10	37	5,59	100
4	0,21	13,32	22	0,76	45,42	36	3,78	100
5	0,13	8,03	22	0,51	30,36	36	5,02	100
6	0,13	8,70	22	0,37	22,37	36	2,18	100
7	0,03	2,12	22	0,21	11,76	38	1,67	100
8	0,11	6,90	23	0,31	18,70	38	1,89	100
9	0,10	6,82	23	0,32	18,91	38	1,89	100
10	0,03	1,88	22	0,19	11,50	38	1,32	100
11	0,02	1,21	22	0,21	12,78	39	1,38	100

Table 11-23. Summary of Static NO_x test on Vehicle No. 8.

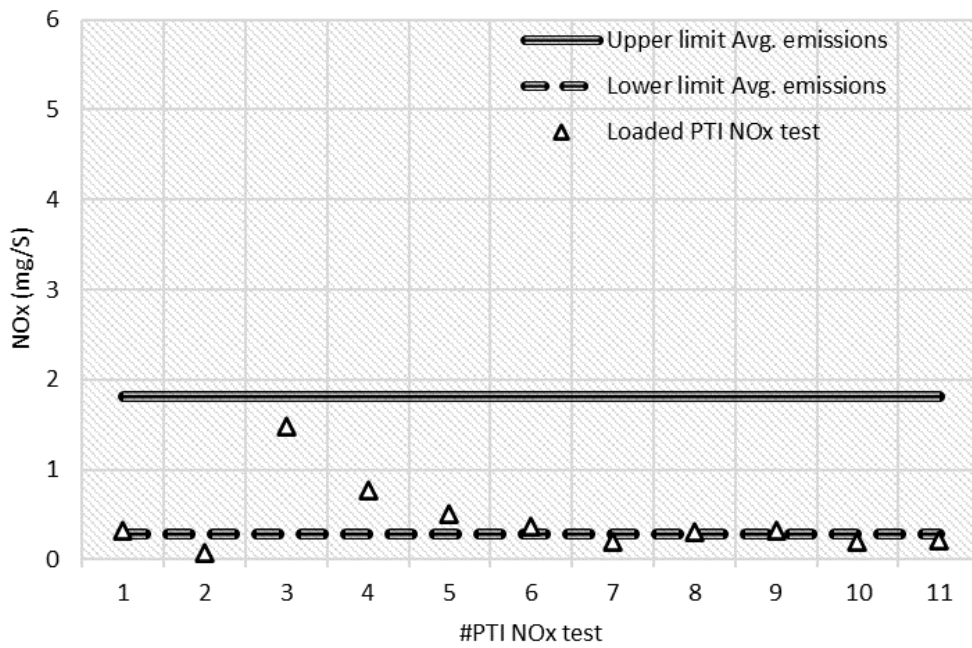


Figure 11-43. Range of Avg. On-road emissions and Loaded PTI test result for Vehicle No. 8.

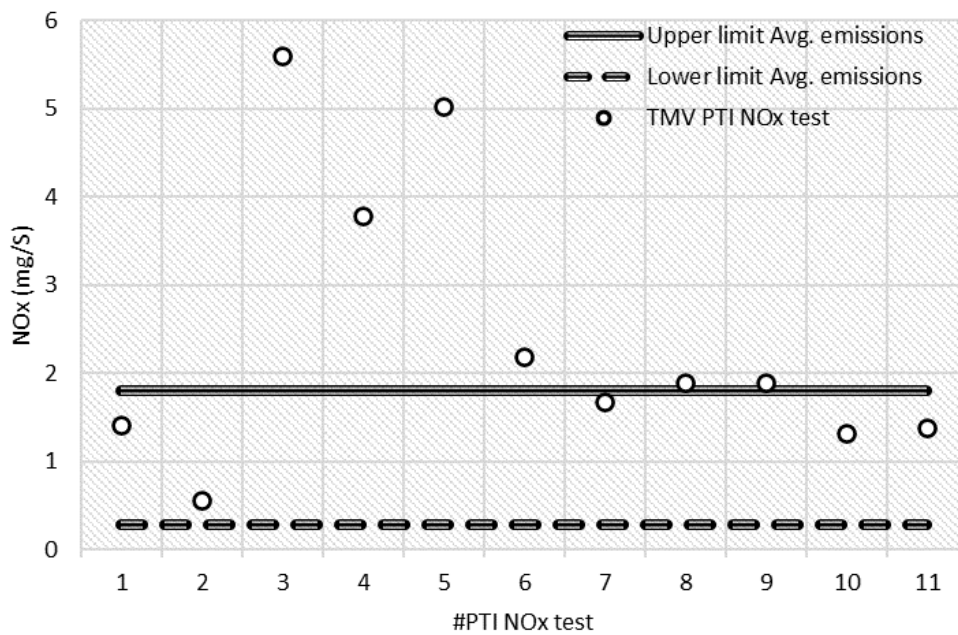


Figure 11-44. Range of Avg. On-road emissions and TMV PTI test results for Vehicle No. 8.

The next step in the analysis is the comparison of the TMV values obtained in the static test with respect to the average emission range of the vehicle.

As can be seen in Figure 11-44, part of these values are included in the range of average emissions. Specifically, the measurements in Figure 11-43 presented a lower

value in the static test under load, providing a TMV value located within the range of average emissions.

On the other hand, those measurements that presented a static load test value within the average emissions range, when comparing the corresponding TMV value, appear above the average emissions range of the vehicle.

To conclude the analysis, Figure 11-45 compares the TMV values obtained by the vehicle with the range of maximum emissions of Vehicle No. 8.

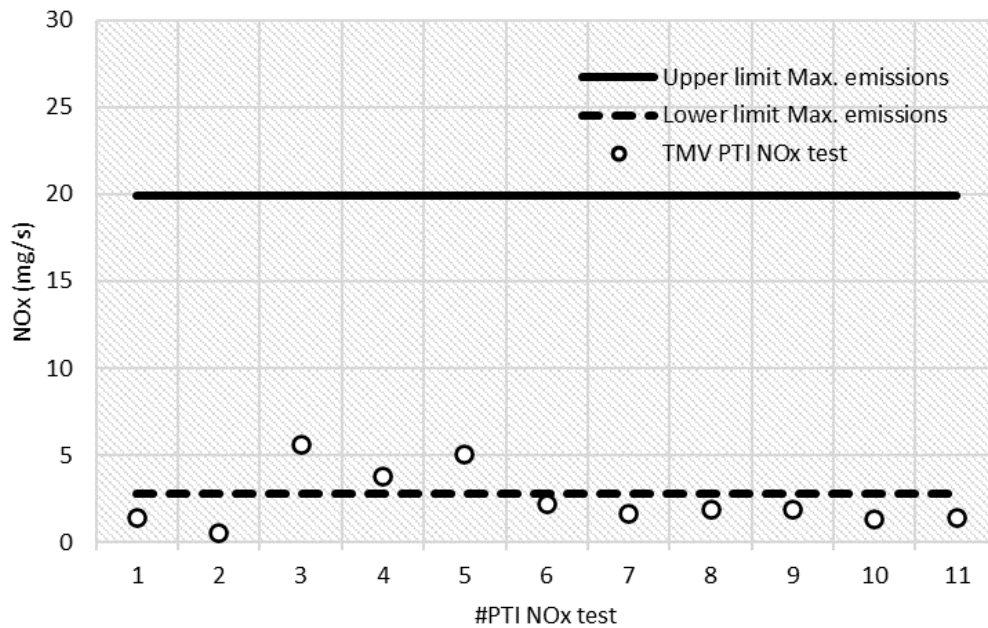


Figure 11-45. Range of Max. On-road emissions and TMV PTI test results for Vehicle No. 8.

This analysis reveals that the highest values observed fall within the scope of the maximum emissions range, while the remaining values are in close proximity to the lower boundary of this range. Notably, none of the values surpass the upper threshold of the maximum emissions range, mirroring the trend observed in the other scrutinized vehicles. This assurance reinforces the notion that the static test does not yield results that surpass the actual emission values exhibited by the vehicle.

CAPÍTULO 12

CONCLUSIONES

12. CONCLUSIONES

12.1. INTRODUCCIÓN

En este capítulo final, después de un breve resumen de la metodología, la validación y la verificación experimental del método en el contexto de la ITV, se proporcionará una visión general sobre la viabilidad de la implementación del método propuesto.

Al mismo tiempo, se llevará a cabo una evaluación de los objetivos que la investigación tenía inicialmente establecidos para comprobar su cumplimiento. Además, se explicará el impacto global de los esfuerzos realizados a lo largo de la realización de la tesis. Tras esta evaluación, se analizarán las posibilidades para futuras propuestas de investigación que surgen a partir de esta tesis. Para finalizar, se hará una revisión de la visibilidad que la investigación ha producido.

12.2. RESUMEN

Dado que el objetivo final de la Tesis es definir un método de medición de NO_x válido para ser usado en ITV, hay una serie de pasos, que han sido descritos a través de los diferentes capítulos de esta Tesis, que deben seguirse para que el método sea totalmente validado.

En el **Capítulo 1**, se ha presentado la motivación que ha llevado a producir la Tesis con el objetivo de proporcionar una herramienta que pueda contribuir a resolver la problemática planteada por las emisiones de NO_x . Además, se han definido los objetivos que serán abordados en el desarrollo de la Tesis.

Para continuar, se ha mostrado el Estado del Arte en el **Capítulo 2**. En él, se demuestra que a pesar de existir una amplia gama de métodos y sistemas empleados para la medición de NO_x en diferentes ámbitos, actualmente no existe un método universalmente aceptado o utilizado que proporcione una medición de NO_x rápida, sencilla y confiable adecuada para su uso en ITV. Dicho método, de existir, se debería poder implementar fácilmente, a gran escala, y para una amplia gama de vehículos. El capítulo incluye una lista de métodos que se emplean para la medición de NO_x , algunos aplicados dentro del ámbito de la ITV, mientras que otros son utilizados para la homologación o para propósitos de investigación. También incluye una descripción de las tecnologías actuales utilizadas para la medición de NO_x , junto con una recopilación de los últimos avances en la medición de NO_x propuestos durante el proceso de la investigación presentada en esta tesis.

En el **Capítulo 3**, el método ha sido formulado teóricamente, de modo que asegure el cumplimiento de los requisitos técnicos necesarios en una medición diseñada para su implementación en ITV. Se ha establecido una hipótesis de trabajo, que permite la fundamentación técnica del método, y se ha descrito el proceso de generación de NO_x en los motores de combustión, incluyendo cómo las características de este proceso han sido utilizadas para definir y desarrollar el método de medición.

Finalmente, se han señalado las principales características y ventajas de este método de medición.

En el **Capítulo 4** se describe y se detalla el método, proporcionando información específica tanto sobre el proceso de medición como sobre el uso de los datos obtenidos durante la medición. Con el contenido de este capítulo, se puede replicar el método de medición. Además, se explican los resultados obtenidos del proceso de medición, junto con las herramientas utilizadas para evaluar la calidad y la significancia de la relación entre las variables utilizadas por el método de medición: la concentración de NO_x en los gases de escape y el valor de "% de carga del motor".

El equipo utilizado para la medición de NO_x también tiene una gran importancia, y la validez del método de medición puede depender de la idoneidad, capacidad y precisión del equipo empleado. Por lo tanto, en el **Capítulo 5** se ha evaluado la idoneidad del equipo utilizado, comparando su rendimiento y resultados con un equipo de medición de referencia, utilizado en laboratorios destinados a la homologación. Se han realizado varias pruebas para verificar si el equipo es válido y adecuado para el propósito para el que ha sido destinado, la medición de NO_x en ITV. A lo largo del capítulo se ha demostrado que el equipo utilizado cumple con los requisitos necesarios para su uso en ITV, y además proporciona mediciones con un nivel de certeza y precisión apropiado para su uso previsto, tomando como referencia el equipo de laboratorio. Un *paper* revisado por pares fue publicado con la información completa del equipo probado [180].

En el **Capítulo 6** se verificó y validó el método, se comprobó la hipótesis de partida, y se demostró la fiabilidad del método a través de unos valores de reproducibilidad adecuados y una precisión en la medición suficiente. El método ha sido validado mediante la realización de pruebas sobre un conjunto de 23 vehículos, con numerosas mediciones realizadas sobre cada vehículo. En base a los resultados obtenidos, se verificó la validez del método en términos de significancia, representatividad, precisión y reproducibilidad. Un resumen de este capítulo y el capítulo 4 fue publicado en un *paper* revisado por pares [175].

Una vez que el método de medición se ha demostrado como válido, justificado técnicamente y adecuado para el propósito previsto, asegurando que proporciona mediciones fiables, precisas y exactas, el siguiente paso es evaluar si los resultados obtenidos al aplicar el método están relacionados con las emisiones reales de los vehículos en condiciones de circulación urbana. El **Capítulo 7** describe el proceso de medición de emisiones reales en un grupo de vehículos en condiciones de circulación urbana. Los resultados obtenidos se han comparado con los límites de emisiones teóricos de los vehículos basados en su nivel Euro de emisiones, así como con los resultados obtenidos a través de la aplicación del método de medición propuesto. Los hallazgos demuestran que los resultados de las mediciones en ITV ofrecen información valiosa, representativa y válida, tanto de las emisiones promedio como de las emisiones máximas de los vehículos en condiciones de circulación urbana.

Tras esto, el último paso que queda para terminar de validar el método de medición propuesto es aplicarlo y, por lo tanto, llevar a cabo mediciones con él en diversas estaciones de ITV, incorporando la prueba en el proceso de inspección. Con este propósito, se ha realizado una campaña de medición de NO_x en ITV, aplicando el método propuesto a los vehículos que acuden a las estaciones, es decir, en los

vehículos que acuden diariamente a ser inspeccionados, no en vehículos preparados *ad hoc*. Los vehículos fueron seleccionados al azar entre los vehículos diésel Euro 4, Euro 5 y Euro 6 que acudieron a las estaciones involucradas en la campaña de medición. Los resultados de esta campaña de medición se detallan en el **Capítulo 8**.

Tanto el propio método, como la campaña de medición, generan una cantidad tan grande de datos que no solo permiten la validación del método, sino que también proporcionan información adicional que puede ser utilizada en la formulación de políticas de gestión de la flota de vehículos y de protección del medio ambiente. El **Capítulo 9** analiza la relación entre varias variables medidas en el conjunto de vehículos analizados y las emisiones de NO_x. También compara los resultados obtenidos al aplicar el método propuesto y los obtenidos con otro método de medición basado en el uso de un banco dinamométrico, para analizar las diferencias entre ambos. Finalmente, se ha realizado el modelado de las emisiones de tres vehículos en una ruta urbana basándose en los resultados de las mediciones para demostrar la utilidad de la información obtenida en la estimación de las emisiones reales de los vehículos.

Resumiendo, a lo largo de estos capítulos se ha definido un método válido y adecuado para medir las emisiones de NO_x, se ha justificado técnicamente y se ha validado a través de diversos resultados experimentales. Este método puede ser implementado de manera rápida, sencilla y económica en ITV para controlar las emisiones de NO_x de toda la flota de coches de pasajeros y vehículos ligeros de carga diésel, identificando así a los vehículos con las emisiones más altas. Esto proporcionaría una herramienta, es decir, información adecuada, para formular políticas destinadas a mitigar las consecuencias de la exposición de la población a las emisiones de NO_x de los vehículos.

12.3. CONCLUSIONES

En esta sección se lleva a cabo una revisión de los objetivos definidos en el Capítulo 1 para determinar si han sido alcanzados. En caso de que algún objetivo no haya sido alcanzado, se analizarán los factores que impidieron su consecución.

Después de verificar la consecución de estos resultados, se analizarán los resultados obtenidos y el cumplimiento de las hipótesis inicialmente formuladas.

Objetivo #1: Definición de un procedimiento para la medición de NO_x

El primer objetivo marcado fue definir un nuevo procedimiento de medición que cumpliera con todos los requisitos necesarios para su implementación en el proceso de inspección en ITV, tanto en términos técnicos como económicos.

Es evidente que la investigación ha conseguido plenamente este primer objetivo indicado en la tesis. El método propuesto, que ha introducido un enfoque novedoso que previamente no se había explorado, cumple los requisitos marcados.

Basado en los principios de generación de NO_x en motores de compresión, el método ha sido diseñado en base a la correlación entre un parámetro de funcionamiento del

motor fácilmente accesible, que se obtiene a través del sistema OBD, y las emisiones de NO_x durante una prueba estática en ralentí.

A través de un examen meticuloso del desarrollo y aplicación del método, se ha demostrado la idoneidad del método para su integración en el proceso de ITV, tanto en términos de su viabilidad económica (costos mínimos de equipo y de personal) como de su alineación técnica con los requisitos necesarios. Además, el método es aplicable en todo tipo de vehículos de las categorías M1 y N1, como evidencia el extenso análisis y la campaña de medición explicada en el Capítulo 8.

Si bien el método teóricamente también se puede aplicar a categorías de vehículos más pesados (M2, M3, N2, N3, etc.), este investigador reconoce la necesidad de una investigación adicional para comprobarlo. El desafío principal radica en lograr un aumento sustancial de la carga sobre el motor mientras el motor del vehículo está en ralentí, especialmente en vehículos con motores más grandes y potentes, como camiones y autobuses.

Aunque este aspecto final requiere un análisis más profundo, se puede afirmar que el primer objetivo se ha cumplido en gran medida, al mismo tiempo que se reconoce la necesidad de una investigación continua para abordar los desafíos únicos planteados por los vehículos pesados.

Objetivo #2: Representatividad de los resultados

La investigación ha demostrado también la consecución del segundo objetivo, que tenía como finalidad asegurar que los resultados obtenidos a través del nuevo método de medición son efectivamente representativos de las emisiones reales de NO_x de los vehículos (en condiciones de circulación urbana).

A lo largo de la tesis, se ha llevado a cabo un proceso de análisis exhaustivo para confirmar que los valores obtenidos de las mediciones de NO_x utilizando este método se corresponden con los valores promedio de las emisiones de NO_x que presentan los vehículos durante condiciones de conducción urbana (como se observa en estado cargado), según los resultados del Capítulo 7. Esto se ha verificado tanto para el conjunto de 23 vehículos utilizados en la validación del método como en las mediciones realizadas durante la campaña de PTI.

Además, se ha justificado la importancia de medir las emisiones en ralentí, cuando el vehículo está detenido durante la conducción urbana, en relación con la representatividad de la medición propuesta.

Finalmente, el valor máximo alcanzado en la medición (TMV) a través de este método se encuentra dentro del rango de emisiones máximas producidas por los vehículos durante la conducción urbana. Esto demuestra que TMV es un indicador válido del máximo nivel de emisiones de NO_x del vehículo. Su aplicación permite la comparación del nivel de emisiones entre diferentes vehículos.

Por lo tanto, se puede afirmar con rotundidad que se ha logrado completamente el objetivo de obtener resultados representativos de las pruebas.

Objetivo #3: Cumplimiento de los requisitos de la ITV

La investigación ha abordado de manera satisfactoria el tercer objetivo, cumplir los requisitos de equipos y personal con respecto a lo requerido por la ITV, tanto desde un punto de vista técnico como económico.

El equipo utilizado, que ya se emplea para la medición de CO en las inspecciones, cumple con todos los requisitos de la ITV, lo que respalda su idoneidad técnica y económica. Además, la precisión del equipo para la medición de NO_x se ha validado en el Capítulo 5, donde se comparó su rendimiento con el de un analizador de gases de referencia utilizado en laboratorios de investigación y homologación.

En cuanto a los requisitos de personal, la sencillez y simplicidad del método han sido ampliamente confirmadas. Los miembros del personal de una estación de ITV no necesitan recibir una formación compleja, y la ejecución del método y su posterior implementación diaria en el proceso de inspección no requieren un tiempo excesivo, como se ha demostrado en el Capítulo 8.

Además, como ventaja adicional, los niveles de seguridad tanto para los vehículos, el equipo y el personal cumplen con los mismos estándares que el resto de las pruebas en el proceso de inspección.

En este sentido, queda claro que se ha cumplido completamente el tercer objetivo.

Objetivo #4: Comparación con otros métodos

La investigación ha cumplido completamente el cuarto objetivo, centrado en lograr al menos el mismo nivel de representatividad y precisión en los resultados de medición de NO_x que otros métodos, al mismo tiempo que mantiene requisitos iguales o inferiores para el proceso de medición.

A través de una comparación meticulosa con otros métodos alternativos propuestos para la medición de NO_x en ITV, como se puede comprobar en el Capítulo 9, se ha demostrado de manera concluyente que los resultados obtenidos a través del método propuesto no solo tienen igual representatividad, sino que en realidad presentaron una representatividad superior. Esta superioridad se debió a abordar y corregir las deficiencias identificadas en el método comparado.

Además, los requisitos del método propuesto en cuanto a equipo (tanto en coste económico como en complejidad) y el proceso de medición (incluyendo complejidad del proceso y la demanda de tiempo) fueron indudablemente favorables en comparación con otros métodos competidores. La investigación también validó la precisión adecuada del equipo de medición al compararlo con equipos más complejos y costosos.

Discusión de los resultados

Es evidente que los cuatro objetivos especificados en el Capítulo 1 han sido alcanzados con éxito durante el desarrollo de la investigación. Por ello, se puede concluir que la investigación ha finalizado con éxito.

La investigación realizada es innovadora debido a que presenta un enfoque distintivo en el contexto de ITV. Aunque existe una gran cantidad de literatura científica sobre las emisiones de NO_x de motores de combustión, la novedad de esta investigación radica en que está dedicada a la medición de estas emisiones dentro del marco de la ITV, así como el enfoque teórico empleado para el análisis de las emisiones de NO_x.

Antes de esta investigación, existía una ausencia casi total en cuanto a investigaciones académicas dirigidas específicamente a la medición de tales emisiones desde el punto de vista de los protocolos de ITV.

En el momento de la publicación de esta tesis, la medición de NO_x en el contexto de la ITV está siendo considerada por parte de la Comisión Europea, analizando la posible inclusión de la medición de NO_x en el proceso de la inspección periódica.

Como resultado, esta investigación se está desarrollando de manera simultánea al proceso de toma de decisiones llevado a cabo por la autoridad pertinente en este asunto. Dada esta alineación temporal, se hace evidente que existe muy poco trabajo previo sobre el cual fundamentar la investigación. Como consecuencia, la investigación depende principalmente de los avances logrados de manera orgánica a lo largo de su desarrollo, sirviendo como base primaria para sus hallazgos e implicaciones.

Por otro lado, este escenario concurrente ha generado una situación en la que el progreso de la investigación ha estado accesible de manera inmediata a las partes interesadas involucradas en el proceso de toma de decisiones. Por lo tanto, existe el potencial para que la presente investigación ejerza una influencia tangible en tiempo real sobre la determinación final relacionada con la incorporación de la medición de NO_x dentro del marco de la ITV.

La propuesta para Euro 7 [196] que está siendo actualmente preparada (aún en forma de borrador) establece como algunos objetivos específicos: a) reducir la complejidad de los actuales estándares de emisiones Euro, b) modificar y actualizar los límites actuales de los contaminantes más relevantes (incluyendo NO_x), y c) mejorar el control de las emisiones reales de los vehículos.

La implementación del método de medición descrito en esta tesis tiene potencial para contribuir significativamente a la consecución de estos tres objetivos.

A pesar de los cambios legislativos implantados por la Unión Europea que tienen como objetivo eliminar gradualmente los vehículos de motor de combustión interna y limitar su comercialización para 2035, es crucial reconocer que el desafío de las emisiones de NO_x no se resolverá automáticamente con la eliminación de vehículos contaminantes para esa fecha.

El método de medición propuesto es pertinente porque aborda las emisiones de los vehículos existentes, garantizando el cumplimiento continuo de los objetivos de

protección ambiental y de salud, incluso más allá de la eliminación gradual de los vehículos de motor de combustión interna.

En efecto, la prohibición de registrar vehículos nuevos no conducirá a la desaparición instantánea de los vehículos existentes, ya que estos seguirán circulando y emitiendo contaminantes a lo largo de su vida útil operativa hasta que finalmente sean reemplazados por vehículos que utilicen tecnologías alternativas.

Además, este proceso de reemplazo de vehículos es poco probable que ocurra rápidamente, y se extenderá a lo largo de un período prolongado.

Por otro lado, también se está planteando el uso de opciones alternativas al veto absoluto de los vehículos de motor de combustión interna. Entre estas alternativas se encuentra la utilización de los llamados *e-fuels* producidos a través de la hidrogenación del CO₂ capturado de la atmósfera. Este enfoque permitiría la venta y operación continuada de vehículos equipados con motores de combustión con un teórico balance neto cero de emisiones de CO₂. Como contrapartida, esta alternativa prolongaría la vida útil de tales vehículos, lo que resultaría en la emisión continua de contaminantes como el NO_x, a pesar de su estatus neutro en cuanto a CO₂.

Otra potencial alternativa sería la adopción de motores de combustión interna alimentados con hidrógeno. Aunque esta tecnología no ha experimentado una adopción generalizada debido a sus limitados beneficios de rendimiento en comparación con los motores de combustión interna convencionales y los desafíos asociados con la adquisición y utilización del hidrógeno, en un escenario futuro podría experimentar un resurgimiento.

Este resurgimiento podría ocurrir en un escenario donde la accesibilidad y disponibilidad del hidrógeno como combustible, especialmente para celdas de combustible, lo hiciera económicamente viable, convirtiendo a los motores de combustión impulsados por hidrógeno en una opción tecnológica atractiva y factible.

En esta situación, las emisiones de NO_x continuarán como uno de los principales contaminantes a mitigar en estos motores, de forma similar a otros vehículos basados en motores de combustión interna. Abordar las emisiones de NO_x en estos motores requiere la implementación de los mismos sistemas de reducción de emisiones de escape que se aplica a los vehículos de combustión tradicionales [197].

Además, hay sectores que abogan por estrategias de descarbonización de la sociedad que abarquen un espectro de tecnologías más amplias, en lugar de priorizar exclusivamente la electrificación del transporte. Sostienen que descartar la tecnología de motores de combustión podría no ser prudente debido a posibles ventajas ambientales.

En una evaluación exhaustiva "de la cuna a la tumba", los motores de combustión podrían exhibir emisiones de CO₂ más bajas y enfrentar menos desafíos en el suministro de materias primas críticas en comparación con los vehículos eléctricos, dependiendo del *mix* energético europeo existente y los contextos nacionales [198]. En consecuencia, se vuelve crucial considerar meticulosamente y analizar científicamente la prolongación de la presencia de estos vehículos dentro de un contexto más amplio de sostenibilidad e impacto ambiental.

Por todo ello, es razonable anticipar que la presencia de vehículos de combustión interna emitiendo NO_x persistirá de manera constante y prominente durante al menos las dos próximas décadas, si no es que se extiende incluso más allá de ese período. Esta proyección se refiere exclusivamente a la Unión Europea, ya que es esperable que, en otras regiones del globo, la longevidad de estos vehículos emisores de NO_x se extienda aún más.

Por lo tanto, la regulación y el control de las emisiones de NO_x provenientes de vehículos de combustión interna a través de la ITV puede ser un instrumento crucial, por una duración extendida de la presencia de estos vehículos, superando las perspectivas iniciales.

La tesis ha demostrado eficazmente que el método propuesto, desde un punto de vista técnico, cumple con los dos requisitos fundamentales para su aplicación práctica en ITV:

1. Los resultados de la medición son fiables y representan con precisión las emisiones reales de NO_x de los vehículos en circulación urbana.

2. Las características del método lo hacen altamente adecuado para su integración en el marco de la ITV: es rápido, sencillo, económico y efectivo.

La integración de la medición de NO_x en el proceso de la ITV, ya sea utilizando este método u otro alternativo, constituiría un desarrollo altamente prometedor. Esta incorporación tiene el potencial de generar mejoras sustanciales y duraderas, especialmente en lo que respecta a la protección de la salud pública a mediano y largo plazo.

Si esta investigación ha ejercido algún tipo de influencia para contribuir a la culminación de este objetivo, esto representaría el logro más destacado del propósito global de la investigación.

12.4. PERSPECTIVAS

Esta investigación no pretende ser un esfuerzo terminado, sino más bien un primer paso en una línea de investigación más amplia. El objetivo es acelerar la implementación de mejoras en el proceso de inspección técnica de vehículos, que permita aumentar su efectividad y fortalecer su papel en la protección del medio ambiente y la salud pública.

Aún más, también se aspira a optimizar la eficiencia de la inspección al minimizar el gasto de recursos, incluyendo tiempo y equipo.

Esta investigación sirve como la base para una búsqueda continua de refinar y mejorar las prácticas de inspección de vehículos, aspirando a los más altos estándares de protección ambiental y eficiencia operativa.

El siguiente proceso de investigación que surge de forma natural de este trabajo implica explorar la viabilidad de integrar la medición de NO_x , utilizando el método propuesto, con la medición de las emisiones de particulado sólido (PN) de los motores. Esto se facilitaría a través de procedimientos de medición de PN en ralentí, como los métodos propuestos recientemente en Bélgica y Alemania. Al combinar

estas mediciones, se podría crear una evaluación más completa de las emisiones durante el proceso de inspección.

Este es un prometedor camino de investigación, al explorar la sincronización entre los procesos de medición de emisiones de particulado sólido (PN) y las condiciones de ralentí propuestas por el método de medición de NO_x. La realización de ambas mediciones mientras el motor está en ralentí abre la posibilidad de llevar a cabo una prueba robusta y sólida. Un enfoque integrado como este ofrecería un ahorro de tiempo considerable al combinar la evaluación de las emisiones de NO_x y PN en un solo proceso.

La perspectiva de armonizar las mediciones de NO_x y PN dentro de una sola prueba tiene una importancia inmensa. Esta innovación podría reducir significativamente el tiempo total de la prueba, al tiempo que mejoraría la detección de vehículos con emisiones elevadas de PN y NO_x durante la ITV. Este enfoque de medición dual podría convertirse en una herramienta fundamental para disminuir las emisiones de contaminantes en entornos urbanos, aliviando así los impactos perjudiciales en la salud pública que se detallan en el Capítulo 1.

Para desarrollar completamente el potencial de este concepto, es esencial llevar a cabo investigaciones adicionales y en profundidad para determinar su viabilidad, precisión e implementación práctica.

Para otra posible vía de investigación, si la propuesta de CITA ante la Comisión para respaldar este método de medición avanza y obtiene aprobación a nivel de la Unión Europea, serían imperativas varias acciones posteriores. Antes de la implementación del método, se requeriría llevar a cabo una serie más extensa de mediciones. Este esfuerzo tiene como objetivo establecer umbrales de rechazo meticulosamente ajustados y definitivos. Estos límites podrían variar según los distintos niveles de emisión, reflejando las diversas características de emisión de varios vehículos.

Además, sería esencial llevar a cabo una evaluación integral de la idoneidad de equipos de medición alternativos. La lógica detrás de este enfoque es evitar depender de un único equipo, asegurando una variedad de opciones viables para la implementación.

Proponer plazos factibles y bien definidos para la ejecución sería otro paso crítico. Estos plazos deben tener en cuenta tanto la preparación de los diferentes organismos reguladores como las capacidades operativas de las instalaciones de inspección (que son distintos en cada país).

Es importante señalar que, si bien el diseño fundamental del método está adaptado para examinar las emisiones de NO_x de los motores de compresión (diésel), aprovechando los principios teóricos fundamentados en sus características de funcionamiento, también se han obtenido resultados prometedores al aplicar el método a vehículos equipados con motores de explosión (gasolina). Sin embargo, sería indispensable realizar una evaluación más extensa de la idoneidad del método para estos motores, allanando el camino para su posible aplicación en este tipo de vehículos también.

Para concluir, también existe una necesidad crítica de explorar la adaptación del método propuesto para vehículos de servicio pesado (camiones y autobuses), ya que

estos vehículos contribuyen significativamente a las emisiones totales de NO_x en entornos urbanos.

El método, tal y como está actualmente definido, podría no ser directamente transferible a estos vehículos debido a que las variaciones relativas en la demanda de potencia en los motores son potencialmente insuficientes con el diseño actual del método. Sin embargo, una investigación dedicada sobre métodos para generar mayores demandas de potencia en los motores de estos vehículos podría abrir el camino hacia la aplicación del mismo concepto de medición. Esto implicará la elaboración de métodos para lograr dos niveles distintos de demanda de potencia mientras el motor está en ralentí, extendiendo así la aplicabilidad del método a vehículos pesados. Este camino de investigación tiene el potencial de mejorar las estrategias de control y medición de emisiones para esta importante fuente de contaminación urbana.

Resumiendo, esta investigación sienta las bases para un abanico de posibles futuros estudios de gran relevancia e importancia, todos intrínsecamente vinculados al bienestar y la salud de la sociedad. Así, también se presentan varias vías para investigaciones adicionales:

- Impactos en la Salud y la Economía: Analizar las posibles repercusiones de implementar este o métodos alternativos de medición de NO_x (y PN) dentro de las inspecciones técnicas periódicas. Esto podría abarcar la cuantificación de la reducción esperada de enfermedades y mortalidad relacionadas con las condiciones medioambientales (exposición a la polución), así como evaluar el impacto económico de la disminución de estos contaminantes atmosféricos, lo que en última instancia conllevaría a ahorros en el sistema de atención médica.
- Implicaciones Económicas: Analizar las repercusiones económicas asociadas con la implementación del método en la Inspección Técnica de Vehículos. Esto podría abarcar la evaluación de los cambios en frecuencias de reparación y sus implicaciones económicas en talleres mecánicos, empresas de fabricación de repuestos, ventas de vehículos nuevos y el mercado de vehículos de segunda mano.
- Efectividad de las Restricciones de Emisiones: Cuantificar la efectividad de las medidas de restricción de emisiones, como el establecimiento de Zonas de Bajas Emisiones (LEZ), a través de una comparación de las emisiones medidas durante la ITV para los vehículos autorizados a circular dentro de estas zonas (por ejemplo, residentes y vehículos de reparto) con los niveles de contaminantes registrados mediante equipos de medición ambiental dentro de estas zonas.
- Análisis Coste-Beneficio Integral: Llevar a cabo un Análisis Coste-Beneficio (ACB) integral de las medidas propuestas o análogas. Dicho análisis debería contemplar todas las diversas áreas de mejora en la salud, ganancias económicas y resultados ambientales mejorados.

El impacto de esta investigación va por tanto más allá de su alcance inmediato, fomentando la perspectiva de futuras investigaciones que puedan influir en decisiones de políticas medioambientales y amplificando los esfuerzos para fortalecer la salud pública, la estabilidad económica y la sostenibilidad ambiental.

12.5. INFLUENCIA Y VISIBILIDAD

Si bien el desarrollo de la tesis representa una labor académica, la participación directa del autor en el campo de la ITV ha facilitado la difusión de los hallazgos de la investigación a los organismos pertinentes encargados de crear, integrar y gestionar los procedimientos de inspección. Esta difusión se ha realizado en varias instancias dentro del ámbito institucional, abarcando tanto la esfera nacional como europea, a través de las cuales el método ha sido compartido.

En primer lugar, en noviembre de 2017 el método fue presentado a miembros del Ministerio de Industria de España en la estación de ITV que GRUPO ITEVELESA tiene en Las Rozas (Madrid).

En mayo de 2018, el método fue presentado públicamente en las XXVII Jornadas Nacionales de ITV, celebradas en Santander (Figure 10-1). Esta presentación destacó los desafíos relacionados con la medición de las emisiones de NO_x al mismo tiempo que presentó los principios utilizados para el diseño y el potencial del método de medición propuesto.

El año siguiente, en octubre de 2019, durante las XXVIII Jornadas Nacionales de ITV celebradas en Zaragoza (Figure 10-2), se mostraron los avances alcanzados en el desarrollo del método hasta ese momento. En esta presentación se detallaron los resultados obtenidos a partir de mediciones realizadas en vehículos en circulación urbana, seguido de una comparación de estos con los resultados generados por el procedimiento de medición propuesto.

A nivel internacional, la primera presentación del método tuvo lugar en la 13^a Conferencia SDEWES celebrada en Palermo en octubre de 2018.

En marzo de 2019, el autor de esta tesis participó activamente en la 15^a reunión del Grupo de Trabajo nº 2 de CITA. Durante esta participación, el autor realizó una exhaustiva presentación ante el grupo de trabajo, presentando el progreso realizado en el desarrollo del método de medición.

Exactamente un año después, en marzo de 2020, los resultados derivados de la campaña de medición que se realizó para validar el método sugerido fueron compartidos con el mismo Grupo de Trabajo nº 2 de CITA. Esta presentación ofreció las perspectivas generadas por los hallazgos de la campaña.

Con el fin de formular la recomendación de CITA sobre la mejor opción para realizar la medición de NO_x en la ITV, este organismo estableció un subgrupo de trabajo dedicado a ello. El mandato de este subgrupo era evaluar las opciones disponibles para la medición de NO_x en el contexto de la ITV y posteriormente definir la postura de CITA sobre la mejor opción para resolver el problema.

Gracias a la difusión de los trabajos realizados, mediante las presentaciones mencionadas anteriormente, el autor de esta tesis tuvo la oportunidad de participar en este grupo de trabajo. En él, colaboró junto a expertos destacados provenientes de diversos sectores relacionados con la ITV, puesto que este grupo incluyó a profesionales que representaban a proveedores de servicios de ITV de múltiples naciones europeas, fabricantes de equipos de ITV, instituciones públicas y entidades indirectamente involucradas, así como a proveedores técnicos de gas.

Dentro de este grupo de trabajo colaborativo, se llevó a cabo un examen exhaustivo de 7 metodologías distintas para la medición de NO_x en ITV a lo largo de múltiples reuniones que abarcaron un año y medio. La culminación de estos esfuerzos resultó en un informe denominado *Position Paper* por parte de CITA [199]. Este documento destaca el método propuesto en esta tesis como el más adecuado entre los examinados en el documento para la medición de NO_x en los vehículos actualmente en circulación. En consecuencia, **se consideró que este método era apto para su integración inmediata en el proceso de ITV a nivel europeo.**

Indudablemente, la afirmación hecha en el *Position Paper* de CITA posee una gran importancia, dada la entidad y autoridad de la organización. El reconocimiento de la validez y viabilidad práctica del método propuesto, demostrada a través de su potencial de implementación en el mundo real, tiene un gran peso, dado que CITA adoptó la conclusión del grupo de trabajo e incorporó formalmente esta postura como la suya propia. Esta crucial aprobación fue presentada el 6 de abril de 2022, durante una reunión híbrida de CITA celebrada en Nitra, Eslovaquia.

En 2020, el método también fue presentado en una reunión con un Oficial de Política de la Comisión Europea, el Dr. Vicente Franco. Esta presentación ofreció una vía para comunicar los detalles y el potencial del método. Además, en octubre de 2021, el método fue expuesto también a miembros del JRC (Joint Research Centre).

Además, el método detallado en esta investigación fue sometido a una evaluación independiente por parte de la Universidad Carlos III de Madrid. Esta evaluación se llevó a cabo en un informe encargado por AECA-ITV, un informe que exploró diversas alternativas para medir NO_x y PM en el contexto de la ITV.

El informe, presentado oficialmente el 20 de abril de 2022, durante la Feria MOTORTEC 2022 celebrada en Madrid, mostró una evaluación favorable de los resultados obtenidos mediante la aplicación de este método. El informe comparó sus hallazgos con los derivados de otros métodos más "convencionales", como las mediciones en banco de rodillos. Como dato destacado, el informe enfatizó las ventajas del método tal como se detalla a lo largo de la tesis, en cuanto a su idoneidad para integrarse en el proceso de ITV [150]. Esta evaluación puso de relieve la conclusión de que un enfoque de medición estática con aplicación de carga destaca como la opción más preferible y efectiva para llevar a cabo mediciones de NO_x en el contexto de la ITV.

En otro esfuerzo paralelo no relacionado con esta investigación, GOCA Vlaanderen en Bélgica llevó a cabo una investigación independiente que involucró varios métodos para la medición de NO_x en ITV. Esta investigación, que culminó en un informe presentado en agosto de 2022 [149], incluyó varios métodos examinados en detalle, incluyendo el método presentado en esta tesis, y arrojando resultados favorables. Es notable que GOCA Vlaanderen es una organización con una considerable experiencia en la evaluación e implementación de métodos de inspección en el contexto de la ITV, y que ya había sido responsable de evaluar e incorporar procedimientos de medición de PN en Bélgica en 2022.

Hasta hace poco, la opinión generalizada era que las mediciones en banco de rodillos representaban la cúspide de la técnica para evaluar las emisiones reales de NO_x de un vehículo. Sin embargo, en los últimos años se ha generado un conjunto

significativo de literatura científica que rebate esta perspectiva. Esto es especialmente evidente comparando los resultados observados a partir de los ciclos NEDC (New European Driving Cycle) y WLTP (Worldwide Harmonized Light Vehicles Test Procedure), ambos muy sofisticados y meticulosamente realizados, y los niveles reales de emisiones exhibidos por los vehículos en condiciones reales de circulación.

La aparición de metodologías como la definida en esta investigación, junto con otras que probablemente surjan basadas en otros datos disponibles de los vehículos, ha puesto de manifiesto las insuficiencias de un sistema de medición en ITV dependiente de la tecnología de banco de rodillos. Además de ser económicamente insostenibles y demandantes de excesivos recursos (en términos de tiempo y personal), las mediciones basadas en banco de rodillos se han demostrado menos representativas que otros métodos de medición alternativos.

En lo que respecta a la identificación de manipulaciones o fallos relacionados con las emisiones de NO_x en vehículos, no existe evidencia concluyente que respalde la superioridad de las mediciones en banco de rodillos ni demuestre ventajas inherentes sobre métodos alternativos.

Un estudio realizado en Alemania [147] llegó a la conclusión de que el uso de un banco dinamométrico era más sensible para identificar casos de manipulación o mal funcionamiento, sugiriendo una medida numérica como indicador de la sensibilidad del método en relación con la disparidad de emisiones entre un vehículo manipulado y uno no manipulado.

Sin embargo, este análisis se enfrenta a un problema fundamental. En el contexto de la ITV, no se sabe de antemano si un vehículo ha sido manipulado. Por lo tanto, al carecer de un valor de referencia preestablecido para la comparación, se vuelve imposible deducir solo a partir del resultado de la prueba si un vehículo ha sido manipulado. Este desafío surge debido a la considerable variabilidad exhibida por las emisiones de NO_x en respuesta a alteraciones en las condiciones de la prueba.

Ciertamente, este desafío es igualmente aplicable a cualquier técnica de medición. Sin embargo, el método expuesto en esta investigación, como se explica a lo largo de la tesis, posee una notable ventaja al mitigar significativamente las variables capaces de influir en los resultados de la medición. Por lo tanto, este método reduce la variabilidad inherente en los resultados de la medición.

En resumen, el método de medición de NO_x propuesto en esta tesis, aunque requerirá un mayor refinamiento para su aplicación efectiva, ha ejercido una influencia sustancial tanto a nivel nacional como europeo. Ha introducido una perspectiva novedosa en la medición de NO_x en el contexto de la ITV, a pesar de las limitaciones intrínsecas asociadas con su ejecución.

Por último, cabe señalar que la investigación ha generado documentación relevante que contribuye a su visibilidad. Entre estos documentos se incluye la publicación por parte del investigador de dos *papers* revisados por pares. Uno de ellos fue publicado en 2021 y describe el método propuesto para medir NO_x en la ITV [175], y otro fue publicado en 2022, evaluando la idoneidad del equipo utilizado para la medición de NO_x en la ITV [180]. Estos documentos están incluidos en esta tesis como productos directos generados por la investigación.

Además, los documentos mencionados anteriormente en esta sección (principalmente el *Position Paper* de CITA [199], así como el informe de la Universidad Carlos III [150], y el informe de GOCA Vlaanderen[149]) también contribuyen a la visibilidad del método propuesto.

Para concluir, la visibilidad proporcionada por la difusión de información sobre el desarrollo del método propuesto en los diversos foros mencionados ha llevado al autor a ser invitado como ponente en varios eventos, en calidad de experto en emisiones de vehículos de combustión y su control a través de la ITV.

Entre los eventos más recientes, cabe destacar la participación del autor como ponente en una serie de *Split Sessions* durante la Conferencia Internacional de CITA de 2023, celebrada en Róterdam del 6 al 8 de junio de 2023 (Figure 10-3).

Adicionalmente, el autor también participó en la conferencia "*Vehicle Inspection and Society: Beyond Technology*" organizada conjuntamente por CITA y la Presidencia Española del Consejo de la Unión Europea, celebrada en Bruselas el 26 de septiembre de 2023 (Figure 10-4).

CHAPTER 13

REFERENCES

13. REFERENCES

- [1] EEA, "Air quality in Europe 2021 Key messages." Accessed: Feb. 18, 2022. [Online]. Available: <https://www.eea.europa.eu/publications/air-quality-in-europe-2021>
- [2] I. A. Reşitoglu, K. Altınışik, and A. Keskin, "The pollutant emissions from diesel-engine vehicles and exhaust aftertreatment systems," *Clean Technol Environ Policy*, vol. 17, no. 1, pp. 15–27, 2015, doi: 10.1007/s10098-014-0793-9.
- [3] N. Hooftman, M. Messagie, J. van Mierlo, and T. Coosemans, "A review of the European passenger car regulations – Real driving emissions vs local air quality," *Renewable and Sustainable Energy Reviews*, vol. 86. Elsevier Ltd, pp. 1–21, Apr. 01, 2018. doi: 10.1016/j.rser.2018.01.012.
- [4] EEA, "Sources and emissions of air pollutants in Europe — European Environment Agency." Accessed: Feb. 18, 2022. [Online]. Available: <https://www.eea.europa.eu/publications/air-quality-in-europe-2021/sources-and-emissions-of-air>
- [5] T. Lee, J. Park, S. Kwon, J. Lee, and J. Kim, "Variability in operation-based NO_x emission factors with different test routes, and its effects on the real-driving emissions of light diesel vehicles," *Science of the Total Environment*, vol. 461–462, no. 2, pp. 377–385, 2013, doi: 10.1016/j.scitotenv.2013.05.015.
- [6] X. Wang *et al.*, "On-road diesel vehicle emission factors for nitrogen oxides and black carbon in two Chinese cities," *Atmos Environ*, vol. 46, pp. 45–55, 2012, doi: 10.1016/j.atmosenv.2011.10.033.
- [7] R. O'Driscoll, M. E. J. Stettler, N. Molden, T. Oxley, and H. M. ApSimon, "Real world CO₂ and NO_x emissions from 149 Euro 5 and 6 diesel, gasoline and hybrid passenger cars," *Science of the Total Environment*, vol. 621, no. x, pp. 282–290, 2018, doi: 10.1016/j.scitotenv.2017.11.271.
- [8] G. A. Bishop and D. H. Stedman, "Reactive Nitrogen Species Emission Trends in Three Light-/Medium-Duty United States Fleets," *Environ Sci Technol*, vol. 49, no. 18, pp. 11234–11240, Sep. 2015, doi: 10.1021/acs.est.5b02392.
- [9] Agency for Toxic Substances and Disease Registry, "NITROGEN OXIDES (nitric oxide, nitrogen dioxide, etc.) CAS #10102-43-9 (nitric oxide); CAS #10102-44-0 (nitrogen dioxide)," U.S. Department of Health and Human Services, Apr. 2002. [Online]. Available: <http://www.atsdr.cdc.gov/toxfaq.html>
- [10] N. Morris, K. Lynch, and S. A. Greenberg, "Severe Motor Neuropathy or Neuronopathy due to Nitrous Oxide Toxicity after Correction of Vitamin B12 Deficiency," *Muscle Nerve*, vol. 51, no. 4, pp. 614–616, 2015.
- [11] World Health Organization. Occupational and Environmental Health Team., "WHO Air quality guidelines for particulate matter, ozone, nitrogen dioxide and sulfur dioxide : global update 2005 : summary of risk assessment," 2006. [Online]. Available: <https://apps.who.int/iris/handle/10665/69477>
- [12] F. de Leeuw, A. González Ortiz, and C. Guerreiro, "Air quality in Europe — 2017 report," *Publications Office of the European Union*, no. 13, p. 74, 2017, doi: 10.2800/850018.

- [13] "Global Burden of Disease (BGD)," Institute for Health Metrics and Evaluation. Accessed: Nov. 11, 2022. [Online]. Available: <http://www.healthdata.org/gbd/2019>
- [14] E. Mulholland, J. Miller, Y. Bernard, K. Lee, and F. Rodríguez, "The role of NO_x emission reductions in Euro 7 / VII vehicle emission standards to reduce adverse health impacts in the EU27 through 2050," *Transportation Engineering*, vol. 9, no. x, p. 100133, 2022, doi: 10.1016/j.treng.2022.100133.
- [15] EEA, "Air quality in Europe - 2020 report," 2020, doi: 10.2800/786656.
- [16] World Health Organization. Occupational and Environmental Health Team., "WHO global air quality guidelines. Particulate matter (PM_{2.5} and PM₁₀), ozone, nitrogen dioxide, sulfur dioxide and carbon monoxide.," Geneva, 2021. [Online]. Available: <https://apps.who.int/iris/handle/10665/345329>
- [17] EEA, "Health impacts of air pollution in Europe 2021." Accessed: Feb. 19, 2022. [Online]. Available: <https://www.eea.europa.eu/publications/air-quality-in-europe-2021/health-impacts-of-air-pollution>
- [18] I. Assessment, "EEA Nitrogen oxides (NO_x) emissions assesment," 2014. Accessed: Jul. 28, 2019. [Online]. Available: <https://www.eea.europa.eu/data-and-maps/indicators/eea-32-nitrogen-oxides-nox-emissions-1/assessment.2010-08-19.0140149032-3>
- [19] EEA, "EMEP/EEA air pollutant emission inventory guidebook 2016: Technical guidance to prepare national emission inventories," *EEA Technical report*, no. 09/30/2016, 2016, doi: 10.2800/92722.
- [20] EEA, "Air quality in Europe - 2018 report," 2018, doi: 10.2800/777411.
- [21] EEA, "Air quality in Europe — 2019 report," 2019, doi: 10.2800/822355.
- [22] J. TAN *et al.*, "Chemical characteristics of PM_{2.5} during a typical haze episode in Guangzhou," *Journal of Environmental Sciences*, vol. 21, no. 6, pp. 774–781, 2009, doi: 10.1016/S1001-0742(08)62340-2.
- [23] M. Jia *et al.*, "Inverse Relations of PM_{2.5} and O₃ in air compound pollution between cold and hot seasons over an urban area of East China," *Atmosphere (Basel)*, vol. 8, no. 3, pp. 1–12, 2017, doi: 10.3390/atmos8030059.
- [24] T. Larssen *et al.*, "Acid deposition and its effects in China: An overview," *Environ Sci Policy*, vol. 2, no. 1, pp. 9–24, 1999, doi: 10.1016/S1462-9011(98)00043-4.
- [25] L. Garcés and M. Hernández, "La lluvia ácida: un fenómeno fisicoquímico de ocurrencia local," *Rev Lasallista Investig*, vol. 1, no. 2, pp. 67–72, 2004. Accessed: Nov. 29, 2021. [Online]. Available: <http://www.redalyc.org/articulo.oa?id=69510211>
- [26] S. Khomenko *et al.*, "Premature mortality due to air pollution in European cities: a health impact assessment," *Lancet Planet Health*, vol. 5, no. 3, pp. e121–e134, Mar. 2021, doi: 10.1016/S2542-5196(20)30272-2.
- [27] D. C. Carshaw, S. D. Beevers, J. E. Tate, E. J. Westmoreland, and M. L. Williams, "Recent evidence concerning higher NO_x emissions from passenger cars and

- light duty vehicles," *Atmos Environ*, vol. 45, no. 39, pp. 7053–7063, 2011, doi: 10.1016/j.atmosenv.2011.09.063.
- [28] M. L. Williams and D. C. Carslaw, "New Directions: Science and policy - Out of step on NO_x and NO₂?", *Atmos Environ*, vol. 45, no. 23, pp. 3911–3912, 2011, doi: 10.1016/j.atmosenv.2011.04.067.
- [29] S. K. Hoekman and C. Robbins, "Review of the effects of biodiesel on NO_x emissions," *Fuel Processing Technology*, vol. 96, pp. 237–249, 2012, doi: 10.1016/j.fuproc.2011.12.036.
- [30] M. Pujadas, A. Domínguez-Sáez, and J. de la Fuente, "Real-driving emissions of circulating Spanish car fleet in 2015 using RSD Technology," *Science of The Total Environment*, vol. 576, pp. 193–209, 2017, doi: 10.1016/j.scitotenv.2016.10.049.
- [31] Y. Chen and J. Borken-Kleefeld, "Real-driving emissions from cars and light commercial vehicles - Results from 13 years remote sensing at Zurich/CH," *Atmos Environ*, vol. 88, pp. 157–164, 2014, doi: 10.1016/j.atmosenv.2014.01.040.
- [32] S. Hausberger, M. Rexeis, M. Zallinger, and R. Luz, "Emission Factors from the Model PHEM for the HBEFA Version 3," *University of Technology, Graz, Report*, vol. Nr. I-20/2, no. Haus-Em 33/08/679, p. 76, 2009, [Online]. Available: <http://scholar.google.com/scholar?hl=en&btnG=Search&q=intitle:Emission+Factors+from+the+Model+PHEM+for+the+HBEFA+Version+3#1>
- [33] G. Triantafyllopoulos, A. Dimaratos, L. Ntziachristos, Y. Bernard, J. Dornoff, and Z. Samaras, "A study on the CO₂ and NO_x emissions performance of Euro 6 diesel vehicles under various chassis dynamometer and on-road conditions including latest regulatory provisions," *Science of the Total Environment*, vol. 666, pp. 337–346, May 2019, doi: 10.1016/j.scitotenv.2019.02.144.
- [34] A. Ramos, J. Muñoz, F. Andrés, and O. Armas, "NO_x emissions from diesel light duty vehicle tested under NEDC and real-world driving conditions," *Transp Res D Transp Environ*, vol. 63, no. April, pp. 37–48, 2018, doi: 10.1016/j.trd.2018.04.018.
- [35] M. Weiss *et al.*, "Will Euro 6 reduce the NO_x emissions of new diesel cars? - Insights from on-road tests with Portable Emissions Measurement Systems (PEMS)," *Atmos Environ*, vol. 62, no. 2, pp. 657–665, 2012, doi: 10.1016/j.atmosenv.2012.08.056.
- [36] J. Pielecha, J. Merkisz, J. Markowski, and J. Remigiusz, "Analysis of Passenger Car Emission Factors in RDE Tests," *Web of Conferences*, vol. 10, no. 00073, pp. 1–7, 2016, doi: 10.1051/c3sconf/2016101000073.
- [37] V. Franco and P. Mock, "ICCT Real driving Emissions: Challenges to Regulating Diesel Engines in Europe," in *Anil Agarwal Dialogue*, New Delhi, 2015, p. 33.
- [38] V. Franco, F. Posada Sánchez, J. German, and P. Mock, "ICCT Real-world exhaust emissions from modern diesel cars. A meta-analysis of PEMS emissions data from EU (Euro 6) and US (Tier 2 Bin 5/ULEV II) diesel passenger cars. Part 1: Aggregated results," *The International Council on Clean Transportation*, no. October, p. 59, Oct. 2014, [Online]. Available:

- http://www.theicct.org/sites/default/files/publications/ICCT_PEMS-study_diesel-cars_20141010.pdf
- [39] B. Degraeuwe and M. Weiss, "Does the New European Driving Cycle (NEDC) really fail to capture the NO_x emissions of diesel cars in Europe?," *Environmental Pollution*, no. X, pp. 1–8, 2016, doi: 10.1016/j.envpol.2016.12.050.
- [40] G. J. Thompson, D. K. Carder, M. C. Besch, A. Thiruvengadam, H. K. Kappanna, and F. Posada, "In-Use Emissions Testing of Light-Duty Diesel Vehicles in the United States," Morgantown, May 2014.
- [41] M. Rexeis, S. Hausberger, J. Köhlwein, and R. Luz, "Update of Emission Factors for EURO 5 and EURO 6 vehicles for the HBEFA Version 3.3," *University of Technology, Graz, Report Nr. I-31/2013 Rex-EM-I*, vol. 43, no. 316, pp. 1–31, 2013, doi: Report No. I-25/2013/ Rex EM-I 2011/20 679.
- [42] J. Poliscanova, "Diesel, the true (dirty) story," *Transport & Environment*, p. 63, Sep. 2017, [Online]. Available: https://www.transportenvironment.org/wp-content/uploads/2021/07/2017_09_Diesel_report_final.pdf
- [43] C. Air Resources Board - Mobile Source Control Division, "Facts about the Low NO_x Heavy-Duty Omnibus Regulation Proposed regulation will ensure reductions in smog-forming NO_x, protect communities most impacted by air pollution." 2021. Accessed: Feb. 27, 2022. [Online]. Available: https://ww2.arb.ca.gov/sites/default/files/classic/msprog/hdlownox/files/HD_NOx_Omnibus_Fact_Sheet.pdf
- [44] L. Yang, V. Franco, A. Campestrini, J. German, and P. Mock, "NO_x control technologies for Euro 6 diesel passenger cars: Market penetration and experimental performance assessment (white paper)," *International Council on Clean Transportation*, vol., no. X, p. 29, 2015.
- [45] V. BOURGEOIS and Eurostat, "Just over 40% of the EU population lives in cities Urban population in the Nordic Member States most satisfied with public spaces," Oct. 2015. Accessed: Feb. 27, 2021. [Online]. Available: <https://ec.europa.eu/eurostat/documents/2995521/7020151/3-05102015-BP-EN.pdf/bf18a8b3-998c-476d-b3af-58292b89939b>
- [46] EEA, "National emissions reported to the Convention on Long-range Transboundary Air Pollution (LRTAP Convention)." 2021. [Online]. Available: <https://www.eea.europa.eu/data-and-maps/data/national-emissions-reported-to-the-convention-on-long-range-transboundary-air-pollution-lrtap-convention-15>
- [47] E. Commission and D.-G. for M. and Transport, *EU transport in figures: statistical pocketbook 2020*. Publications Office of the European Union, 2020. doi: doi/10.2832/491038.
- [48] European Commission, "Commission Regulation (EU) 2017/1151," *Official Journal of the European Union*, no. 692, pp. 1–643, 2017, Accessed: Dec. 03, 2021. [Online]. Available: <https://eur-lex.europa.eu/legal-content/EN/TXT/PDF/?uri=CELEX:32017R1151&from=ES>
- [49] European Commission, "Commission Regulation (EU) 2017/1154," *Official Journal of the European Union*, no. 715, pp. 708–732, 2017, Accessed: Dec. 03,

2021. [Online]. Available: <https://eur-lex.europa.eu/legal-content/EN/TXT/PDF/?uri=CELEX:32017R1154&from=ES>
- [50] P. Söderena *et al.*, "Monitoring Euro 6 diesel passenger cars NOx emissions for one year in various ambient conditions with PEMS and NOx sensors," *Science of the Total Environment*, vol. 746, Dec. 2020, doi: 10.1016/j.scitotenv.2020.140971.
- [51] J. European Union, "COMMISSION REGULATION (EU) 2017/1347 of 13 July 2017," *Official Journal of the European Union*, vol. L192, pp. 1–22, 2017, Accessed: Dec. 03, 2021. [Online]. Available: <https://eur-lex.europa.eu/legal-content/EN/TXT/PDF/?uri=CELEX:32017R1347&from=ES>
- [52] Y. I. Zhang, D. H. Stedman, G. A. Bishop, P. L. Guenther, and S. P. Beaton, "Worldwide On-Road Vehicle Exhaust Emissions Study by Remote Sensing," *Environ Sci Technol*, vol. 29, no. 9, pp. 2286–2294, 1995. [Online]. Available: <https://pubs.acs.org/sharingguidelines>
- [53] Roadworthiness package Commission Staff Working Paper and European Commission, "Impact Assessment SWD(2012) 206 final," Brussels (Belgium), SWD(2012) 206 final, 2012. Accessed: Dec. 03, 2021. [Online]. Available: https://ec.europa.eu/transport/road_safety/sites/default/files/pdf/road_worthiness_package/impact_assessment_study_en.pdf
- [54] CITA, "AUTOFORE: Study on the Future Options for Roadworthiness Enforcement in the European Union," 2007. [Online]. Available: https://citainsp.org/wp-content/uploads/2016/01/Autofore_Final_report_without_links.pdf
- [55] The European Commission, "Road Safety : The Roadworthiness Package – Tougher vehicle checks to save lives," *Spokespersons' Service*, no. MEMO/12/555, p. 9, 2012, Accessed: Dec. 02, 2021. [Online]. Available: https://ec.europa.eu/commission/presscorner/api/files/document/print/en/memo_12_555/MEMO_12_555_EN.pdf
- [56] The Council of the European Communities and European Parliament, "Directive 2014/45/EU of 3 April 2014 on periodic roadworthiness tests for motor vehicles and their trailers and repealing Directive 2009/40/EC," *Official journal of the European Union*, vol. 127, pp. 51–128, 2014, [Online]. Available: <http://eur-lex.europa.eu/legal-content/EN/TXT/PDF/?uri=CELEX:32014L0045&from=HR>
- [57] Gobierno de España, "RD 920/2017 por el que se regula la inspección técnica de vehículos," *BOE (Boletín Oficial del Estado)*, vol. 271, no. I, pp. 107068–107133, 2017, doi: BOE-A-2012-5403.
- [58] G. de E. Ministerio de Industria, Comercio y Turismo, "MANUAL DE PROCEDIMIENTO DE INSPECCION DE ESTACIONES ITV Versión 7.4.1," *Catálogo de Publicaciones de la Administración General del Estado*, p. 654, 2020, [Online]. Available: <https://publicacionesoficiales.boe.es/>
- [59] P. Boulter *et al.*, "TEDDIE: A new roadworthiness emission test for diesel vehicles involving NO, NO₂ and PM measurements, Final Report," *Cita*, no. 1, pp. 1–105, 2011, [Online]. Available: https://citainsp.org/wp-content/uploads/2016/01/teddie_final_report.pdf

- [60] T. Barlow *et al.*, "CITA PROJECT: SET – Sustainable Emissions Test: Final Report," Brussels, Sep. 2015. [Online]. Available: www.citainsp.org
- [61] P. Buekenhoudt *et al.*, "CITA SET II Project, Sustainable Emission Test for diesel vehicles involving NO_x measurements, Final Report," Brussels (Belgium), Jan. 2019.
- [62] P. Buekenhoudt *et al.*, "CITA SET II Project, Sustainable Emission Test for diesel vehicles involving NO_x measurements, Annexes to the Final Report," Brussels (Belgium), Jan. 2019.
- [63] S. Ro, J. Park, M. Shin, and J. Lee, "Developing on-road nox emission factors for euro 6b light-duty diesel trucks in korean driving conditions," *Energies (Basel)*, vol. 14, no. 4, 2021, doi: 10.3390/en14041041.
- [64] R. Verbeek, R. Vermeulen, W. Vonk, and H. Dekker, "Real world NO_x emissions of Euro V vehicles (MON-RPT-2010-02777)," Delft, 2010.
- [65] A. M. Gómez Amador, J. L. San Román García, and V. Díaz López, "Contribución de la Inspección Técnica de Vehículos (ITV) a la seguridad vial y al medioambiente," Madrid, 2022.
- [66] Y. Chen and J. Borken-Kleefeld, "NO_x Emissions from Diesel Passenger Cars Worsen with Age," *Environ Sci Technol*, p. 10, 2016, doi: 10.1021/acs.est.5b04704.
- [67] Y. Zeldovich, "The oxidation of nitrogen in combustion explosions," in *Acta Physicochimica USSR*, 1946, pp. 577–628.
- [68] C. P. Fenimore and G. W. Jones, "Nitric oxide decomposition at 2200–2400K," *J Phys Chem*, vol. 61, pp. 654–657, 1957, doi: <https://doi.org/10.1021/j150551a034>.
- [69] O. K. Obayes, M. Aldhaidhawi, and M. Najee, "Effect of cylinder head temperature on performance and emissions of a spark ignition engine operating on different fuels," 2023, p. 050022. doi: 10.1063/5.0136366.
- [70] M. Semakula and P. F. Inambao, "The Formation, Effects and Control of Oxides of Nitrogen in Diesel Engines," *International Journal of Applied Engineering Research*, vol. 13, no. 6, pp. 3200–3209, 2018, [Online]. Available: <http://www.ripublication.com3200>
- [71] Moats and Ryan Delacy, "FORMATION OF NO_x DURING FUEL OIL COMBUSTION," 1974.
- [72] J. J. Chong, A. Tsolakis, S. S. Gill, K. Theinnoi, and S. E. Golunski, "Enhancing the NO₂/NO_x ratio in compression ignition engines by hydrogen and reformat combustion, for improved aftertreatment performance," *Int J Hydrogen Energy*, vol. 35, no. 16, pp. 8723–8732, 2010, doi: 10.1016/j.ijhydene.2010.06.008.
- [73] C. D. Rakopoulos and G. C. Mavropoulos, "Experimental instantaneous heat fluxes in the cylinder head and exhaust manifold of an air-cooled diesel engine," *Energy Convers Manag*, vol. 41, no. 12, pp. 1265–1281, 2000, doi: 10.1016/S0196-8904(99)00179-X.

- [74] M. A. Ghadikolaei, L. Wei, C. S. Cheung, and K. F. Yung, "Effects of engine load and biodiesel content on performance and regulated and unregulated emissions of a diesel engine using contour-plot map," *Science of the Total Environment*, vol. 658, pp. 1117–1130, 2019, doi: 10.1016/j.scitotenv.2018.12.270.
- [75] M. Nowak, Ł. Rymaniak, P. Fuć, M. Andrzejewski, and P. Daszkiewicz, "Gaseous compounds and particulate matter exhaust emission measurements from light duty vehicle in real driving conditions.," *Autobusy*, no. 12, pp. 327–331, 2017.
- [76] W. W. Pulkrabek, *Engineering Fundamentals of the Internal Combustion Engine*. Upper Saddle River, NJ: Pearson Prentice Hall, 2014.
- [77] C. T. Bowman, "Control of Combustion-Generated Nitrogen Oxide Emissions: Technology Driven by Regulation," in *Twenty Fourth Symposium (International) on Combustion*, Pittsburgh: The Combustion Institute, 1992.
- [78] P. Cabrera, "Aplicación de la medida de NOx para el control de motores diesel sobrealimentados," 2013.
- [79] R. C. Flagan and J. H. Seinfeld, *Pollutant formation and control in combustion. i Fundamentals of air pollution engineering*. Englewood Cliffs, USA: Prentice-Hall, 1988.
- [80] British Standard, "BS ISO 15031-5:2006 Road vehicles — Communication between vehicle and external equipment for emissions related diagnosis, Part 5: Emissions-related diagnostic services," *British Standard*, no. 15031-5:2006, Art. no. 15031-5:2006, 2006.
- [81] The European Parliament and the Council of the European Union, "DIRECTIVE 98/69/EC OF THE EUROPEAN PARLIAMENT AND OF THE COUNCIL of 13 October 1998 relating to measures to be taken against air pollution by emissions from motor vehicles and amending Council Directive 70/220/EEC," *Official Journal of the European Communities*, vol. L350, pp. 1–56, 1998.
- [82] E. P. Management, "NGA 2000 Heated NO / NO x Analyzer Module Wet Chemiluminescence Detection (WCLD)," *Rosemount Analytical Inc.* Emerson Process Management Rosemount Analytical Inc., Solon, Ohio, USA, pp. 1–8, 2006.
- [83] S. Gluck, C. Glenn, T. Logan, B. Vu, M. Walsh, and P. Williams, "Evaluation of nox flue gas analyzers for accuracy and their applicability for low-concentration measurements," *J Air Waste Manage Assoc*, vol. 53, no. 6, pp. 749–758, 2003, doi: 10.1080/10473289.2003.10466208.
- [84] R. Suarez-Bertoa *et al.*, "On-road emissions of Euro 6d-TEMP passenger cars on Alpine routes during the winter period," *Environmental Science: Atmospheres*, vol. 1, no. 3, pp. 125–139, Feb. 2021, doi: 10.1039/d0ea00010h.
- [85] R. Higashi, Y. Taniguchi, K. Akao, K. Koizumi, N. Hirayama, and Y. Nakano, "A NOx and SO2 gas analyzer using deep-UV and violet light-emitting diodes for continuous emissions monitoring systems," *Proceedings os SPIE - The INternational Society for Optical Engineering*, vol. 9003, no. June 2015, p. 7, 2014, doi: 10.1117/12.2036159.

- [86] B. Giechaskiel and M. Clairotte, "Fourier Transform Infrared (FTIR) Spectroscopy for measurements of vehicle exhaust emissions: A review," *Applied Sciences (Switzerland)*, vol. 11, no. 16, 2021, doi: 10.3390/app11167416.
- [87] J. M. Rheaume, "Solid State Electrochemical Sensors for Nitrogen Oxide (NO_x) Detection in Lean Exhaust Gases," 2010. [Online]. Available: <https://escholarship.org/uc/item/98384265>
- [88] M. Campolo, A. Sclabi, and D. Molin, "TEDDIE project - Final report," 2010.
- [89] The Council of the European Communities, "Directive 72/306/EEC of 2 August 1972 on the approximation of the laws of the Member States relating to the measures to be taken against the emission of pollutants from diesel engines for use in vehicles," *Official Journal of the European Communities*, vol. 190, no. 1, pp. 889–908, Aug. 1972.
- [90] KNESTEL, "Kick-Down NO_x White Paper. Innovative NO_x measurement method for cycling exhaust emission testing." KNESTEL Technologie & Elektronik GmbH, Hopferbach. [Online]. Available: <https://knestel.de/en/solutions/automotive/kick-down-nox-measurement/>
- [91] Z. Samaras and T. Zachariadis, "The Inspection of In-Use Cars in Order to Attain Minimum Emissions of Pollutants and Optimum Energy Efficiency, LAT Report 9502," *Laboratory of Applied Thermodynamics/Aristotle University Thessaloniki*, vol. LAT, no. Report 9502, p. 45, 1995, Accessed: Dec. 02, 2021. [Online]. Available: <https://ec.europa.eu/environment/archives/air/pollutants/inusecars1.pdf>
- [92] J. Norris, "Low Emission Diesel Research CP17/18/770 Phase 3-Report," *AEA Technology*, no. netcen/ED48626P3/Issue 1, p. 63, Feb. 2005.
- [93] P. Anyon *et al.*, *Proposed Diesel Vehicle Emissions National Environment Protection Measure Preparatory Work. In-Service Emissions Performance - Drive Cycles. Volume 1*. Adelaide: National Environment Protection Council Service Corporation, 2000. Accessed: Dec. 07, 2021. [Online]. Available: <http://www.nepc.gov.au>
- [94] EPA (United States Environmental Protection Agency), "Acceleration Simulation Mode Test Procedures, Emission Standards, Quality Control Requirements, and Equipment Specifications - Final Technical Guidance (EPA-420-B-04-011, July 2004)," Jul. 2004. Accessed: Dec. 02, 2021. [Online]. Available: <https://nepis.epa.gov/Exe/ZyNET.exe/P10006DI.TXT?ZyActionD=ZyDocument&Client=EPA&Index=2000+Thru+2005&Docs=&Query=&Time=&EndTime=&SearchMethod=1&TocRestrict=n&Toc=&TocEntry=&QField=&QFieldYear=&QFieldMonth=&QFieldDay=&IntQFieldOp=0&ExtQFieldOp=0&XmlQuery=&File=D%3A%5Czyfiles%5CIndex%20Data%5C00thru05%5Ctxt%5C00000013%5CP10006DI.txt&User=ANONYMOUS&Password=anonymous&SortMethod=h%7C-&MaximumDocuments=1&FuzzyDegree=0&ImageQuality=r75g8/r75g8/x150y150g16/i425&Display=hpfr&DefSeekPage=x&SearchBack=ZyActionL&Back=ZyActionS&BackDesc=Results%20page&MaximumPages=1&ZyEntry=1&SeekPage=x&ZyPURL#>

- [95] Technical Committee : ISO/TC 22 Road vehicles, "ISO 7644:1988 Road vehicles — Measurement of opacity of exhaust gas from compression-ignition (diesel) engines — Lug-down test," *International Organization for Standardization*, 1988, Accessed: Dec. 02, 2021. [Online]. Available: <https://www.iso.org/standard/14461.html>
- [96] ICCT, "China's vehicle emissions inspection and maintenance program," *International Council on Clean Transportation*, no. December, 2020. Accessed: Sep. 05, 2023. [Online]. Available: <https://theicct.org/wp-content/uploads/2021/06/China-IM-policy-update-dec2020.pdf>
- [97] The Council of the European Communities, "Directive 70/220/EEC of 20 March 1970 on the approximation of the laws of the Member States relating to measures to be taken against air pollution by gases from positive-ignition engines of motor vehicles," 1970. Accessed: Dec. 07, 2021. [Online]. Available: <https://eur-lex.europa.eu/legal-content/EN/TXT/PDF/?uri=CELEX:31970L0220&from=EN>
- [98] W. M. Pidgeon *et al.*, "Evaluation of a Four-Mode Steady-State Test with Acceleration Simulation Modes as an alternative Inspection and Maintenance Test for Enhanced I/M Programs," Ann Arbor, MI, May 1993.
- [99] J. Gieseke and G.-J. Gerbrandy, "Working Document No . 11 on the inquiry into emission measurements in the automotive sector –Appendix D: Timeline," *Committee of Inquiry into Emission Measurements in the Automotive Sector*, no. PE594.081v01-00, p. 13, 2016, Accessed: Dec. 07, 2021. [Online]. Available: https://www.europarl.europa.eu/doceo/document/EMIS-DT-594081_EN.pdf?redirect
- [100] European Parliament and Council of the European Union, "Regulation (EC) No 443/2009 of 23 April 2009 setting emission performance standards for new passenger cars as part of the Community's integrated approach to reduce CO₂ emissions from light-duty vehicles," *Official Journal of the European Union*, vol. 140, no. 1, pp. 1–15, 2009, doi: 10.1524/zkri.2009.1105.
- [101] E. C. for E. of the U. N. (UN/ECE), "Regulation No 101 - Uniform provisions concerning the approval of passengers cars equipped with an internal combustio engine with regard to the measurement of the emissio of carbon dioxide and fuel consumption an of categories M1 and N1 vehicles equipped ,," *Official Journal of the European Union*, vol. 4, no. 101, pp. 89–139, 2004.
- [102] UN/ECE, "UN/ECE Regulation No 83 of the Economic Commission for Europe of the United Nations (UN/ECE) – Uniform provisions concerning the approval of vehicles with regard to the emission of pollutants according to engine fuel requirements," *Official Journal or the European Union*, vol. L 375, pp. 223–495, Dec. 2006, Accessed: Aug. 29, 2022. [Online]. Available: [http://data.europa.eu/eli/reg/2006/83\(2\)/oj](http://data.europa.eu/eli/reg/2006/83(2)/oj)
- [103] E. Commission, "Commission Regulation (EU) 2016/427 of 10 March 2016 amending Regulation (EC) No 692/2008 as regards emissions from light passenger and commercial vehicles (Euro 6)," *Official journal of the European Union*, vol. 82, no. 31/03/2016, pp. 1–98, 2016, [Online]. Available: <http://data.europa.eu/eli/reg/2016/427/oj>

- [104] The European Commission, "Commission Regulation (EU) 2016/646 of 20 April 2016 amending Regulation (EC) No 692/2008 as regards emissions from light passenger and commercial vehicles (Euro 6)," *Official Journal of the European Union*, vol. 109, no. 1, pp. 1–22, 2016, [Online]. Available: <http://data.europa.eu/eli/reg/2016/646/oj>
- [105] United Nations, "GTR 15 - Global Registry Worldwide harmonized Light vehicles Test Procedure," *Global Registry*, no. 15, pp. 17, 49–58, 2014, [Online]. Available: <http://www.unece.org/fileadmin/DAM/trans/main/wp29/wp29r-1998agr-rules/ECE-TRANS-180a15e.pdf>
- [106] V. Franco García, "Evaluation and improvement of road vehicle pollutant emission factors based on instantaneous emissions data processing," Valencia. [Online]. Available: <https://www.researchgate.net/publication/263843116>
- [107] G. Fontaras, V. Franco, P. Dilara, G. Martini, and U. Manfredi, "Development and review of Euro 5 passenger car emission factors based on experimental results over various driving cycles," *Science of the Total Environment*, vol. 468–469, no. 2014, pp. 1034–1042, 2014, doi: 10.1016/j.scitotenv.2013.09.043.
- [108] M. André, "The ARTEMIS European driving cycles for measuring car pollutant emissions," *Science of the Total Environment*, vol. 334–335, pp. 73–84, 2004, doi: 10.1016/j.scitotenv.2004.04.070.
- [109] Green NCAP, "BAB Motorway Test Cycle," *Green NCAP*. 2019. Accessed: Mar. 07, 2022. [Online]. Available: https://www.greenncap.com/wp-content/uploads/GNT_BAB_Motorway_v1.0.0.pdf
- [110] Y. Chen, R. Sun, and J. Borken-Kleefeld, "On-Road NO_x and Smoke Emissions of Diesel Light Commercial Vehicles-Combining Remote Sensing Measurements from across Europe," *Environ Sci Technol*, vol. 54, no. 19, pp. 11744–11752, Oct. 2020, doi: 10.1021/acs.est.9b07856.
- [111] A. Dimaratos, G. Triantafyllopoulos, L. Ntziachristos, and Z. S. Emisia, "Real-world emissions testing on four vehicles," pp. 1–37, 2017.
- [112] J. Janssen and N. Hagberg, "Plume Chasing A way to detect high NO_x emitting vehicles," no. x, 2020, [Online]. Available: <http://www.avl.com/>
- [113] D. Pöhler, "Report Heavy Duty Vehicle (HDV) NO_x emission measurement with mobile remote sensing (Plume Chasing) and subsequent inspection of high emitters A study in Denmark September / October 2020," *Airyx GmbH*, no. x, 2020.
- [114] J. Janssen and N. Hagberg, "Stationary NO_x measurements. A way to detect high NO_x emitting vehicles," *AVL MTC Motortestcenter AB*, no. x, 2020, [Online]. Available: <http://www.avl.com/>
- [115] G. A. Bishop, J. R. Starkey, A. Ihlenfeldt, W. J. Williams, and D. H. Stedman, "IR long-path photometry: a remote sensing tool for automobile emissions," vol. 61, no. 10, pp. 671A–677A, 1989, doi: 10.1021/ac00185a002.
- [116] H. D. Kuhns *et al.*, "Remote sensing of PM, NO, CO and HC emission factors for on-road gasoline and diesel engine vehicles in Las Vegas, NV," *Science of the*

- Total Environment*, vol. 322, no. 1–3, pp. 123–137, 2004, doi: 10.1016/j.scitotenv.2003.09.013.
- [117] C. Mazzoleni *et al.*, "Correlation between automotive CO, HC, NO, and PM emission factors from on-road remote sensing: Implications for inspection and maintenance programs," *Transp Res D Transp Environ*, vol. 9, no. 6, pp. 477–496, 2004, doi: 10.1016/j.trd.2004.08.006.
- [118] D. C. Carshaw, M. L. Williams, J. E. Tate, and S. D. Beevers, "The importance of high vehicle power for passenger car emissions," *Atmos Environ*, vol. 68, pp. 8–16, 2013, doi: 10.1016/j.atmosenv.2012.11.033.
- [119] D. C. Carshaw and G. Rhys-Tyler, "New insights from comprehensive on-road measurements of NO_x, NO₂ and NH₃ from vehicle emission remote sensing in London, UK," *Atmos Environ*, 2013, doi: 10.1016/j.atmosenv.2013.09.026.
- [120] D. C. Carshaw, N. J. Farren, A. R. Vaughan, W. S. Drysdale, S. Young, and J. D. Lee, "The diminishing importance of nitrogen dioxide emissions from road vehicle exhaust," *Atmos Environ X*, vol. 1, no. 2, p. 100002, 2019, doi: 10.1016/j.aea.2018.100002.
- [121] J. Borken-Kleefeld *et al.*, "Contribution of vehicle remote sensing to in-service/real driving emissions monitoring-CONOX Task 3 report," Stockholm, Mar. 2018. [Online]. Available: www.ivl.se
- [122] H. Jenk, A. Sjödin, Y. Bernard, R. Muncrief, U. Tietge, and D. Carshaw, "The CONOX project: Pooling, sharing and analyzing European remote sensing data," *ICCT*. Accessed: Sep. 05, 2023. [Online]. Available: https://theicct.org/sites/default/files/CONOX%20presentation%20Brussels%2028%20Sep_Final_v4.pdf
- [123] T. Dallmann, Y. Bernard, U. Tietge, and R. Muncrief, "Remote sensing of motor vehicle emissions in Paris," *The Real Urban Emissions Initiative (TRUE)*, no. September, p. 44, 2019, [Online]. Available: https://theicct.org/sites/default/files/publications/TRUE_ParisRS_study_20190909.pdf
- [124] T. Dallmann, Y. Bernard, U. Tietge, and R. Muncrief, "Remote sensing of motor vehicle exhaust emissions in London," *The Real Urban Emissions Initiative (TRUE)*, no. December, p. 34, 2018, [Online]. Available: <https://theicct.org/publications/on-road-emissions-paris-201909>
- [125] Y. Bernard, T. Dallmann, K. Lee, I. Rintanen, and U. Tietge, "Evaluation of real-world vehicle emissions in Brussels," Washington DC, Nov. 2021. Accessed: Mar. 05, 2022. [Online]. Available: <https://theicct.org/wp-content/uploads/2021/12/TRUE-Brussels-report-2021-11-19.pdf>
- [126] Y. Bernard, U. Tietge, and I. Pniewska, "Remote sensing of motor vehicle emissions in Krakow," Washington DC, Sep. 2020. Accessed: Mar. 05, 2022. [Online]. Available: <https://theicct.org/wp-content/uploads/2021/06/Remote-sensing-Krakow-sept2020-1.pdf>
- [127] U. Tietge, Y. Bernard, J. German, R. Muncrief, G.-M. Alt, and J. Sintermann, "A comparison of light-duty vehicle NO_x emissions measured by remote sensing

- in Zurich and Europe," Washington DC, 2019. [Online]. Available: www.theicct.org%7C@TheICCT
- [128] N. Hooftman, M. Messagie, J. van Mierlo, and T. Coosemans, "A review of the European passenger car regulations – Real driving emissions vs local air quality," *Renewable and Sustainable Energy Reviews*, vol. 86, no. January, pp. 1–21, 2018, doi: 10.1016/j.rser.2018.01.012.
- [129] P. Bonnel *et al.*, "EUROPEAN PROJECT ON PORTABLE EMISSIONS MEASUREMENT SYSTEMS: 'EU-PEMS' PROJECT," *Institute for Environment and Sustainability, Joint Research Centre, European Commission*, no. Status and Activity Report 2004-2005, p. 34, 2006, Accessed: Dec. 07, 2021. [Online]. Available: <http://europa.eu.int>
- [130] M. Weiss *et al.*, "Analyzing on-road emissions of light-duty vehicles with Portable Emission Measurement Systems (PEMS)," 2011.
- [131] Y. Wu *et al.*, "The challenge to NO_x emission control for heavy-duty diesel vehicles in China," *Atmos. Chem. Phys. Atmospheric Chemistry and Physics*, vol. 12, pp. 9365–9379, 2012, doi: 10.5194/acp-12-9365-2012.
- [132] M. Fu, Y. Ge, X. Wang, J. Tan, L. Yu, and B. Liang, "NO_x emissions from Euro IV busses with SCR systems associated with urban, suburban and freeway driving patterns," *Science of the Total Environment*, vol. 452–453, no. x, pp. 222–226, 2013, doi: 10.1016/j.scitotenv.2013.02.076.
- [133] S. Zhang *et al.*, "Can Euro V heavy-duty diesel engines, diesel hybrid and alternative fuel technologies mitigate NO_x emissions? New evidence from on-road tests of buses in China," *Appl Energy*, 2014, doi: 10.1016/j.apenergy.2014.07.008.
- [134] European Commission, "COMMISSION REGULATION (EU) 2016/427 of 10 March 2016 amending Regulation (EC) No 692 / 2008 as regards emissions from light passenger and commercial vehicles (Euro 6)," *Official Journal of the European Union*, vol. L82, Mar. 2016.
- [135] V. Franco, M. Kousoulidou, M. Muntean, L. Ntziachristos, S. Hausberger, and P. Dilara, "Road vehicle emission factors development: A review," *Atmos Environ*, 2013, doi: 10.1016/j.atmosenv.2013.01.006.
- [136] G. Kadijk, P. van Mensch, and J. Spreen, "Detailed investigations and real-world emission performance of Euro 6 diesel passenger cars," Delft, May 2015. [Online]. Available: www.tno.nl
- [137] N. Fonseca, J. Casanova, and F. Espinosa, "Influence of Driving Style on Fuel Consumption and Emissions in Diesel Powered Passenger Car," in *18th International Symposium Transport and Air Pollution*, EMPA, 2010, pp. 1–6.
- [138] J. Casanova and N. Fonseca, "ENVIRONMENTAL ASSESSMENT OF LOW SPEED POLICIES FOR MOTOR VEHICLE MOBILITY IN CITY CENTRES," 2012.
- [139] J. Gallus, U. Kirchner, R. Vogt, and T. Benter, "Impact of driving style and road grade on gaseous exhaust emissions of passenger vehicles measured by a Portable Emission Measurement System (PEMS)," *Transp Res D Transp Environ*, vol. 52, pp. 215–226, 2017, doi: 10.1016/j.trd.2017.03.011.

- [140] R. A. Varella, M. v. Faria, P. Mendoza-Villafuerte, P. C. Baptista, L. Sousa, and G. O. Duarte, "Assessing the influence of boundary conditions, driving behavior and data analysis methods on real driving CO₂ and NO_x emissions," *Science of the Total Environment*, vol. 658, pp. 879–894, Mar. 2019, doi: 10.1016/j.scitotenv.2018.12.053.
- [141] J. M. Luján, V. Bermúdez, V. Dolz, and J. Monsalve-Serrano, "An assessment of the real-world driving gaseous emissions from a Euro 6 light-duty diesel vehicle using a portable emissions measurement system (PEMS)," *Atmos Environ*, 2018, doi: 10.1016/j.atmosenv.2017.11.056.
- [142] P. Söderena *et al.*, "Monitoring Euro 6 diesel passenger cars NO_x emissions for one year in various ambient conditions with PEMS and NO_x sensors," *Science of the Total Environment*, vol. 746, no. x, p. 140971, 2020, doi: 10.1016/j.scitotenv.2020.140971.
- [143] Z. Mera, N. Fonseca, J. M. López, and J. Casanova, "Analysis of the high instantaneous NO_x emissions from Euro 6 diesel passenger cars under real driving conditions," *Appl Energy*, vol. 242, no. x, pp. 1074–1089, 2019, doi: 10.1016/j.apenergy.2019.03.120.
- [144] E. Pucher and A. Gruber, "New universal short test procedure for NO_x and Particle number at periodic technical inspection." CITA, Vienna, Oct. 22, 2019.
- [145] G. Kadijk and A. Mayer, "White paper NPTI-the New Periodic Technical Inspection emission test procedure for vehicles with emission control systems," in *ETH Conference*, Zürich, Jun. 2017.
- [146] S. Lipp and J. Blassnegger, "New procedure of NO_x emission test (AU) in a future Periodic Technical Inspection (PTI)," Graz, Feb. 2021. [Online]. Available: <http://fvt.tugraz.at>
- [147] F. Schneider *et al.*, "Further development of exhaust emissions testing. Short version," Dessau-Rosslau, Aug. 2019. [Online]. Available: <http://www.umweltbundesamt.de/publikationen>
- [148] C. Bieth and Y. Sommer, "NO_x study for PTI," *WG2 CITA meeting Tbilissi*. UTAC CERAM, Tbilissi, Mar. 24, 2020.
- [149] P. Buekenhoudt *et al.*, "Ontwikkeling van een NO_x-emissietest voor gebruik tijdens de technische voertuigkeuring," Erembodegem, 2022. Accessed: Oct. 02, 2023. [Online]. Available: <https://www.vmm.be/publicaties/ontwikkeling-van-een-nox-emissietest-voor-gebruik-tijdens-de-technische-voertuigkeuring>
- [150] V. Díaz López, S. Sanz Sánchez, E. Olmeda Santamaría, and S. Satos Cuadros, "PTI METHODOLOGY FOR INSPECTION OF NO_x AND PARTICLE MATTER EMISSIONS," Madrid, 2022. Accessed: Aug. 31, 2022. [Online]. Available: https://www.aeca-itv.com/wp-content/uploads/2022/06/PTI-METHODOLOGY-INSPECTION-NOx-AND-PARTICLE-vf-eng-GB_DocEjec.pdf
- [151] Joint Research Centre, "PTI – DeNO_x systems monitoring. Presented at the CITA Task Force on Emissions on Web/Online Meeting." European Commission, 2023. [Online]. Available: https://citainsp.org/wp-content/uploads/2023/02/220912_PTI_NOx_V5.pdf

- [152] D. Thomas, G. S. Sandhu, T. Nilsson, and S. Bjurkvist, "Investigating the Incorporation of Idle, High Idle, and Driving Acceleration NO_x Emissions Tests into the Periodic Technical Inspection Procedures," *Atmosphere (Basel)*, vol. 14, no. 3, p. 536, 2023, doi: 10.3390/atmos14030536.
- [153] UNE, "UNE 26110 - Vehículos de carretera. Criterios para la evaluación de la equivalencia de métodos de eficacia de frenado con respecto a los definidos en la Norma ISO 21069." pp. 1–21, 2017.
- [154] K. Tucki, R. Mruk, O. Orynycz, K. Botwinska, A. Gola, and A. Baczyk, "Toxicity of exhaust fumes (CO, NO_x) of the compression-ignition (diesel) engine with the use of simulation," *Sustainability (Switzerland)*, vol. 11, no. 8, pp. 1–15, 2019, doi: 10.3390/su11082188.
- [155] N. E. Fonseca González, "Aspectos de la medición dinámica instantánea de emisiones de motores. Aplicación al desarrollo de un equipo portátil y una metodología para estudios de contaminación de vehículos en tráfico real," 2012.
- [156] S. Kwon, Y. Park, J. Park, J. Kim, K. H. Choi, and J. S. Cha, "Characteristics of on-road NO_x emissions from Euro 6 light-duty diesel vehicles using a portable emissions measurement system," *Science of the Total Environment*, 2017, doi: 10.1016/j.scitotenv.2016.10.101.
- [157] L. Yang *et al.*, "Evaluating real-world CO₂ and NO_x emissions for public transit buses using a remote wireless on-board diagnostic (OBD) approach," *Environmental Pollution*, 2016, doi: 10.1016/j.envpol.2016.07.025.
- [158] T. Dallmann, "Real-world emissions in the United States: The TRUE U.S. remote sensing database," *The Real Urban Emissions Initiative (TRUE)*, London, Oct. 2020. [Online]. Available: <https://theicct.org/publications/true-us-database->
- [159] V. Bermúdez, J. R. Serrano, P. Piqueras, J. Gómez, and S. Bender, "Analysis of the role of altitude on diesel engine performance and emissions using an atmosphere simulator," *International Journal of Engine Research*, vol. 18, no. 1–2, pp. 105–117, 2017, doi: 10.1177/1468087416679569.
- [160] Y. Chen, X. Wu, K. Hu, and J. Borken-Kleefeld, "Nox emissions from diesel cars increase with altitude," *Transp Res D Transp Environ*, vol. 115, Feb. 2023, doi: 10.1016/j.trd.2022.103573.
- [161] G. Kadijk, M. Elstgeest, N. E. Ligterink, and P. J. van der Mark, "Emissions of six petrol vehicles with high mileages," The Hague, Jun. 2018. [Online]. Available: www.emissieregistratie.nl.
- [162] N. H. Abu-Hamdeh and K. A. Alnefaie, "A Comparative Study of Almond Biodiesel-Diesel Blends for Diesel Engine in Terms of Performance and Emissions," *Biomed Res Int*, vol. 2015, p. 529808, 2015, doi: 10.1155/2015/529808.
- [163] X. J. Man, C. S. Cheung, Z. Ning, L. Wei, and Z. H. Huang, "Influence of engine load and speed on regulated and unregulated emissions of a diesel engine fueled with diesel fuel blended with waste cooking oil biodiesel," *Fuel*, vol. 180, pp. 41–49, 2016, doi: <https://doi.org/10.1016/j.fuel.2016.04.007>.

- [164] C. Lim, J. Lee, J. Hong, C. Song, J. Han, and J.-S. Cha, "Evaluation of regulated and unregulated emissions from a diesel powered vehicle fueled with diesel/biodiesel blends in Korea," *Energy*, vol. 77, pp. 533–541, 2014, doi: <https://doi.org/10.1016/j.energy.2014.09.040>.
- [165] S. K. Grange, N. J. Farren, A. R. Vaughan, R. A. Rose, and D. C. Carslaw, "Strong Temperature Dependence for Light-Duty Diesel Vehicle NO_x Emissions.," *Environ Sci Technol*, vol. 53, no. 11, pp. 6587–6596, Jun. 2019, doi: [10.1021/acs.est.9b01024](https://doi.org/10.1021/acs.est.9b01024).
- [166] J. Cha, J. Lee, and M. S. Chon, "Evaluation of real driving emissions for Euro 6 light-duty diesel vehicles equipped with LNT and SCR on domestic sales in Korea," *Atmos Environ*, vol. 196, no. February 2018, pp. 133–142, 2019, doi: [10.1016/j.atmosenv.2018.09.029](https://doi.org/10.1016/j.atmosenv.2018.09.029).
- [167] P. G. Boulter, T. Barlow, I. S. Mccrae, and S. Latham, "OSCAR: On-board emission measurements in Central London," *Transport Research Laboratory*, no. TRL Report: UPR/IE/034/06, p. 26, 2006, [Online]. Available: <http://www.eu-oscar.org>
- [168] P. Mock and J. German, "The future of vehicle emissions testing and compliance. How to align regulatory requirements, customer expectations, and environmental performance in the European Union," *ICCT*, vol. White Paper, no. November, p. 36, 2015, [Online]. Available: <http://www.theicct.org/future-of-vehicle-testing>
- [169] European Commission, "Directive 2010/48/EU on roadworthiness tests for motor vehicles and their trailers," *Official Journal of the European Union*, vol. L173, pp. 47–72, 2010, [Online]. Available: <http://ec.europa.eu/transport/>
- [170] European Parliament and The Council of the European Communities, "DIRECTIVE 2009/40/EC on roadworthiness tests for motor vehicles and their trailers," 2009.
- [171] J. Dekoster, U. Schollaert, and N. S. European Commission. Directorate-General for Environment, *Cycling: the way ahead for towns and cities*. Office for Official Publications of the European Commission, 1999. Accessed: Mar. 09, 2022. [Online]. Available: http://ec.europa.eu/environment/archives/cycling/cycling_en.pdf
- [172] K. S. Chen, C. Y. Chung, and S. W. Wang, "Measurement and three-dimensional modeling of airflow and pollutant dispersion in an undersea traffic tunnel," *J Air Waste Manage Assoc*, vol. 52, no. 3, pp. 349–363, 2002, doi: [10.1080/10473289.2002.10470783](https://doi.org/10.1080/10473289.2002.10470783).
- [173] C. Y. Chung and P. L. Chung, "A numerical and experimental study of pollutant dispersion in a traffic tunnel," *Environ Monit Assess*, vol. 130, no. 1–3, pp. 289–299, 2007, doi: [10.1007/s10661-006-9397-0](https://doi.org/10.1007/s10661-006-9397-0).
- [174] Z. Ning, C. S. Cheung, Y. Lu, M. A. Liu, and W. T. Hung, "Experimental and numerical study of the dispersion of motor vehicle pollutants under idle condition," *Atmos Environ*, vol. 39, no. 40, pp. 7880–7893, Dec. 2005, doi: [10.1016/j.atmosenv.2005.09.020](https://doi.org/10.1016/j.atmosenv.2005.09.020).

- [175] E. Fernández, A. Valero, J. J. Alba, and A. Ortego, "A New Approach for Static NO_x Measurement in PTI," *Sustainability (Switzerland)*, vol. 13, no. 23, 2021, doi: 10.3390/su132313424.
- [176] E. K. Nam, "Understanding and Modeling NO_x Emissions from Air Conditioned Automobiles," *SAE Technical Paper Series*, no. 2000-01-0858, Mar. 2000, doi: 10.4271/2000-01-0858.
- [177] D. Vu, J. Szente, M. Loos, and M. Maricq, "How Well Can mPEMS Measure Gas Phase Motor Vehicle Exhaust Emissions?," *SAE International*, Apr. 2020, doi: 10.4271/2020-01-0369.
- [178] N. Ladommatos, S. Abdelhalim, and H. Zhao, "Control of oxides of nitrogen from diesel engines using diluents while minimising the impact on particulate pollutants," *Appl Therm Eng*, vol. 18, pp. 963–980, 1998.
- [179] INTERNATIONAL STANDARD, "ISO 21069-1A:2004 Road vehicles - Test of braking systems on vehicles with a maximum authorized total mass of over 3,5 t using a roller brake tester Part 1 : Pneumatic braking systems." ISO 21069-1:2004(E), pp. 1–16, 2004.
- [180] E. Fernández, A. Ortego, A. Valero, and J. J. Alba, "Suitability Assessment of NO_x Emissions Measurements with PTI Equipment," *Vehicles*, vol. 4, no. 4, pp. 917–941, 2022, doi: 10.3390/vehicles4040050.
- [181] OIML, "OIML R99 - 1 & 2 Edition 2008 (E) Instruments for measuring vehicle exhaust emissions Part 1: Metrological and technical requirements Part 2: Metrological controls and performance tests," , 2008.
- [182] V. Bermúdez, A. García, D. Villalta, and L. Soto, "Assessment on the consequences of injection strategies on combustion process and particle size distributions in Euro VI medium-duty diesel engine," *International Journal of Engine Research*, vol. 21, no. 4, pp. 683–697, Apr. 2020, doi: 10.1177/1468087419865652.
- [183] P. Fernández-Yáñez, J. A. Soriano, C. Mata, O. Armas, B. Pla, and V. Bermúdez, "Simulation of optimal driving for minimization of fuel consumption or NO_x emissions in a diesel vehicle," *Energies (Basel)*, vol. 14, no. 17, Sep. 2021, doi: 10.3390/en14175513.
- [184] B. Pla, P. Piqueras, P. Bares, and A. Aronis, "NO_x sensor cross sensitivity model and simultaneous prediction of NO_x and NH₃ slip from automotive catalytic converters under real driving conditions," *International Journal of Engine Research*, vol. 22, no. 10, pp. 3209–3218, Oct. 2020, doi: 10.1177/1468087420966406.
- [185] ISO and OIML, "ISO 3930:2000(E) / OIML R99:2000(E) Instruments for measuring vehicle exhaust emissions," Geneva, Sep. 2000. [Online]. Available: www.iso.ch
- [186] CFR, "PART 1065: ENGINE-TESTING PROCEDURES," *Code of Federal Regulations (CFR)*, vol. 37, no. 40. Code of Federal Regulations, USA, pp. 46–293, 2021. Accessed: Sep. 05, 2022. [Online]. Available: <https://www.govinfo.gov/content/pkg/CFR-2021-title40-vol37/pdf/CFR-2021-title40-vol37-part1065.pdf>

- [187] EPA (United States Environmental Protection Agency), "PART 1066: VEHICLE-TESTING PROCEDURES," *Code of Federal Regulations (CFR)*, vol. 37, no. 40. pp. 293–393, 2021. Accessed: Sep. 05, 2022. [Online]. Available: <https://www.govinfo.gov/content/pkg/CFR-2021-title40-vol37/pdf/CFR-2021-title40-vol37-part1066.pdf>
- [188] ISO/IEC, "ISO/IEC 17025:2005(E) General requirements for the competence of testing and calibration laboratories," Geneva, 2005.
- [189] A. Inc., *Andros Inc. Model 6900 Product Manual (Compact Automotive Gas)*, no. 891166. Richmond, CA: Andros Incorporated.
- [190] ANFAC, "INFORME ANUAL 2018," 2018. Accessed: Aug. 31, 2023. [Online]. Available: https://anfacs.com/informe_anual_2018/
- [191] ANFAC, "INFORME ANUAL 2019," 2019. [Online]. Available: https://anfacs.com/wp-content/uploads/2020/07/ANFAC_INFORME_ANUAL_2019_VC.pdf
- [192] Z. Mera, N. Fonseca, J. M. López, and J. Casanova, "Analysis of the high instantaneous NO_x emissions from Euro 6 diesel passenger cars under real driving conditions," *Appl Energy*, vol. 242, pp. 1074–1089, May 2019, doi: 10.1016/j.apenergy.2019.03.120.
- [193] European Commission, "COMMISSION REGULATION (EC) No 692/2008 of 18 July 2008," 2008.
- [194] "EUROPEAN VEHICLE MARKET STATISTICS," 2019. [Online]. Available: <http://eupocketbook.theicct.org>
- [195] M. André, "Driving patterns analysis and driving cycles, within the project: European Development of Hybrid Technology approaching efficient Zero Emission Mobility (HYZEM)," *INRETS report*, vol. LEN 9709, p. 47, 1997.
- [196] E. Commission, "Proposal for a REGULATION OF THE EUROPEAN PARLIAMENT AND OF THE COUNCIL," *COM(2022)*, vol. 586 final, no. 2022/0365 (COD), pp. 1–66, 2023.
- [197] S. Roiser, P. Christoforetti, E. Schutting, and H. Eichlseder, "Emission behaviour and aftertreatment of stationary and transient operated hydrogen engines," *International Journal of Engine Research*, May 2023, doi: 10.1177/14680874231172316.
- [198] J. Ramón Serrano, R. Payri, B. Tormos, and A. Gómez Vilanova, "The real necessity of Internal Combustion Engines development for fighting against climatic change crisis from the point of view of Road Transport," *Técnica Industrial, noviembre*, vol. 2019, pp. 48–54, doi: <https://doi.org/10.23800/10329485432>.
- [199] CITA, "Monitoring of NO_x emissions as part of the PTI," Brussels, May 2022. Accessed: May 20, 2022. [Online]. Available: https://citainsp.org/wp-content/uploads/2022/05/CITA-NOx-Position-Paper_FINAL_May_22.pdf
- [200] W. G. 1 (JCGM/WG 1) Joint Committee for Guides in Metrology, "JCGM 100:2008 GUM 1995 with minor corrections, Evaluation of measurement data

- Guide to the expression of uncertainty in measurement," 2008. [Online]. Available: <http://www.bipm.org/en/publications/guides/gum.html>
- [201] E. A. L. Committee, "EA-4 / 02 M : 2013 Evaluation of the Uncertainty of Measurement In Calibration," p. 75, 2013, [Online]. Available: www.european-accreditation.org

ASSESSMENT AND MEASUREMENT OF NO_x EMISSIONS IN LIGHT DIESEL VEHICLES DURING PERIODIC TECHNICAL INSPECTION

Zaragoza, 2023

Eugenio Fernández Cáceres